UNIVERSITY OF SHEFFIELD

Department of Civil and Structural Engineering

A STUDY OF MODEL RETAINING WALLS SUPPORTED BY MULTI-PLATE ANCHORS

By

MAGUED N. ABDEL-MALEK

B.Sc., M.Sc.

Thesis submitted to the University of Sheffield for the Degree of Doctor of Philosophy

July, 1978

To my parents

A STUDY OF MODEL RETAINING WALLS SUPPORTED BY MULTI-PLATE ANCHORS

By

MAGUED N. ABDEL-MALEK

B.Sc., M.Sc.

SUMMARY

The study reported in this thesis forms part of a continuing programme of research on the performance of anchors and anchored supported structures being carried out at the University of Sheffield.

In addition to a review of some of the recent laboratory studies, field observations and analytical investigations, the present study incorporates two main parts. In the first part, the failure mechanism and load carrying capacity of multi-plate anchors were investigated in a series of small scale studies. The study showed the difference in behaviour between single and multi-plate horizontal anchors and led to a better understanding of their failure mechanism. It also provided information for the design of the multi-plate anchors to be used in the second part of the research programme.

In the second part, the behaviour of a 0.6 m high rigid retaining wall in a normally consolidated sand and supported by up to four rows of anchors, was studied.

Different design methods were employed to examine the overall stability of the wall-anchors-soil system. These were investigated experimentally in a series of tests in which field construction procedure was simulated. After construction was completed, the

retained backfill was subjected to surcharge loading in an attempt to approach failure. Normal earth pressure distribution on both sides of the wall, normal and shear components of the wall base reaction, anchor load changes, anchor movements, wall movements, sand surface subsidence and sand movements within the retained sand mass were monitored.

The study showed the reliability of the different design methods and the effect of parameters such as anchor lengths and prestress loads on the overall behaviour of the systems.

ACKNOWLEDGEMENTS

This research was carried out in the Department of Civil and Structural Engineering of the University of Sheffield, where the equipment, materials and facilities used were provided. Financial support was provided by the Egyptian Government.

The author wishes to express his gratitude to Professor T. H. Hanna for initiating the study, for his many valuable suggestions and his vigorous encouragement throughout the study. The author also wishes to thank Dr. W. F. Anderson for his guidance, supervision, assistance, advice and unfailing help throughout all stages of the study.

The author gratefully acknowledges the help and assistance of the technical staff of the Department. In particular he wishes to thank Mr. J. D. Webster, Mr. V. Harrison and Mrs. D. Hutson.

Many thanks are due to the author's colleagues in the Geotechnics Research Laboratory for their constructive comments.

The author wishes also to acknowledge Miss J. Healey for her kind help in typing this thesis.

Finally, the author wishes to express his love and gratitude to his wife Elham, whose understanding and encouragement kept him going through all the difficult periods of his study.

CONTENTS

NOTATIONS USED IN THE THESIS

B = Anchor plate height

b = Anchor plate length

C' = Shear strength parameter

D = Embedment depth

E = Measured horizontal component of earth load on back of wall

F = Factor of safety defined as $\tan \phi' / \tan \phi'_m$

H = Wall height

Km = Mobilized earth pressure coefficient

Ko = Coefficient of earth pressure "at-rest"

L = Free anchor length

L_W = Length of central wall

ℓ = Anchorage length

N_{qu} = Uplift coefficient for anchors in Meyerhof's analysis

P_i = Measured anchor load

P_t = Theoretical prestress load

Q = Ultimate pulling load

S_i = Shear component of reaction at wall base

T_{af} = Measured normal component of the wall base reaction after sand filling

T_i = Measured normal component of the wall base reaction at any testing stage

α = Slope angle of backfill in Coulomb's analysis

β = Angle of wall inclination in Coulomb's analysis

γ = Unit weight

δ = Angle of wall friction

δ_{wm} = Mobilized angle of wall friction

ϕ' = Angle of shearing resistance

ϕ'_m = Mobilized angle of shearing resistance in the retained sand mass

λ = Distance between successive plates in an anchor block

θ = Inclination of the anchors from the horizontal

NOTATIONS USED IN APPENDICES

A = Cross-sectional area of proving ring

B = Proving ring width

F = Resultant force on the rupture line in Dubrova's analysis

f = Predicted stress in the proving ring

h = Function of the geometry of the section of a proving ring

N = Applied force on the proving ring

P = Earth pressure force against the wall in Dubrova's analysis

ro = Mean radius of proving ring

t = Half thickness of proving ring

X_b = True bottom horizontal displacement of the wall

X_{bm} = Measured bottom horizontal displacement of the wall

X_t = True top horizontal displacement of the wall

X_{tm} = Measured top horizontal displacement of the wall

Y_b = True bottom vertical displacement of the wall

Y_c = The distance between the centre of the wall rotation and the toe of the wall

Y_t = True top vertical displacement of the wall

Z = Point where the rupture line intersects the wall in Dubrova's analysis

α = Angle of wall rotation at full excavation

β = The angle between X - X axis and a point on the proving ring circumference

γ = Soil unit weight

θ = Angle of inclination of the wall with the horizontal at full excavation

ψ = Angle between the line of action of the force and the normal to any rupture line in Dubrova's analysis

CHAPTER 1

INTRODUCTION

CHAPTER 1

INTRODUCTION

The increasing tendency to construct buildings with a number of basement floors, which require deep excavations in congested areas, has led to the development of methods of earth support.

The use of anchored retaining walls to support the sides of both temporary and permanent excavations has become fairly common in recent years, and the method is now being employed with increasing frequency. Despite the rapid development in construction techniques for such anchored wall systems, the complicated nature of the structure-anchors-soil interaction is not fully understood. In trying to obtain a better understanding of the design of such systems and to improve the state of knowledge of their performance, it is believed that a combination of good field observations, development of analytical techniques and laboratory model studies is needed.

An important factor in the design of anchored retaining walls is the overall stability. A number of design methods have been proposed but there is little published work on the effectiveness of these design methods. In the present study model tests have been carried out in order to compare the wall-anchors-soil behaviour when the system has been designed according to the various available design methods.

One of the limitations of previous model studies is that the important concept of interaction between the wall, the anchors and the soil has not been allowed for. In most model studies the walls have usually been supported by wires passing through the backfill and tied to the back of the apparatus, thus preventing any interaction between

the soil and the support system. In order to accomplish complete wall-anchors-soil interaction it is necessary to tie anchor wires to the wall and to embed the anchor units in the backfill.

To simulate multi-bell anchors in the present investigation, the anchor units were composed of brass rods which were connected to the wall and to a number of aluminium plates which were embedded in the backfill. The use of such anchors necessitated a preliminary study to be carried out to investigate the failure mechanism and load carrying capacity of multi-plate anchors. This was accomplished by carrying out pull-out tests on multi-plate strip anchors which were embedded at various depths. Two series of tests were carried out. In the first series a two-dimensional pin model analogy was used to study photographically the failure mechanism of horizontally loaded multi-plate anchors. In the second series, tests were carried out in a small sand box to assess quantitatively the carrying capacity of the different arrangements of multi-plates.

In the main part of this study, a smooth rigid wall supported by up to four rows of embedded multi-plate anchor units was tested in a sand flume. Different design methods were employed to check the overall stability of the wall-anchors-soil system. These resulted in a variety of anchor lengths and prestress loads, and the effect of these on the performance of the different systems was monitored. Field construction was simulated and the behaviour of the different elements comprising the wall-anchors-soil system was observed. After construction was completed, an attempt was made to approach failure of the system by applying a uniform surcharge load on the backfill. The behaviour of the different systems, under these loading conditions, was examined.

CHAPTER 2

REVIEW OF INVESTIGATIONS INTO THE BEHAVIOUR OF TIED-BACK RETAINING WALLS

CHAPTER 2

REVIEW OF INVESTIGATIONS INTO THE BEHAVIOUR OF TIED-BACK RETAINING WALLS

2.1 Introduction

In the last few years, there has been a great increase in the use of multi-tied retaining walls to support deep excavations. As has frequently happened in the past, construction practice has developed ahead of theory, and in trying to catch up and to obtain a better understanding of their design, Hanna (1971) suggested a study having the following objectives:

i) The evaluation of the performance of well instrumented laboratory scale walls in which excavation is simulated for a range of design assumptions.

ii) Measurement of the performance of well instrumented field excavations supported by tied-back walls.

iii) Development of analytical models using the finite element method of analysis with appropriate soil constants.

In the following sections some of the laboratory, field and analytical studies are reviewed, followed by a review of the methods of assessing overall stability.

2.2 Laboratory Studies

2.2.1 Progress of laboratory work

Early work on laboratory scale tests on model sheet pile walls started more than forty years ago. Stroyer (1935), Tschebotarioff (1949), Browzin (1948), Rowe (1952) and Rowe (1956) investigated the

problem of a sheet pile wall supported by a single row of ties. In these studies parameters such as anchor level, anchor yield, dredging level, soil type and stress history, surcharge load and distribution of soil pressure were investigated.

Work was continued by Rowe and Briggs (1961) in a series of tests on a model strutted wall 3' 6" (1.07 m) high and 7' (2.14 m) long using loose dry sand for the retained material and varying the number of strut levels. Lateral pressures, bending moments and strut loads were measured. In their concluding comments, they emphasised the need to differentiate between deformation and failure problems. With a single strut, as in a sheet pile wall, the total active load can be calculated on the basis of failure, although the passive fixity is not a failure calculation. However, with several struts, the purpose of which is to prevent soil deformation, not even the active load may be computed on the basis of the failure parameters of the soil.

Recently Breth and Wanoschek (1972) carried out laboratory model tests on strutted walls to investigate the influence of foundation loads upon the earth pressure acting on flexible strutted walls. In the model tests, the process of strutting and dredging in open excavation was simulated, and the foundation load was applied before the excavation started. Their main deductions were: i) earth pressure upon strutted walls - with or without foundation loads - was bigger than the active earth pressure computed according to Coulomb; ii) earth pressure depends mainly upon the dredging process and position of the struts; and iii) only loads adjacent to the wall -

within the wedge formed by an angle of $45° - \phi/2$ with the vertical - affected the pressure distribution. However, loads lying beyond this wedge and up to a certain distance affected the value of the earth pressure but did not affect the distribution.

A literature survey revealed that the vast majority of the documented laboratory studies dealt with single tied and strutted walls, from which the above mentioned were some examples. However, very few laboratory studies - excluding those carried out at Sheffield University - were entirely devoted to multi-anchored walls, among those the work carried out by James and Jack (1974) and Breth and Wolff (1976).

James and Jack (1974) carried out a series of laboratory model tests on flexible and rigid walls. Both walls were 10 ft (3.05 m) wide and 8 ft (2.44 m) deep. They were composed of two panels 4 ft x 8 ft (1.22 m x 2.44 m) and one of 2 ft x 8 ft (0.61 m x 2.44 m). Test measurements were concentrated on the central wall panel. A steel sheet of thickness 0.048 in (1.2 mm) was used to fabricate the flexible wall. Four levels, each containing five anchor rods 0.25 in (6.4 mm) diameter, were employed to support the wall. The rigid wall comprised two steel sheets 0.064 in (1.6 mm) thick bolted at a distance of 0.976 in (25.0 mm) apart. Three layers of five anchors consisting of lengths of threaded rod were used to support the wall. The rods were joined to the metal wall from one end while the other end passed through the rear wall of the apparatus and connected to flexible rings. These rings were instrumented to act as proving rings to set the prestress level in the anchors as well as to monitor anchor load changes

in the central wall. Bending stresses in the wall, wall movements, sand surface movements and anchor load changes were monitored.

One of the main purposes of this study was to assess the validity of the approach proposed by the writers to estimate anchor forces. However, a comparison of the results with the design values indicated that for the flexible wall tests, the proposed method predicted only 50% of the anchor load actually developed at the upper row, while it overestimated the loads at each of the remaining rows by an average of 27%. For the rigid wall tests a similar comparison showed that the final loads developed exceeded the design predictions for all rows, and the greatest deviations occurred in the top row (Fig. 2.1 shows anchor load variation with construction stages for the rigid wall). It was also concluded that anchor stressing had a direct influence on the settlement of the retained sand surface (Fig. 2.2). With anchor stressing the rate of settlement was reduced. It was also observed that the sand settlement for both the rigid wall and the flexible one was almost identical.

Breth and Wolff (1976) carried out model tests in which they simulated the anchors by wires fixed to thin steel plates coated with sand. These were placed in the sand - when filling the model - to imitate the grouted zone of anchors. The model wall was 1.0 m high and composed of horizontal steel elements of very stiff tubes of rectangular section. The elements were suspended on thin wires thus forming a stack chain of 15 parts. Between these chains two vertical flexible beams were fixed to give the required flexural stiffness of the wall. The wall was supported by three rows of

anchors. These were of the same length for each test, and varied from 0.395 m to 0.695 m for the different tests. Earth pressures, anchor forces, wall displacement and deformation of the sand surface were measured.

From their work Breth and Wolff concluded that the earth pressure decreased with increasing the anchor lengths and increased with increasing the prestress force (Fig. 2.3(a)). With longer anchors wall displacements were smaller (Fig. 2.3(b)). They also said that with the embedded anchors interaction between the wall, the ground and the anchors was possible, and differences in performance were to be expected when using embedded anchors and when using anchor wires fixed to the back of the apparatus. In the latter, they said, the anchors are stiff-like struts, and illustrated the fundamental differences between the two cases by presenting the results of two tests; embedded anchor units were used in the first and struts in the second (Fig. 2.3(c)). The figure shows the wall movements, where tests with embedded anchors exhibited larger movements than those with struts. Also, with struts, higher values of earth pressure were observed in the region between the top of the wall and the bottom strut, while the anchored wall showed higher values of earth pressure in the region between the bottom anchor and the toe of the wall. Anchor and strut load variations are also shown. Struts at the upper two rows attained higher load values at final excavation and during the different stages than those attained by embedded anchors, while the third row showed the reverse.

2.2.2 Research work at Sheffield University

Work has been in progress at Sheffield University for some time investigating the behaviour and performance of laboratory scale model retaining walls supported by multiple rows of prestressed anchors. Instrumentation was developed to measure parameters such as the earth pressure distribution on the wall, the anchor forces and the soil and wall movements.

The first in the series of studies was carried out by Matallana (1969), who examined the influence of the initial earth pressure design assumption on the behaviour of a retaining wall supported by three levels of anchors. Abu-Taleb (1971) modified the apparatus used by Matallana to enable additional quantities to be measured. The different variables examined by Abu-Taleb were: i) the geometrical arrangement of the anchor wires; ii) the flexibility of the anchor wires; and iii) the presence of a rigid boundary at the wall base level. He also studied the effect of anchor inclination and design pressure distribution on the above variables. Comprehensive discussion on both studies was presented by Hanna and Matallana (1970) and Hanna and Abu-Taleb (1972).

The next study was carried out by Plant (1972), who studied the behaviour of a 0.6 m high, 0.91 m long rigid retaining wall in a normally consolidated dry sand. The wall was supported by two to four levels of anchors and these were either anchor wires (part I of the study) or embedded anchor units (part II). The main variables considered by Plant were: i) the anchor inclination; ii) the anchor geometry; iii) the wall design assumption; iv) the number

of anchor levels; and v) the anchor lengths.

Plant concluded that the magnitudes of wall and sand movements were affected by the number of anchor rows, the anchor inclination, the anchor geometry, the initial design assumption and the anchor lengths where embedded anchor plates were used. He also said that the normal earth pressure distribution against the back of the wall was a function of the lateral wall displacement. In tests with embedded anchor units he found that the most significant load reductions were associated with the longest anchors.

The earth pressure distribution measured by the earth pressure cells as well as the measured anchor forces, shear and normal forces on the wall base enabled the calculations of the average angle of wall friction, the coefficient of earth pressure mobilized and consequently the average angle of friction mobilized in the sand mass. From these calculated values Plant said that tests with embedded anchors did not establish any definite trend for the mobilized angle of wall friction or the mobilized angle of friction in the sand mass.

He also mentioned that the Kranz method (1953) for anchor length determination is far from ideal since it takes no account of the strain or stress distribution in the retained backfill as it assumes a specific rupture surface. However, he stated that the method is a practical solution in designing the anchor lengths at the present time. Plant criticized the slip circle method which, he said, neglects the effect of anchor forces and gives rise to much larger wall movements compared with the Kranz method.

Kurdi (1973) studied the behaviour of five tied-back retaining walls having different flexibilities. The wall was supported by three levels of anchors, the main variables considered were: i) the flexibility of the wall; ii) the anchor geometry; and iii) the anchor inclinations. Hanna and Kurdi (1974) presented a comprehensive discussion about this study, in which they concluded that: i) the greatest anchor load changes were associated with inclined anchor supports or very flexible walls; ii) the earth pressure behind a flexible wall was reduced by the wall moving away from the retained soil. It was also redistributed by sand arching and concentrated near to the anchorage levels; iii) the maximum bending moment in a wall decreased with wall flexibility increase; iv) surface subsidence extended to more than two wall heights away from the wall; v) lateral wall movements were regulated by its flexibility and by anchor inclination. The movements were considerably greater than those for a similar rigid wall; and vi) the design approach using a rectangular earth pressure distribution appeared reasonable.

Dina (1973) approached the problem in two ways. Firstly, using a pin model analogy, he carried out a photographic study of the failure surfaces developed in the soil behind a tie-back retaining wall. The model wall varied in inclination between -30° and +30° to the vertical, and several modes of wall rotation and translation were investigated. Secondly, the behaviour of a rigid inclined wall supported by three levels of prestressed anchor wires in a sand medium, was studied. Variables such as earth pressure design assumption, wall inclination and anchor wire inclination were investigated. The following

conclusions were listed by Dina: i) earth pressure distribution against the back of the wall was a function of the lateral wall displacement; ii) large lateral movements at the top of the wall were associated with positively inclined walls, while with negatively inclined walls the largest movement was at the wall base; iii) negatively inclined walls experienced a decrease in the base normal reaction throughout the construction stages, while an increase in the base normal reaction was observed with positively inclined walls; iv) from the photographic study it was found that the inclination of the wall, the mode of wall movement, the length of the anchors and their size and inclination all had a large effect on the failure mechanism. The failure zones were not plane but were the result of the interaction of a number of individual failure surfaces.

The next study in the continuing programme of research was carried out by Ponniah (1973). He studied the effect which surcharge load had on the performance of anchored retaining walls. The principal variables he considered were: i) the intensity of the uniformly distributed surcharge; ii) the anchor inclination. He summarised the results of his work in the following conclusions: i) increases in either the anchor inclination or the surcharge intensity increased the wall movements, the surface subsidence, the anchor load changes, the normal component of the base reaction and the range of values of base shear; ii) Coulomb's failure theory, used to compute the mobilized angle of internal friction, was found to be inapplicable to sands which were surcharged; iii) from the pressure distributions obtained a design earth pressure distribution for a uniformly

distributed surcharge was suggested.

Shah (1975) continued the research on laboratory scale model walls. In the first part of his work he repeated some of Plant's tests to examine the effect of varying the overconsolidation ratio on the behaviour of the wall. He also studied the effect of anchor inclination when the wall supported overconsolidated sand. In the second part he studied the behaviour of the wall under the effect of a strip loading which was varied in magnitude and position. A total of ten tests was performed with an overconsolidation ratio varying between 1 and 4, anchor inclination between 0°-30°, line load pressure between 0 and 12 KN/m^2 at a distance from the wall varying between 90 mm and 240 mm. He summarised his conclusions as: i) anchor inclination has a significant effect on wall movements in overconsolidated sand, where the wall movements were of the order of three times those in normally consolidated sand; ii) for both normally and overconsolidated sands, the sand subsidence at full excavation depth and the variations of anchor loads were of the same order; iii) strip loads close to the wall affected the earth pressure distribution, but this effect was not too apparent with increased distance of the strip load from the wall; iv) anchor load changes increased with increasing the intensity of strip loading and decreased with increasing the distance of the strip loading from the wall; v) determination of the mobilized angle of internal friction using Coulomb's failure theory was found to be inapplicable in the case of both overconsolidated sand and normally consolidated sand with strip loading. A full discussion of Shah's work was presented by Anderson et al. (1977).

2.3 Field Studies

2.3.1 General

Due to the complexities involved in the behaviour of multi-anchored retaining walls, there are considerable difficulties in theoretically predicting their performance. This emphasises the importance of field studies, where every possible opportunity should be taken to instrument prototype structures and observe their performance.

There are at least three important benefits from such an approach (Burland, 1977). Firstly, the accuracy of present analytical and predictive techniques can be evaluated and modified as necessary. Secondly, the in situ properties of the ground can be deduced by back analysis and compared with laboratory and in situ determinations. Thirdly and perhaps most important, the measurements provide quantitative data which can be used as an aid to judgement in future design and construction works.

Plant (1972) and Ponniah (1973) reported and discussed in detail some very useful examples of well documented field studies such as Pierre Lacland Building in Missouri (Mansur and Alizadeh, 1970), Emo Building in Madrid (Maestre, 1969), Societe General de Belgique in Brussels (Vander Linden, 1969), Seattle's First National Bank building in the U.S.A. (Shannon and Strazer, 1970), Pickering Generating Station, Ontario, Canada (Hanna and Seeton, 1967) and The National Arts Centre, Ottawa, Canada (McRostie et al., 1972).

2.3.2 Review of recent field studies

A diaphragm wall, 0.61 m thick was constructed to retain 14.5 m of soil of the large double basement excavation for the Keybridge House, Vauxhall, in London. Littlejohn and MacFarlane (1974) presented a detailed study of the instrumentation and performance of the wall which was tied back by three rows of anchors. Figure 2.4 shows a section through the instrumented panel of the wall, and the soil profile.

Wall deformations were measured mid-way between two vertical rows of anchors. Also, anchor loads were measured using load cells that were connected between the stressing head and the loading plate.

Fig. 2.5 illustrates the wall displacement profiles relative to the toe of the wall, the overall displacements shown being taken only at the times when a general survey was performed. Profile (a) shows that an overall rotation of the wall occurred at an excavation depth of 3.05 m. Profile (b) was monitored when all anchors at the first level had been installed and stressed for one week except for one anchor immediately adjoining the inclinometer duct. As can be seen, the wall has been drawn back with apparent toe rotation. After a further 29 days when all upper level anchors were stressed, the wall deflection (profile (c)) reverted to the shape of profile (a) with no major change in prestress load being monitored. With two levels stressed a further wall displacement towards the excavation occurred (profile (e)). Following excavation to 10.4 m and the stressing of all anchors the differential displacement between the upper anchor levels increased from 0.77 mm to 2.04 mm with a further overall

rotation of 5 minutes of arc. At final excavation further rotation was indicated and the general survey showed an overall displacement of 10 mm and 0.5 mm into the excavation for the crest and toe respectively (profile (g)). Vertical displacement indicated that the crest moved down 12.2 mm. After the final stage was reached a delay of three months occurred in the construction programme, and profile (h) shows that differential displacement between crest and toe doubled, although the central anchor load exhibited only a slight loss of prestress. This indicated possible consolidation of the highly stressed soil surrounding the fixed anchor, or more likely that overall movement of the retained soil mass containing the anchors occurred. The total displacement of the crest was estimated to be 22.0 mm.

For the final two profiles (g, h), the calculated bending moment curves are given together with the design values for the corresponding stage of excavation in Fig. 2.6. Design values for the initial cantilever condition are also shown. It can be observed that the magnitudes of the bending moment maxima are in good agreement with the design values. The magnitudes of peak bending moment measured are less than the design values by about 23%. However, it should be noted that the measured moments relate to the normal groundwater level whereas the design curves have been established on the basis of flood level.

Regarding the overall behaviour, the profiles indicated that more efficient anchoring was obtained with the gravel anchors (first level) and the wall panel exhibited a rotation about the upper anchor

regions. For the two anchors successfully monitored on the panel, a drop in load occurred over a period of six months. These reductions were small, being 2.8% for level 2 and 12.7% for level 3.

It was also pointed out that the displacement and overall rotation of the wall over the cantilever stage represented a large proportion (50%) of the corresponding movements at full excavation, thus illustrating the need for early support if wall movements are to be kept to a minimum.

Gould (1970) and Saxena (1974) documented the measured behaviour of the few instrumented panels of the World Trade Centre's perimeter wall constructed by the slurry trench method. A concrete wall 3 ft (0.90 m) thick was constructed to allow the excavation and construction of six basement floors about 70 ft (21.0 m) below the ground elevation. The wall was supported by tie-back rock anchors during the construction stage; final support was provided by the floor system, and the ties were destressed. Fig. 2.7 shows the main features of the wall at two instrumented panels.

Panel W35 had six ties evenly distributed over the height of the wall, with the upper tie about 7 ft (2.10 m) below the top of the wall. The ties were installed at 100% of their design load except for the top level, which was installed at 90% of its design load. The observations showed that the wall moved continuously into the soil as excavation proceeded and the lower ties were installed. The maximum movement was about 0.2 ft (60 mm) and this was observed about a year and a half after the start of excavation (Fig. 2.8(a)). After lock-off the tie loads decreased continuously and reached the values shown in Fig. 2.8(a). Bending moments and horizontal pressures on the wall

were developed and are shown in Fig. 2.8(b), (c), together with the earth pressure distribution used in the design. Total horizontal pressures were slightly higher than the at-rest plus water pressures, except at the top of the wall and opposite the central group of four anchors.

The bending moment diagram shows that below the upper tie the moments were large and positive at the early stages of excavation. Negative moments opposite the central group of four ties, and a large positive moment at the wall base, developed as excavation progressed.

For Panel G21, due to the presence of a subway structure adjoining this panel, the first anchor was installed at a lower elevation than most panels. Furthermore, to avoid over-stressing the wall of the subway structure, the anchor was locked-off at 40% of its design load. A temporary brace held the wall until the first anchor was in its place. The remaining three ties were installed at 100% of their design load.

Fig. 2.9(a) shows that the wall moved continuously towards the excavation during construction. The maximum deflections were slightly more than 0.2 ft (60 mm). Bending moments and pressure diagrams for the completion of excavation are shown in Fig. 2.9(b) and (c). The total pressure was in the same order of the original earth and water pressures at the central part of the wall, but was slightly lower near the base.

A slight increase of load at the top level tie was observed and was attributed to the elastic elongation of the tie. However, the remaining three ties experienced a loss of load - as shown in Fig. 2.9(a) -

even though the movements of the wall were towards the excavation, indicating either slippage between tie and grout or creep at the anchorage.

Another study was carried out by Liu and Dugan (1972) on an excavation for a city block in Boston. Excavation reached a depth of 55 ft (16.5 m) in order to construct the four basements and foundations for a 40-storey office tower. A tied-back soldier pile and lagging scheme was chosen to provide lateral support, with 60-kip (267 KN) capacity tie-backs grouted into either stiff clay, compact sand or glacial till.

A plan of the site is shown in Fig. 2.10. It slopes downwards in an easterly direction from elevation 83'(24.9 m) to elevation 54' (16.20 m) and is bounded on three sides by 9- to 12-storey office buildings, all supported on footing foundations bearing above the final excavation level for the project. Fig. 2.11 shows a typical soil profile at the site. The groundwater table was located below the bottom of the excavation.

A rectangular earth pressure distribution diagram with the intensity of 15 H in lbs/ft^2, was recommended for design (where H is the height of excavation in feet). The minimum grouted anchor length was 15 ft (4.50 m), and no anchor could be placed within the zone formed by the face of excavation and the plane making a 35° angle with the vertical and intersecting the face of excavation at the final excavation grade, as shown in Fig. 2.11.

An instrumentation and monitoring programme was implemented to serve as an early warning system, to reduce the risk of undertaking

such a large and deep excavation and to yield a permanent record of movements. The monitoring system was divided into two categories: i) control survey measurements of the building and ground surrounding the site and ii) measurements of the lateral support system.

Three soldier piles were selected for installation of the soldier pile and tie-back monitoring system. The location of the test section is shown in Fig. 2.10. At these piles, the depth of excavation was greatest, 55 ft (16.5 m), and, consequently the most tie-backs (7 levels) were to be installed (Fig. 2.11).

Inclinometer SI-6 (Fig. 2.11) was installed to monitor the lateral deflection of the soldier pile. Lateral ground movement at 25 ft (7.5 m) behind the excavation was monitored by inclinometer SI-4 (Fig. 2.11). The lateral deflections are presented for selected dates in Fig. 2.12. The levels of excavation at different dates are shown to the left of the soldier pile, and the dates at which various tie-backs were tensioned are listed to the right.

From the deflection profiles Liu and Dugan concluded that: i) as the excavation proceeded, the soldier pile gradually deflected towards the excavation; ii) the soldier pile movements were not generally affected by the tensioning of the tie-backs. However, as the top 14 ft (4.20 m) of soil consisted of fairly loose fill, the top level tie-backs had probably pushed the soldier pile a short distance into the soil; and iii) the lateral ground movements are in agreement with the movements of the soldier pile but of a smaller magnitude.

Settlements of the top of the soldier piles were measured and

are presented in Fig. 2.13. Settlement increased as construction progressed. This was attributed mainly to the load imposed by the angled tie-backs and also to the decrease of frictional resistance along the pile due to excavation.

In general, values observed for the lateral movements, and settlements were very small, indicating a rigid and stable system.

Fig. 2.14 presents typical plots of tie-back loads versus time. Loads measured in the three tie-backs on the uppermost level (A) are contained in the middle portion of Fig. 2.14. It shows an overall trend of gradual, but small, decrease in load with time. These results were typical of load variations measured in the tie-backs on the upper four levels, (A) to (D). The loads measured in level (E) are summarized in the lower portion of Fig. 2.14. The trend of tie-back loads decreasing with time is more pronounced. The tie-backs on the next two levels, (F) and (G), underwent even larger decreases in load with time. The decrease in loads was attributed to creep of the grouted anchor, stress relaxation of the tie-back cables, slipping or creep of the cables in the locking chucks or inward deflection of the soldier pile due to loading a lower level tie-back.

Soldier pile settlements were also measured over the entire lateral support system. The authors reported settlement values ranging between 0.01 ft (3 mm) to 0.06 ft (18 mm). Values of the lateral deflection of the top of the piles varied generally from 0.02 ft (6 mm) away from the excavation to 0.06 ft (18 mm) towards the excavation.

Ground outside the excavation suffered minor horizontal movements towards the excavation, ranging up to 0.5 inch (12.7 mm). Sidewalk

settlements varied from 0.0 to 0.09 ft (27 mm).

Movements of adjacent buildings were monitored and found to be small and insignificant with only one exceptional point which settled 0.02 ft (6 mm).

A concrete diaphragm wall was formed as part of the foundation for the west wing of the Guildhall precincts construction in London. James and Phillips (1971) documented the results of instrumentation of this diaphragm wall which was formed in Thames ballast underlain by London clay and supported by two levels of prestressed anchors (Fig. 2.15). The retaining wall comprised twenty-four panels varying in depth from 9.8 m to 11.3 m. One of these panels was selected for instrumentation because of its remoteness from the stiffening effects of the corners. This panel had an overall depth of 9.8 m, a length of 4.5 m and a thickness of 0.5 m and contained two vertical lines of anchors spaced 2.25 m apart. The anchors were initially taken to a test load of 620 KN and subsequently the upper and lower anchors were locked-off at 550 KN and 240 KN respectively. The instrumentation consisted of an inclinometer to record the deflection profiles of the wall at various construction stages. In addition, load cells measured the anchor loads and surveys were carried out to determine the overall wall movement.

The deflected profiles of the wall, calculated from the inclinometer, are shown in Fig. 2.16 for six stages of construction. In each case the deflection has been plotted relative to the base of the wall. Overall movements of the wall obtained from optical surveys have been superimposed in profiles (d) and (h). Profile (a) shows an

overall rotation towards the excavation together with a superimposed cantilever action above the excavated depth. The maximum differential displacement (10 mm) between the crest and toe of the wall occurred during this initial cantilever stage of construction. The effect of stressing the top anchors is shown in profile (b), where the wall has been drawn back towards its original profile. The difference between profiles (b) and (c) corresponds to a time lapse of four days. During this period there has been an overall movement towards the excavation and a bulging deflexion below excavation level. Profiles (d), (e), (f), (g) and (h) represent the remaining construction stages until full excavation. From the general survey the overall displacements monitored (profiles (d) and (h)) show a displacement into the retained soil mass and some conflict appears to exist between these wall movements and the inclinometer profiles. The apparent error was probably due to movement of the base line joining the fixed stations. The maximum vertical movements measured with a geodetic level were 0.25 mm and were not considered significant. The authors reported that the four anchors in this panel exhibited less than 5% loss of prestress during the test period of one hundred days. Bending moments predicted by the design method were also compared with the observed bending moment (Littlejohn and MacFarlane, 1974). Fig. 2.17 shows the bending moments at different construction stages with the predicted profiles superimposed. A similar pattern is observed especially at the final excavation stages.

The performance of an anchored tie-back system supporting the excavation of the Operations Control Centre Building in Washington

has been described by Ware et al. (1973). The excavation pit measured 78 by 57 m in plan and varied in depth from 10.7 to 15.2 m. The average ground surface elevation of the site was +12 m. The uppermost 1.5 to 3.0 m was fill material, below which the soil consisted of Pleistocene terrace deposits of clay and sand to about elevation -10.7 m to -12.2 m where Cretaceous Potomac formation was encountered (Table 2.1 summarises the subsurface conditions).

The excavated soil face was supported with a system of soldier piles, timber lagging, wales and tie-backs, as shown in Fig. 2.18. One hundred and forty four soldier piles were installed around the perimeter of the excavation. Piles were spaced at 1.7 m to 1.9 m centres, and were driven to lengths varying from 15.2 m to 18.3 m with an average embedment of 3.7 m below structure subgrade.

A 3.1 m excavation was then made inside the soldier piles. Timber lagging was installed between the piles as the excavation proceeded and was generally placed behind the exposed flanges of the soldier piles. Wale sections and tie-backs were then installed. For each tie-back, three tendons of 7-wire strand construction were used. An angle of 15° with the horizontal was selected for inclination of the tie-backs, to minimize the vertical component of load on the soldier piles. The length of the tie-backs at each level was equal to the distance from the soldier pile to an assumed influence line in the soil, plus the required anchorage length beyond the influence line which sloped upward from the base of the excavation at an angle of 40° from vertical (Fig. 2.18).

It was found necessary due to the proximity of surrounding

buildings to closely monitor both vertical and horizontal movements of the tied-back walls and settlement around the excavation.

Prior to any excavation, an accurate survey was made to determine the elevation and horizontal location of each soldier pile. These surveys were repeated weekly during the period of excavation. Additional surveys were made to determine the horizontal location of the soldier piles at each tie-back level. However, the readings on lower tie-back levels were discontinued due to inconvenience. Since readings at the tops of the soldier piles consistently showed the greatest lateral movements, they were considered to be most significant.

The maximum recorded horizontal and vertical movement of each soldier pile is summarized in Figs. 2.19-2.22, together with three sections showing representative soldier piles for each end and the middle of the wall (refer to Table 2.1 for soil profile legend).

In general, the maximum horizontal movement occurred on the north wall, while the west wall experienced the greatest settlement. The relatively large horizontal movement of the north wall resulted from the fact that the upper two tie-back levels were anchored almost entirely in cohesive soil. Although this soil held the tie-back test loads adequately, it allowed some creep with time. The large settlement experienced on the west wall can be attributed to the fact that the uppermost tie-backs were actually installed at an angle of 25° below the horizontal, in order to clear utilities, instead of 15°. Although the angle at lower levels was decreased from 15° to 10° to compensate, the net effect was to increase the average vertical loads on these soldier piles by about 10%.

Relatively large horizontal and vertical movements of the soldier piles occurred in the central section of the west wall, as Fig. 2.21 indicates. This was due to the excavation of an elevator pit down to elevation -2.4 m in front of this panel of the wall, which brought the total excavation depth to a maximum of 15.2 m in the project. Soldier pile W-22 (Fig. 2.21) settled appreciably throughout the excavation process and it was finally decided to install supporting rakers after the excavation had been advanced to elevation +0.6 m. After completion of excavation it was found that the bottom of this pile crumpled during driving and the pile top did not extend below elevation -1.5 m.

A total of 200 settlement points was set in the streets and sidewalks surrounding the site. Fig. 2.23 presents a summary of average surface settlements in terms of distance from the face of the excavation versus settlement. It can be seen that the average surface settlement was extremely small; the maximum measured settlement was 16 mm. This was directly opposite the deepest portion of the excavation. Street settlements were not considered excessive or detrimental to either the streets or nearby utilities. No damage to utilities was discovered which could be attributed to settlement.

Henauer and Otta (1976) presented the results of their field measurements of the walls supporting a 16 m deep excavation (Fig. 2.24), which was situated in an urban area with unfavourable soil conditions. The excavation was retained partially by slurry trench walls tied back by two rows of anchors (Figs. 2.24, 2.27) and partly by anchored sheet piles which were placed into a trench (Figs. 2.24, 2.25). The trench behind the sheet pile walls was refilled with

filter gravel. The piles were tied back by four rows of anchors.

Deformations of the sheet pile wall, as well as ground movements at section 1-1 (Fig. 2.24) were monitored and are presented in Fig. 2.25 for different construction stages. The maximum wall deflection was 80 mm toward the excavation, and the maximum ground subsidence was 35 mm at a distance of 9.0 m from the back of the wall. The major part of this deformation occurred during the second and third excavation stages.

Variations of anchor forces for the four rows are plotted in Fig. 2.26 for different construction stages. At full excavation (218 days), the final anchor forces in the upper three rows were slightly higher than the initial prestress value induced in them. However, the fourth row attained a value slightly less than its initial prestress value.

Horizontal deformations less than 10 mm were observed for the anchored slurry trench wall (section 6-6 in Fig. 2.27). The maximum vertical ground deformation was 8.0 mm at a distance of 5.0 m from the back of the wall.

Top displacements, for the section of the wall between points 1 and 12 (Fig. 2.24), are summarised in Fig. 2.28. Values of the measured displacement varied between 15 mm above the initial top elevation of the wall, and 55 mm below it.

A case study has been described by Clough (1976) for the construction of the Entertainment Centre and Theme Towers, Los Angeles, U.S.A. The excavation for this project was exceptionally large and deep. In plan it covered an area approximately 720 ft^2

(67 m^2), and it ranged from 70 ft (21.35 m) to 110 ft (33.55 m) deep. The soil profile consisted of 20 ft (6.1 m) of silt and clay underlain by a considerable depth of slightly cemented sand and silty sand.

To support the excavation a tied-back composite diaphragm wall was employed. Soldier piles, 8WF32, were set into drilled holes at 6 foot (1.83 m) centres; the soldier piles extended 15 ft (4.58 m) below the level of the excavation. Structural concrete was used to fill the holes up to the excavation level and lean concrete was used thereafter.

Following installation of the soldier piles, the excavation was carried out to full depth in the central area, leaving a peripheral berm with a 50 foot (15.25 m) wide bench to support the wall. The bench was cut down in five foot (1.53 m) increments whereupon a level of tie-backs was installed. Sixteen inch (0.4 m) diameter friction anchors were employed. Prestress loads applied to the anchors were calculated from the design diagram shown in Fig. 2.29.

With the anchors in place, the exposed soil between the soldier piles was gunited to form a diaphragm wall.

This sequence of operations was repeated to the full depth of excavation. A total of nine levels of tie-backs was eventually installed. The diaphragm wall was incorporated as a part of the final structure.

Performance of the wall system was observed by a survey net and load cells on the anchors. Lateral movements of the wall and street subsidence was a maximum of three inches (76 mm) with typical values much less. These values were considered tolerable for this site.

Sills et al. (1977) described the behaviour of an anchored diaphragm wall supporting a 8.0 m deep excavation for the Neasden Lane Underpass in north London. The soil profile consisted of stiff brown fissured London clay which at a depth of 8.0 m grades into grey-blue fissured London clay. At a depth of 30 m, the Woolwich and Reading beds are encountered.

Four rows of anchors were installed in the diaphragm wall. Each panel, of nominal thickness 600 mm and width 4.57 m, contained eight anchors. The optimum angle of inclination of the anchors to the horizontal was 20°, although in some panels inclinations up to 40° were used to minimise the encroachment beneath nearby houses.

The deformation of the ground mass behind the diaphragm wall was studied in two parts. The vertical and horizontal movements at the surface were measured with reference to two datum points A and B shown in Fig. 2.30. The movements of points beneath the ground surface were measured by magnet extensometers and inclinometers. These internal movements were then related to the surface movements. Three inclinometer guide tubes - each 13 m long - were installed, the first two in the ground behind the line of the cutting, while the third one was fastened to the reinforcing cage before lowering it into the slurry filled diaphragm wall trench.

Pore water pressure was also monitored during and after the excavation. Four pneumatic piezometers were installed at depths $3\frac{1}{2}$ m, 7 m, 10 m and 13 m, in each of three boreholes. One of these was just behind the wall, and the others were at distances 7 m and 16 m back from the wall. In addition, Casagrande standpipes were installed

at the locations shown in Fig. 2.31.

The anchors in the test panel were inclined at an angle of 20° to the horizontal, with seven underreams giving a design load of 400 KN. Loads carried by the anchors were recorded using vibrating wire load cells. These were fixed between pairs of purpose made anchor plates against which the tendons were stressed.

The trench for the diaphragm wall in the region of the test panel was excavated in January 1972. The diaphragm wall was cast complete by the end of that month. Fig. 2.32 shows the detailed progress of excavation in the plane normal to the test panel.

Fig. 2.33 shows the development of surface movement at various times during and after excavation. The movement was initially inward and horizontal. Settlement occurred mainly after the completion of the excavation, and was, at all points, less than the horizontal movement. Within 14 months of the end of the excavation, the inward and downward movements appear to have ceased, having reached maximum values of about 50 mm and 30 mm respectively. It can be seen that one third to one half of this total displacement had occurred by the time the excavation was complete.

The surface movements have been combined with the inclinometer results to give the total horizontal movements at three locations behind the wall down to a depth of 13 m. As shown in Fig. 2.34, the displacement of the wall and the displacement 4 m behind the wall followed the same pattern; the movement is largely translation during excavation followed by some rotation after completion of the excavation. Further back from the wall at a distance of 19 m, the

movement was almost entirely translation.

Fig. 2.35 shows trajectories of movement obtained by linking together survey movements and those measured with the inclinometers and extensometers. Little settlement occurred during the first 5 m of excavation, while horizontal displacements were one third of the total. By the time the excavation had reached its full depth of 8 m, an appreciable vertical settlement occurred at and just behind the wall, both at ground level and at a depth of 13 m. Ten months after the completion of excavation the ratio of horizontal to vertical components of the movements of the top of the wall was about two to one and slightly more than one to one at the bottom of the wall. Movements having the same ratio were observed by Littlejohn and MacFarlane (1974), in their study of the excavation at Keybridge House described earlier. It is worthwhile mentioning that similar displacement measurements were made for two other excavations in London clay, the Y.M.C.A. building in London (Burland, 1975) and the underground car park at Westminster (Burland and Hancock, 1977), where diaphragm walls were supported by struts acting horizontally. In neither of these cases has any downward movement of the wall been observed. It would therefore seem that the observed wall settlement at Neasden Lane is almost certainly due to the downward pull of the anchors.

Measurements showed that the top two rows of anchors decreased in load as the row beneath was stressed and then they recovered their initial value which was maintained constant. The loads in the third row dropped following completion of excavation, and then also became

constant. The loads in the fourth row continued to drop for about 8 months after completion of excavation. The authors considered the performance of these ground anchors to be consistent with fairly high horizontal movements.

Considerable difficulty was experienced with the operation of the piezometers, and it was only possible to draw some general conclusions. The pore pressure began to drop at the start of the excavation, and continued to fall, more slowly, after completion of the excavation until it reached a minimum some 8 to 10 months after the end of excavation. Later readings indicated a gradual increase in pore pressure, but even after 44 months the values were considerably lower than the original ones.

The study has provided a useful insight into the mechanism of behaviour of ground anchors. The authors concluded that the installation of ground anchors does not preclude the possibility of high horizontal and vertical movements. However, it appears that a block movement of ground has occurred, with translational and tilt components. Within the block, the horizontal movements have become quite high, notwithstanding the satisfactory performance of the anchors.

2.4 Analytical Studies

2.4.1 General

Along with field studies and laboratory scale model tests, modern analytical methods using the finite element technique have been developed. These have the advantage over conventional limit

state methods in that (Wittke and Semprich, 1973) they account for complex geometrical and loading boundary conditions. Also, they consider the interaction between structures and soil, with complex stress-strain characteristics.

Calculations begin with a subdivision of the continuum into elements of finite size, usually triangles for two dimensional continua and tetrahedra for three dimensional cases. These elements are assumed to be interconnected only at the corner points. At these nodal points, the internal stresses are assumed to be transmitted from one element to the other by means of substitute nodal forces. Also, volume forces and external loads such as self weight and anchor forces can only be applied to the system forces concentrated at the nodes. Another assumption is that the displacements within one element are linearly dependent on the co-ordinates. The coefficients of these linear relationships can be expressed by the corresponding nodal co-ordinates and displacements, the latter ones being the unknowns of the system. By simple partial differentiation, the strains and, applying Hook's law, also the stresses, can be determined as functions of the nodal displacements. A relationship between the nodal forces and the stresses and consequently also the nodal displacements can be determined by applying the principle of virtual work to each element. Fulfilling the equilibrium conditions at every node of the system, as well as the boundary conditions, finally results in a system of linear equations for the unknown nodal displacements, from which the stress field can also be evaluated.

In the next section, some of the case studies are reviewed, and

whenever possible, theoretical predictions are compared with field measurements.

2.4.2 Review of analytical studies

Clough, Weber and Lamont (1972) described the use of the finite element method in the design of a 65 ft (19.83 m) high tied-back soldier pile wall for the Bank of America building in Seattle, Washington. During construction of the wall and the excavation a thorough instrumentation programme was undertaken consisting of heave gauges, wall inclinometers, anchor load cells and behind-the-wall surface settlement surveys which allowed comparison of observed to predicted behaviour.

The excavation was made in a deposit of a saturated, highly overconsolidated clay which consisted of two strata. The upper stratum was about 20 ft (6.1 m) thick and is harder than the lower stratum, known as Seattle clay, which was about 60 ft (18.3 m) thick. A cross-section through the high side of the excavation at the final depth is shown in Fig. 2.36. Six rows of anchors were employed and prestressed to loads of 120 to 200 kips (534 KN to 890 KN).

Preconstruction finite element analyses were conducted to confirm the design of the wall as established by past experience, and to predict surface settlement behind the wall.

In simulating the actual sequence of construction 13 steps were employed, seven for excavation and six for anchor prestressing. Every excavation step was followed by an increment simulating anchor prestressing and installation except for the final excavation step.

The tie-rods were assumed grouted over the entire length. The section modulus of the wall in the finite element analyses was made equivalent to that of the actual soldier pile wall. The soil was modelled by the non-linear elastic approach, described by Clough and Duncan (1971). The soil parameters utilized in the preconstruction analysis were used without change in the six anchor analysis.

By the date this study was documented, February 1972, the wall was not yet completed. The excavation was at a depth of 55 ft (16.78m) and five rows of tie-backs were installed. However, comparisons between the observed and predicted behaviour at that stage were made. Wall deflections observed are compared with those calculated in Fig. 2.37. A similar comparison is also made for surface settlements in Fig. 2.38. The observed and predicted behaviour was reasonably similar in form but the predicted movements were somewhat larger than those observed. The degree of agreement, however, was considered encouraging.

The predicted lateral earth pressures on the wall are shown in Fig. 2.39. Also superimposed are the original at-rest pressures (K_o = 1.3) and the recommended design pressures by Terzaghi and Peck (1967) for overconsolidated clays. The predicted results were higher than the at-rest pressures in the upper stratum of very hard clay and less than the at-rest values in the lower stratum of Seattle clay. There was a localized zone of high pressure in the Seattle clay at the level of the last anchor reflecting the effect of the last prestress load.

Barla and Mascardi (1974) described the construction and

behaviour of an anchored wall in Genoa, Italy. The work required an excavation 34 m deep with a total length of 147 m and a minimum distance of 3 m from existing buildings, as shown in Fig. 2.40. Fig. 2.41 and Table 2.2 show the results of soil investigations at the site.

The choice of the retaining wall finally adopted was based on the following: i) the need for varying as little as possible the existing stresses in the soil, in order to minimize related strains in the existing buildings around the excavation; ii) the need for flexibility of wall design, in order to allow for significant variations in the retaining structure, as additional information about the final state of equilibrium of the soil was to be provided by repeated measurements during construction.

The retaining structure was composed of a reinforced concrete wall, 0.5 m thick, 358 vertical bored piles spaced 0.6-0.8 m and reinforced with steel H-beams. The wall was tied by 658 grouted anchors, inclined at 20° to the horizontal and having nominal service loads of 569 and 853 KN.

The initial design of the wall was based on the assumption of a triangular distribution of horizontal pressure with depth, referring to an ideal active state of stress, affected by a factor of safety and checked according to a limit equilibrium analysis.

The excavation proceeded step by step as anchors and horizontal beams were installed. Vertical and horizontal displacements of the crest of the wall were measured to an accuracy of 1 mm.

When the excavation reached elevation 21 m some cracks appeared

in the old buildings along the longer side of the excavation. A check of the tension in the cables of the anchorages showed increases of about 10%. Work was stopped and supplementary boreholes were drilled. These boreholes showed the presence of a heavily overconsolidated clay which was not found in the previous site investigation. The measurement of overconsolidation pressure, and the use of the diagram of K_o versus OCR (Brooker and Ireland, 1965) allowed an evaluation of the original horizontal pressure in the overconsolidated clay.

Work was then continued and wall displacements were measured at a number of vertical sections as well as tension forces in 12 anchorages.

A finite element study of the anchored wall was carried out when the excavation reached approximately mid-depth. Excavation was simulated, anchors were represented in the model by bar elements. The soil-anchor interaction was accounted for by distribution of the anchor load between points situated at the two extremes, avoiding irregular stress concentrations in the soil.

The finite element model used to represent the wall section (G) of Fig. 2.42 is shown in Fig. 2.43. It consisted of 201 nodal points and 174 elements. Plane strain conditions were assumed. The soil was taken as linearly elastic and isotropic. The nodal points along the vertical outer boundaries were set as free to move in the vertical direction. The nodal points along the horizontal boundary were taken as fixed. The initial state of stress in the soil was assumed to be given by a vertical stress due simply to the gravity load and a horizontal stress distribution as shown in Fig. 2.44.

Eight different excavation steps were considered in the finite element analysis. The actual construction sequence for placing the anchorages was reproduced as closely as possible.

Fig. 2.44 shows the distribution of stresses in the soil adjacent to the anchored wall for excavation level at elevation 9.4 m. Also shown are the elements subjected to tensile stresses. Tensile stresses developed in the silty clay as the excavation proceeded (Fig. 2.45) and first arose close to the wall and propagated towards the right vertical boundary of the model.

A safety factor, F_{SL}, defined as the ratio of the deviator stress at failure to the mobilized deviator stress, was evaluated for each element of the structure in its final configuration. Fig. 2.45 shows that F_{SL} is less than 1.5 only in the silty clay, and generally reaches extremely high values in the remaining areas.

Fig. 2.46 shows a comparison between measured and computed values for the vertical and horizontal displacements at the crest of the wall of section (G) at each stage of excavation. For the horizontal displacements of point A in the soil, the values computed matched field observations made during wall construction and on completion of the work.

For the vertical displacements, a distinction is made between displacements for point A, pertaining to the soil, and point B, considered as joined to the vertical piles. The displacement of B was evaluated under the assumption that this point follows the behaviour of a point located on the same vertical at the base of the wall. Values predicted in this way for point B agreed remarkably well

with the measured vertical displacements at the crest of the wall.

The agreement between field observations and numerical predictions for displacement values confirmed that an appropriate choice was made for the material parameters and natural stress distribution in the soil.

To assess the effect of different parameters such as prestress load, wall stiffness, excavation depth and tie-back stiffness on the wall performance, Clough and Tsui (1974) presented a study on two hypothetical examples. Two excavations supported by four tiers of tie-backs were considered in the analysis as shown in Fig. 2.47. Excavation I was a 32.5 ft (9.91 m) deep cut in a homogeneous deposit of normally consolidated clay 50 ft (15 m) thick and was 40 ft (12 m) wide. Excavation II had dimensions exactly 1.5 times those of excavation I; it was 49 ft (15 m) deep, 60 ft (18 m) wide, and the clay deposit into which the excavation was made was 75 ft (32 m) thick. In both cases the homogeneous clay was assumed to be underlain by rock, and the tie-backs were assumed to be anchored to the underlying rock.

The creation of the excavation and prestressing effects were modelled in nine steps as shown in Fig. 2.48. The sequence followed closely that employed in the field with tied-back walls.

The finite element mesh employed was composed of 361 elements and 380 nodes as shown in Fig. 2.49. As the anchorage was in the rock, represented at the base of the mesh as a rigid material, the prestressing effect could not influence the surrounding soil. Accordingly, no special elements were included in the mesh to

represent the tie cables or the anchors. Instead, they were represented as inclined springs restraining the outward movements of the wall, and were installed after the prestressing force was applied to the wall.

The results of the analysis, and the effect of the different parameters are summarised as follows:-

i) Effect of prestressing: The parametric variations considered in the design prestress diagram are shown in Fig. 2.50. Four different diagrams were used to calculate prestress loads; three were trapezoidal and one was triangular. The trapezoidal diagrams were similar in shape to those recommended by Peck (1969). The maximum ordinate of the diagrams was varied as 0.2 γH, 0.4 γH and 0.7 γH. The triangular diagram corresponded exactly to the "at-rest" distribution.

The predicted soil and wall deformations for excavations I and II are shown in Fig. 2.51. The use of higher prestressing loads resulted in decreasing the wall and soil movements. The effect of prestressing on the wall movement was particularly dominant near the top of the wall where the largest of the trapezoidal loadings managed to eliminate wall movement entirely. However, none of the prestress loads was able to prevent wall movement near the bottom of the excavation and as a result soil settlements occurred for all conditions. The triangular "at-rest" design assumption was less effective than most of the trapezoidal assumptions in reducing movements.

ii) Effect of wall rigidity: Three values of wall flexural stiffness

were considered in both cases I and II. These were 288,000 kip.sq ft/ft, 36,000 kip.sq ft/ft and 9,000 kip.sq ft/ft (390,000 KN.m^2/m, 48,500 KN.m^2/m and 12,100 KN.m^2/m); and were referred to as S, M and F consequently.

The predicted wall and soil movements for excavations I and II for the three different wall rigidities are shown in Fig. 2.52. Wall deformations and soil settlements were reduced by increasing the wall rigidity. However, the decrease in movements was not in direct proportion to the increase in rigidity.

iii) Effect of tie-back stiffness: In the analysis, tie-backs were given stiffness values corresponding to 3 sq in (1936 mm^2) tie rods and cable bundles with a total area of 0.3 sq in (194 mm^2). The predicted wall and soil movements for excavation I for the different tie-rod stiffness values are shown in Fig. 2.53. Stiffer tie-backs reduced the movements by about 50%. Again the reduction is not in proportion to the stiffness change, since an increase in tie-back stiffness by a factor of 10 caused a 50% reduction in movements.

iv) Effect of excavation depth: The effect of excavation depth can be seen in all of the plots of movements, Figs. 2.51-2.54, by comparing movements for excavation I and excavation II. The deeper excavation yielded more soil settlement and wall movement under all circumstances.

In Fig. 2.54 the predicted net earth pressures are shown for excavation I with a four tier tie-back and for excavation II with a

four and a three tie-back support system. Results are shown for both the flexible wall and the medium wall. The results indicated that the excavation depth did not have a significant effect on the earth pressure distribution. Also earth pressures for both excavations showed a reasonably close similarity to the design prestress pressure diagram above the excavation bottom. Below the excavation bottom both showed reduction due to the pressure on the excavation side of the wall, with the reduction being greatest for the flexible wall. The only difference between the pressures for excavations I and II was that the pressures for excavation II showed bulges at the locations of the prestress loads. This effect became extremely prominent for the three tier system and was more pronounced for the flexible wall than the medium stiff wall. The reason for the differences in these diagrams lay in the vertical spacing between the tie-backs and the wall flexibilities. The spacing in the three cases were 6.5 ft, 10 ft and 16 ft (2 m, 3 m and 4.9 m). In the first case with the smallest spacing, the pressure concentrations were masked since the concentrations overlapped significantly, whereas with the largest spacing, the concentration under one tie-back did not overlap with the others which gave a pressure distribution substantially different than the assumed prestress diagram.

A flexible sheet pile wall and a stiff cast in situ diaphragm, both supported by a single row of anchors, were considered in a finite element analysis by Egger (1972). His analysis showed the important influence of the wall flexibility on the earth pressure distribution. It also showed that the anchor prestressing force had

an effective influence on the ground and wall movements. He emphasised the importance of using a stiff wall, and of a high anchor prestressing value for the prevention of damage to adjacent structures by ground movements. The work of Egger (1972) was reviewed in detail by Kurdi (1973).

2.5 Overall Stability

2.5.1 General

Checking the overall stability of the wall-anchor-soil system requires a number of simplifying assumptions to be made. Most methods of analysis are based on a limit state whereby a surface of failure is assumed and disturbing forces are compared with the resisting forces to give the overall factor of safety.

The main drawback of such methods of limit analysis is that they do not predict the deformations and the stresses within the retained soil mass. The most promising and logical method of analysis is to model the wall construction sequence using the finite element method (Section 2.4). However, because of the size of the computer programmes and the computing time involved, only very large schemes are likely to be analysed by this method.

2.5.2 Design earth pressure distribution

The choice and determination of the appropriate earth pressure distribution is a first stage in the design. Earth pressures acting upon a strutted or a tied-back retaining wall are bigger than the active earth pressures calculated by Coulomb's method. Deviations

are reasoned to wall movement being different from those necessary to mobilize the active pressure (Breth and Wanoschek, 1972; Casagrande, 1973). The earth pressure is somewhere in between the active and the at-rest values and may be known as the partially mobilized active pressure (Larsen et al., 1972).

The methods recommended for estimating the earth pressure on tied-back walls are generally based on semi-empirical pressure diagrams that were originated by Terzaghi (1941) and Peck (1943) for strutted excavations. These were based on the experience and comprehensive measurements on subway constructions in Berlin and Chicago.

Fig. 2.55(a) shows the pressure diagrams suggested by Terzaghi and Peck (1967). These are not intended to represent the real distribution of earth pressure, but to provide a means of calculating loads which might be approached but not exceeded. Peck (1969) stated that these diagrams were applicable for sands but gave rise to some discrepancies for shallow excavations in soft to medium clay. He also suggested a value of m (see Fig. 2.55) varying from 0.4 to 1.0 according to different soil conditions.

The original pressure diagrams suggested by Terzaghi and Peck were modified by other workers (Tschebotarioff, 1951; Broms, 1968) and also in the different codes of practice (e.g. CP 2, 1951 and French Code of Practice T.A., 1972). The different modifications and recommendations are summarised in Fig. 2.55(b, c, d).

James and Jack (1974) suggested another empirical method for the determination of the pressure distribution. The method carries

through a stage by stage analysis simulating the method of construction carried out in the field. Each stage of excavation is analysed by assuming an equivalent single-tied wall method of analysis using a new centre of rotation for each excavation depth. The method is based on the following assumptions: a) the mobilizing and resisting soil forces are those determined from Rankine's earth pressure; b) at failure there is a unique point of rotation in the plane of the wall; c) the wall is only of sufficient length to mobilize a factor of safety of unity against rotation at any stage of excavation. Fig. 2.55(e) illustrates the principle of the method proposed.

2.5.3 Review of stability methods

The original method, and one of the most commonly used methods, is that due to Kranz (1953), in which a composite failure surface, made up of an active wedge zone behind the anchors, a passive wedge zone in front of the anchors and a connecting plane between these surfaces is assumed. The method of Kranz formed the basis of stability check for anchor walls in the recommendation of the Committee for Water Front Structures (1966). The method is illustrated in Fig. 2.56(a) and is valid for free support sheet piling and anchor walls in uniform soils, with a single line of anchors. The soil wedge, BFH, with dead weight W_a and slip surface BF, loads the sheet piling and supports itself on the anchoring section BCDF with force R_a. The anchoring section BCDF lies on the "failure plane" which extends from the lower edge of the anchor plate to the lower edge of the sheet piling, being held by the force R_1, which is inclined to the normal

to the failure plane DF by the angle of friction, ϕ'. It is loaded by the anchor tension, which is transmitted through the deadman or anchor plate, by its own dead weight W_1 and by the soil pressure P_1, which the slip wedge CDI exerts on the rear surface of the deadman or anchor plate. The anchoring is stable when the average force acting on the anchoring section BCDF in the direction of the anchor, is greater than the actual force which results from the calculations of the sheet piling, i.e. when the potential anchor force is greater than the actual. The ratio of the potential to the actual anchor force is defined as the Factor of Safety which must be greater than 1.5. If this condition is not satisfied, the anchor must be lengthened or the deadman or anchor plate placed deeper.

The investigation of the stability is made by drawing a vector polygon from the known magnitude R_a, W_1 and P_1, the direction of R_1 and the anchor direction. Thus the potential anchor force A_{poss} is obtained (Fig. 2.56(b)). The calculation is simplified if the force R_a which supports the slip wedge BFH, is replaced by the two forces which are in equilibrium with it, the weight W_a of the slip wedge and its supporting reaction force, the soil pressure P_a, which acts on the sheet piling from F to H. The force R_a is thus eliminated from the calculations and the slip surface BF does not need to be determined. The calculation is now concerned with the entire section of earth CDFH. The simplified force polygon is shown in Fig. 2.56(c).

This method of analysis has been modified by Broms (1968) to allow for the axial force in the wall. In Fig. 2.57(a) the rupture surface is assumed to extend from a point B located 2 m from the

lower end of the anchor zone to a point C on the sheet pile wall. Point C corresponds to the minimum penetration depth required to prevent failure. The forces initiating failure are the force P_1 which acts along AB and the weight W of the sliding mass of the soil. The forces preventing failure are the reaction force Q, the anchor force T, the toe resistance V and the passive earth pressure P_p at the lower part of the sheet pile wall above point C. The anchor force T acting along B-F, the section of anchor zone located between the assumed failure surface and the end of the anchor zone, is generally neglected in the calculations. The force $(P_p)_{required}$ which is necessary to prevent failure along the assumed failure surface, can be calculated from the force polygon shown in Fig. 2.57(b). This force should be less than $(P_p)_{available}/F$ where $(P_p)_{available}$ is the passive Rankine earth pressure force above point C, and F is a safety factor which is generally assumed equal to 1.5.

In both stability methods reviewed, an additional requirement is that no part of the anchor zone should be located within the active earth zone which affects the earth pressure on the sheet pile wall. This zone is determined by drawing a line from point C (Fig. 2.57(a)) inclined at $(45 + \phi/2)$ with the horizontal.

The use of the method of Kranz (1953) in the recommendation of the Committee for Water Front Structures (1966) was limited to walls with a single line of anchors, whereas the original work of Kranz (1953) considered multiple rows of anchors and is supported by the findings of Ranke and Ostermayer (1969).

For multiple anchored walls, Kranz provided two solutions:

1) Fig. 2.58(a). The possible anchor force in the upper anchor, A_1, is found from stability of the wedge BDEC lying between the active slip surface BC and the, so-called, affected slip surface BDE. The possible anchor force in the lower anchor, A_2, is found from the stability of the wedge BFGC lying between the slip surfaces BC and BFG.

2) The second solution given by Kranz is the so-called step system (Fig. 2.58(b)). For the calculations of A_1, for example, only the upper part of the wall to A_2 (wedge BDEC) is considered, while it is assumed temporarily that A_2 and A_3 have an unyielding point of support. This method has not been generally adopted and was rejected by researchers (see Plant, 1972).

A good guide for the application of the Kranz method to multi-levels of anchors in non-uniform soils and for different combinations of anchor positions is given in the French Code of Practice (1972). The code recommends that the minimum free anchor length should be ensured before carrying out stability calculations. This was defined as the greatest of:- (see Fig. 2.59) 1) l_1: the length required to fix the anchorage in a firm stratum incapable of resistance; 2) l_2: far than a line of failure, assumed making an angle = $(\frac{\pi}{4})$ and passing through the base point.

To ensure general stability it is recommended that individual equilibrium for each layer should be carried out, and should satisfy the general condition of stability. The French Code of Practice indicates that the influence of an anchor on the stability of another one should also be taken into consideration. Examples of different

cases illustrated in the code are shown in Figs. 2.60, 2.61 and 2.62.

Fig. 2.60 represents the case of two independent anchors. The two equilibrium conditions are independent and may be carried out in any order.

In Fig. 2.61, two cases are represented. In the first (Fig. 2.61(a)) the point of fixity of the first row C_1 is internal to the mass M_2, while the point of fixity of the second row C_2 is external to the mass M_1. The two equilibrium conditions are independent and may be considered in any order as shown in the figure. In the second (Fig. 2.61(b)), C_2, the point of fixity of the second row, is internal to the mass M_1, while C_1 is external to the mass M_2.

Fig. 2.62 represents the case where C_2, the point of fixity of the second row, is close to the limit of the mass M_1. A complex fracture surface is assumed, as shown in the figure. The first polygon of forces (equilibrium of $c_2c_1e_1e_2$) is drawn from the origin, which leads to the intermediate point I. From I, the second polygon of forces (equilibrium of bc_2e_2f) is drawn which leads to the final point F. The two stability conditions alongside are verified simultaneously.

Broms' method (1968) was modified (Locher, 1969) to allow for a new definition of the factor of safety. In Fig. 2.63(a) the earth pressure E, on the vertical cut through the mid-point of the fixed anchor, is calculated with a nominal friction angle ϕ_n, and the resultant force R_n on the inclined plane of the sliding wedge must form the same angle ϕ_n with the normal to the sliding plane. ϕ_n has been correctly assumed if the weight G and the forces E and R_n' are in equilibrium. If this is not the case, then ϕ_n has to be altered and

when equilibrium is achieved the factor of safety is defined as

$$F = \frac{\tan \phi}{\tan \phi_n}$$

where ϕ is the actual angle of internal friction.

So far, the modified Broms method was only suggested for single anchored walls. However, Ostermayer (1976) and Schulz (1976) generalized the method so that it could be applied to multi-tied walls. It was also recommended to consider the passive resistance on the embedded depth of the wall into the stability analysis. The equilibrium is carried out as shown in Fig. 2.63(b). A factor of safety, $F = \tan \phi / \tan \phi_n$ greater than, or equal to, 1.2 is recommended.

Many workers prefer to use a much simpler failure surface such as a Coulomb wedge, a circular arc or a log-spiral surface, especially in the case of multi-level anchors where the shape of the sliding surface is not known.

Littlejohn (1972) suggested a stability analysis using a spiral shaped sliding surface as shown in Fig. 2.64. A logarithmic spiral has the property that the radius from the spiral centre to any point on the curve forms a constant angle ϕ with the normal line to the curve. If a nominal friction angle of the soil ϕ_n is employed where

$$\tan \phi_n = \frac{\tan \phi}{F}$$

then the line of action of the resulting forces on each part of the sliding surface will pass through the spiral centre. None of the forces along the sliding line will therefore create a moment around

this point and they can therefore be neglected when considering the equilibrium of moments around the point.

The safety factor F is correct when the moments of the remaining weights and forces on the sliding body total zero. As shown in Fig. 2.64, when the moments produced by G_t and G_s balance, a conservative value of F is then defined as $\tan\phi/\tan\phi_n$.

Ostermayer (1976) also recommended a conventional overall stability analysis with a circle or a logarithmic spiral to be carried out, to ensure the safety against rotational sliding. However, he recommended that tilting of the wall should be checked as well using both the Kranz method and the modified Broms method.

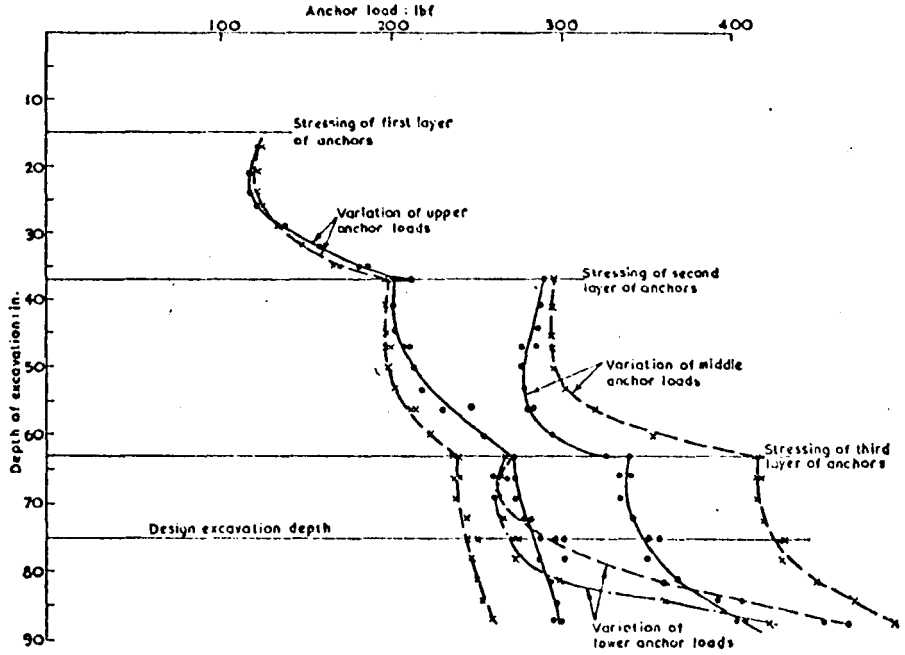

FIG. 2.1 ANCHOR LOAD MEASUREMENTS FOR THE RIGID MODEL WALL TEST (After James and Jack, 1974)

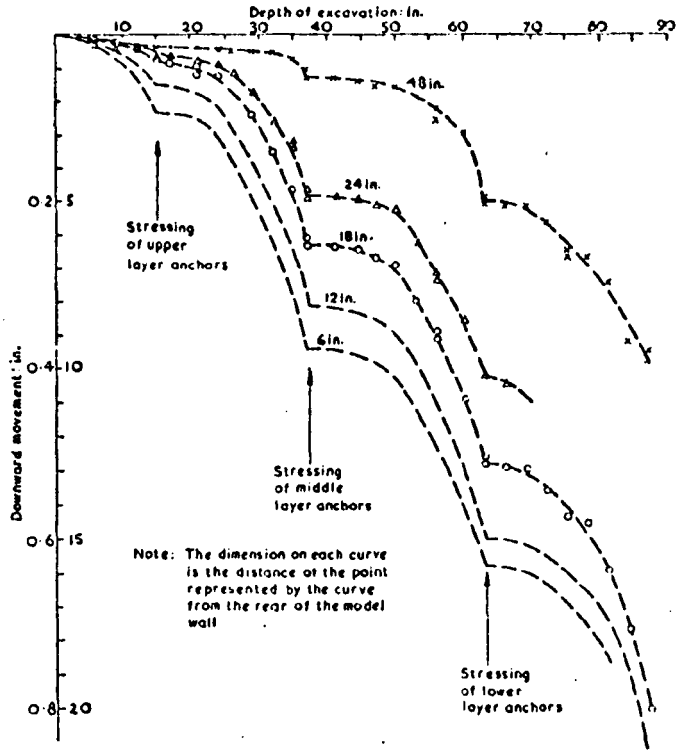

FIG. 2.2 SETTLEMENT OF THE RETAINED SOIL SURFACE FOR THE RIGID MODEL WALL TEST (After James and Jack, 1974)

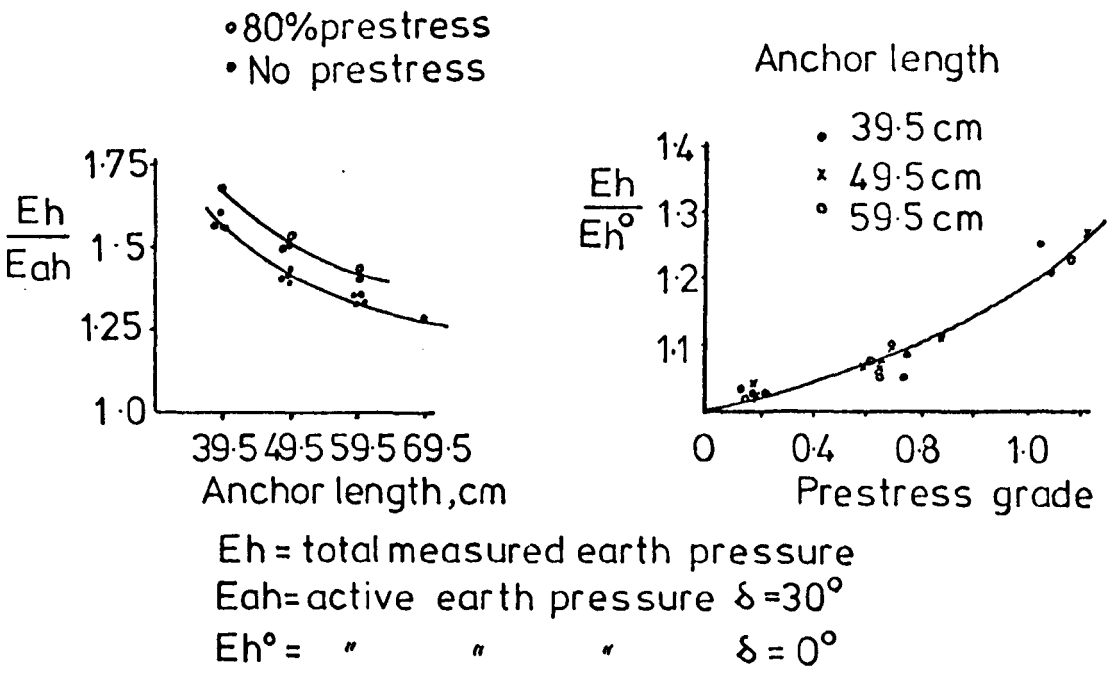

Eh = total measured earth pressure
Eah = active earth pressure $\delta = 30°$
Eh° = " " " $\delta = 0°$

(a) Dependence of earth pressure on anchor length and prestress load

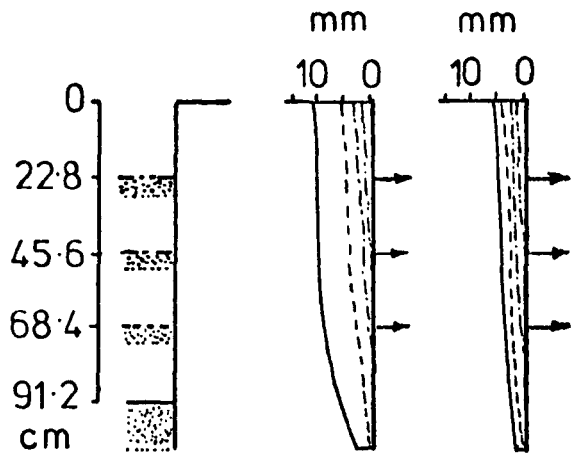

Anchor length 39·5 cm 69·5 cm

(b) Dependence of wall displacement on anchor length

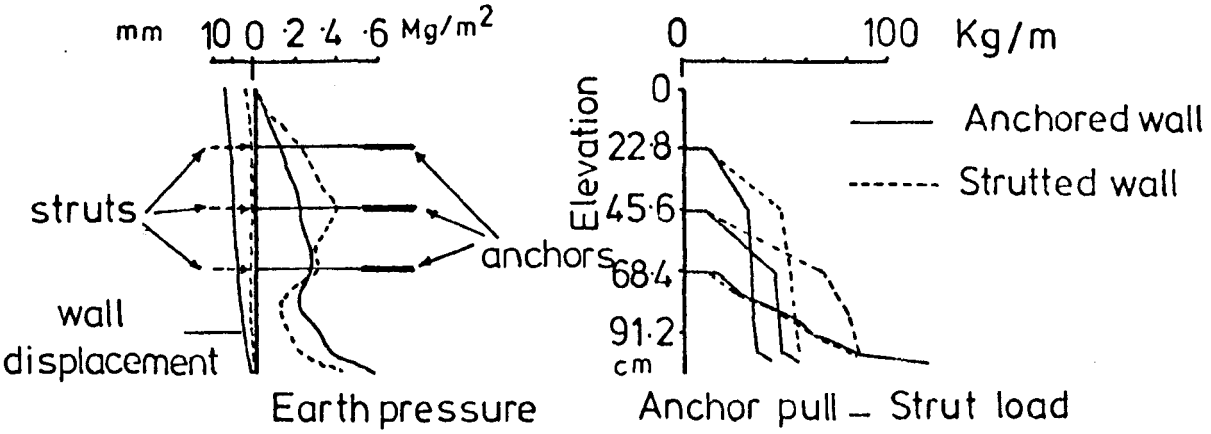

(c) Difference in behaviour between anchored and strutted walls

FIG.2·3 EXPERIMENTAL RESULTS OF MODEL TESTS ON ANCHORED AND STRUTTED WALLS (After Breth and Wolff 1976)

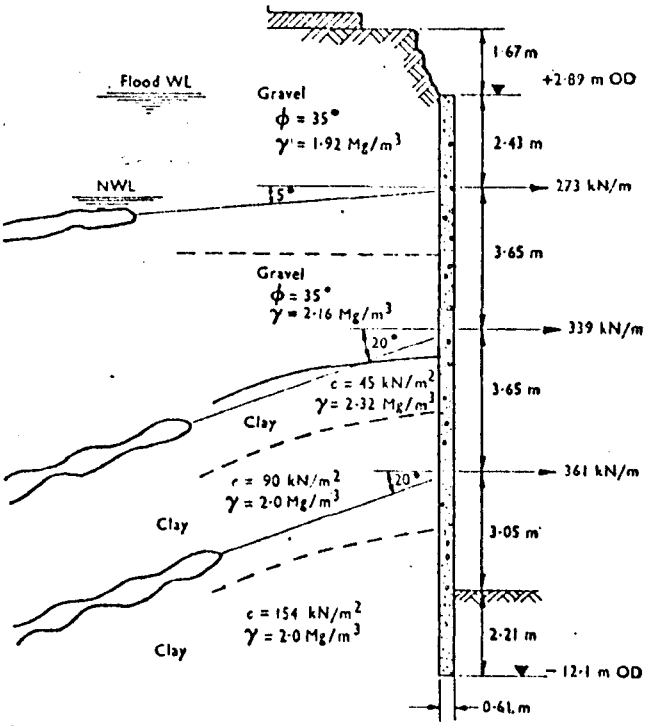

FIG. 2.4 SECTION DD THRCUGH PANEL 9-VAUXHALL (After Littlejohn and MacFarlane, 1974)

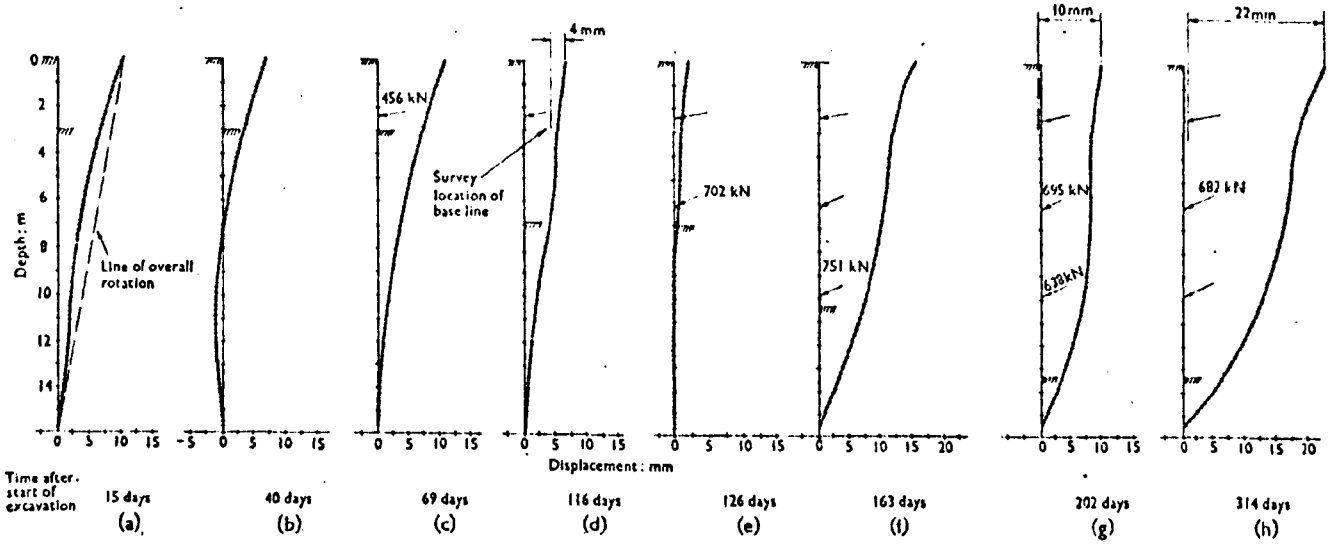

FIG. 2.5 DISPLACEMENT PROFILES OF PANEL 9 AT VARIOUS CONSTRUCTION STAGES (After Littlejohn and MacFarlane, 1974)

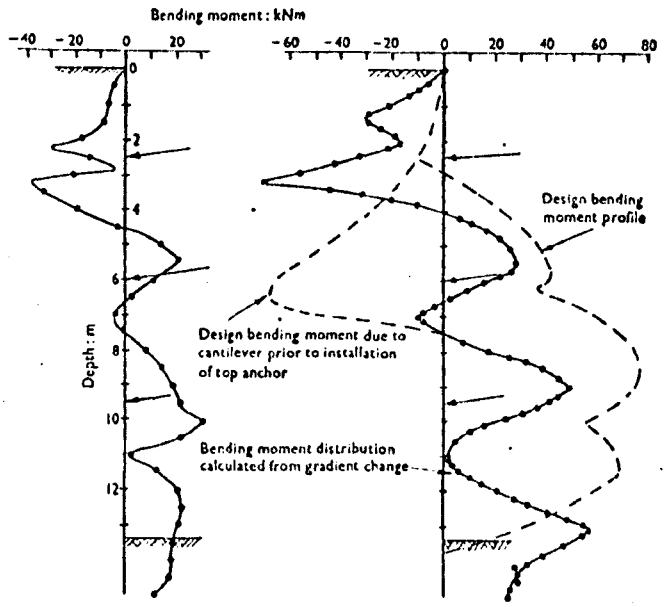

FIG. 2.6 BENDING MOMENT PROFILES OF PANEL 9 AT FINAL EXCAVATION STAGE (After Littlejohn and MacFarlane, 1974)

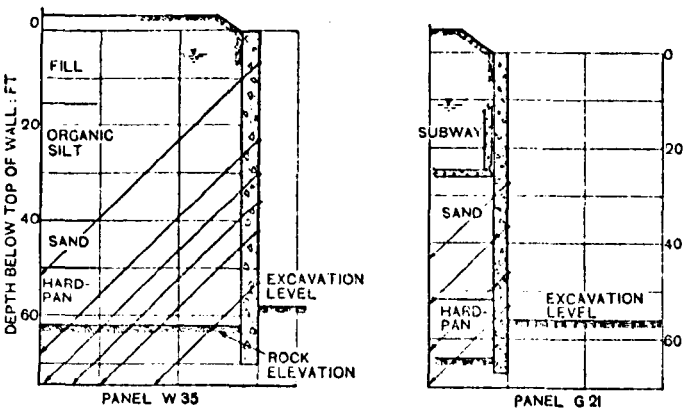

FIG. 2.7 PANEL SECTIONS
(After Gould, 1970
and Saxena, 1974)

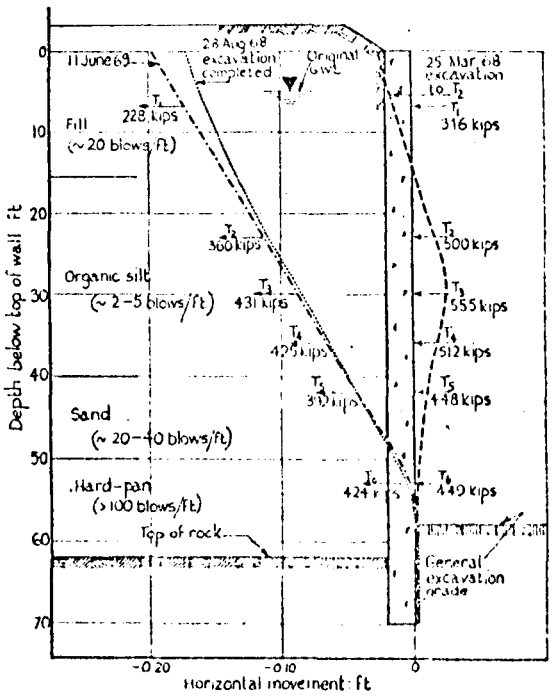

FIG. 2.8(a) HORIZONTAL MOVEMENTS

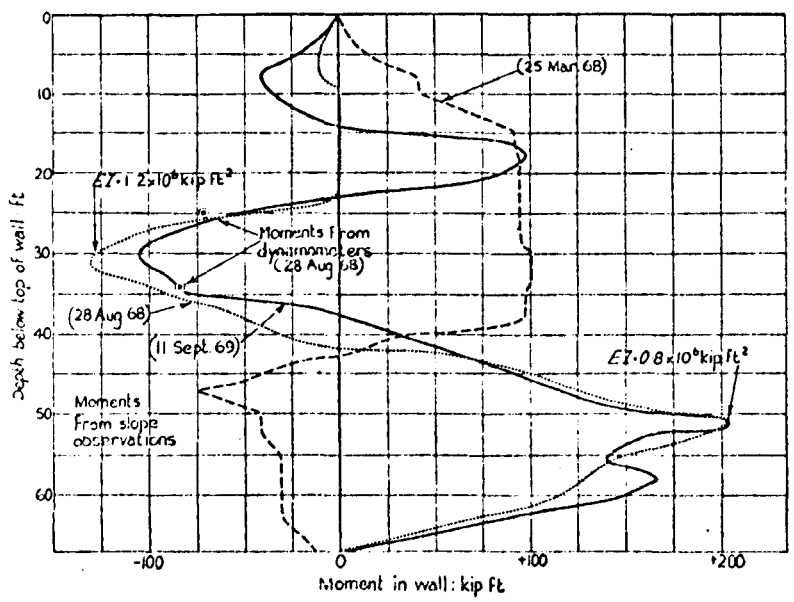

FIG. 2.8(b) BENDING MOMENTS

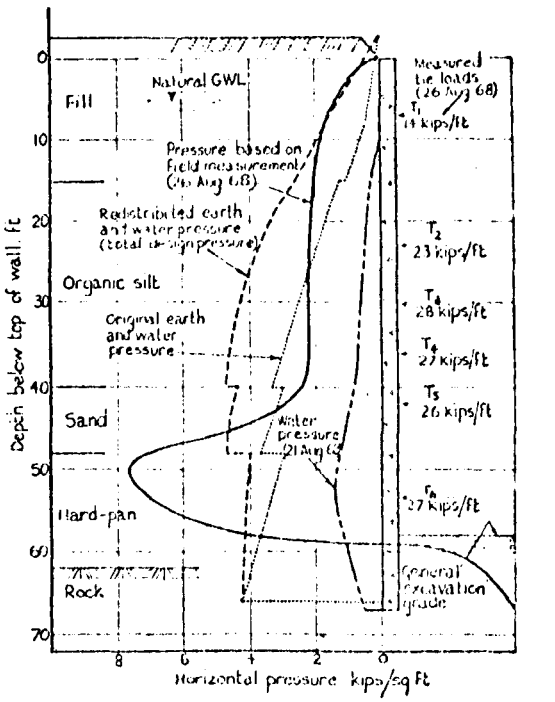

FIG. 2.8(c) HORIZONTAL PRESSURE

FIG. 2.8 OBSERVATIONS ON PANEL W35
(After Gould, 1970 and Saxena, 1974)

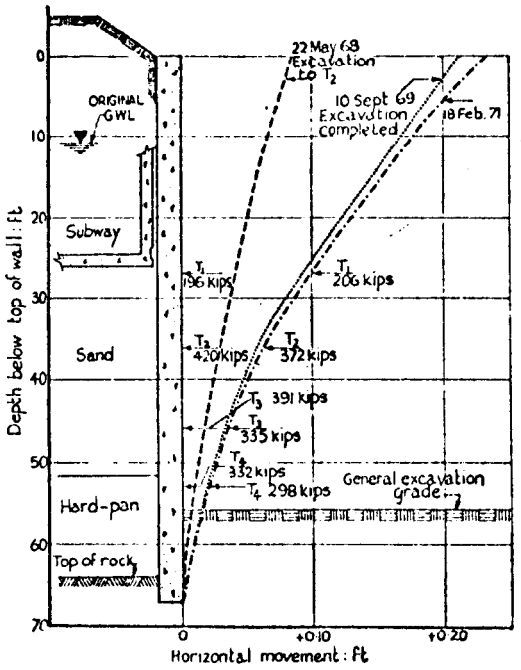

FIG. 2.9(a) HORIZONTAL MOVEMENTS

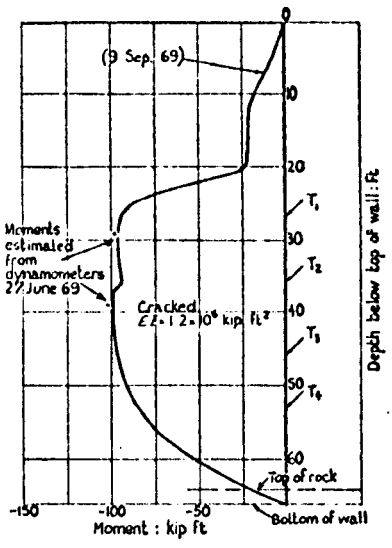

FIG. 2.9(b) BENDING MOMENTS

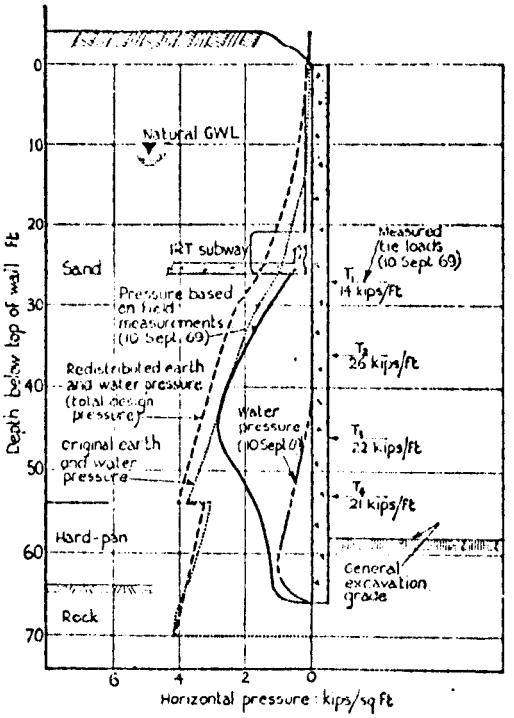

FIG. 2.9(c) HORIZONTAL PRESSURE

FIG. 2.9 OBSERVATIONS ON PANEL G21
(After Gould, 1970 and Saxena, 1974)

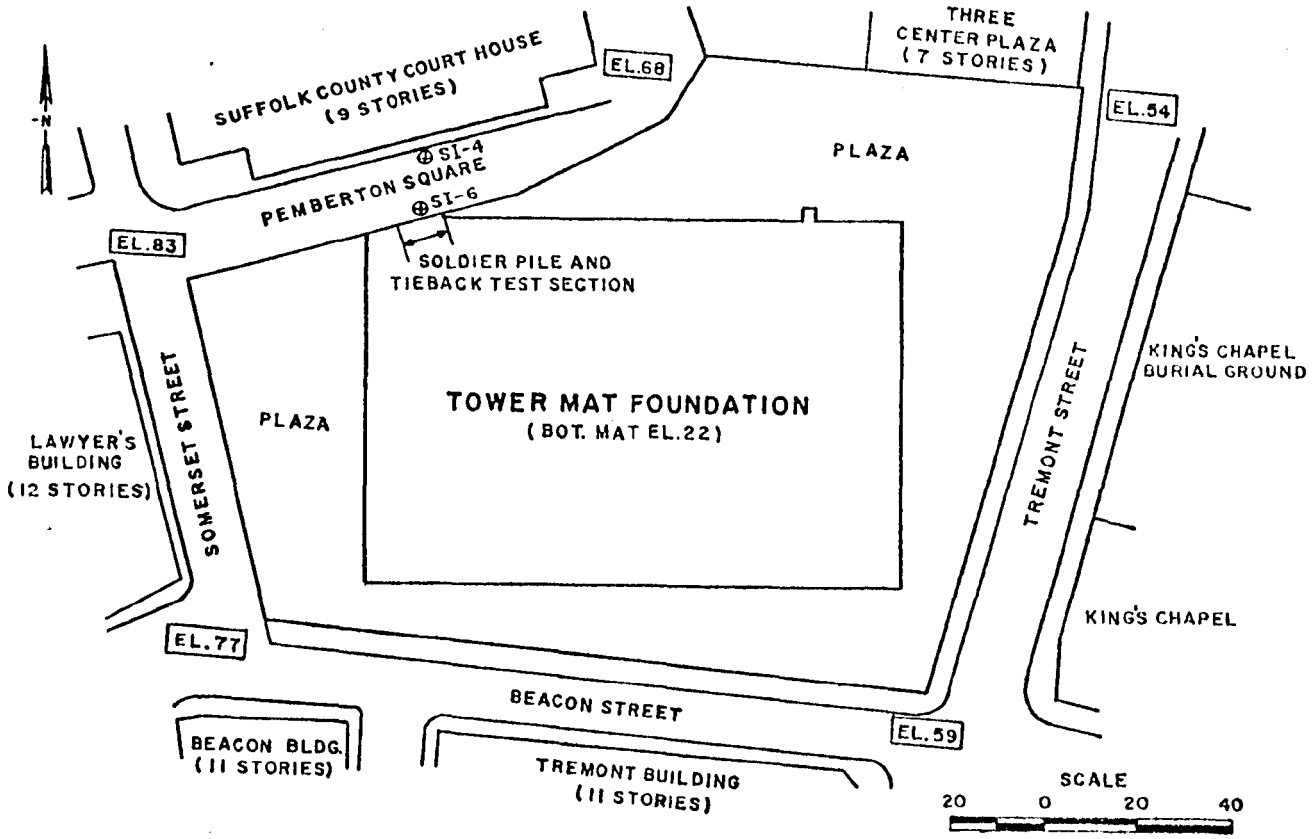

FIG. 2.10 SITE PLAN (After Liu and Dugan, 1972)

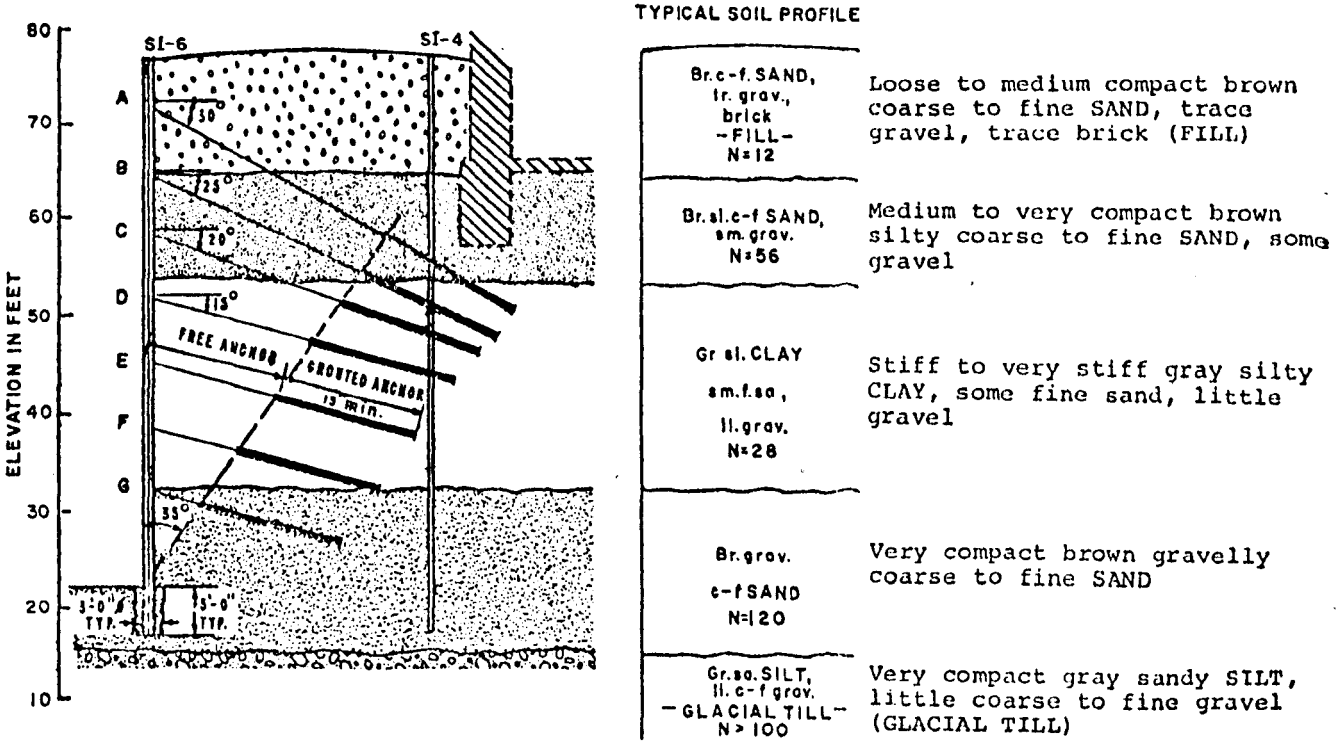

FIG. 2.11 SOLDIER PILE AND TIEBACK TEST SECTION (After Liu and Dugan, 1972)

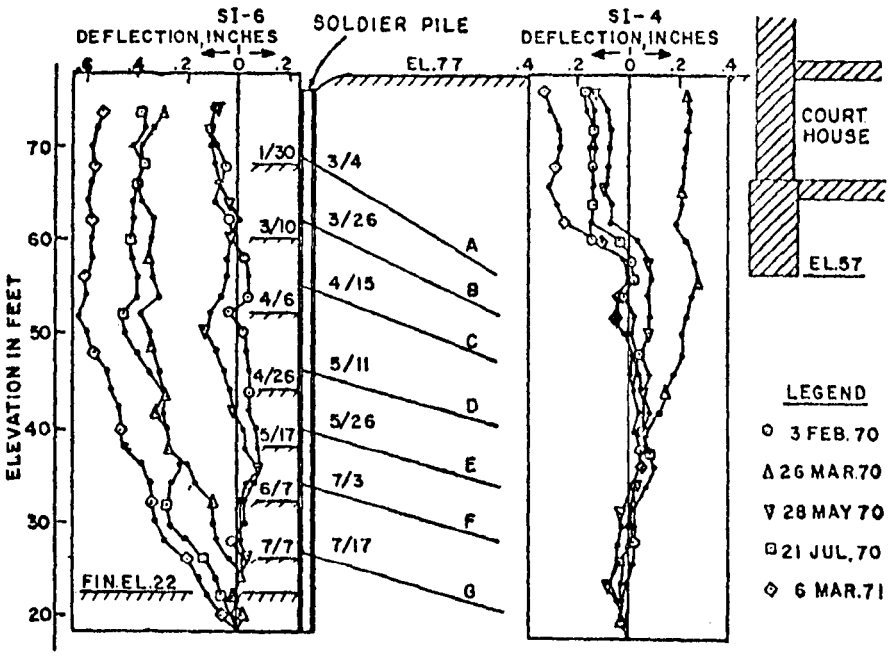

FIG. 2.12 LATERAL DEFLECTIONS AT THE TEST SECTION (After Liu and Dugan, 1972)

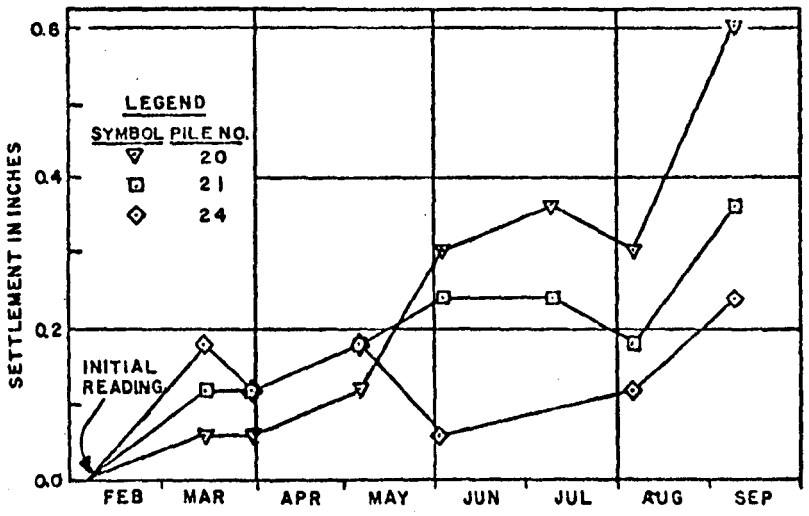

FIG. 2.13 SOLDIER PILE SETTLEMENT (After Liu and Dugan, 1972)

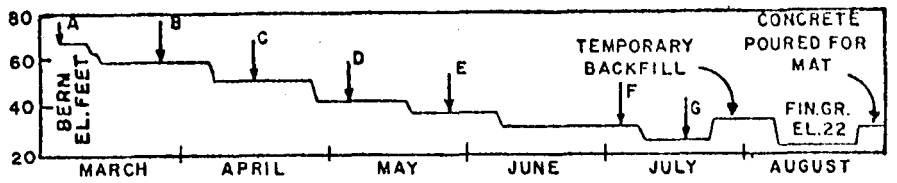

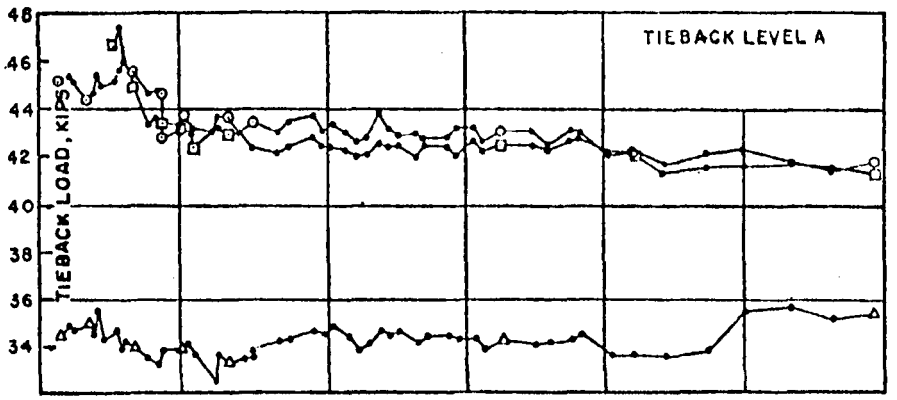

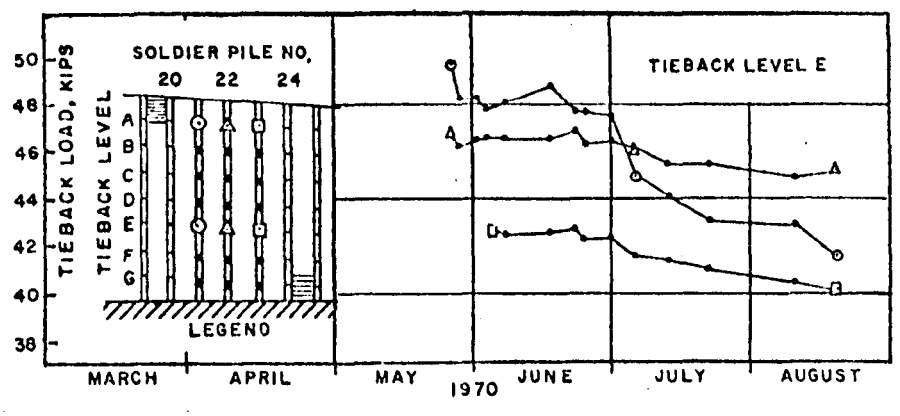

FIG. 2.14 TIEBACK LOAD VS. TIME
(After Liu and Dugan, 1972)

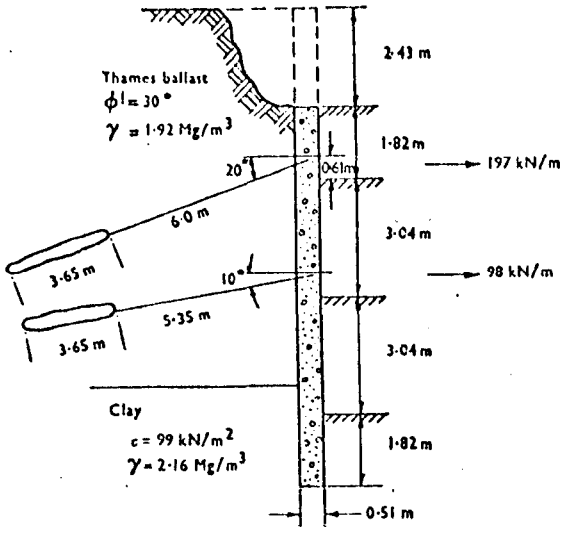

FIG. 2.15 SECTION AA THROUGH PANEL A12-GUILDHALL (After James and Phillips, 1971)

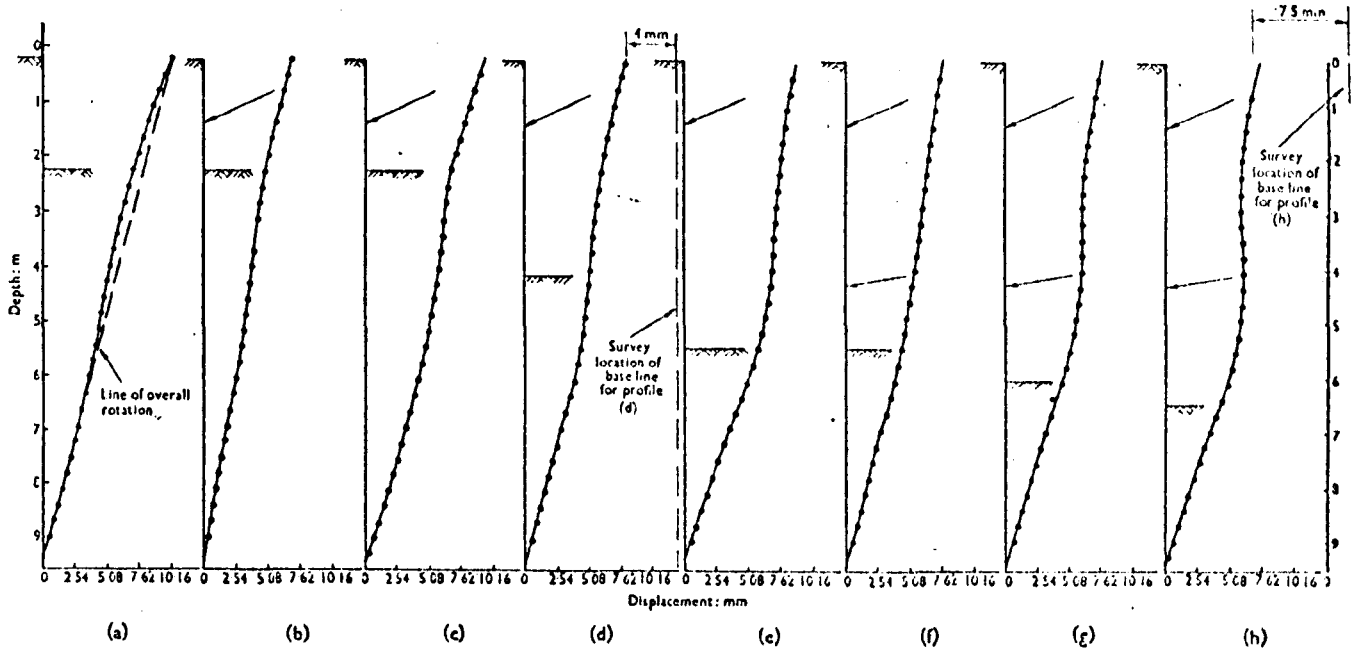

FIG. 2.16 DISPLACEMENT PROFILES OF PANEL A12 AT VARIOUS CONSTRUCTION STAGES (After James and Phillips, 1971)

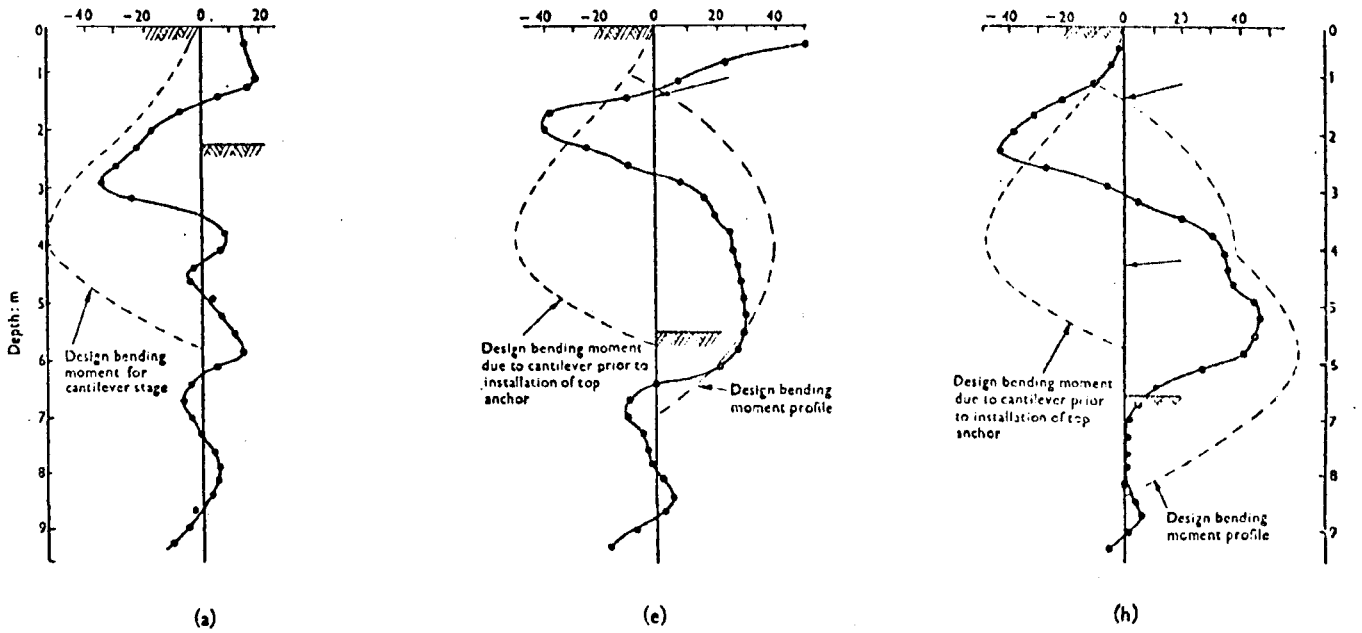

FIG. 2.17 BENDING MOMENT PROFILES OF PANEL A12 AT CONSTRUCTION STAGES (a), (e) and (h) (After James and Phillips, 1971)

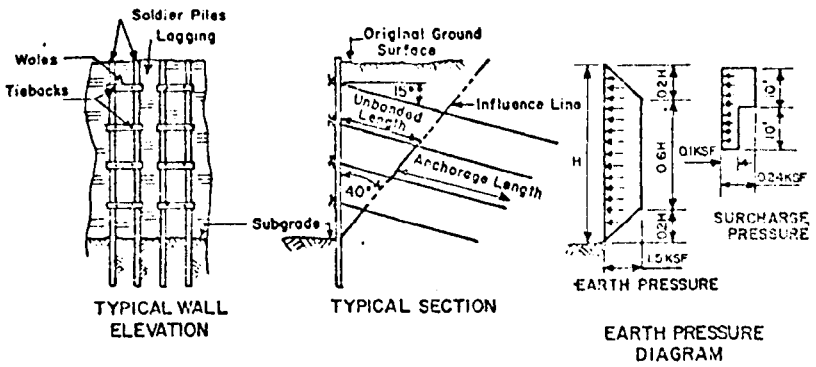

FIG. 2.18 STRUCTURAL ELEMENTS
(After Ware et al,1973)

SYMBOL	DESCRIPTION	SHEAR STRENGTH C(PSF)	SHEAR STRENGTH φ EFF	UNIT WT.(PCF)
	FILL MATERIAL(F)			130
	SILTY SAND & SAND, SOME GRAVEL, (SM & SP)		32°	130
	CLAY (CL)	1500 TO 2000	25°	130
	SILTY SAND, OCC LENSES OF ORGANIC, (SM & SP)		32°	130

TABLE 2.1 SUBSURFACE CONDITIONS
(After Ware et al,1973)

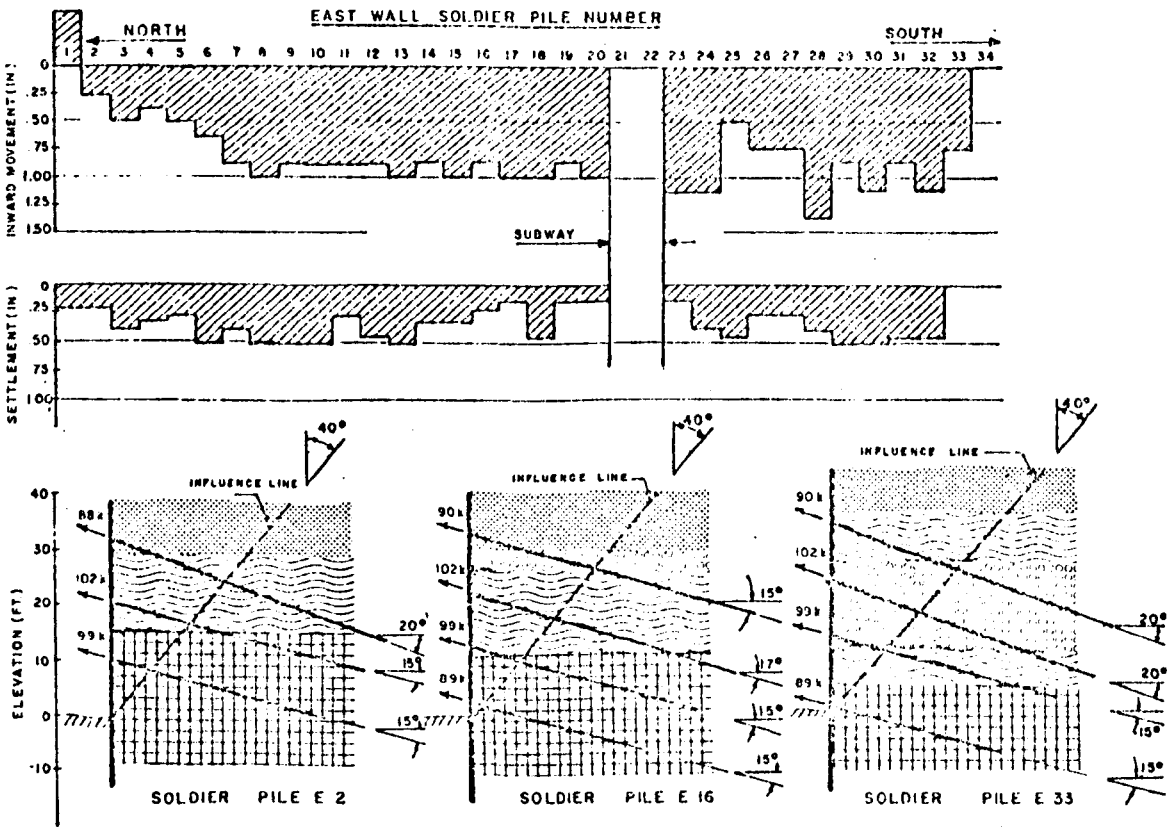

FIG. 2.19 PILE MOVEMENT AND TIEBACK LOCATION-EAST WALL
(After Ware et al,1973)

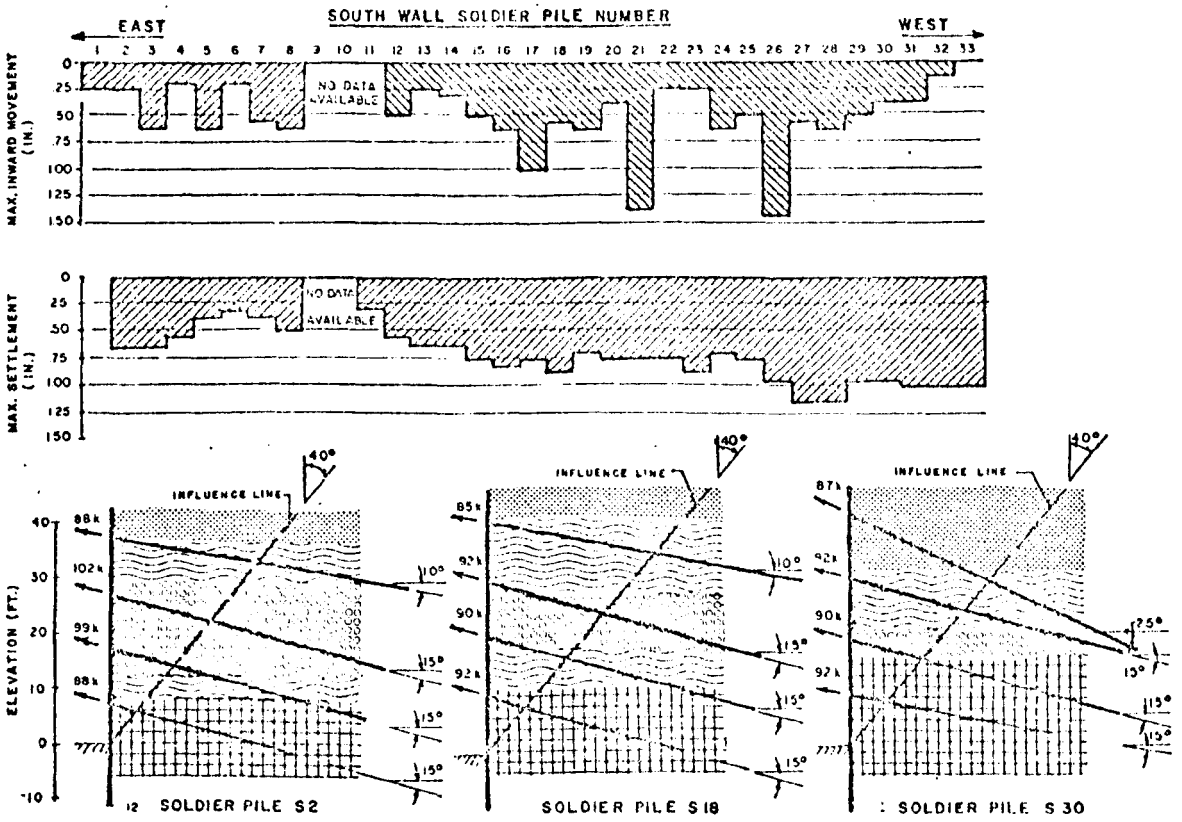

FIG. 2.20 PILE MOVEMENT AND TIEBACK LOCATION-SOUTH WALL
(After Ware et al, 1973)

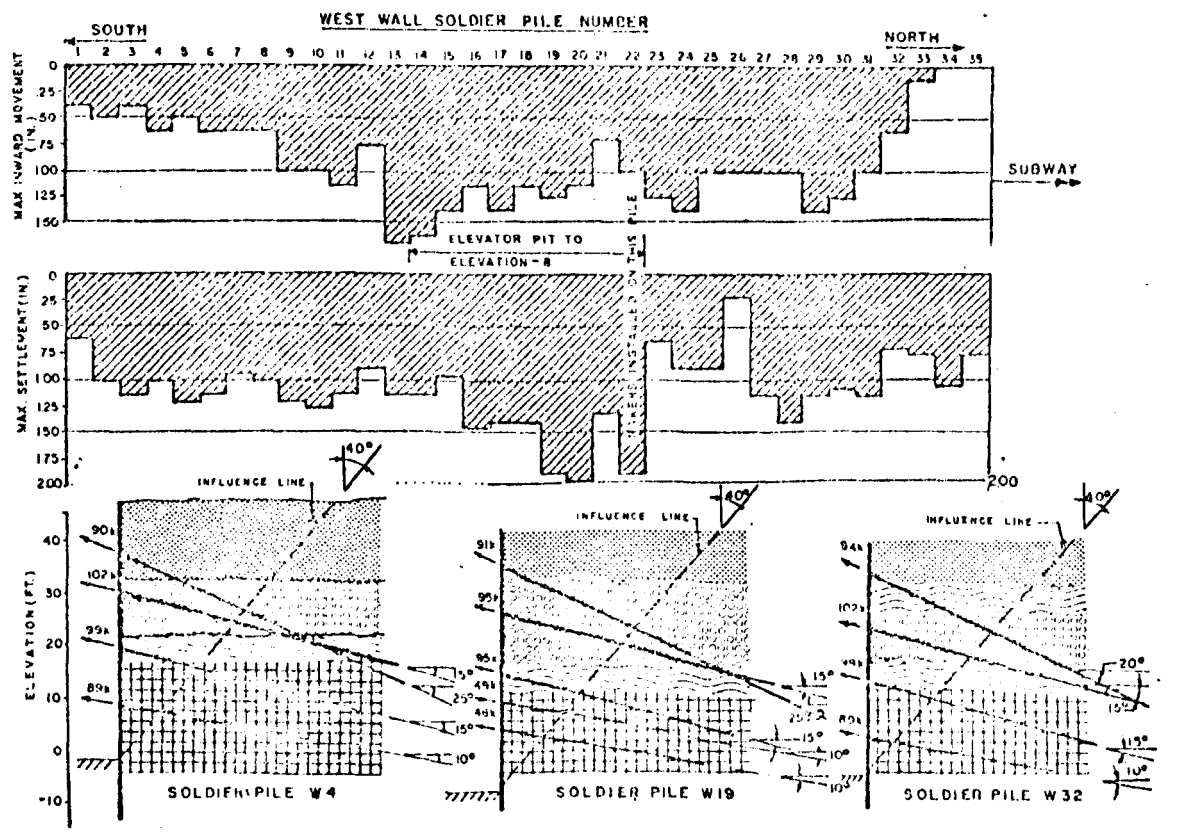

FIG. 2.21 PILE MOVEMENT AND TIEBACK LOCATION-WEST WALL
(After Ware et al, 1973)

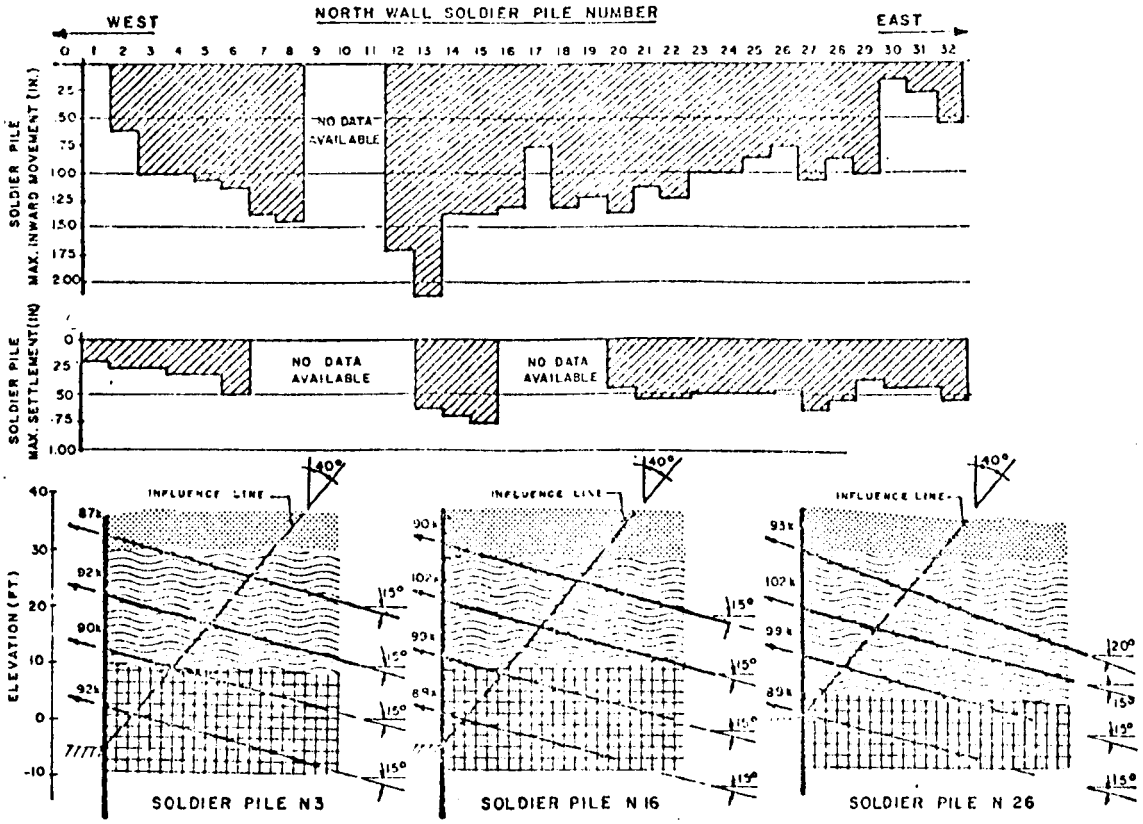

FIG. 2.22 PILE MOVEMENT AND TIEBACK LOCATION-NORTH WALL
(After Ware et al,1973)

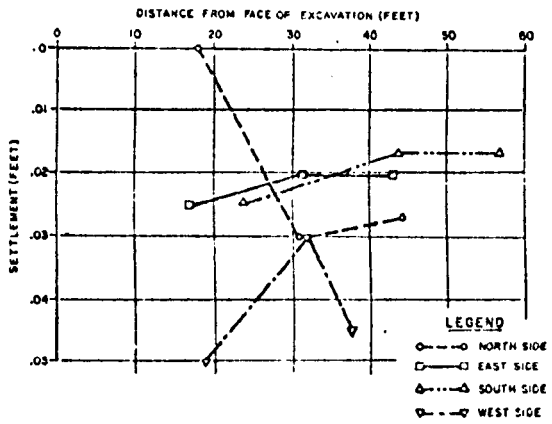

FIG. 2.23 AVERAGE STREET SETTLEMENT
(After Ware et al,1973)

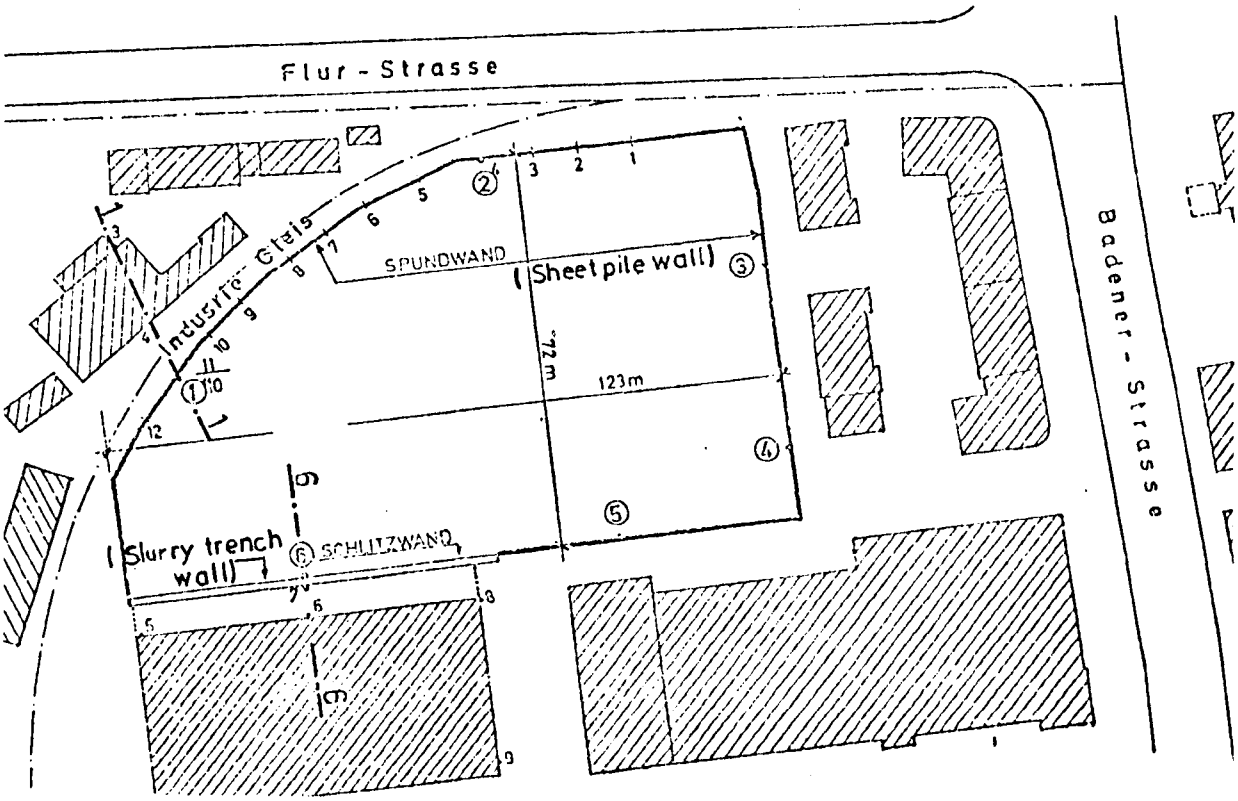

FIG. 2.24 SITE PLAN (After Henauer and Otta, 1976)

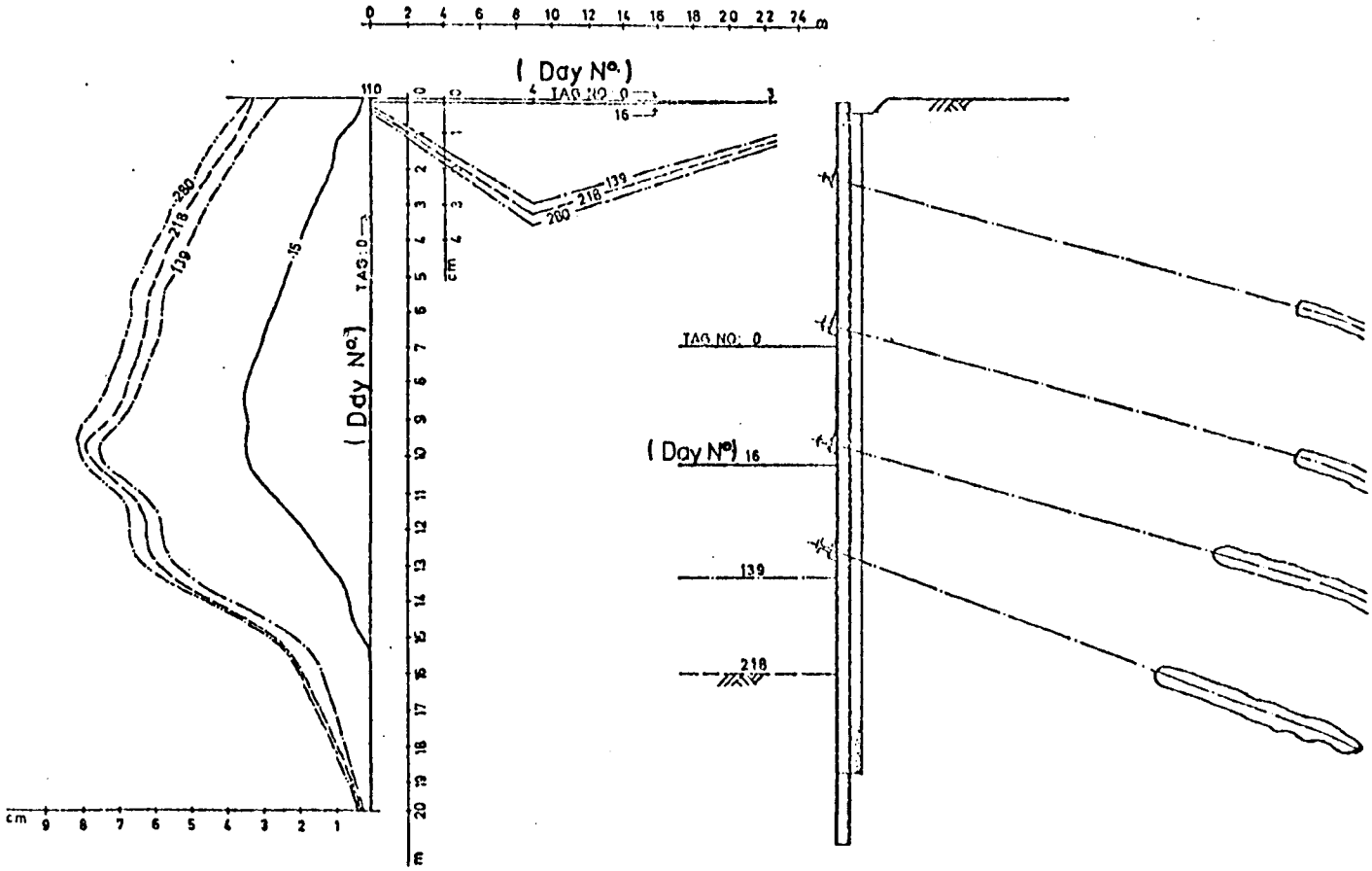

FIG. 2.25 SECTION 1 WITH MEASURED DEFORMATIONS (After Henauer and Otta, 1976)

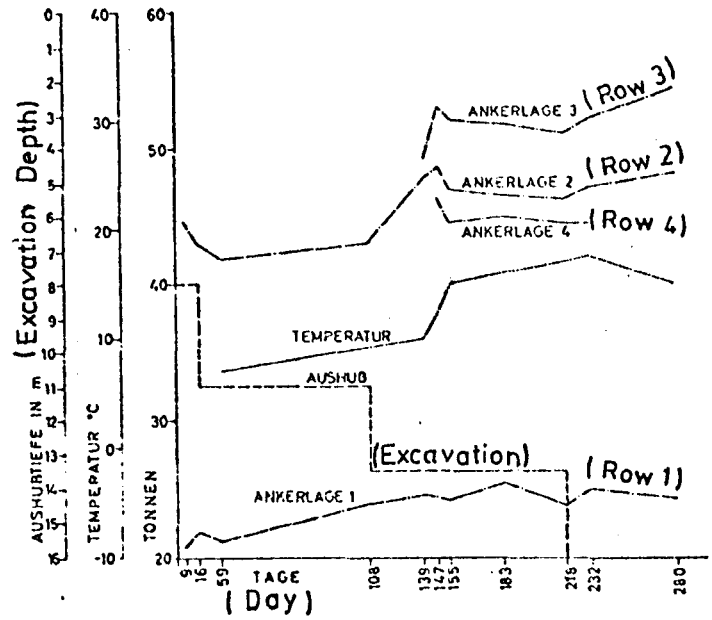

FIG. 2.26 ANCHOR FORCES IN SECTION 1
(After Henauer and Otta, 1976)

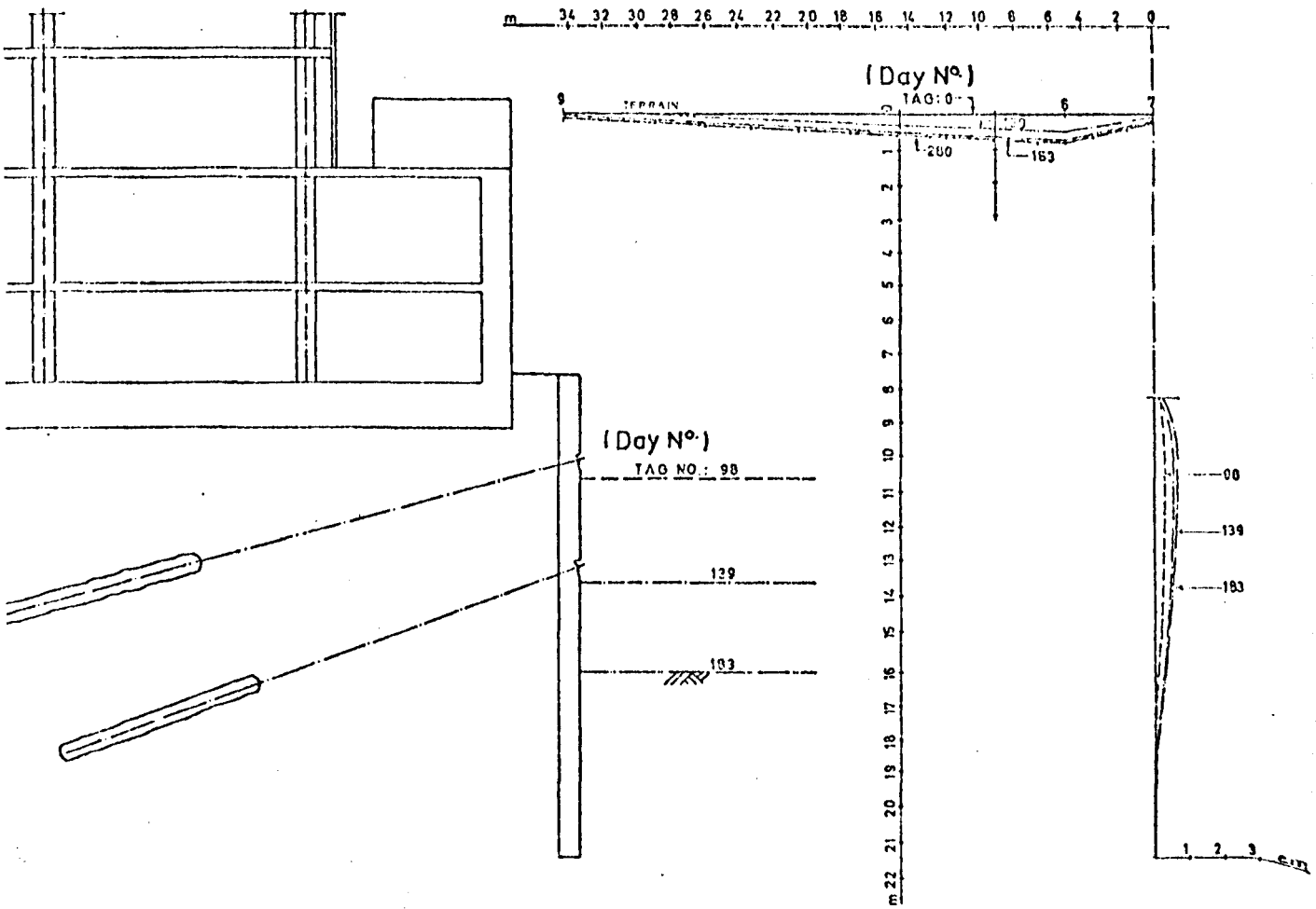

FIG. 2.27 SECTION 6 WITH MEASURED DEFORMATIONS (After Henauer and Otta, 1976)

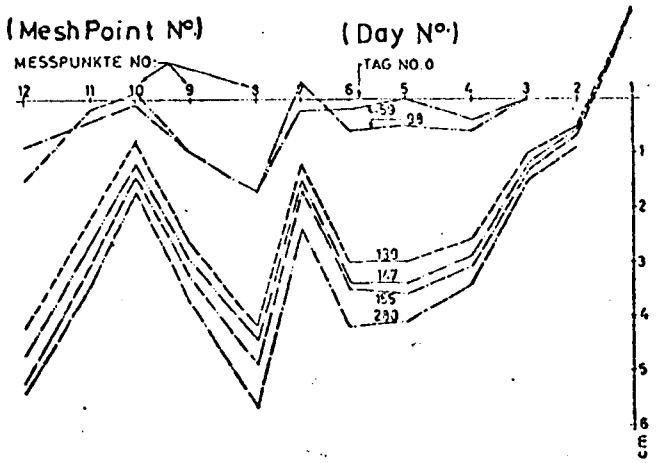

FIG. 2.28 DISPLACEMENT OF WALL- TOP BETWEEN POINTS 1-12 (after Henauer and Otta, 1976)

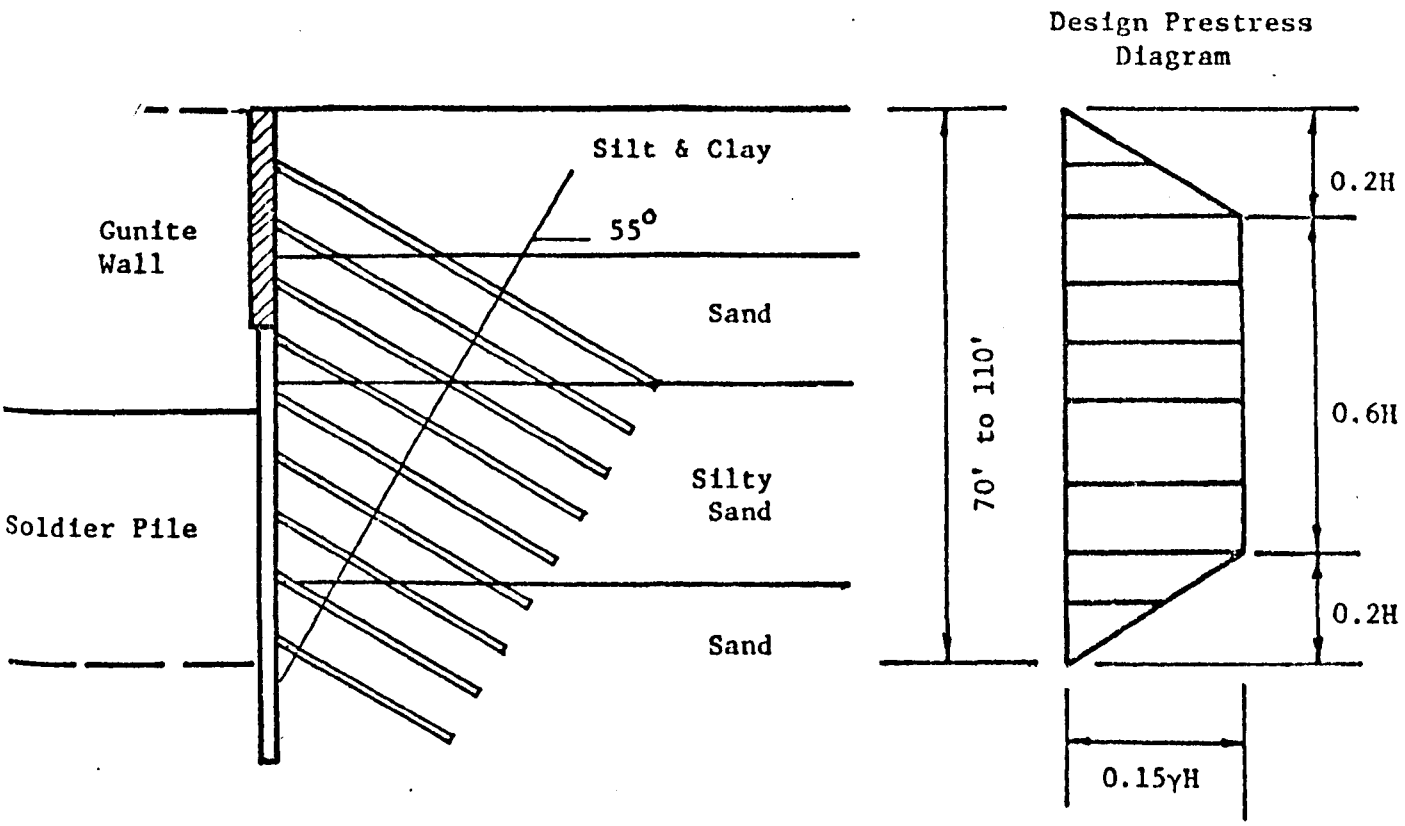

FIG. 2.29 ENTERTAINMENT CENTER AND THEME TOWERS EXCAVATION, LOS ANGELES, CALIFORNIA (After Clough, 1976)

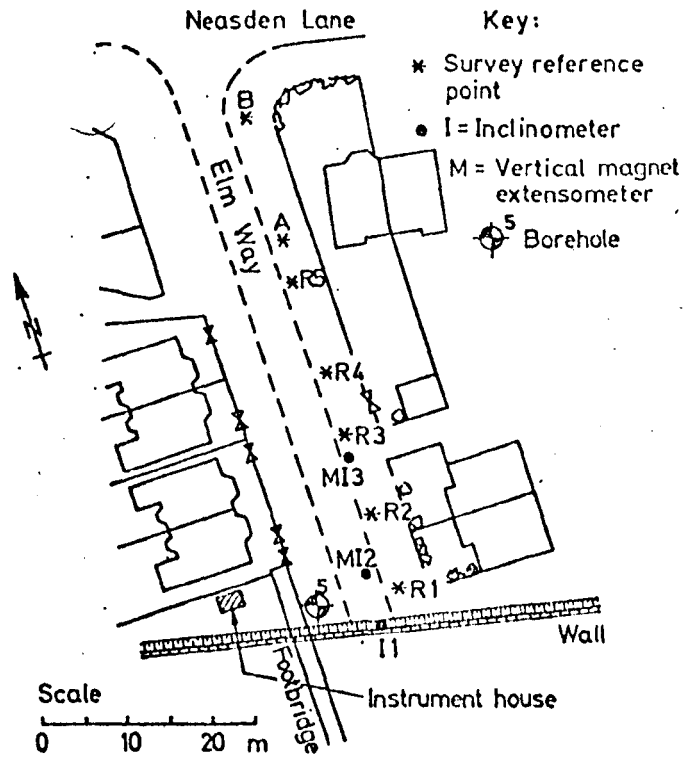

FIG. 2.30 PLAN OF INSTRUMENTED AREA (After Sills et al, 1977)

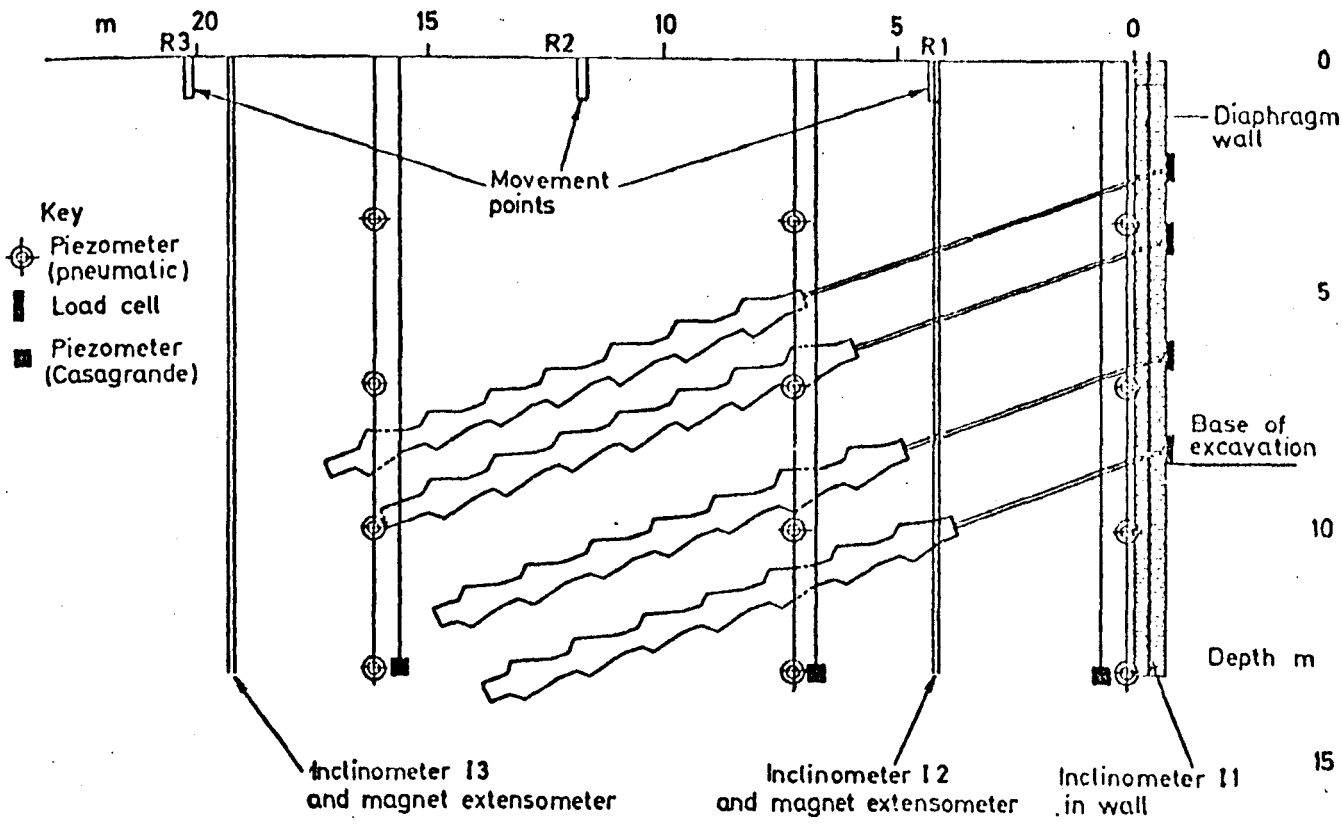

FIG. 2.31 SECTION THROUGH INSTRUMENTATION (After Sills et al, 1977)

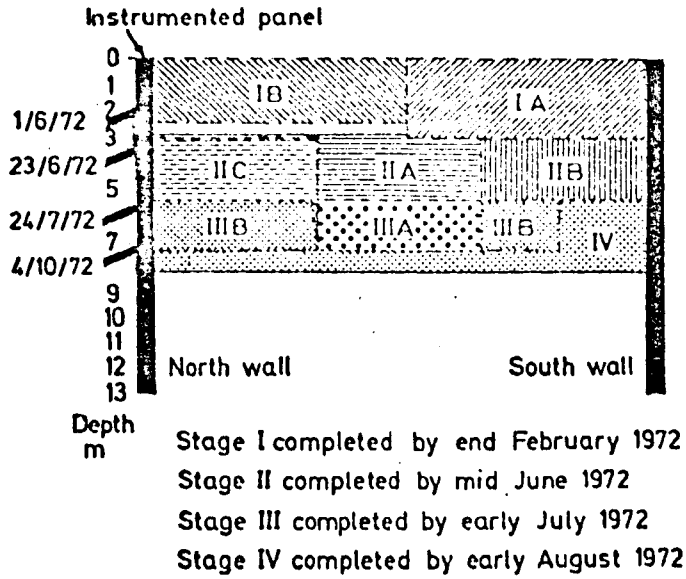

FIG. 2.32 PROGRESS OF EXCAVATION (After Sills et al, 1977)

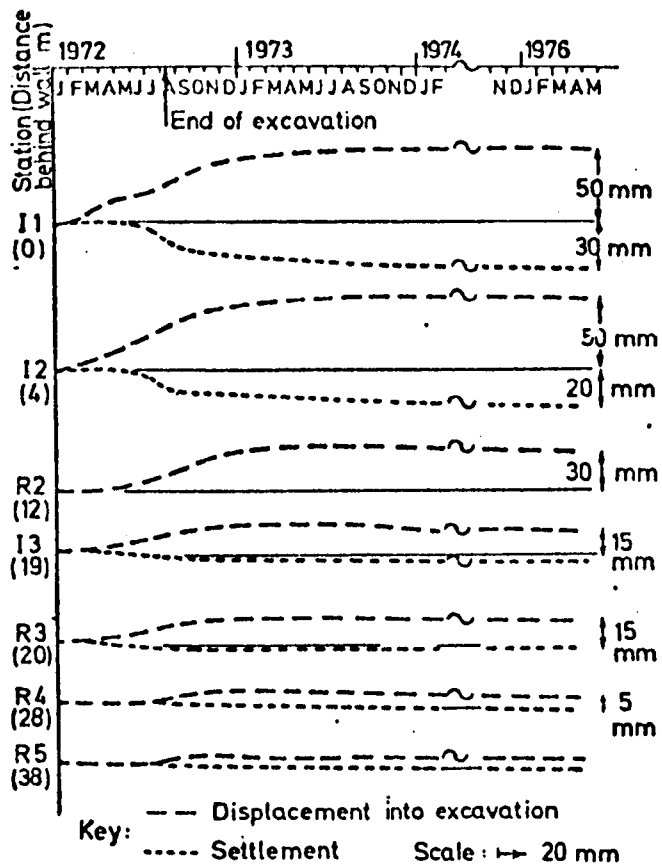

FIG. 2.33 SURFACE MOVEMENTS BEHIND THE WALL (After Sills et al, 1977)

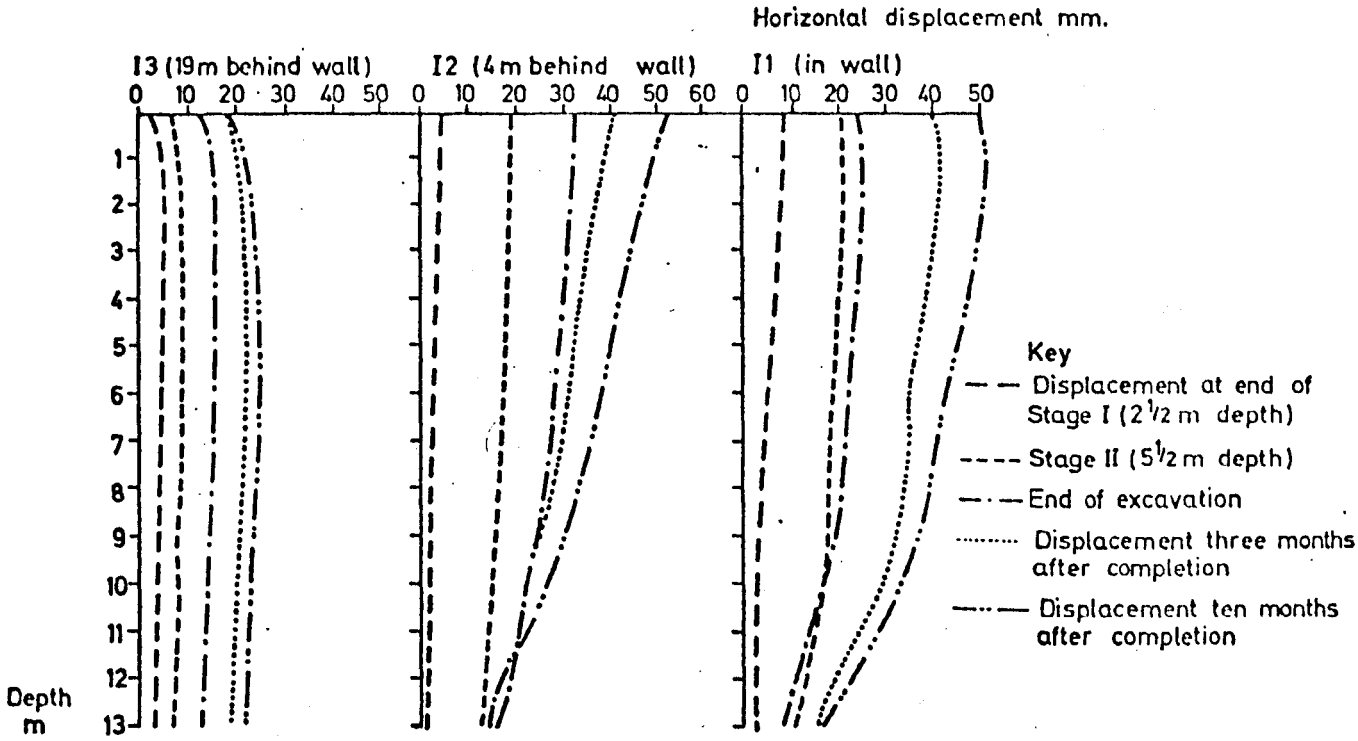

FIG. 2.34 HORIZONTAL MOVEMENTS OF WALL AND GROUND (After Sills et al, 1977)

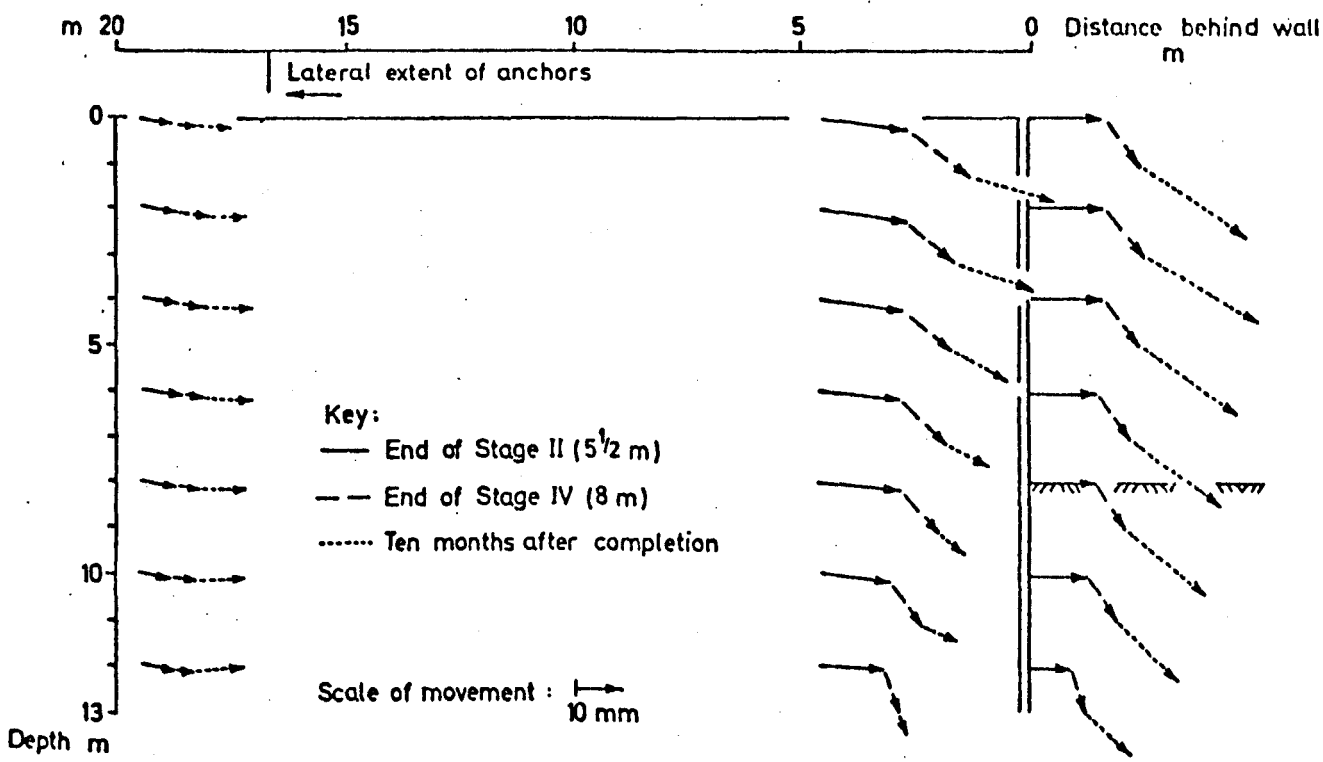

FIG. 2.35 VECTORS OF MOVEMENT (After Sills et al, 1977)

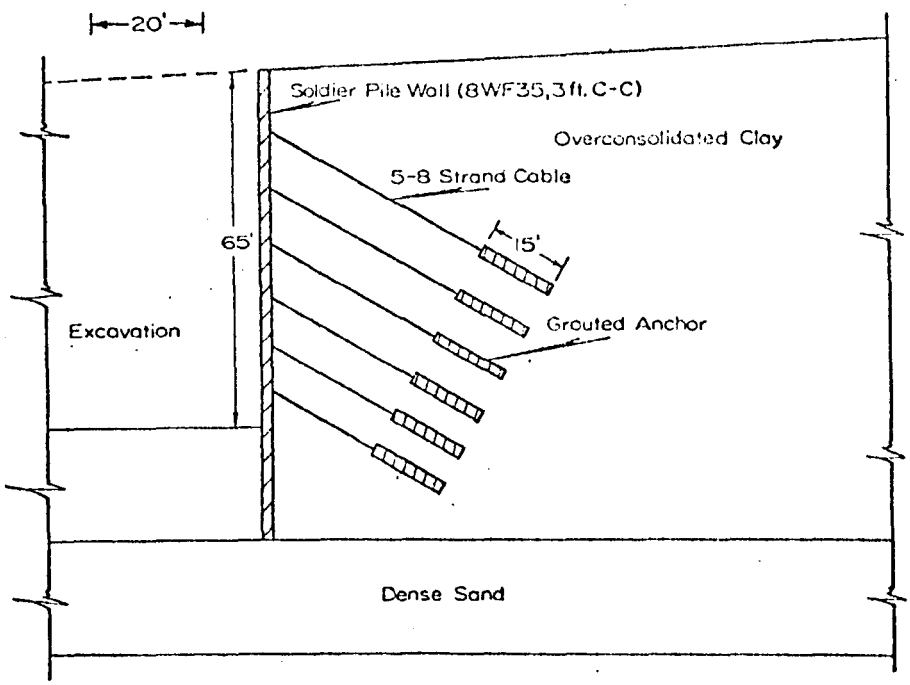

FIG. 2.36 CROSS-SECTION THROUGH BANK OF CALIFORNIA TIED-BACK WALL (After Clough et al, 1972)

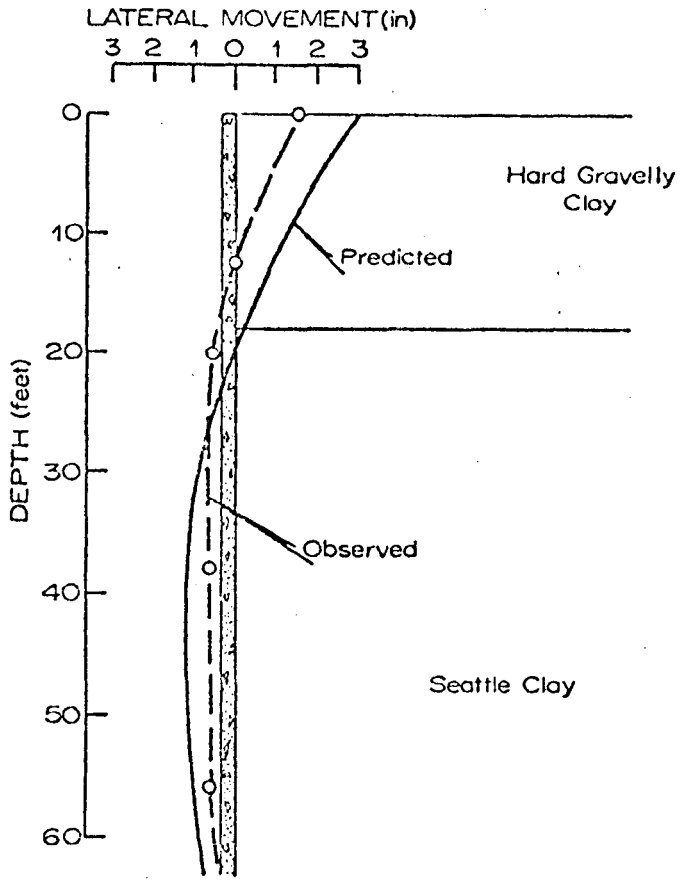

FIG. 2.37 PREDICTED AND OBSERVED WALL DEFLECTIONS-BANK OF CALIFORNIA EXCAVATION (After Clough et al, 1974)

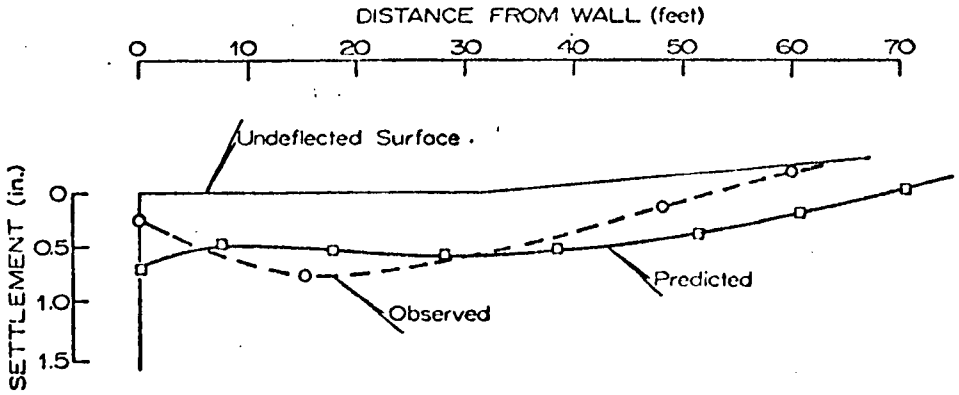

FIG. 2.38 PREDICTED AND OBSERVED SURFACE SETTLEMENTS-BANK OF CALIFORNIA EXCAVATION (After Clough et al, 1972)

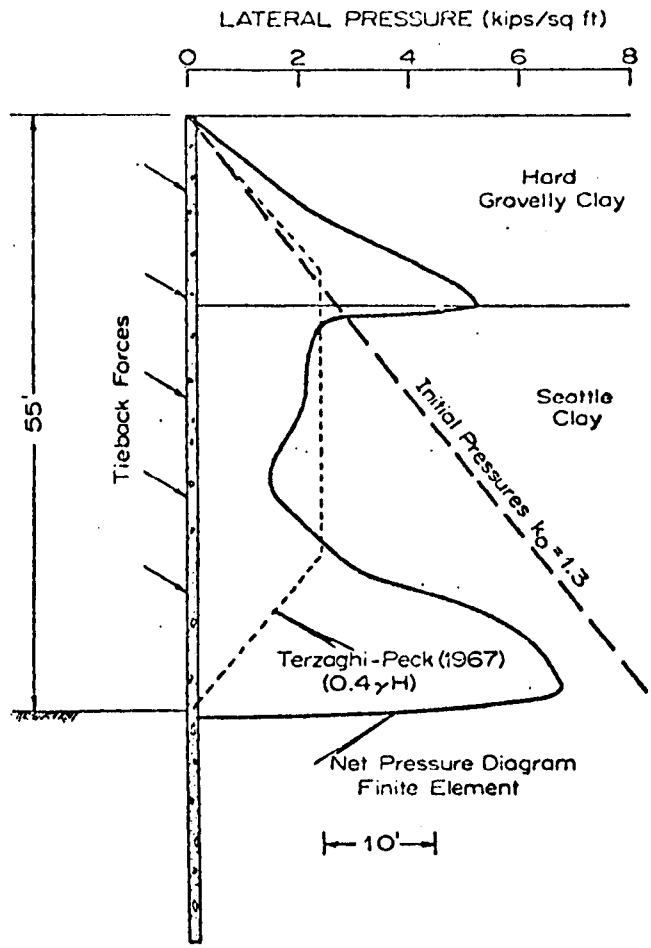

FIG. 2.39 PREDICTED EARTH PRESSURE-BANK OF CALIFORNIA EXCAVATION (After Clough et al, 1972)

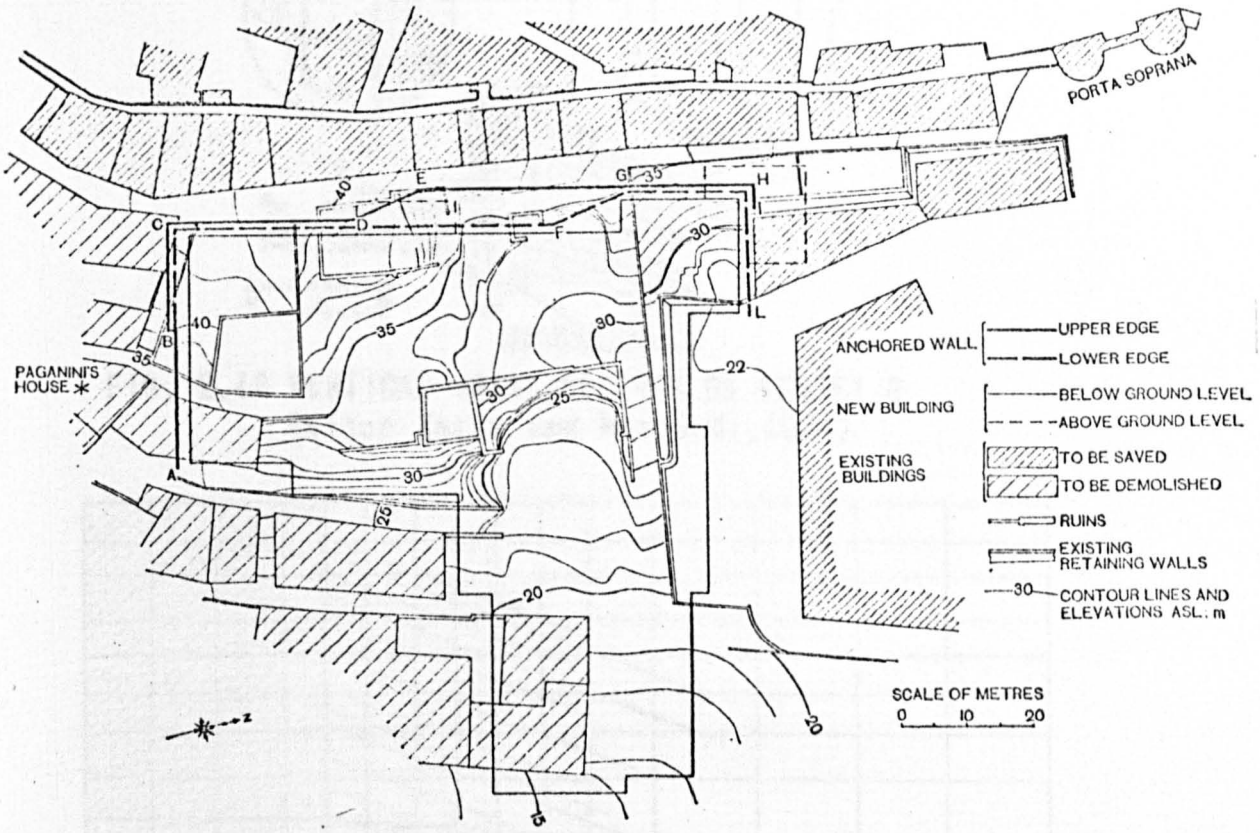

FIG. 2.40 PLAN OF THE SITE (After Barla and Mascardi, 1974)

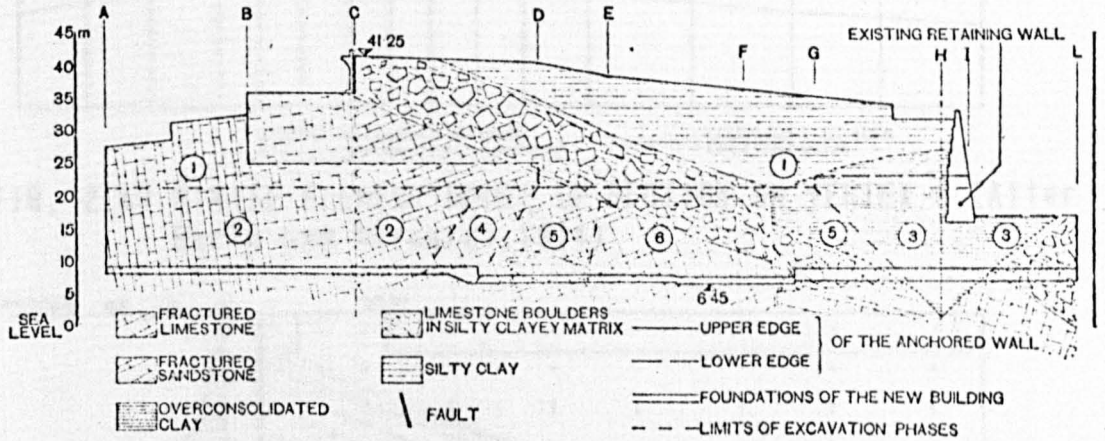

FIG. 2.41 VERTICAL SECTION ALONG THE WALL: NUMERALS INDICATE THE ORDER OF MAIN PHASES OF EXCAVATION (After Barla and Mascardi, 1974)

Soil	Deformation modulus E, MN/m^2	Poisson's ratio ν	Cohesion c, MN/m^2	Angle of friction ϕ, degrees
Silty clay	19·6	0·40	0·0196	27
Overconsolidated clay	58·8	0·40	0·0588	31·5
Limestone boulders in silty clay matrix	78·5	0·30	0·098	46
Fractured limestone or sandstone	1177	0·15	0·098	46

TABLE 2.2 SOIL PARAMETERS USED IN FINITE ELEMENT ANALYSIS (After Barla and Mascardi, 1974)

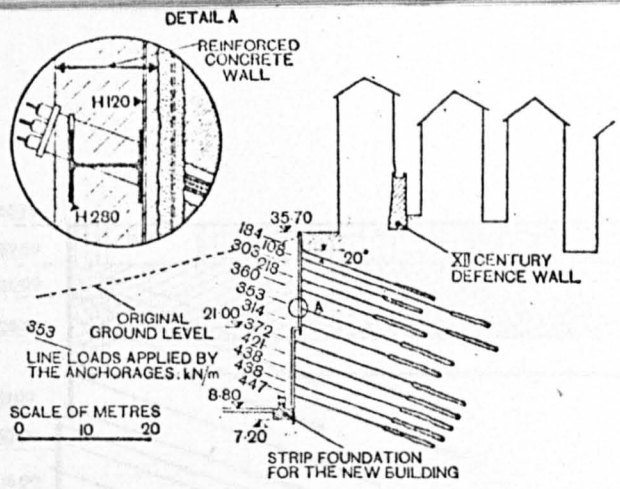

FIG. 2.42 VERTICAL CROSS-SECTION ON VERTEX G (After Barla and Mascardi, 1974)

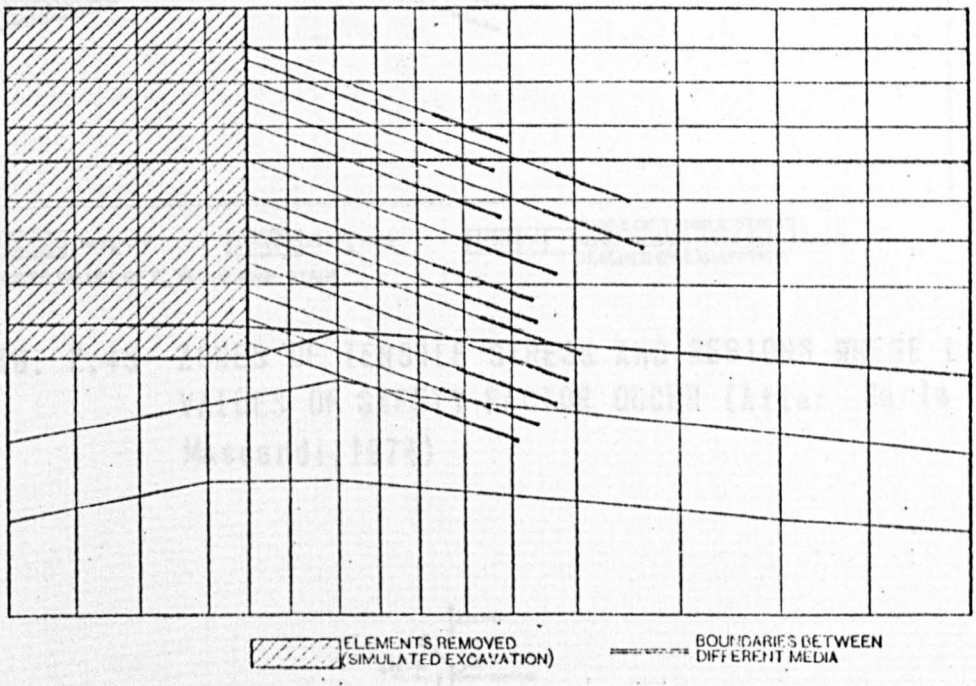

FIG. 2.43 FINITE ELEMENT MODEL OF SECTION ON VERTEX G (After Barla and Marcardi, 1974)

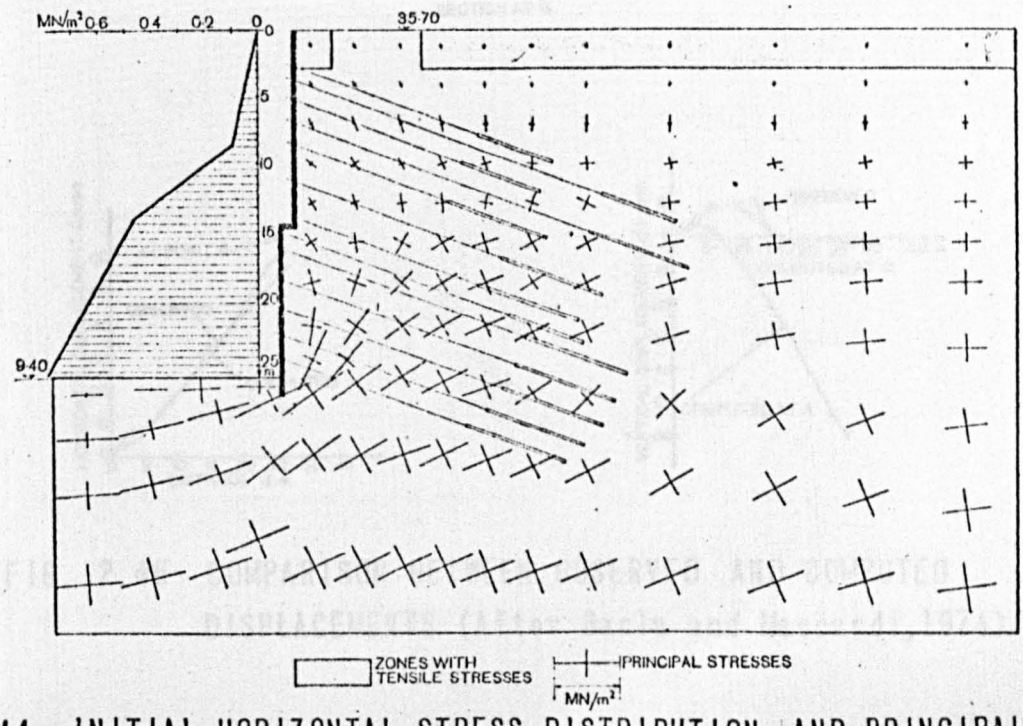

FIG. 2.44 INITIAL HORIZONTAL STRESS DISTRIBUTION, AND PRINCIPAL STRESS IN THE SOIL IN THE FINAL STAGE OF EXCAVATION (After Barla and Mascardi, 1974)

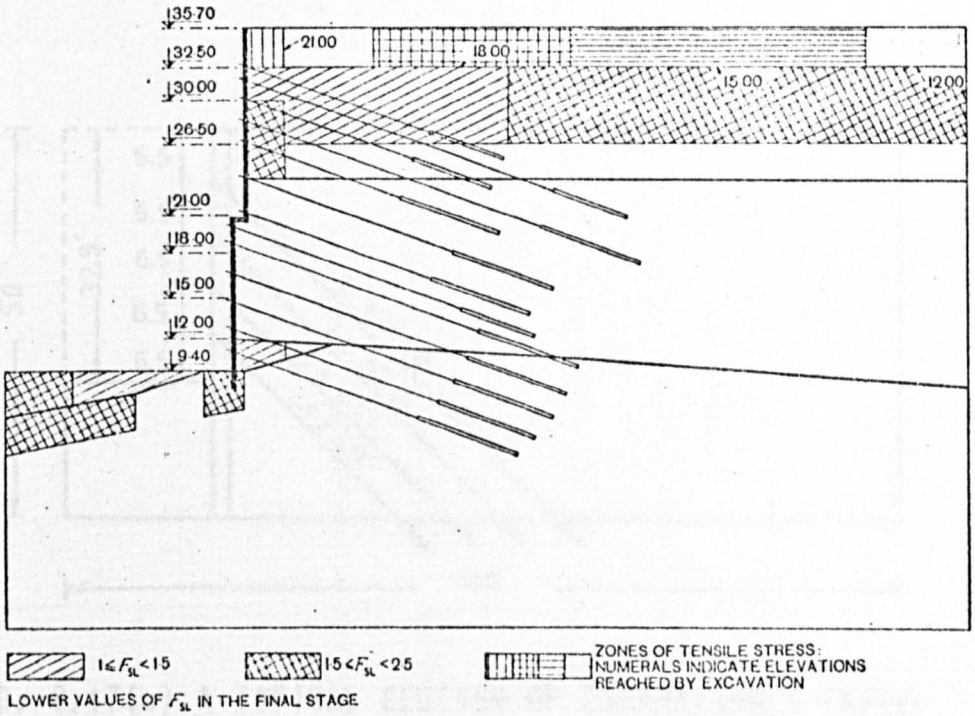

FIG. 2.45 ZONES OF TENSILE STRESS AND REGIONS WHERE LOWER VALUES OF SAFETY FACTOR OCCUR (After Barla and Mascardi, 1974)

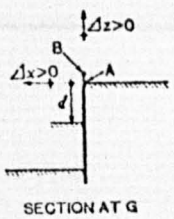

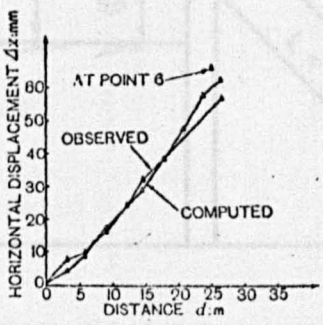

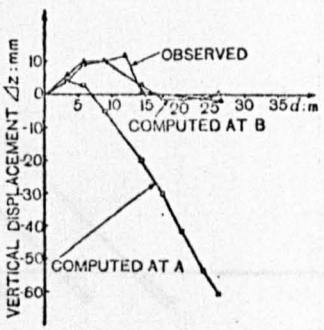

FIG. 2.46 COMPARISON BETWEEN OBSERVED AND COMPUTED DISPLACEMENTS (After Barla and Mascardi, 1974)

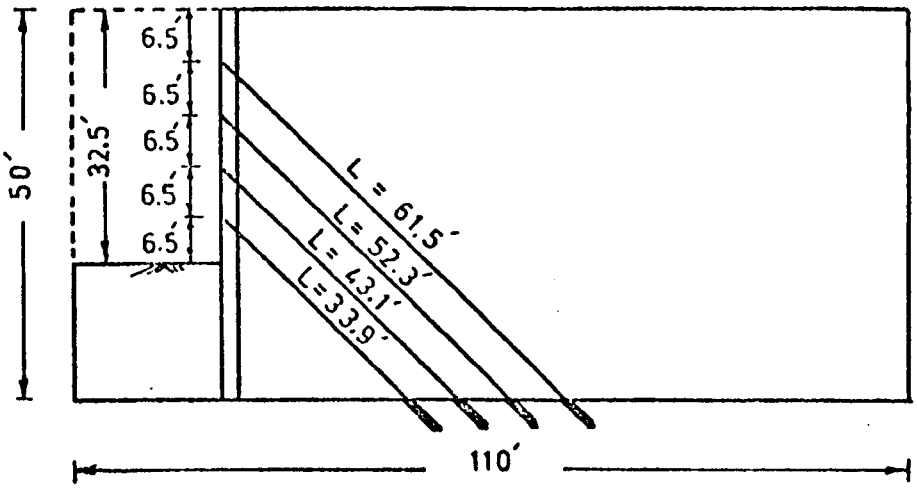

FIG. 2.47(a) A TYPICAL SECTION OF EXCAVATION I (After Clough and Tsui, 1974)

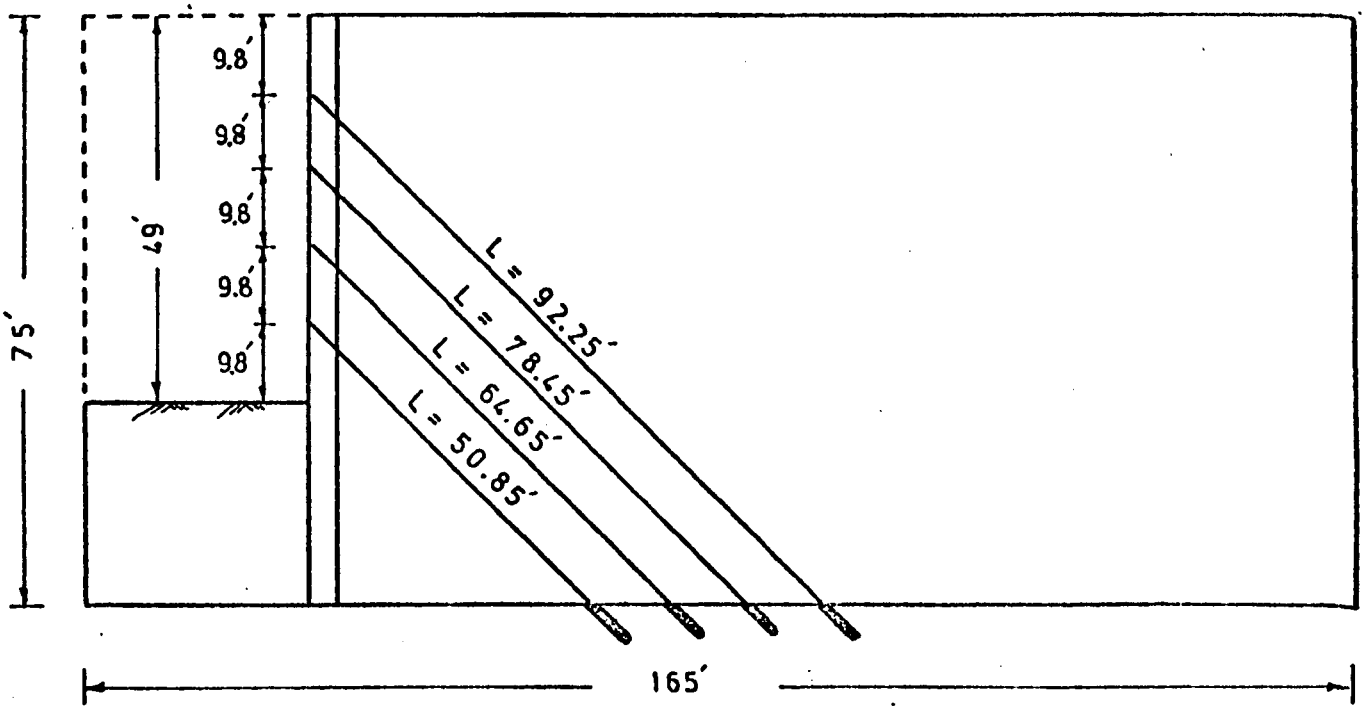

FIG. 2.47(b) A TYPICAL SECTION OF EXCAVATION II (After Clough and Tsui, 1974)

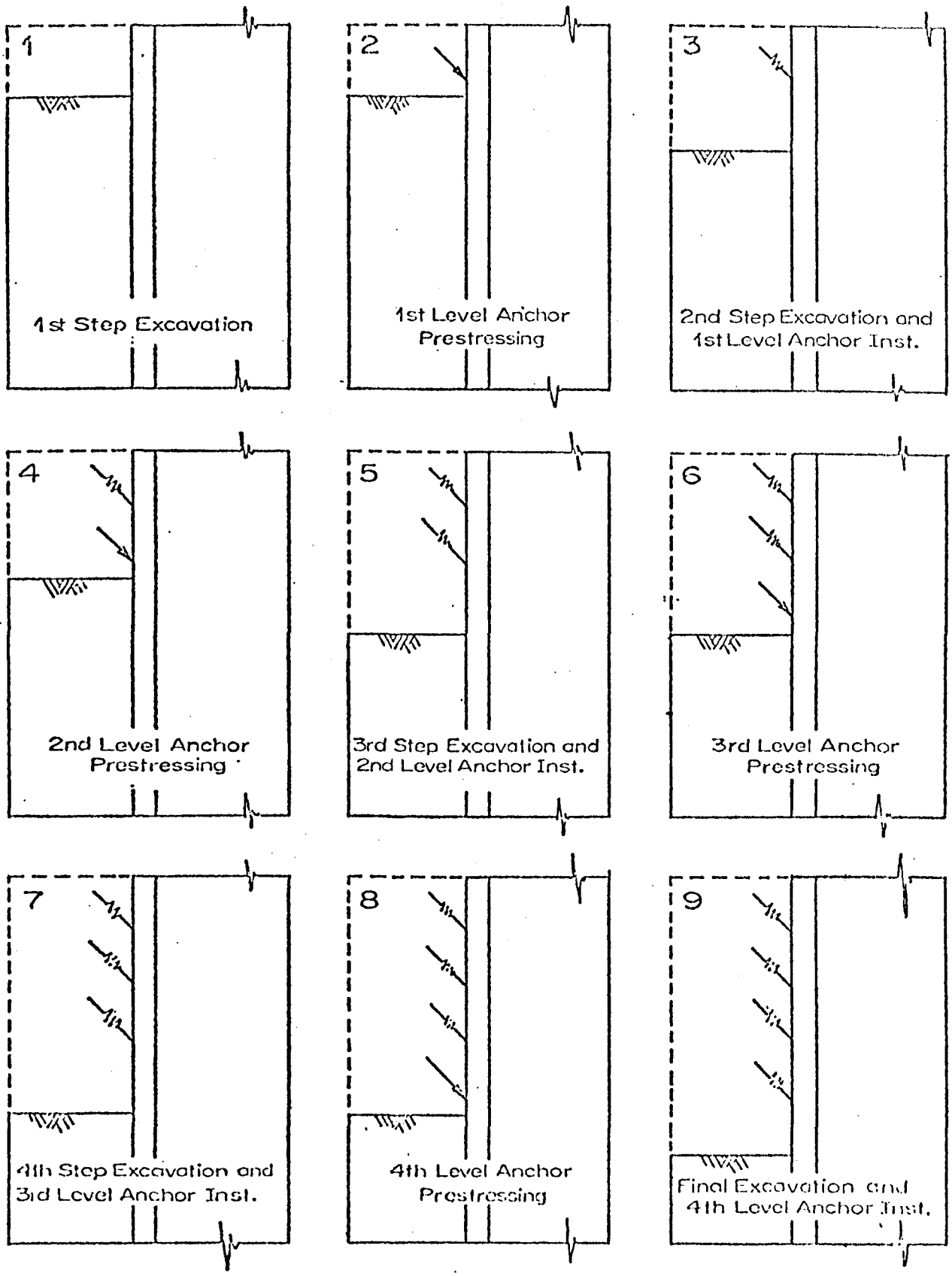

FIG. 2.48 CONSTRUCTION SEQUENCES FOR TIED-BACK EXCAVATION (After Clough and Tsui, 1974)

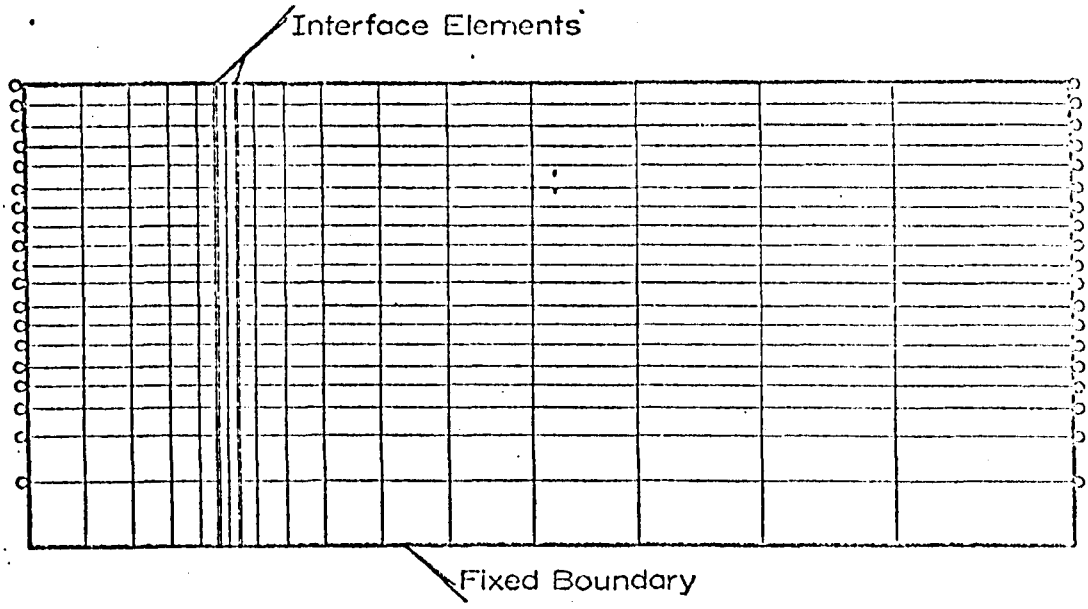

FIG. 2.49 FINITE ELEMENT MECH FOR TIED- BACK EXCAVATION ANALYSIS (After Clough and Tsui, 1974)

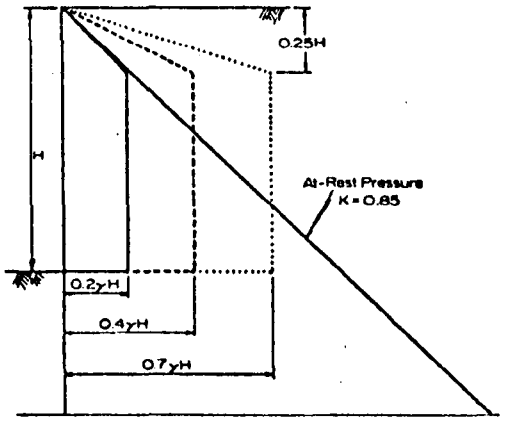

FIG. 2.50 DESIGN PRESTRESS DIAGRAMS USED IN PARAMETRIC STUDY (After Clough and Tsui, 1974)

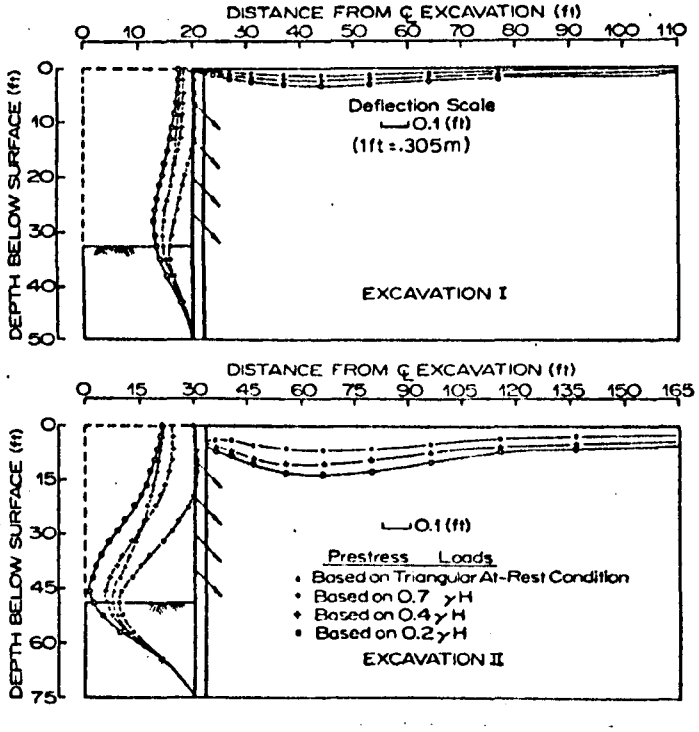

FIG. 2.51 EFFECT OF PRESTRESS ON SOIL AND WALL MOVEMENTS (After Clough and Tsui, 1974)

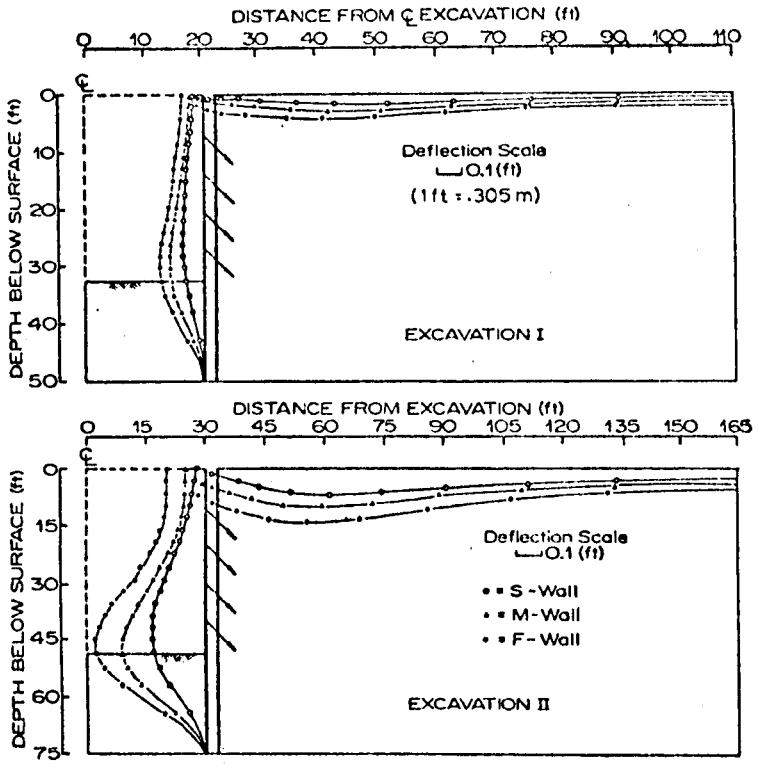

FIG. 2.52 EFFECT OF WALL RIGIDITY ON SOIL AND WALL MOVEMENTS (After Clough and Tsui, 1974)

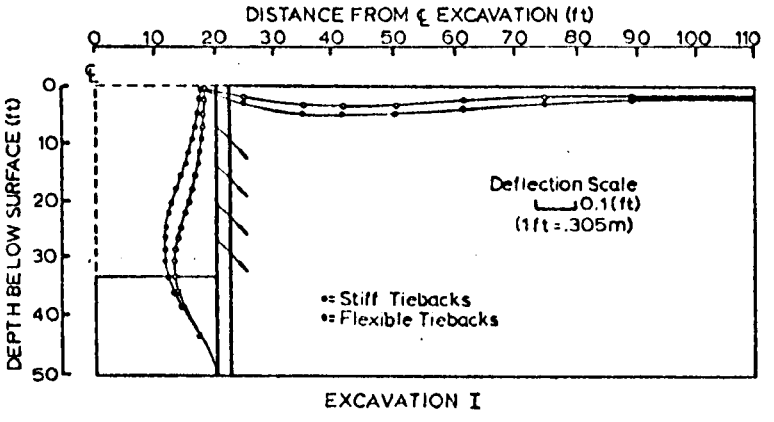

FIG. 2.53 EFFECT OF TIE-BACK STIFFNESS ON SOIL AND WALL MOVEMENTS (After Clough and Tsui, 1974)

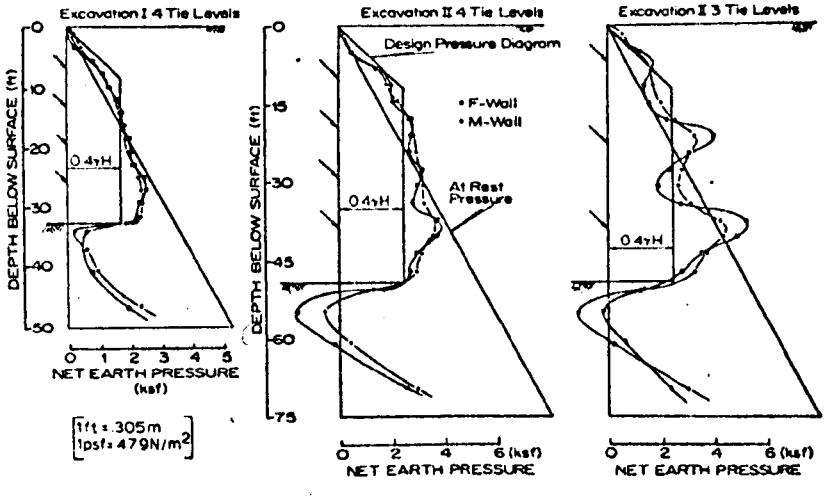

FIG. 2.54 PREDICTED NET EARTH PRESSURES FOR DIFFERING TIE-BACK ARRANGEMENTS AND WALL FLEXIBILITIES

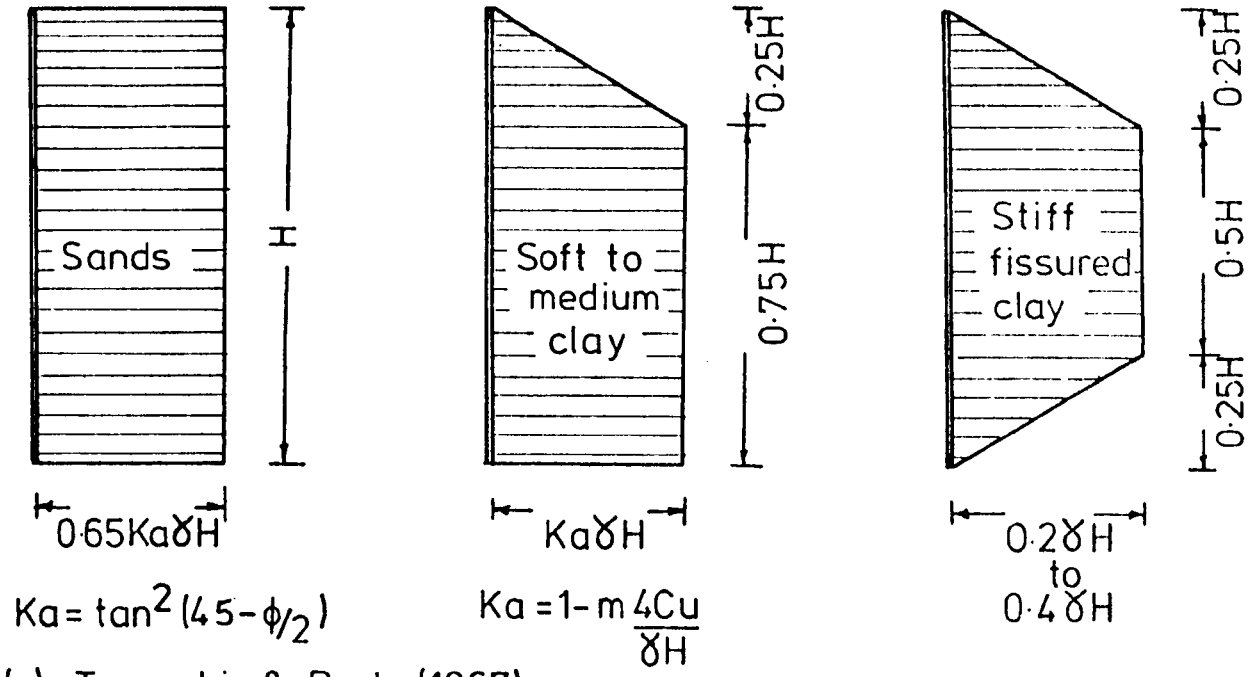

$Ka = \tan^2(45 - \phi/2)$ $\quad Ka = 1 - m\frac{4Cu}{\gamma H}$

(a) Terzaghi & Peck (1967)

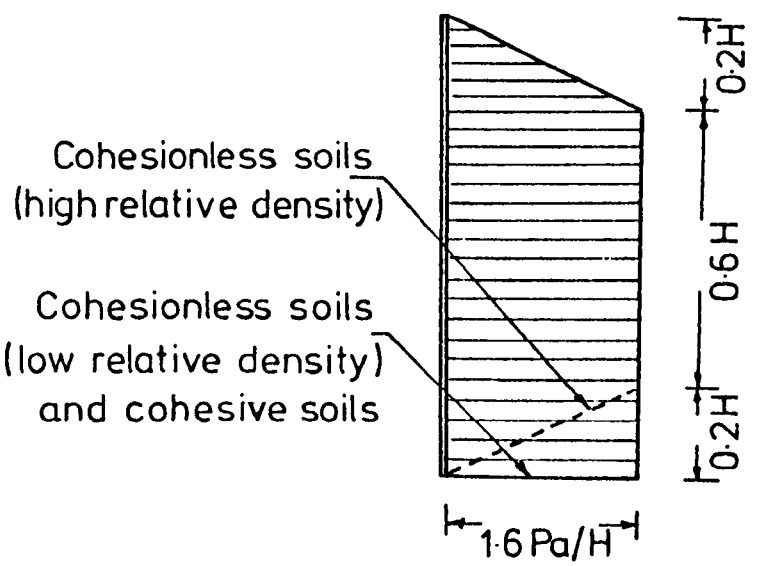

(b) C.P.2 (1951) & Broms (1968)

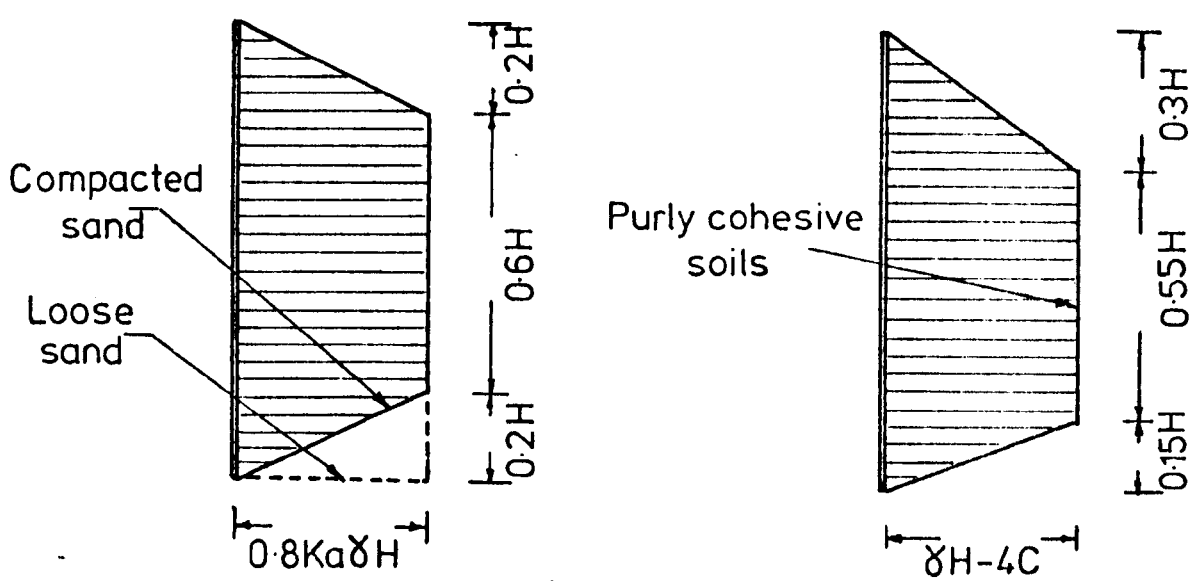

(c) French code of practice T.A (1972)

FIG. 2·55 CONVENTIONAL PRESSURE DISTRIBUTIONS

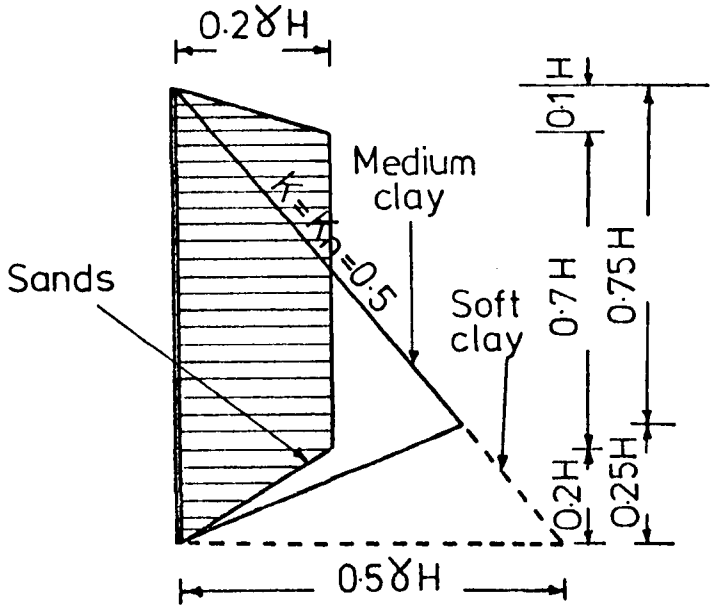

(d) Tschebotarioff (1951)

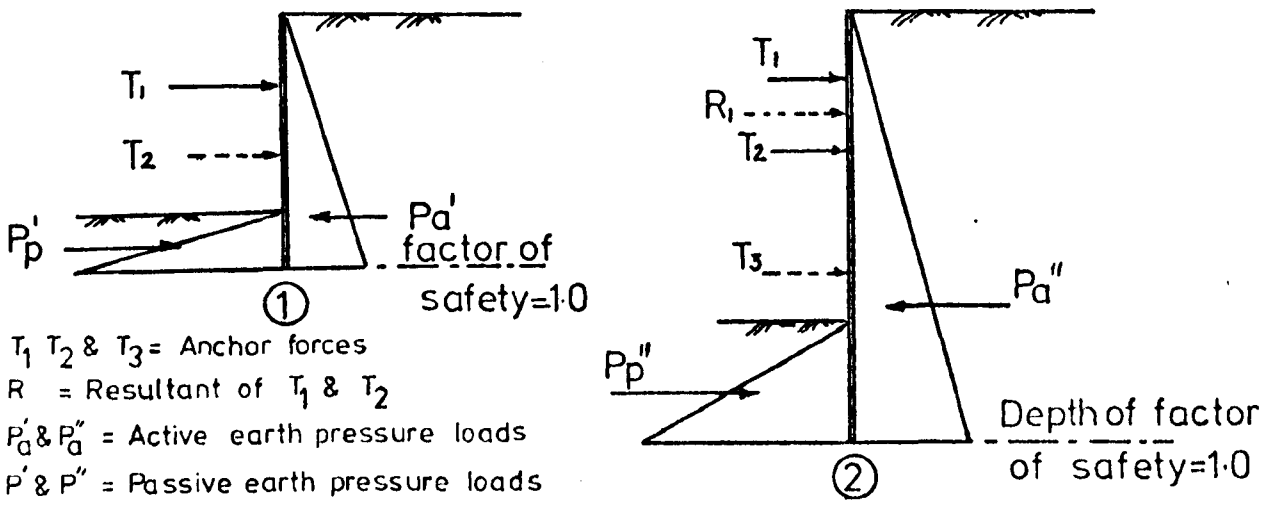

Equilibrium of ①

$\Sigma H=0$ when $T_1=Pa'-Pp'$

$\Sigma M=0$ when $Mp=Ma$

(about position of T_1)

Equilibrium of ②

$\Sigma H=0$ when $T_1+T_2=Pa''-Pp''$

$\Sigma M=0$ when $Mp''=Ma''$

(about the centroid of T_1 and T_2)

(e) James & Jack (1974)

Cont. FIG. 2·55 CONVENTIONAL PRESSURE DISTRIBUTIONS

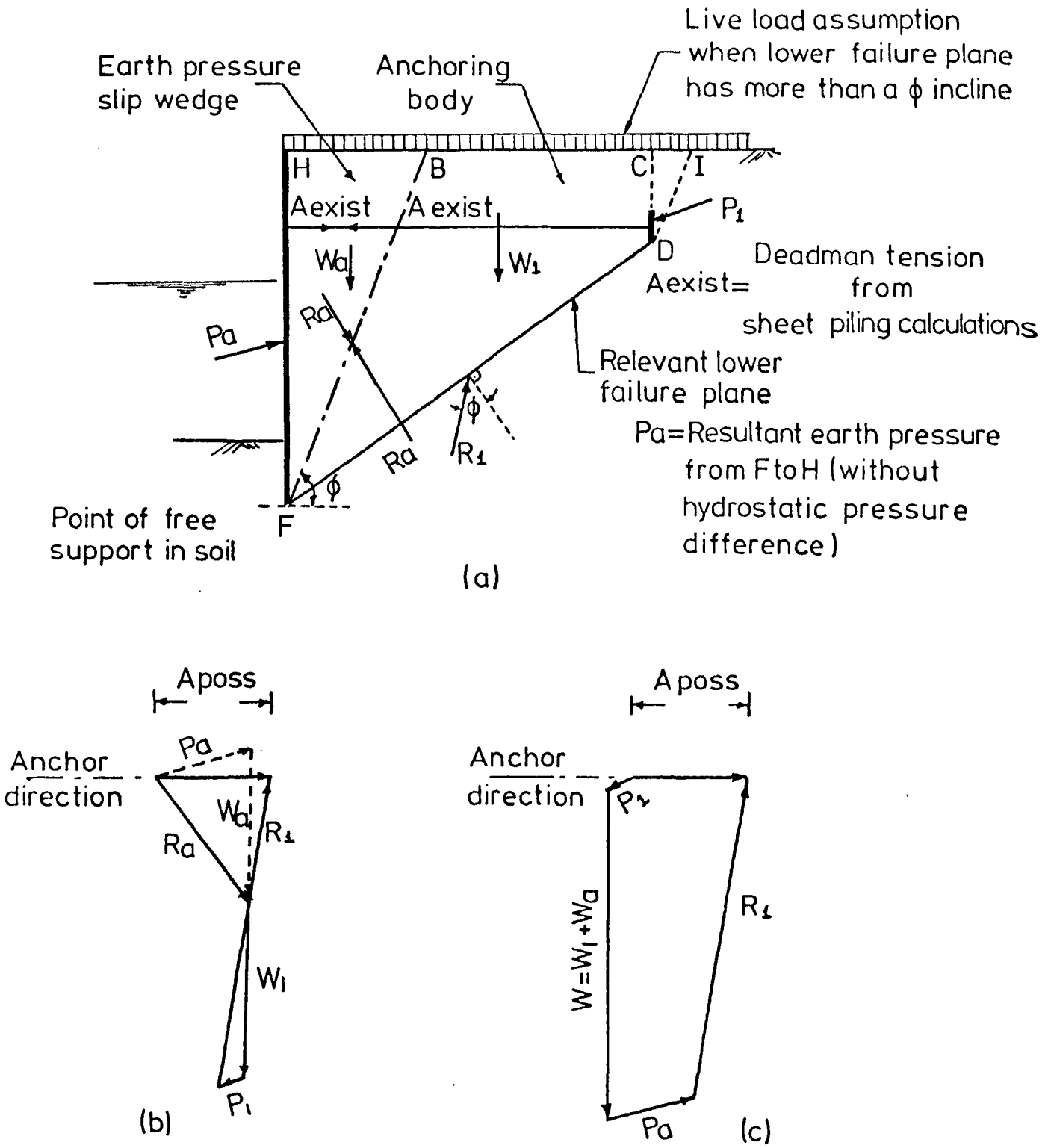

FIG 2·56 DETERMINATION OF DEADMAN STABILITY AT LOWER FAILURE PLANE (After The committee for water front structures)

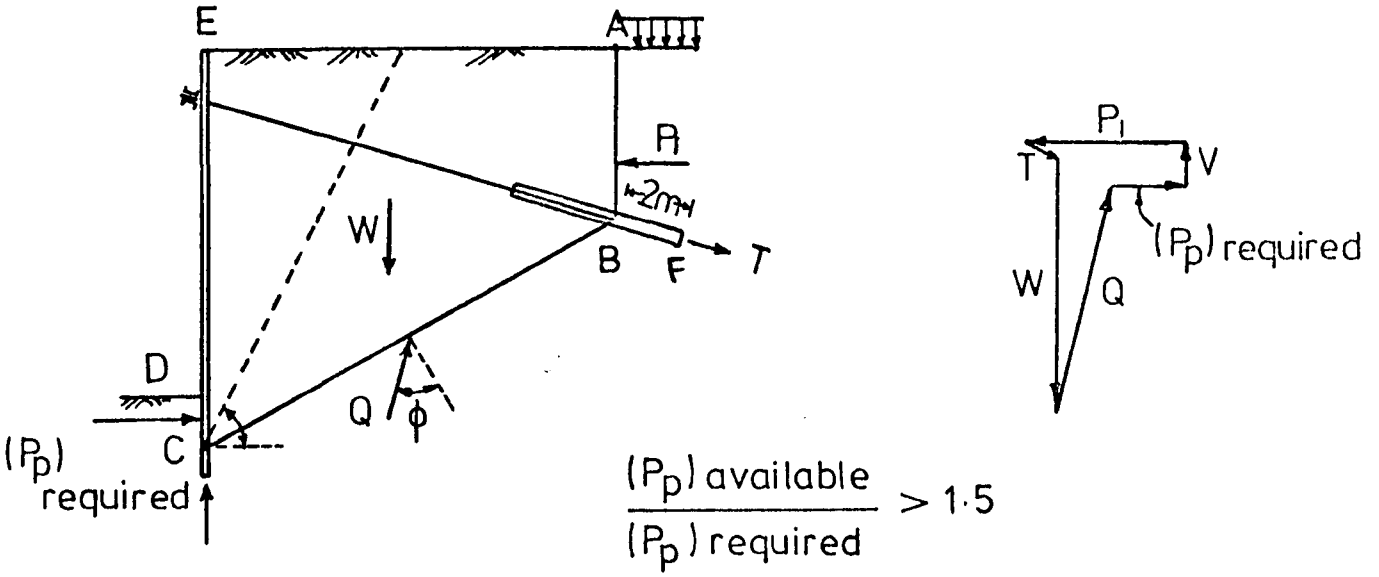

(a) Assumed failure surface (b) Force polygon

FIG. 2·57 FAILURE ALONG DEEP FAILURE PLANE

(After Broms (1968))

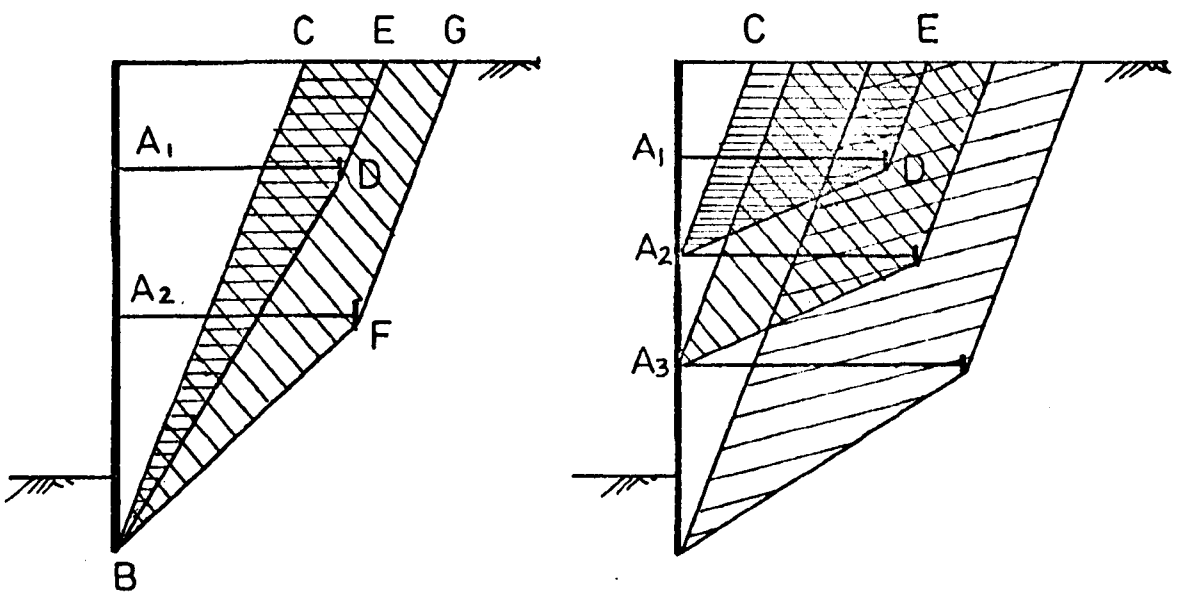

(a) Deep slip plane (b) Step system

FIG. 2·58 SLIP PLANES FOR MULTIPLE ANCHORED WALL

(After Krandtz 1953)

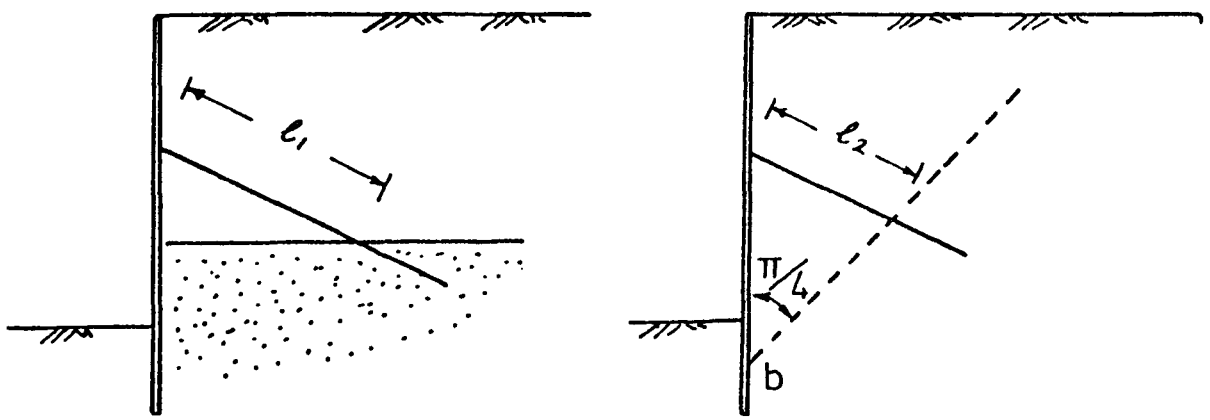

FIG. 2·59 FREE ANCHOR LENGTH

(After French code of practice)

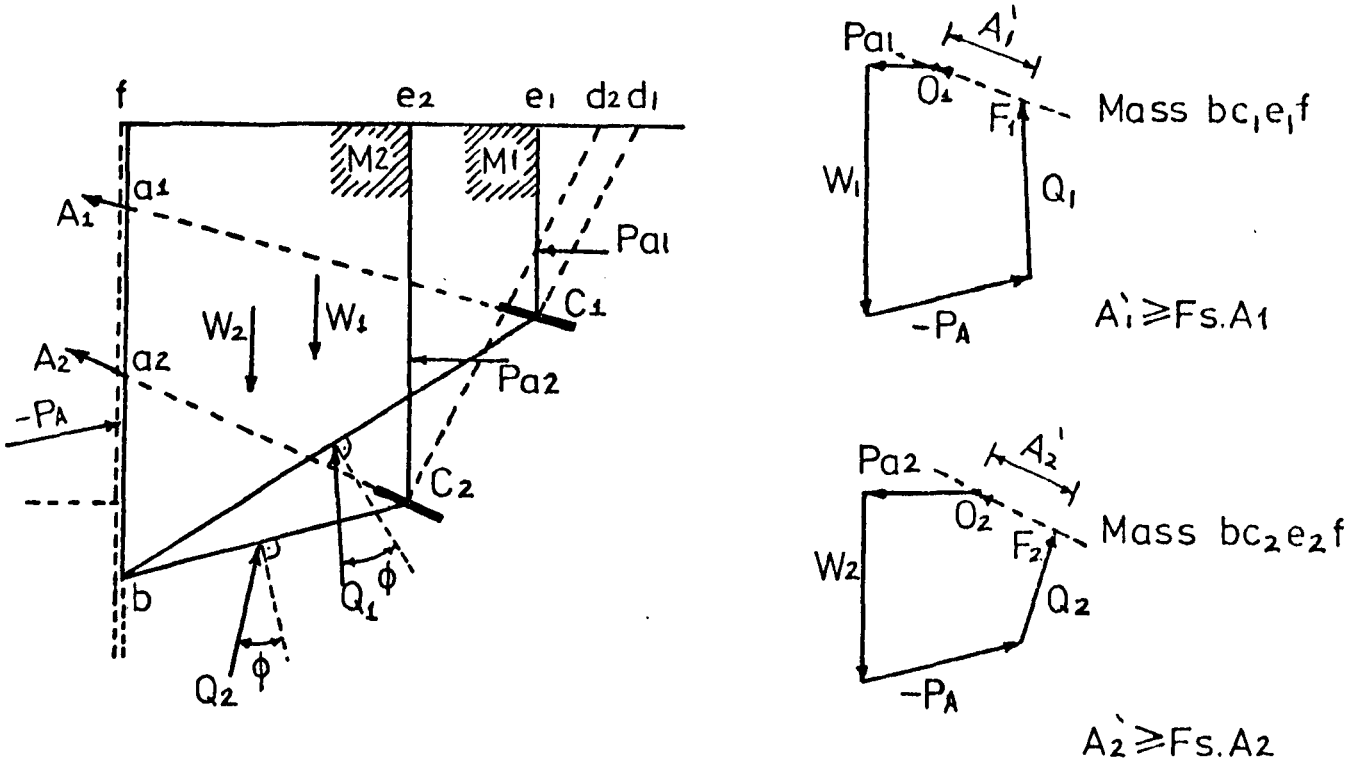

FIG. 2·60 TWO COMPLETE INDEPENDENT ANCHORS

(After French code of practice)

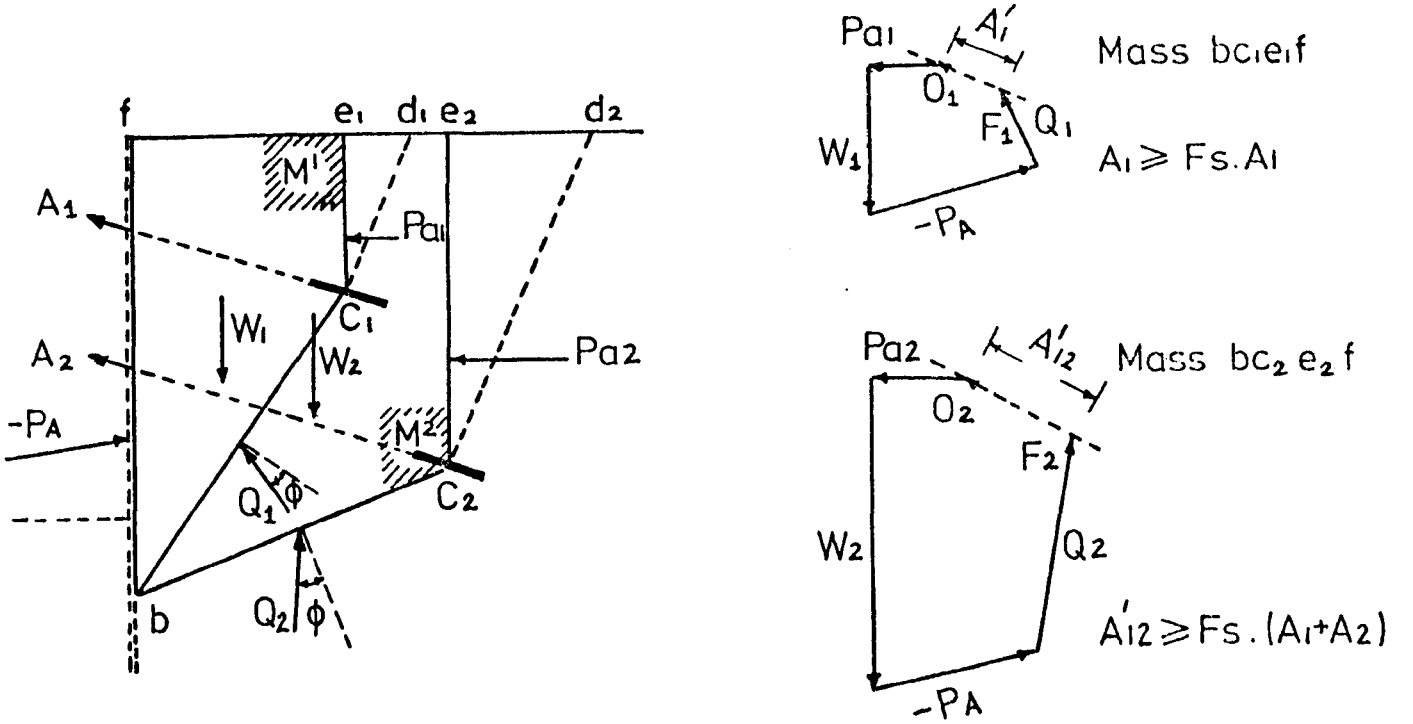

FIG. 2·61 (a) TWO ANCHORS, ONE INDEPENDENT
(After French code of practice)

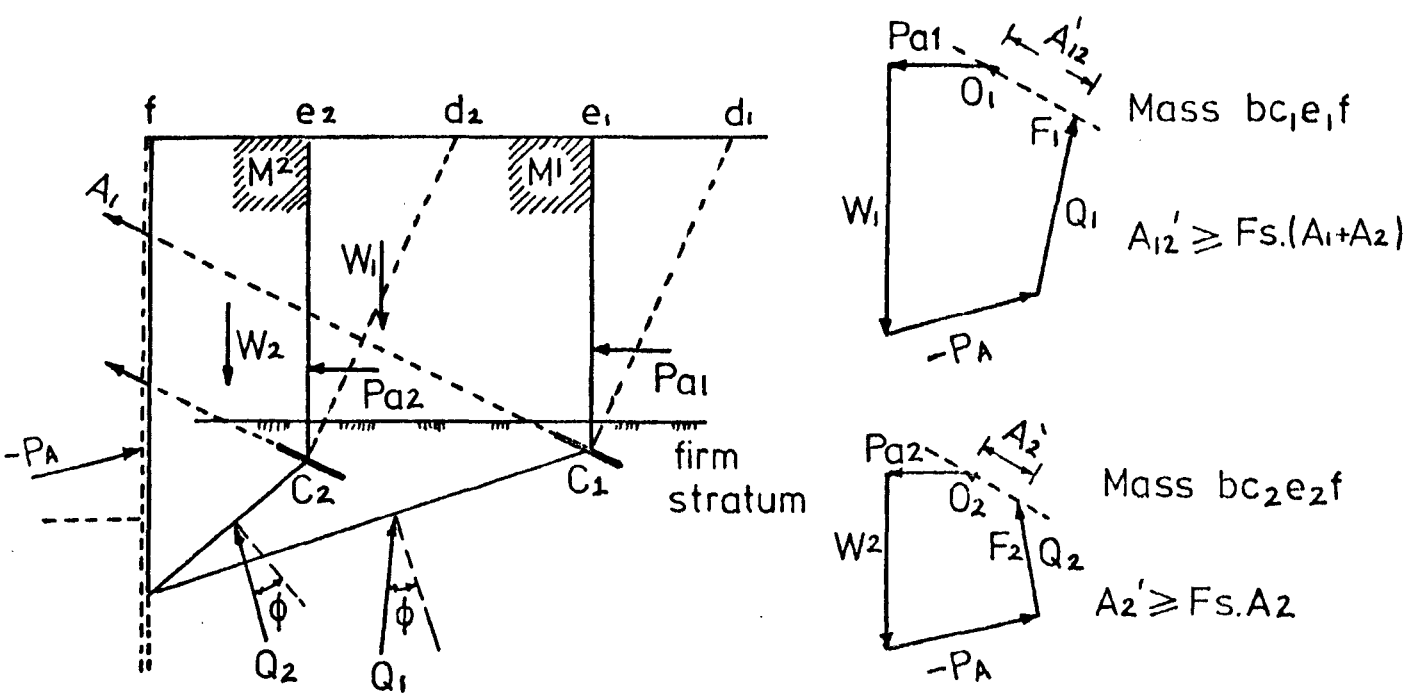

FIG. 2·61(b) TWO ANCHORS ONE INDEPENDENT
(After French code of practice)

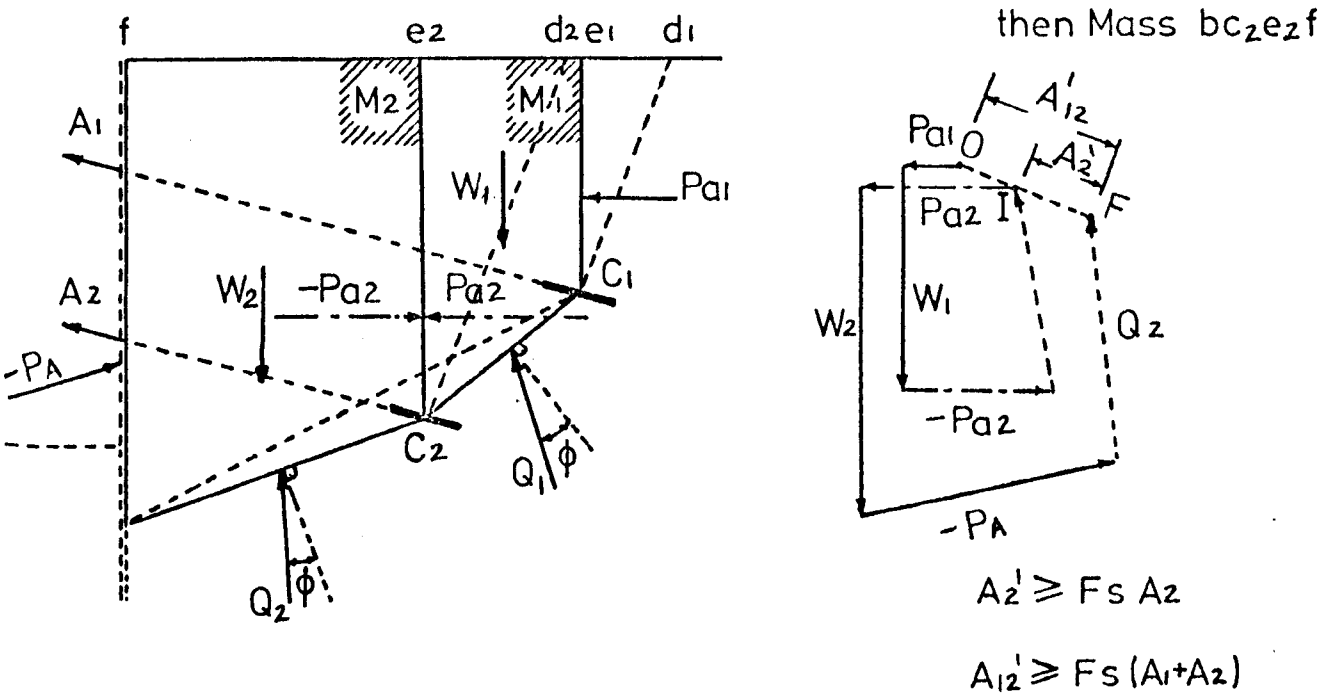

FIG. 2·62 COMPLEX FRACTURE SURFACE
(After French code of practice)

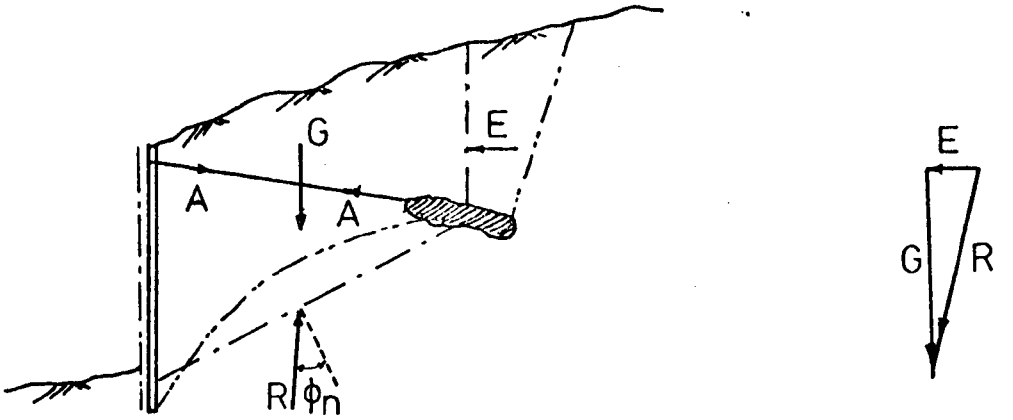

$$F = \frac{\tan \phi}{\tan \phi_n}$$

FIG. 2·63(a) STABILITY OF WALL WITH ONE ROW OF ANCHORS (After Locher 1969)

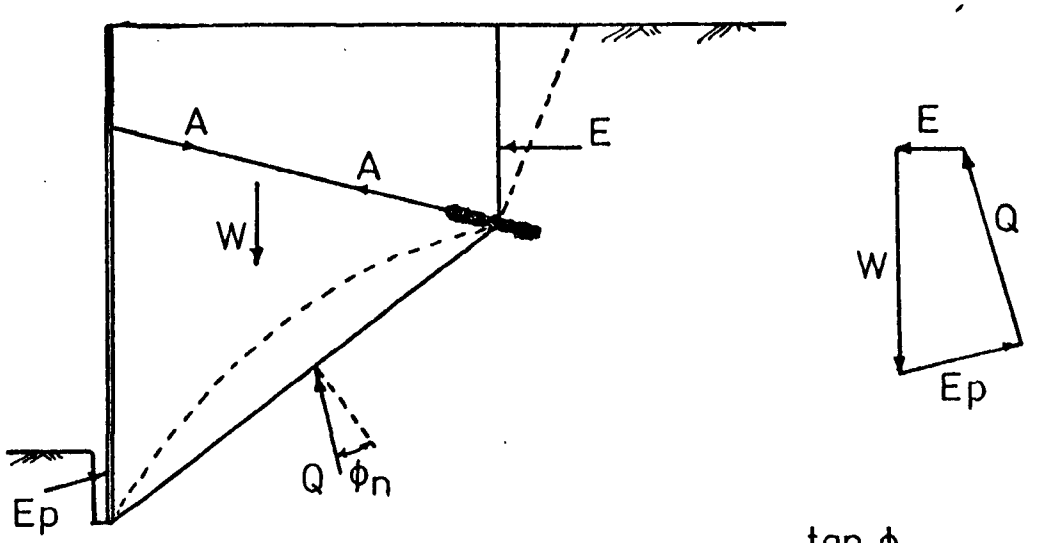

$$F = \frac{\tan \phi}{\tan \phi_n}$$

FIG. 2·63(b) STABILITY ANALYSIS FOR A SECTION OUTSIDE THE WALL (After Ostermayer 1976)

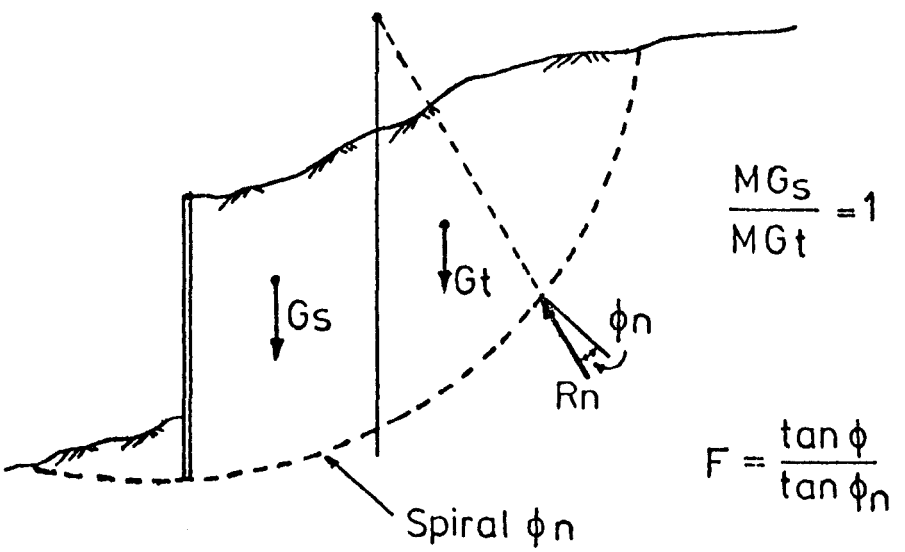

FIG. 2·64 STABILITY ANALYSIS – SPIRAL SHAPED SLIDING SURFACES (After Littlejohn 1972)

CHAPTER 3

SMALL SCALE STUDIES

CHAPTER 3

SMALL SCALE STUDIES

3.1 General

The purpose of carrying out these studies was to provide information on the behaviour and load carrying capacity of multi-bell horizontal anchors to be used as a supporting system in the retaining wall tests.

The study incorporates two main parts. In part ONE, a two-dimensional pin model analogy was used, in which steel pins were used to simulate the granular soil mass and multi-plate anchors to simulate multi-bells. The main aim of this analogy was to achieve a better understanding of the behaviour of horizontally loaded anchors by photographically studying the soil failure mechanism around the anchors.

In part TWO, tests were carried out in a small sand box using multi-plate strip anchors at different depths. Different arrangements of multi-plates were considered. The quantitative results of these tests are explained in the light of the quantitative results of the pin model analogy.

3.2 Pin Model Analogy

3.2.1 Introduction

Many different techniques have been used for the study of the shape of rupture surfaces in soils, among these:

i) Glass fronted boxes containing a model foundation embedded in soil were used by El-Rayes (1965), Carr (1970), Yilmaz (1971) and others. A camera in front of the glass side was used to photograph

the rupture zones at different times during testing.

ii) Coloured or smoked layers of soil around a foundation were used by Baker and Kondner (1966) and El-Rayes (1965). These techniques resulted in the formation of well defined rupture zones.

iii) Coloured layers of sand mixed with cement were used by De Beer and Ladanyi (1961). After the test, water was introduced into the cement-sand mix which was then allowed to set. It was then sawn in line along the axis of the model and the cross-section exposed for examination.

iv) A more sophisticated method was used by Roscoe et al. (1963) and James and Bransby (1971), in which lead shot was embedded in the soil and movements of the shot traced by X-ray photography.

These last two methods have the advantage that the movement of the soil is not restricted by artificial boundaries. The movement is, in fact, three-dimensional, whereas in the narrow glass-sided boxes the movement is restricted to two dimensions.

v) Schneebeli (1957) suggested an attractive method in which planar conditions in a frictional soil can be effectively simulated by using steel pins to represent the soil. This method has proved its reliability and capability of indicating trends that are similar in many aspects to those obtained with real granular soils (Boucraut, 1964; Mazurkiewicz, 1972).

It was decided to use the "Taylor-Schneebeli" pin model apparatus in this part of the study. This method of soil analogy, besides its reliability, has the following advantages (Abu-Taleb, 1974):

a) it is free from boundary effect,

b) it eliminates the intermediate principal stress,

c) the piles of rods have similar mechanical properties to those of a cohesionless medium,

d) the angle of internal friction seems to be chiefly dependent on the surface roughness of the rods, and

e) photographic recording is possible.

3.2.2 Apparatus and equipment

A rigid steel frame (Fig. 3.1) 0.8 m wide by 1.0 m high was used to accommodate the pins. A variable speed motor was attached to one side of the rigid frame, and was used to pull out the anchors. Duralumin rectangular anchor plates 8 mm thick by 75 mm wide and of two different heights (25 mm, 50 mm) were used. The anchor plates were pulled by two steel rods, 10 mm x 2.5 mm in cross-section. These were connected to the motor via a load transducer. Two sizes of steel load transducers were designed (see Appendix I) to suit the different load values in each series of tests.

The load transducers were instrumented with four strain gauges, type P S 5, which were connected to form a full bridge.
A constant voltage supply was used to feed the circuit, and the output wires were connected to a multi-point recorder (Honeywell chart recorder) via an apex unit. Fig. 3.2 illustrates details of the electric circuit.

A camera loaded with a micro-negative film was used for the photographic study. This was always fixed at a constant distance from the test frame.

Following the recommendations put forward by early researchers (Ovesen, 1962, 1964), the pin material used had to be a mixture of two different steel pins of diameters 5 mm and 3 mm and of length 75 mm and were intermixed in proportion of 2 to 1 by weight of large to small pins respectively.

The method of placement and compaction of the pins ensured repeatability of the tests and gave the following properties:

$$\text{Density} = 6.40\ \text{Mg/m}^3,$$
$$\phi' = 23.65^\circ, \quad \text{and}$$
$$c' = 0.$$

3.2.3 Test programme

Two preliminary series of tests, A and B, were carried out with a single anchor plate, 50 mm high. In series A, the relation between embedment depth D, pulling load Q and mode of failure was studied. In series B, the boundary effect on ultimate load was investigated, by varying the anchor length L and examining its effect on both the ultimate pulling load Q , and the failure mechanism.

Series C was devoted to multi-plate anchors. Different arrangements of anchor plates were experimented with, all plates being 50 mm high.

The extent to which the experiments of this series could be carried out was limited by the dimensions of the testing rig as well as the anticipated width of failure zone that would result if this was not to be affected by the boundaries of the test frame. Consequently it was decided to carry out a fourth group (series D) with smaller anchor plates.

In series D, anchor plates 25 mm high were used. The series was confined to the behaviour of double-plate anchors.

Tables 3.1, 3.2, 3.3 and 3.4 give details of all the tests in each series.

3.2.4 Test procedure

Before starting the tests, the load transducers were calibrated using dead weights. A straight line relationship was achieved, from which the load corresponding to each division on the chart of the Honeywell recorder was calculated (see Fig. 3.3). These load values calculated from the calibration chart were supposed to be constant for each transducer providing that the voltage input during the calibration and throughout the tests was constant. This was checked by a voltmeter before starting each experiment.

A perspex backboard marked with the position of the anchor plate or plates, centre line of the anchor rod and several depths of embedment, was clamped to the back of the steel frame.

The pins were packed against this backboard in equal layers, each 50 mm thick. The same technique of packing, which consisted of rolling and tapping the pins with a perspex block, was used through all the tests.

The anchor plate or plates were placed in position, and packing was then continued to the required depth. In some of the tests a spray paint was used to form a grid on the pins to help define the failure zone in photographs.

The perspex board was then removed; the anchor plate or plates

were connected to the anchor rods, and these in turn connected to the motor via the load transducer.

A 4.0 volt input was introduced to the electrical circuit and the zero reading on the chart recorder was adjusted using the apex unit. The anchor was then tested by pulling it with a constant strain rate of 2.8 mm/min, until the maximum load was reached. The motor speed was then changed to a higher one of 31.75 mm/min and the anchor was pulled while a time exposure photograph was taken. The camera shutter setting was at an aperture of f. 8, with an exposure time of one minute using normal room lighting.

3.2.5 Results and discussion

i) Series A

Table 3.1 summarises the results of the ten tests carried out in this series. The results are plotted in Fig. 3.4 as a relationship between the ultimate load Q and the dimensionless ratio D/B (embedment depth/anchor plate height). In Fig. 3.5 typical post-failure grain movements are shown for three tests in which the D/B value was 2, 6 and 12.

A correlation between the photographic study, Fig. 3.5, and the quantitative results, Fig. 3.4, shows that the failure mechanism changes for different values of D/B. The curve follows a certain trend up to a value of D/B about equal to 4, and then tends to be a straight line. In the photographs, up to D/B = 4, a general shear failure was observed with both the active and passive zones fully mobilized and with the top surface of the pins greatly disturbed. Beyond D/B = 4,

the failure tended to be a local shear failure, but there was still a little surface disturbance above the passive side which vanished at D/B = 10. It should be noted that the critical ratio D/B = 4 is not a general criterion, as it is dependent on many factors such as the anchor geometry (anchor plate shape), kind of soil and its relative density.

ii) Series B

In all tests carried out in this series the ratio D/B was kept constant and equal to 6. Eight tests were carried out, the anchor length being different in each test, the results of which are given in Table 3.2.

Fig. 3.6 shows photographs of the failure zones for two tests where the L/B values were 4 and 10, while Fig. 3.7 shows the relationship between the ultimate load Q and the ratio L/B, anchor length/anchor plate height. It is evident from both figures that the ultimate load is higher for smaller values of L/B up to an L/B value about equal to 5, where the passive mobilized zone was confined between the rigid frame boundary and the anchor plate. This gave more resistance to the pulling force. It was also noticed when L/B was less than 5, that due to the confinement of the pins, the top surface above the passive zone is more affected than in the tests with L/B greater than 5.

For L/B values greater than 5, the ultimate load was almost constant, and it could be concluded that beyond the limit L/B = 5, the anchor length has no effect on the ultimate pulling load.

It could also be concluded that the use of very short anchors in

supporting a retaining structure could result in "short-circuiting" the prestress force from the anchor block back to the retaining wall.

It is worth mentioning that this value of L/B = 5 could also be affected by parameters such as embedment depth, the kind of soil and its relative density, and the anchor geometry.

iii) Series C

In this series the behaviour of multi-plate anchors was examined. As mentioned before, the size of the apparatus and the relatively large dimensions of the anchor plates limited the number of tests carried out in this group. Table 3.3 summarises the results of the thirteen tests carried out in this series.

Seven tests were carried out with two anchor plates. The distance between the two plates, ℓ, varied from a minimum of $\frac{1}{2}$B to a maximum of 5B. The results indicated an increase in the ultimate loads with increasing distance between the two plates. For values of ℓ equal to or greater than 3B a complete shear failure was observed (Fig. 3.8(a)). This extended to reach both sides of the frame when ℓ was equal to 5B (see Fig. 3.8(b)). Whereas, for values of ℓ less than 3B, only the passive zone was fully mobilized and the failure was likely to be a local shear failure (Fig. 3.8(c)).

Three tests were carried out with three anchor plates and three with four plates, with a minimum anchorage length of ℓ = B = 50 mm and a maximum of ℓ = $4\frac{1}{2}$B = 225 mm. The introduction of the third or fourth plate within this limited anchorage length did not affect the failure shape. Fig. 3.9 indicates that, similar to tests with two

plates, for ℓ equal to or greater than 3B, a complete shear failure occurs, while for ℓ less than 3B only the passive zone was mobilized and a local shear failure was observed.

The ultimate pulling capacity was increased slightly by introducing the third or the fourth plate, the increase being dependent on the value of the total anchorage length. When the anchorage length ℓ was equal to B (tests C_2, C_8), introducing the third plate increased the ultimate load by 1.9%. When ℓ was $1\frac{1}{2}$B (tests C_3, C_{11}), introducing an extra two plates increased the ultimate load by 4.2%. In tests C_5, C_{10} and C_{12}, where the anchorage length ℓ was 3B, the third plate in C_{10} increased the ultimate load by 3.4% and the fourth in C_{12} increased it by 6.8%.

These slight increases are mainly attributed to more confinement of the pins between the plates leading to an increase in the frictional resistance between the moving block of pins and the neighbouring stationary ones, and that is why for small values of ℓ, where the pins were initially confined, the increase is less significant.

It is worth mentioning also that with multi-plates the position defining deep and shallow anchors is not unique, but is dependent on the anchorage length, ℓ.

iv) Series D

Anchor plates 25 mm high were used in this series. Twenty tests were carried out at two different depths, 250 mm and 500 mm, i.e. at D/B ratios of 10 and 20. Test results are given in Table 3.4 and Fig. 3.10.

A correlation between the photographic study (see Fig. 3.11(a))

and the quantitative results (curve 1, Fig. 3.10) shows that for a depth D = 10B, the ultimate load increased by increasing the length ℓ. However, in considering the rate with which the ultimate load increased, the curve could be divided into three regions. The first region extends up to an anchorage length ℓ = 3B, during which the rate of ultimate load increase is increasing. The second region lies between ℓ = 3B and ℓ = 6B, where the rate of ultimate load increase is decreasing and the third region is for anchorage lengths greater than ℓ = 6B where the rate is increasing again. Examining the photographs (Fig. 3.11(a)), the behaviour can be explained as follows. With a single plate anchor a local shear failure was observed while with double plate anchors, having anchorage lengths $\ell \succ$ 3B, a complete shear failure was observed. In changing from a local shear failure to a complete shear failure, the passive zone was immediately mobilized after adding the second plate at ℓ = B. This provided more resistance to pull-out, causing an increase in the rate of ultimate load increase. For anchorage lengths $\ell \succ$ 3B, both the active and passive zones were fully mobilized. The mobilization of the active zone tended to decrease the pull-out resistance and consequently decrease the rate of the ultimate load increase. During this stage the anchor developed its resistance to pull-out through shearing resistance along the failure surfaces and frictional forces along the anchorage length, the latter being less pronounced at anchorage lengths less than 6B. When ℓ reached 6B more frictional forces developed along the anchorage length between moving particles and adjacent stationary ones. The development of these frictional forces, in addition to the shearing resistance along the failure surfaces,

added more resistance to pull-out, causing the rate of ultimate load increase to increase again. At this depth, D = 10B, and up to an anchorage length = 9B, the two plates were still working together and forming one failure zone.

Considering curve 2 (Fig. 3.10), which represents the second set of tests at a depth D equal to 20B, the behaviour is different but with the same three regions existing as in curve 1.

The first region includes single plate anchor and double-plate anchors with anchorage lengths ℓ up to ℓ = 3B. In this region a local shear failure encompassing the two plates was observed (see Fig. 3.11 (b)). This was identical in shape in each test. An increase in the failed area was observed with increasing the spacing. This was accompanied by an increase in the ultimate load. The second region lies between ℓ = 3B and 6B. With increasing the anchorage length, ℓ, the pins confined between the two plates develop some frictional forces with the adjacent ones, whereas the common failure zone encompassing the two plates no longer exists. As a result the anchor will develop its resistance to pull-out through frictional forces along the anchorage length which compensates for the loss of resistance along the failure surfaces. A very slight increase in the ultimate load accompanies this stage. The third region includes double-plate anchors with anchorage lengths $\ell > 6B$. At this stage each of the two plates starts to behave separately, and the rear plate develops its own passive zone. Also, there is still some frictional resistance between moving and stationary pins. A notable increase in the ultimate load accompanies this stage, and this ultimate load reaches its maximum value at ℓ = 9B where a

complete separation occurs with isolated local shear failure zones around each plate and no frictional forces (see Fig. 3.11(b)). Beyond this limit the ultimate load tends to remain constant whatever the increase in the anchorage length, .

3.2.6 Concluding comments

While the failure mechanism in the case of single plate anchors is unique and characterised by the ratio D/B, the case of multi-plates is different where a new parameter is introduced which is the anchorage length, ℓ.

As with single plate anchors, the failure mechanism of shallow multi-plate anchors was different from that of deep multi-plate anchors. However, with the limited number of tests carried out, the limitations between shallow and deep were not defined.

In tests using single plate anchors and in multi-plate anchor tests in which each single plate behaved separately, no portion of the failure zone extended below the base of the anchor plate. However, in all other multi-plate anchors, with frictional forces developing along the anchorage length, slight movements of the particles just below the anchor plates were observed.

For multi-plate anchors with anchorage length greater than ℓ = 3B, frictional forces develop above and below the anchor block. While those developing below the anchor block are solely dependent on the confinement of the pins and the anchorage length, the frictional forces above the anchor block depend on the state of neighbouring pins. If these are in a state of plastic flow (see Fig. 3.11(a), test No. 5),

there will be less opportunity for frictional forces to develop, whereas if they are in a stationary condition (see Fig. 3.11(a), test No. 10) more frictional forces are likely to develop.

Multi-plate anchors carried more load than single plate anchors at the same depth and with the same anchor plate height. The difference is mainly attributed to both the increase in the failed surfaces and the frictional forces developing along the anchorage length.

The assumption of L (the anchor free length) = 5B as a minimum safe distance between the face of the anchor block and the retaining wall seems to be reasonable and applicable for deep multi-plate anchors. However, for shallow multi-plate anchors a higher conservative value must be adopted.

Although a well detailed study of the behaviour of multi-bells is needed, the present investigation highlighted their general behaviour at different depths, and this helped in assessing and explaining some other results throughout the research programme.

3.3 Small Sand Box Tests

3.3.1 Introduction

Most publications describing model studies using anchors have been devoted to the behaviour of uplift anchors (for example, Balla, 1961; Baker and Kondner, 1966; Meyerhof and Adams, 1968; Vesic, 1971; Yilmaz and Hanna, 1971; Hanna et al., 1972; Hanna and Spark, 1973).

Comparatively few studies on horizontal and inclined anchors have been reported. Most of the work on horizontal anchors has been concerned mainly with shallow anchors (e.g. Hueckel, 1957; Ovesen, 1972). Studies

on deep horizontal anchors were reported by Boucraut (1964) and Biarez et al. (1965). The effect of anchor inclination on its ultimate pull-out capacity was studied in laboratory model tests and reported by Larnach (1972, 1973) and Das and Seely (1975). Meyerhof (1973) extended his earlier work on vertical anchors (1968) to examine the load carrying capacity of inclined piles and anchors.

In the above mentioned studies, the anchors were simply represented by plates (horizontal, vertical or inclined) of different shapes that were pulled vertically, laterally or at an angle.

A survey of all these studies and others failed to reveal knowledge of the behaviour of multi-plate strip anchors, or to provide satisfactory formulae to be applied to it. However, it was essential that a logical approach be adopted in seeking a practical solution to their design for the retaining wall tests.

Sixty tests on individual multi-plate strip anchors were carried out in a small testing box. Details of these tests are given in Tables 3.5, 3.6 and 3.7.

3.3.2 Test materials

Air dried sand passing through sieve No. 72 and retained on sieve No. 14 was used throughout the test programme. The average density of $1.52\,Mg/m^3 \pm 0.005\,Mg/m^3$ was obtained by slight stirring of the sand (see section 4.4 for full details of physical and mechanical properties of the sand material).

3.3.3 Test equipment

(i) Small testing box

The box consisted of a steel frame with a timber lining. It was 600 mm deep and 605 mm square. Three holes were drilled through the front face of the box to guide the anchor rods. Another hole was drilled in the back face to accommodate a brass conducting tube through which a rod for measuring the anchor plate displacement passed. Fig. 3.12 shows the general arrangement of the box partially filled with sand and with the anchors set in position. The anchor rods were connected to proving rings at the front face of the box and a mechanical dial gauge was fixed to the displacement rod which was attached to the back of the anchor plate.

(ii) Anchors

a. Anchor plates: Duralumin strip plates 388 mm long, 25 mm high and 3 mm thick were used. Different numbers of plates were used in each test giving different total anchorage lengths, ℓ (see Tables 3.5, 3.6 and 3.7 for details of the different arrangements).

b. Anchor rods: The system was pulled by three brass rods 2.4 mm in diameter. These had a total length of 500 mm, the end 30 mm having a screw thread to attach the proving rings. A length of 225 mm at the other end also had a screw thread to facilitate fixing the anchor plates at different spacings according to the individual test requirements. The plates were fixed in position using a washer and a nut on each side of the plate.

(iii) Loading system

Duralumin proving rings were used having the dimensions shown in Fig. 3.13 (see Appendix II for the design of the rings). These were instrumented with four strain gauges, type PL 2, which were connected to form a full bridge. The proving rings were calibrated - using a "Peekel" strain indicator - by dead weights, and a calibration curve was obtained for each one (see Fig. 3.14 for a typical calibration curve).

A duralumin cylindrical tube 40 mm long and 25 mm external diameter slotted from one end was used to accommodate the proving ring. This had a circular duralumin end plate with a central hole and slotted at the perimeter to allow the strain gauge wires to pass through. A brass screwed rod was fixed to the proving ring and passed through the hole in the end plate. A nut on this rod was used to apply load to the anchors (see Fig. 3.13).

3.3.4 Test programme

A total of sixty tests was carried out in which the total anchorage length varied from 25 mm to 200 mm, and the number of plates fixed along this anchorage length varied from a single plate up to nine plates.

The programme was divided into six groups (see Tables 3.5, 3.6 and 3.7). Groups A, B, C and D were devoted to anchors with single and double plates and were carried out at depths of 100, 200, 300 and 400 mm respectively. Groups E and F were carried out at depths of 100 and 300 mm respectively, using anchors with the number of plates ranging

from two up to nine.

3.3.5 Sand placement and test preparation

Sand was weighed and placed manually in 50 mm layers. Each layer was carefully stirred in parallel lines at approximately 20 mm spacing with a 3 mm diameter steel rod which just penetrated the immediately previous layer to reduce stratification. When the sand surface reached the anchor level, the anchor plates and three anchor rods were placed carefully in position and the rods inserted through their guide holes in the front face of the box. The small proving rings were attached at this stage, together with the movement rod which was attached to the centre of the back anchor plate. Both the brass rod and its conductor tube were put through the hole in the back face of the box (Fig. 3.12 shows a typical test at this stage of preparation).

Sand filling was continued with careful stirring around the anchor plates, until the required depth was reached and the sand surface was then carefully levelled.

A mechanical dial gauge was attached outside the back side of the box, positioned on the brass movement rod and zeroed. Zero readings of the three proving rings were recorded and then the remaining components of the loading system were carefully attached.

3.3.6 Anchor stressing

Each anchor rod was stressed in increments of 5 Newtons, a "Peekel" strain indicator being used to monitor the load, i.e. a total load of 15 N was applied to the anchor plates at each stage. After

each load increment, the movement of the anchor plates was obtained from the dial gauge reading. The incremental loading continued until a total load of 600 N was reached. This corresponds to the maximum capacity of the proving rings.

3.3.7 Test results

i) General

It was realised that a complete study and investigation of laterally loaded multi-bell anchors would be a major task and would form a major branch of a research programme. However, with the limited number of tests carried out, a practical and logical solution was established.

In analysing the results, it was considered more appropriate to have similarity in anchor plate deformation rather than a constant factor of safety with respect to the ultimate load carrying capacity. An anchor plate deformation of 1.0 mm was adopted and the corresponding value of the pull-out load was worked out from the load-deformation curve obtained from each test. These pull-out load values are plotted against the anchorage length in Fig. 3.15 (for groups A, B, C and D) and in Fig. 3.16 (for groups E and F).

ii) Groups A, B, C and D

It can be deduced from curves 1, 2 (Fig. 3.15) that for shallow embedment depths (D/B = 4, 8) the pull-out load is increasing with increasing the anchorage length. In considering the rate of this increase it will be noticed that up to ℓ = 3B, this rate is increasing,

while beyond this limit the rate of increase is decreasing. When ℓ reached 7 to 8B, a very slight increase was monitored. The behaviour is more or less identical with the group of shallow anchors in the pin model tests (a more complete explanation is given in section 3.2.5(iv)), with the exception that the third region of the curve showing an increase in the rate of anchor load increasing - due to the development of frictional forces - does not exist in the sand box tests. This could be explained as follows: in the pin model tests with the size of the pins being relatively large compared to the sand particles, and also with a comparatively higher unit weight and more compaction of the pins between the plates, the possibility of frictional forces developing along the anchorage length was more likely in the pin model tests than in the small sand box tests.

The pull-out loads in tests A_8 and A_9 - (small sand box, series A, with ℓ = 8B and ℓ = 9B) - were less than those in test A_7 (ℓ = 7B). This trend is contrary to that found for group B tests and also with the pin model results. This might be attributed to the fact that at this very shallow depth (D = 4B) with ℓ increased to 8B-9B, the failure planes interfered with the back wall of the sand box. This may have reduced the area developing shearing resistance and consequently reduced the pull-out load.

Considering curves 3 and 4 in Fig. 3.15, where the embedment depths were 300 and 400 mm respectively, the trend is the same as in series A and B with the pull-out load increasing with increasing the anchorage length, ℓ, up to ℓ = 3B. The rate of increase started to decrease beyond this ℓ/B value and it seems that for a value of ℓ greater than 3B

and less than 6B the pull-out load is only slightly affected by increasing the anchorage length. This could be due to the effect of frictional forces developing along the anchorage length and the dependence of these forces on the unit weight, the size and the confinement of the material between the two plates. In the pin model tests, confinement of the pins between the plates was possible due to the way they were placed. Also, the density was higher and the size of the pins was relatively large. In the sand box tests stirring of the sand between the plates was impossible resulting in less confinement. Also the unit weight and the size of the particles were both small compared to those of the pins. As a result greater forces developed in the pin model resulting in a slightly higher increase in the pull-out load.

As ℓ continued to increase to values greater than ℓ = 6B, each plate tried to behave separately and develop its own failure zone. Meanwhile there will be still some movements of the soil confined between the two plates. With increasing ℓ, complete separation occurs and each plate will develop its own local failure zone, frictional forces will disappear and the pull-out capacity of the anchor will reach a constant value.

iii) Groups E and F

Fig. 3.16(a) shows the results of groups A and E and Fig. 3.16(b) shows the results of groups C and F. These show results for different arrangements for anchor plates at two depths, 100 and 300 mm respectively.

From both families of curves it can be concluded that introducing more plates will affect the confinement of the soil along the anchorage length and this in turn will tend to increase the frictional forces and consequently the pull-out forces.

3.3.8 Dimensional analysis

In Fig. 3.16(a,b), points of equal number of anchor plates were connected and values of pull-out forces corresponding to different anchorage lengths were interpolated. Using these values, together with the results in Fig. 3.15, the group of curves shown in Fig. 3.17 was constructed giving a relation between the pull-out load and the depth for different arrangements.

From these curves values for the pull-out loads corresponding to different arrangements at depths varying from 100 mm up to 500 mm (expected depth limits of anchor rows during retaining wall tests) could be worked out.

Different parameters were introduced to express the relation between the pull-out load and anchor arrangement in a dimensionless form. The pull-out load was expressed as "(pull-out stress)/(soil unit weight x anchor plate height)", i.e. $(Q/bB^2\gamma)$, and related to the anchor geometry "(anchorage length)/(anchor plate height)", i.e. (ℓ/B), where

- Q is the ultimate load,
- B is the anchor plate height,
- b is the anchor plate length,
- ℓ is the anchorage length, and
- γ is the soil unit weight.

A chart representing this relationship is presented for each depth for values of D = 100, 200, 300, 400 and 500 mm in Fig. 3.18.

With the aid of this last group of dimensionless curves and for a particular value of a pull-out load at a certain depth, the suitable arrangement that could sustain the load could be established.

3.3.9 Contribution for inclined anchors

Because the retaining wall tests were to include some tests with 30^{o} inclined anchors as a supporting system, it was necessary to modify the results of the tests carried out on horizontal anchors to be applied to inclined systems.

Meyerhof (1973) found that the uplift resistance of inclined anchors and piles under axial load can be expressed in terms of uplift coefficients, which he evaluated by extending his previous work for vertical uplift of foundation (Meyerhof, 1968). His theory and test results indicated that the uplift coefficients of anchors in sand and clay generally increase with inclination, from a minimum for vertical uplift to a maximum for horizontal pull.

A chart representing the relationship between the values of the uplift coefficients and angles of shearing resistance for different angles of load inclinations was presented by Meyerhof (see Fig. 3.19(a)).

Values of the uplift coefficient N_{qu} (for deep anchors) corresponding to an angle of internal friction $\phi' = 37^{o}$ (see section 4.4.2 for sand properties), and for different anchor inclinations were found from the chart and plotted (see Fig. 3.19(b)). From the plotted relationship a

drop in the value of N_{qu} of 21% was observed between horizontal anchors and 30° inclined anchors, which would indicate a drop of 21% in pull-out load.

On the assumption that multi-bell strip anchors will behave in the same manner as strip anchors, a reduction factor of 21% was applied to values of pull-out loads obtained from the horizontal anchor tests. The same dimensional analysis described before was adopted and a family of curves for different depths was obtained for use in designing inclined anchors for the retaining wall tests.

Test Number	Anchor Plate Height B (mm)	Embedment Depth D (mm)	Anchor Length L (mm)	Ratio D/B	Ultimate Load Q (N)
1	50	25	400	1/2	59
2	50	100	400	2	103
3	50	200	400	4	275
4	50	250	400	5	363
5	50	300	400	6	455
6	50	350	400	7	544
7	50	400	400	8	627.8
8	50	450	400	9	741
9	50	500	400	10	839
10	50	600	400	12	1030

Table 3.1. Pin Model Tests Series A.

Test Number	Anchor Plate Height B (mm)	Embedment Depth D (mm)	Anchor Length L (mm)	Ratio L/B	Ultimate Load Q (N)
1	50	300	100	2	520
2	50	300	150	3	520
3	50	300	200	4	490.5
4	50	300	250	5	458
5	50	300	300	6	437
6	50	300	400	8	456
7	50	300	500	10	448
8	50	300	600	12	431

Table 3.2. Pin Model Tests Series B.

Test Number	Number of Plates	Anchor Plate Height B (mm)	Distance Between Successive Plates λ (mm)	Total Anchorage Length ℓ (mm)	Ultimate Load Q (N)	Remarks
1	2	50	$\frac{1}{2}$ B = 25	25	687	In all tests D was 400 mm and L was 350 mm
2	2	50	1 B = 50	50	741	
3	2	50	$1\frac{1}{2}$ B = 75	75	785	
4	2	50	2 B = 100	100	819	
5	2	50	3 B = 150	150	873	
6	2	50	4 B = 200	200	1069	
7	2	50	5 B = 250	250	1020	
8	3	50	$\frac{1}{2}$ B = 25	50	755	
9	3	50	1 B = 50	100	834	
10	3	50	$1\frac{1}{2}$ B = 75	150	903	
11	4	50	$\frac{1}{2}$ B = 25	75	824	
12	4	50	1 B = 50	150	932	
13	4	50	$1\frac{1}{2}$ B = 75	225	1030	

Table 3.3. Pin Model Tests Series C.

Test Number	Depth D (mm)	Anchor Plate Height B (mm)	Anchorage Length ℓ (mm)	Ultimate Load Q (N)	Test Number	Depth D (mm)	Anchor Plate Height B (mm)	Anchorage Length ℓ (mm)	Ultimate Load Q (N)
1	250	25	Single	264.9	11	500	25	Single	606.3
2	250	25	25	270.0	12	500	25	25	613.0
3	250	25	50	319.0	13	500	25	50	723.0
4	250	25	75	343.4	14	500	25	75	814.2
5	250	25	100	353.0	15	500	25	100	864.6
6	250	25	125	374.0	16	500	25	125	884.0
7	250	25	150	392.4	17	500	25	150	884.4
8	250	25	175	441.5	18	500	25	175	1018.0
9	250	25	200	433.0	19	500	25	200	1118.3
10	250	25	225	431.6	20	500	25	225	1105.0

Table 3.4. Pin Model Tests Series D.

Group	Test Number	Depth D (mm)	Number of Plates	Distance Between Plates λ (mm)	Total Anchorage Length e (mm)	Load Corresponding to 1 mm Deformation (N)	Remarks
A	A-1	100	1	-	-	143.2	
	A-2	100	2	25	25	150.0	
	A-3	100	2	50	50	160.0	
	A-4	100	2	75	75	169.7	
	A-5	100	2	100	100	180.5	
	A-6	100	2	125	125	190.3	
	A-7	100	2	150	150	202.1	
	A-8	100	2	175	175	191.3	
	A-9	100	2	200	200	191.0	
B	B-1	200	1	-	-	240.4	
	B-2	200	2	25	25	258.0	
	B-3	200	2	50	50	276.6	
	B-4	200	2	75	75	302.0	
	B-5	200	2	100	100	315.9	
	B-6	200	2	125	125	335.5	
	B-7	200	2	150	150	350.2	
	B-8	200	2	175	175	353.0	
	B-9	200	2	200	200	360.0	
C	C-1	300	1	-	-	323.7	
	C-2	300	2	25	25	369.8	
	C-3	300	2	50	50	432.6	
	C-4	300	2	75	75	450.3	
	C-5	300	2	100	100	451.3	
	C-6	300	2	125	125	446.4	
	C-7	300	2	150	150	456.2	
	C-8	300	2	175	175	500.0	
	C-9	300	2	200	200	508.2	
D	D-1	400	1	-	-	370.8	
	D-2	400	2	25	25	428.7	
	D-3	400	2	50	50	523.9	
	D-4	400	2	75	75	566.0	
	D-5	400	2	100	100	576.8	
	D-6	400	2	125	125	578.8	
	D-7	400	2	150	150	578.8	
	D-8	400	2	175	175	589.6	
	D-9	400	2	200	200	615.1	

Table 3.5. Small Sand Box Tests Series A, B, C and D.

Group	Test Number	Depth D (mm)	Number of Plates	Distance Between Plates λ (mm)	Total Anchorage Length ℓ (mm)	Load Corresponding to 1 mm Deformation (N)	Remarks
E_I	EI-2	100	2	25	25	150.0	test A-2
	EI-3	100	3	25	50	196.0	
	EI-4	100	4	25	75	215.8	
	EI-5	100	5	25	100	225.6	
	EI-6	100	6	25	125	240.4	
	EI-7	100	7	25	150	255.0	
	EI-8	100	8	25	175	270.0	
	EI-9	100	9	25	200	279.6	
E_{II}	EII-2	100	2	50	50	160.0	test A-3
	EII-3	100	3	50	100	215.8	
	EII-4	100	4	50	150	235.4	
	EII-5	100	5	50	200	264.9	
E_{III}	EIII-2	100	2	75	75	169.7	test A-4
	EIII-3	100	3	75	150	220.7	
E_{IV}	EIV-2	100	2	100	100	180.5	test A-5
	EIV-3	100	3	100	200	247.7	

Table 3.6. Small Sand Box Tests Series E.

Group	Test Number	Depth D (mm)	Number of Plates	Distance Between Plates λ (mm)	Total Anchorage Length ℓ (mm)	Load Corresponding to 1 mm Deformation (N)	Remarks
F_I	FI-2	300	2	25	25	369.8	test C-2
	FI-3	300	3	25	50	485.6	
	FI-4	300	4	25	75	515.0	
	FI-5	300	5	25	100	559.0	
	FI-6	300	6	25	125	608.0	
	FI-7	300	7	25	150	647.5	
	FI-8	300	8	25	175	686.7	
	FI-9	300	9	25	200	725.9	
F_{II}	FII-2	300	2	50	50	432.6	test C-3
	FII-3	300	3	50	100	549.4	
	FII-4	300	4	50	150	622.9	
	FII-5	300	5	50	200	686.7	
F_{III}	FIII-2	300	2	75	75	450.3	test C-4
	FIII-3	300	3	75	150	603.3	
F_{IV}	FIV-2	300	2	100	100	451.3	test C-5
	FIV-3	300	3	100	200	662.2	

Table 3.7. Small Sand Box Tests Series F.

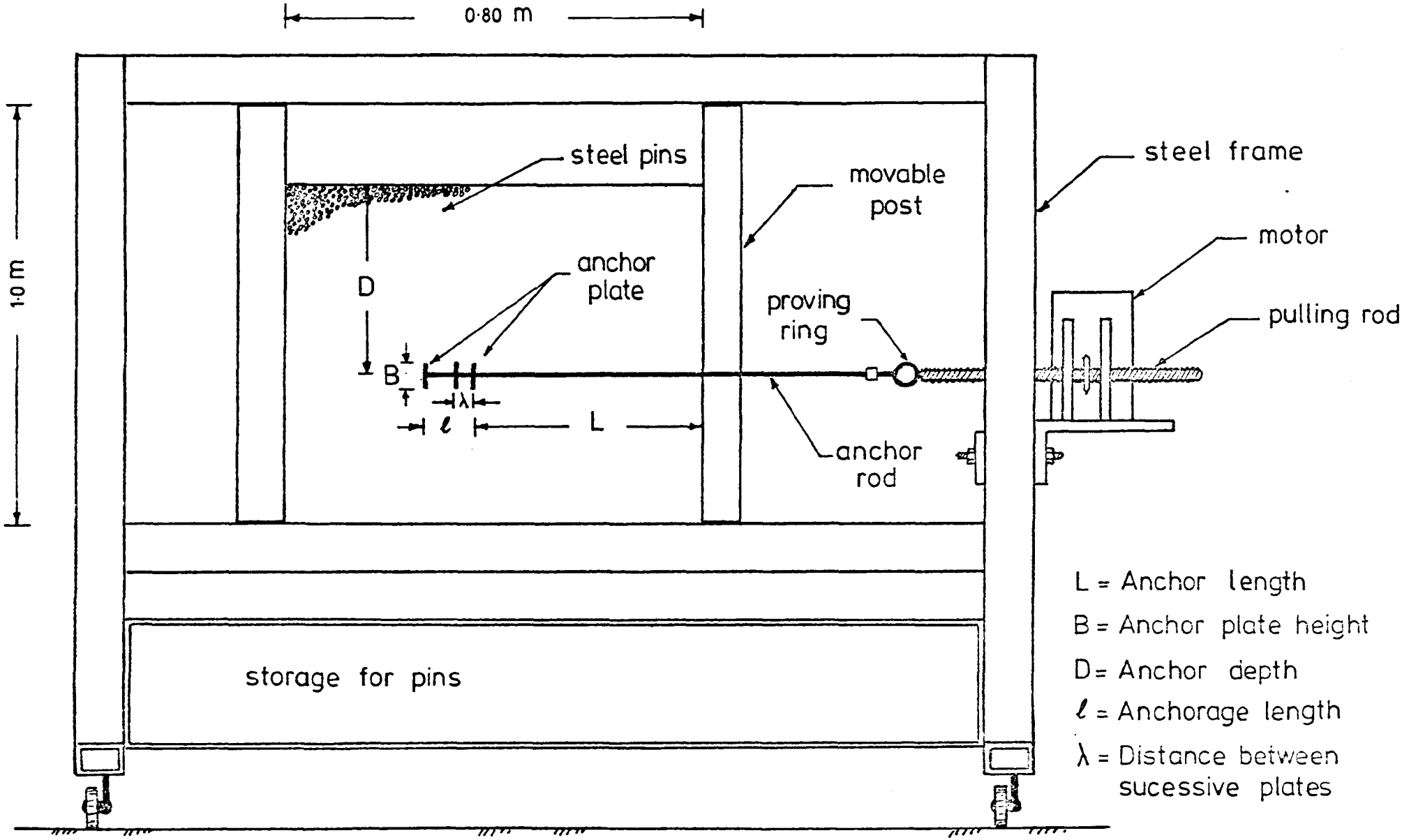

FIG. 3·1 GENERAL LAYOUT OF THE PIN MODEL TEST RIG

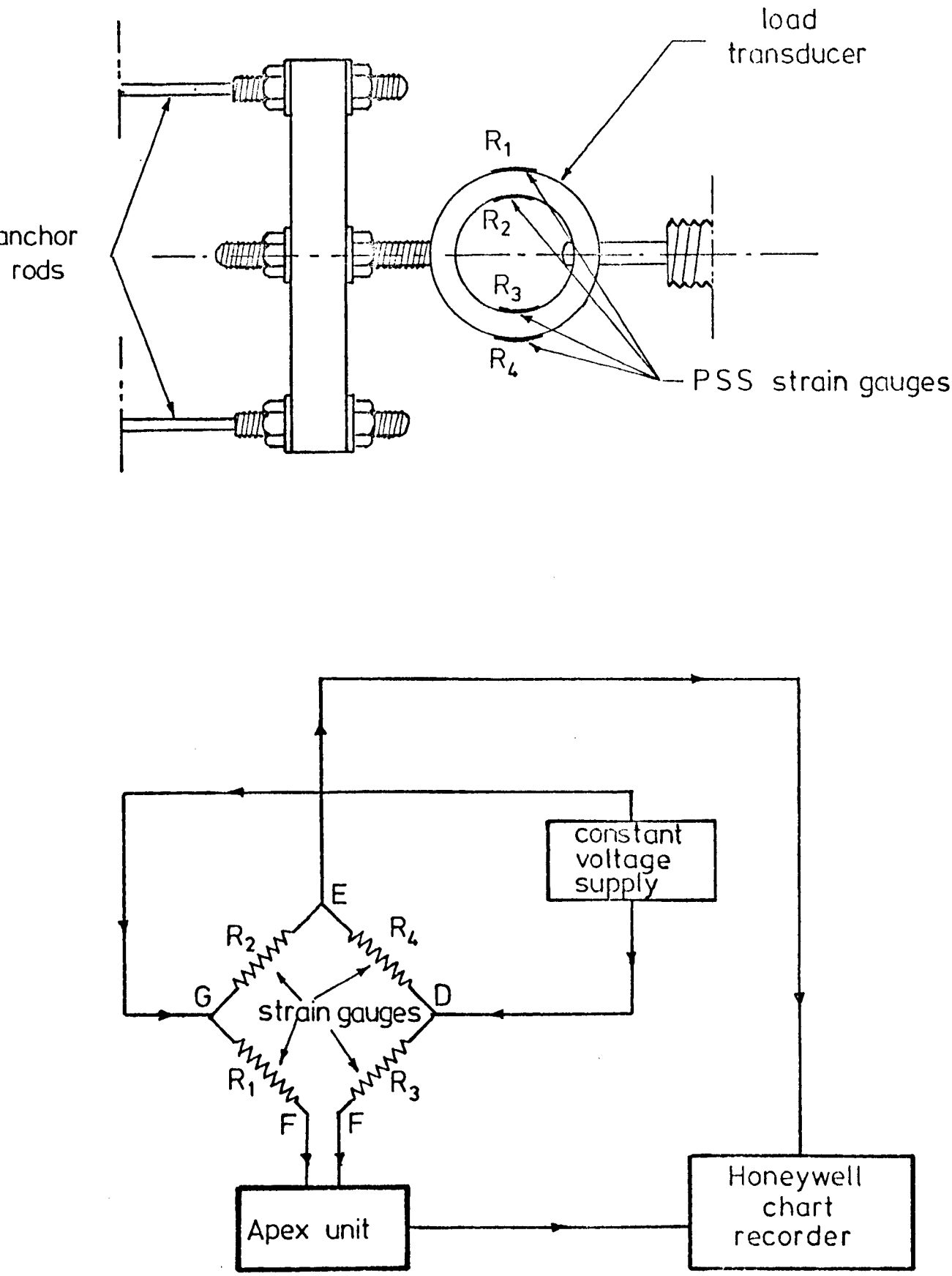

FIG. 3·2 DETAILS OF THE ELECTRIC CIRCUIT USED FOR LOAD MEASUREMENT IN THE PIN MODEL TESTS

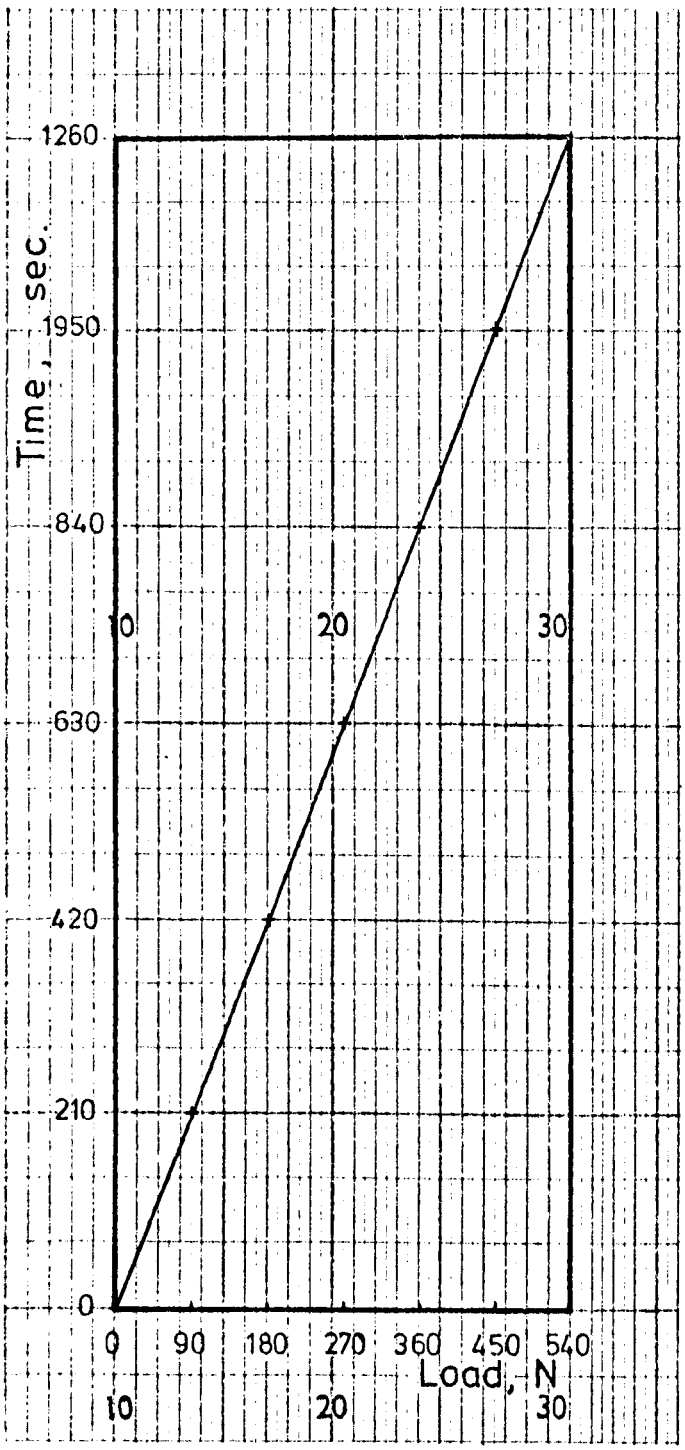

RING 1

(Chart division = 25.7 N)

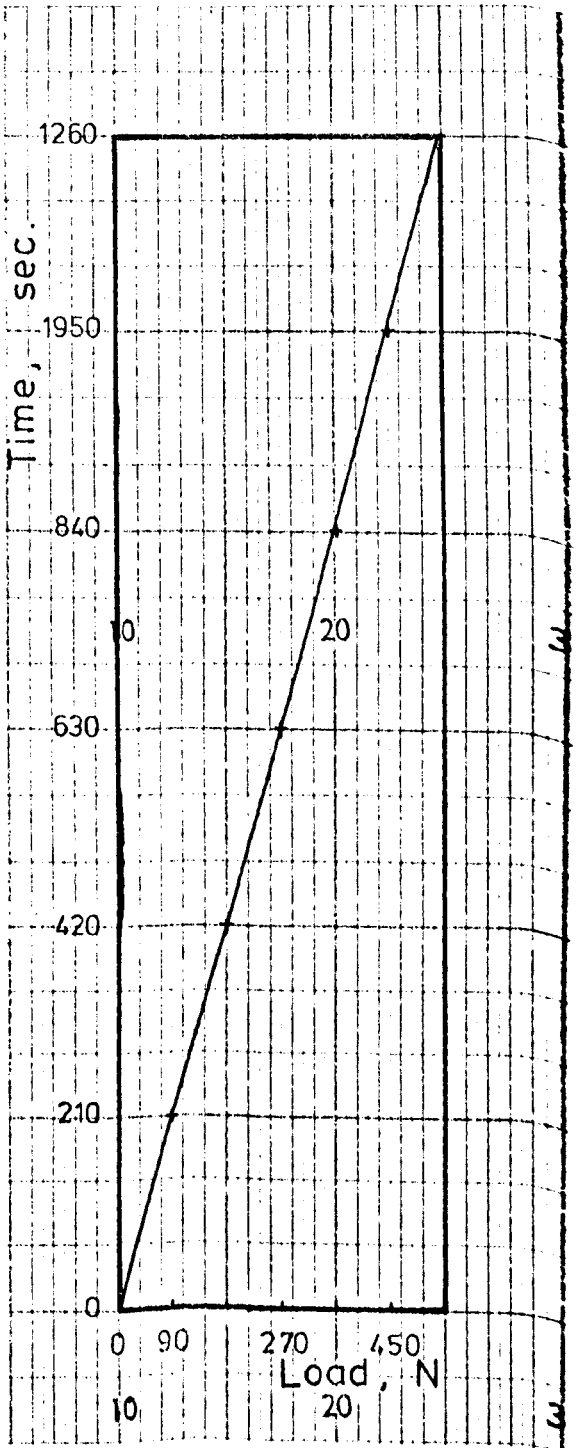

RING 2

(Chart division = 36.0 N)

Volt input = 4.0

FIG. 3.3 CALIBRATION CURVES FOR STEEL PROVING RINGS

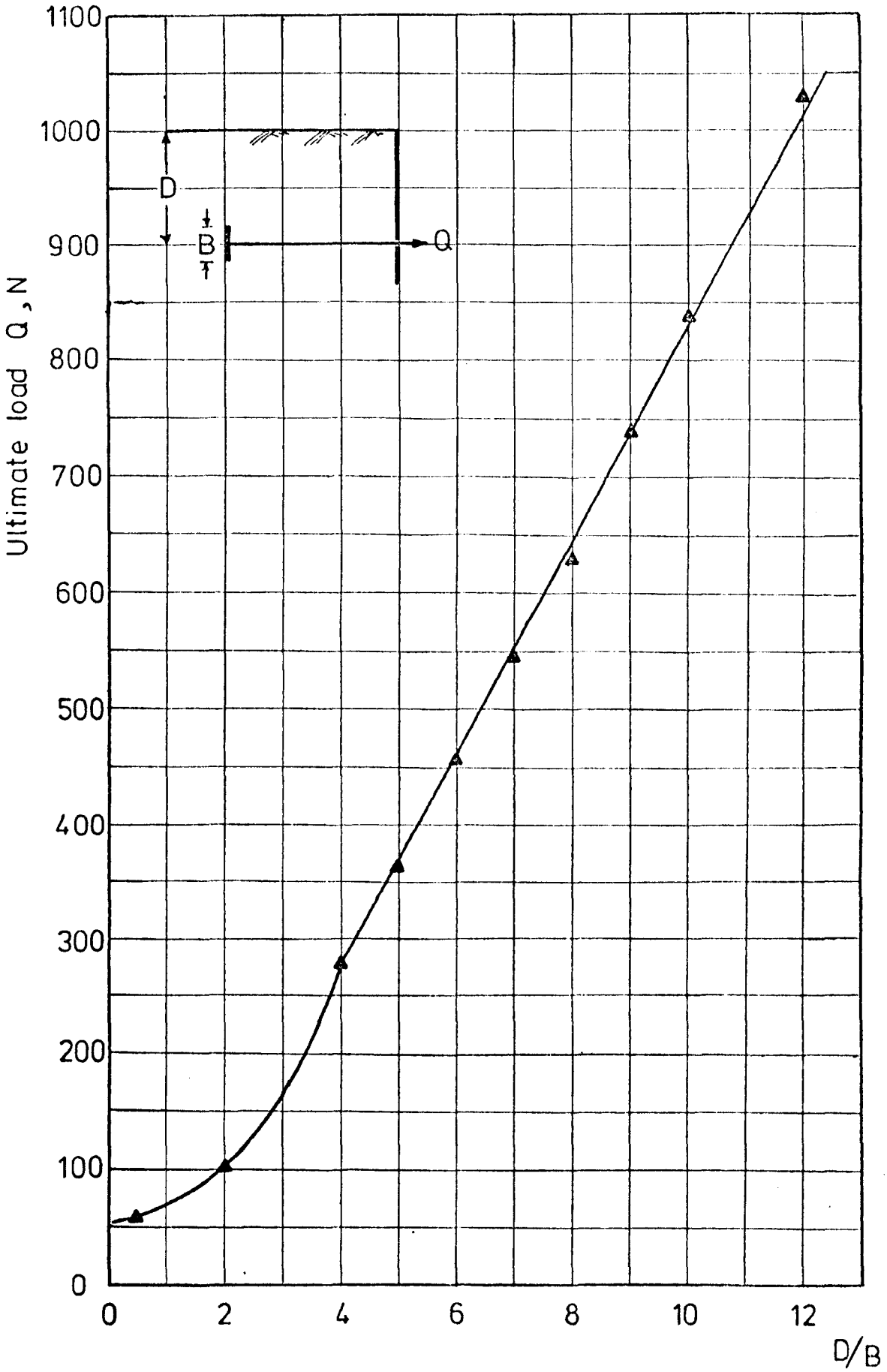

FIG. 3·4 ULTIMATE LOAD (Q) V. DEPTH/HEIGHT (D/B) FOR GROUP A PIN MODEL TESTS

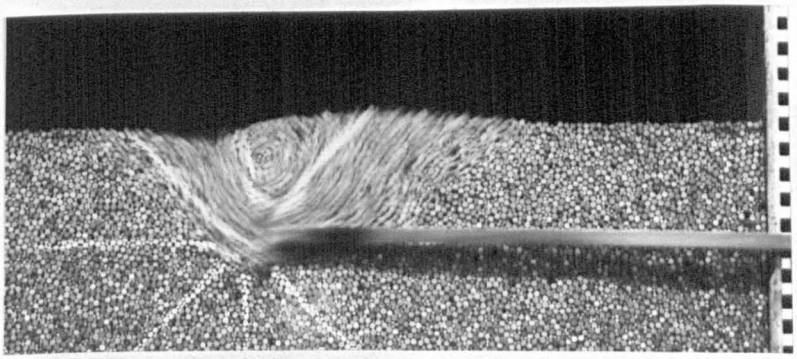

TEST NO. 2 D/B = 2

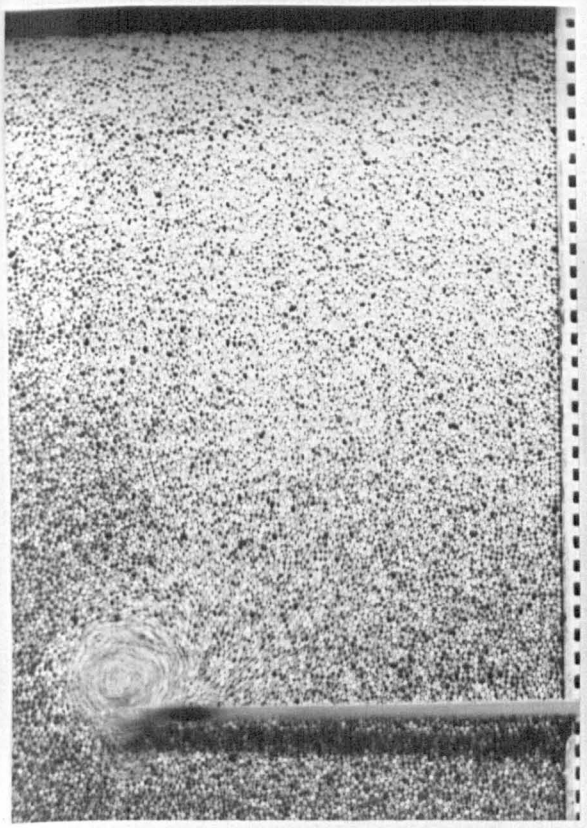

TEST NO. 10 D/B = 12

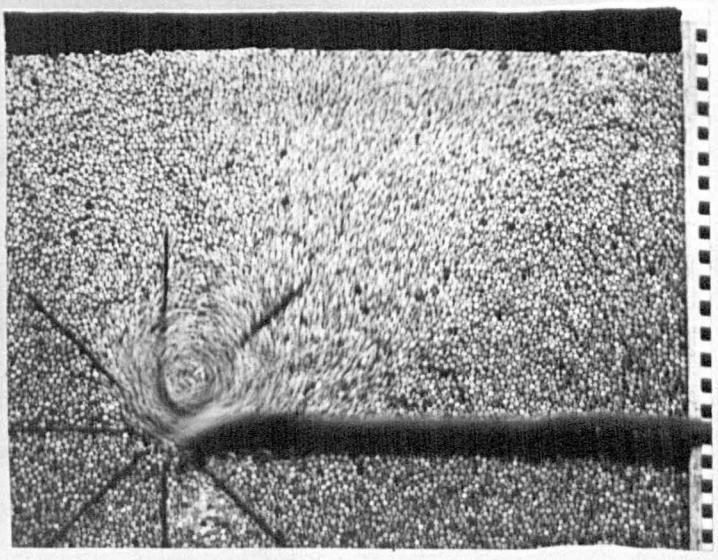

TEST NO. 5 D/B = 6

FIG. 3.5 TYPICAL FAILURE MECHANISM FOR SINGLE PLATE ANCHORS (GROUP A)

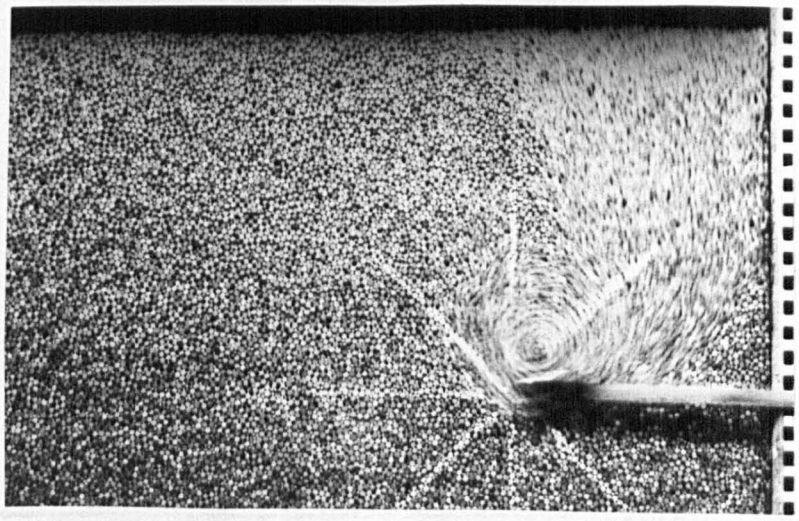

TEST NO. 3 L/B = 4

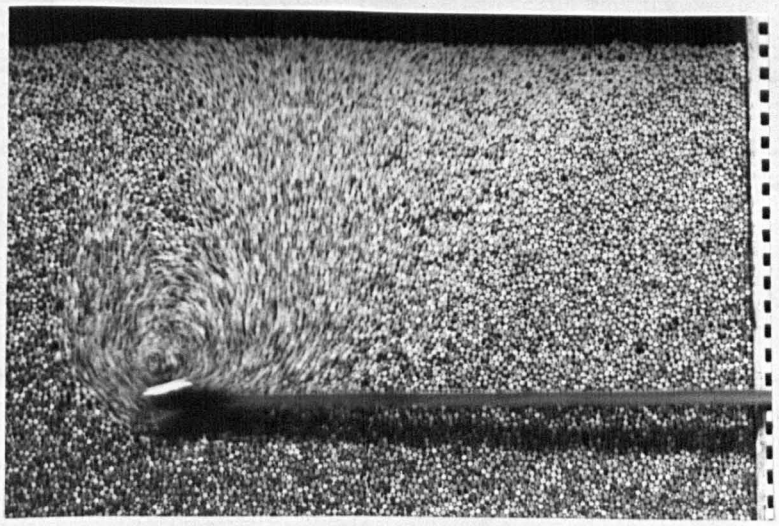

TEST NO. 7 L/B = 10

FIG. 3.6 TYPICAL FAILURE MECHANISM FOR SINGLE PLATE ANCHORS (GROUP B)

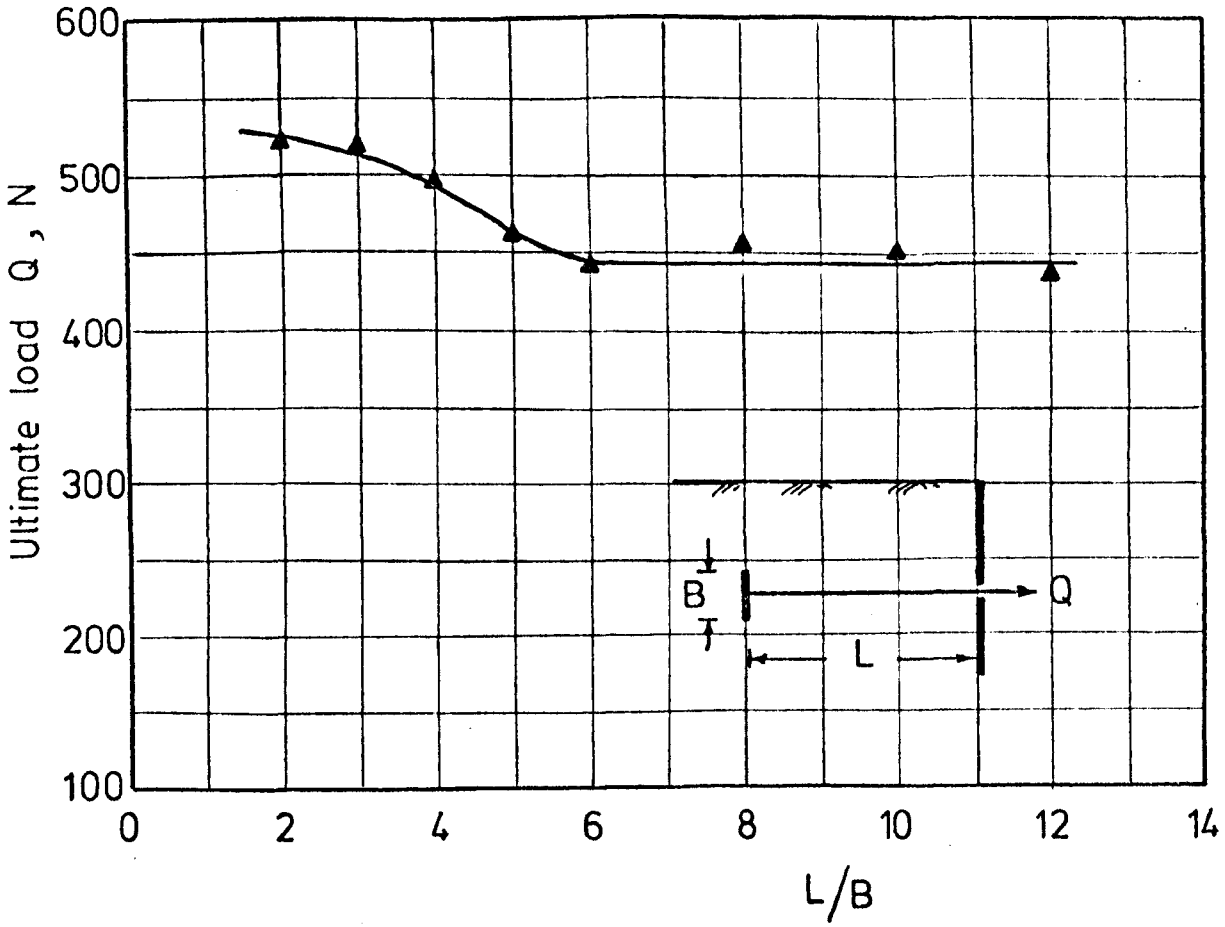

FIG. 3·7 ULTIMATE LOAD (Q) V. LENGTH/HEIGHT (L/B) FOR GROUP B PIN MODEL TESTS

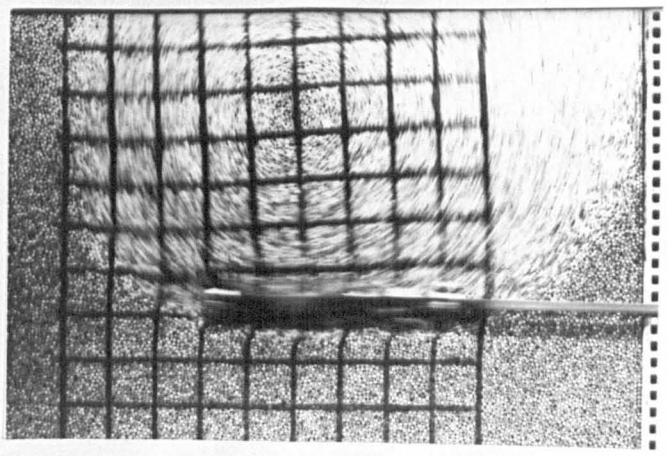

a) TEST NO. 5 ℓ = 3B

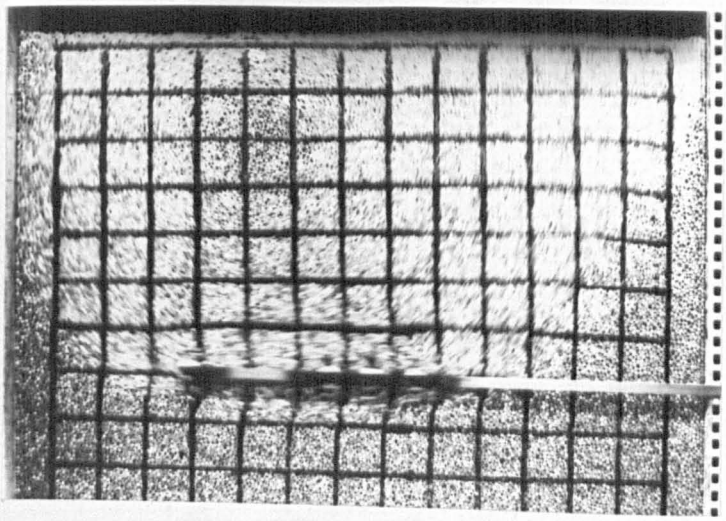

b) TEST NO. 7 ℓ = 5B

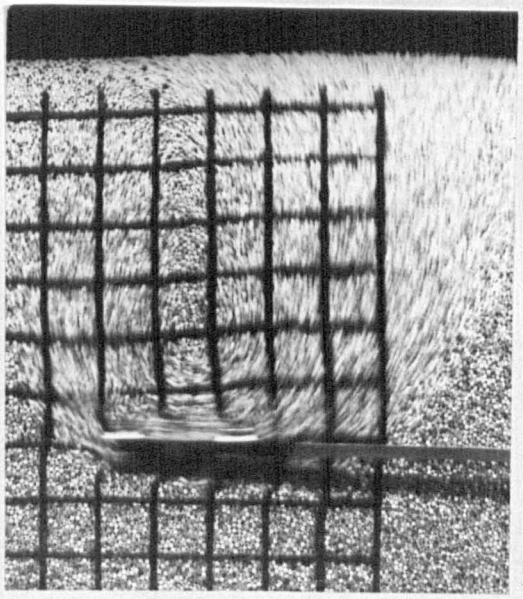

c) TEST NO. 4 ℓ = 2B

FIG. 3.8 TYPICAL FAILURE MECHANISM FOR MULTI-PLATE ANCHORS (GROUP C-TWO PLATES)

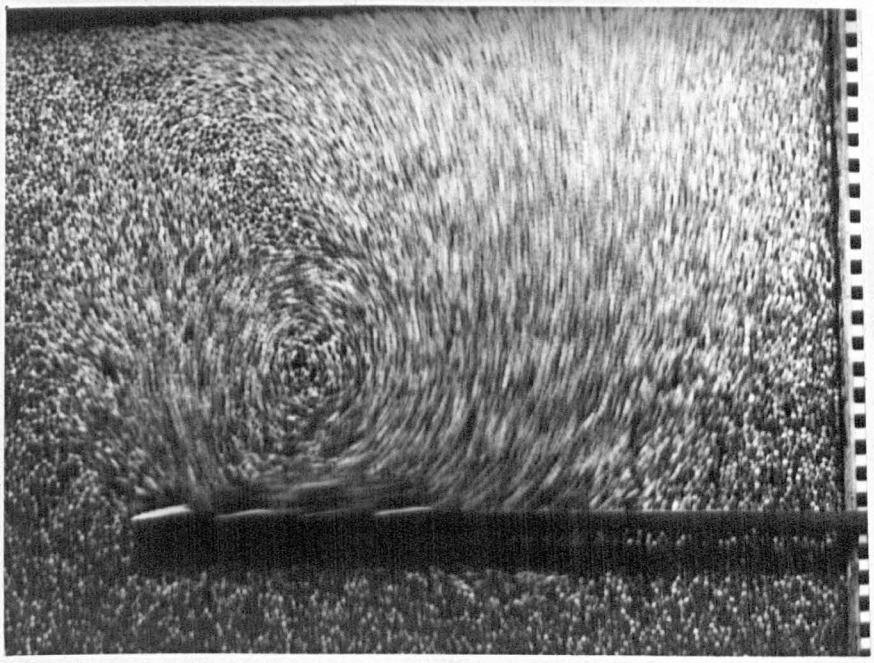

TEST NO. 9 ℓ = 2B (THREE PLATES)

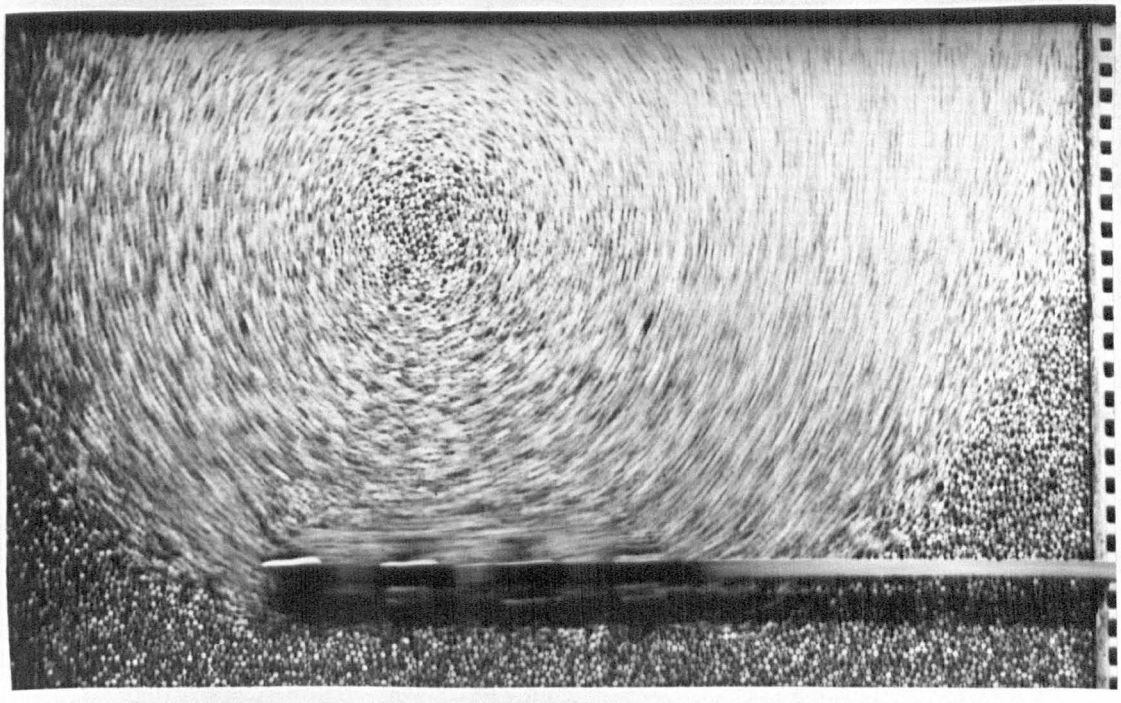

TEST NO. 13 ℓ = 4.5B (FOUR PLATES)

FIG. 3.9 TYPICAL FAILURE MECHANISM FOR MULTI-PLATE ANCHORS (GROUP C)

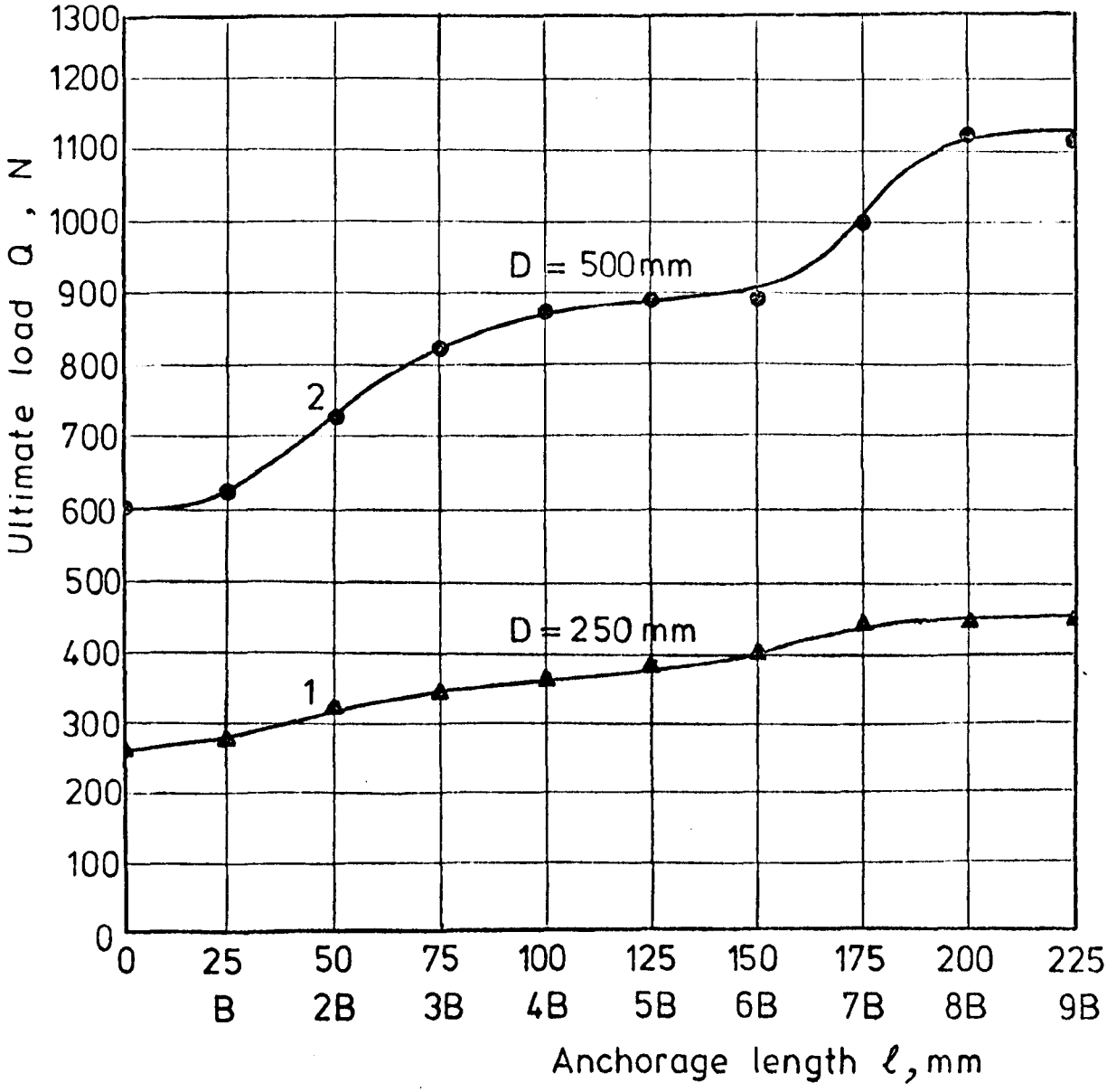

FIG. 3·10 ULTIMATE LOAD — ANCHORAGE LENGTH RELATIONSHIP FOR GROUP D PIN MODEL TESTS (TWO PLATES)

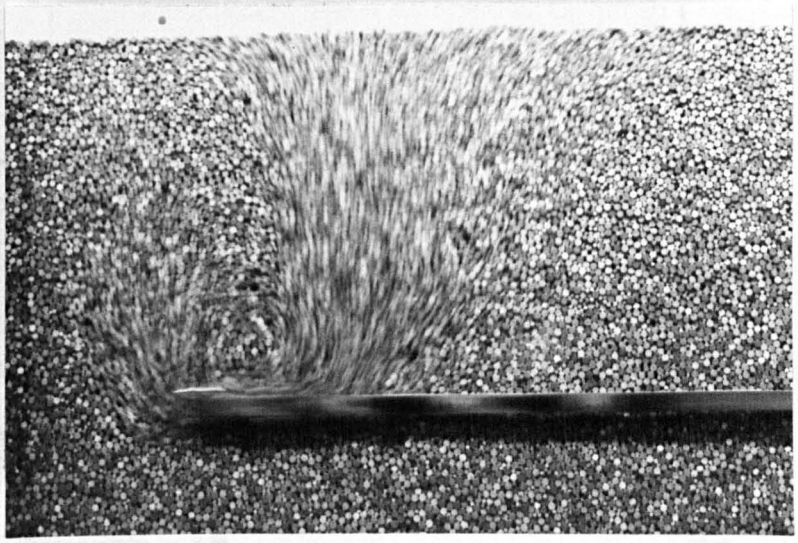

TEST NO. 3 ℓ = 2B

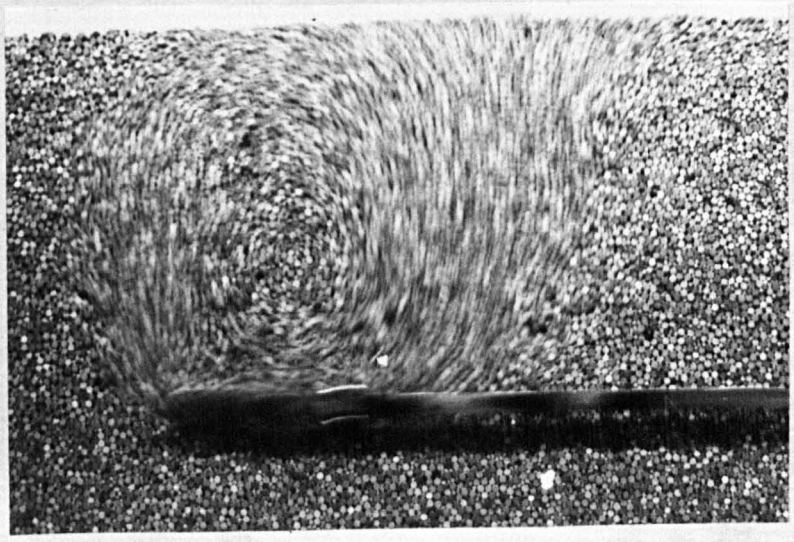

TEST NO. 5 ℓ = 4B

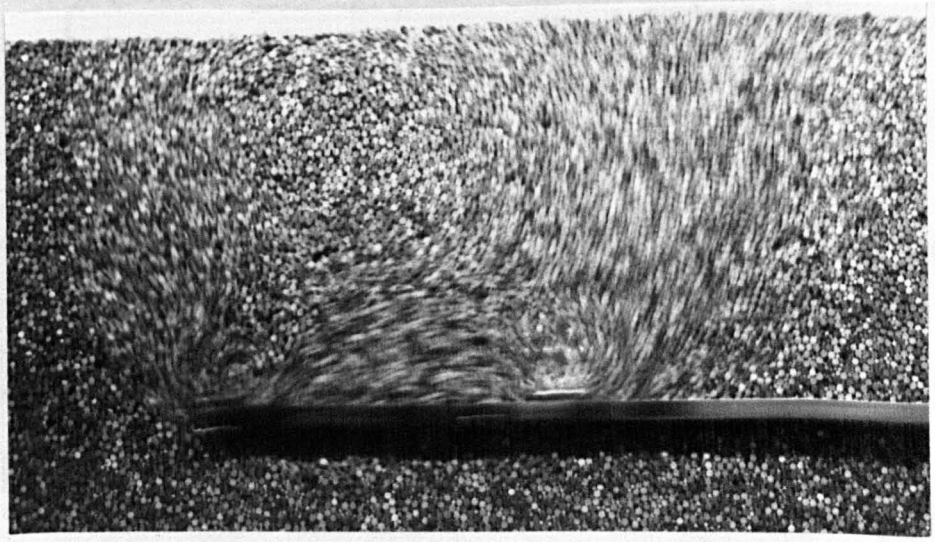

TEST NO. 10 ℓ = 9B

FIG. 3.11 (a) TYPICAL FAILURE MECHANISM
DOUBLE-PLATE ANCHORS (GROUP D)

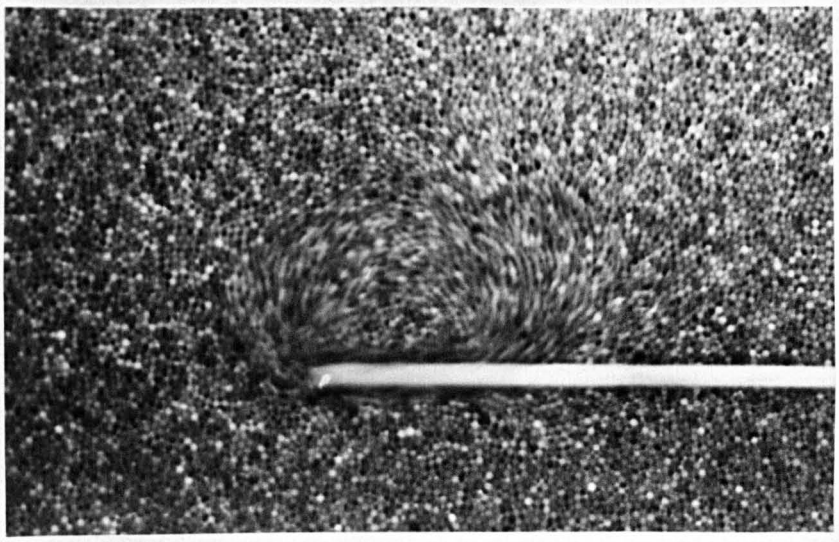

TEST NO. 14 ℓ = 3B

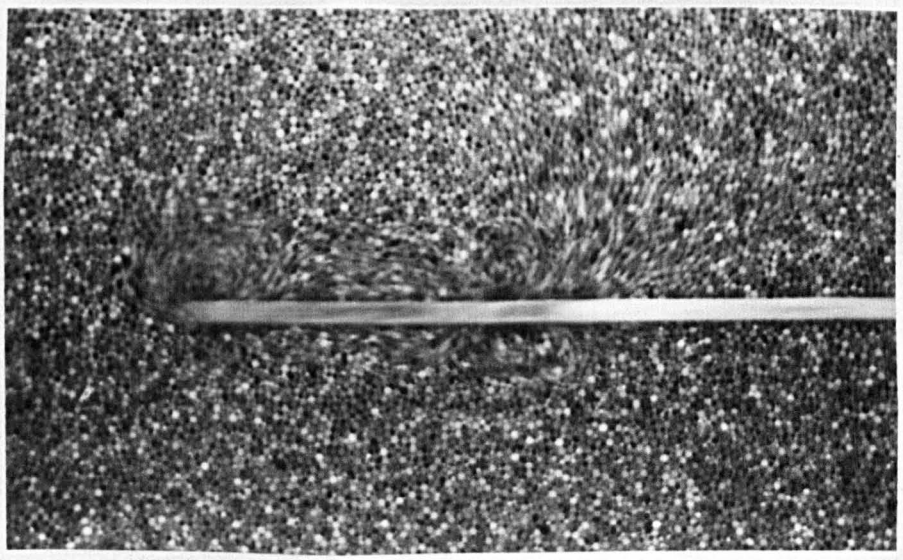

TEST NO. 18 ℓ = 7B

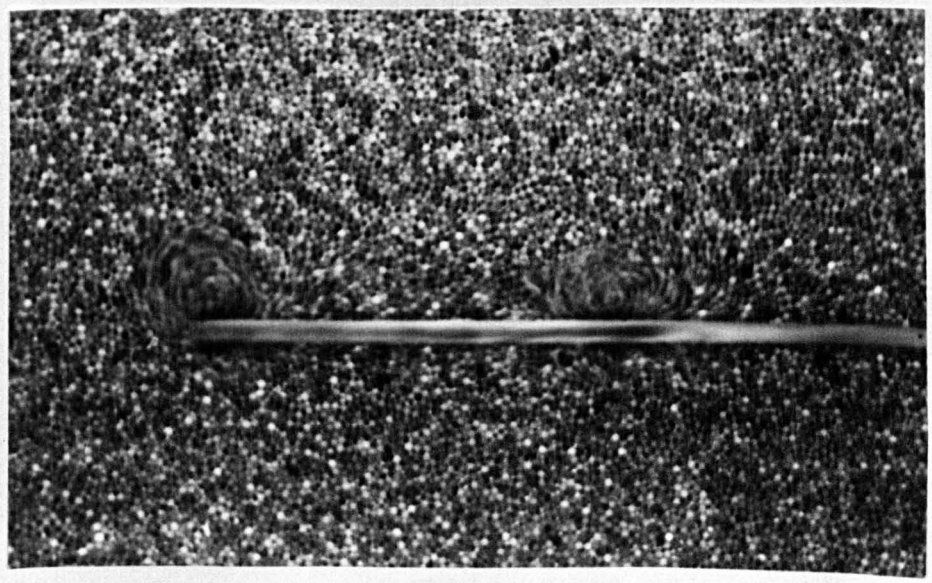

TEST NO. 20 ℓ = 9B

FIG 3.11 (b) TYPICAL FAILURE MECHANISM FOR DOUBLE-PLATE ANCHORS (GROUP D)

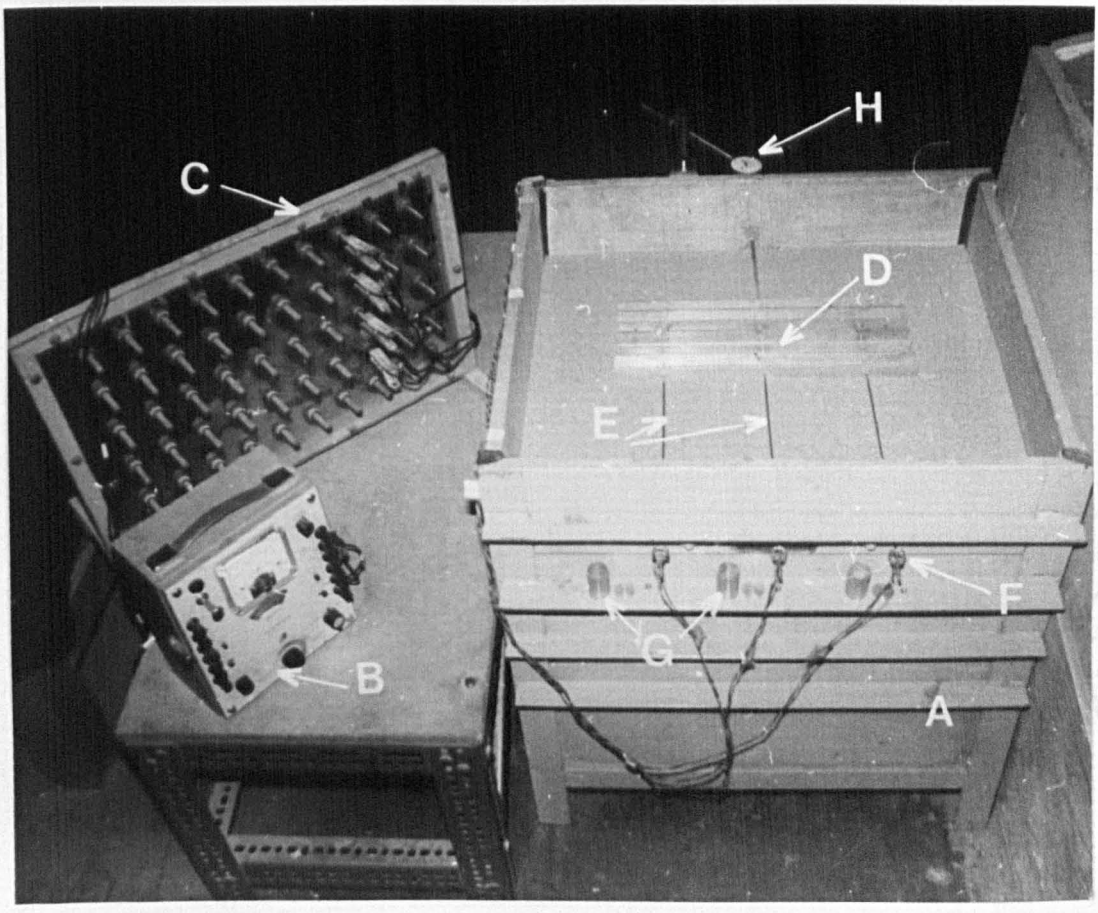

A - Small Sand Box

B - Strain Indicator

C - Terminal Board

D - Anchor Plates

E - Anchor Rods

F - Proving Rings

G - Components of the Load Transducers

H - Dial Gauge

FIG. 3.12 GENERAL ARRANGEMENT OF THE SMALL SAND BOX

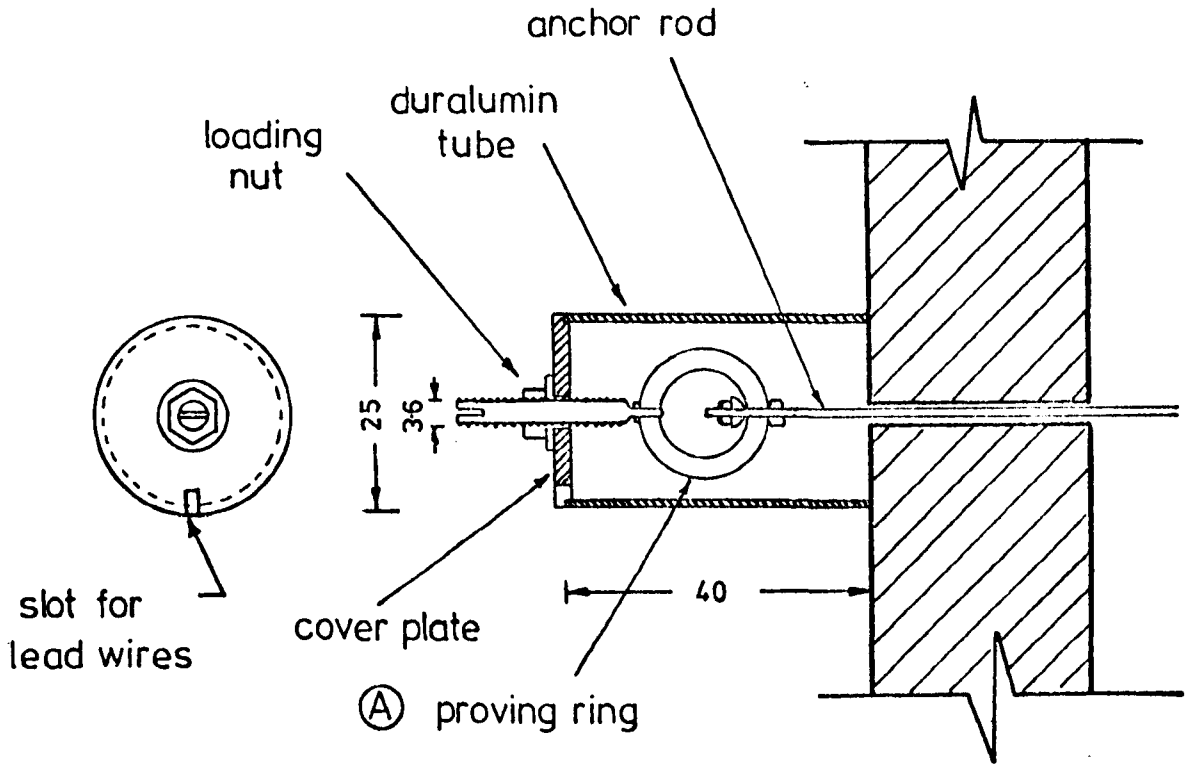

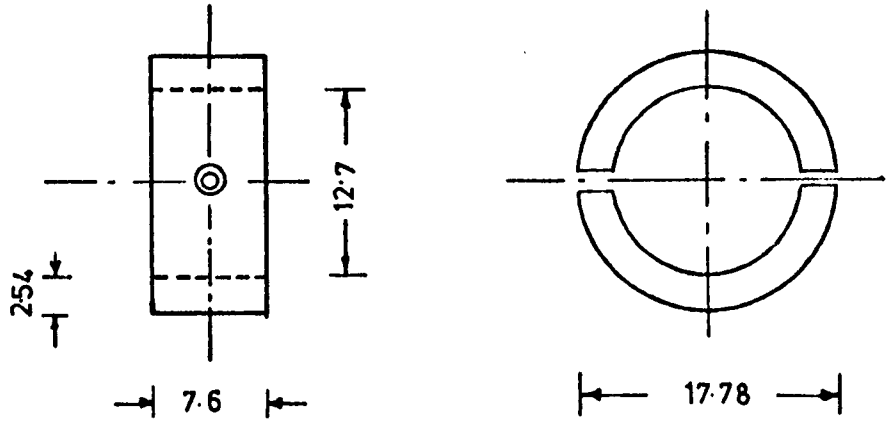

Detail Ⓐ

FIG. 3·13 COMPONENTS OF THE LOADING SYSTEM FOR SMALL SAND BOX TESTS

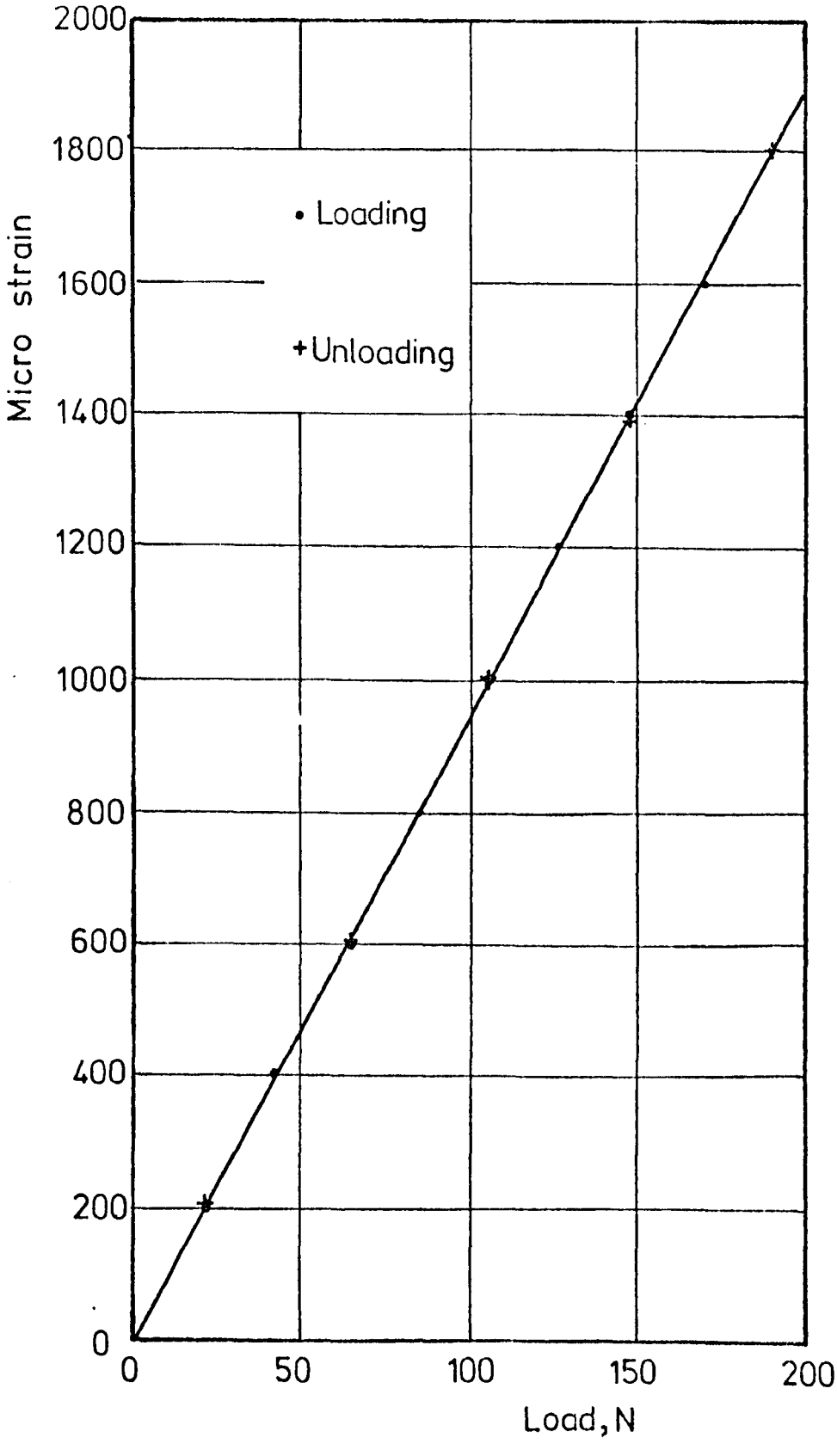

FIG. 3·14 TYPICAL CALIBRATION CURVE FOR A DURALUMIN PROVING RING

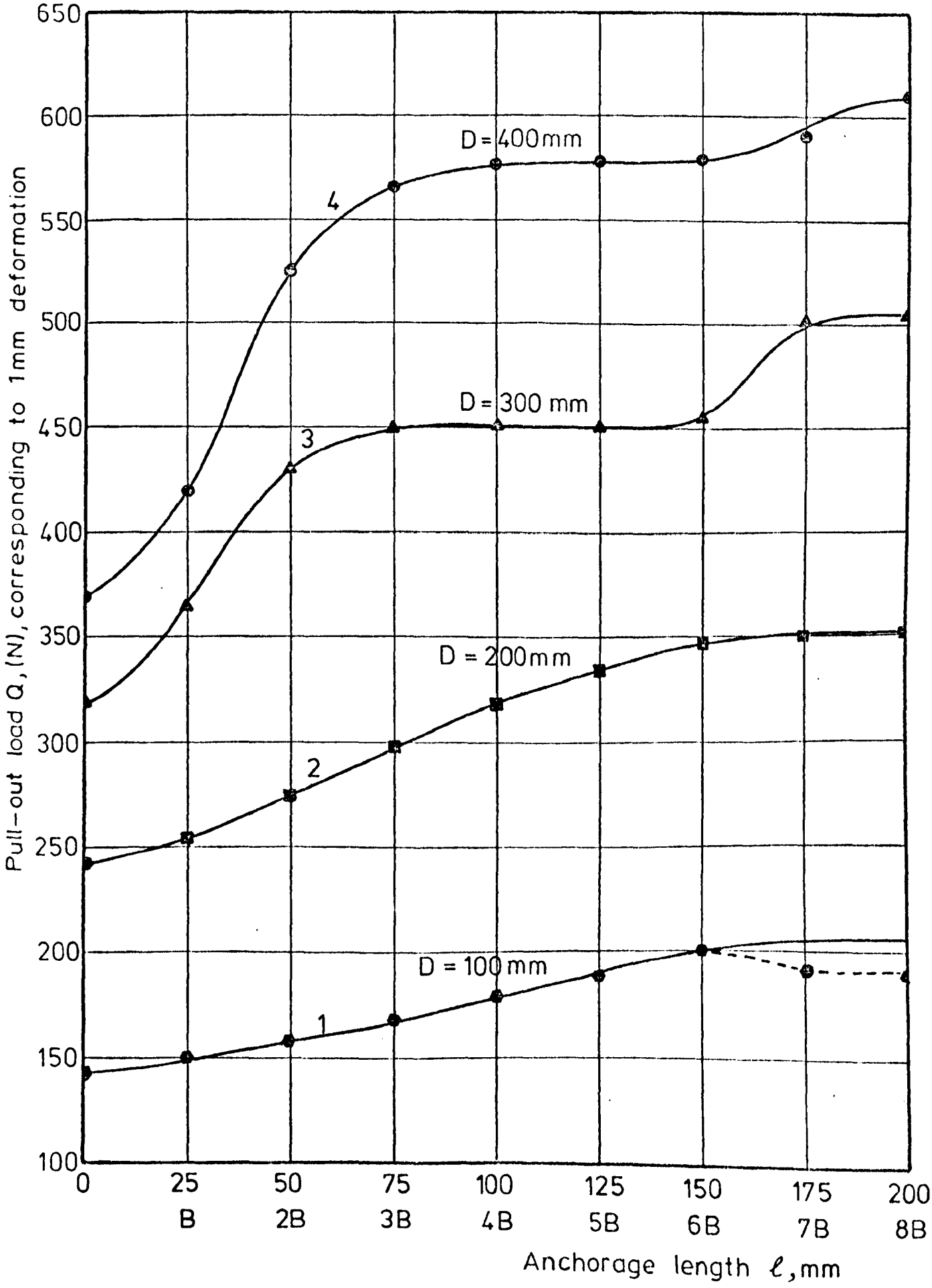

FIG. 3·15 PULL-OUT LOAD-ANCHORAGE LENGTH RELATIONSHIP FOR DOUBLE-PLATE ANCHORS AT DIFFERENT EMBEDMENT DEPTHS (Groups A,B,C & D, small sand box)

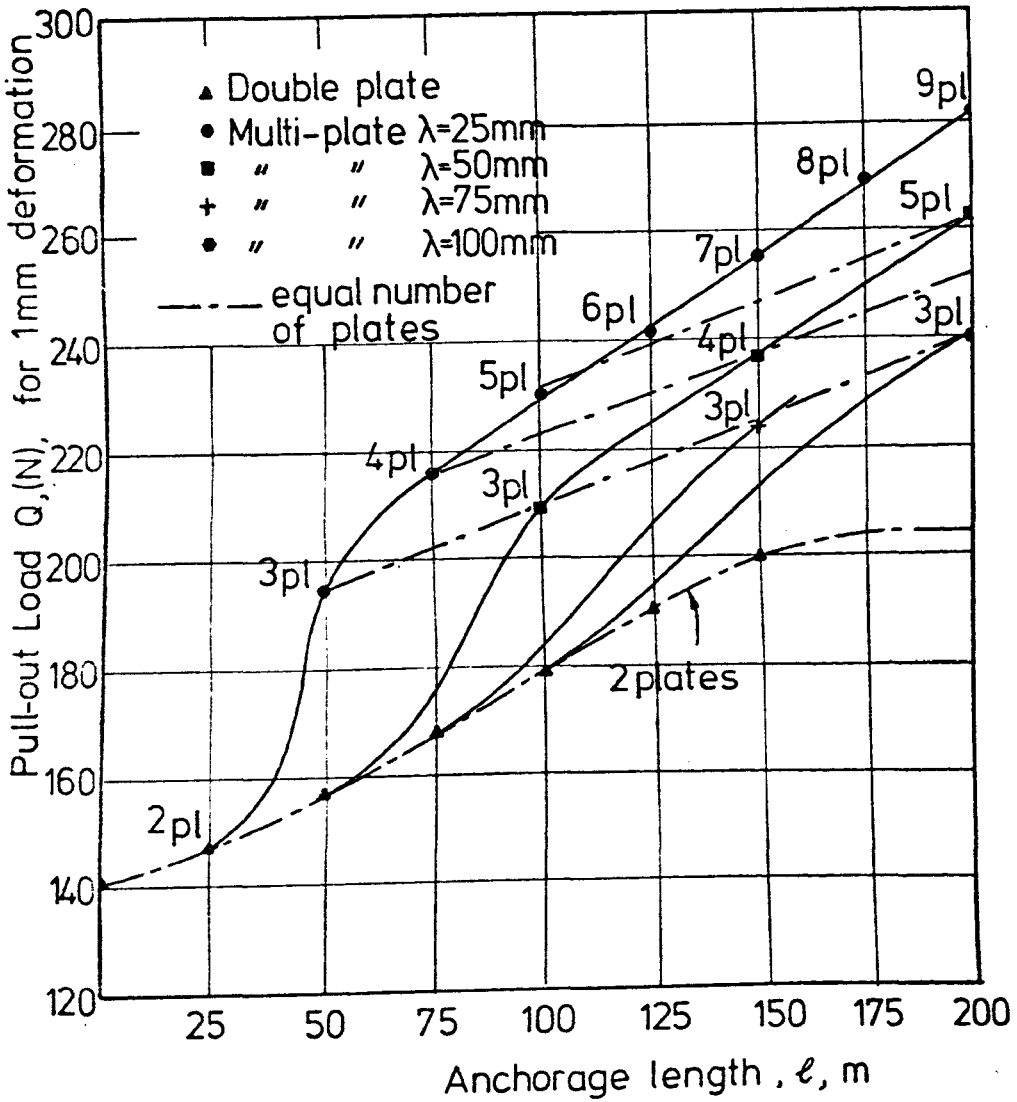

(a) Depth D=100mm

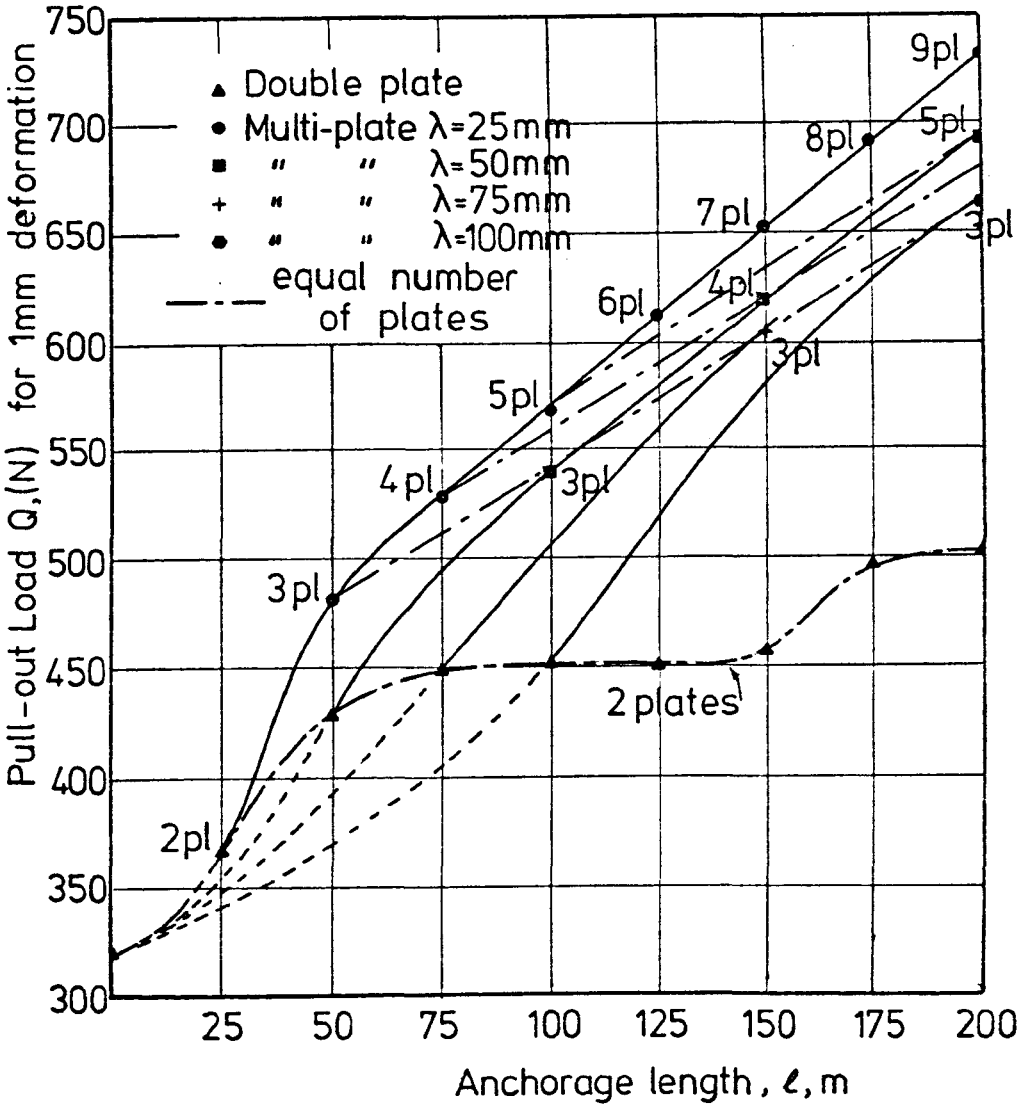

(b) Depth D=300mm

FIG. 3·16 PULL-OUT LOAD ANCHORAGE LENGTH RELATIONSHIP FOR DIFFERENT NUMBER OF ANCHOR PLATES (Group E & F small sand box)

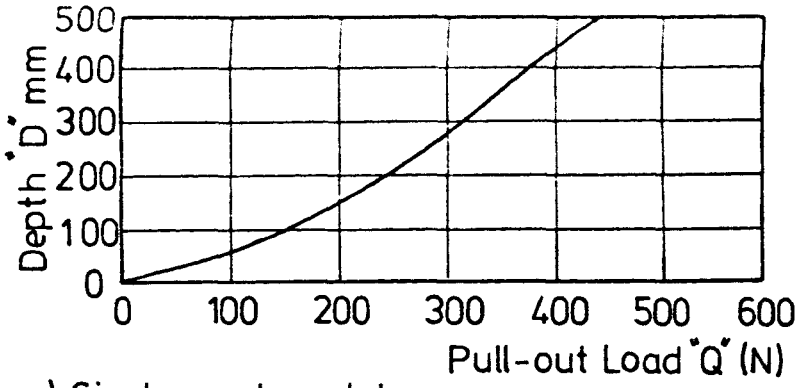

a.) Single anchor plate

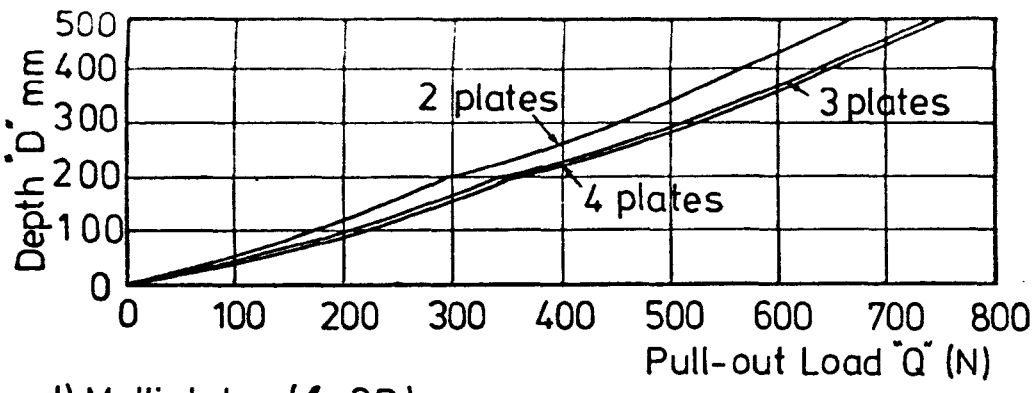

d.) Multi-plate ($\ell = 3B$)

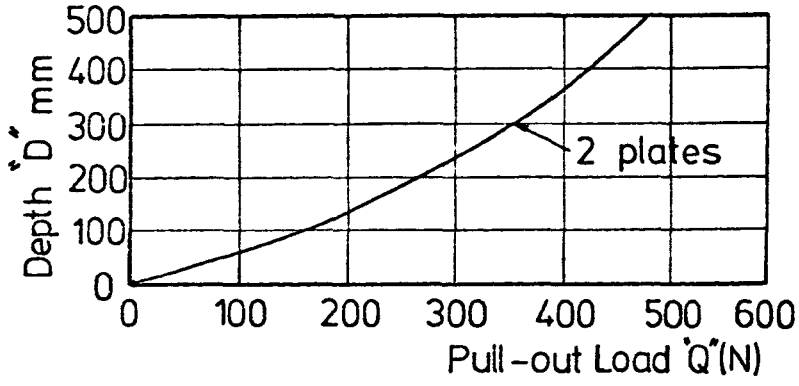

b.) Multi-plate ($\ell = 1B$)

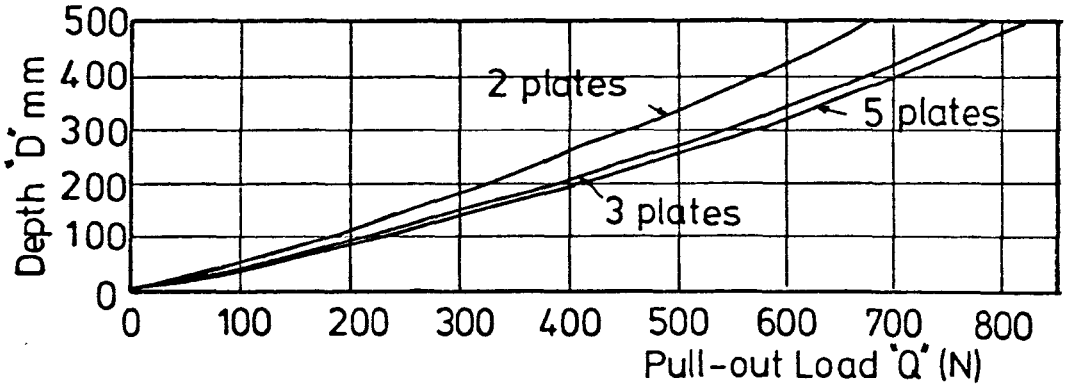

e) Multi-plate ($\ell = 4B$)

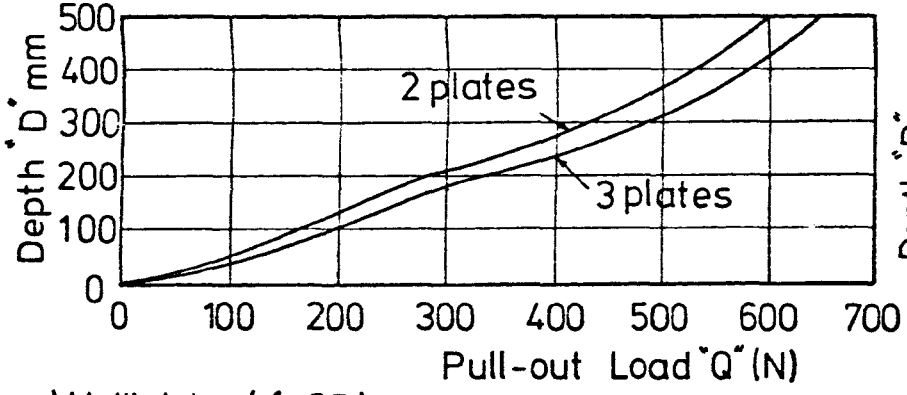

c.) Multi-plate ($\ell = 2B$)

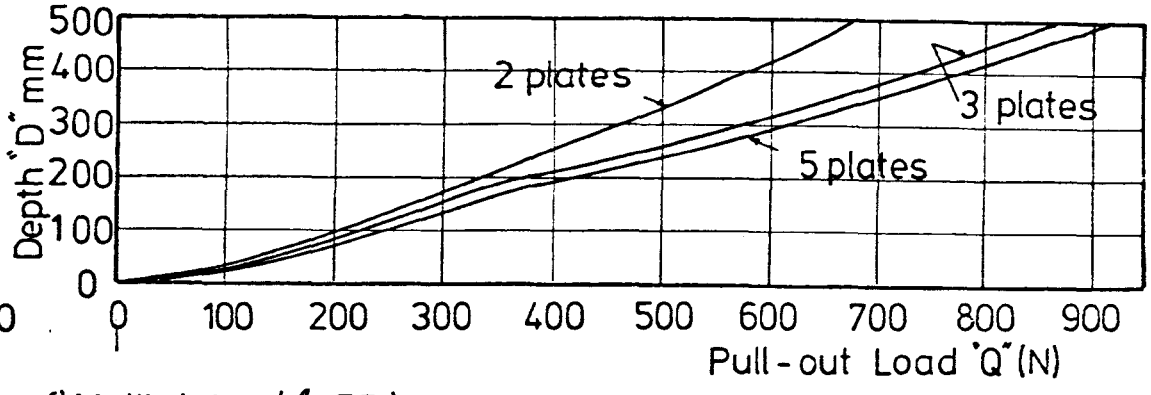

f.) Multi-plate ($\ell = 5B$)

FIG. 3·17 DEPTH–PULL-OUT LOAD RELATIONSHIP FOR DIFFERENT ARRANGEMENTS (Small sand box tests)

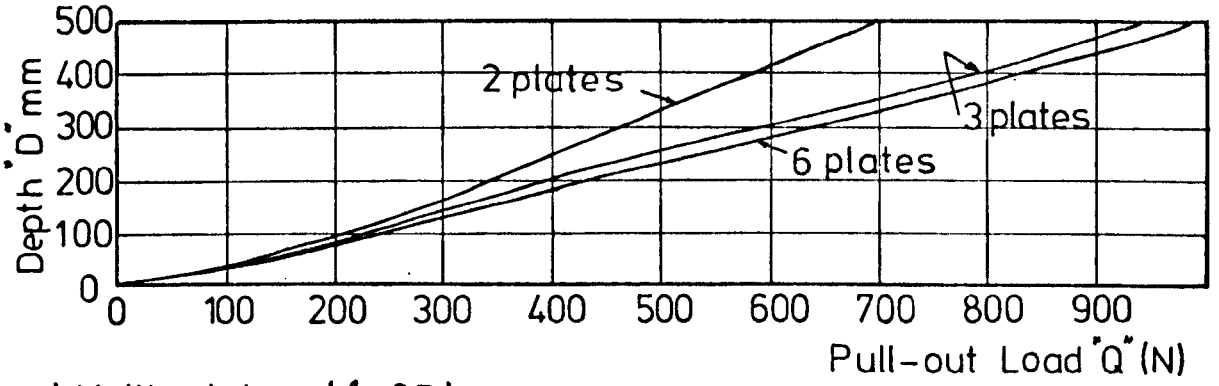

g.) Multi-plate (ℓ = 6B)

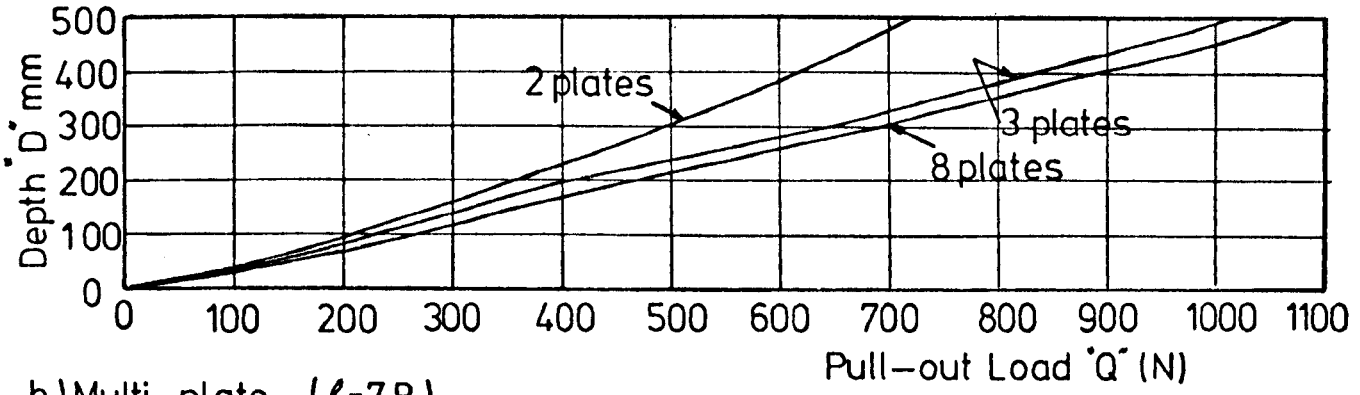

h.) Multi-plate (ℓ = 7B)

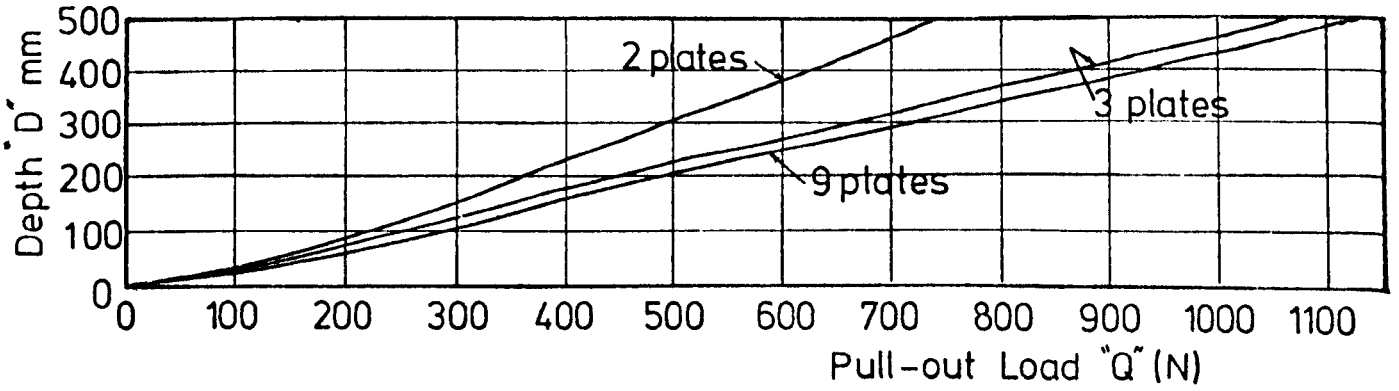

i.) Multi-plate (ℓ = 8B)

cont. FIG. 3·17 DEPTH – PULL-OUT LOAD RELATIONSHIP FOR DIFFERENT ARRANGEMENTS (Small sand box tests)

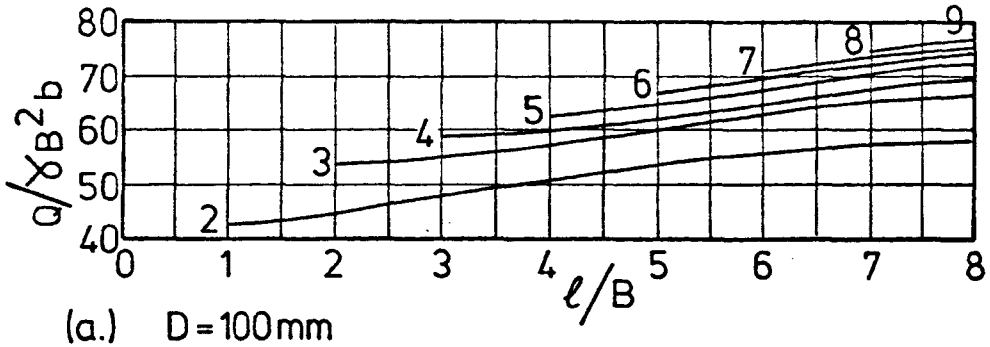

(a.) D = 100 mm

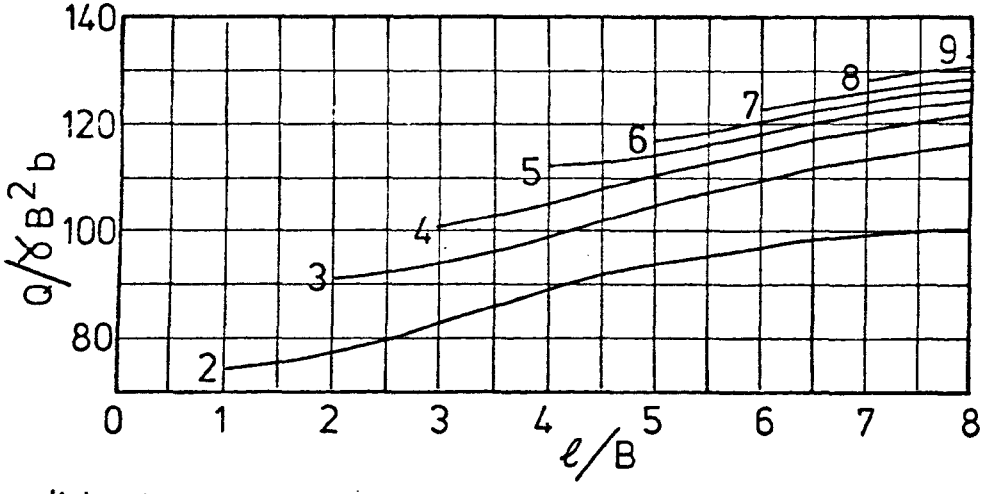

(b.) D = 200 mm

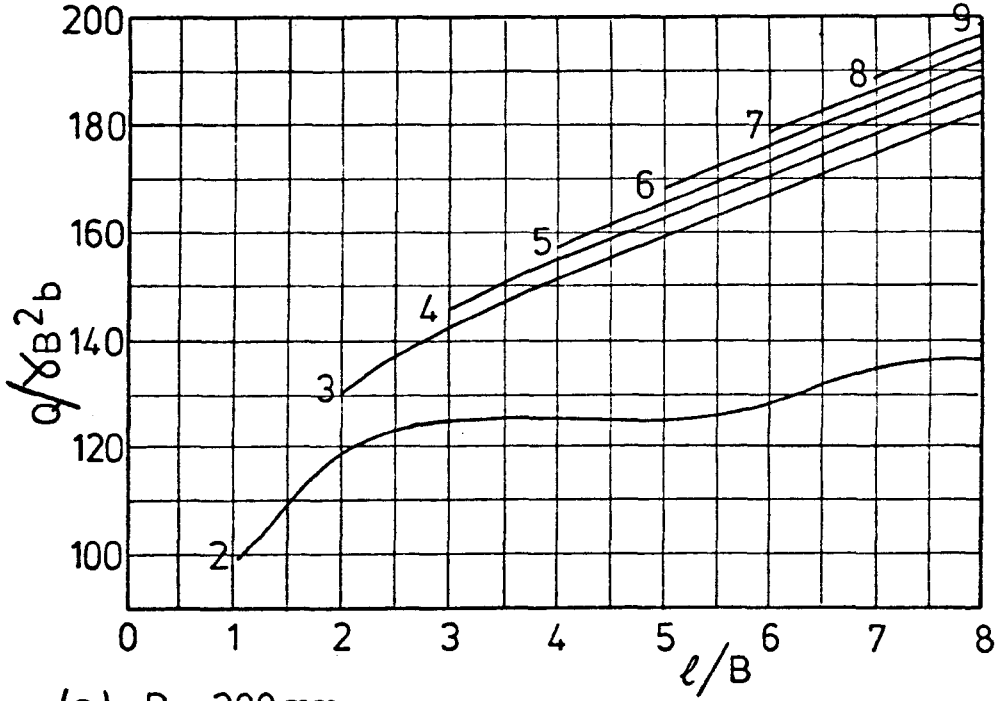

(c.) D = 300 mm

FIG. 3·18 $Q/\gamma B^2 b$ v. ℓ/B RELATIONSHIP FOR MULTI-PLATE ANCHORS (Small sand box tests)

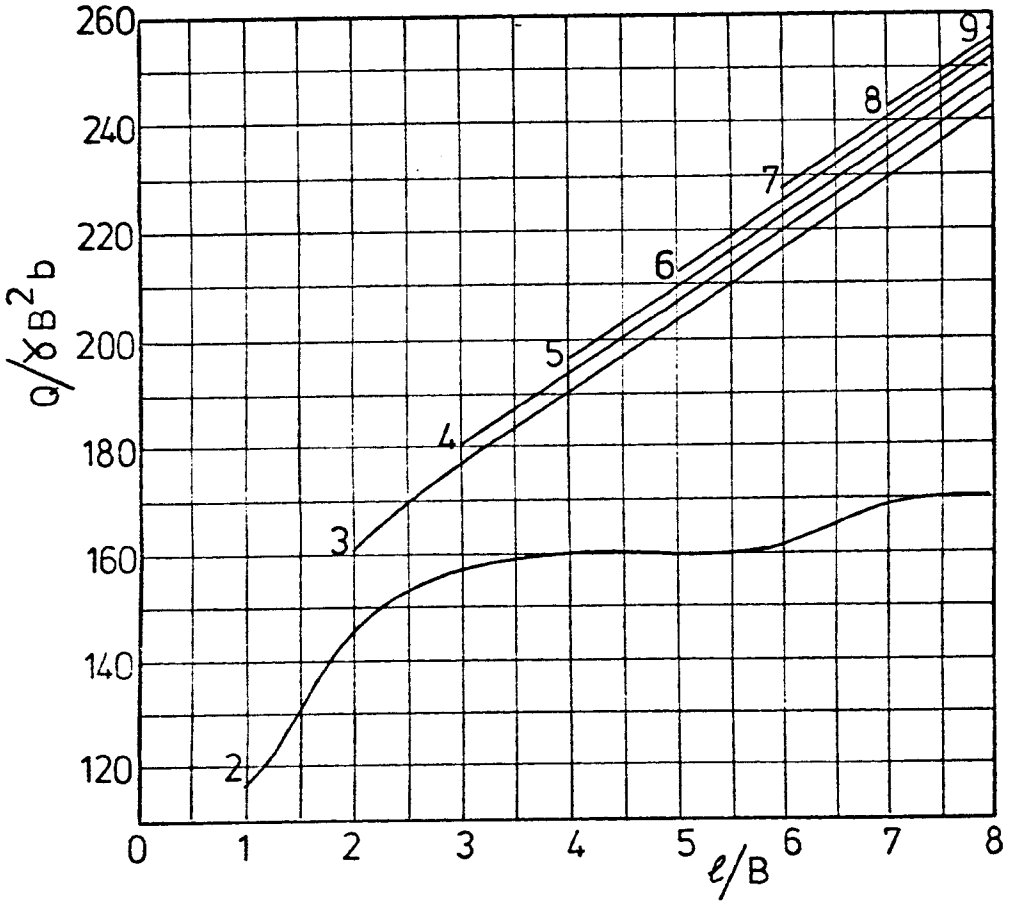

(d.) D = 400 mm

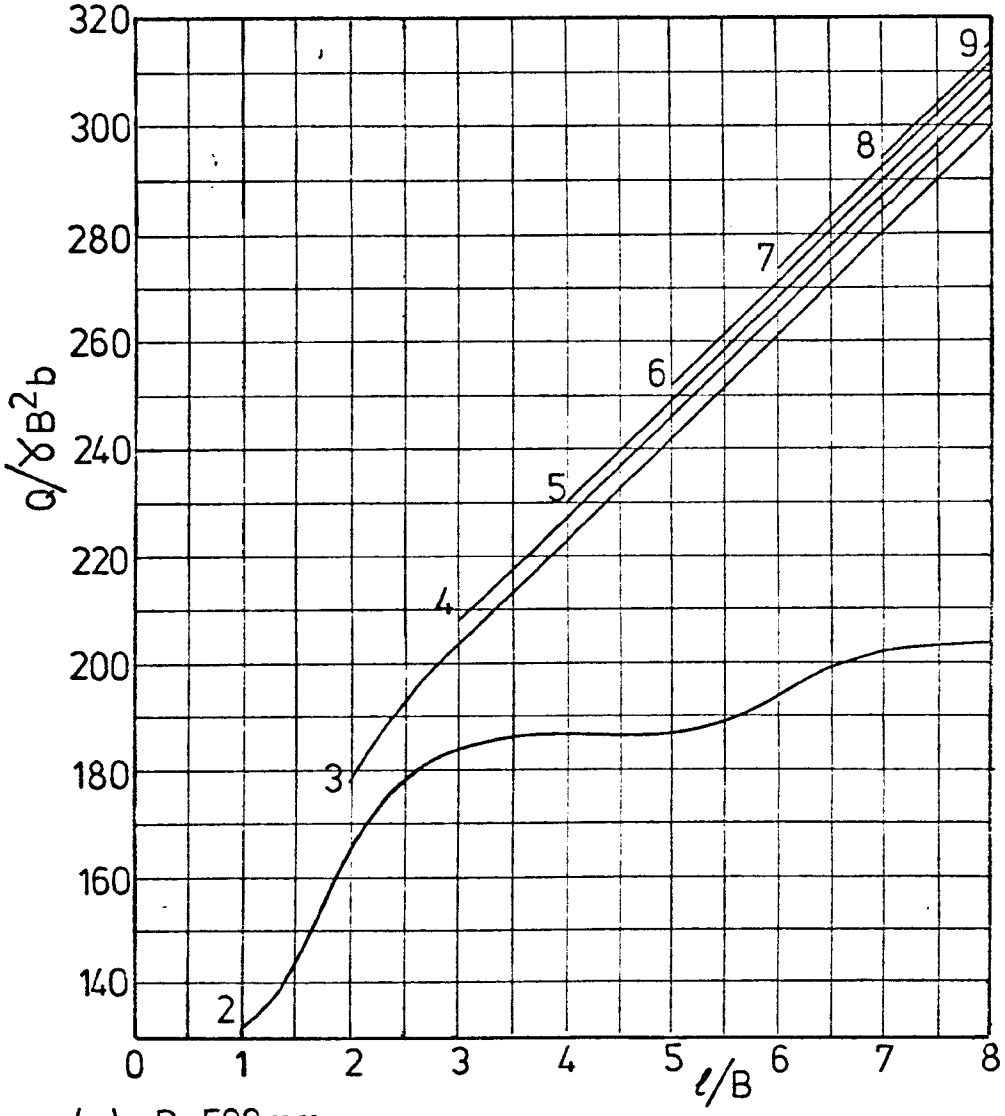

(e.) D = 500 mm

Cont. FIG. 3·18 $Q/\gamma B^2 b$ — ℓ/B RELATIONSHIP FOR MULTI-PLATE ANCHORS (Small sand box tests)

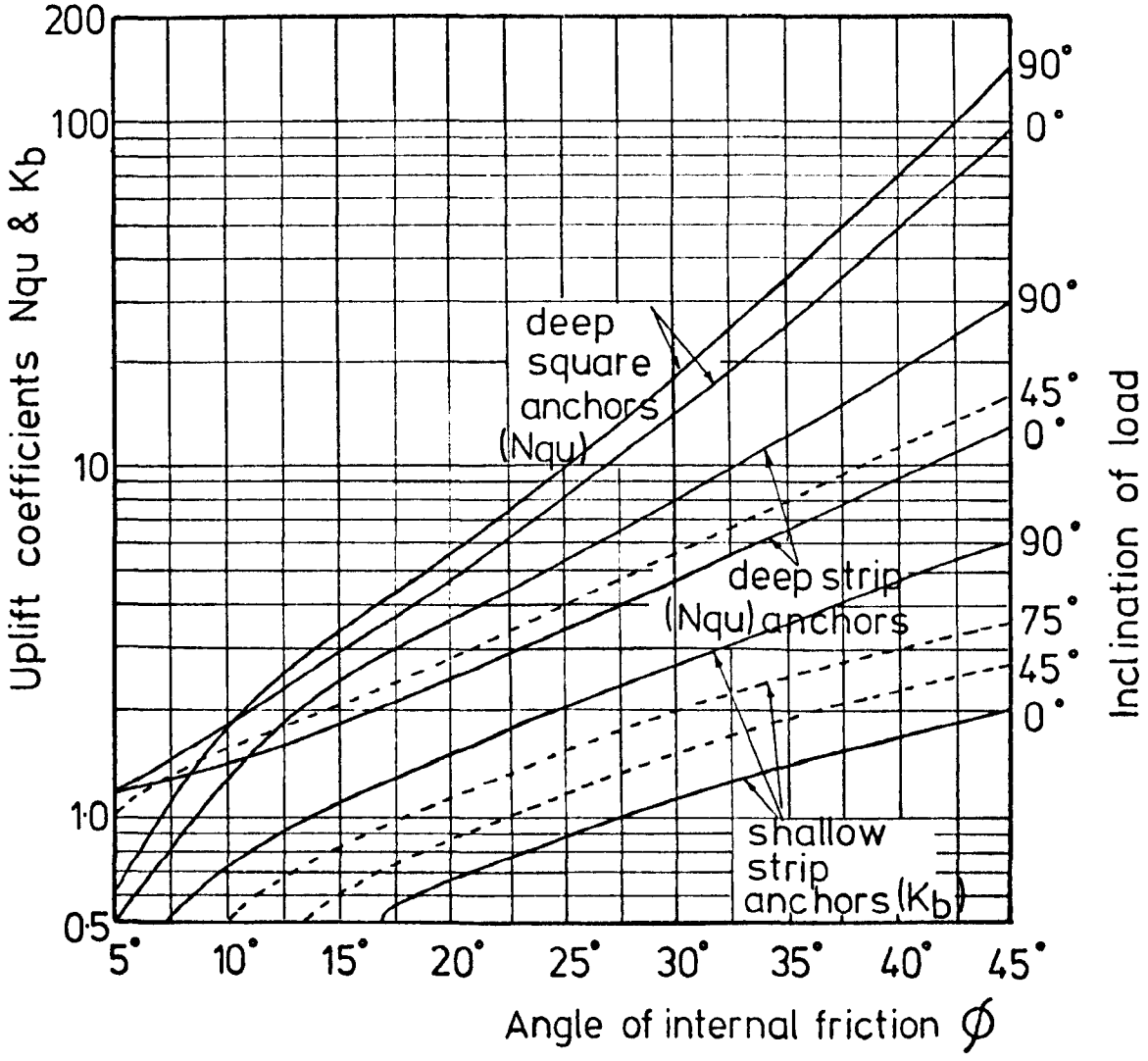

FIG. 3·19 (a.) THEORETICAL UPLIFT COEFFICIENTS FOR ANCHORS (After Meyerhof 1973)

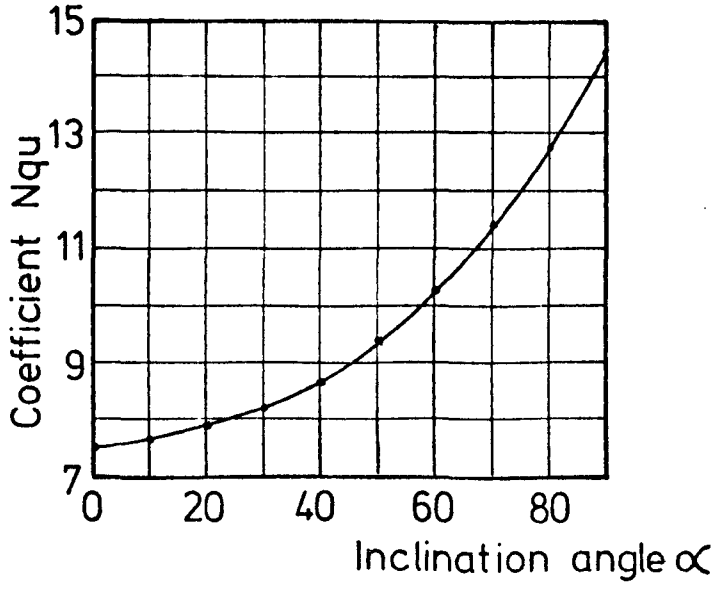

FIG. 3·19 (b.) Nqu – α RELATIONSHIP FOR ϕ = 37

CHAPTER 4

MAIN APPARATUS AND TEST MATERIALS

CHAPTER 4

MAIN APPARATUS AND TEST MATERIALS

4.1 General

In this chapter the experimental equipment and materials used in the retaining wall tests are described. The behaviour of a laboratory scale multi-anchored retaining wall was examined in an apparatus which was used previously by Plant (1972), Ponniah (1973) and Shah (1975). Slight modifications were made to the apparatus to allow for some extra measurements and to facilitate the testing procedure. The wall retained dry sand and was supported by embedded anchor units. In order to assess the behaviour of the wall, the anchors and the retained sand, the instrumentation developed by previous workers was used. Earth pressure distribution on both sides of the retaining wall, movement of the wall, the anchors and the retained sand, anchor loads and reaction on the base of the wall were all monitored.

4.2 Description of Apparatus

4.2.1 Testing flume

The flume measured 1.05 m high, 0.91 m wide and 1.83 m long at the top, with its back sloping at 45° (Fig. 4.1). The flume had a sloping back for two reasons. Firstly, it limited the already considerable amount of sand required and secondly, it allowed access for the attachment of mechanical dial gauges for some of the sand movement gauges. The flume was constructed of mild steel channel

sections which were welded together to form a rigid frame. The frame was lined with 25 mm thick timber which was painted with varnish on the inside. The front vertical face of the flume was removable to facilitate sand filling and emptying after the completion of each test.

4.2.2 The retaining wall

The retaining wall was suspended at a distance of 600 mm from the front of the flume. It was supported by steel cables, and its weight counterbalanced by steel cylinders filled with lead shot. The steel cables ran over pulleys set within a central box section for dust protection, and this was supported by a rigid frame independent of the flume sides. The wall consisted of three panels, the central one being 390 mm wide and the dummy walls on either side were each 260 mm wide (Fig. 4.2). The purpose of using three sections was to produce a plane state of deformation behind the central wall and eliminate boundary effects. The wall sections were of 29 mm thick duralumin (for choice of wall thickness see Plant, 1972) 660 mm high, 600 mm being embedded in the sand while the remaining 60 mm allowed for positioning of mechanical dial gauges to measure wall displacements.

4.2.3 Earth pressure cells

It was considered necessary to have the capability of measuring the earth pressure distribution on both the front and back faces of the central wall at different construction stages. An indirect method was used for these measurements in which the strains were

measured at different points on both the front and back faces of the wall and then the stresses worked out.

Ten measuring points on each face were considered appropriate to provide a representative distribution of earth pressure. The pressure cells used were machined in one piece from duralumin and were 20 mm wide with an overall length of 90 mm. The pressure responsive diaphragm, 1 mm in thickness, was 50 mm long, to the underside of which two PL2 strain gauges were attached. The design range of the pressure cells was 0 to 7.5 KN/m^2 and at the upper limit the deflection to span ratio of the pressure cell was 1 : 2500 (for the limitations, and design of the pressure cells, see Plant, 1972). Ten grooves were machined on either side of the wall to accommodate the pressure cells. Dummy cells of the same flexibility were positioned between the strain gauged cells to give continuity.

4.2.4 Wall base load transducers

Normal and shear components of reaction at the wall base were also measured to give a better understanding of the overall force system acting on the wall. Two load transducers were installed at the toe of the central wall for that purpose.

The normal load transducer consisted of a thin-walled duralumin tube with a base plate attached to the wall (Fig. 4.3(a)). A central rigid rod transferred the applied load from a footing (50 mm long by 29 mm wide) to the tube. Eight electrical resistance strain gauges were mounted longitudinally and transversely on the peripheral surface of the tube to provide temperature compensation and eliminate possible

bending effects. For the measurement of the shear component of reaction at the wall base, a footing (50 mm long by 29 mm wide) was attached to the end of a strain gauged cantilever machined from duralumin (Fig. 4.3(b)). Temperature compensation was achieved by mounting two strain gauges on each face of the cantilever. Lead wires from the strain gauges for each transducer were carried up in grooves machined in each vertical edge of the central wall (Fig. 4.3(b)).

4.2.5 Anchor load transducers

As the anchor load transducers were to be connected at the front face of the wall, and to avoid excessive excavation below the level of each row of anchors, it was appropriate to use very small proving rings to monitor anchor load changes.

Small duralumin proving rings were designed. These had the same dimensions as those used in the small sand box tests (see Section 3.3.3(iii) and Appendix II). The anchor load which was measured by a small proving ring was transferred to the retaining wall by a duralumin tube. The duralumin tubes used for tests with horizontal anchors were similar to those described earlier in Chapter Three (see Section 3.3.3 and Fig. 3.13), while those used for tests with inclined anchors are shown in Fig. 4.4.

4.2.6 Measurement recording

The lead wires from the earth pressure cells, the wall base load transducers and the anchor load transducers were connected to a

series of brass terminals mounted on terminal boards. These were fed by a 2 volt current using a heavy duty voltage stabilizer. The output from the terminals was fed to fifty channels in a data logger (SOLARTRON LM1426), where the readings were recorded during the different construction stages (Fig. 4.5). In addition a digital voltmeter (SOLARTRON A200) was connected successively to each set of the anchor load transducer terminals to get direct readings during stressing of the anchors.

4.2.7 Embedded anchor units

The anchor units consisted of duralumin strip anchor plates connected via brass anchor rods to the retaining wall. The anchor plates were 388 mm and 258 mm long for the central wall and the dummy walls respectively. The anchor plates were 2.0 mm thick and varied in height and number depending on the required anchor load and depth of embedment. Anchor rods were made of brass and were 2.4 mm in diameter. These varied in length according to the test requirements. Seven rods were used for each row, three for the central wall and two for each dummy side. These passed through the retaining wall and were connected to the small anchor load transducers at the front face of the wall (see Fig. 4.6 for typical anchor units).

4.2.8 Wall movements

Movements of the wall were measured using mechanical dial gauges reading directly to 0.01 mm. At the top of the wall vertical and horizontal displacements were measured by two pairs of dial

gauges. These were fixed by magnetic stands to a cross beam that was connected to the independent frame (see Fig. 4.7). Near the toe of the wall a single dial gauge was connected to the wall via a brass rod set within a brass tube 3 mm in diameter (see Fig. 4.1).

4.2.9 Surface subsidence

The sand surface movements were measured by nine mechanical dial gauges reading to 0.002 mm. These were supported via threaded brass rods from a mild steel frame independent of the test flume. The dial gauge stems rested on small perspex footings 25 mm in diameter and 3 mm thick having four legs, 15 mm long. These were pushed into the sand at nine predetermined positions at distances from the back of the central wall ranging from 60 mm and to 860 mm (Fig. 4.8).

4.2.10 Sand movements

Sand movements within the retained soil behind the central wall were measured in all tests. The sand movement gauges used were a combination of those developed by Carr (1970) and those used by Arber (1976).

Eight horizontal and eight vertical movement gauges were used, giving vectorial displacements at eight locations. The eight locations were at two different distances (200mm and 400 mm) from the back of the wall on each of four levels (150, 250, 450 and 600 mm) below the top sand surface (see Fig. 4.9). These were accurately chosen after establishing the anchor lengths and anchor block

dimensions for the various tests. Care was taken not to obstruct any of the anchors and that is why it was necessary to use two kinds of vertical movement gauges. The displacements of the movement rods were measured using 0.001 in (0.025 mm) mechanical dial gauges.

Horizontal movement gauges comprised a brass conductor tube (4.8 mm in diameter), a brass movement rod (1.6 mm in diameter) and a movement perspex footing, 20 mm diameter, 2 mm thick, which was attached to the tip of the brass rod (Fig. 4.10).

Two kinds of vertical movement gauges were used. In the first, perspex footings similar to those of the horizontal movement gauges were fixed to the tip of the 1.0 mm diameter movement rod and a special sponge rubber attachment was provided at the tip of the 2.0 mm aluminium conducting tube to prevent sand particles from hindering free movement. In the second type, the movement footing was a 6 mm diameter 30° cone which was fixed at the end of the brass movement rods (1.6 mm diameter) which passed through a 4.8 mm diameter brass conducting tube (Fig. 4.10).

The horizontal movement gauges were placed in the sand mass at the required positions during sand filling and the conductor tubes passed through accurately located bushings in the sloping back of the test flume. The first kind of the vertical movement gauges was placed prior to sand filling. These were introduced through vertical bushings located at the sloping back of the flume. The second type of the vertical movement gauges was placed in position after sand filling via guide bushings supported in two rigid steel bars fixed above the sand surface across the flume.

4.2.11 Anchor movements

Anchor movements were measured using brass rods 1.6 mm diameter threaded at one end, and screwed into special drilled holes in the back anchor plate of each anchor block. The brass rods were inside a 2.4 mm aluminium conducting tube. These were passed through bushings located in the sloping back of the sand flume. Mechanical dial gauges were connected to the brass rods outside the flume to measure the anchor movement to an accuracy of 0.001 in (0.025 mm).

4.2.12 Surcharge load

A uniformly distributed surcharge load over an area of 0.4 m by 0.91 m (the width of the flume), and 0.44 m away from the back of the retaining wall, was applied after full excavation to examine the post-construction behaviour of the wall.

A steel frame (Fig. 4.11) constructed from channel sections and a steel plate, 6.35 mm thick, was used to accommodate a pressure bag made of rubber. The bag was confined between the steel plate and the sand surface. The bag was connected via a flexible tubing to a pressure system (regulating valve and pressure gauge), and this in turn to a compressor. The bag was inflated by pressure increments of 5 KN/m^2.

4.3 Calibration of the Measuring Devices

4.3.1 Earth pressure cells

The pressure cells were calibrated over the design pressure range of 0-7.5 KN/m^2. The mild steel frame shown in Fig. 4.12 was

specially made for that purpose. The wall was set in the frame with a polythene air bag between the pressure cells and the upper steel plate. The bag, 750 mm long and 200 mm wide, was made by heat-sealing polythene sheeting 0.006 mm thick. The bag was connected via flexible tubing to a paraffin manometer and air supply cylinder (Fig. 4.13(a)). Zero strain gauge readings were recorded for all cells before placing the polythene bag. The bag was then placed in position and inflated by pressure increments of approximately 1.5 KN/m^2 (Fig. 4.13(b)), care being taken that no creases formed in the polythene. The strain gauge readings were recorded for each increment using the data logger. Finally the bag was deflated by decrements of 1.5 KN/m^2 to zero, and the unloading strain gauge readings were also recorded.

The whole procedure was carried out twice, for the front and back faces of the wall. A calibration curve for each cell was plotted and a straight line relationship was achieved (see Fig. 4.14 for a typical calibration curve). The pressure cells were re-calibrated twice, once mid-way through the testing programme and finally on completion of the test programme. The changes in calibration varied by about $\pm$ 3 per cent.

4.3.2 Wall base transducers

After both transducers were fixed in position in the wall they were calibrated by dead loading.

For calibrating the normal load transducer, the wall had to be held upside down. A special attachment (see Fig. 4.15) was made to

be connected to the central rigid rod of the transducer. Dead weights were placed carefully on the top circular plate of the attachment in increments of 9.81 N (1 kg) up to a maximum of 98.1 N and then reloaded in stages. The output voltage readings were recorded during both loading and unloading stages. A calibration curve was then plotted (see Fig. 4.16).

A special hanger was used to calibrate the shear load transducer (Fig. 4.17). As the transducer was to be subjected to a transverse force from two opposite directions, it had to be calibrated twice, once for each direction. Loading and unloading was carried out in increments of 9.81 N and the calibration curve was plotted (see Fig. 4.18).

4.3.3 Anchor load transducers

All proving rings were stress relieved before calibration in common with all other load transducers.

A brass rod provided with a circular duralumin plate at one end was threaded from its other end and attached to each proving ring in turn. The proving ring was then accommodated in its special duralumin cylinder and suspended in a slotted beam to be calibrated (see Fig. 4.19). Calibration was carried out in increments of loading and unloading cycles.

The output voltage was recorded using both the data logger and the digital voltmeter, the latter being directly connected to the terminals of the proving ring. As the output scales of both the data logger and the digital voltmeter were different, and because

there was a very slight loss in voltage between the terminals and the data logger heads, two calibration curves were obtained. The one associated with the data logger was used when analysing the results and the other during stressing the anchors (see Fig. 4.20 for a typical calibration curve).

4.4 Test Material

4.4.1 Physical properties

The sand used throughout the test programme was obtained from a pit in Derbyshire. The dry sand was passed through a No. 14 sieve (1.18 mm) to remove the fine gravel sizes, and through a No. 72 (212 μm) sieve to remove dust. The material passing through the No. 14 sieve and retained on the No. 72 sieve was used for the tests.

A sieve analysis was carried out and a grading curve was plotted and is shown in Fig. 4.21. The sand had a uniformity coefficient of 1.9 and the mean specific gravity was found to be 2.68. Maximum and minimum densities corresponding to porosities of 33% and 47% were found by previous researchers (Plant, 1972) to be 1.790 Mg/m^3 and 1.42 Mg/m^3 respectively.

4.4.2 Mechanical properties

Standard constant rate of strain shear box tests were carried out on the sand material. The sand samples were slightly stirred to give an average density of 1.52 Mg/m^3. Three tests were performed with normal stress values of 23.8, 34.7 and 45.6 KN/m^2. Results are plotted in Fig. 4.22 indicating a value of the angle of shearing

resistance ϕ' of 37°. Values of ϕ' for the same sand material at a similar density obtained from drained triaxial tests (Plant, 1972; Shah, 1975) were found to vary from 36.4° to 37.2°. Accordingly, the value of 37° was found to be satisfactory and was used in all the calculations throughout the research programme.

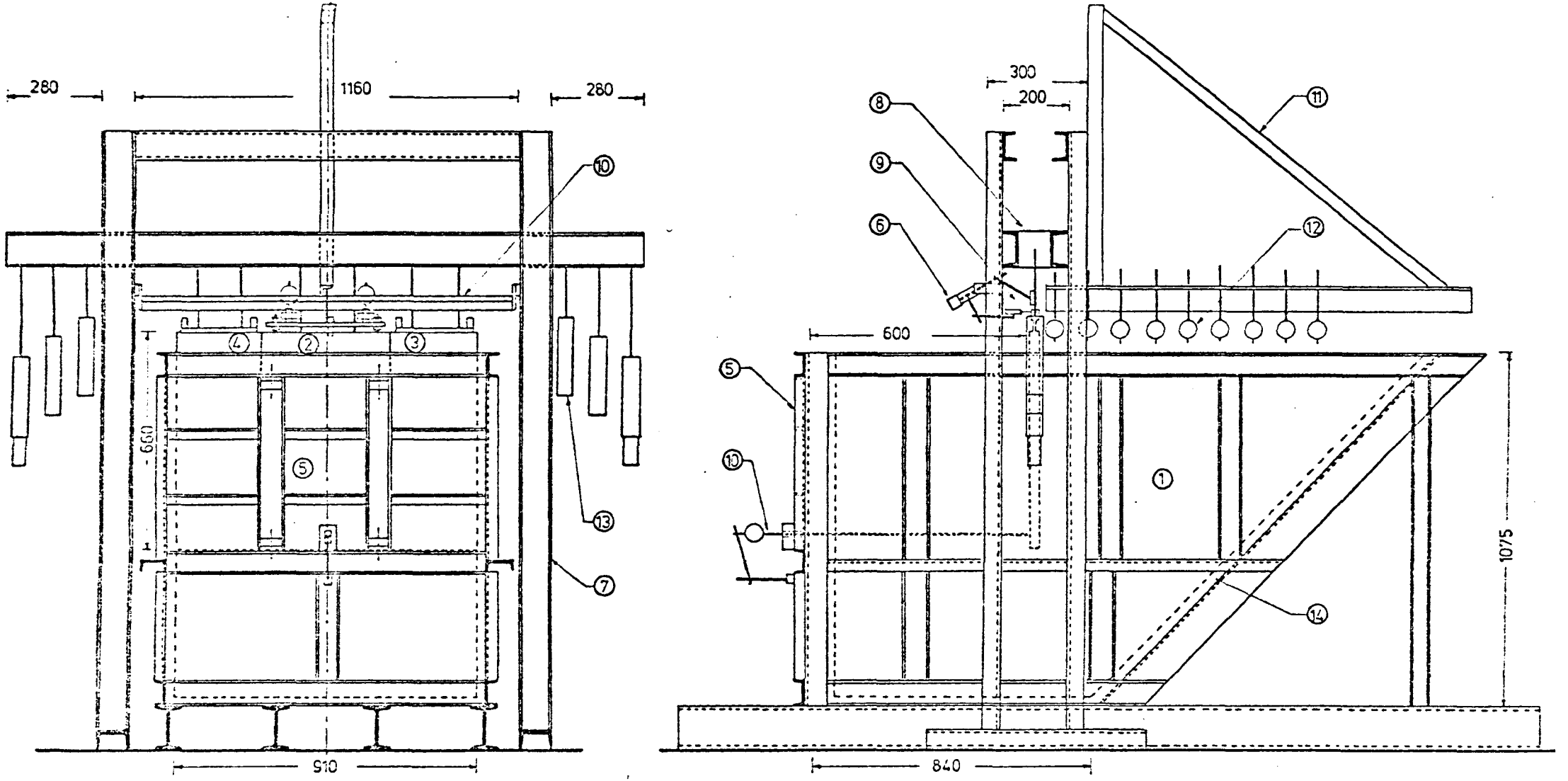

1. MAIN TESTING FRAME
2. MAIN TESTING WALL
3. DUMMY WALL
4. DUMMY WALL
5. REMOVABLE FRONT FACE
6. CROSS BEAM
7. INDEPENDENT FRAME
8. PULLIES COMPARTMENT
9. WALL TOP MOVEMENT GAUGES
10. WALL BOTTOM MOVEMENT GAUGES
11. FRAME SUPPORTING SAND MOVEMENT GAUGES
12. SAND SUBSIDENCE GAUGES
13. COUNTER GAUGES
14. TIMBER LINING

ALL DIMENSIONS IN mm

FIG. 4-1. GENERAL LAYOUT OF THE TESTING FLUME

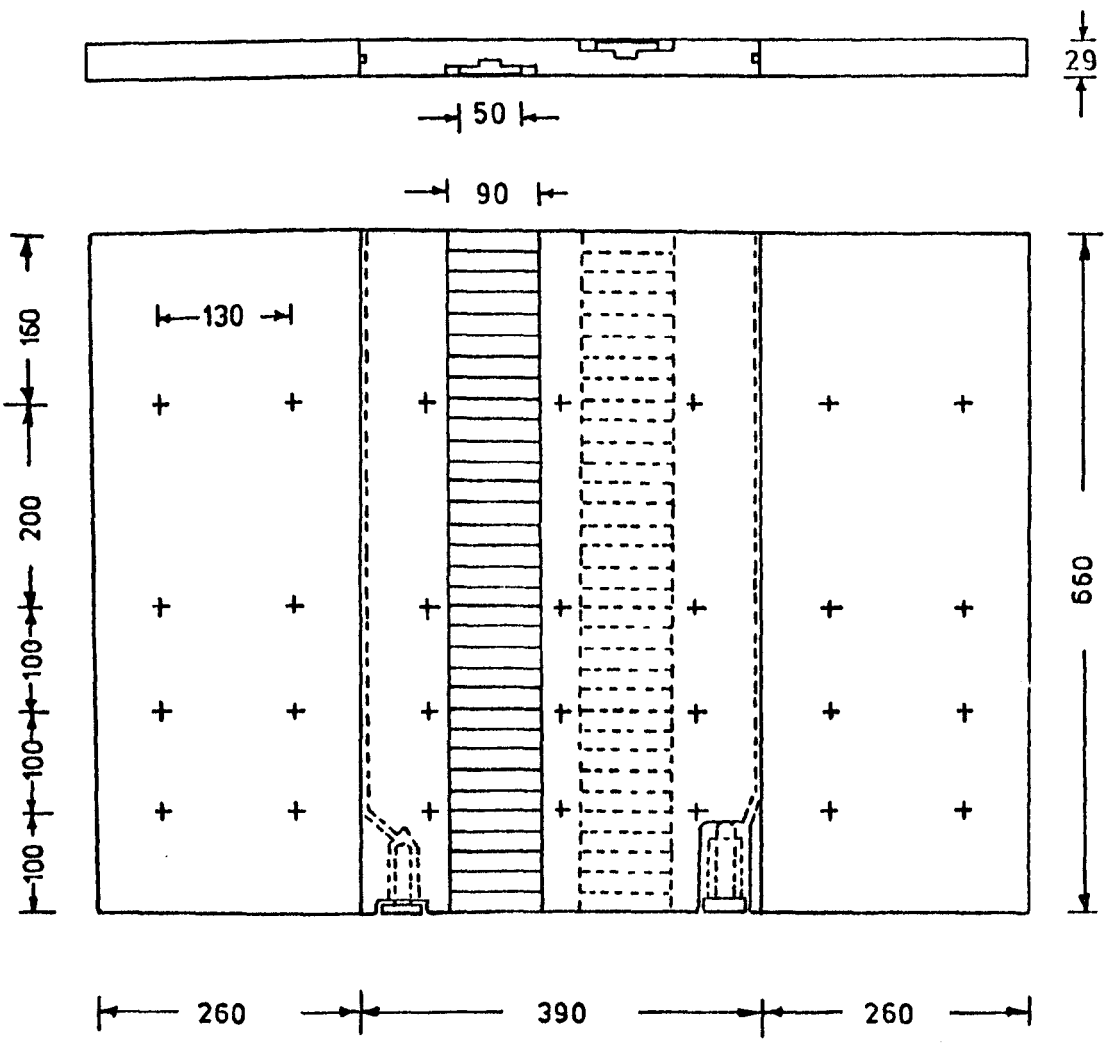

All dimensions in mm

FIG. 4·2 THE TEST WALL

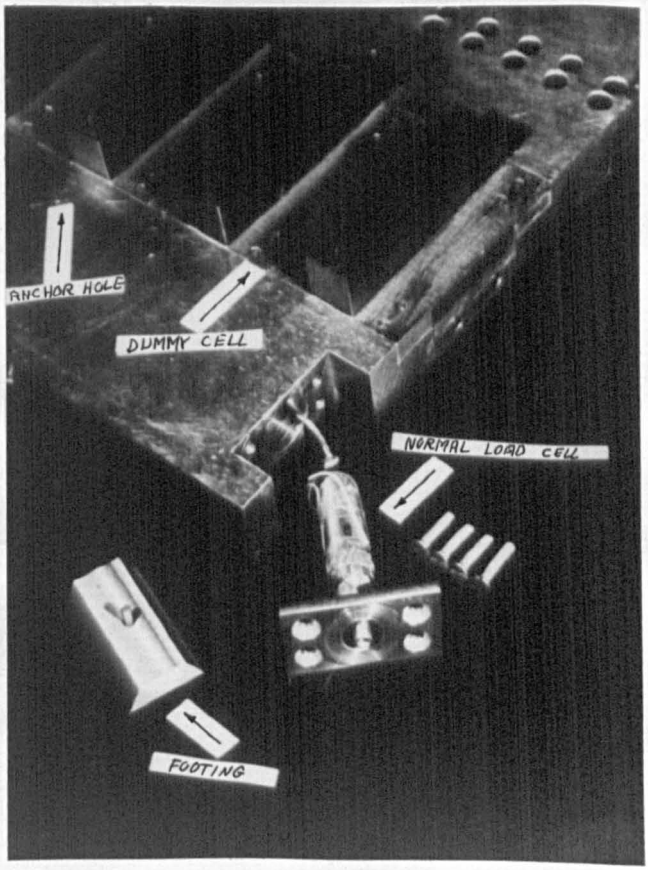

FIG. 4.3 (a) NORMAL LOAD TRANSDUCER

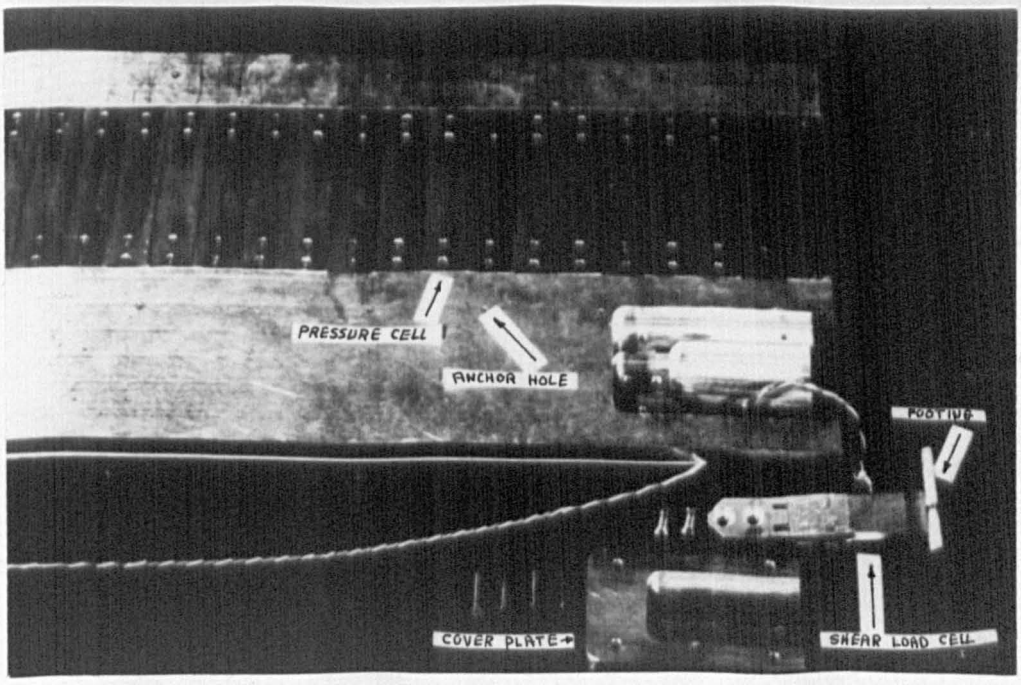

FIG. 4.3 (b) SHEAR LOAD TRANSDUCER

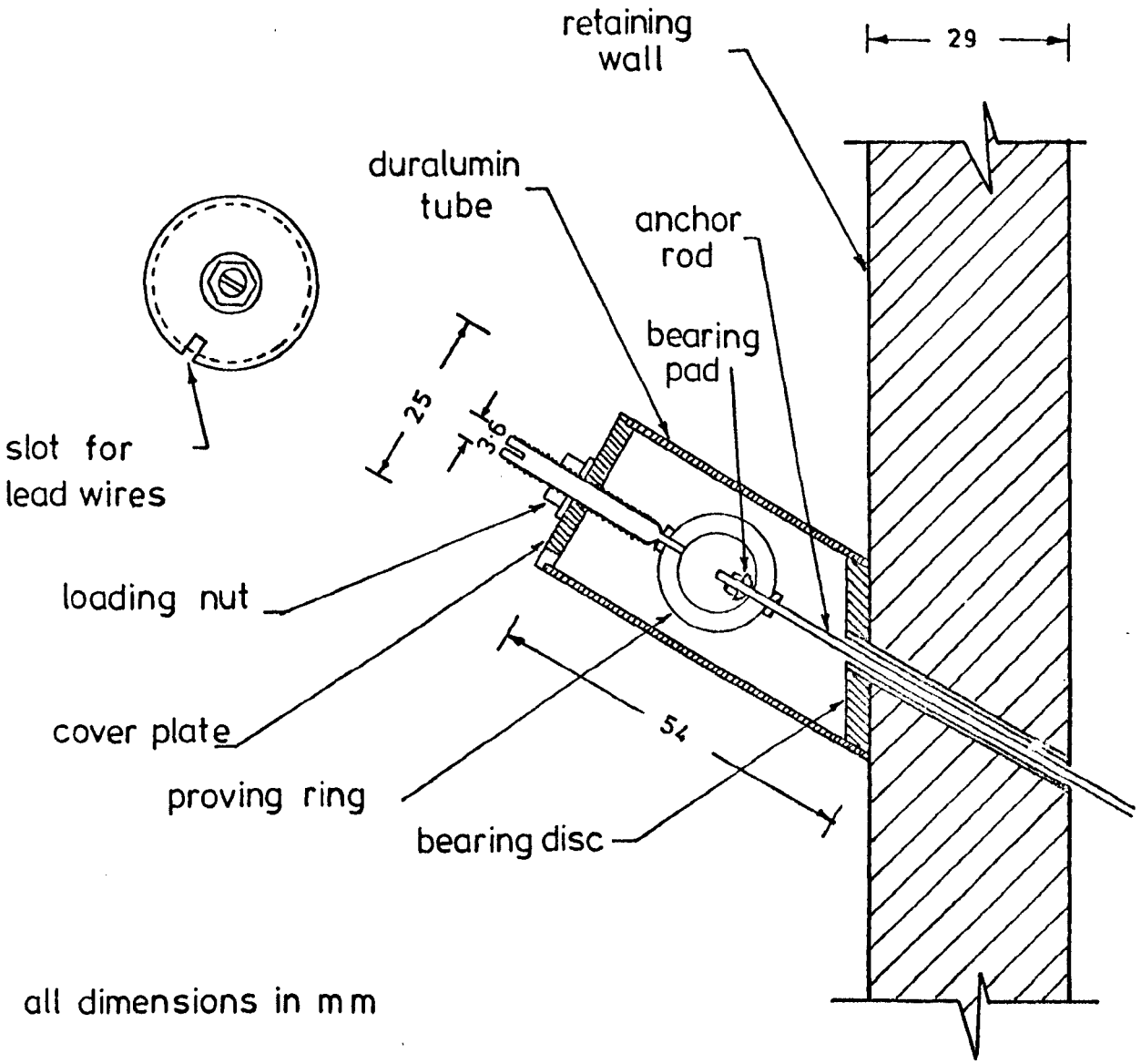

FIG.4·4 LOAD TRANSDUCER ARRANGEMENT FOR 30° INCLINED ANCHORS

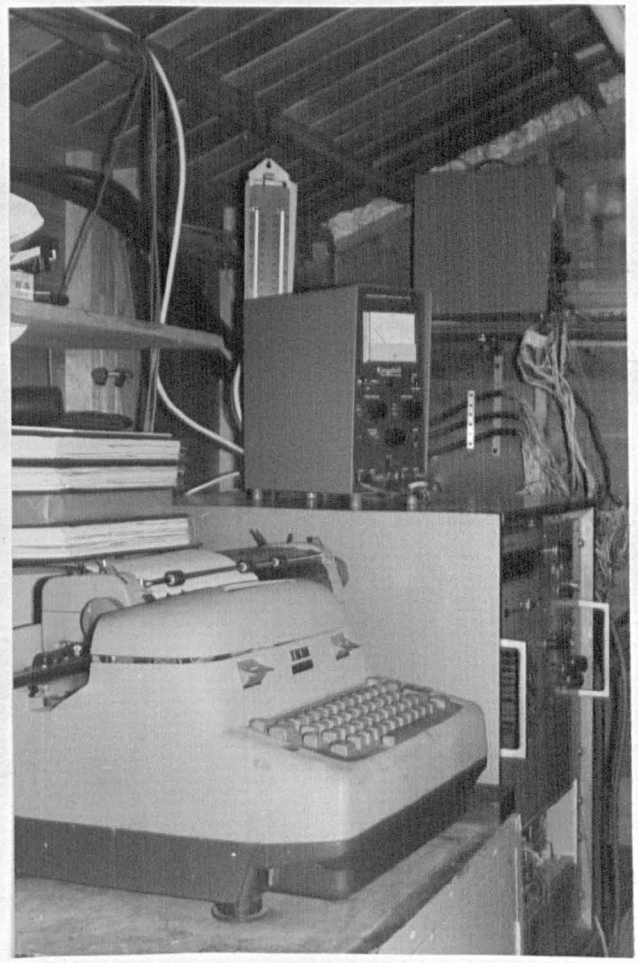

FIG. 4.5 VOLTAGE STABILIZER
AND DATA LOGGER

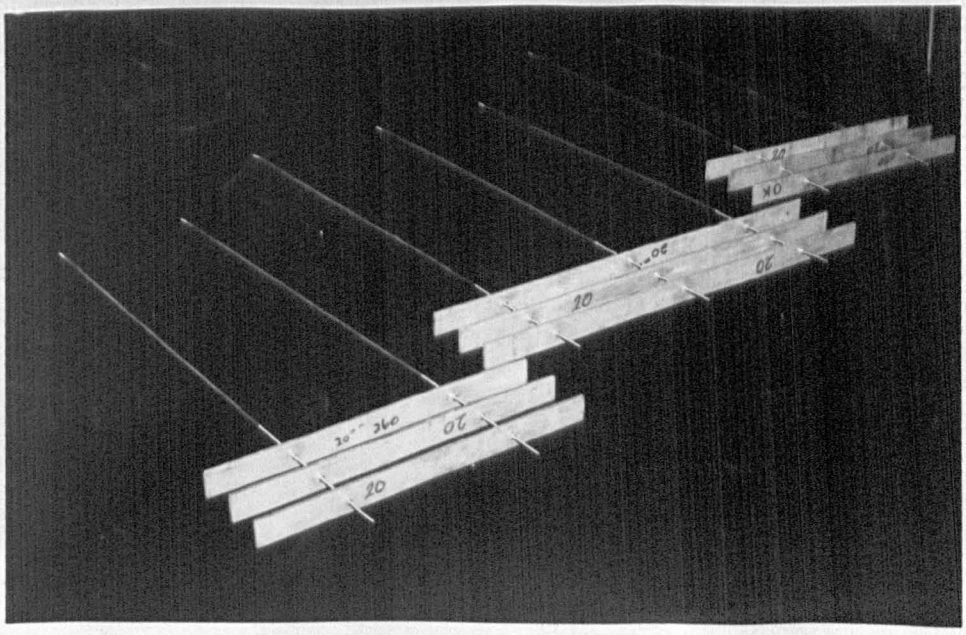

FIG. 4.6 TYPICAL ANCHOR UNITS

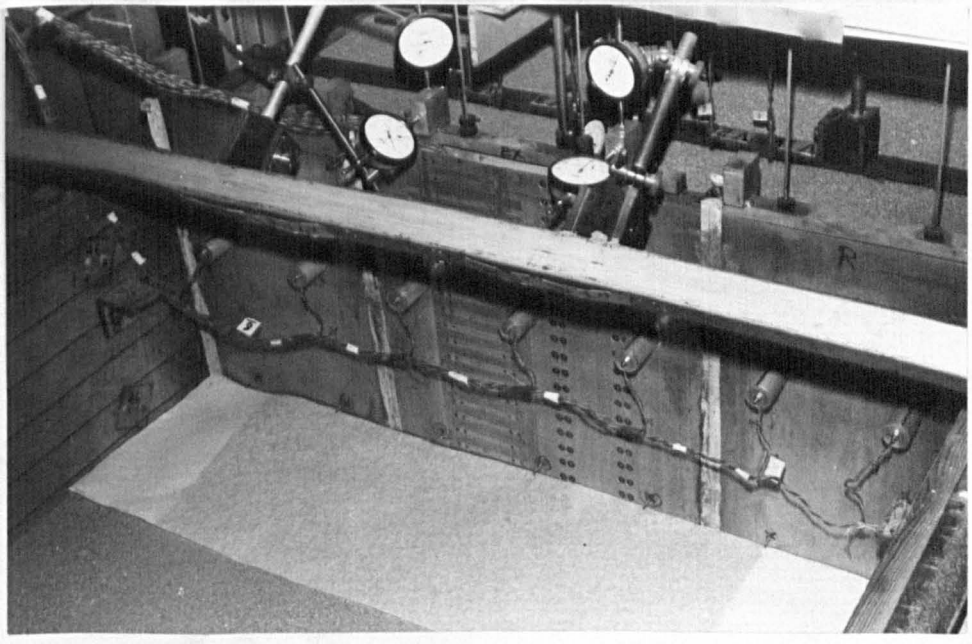

FIG. 4.7 WALL MOVEMENT GAUGES

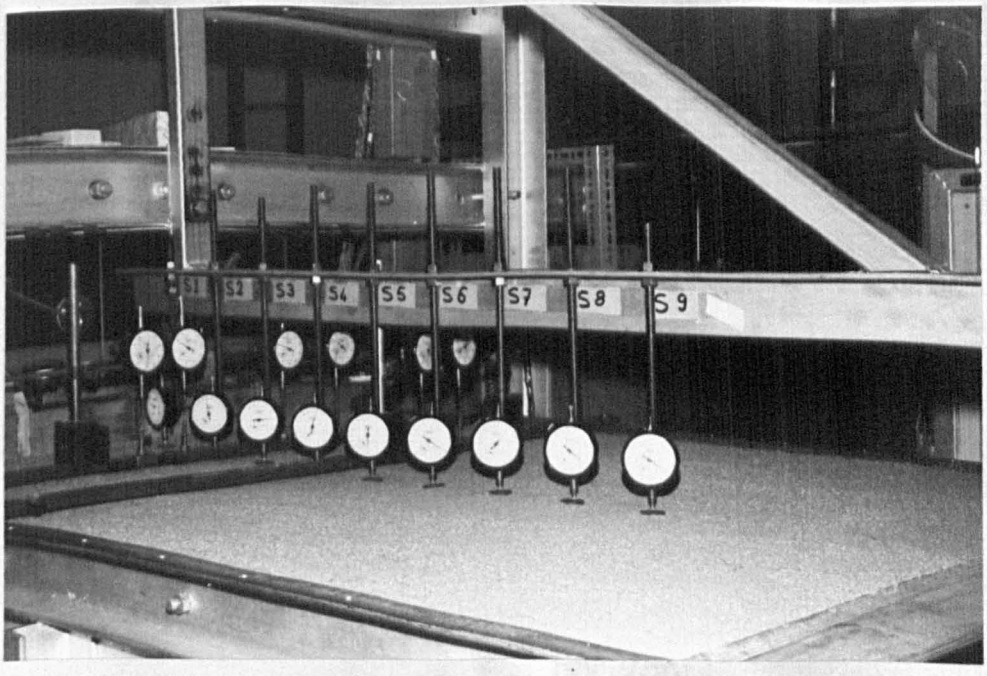

FIG. 4.8 SURFACE SUBSIDENCE GAUGES

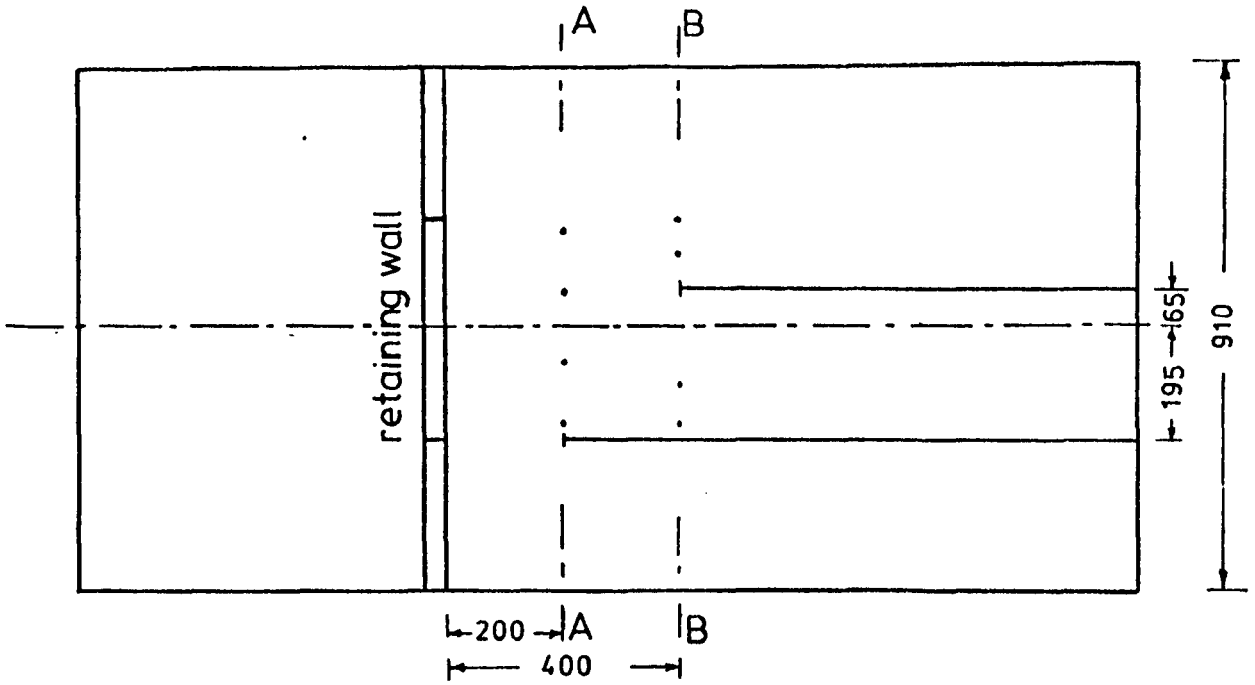

All dimensions in mm

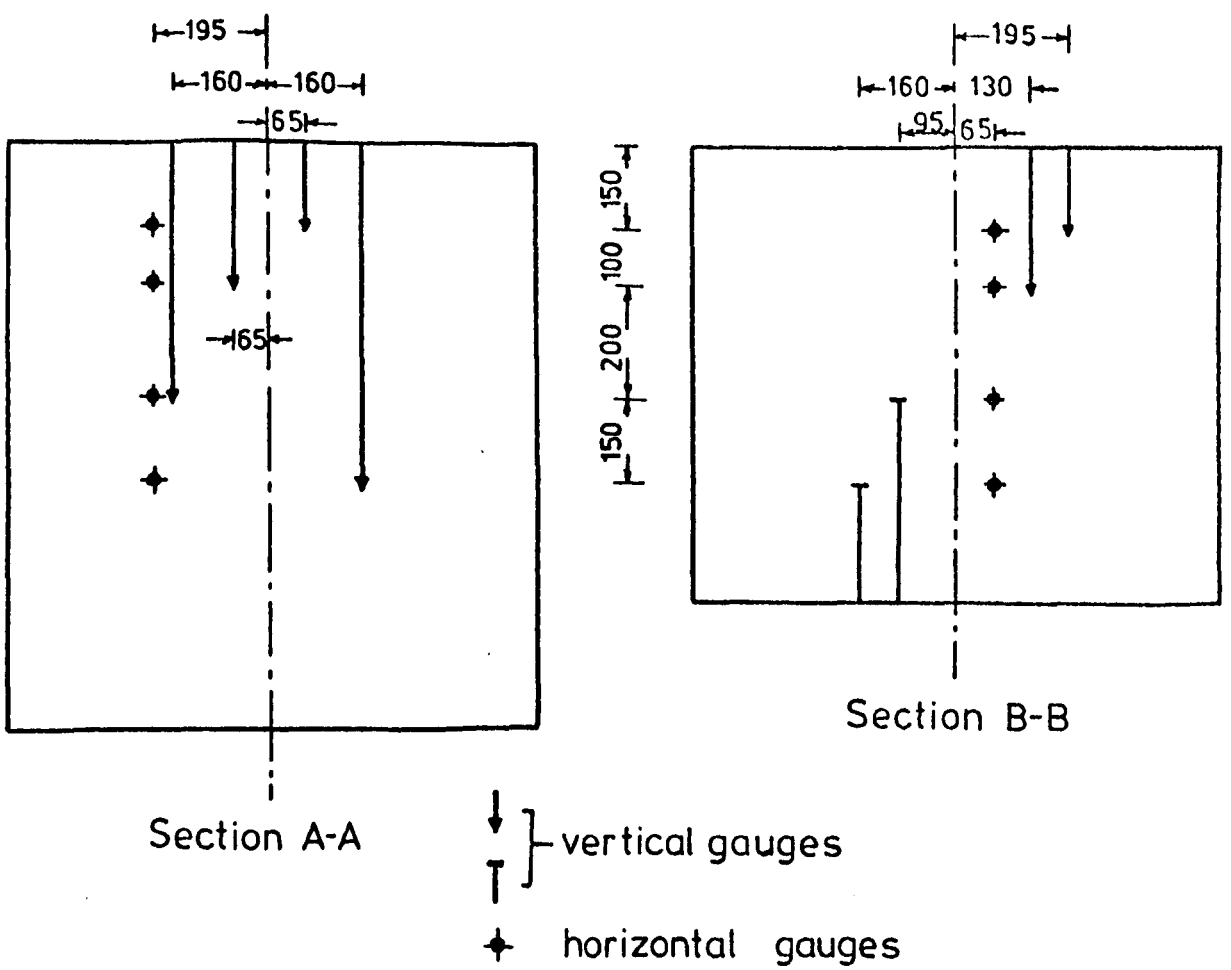

FIG. 4·9 LOCATION OF SAND MOVEMENT GAUGES BEHIND THE CENTRAL WALL

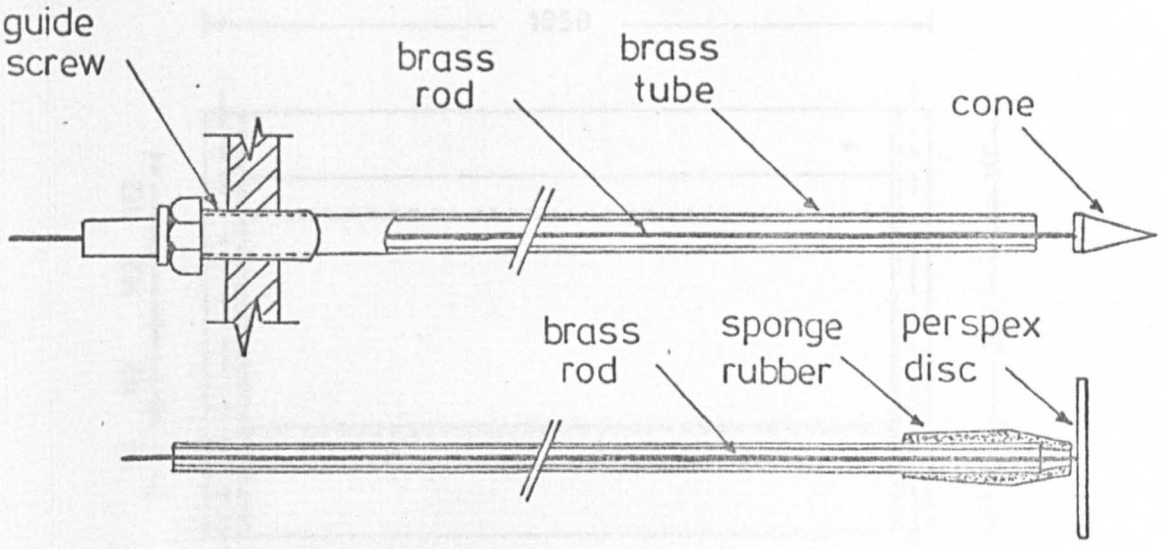

Vertical movement gauges

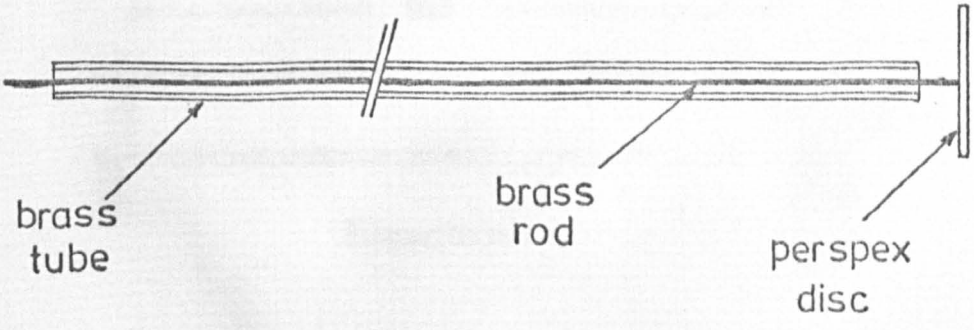

Horizontal movement gauges

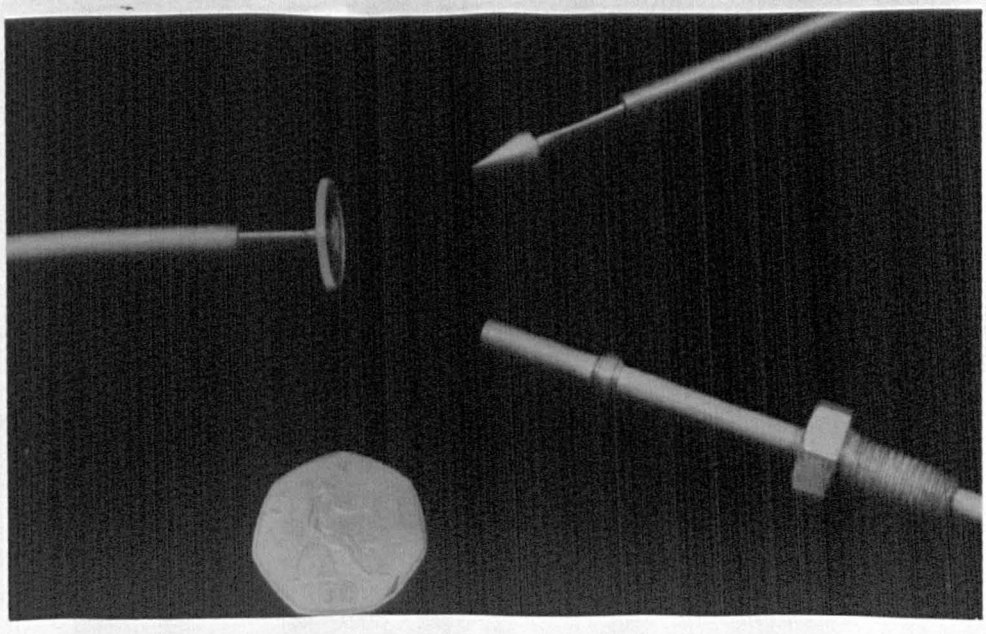

FIG. 4·10 SAND MOVEMENT GAUGES

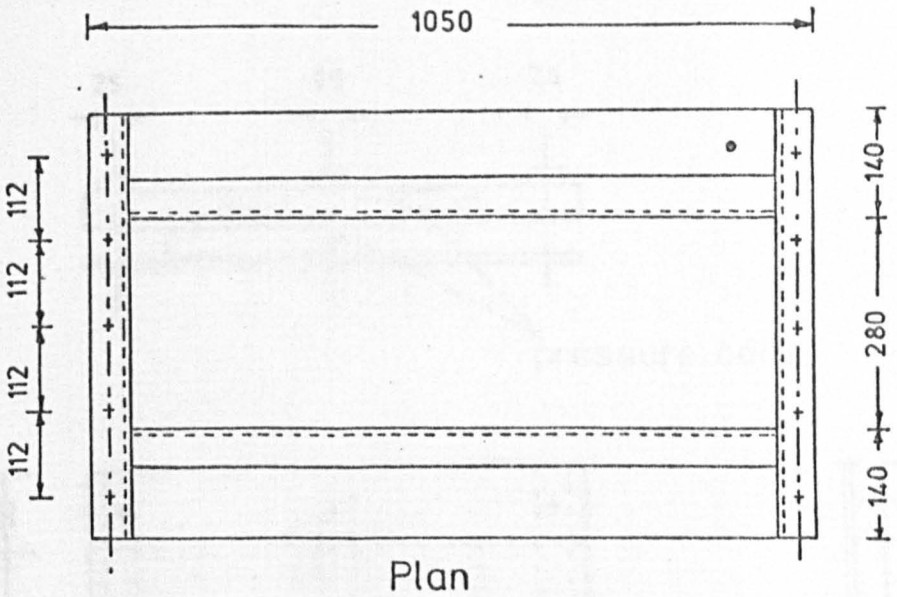

All dimensions in mm

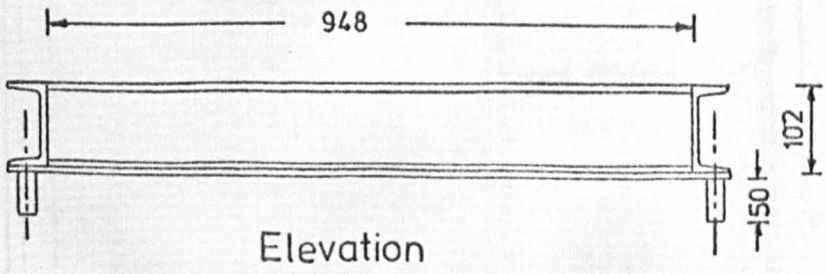

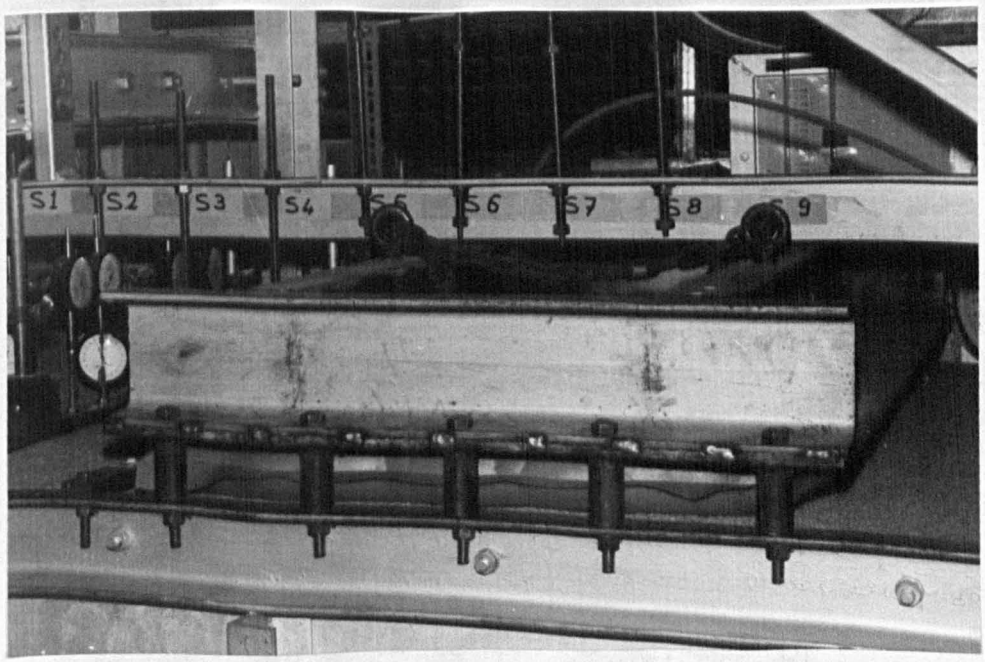

FIG.4·11 SURCHARGE LOAD SYSTEM

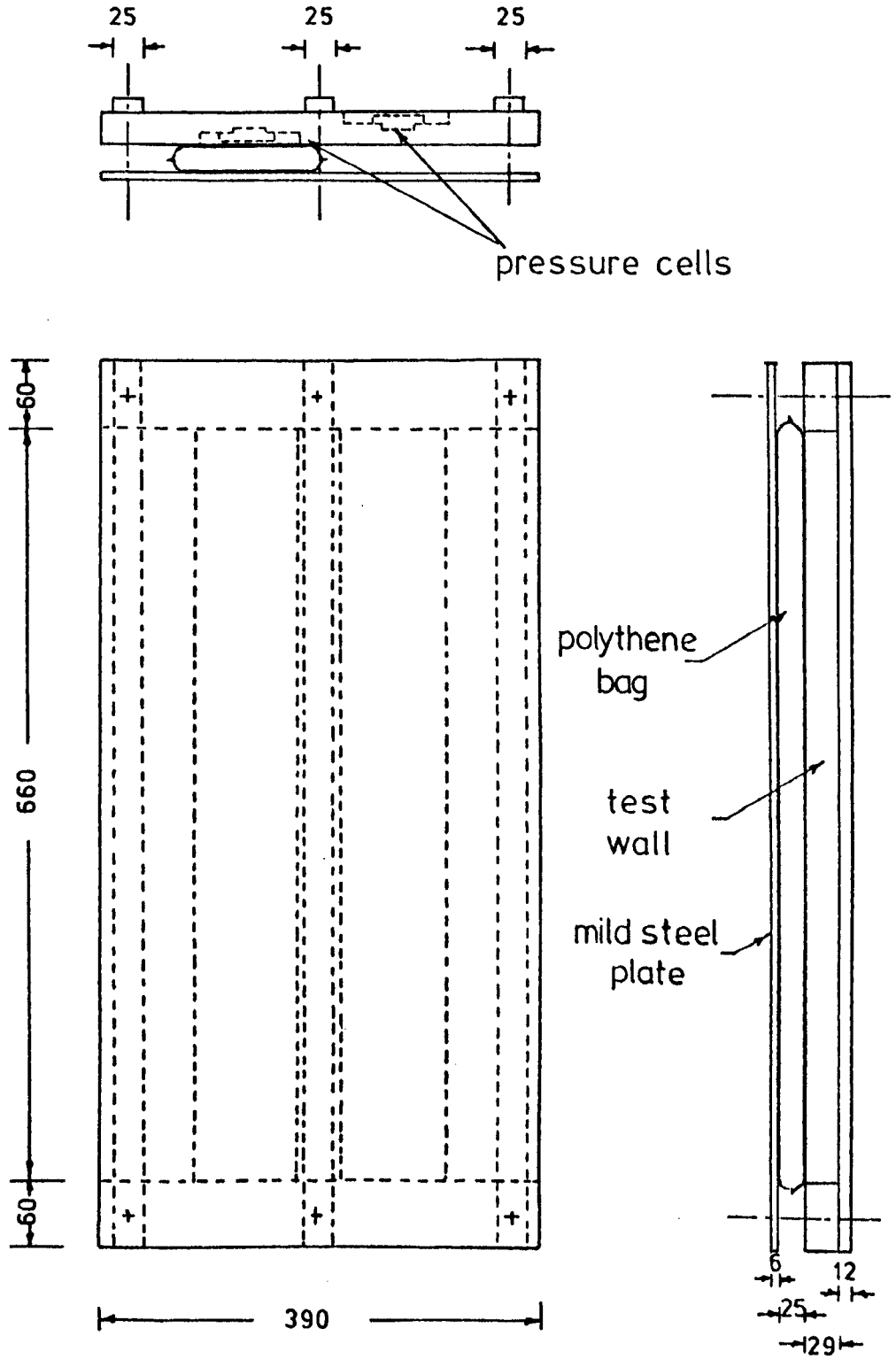

All dimensions in mm

FIG. 412 FRAME FOR CALIBRATION OF EARTH PRESSURE CELLS

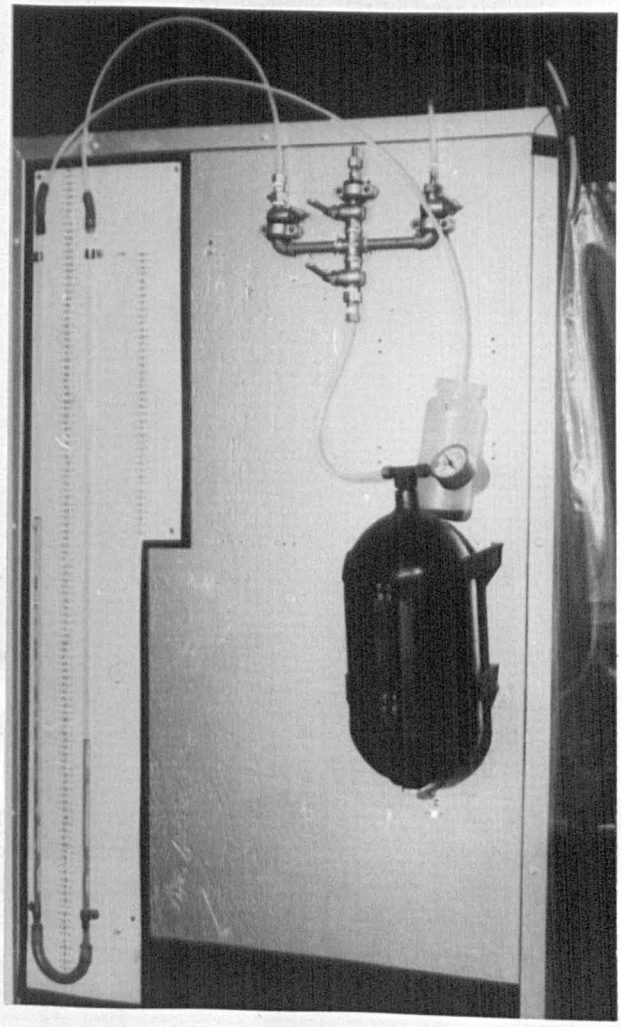

Air supply cylinder, Paraffin manometer and Polythen air bag

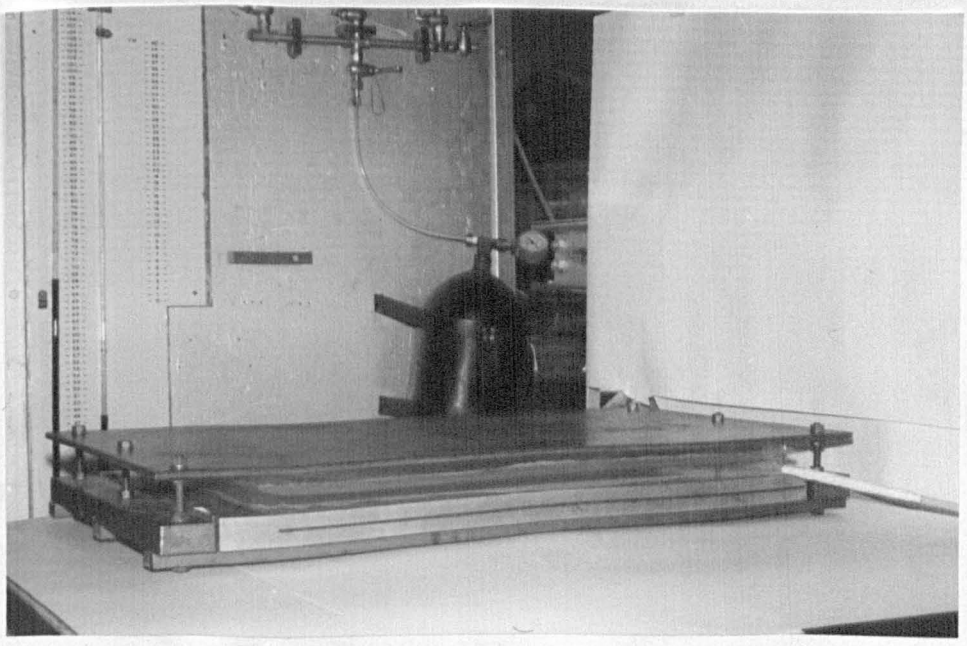

Reaction frame for calibrating pressure cells

FIG. 4.13 CALIBRATION OF THE EARTH PRESSURE CELLS

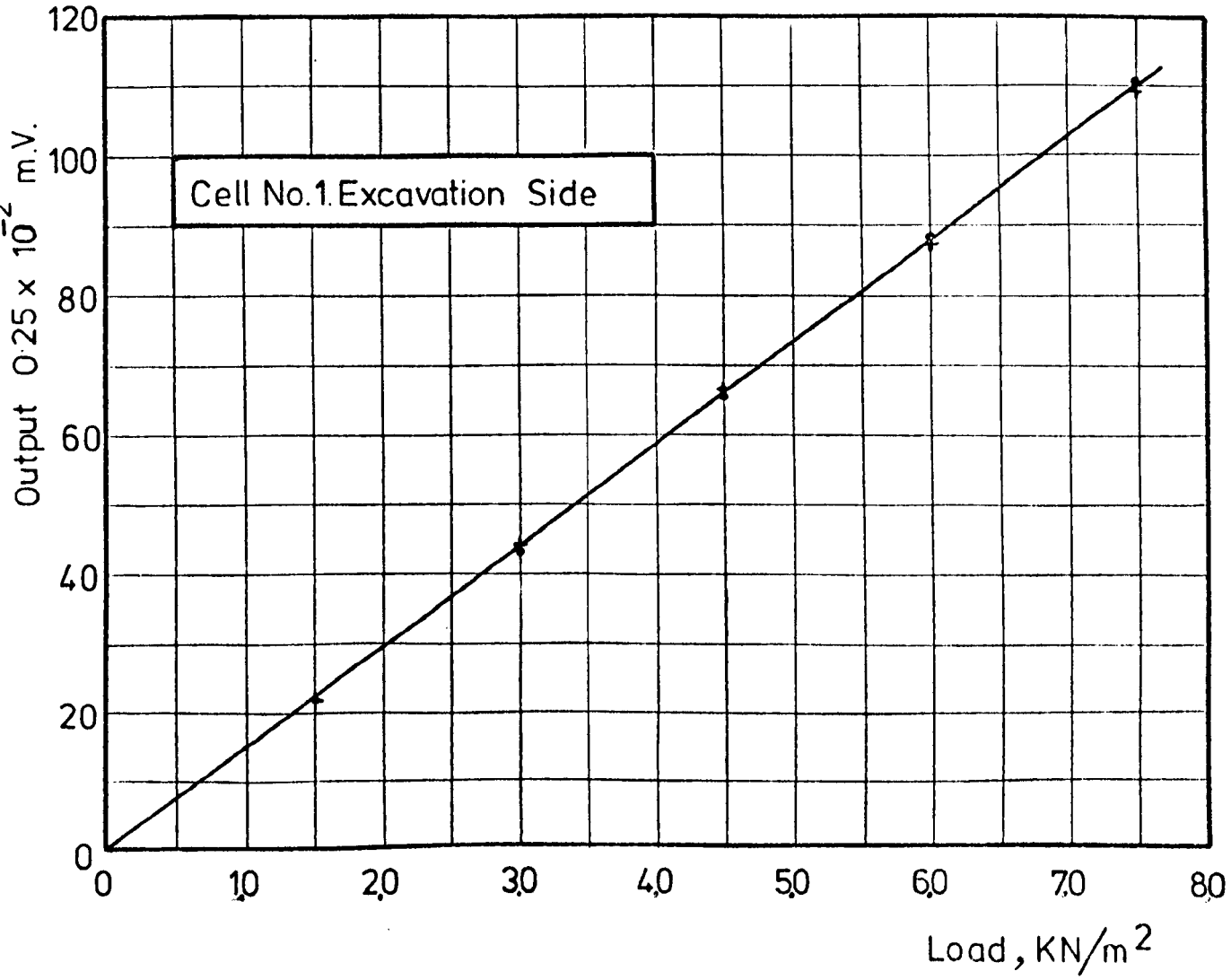

FIG. 4·14 TYPICAL CALIBRATION CURVE FOR A PRESSURE CELL

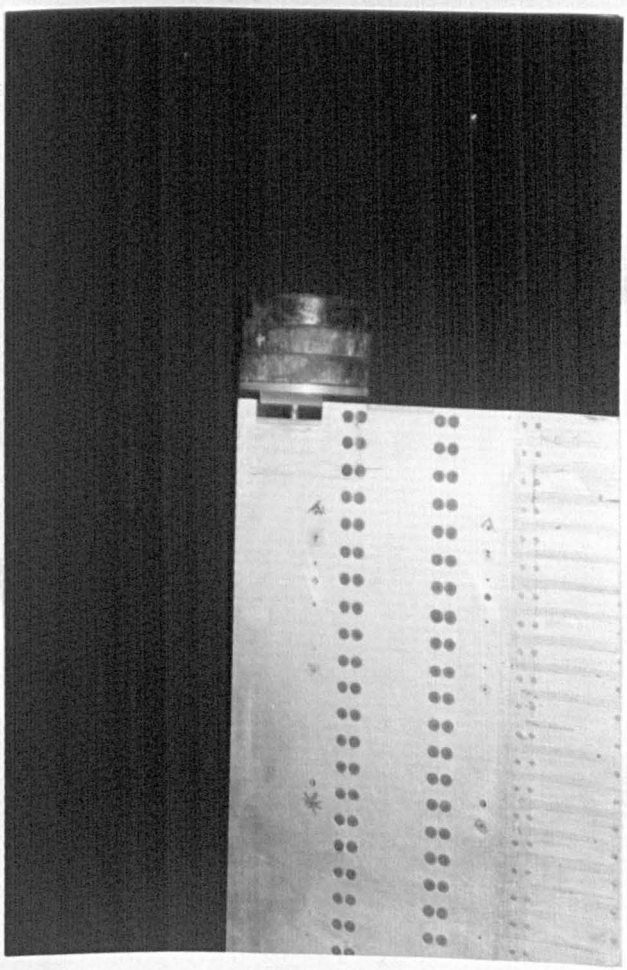

FIG. 4.15 CALIBRATION OF THE NORMAL LOAD TRANSDUCER

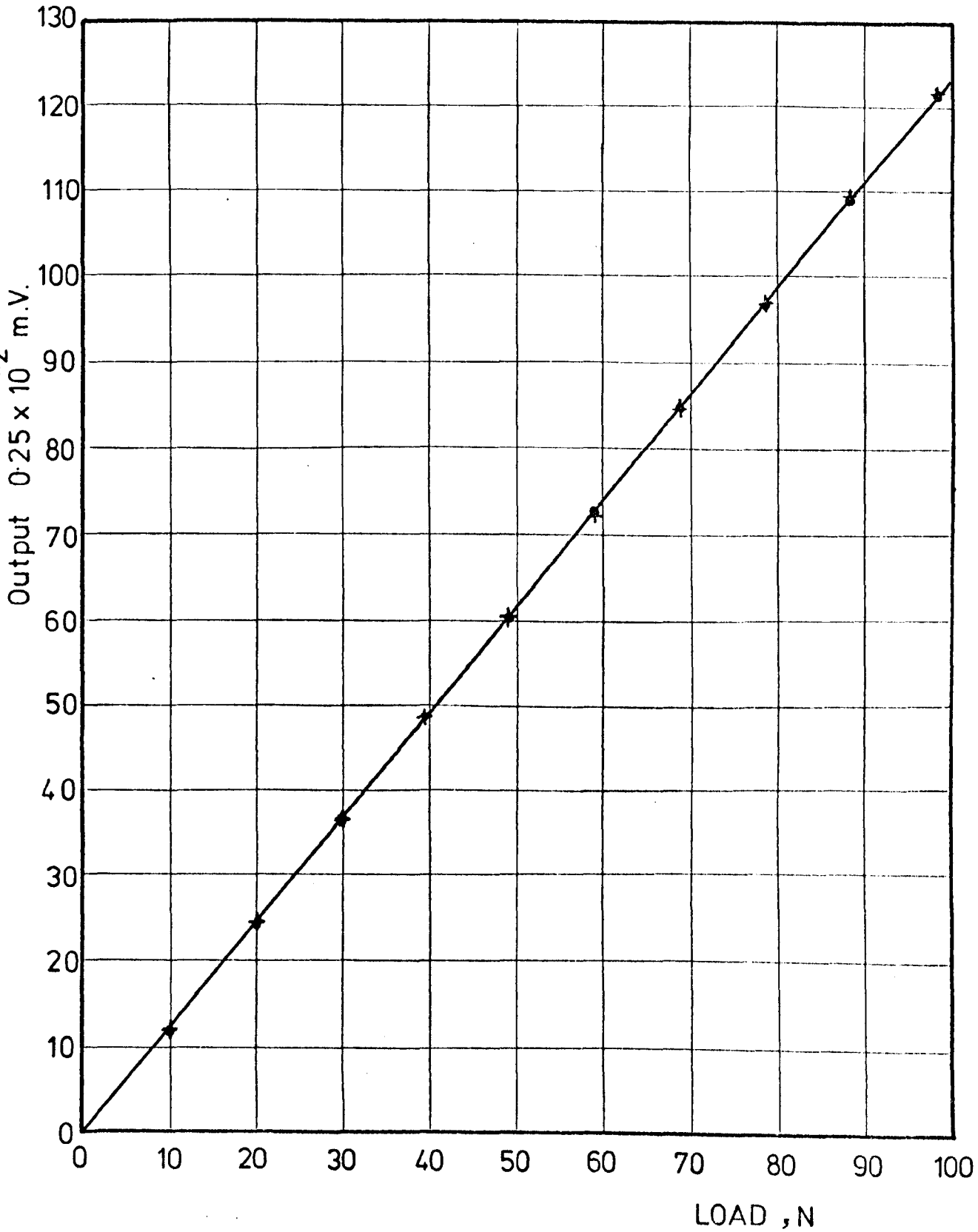

FIG. 4·16 CALIBRATION CURVE FOR NORMAL LOAD TRANSDUCER

all dimensions
in mm

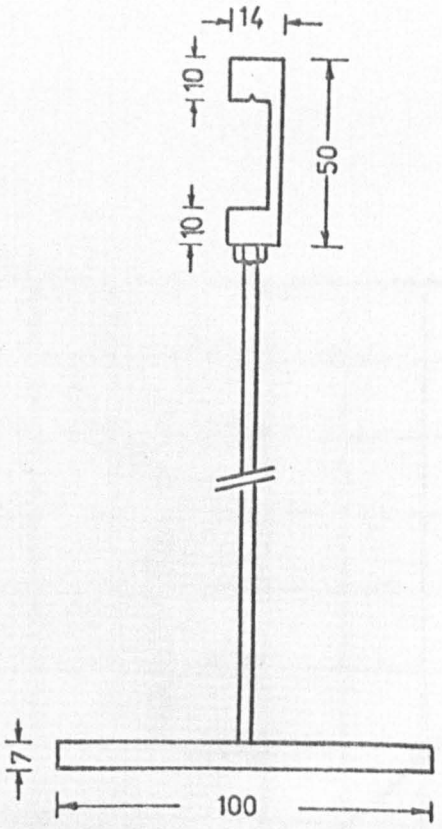

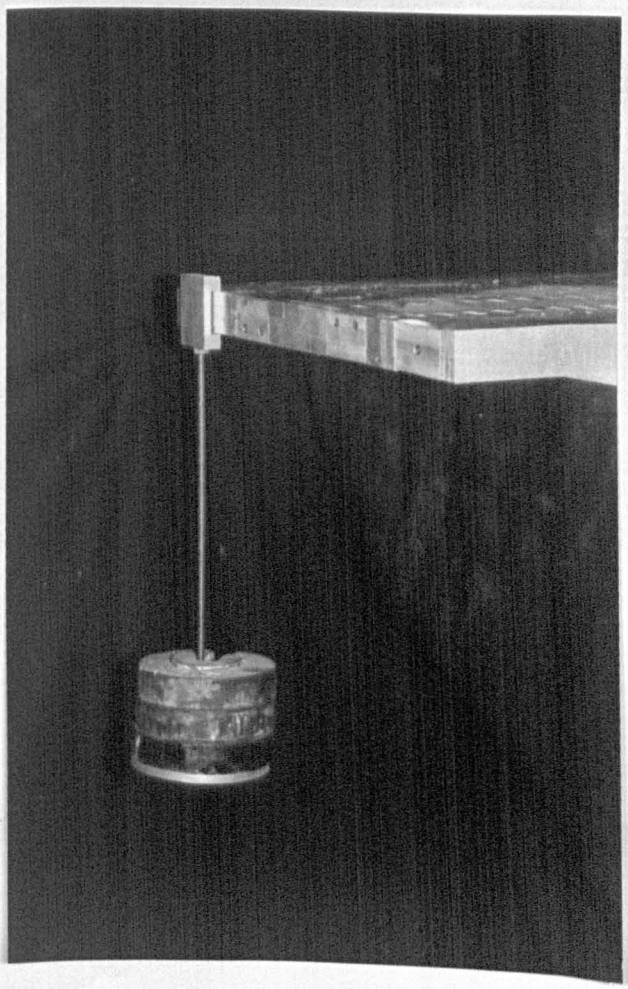

FIG. 4·17 CALIBRATION OF SHEAR LOAD TRANSDUCER

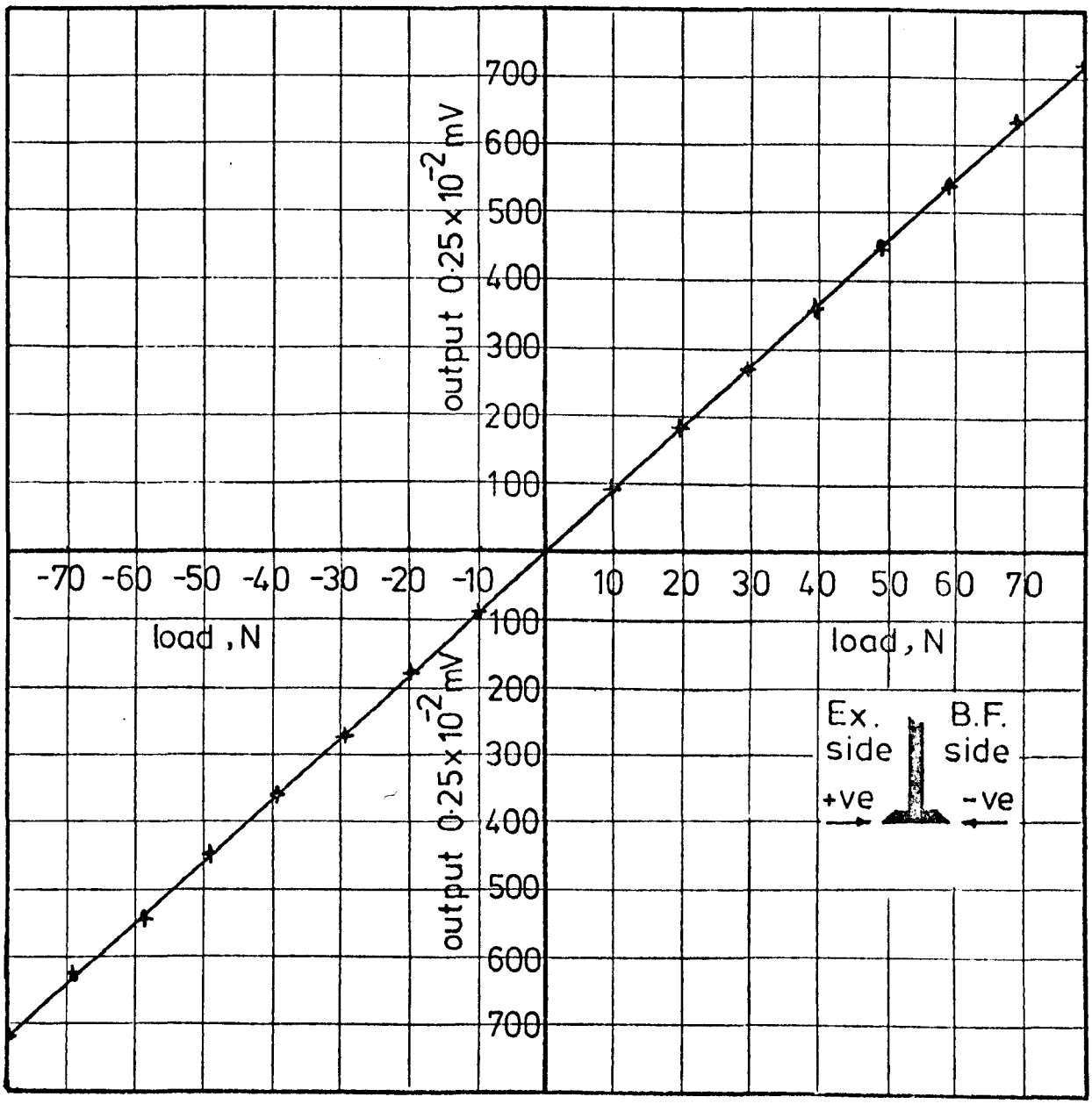

FIG. 4·18 CALIBRATION CURVE OF SHEAR LOAD TRANSDUCER

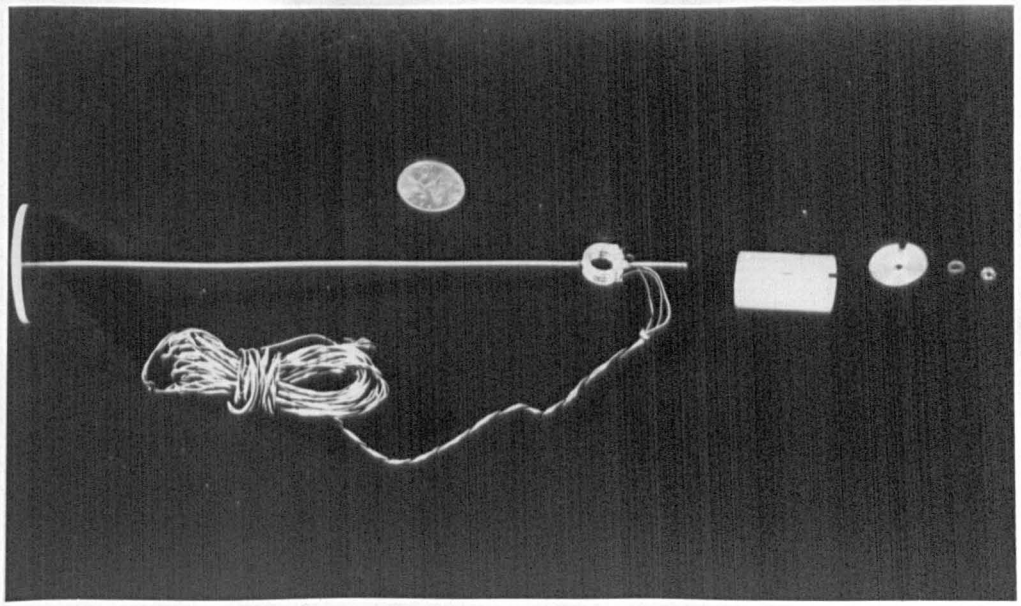

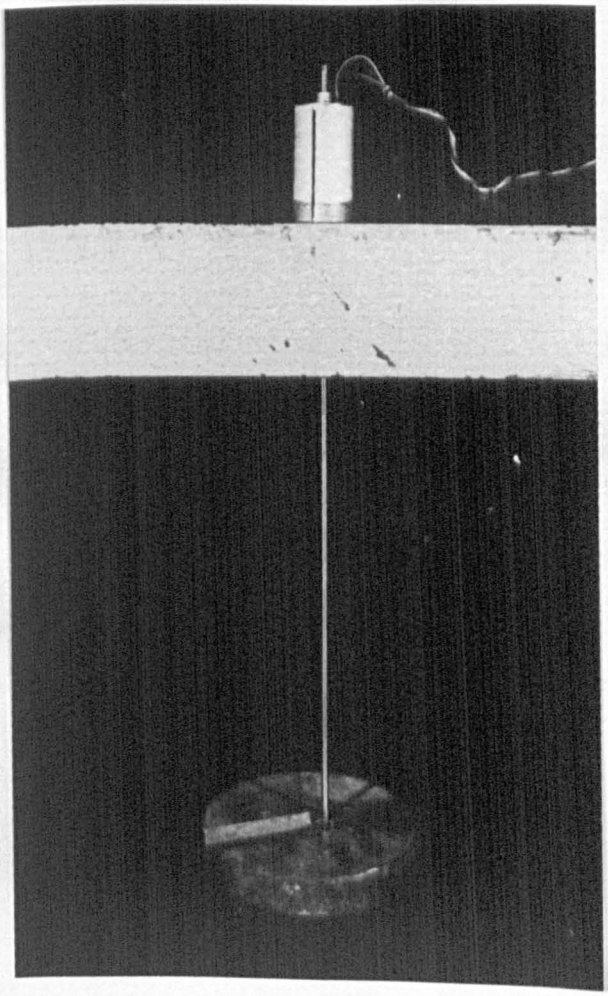

FIG. 4.19 COMPONENTS AND CALIBRATION OF ANCHOR LOAD TRANSDUCERS

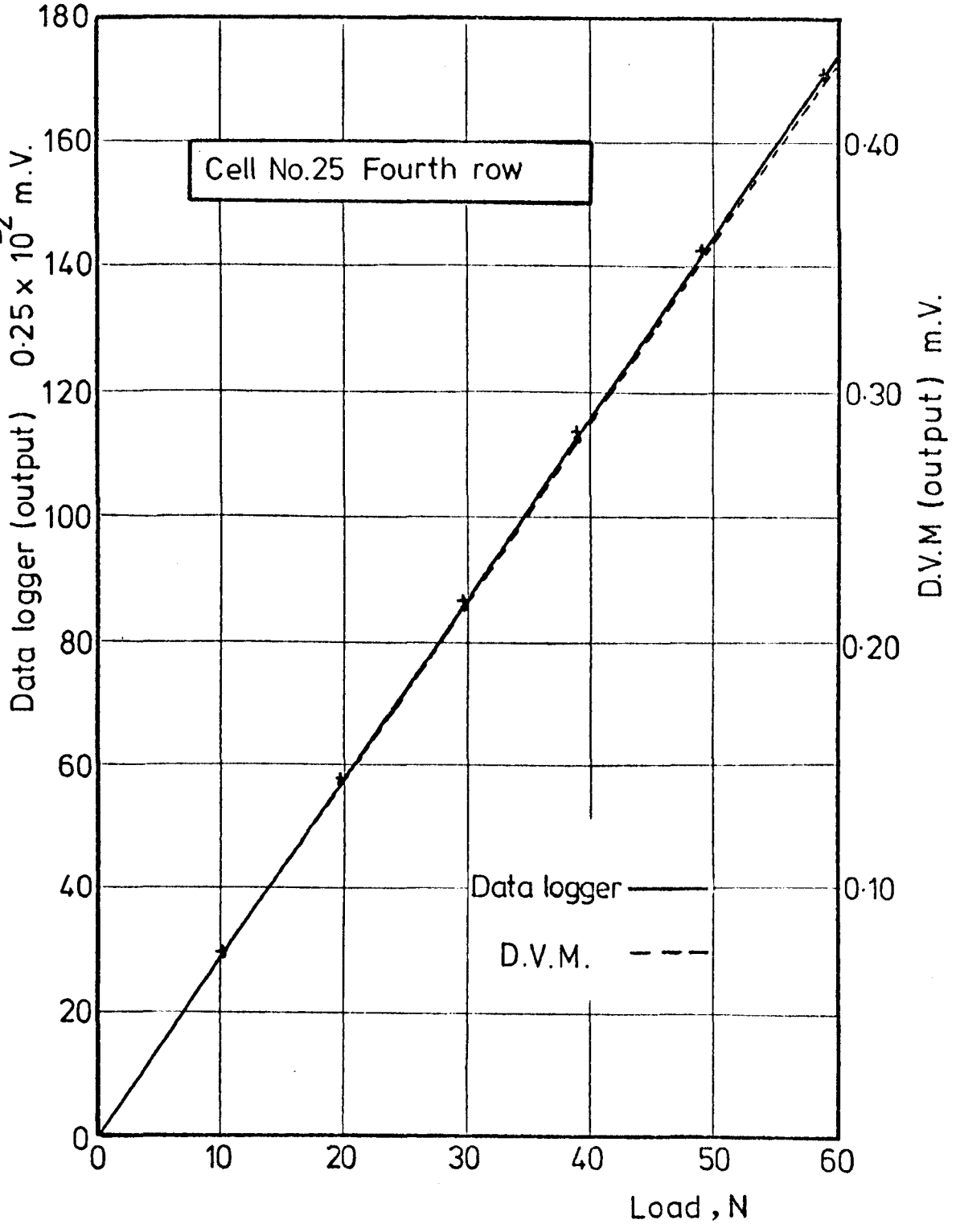

FIG.4·20 TYPICAL "DATA LOGGER" AND "D.V.M." CALIBRATION CURVES FOR A PROVING RING

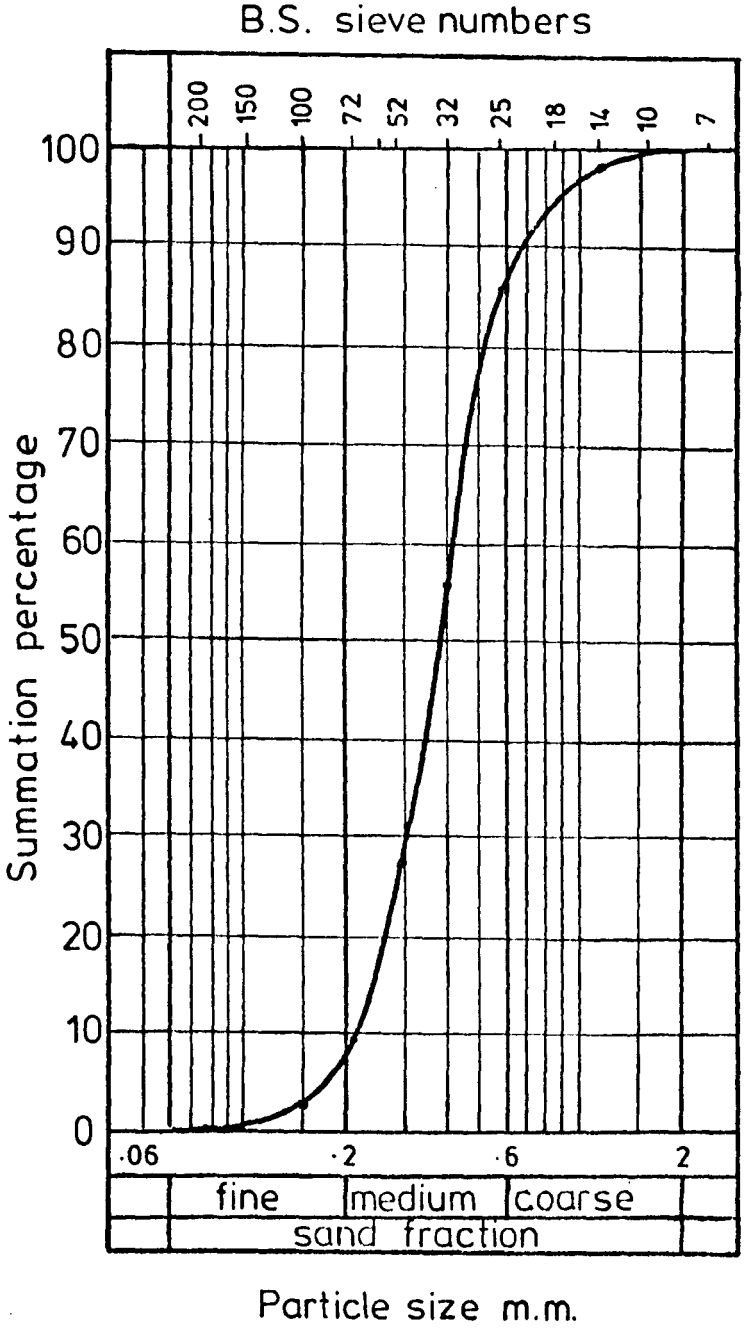

FRI. 4·21 SAND GRADING CURVE

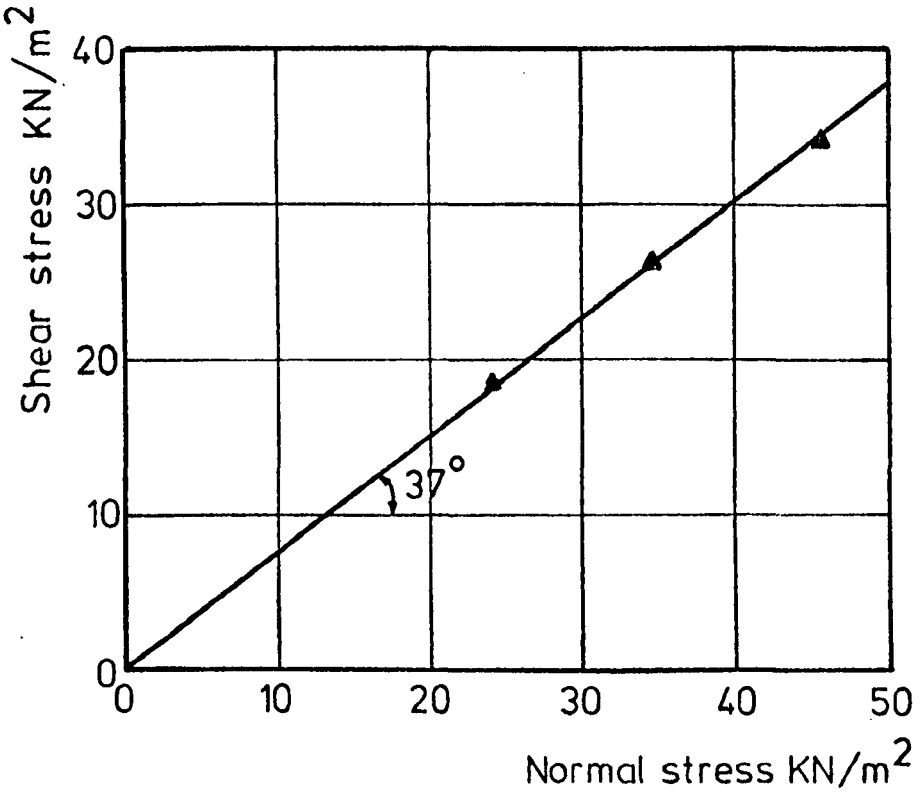

FIG.4·22 MOHR FAILURE ENVELOPE FOR THE SAND MATERIAL

CHAPTER 5

TEST PROGRAMME AND TESTING PROCEDURE

CHAPTER 5

TEST PROGRAMME AND TESTING PROCEDURE

5.1 Introduction

Twenty-three tests were carried out in the main testing apparatus, of which four were of a preliminary nature to assess factors such as the standardization of the method of sand placement and stirring for density control. These tests also allowed minor problems to be overcome. For example, the load transducer readings exhibited hysteresis due to the way they were connected to the anchor rods. This necessitated the modification of the connecting elements. Also rotation of the proving rings occurred during stressing and this necessitated the development of a special stressing device.

Thus the results of nineteen tests are shown in the following chapters, of which three are tests which were performed to check repeatability.

5.2 Test Programme

In the nineteen tests carried out the retaining wall was supported by between two and four rows of prestressed embedded anchor units. The tests were divided into four groups according to the number and inclination of the anchor rows, as follows:

1) Two rows horizontal system,
2) Three rows horizontal system,
3) Four rows horizontal system, and
4) Three rows, 30^{o} inclined system.

In each group four tests were carried out, excluding repeatability tests. In each test a different method was adopted to establish the overall stability of the wall-soil-anchors system.

The design methods adopted were:

Method (A): The anchor forces were determined from a rectangular earth pressure distribution with a value of the coefficient of earth pressure equal to the average of the at-rest coefficient, Ko, and the active coefficient, Ka, as recommended by Hanna and Matallana (1970), and used by previous researchers. The overall stability analysis was carried out according to the method developed by Kranz (1953) and detailed by Plant (1972) (see Chapter Two, Section 2.5.3).

Method (B): Anchor forces were determined as in method (A), while the stability analysis followed the suggestions by Ostermayer (1976) described earlier (see Chapter Two, Section 2.5.3).

Method (C): The same method for determining anchor forces adopted in (A) and (B) was followed. However, the stability analysis was carried out according to the French Code of Practice (1972) (see Chapter Two, Section 2.5.3).

Method (D): Anchor forces were determined using the method developed by James and Jack (1974) and described earlier (Section 2.5.2), while the stability analysis was carried out after the method recommended by Littlejohn (1972) using a spiral failure plane (Section 2.5.3).

The above mentioned four methods when applied to the different systems, yielded a combination of different anchor lengths and anchor loads. These are given in Table 5.1.

5.3 Testing Procedure

5.3.1 Sand placement and test preparation

(a) Preparations before filling

Prior to sand placement, the wall was set in position, and the top of the three panels levelled accurately at 60 mm above the top level of the flume. A thin film of molybdenum disulphide grease was applied to the edges of the wall panels to reduce friction between them, as well as reducing friction between the dummy walls and the timber sides of the flume. Narrow strips (20 mm) of polythene were also provided to prevent sand grains from entering the clearance between the wall sections and the clearance between the dummy walls and the sides of the flume (see Fig. 5.1). The brass rod and its conducting tube for measurement of wall toe displacement was set in position and connected to the wall. Its dial gauge was not connected until the sand filling was completed to avoid any risk of disturbing it.

All anchor units had to be assembled according to the individual test requirements. The required number of anchor plates for each level were connected to the anchor rods at the predetermined spacings at distances from the tips of the anchor rods corresponding to the designed free anchor length plus an allowance of 50 mm which represents the thickness of the wall and a distance of 21 mm for connecting the load cells.

Zero readings of the earth pressure cells and the shear and normal transducers were then recorded.

(b) Sand placement and anchors installation

Sand was weighted out and placed manually in 50 mm layers on either side of the wall, care being taken not to create any pressure difference across the wall. Each layer was carefully stirred in parallel lines of approximately 20 mm spacing with a 3 mm diameter steel rod. The rod was marked at a distance of 60 mm from its end and while stirring the mark was always kept just above the sand surface. This ensured that the rod just penetrated the immediately previous layer to reduce stratification. Stirring was in a direction perpendicular to the retaining wall. The average density obtained by this method was 1.52 Mg/m^3 and the method proved to be satisfactory with a maximum scatter between tests of $\pm$ 0.004 Mg/m^3.

Sand filling was continued until the level of the bottom row of anchors was reached. The assembled anchor units were placed in position. The brass anchor rods passed through the test wall and extended beyond the front face of the wall to enable the load cells to be fitted during the test. Very thin sponge discs 12 mm in diameter were placed over the ends of the brass rods to prevent sand grains entering the clearance holes. Finally, the anchor movement rod and its conducting tube was introduced from the back of the flume and connected to the trailing plate in the anchor block. Fig. 5.2 shows a block of anchors in position prior to further filling. The sand was carefully stirred around each anchor block in the same way as with the preceding sand layers. Sand filling was continued, placing the anchor units at the appropriate levels until the final sand level was reached.

During the filling process the normal load transducer showed a

gradual increase in the normal reaction at the base of the wall. After completion, the shear load transducer was always at or near zero, indicating that no rotation or translation of the wall had occurred.

(c) Positioning of the sand movement gauges

As mentioned before, three kinds of movement gauges were used, one for measuring horizontal movements and two for measuring vertical movements. The horizontal movement gauges were placed while sand filling progressed, whereas two of the vertical movement gauges were placed prior to sand filling and the rest after the completion of filling.

(i) Horizontal Movement Gauges:

The gauges were positioned at four levels at two different distances from the wall (see Fig. 4.10).

When the sand in the flume reached the required level for the horizontal gauges, they were placed in position on the sand surface with the end of the conducting tube in contact with the movement footing. Care was taken to position the movement footing at the correct distance from the wall and to ensure that the conductor tubes were horizontal. A short length of the conductor tube and a longer length of the movement rod were then protruding beyond the guide bushing outside the back wall of the flume. All the horizontal movement gauges were positioned at their predetermined locations during sand filling, particular care being taken during stirring not to disturb any of them.

(ii) Vertical Movement Gauges:

Two out of the eight vertical movement gauges were placed prior to sand filling (see Section 4.2.10). These were introduced through vertical guide bushings at the bottom of the sloping back of the flume and fixed at their predetermined levels, one at the base level of the wall and the other 150 mm above this level. Great care was taken during sand placement and stirring to avoid disturbing them. The rest of the vertical movement gauges were positioned after completion of sand filling using two rigid steel bars fixed across the flume and above the final sand level. The two bars were provided with six tapped holes to fix the guide bushings of the movement gauges and were located at distances of 200 and 400 mm behind the wall.

After the final sand surface was levelled, the steel bars were fixed across the flume and the vertical gauges carefully pushed through the guide bushings into the sand until a collar near the top end of the conductor tube reached the top of the guide bushing. This fixed the correct level of the gauge footings.

The positions of both the horizontal and the vertical movement gauges were chosen in such a manner that none of the gauges interacted and none of them obstructed the movements of the anchor blocks. By combining the vertical and horizontal movement readings and assuming uniform displacement behind the wall, the vectorial sand movements at eight positions were obtained.

(d) Positioning of the sand subsidence, wall movement and anchor movement gauges

(i) Sand Subsidence Gauges:

After the final sand surface was carefully levelled, the mild steel frame supporting the dial gauges for sand subsidence measurements was fixed in position. This was originally removed to facilitate the procedure of sand filling and to provide enough room for adequate stirring. The perspex sand subsidence footings were then placed in position and the dial gauge stems lowered to make contact with these footings. Allowance was made for the dial gauge stems to move either upward or downward.

(ii) Wall Movement Gauges:

Two pairs of mechanical dial gauges supported by magnetic bases were attached to a cross beam (see Section 4.2.8 and Fig. 4.7) and were adjusted to measure the vertical and horizontal wall displacements at two different locations. A fifth dial gauge was connected to the wall toe movement rod and fixed outside the front face of the flume using a magnetic base.

(iii) Sand and Anchor Movement Gauges:

Mechanical dial gauges with the screws removed from the lower end of their stems enabled all movement rods to be fitted within the stems using special brass adaptors. These were placed in position using magnetic stands, and accurately adjusted with the stems perfectly horizontal (for horizontal sand movements and anchor movements) or vertical (for vertical sand movements).

Prior to the start of the test the conductor tubes of the vertical and horizontal sand movement gauges were adjusted so that the movement footings were free to move as the retained sand deformed.

The positioning of the dial gauges and adjusting the conductor tubes completed the test preparation. All zero readings of the dial gauges were recorded, together with all the readings of the earth pressure cells and the shear and normal transducers.

Assembling the anchor units together with filling the flume and doing all the test preparations normally took two days to accomplish.

5.3.2 Excavation and anchor stressing

(a) Excavation

Prior to the start of excavation the at-rest earth pressure distribution against the wall was recorded by the ten pressure cells on each side of the wall, together with the zero readings of both load transducers at the wall base.

The sand at the front of the wall was then excavated manually to a level 20 mm below the first row of the anchors simulating field construction. This space of 20 mm was necessary to accommodate the anchor load transducers. A time interval of 10 minutes was allowed and then all instruments were recorded.

(b) Connecting the load transducers

The thin sponge discs, which prevented sand grains entering the holes in the wall, were removed and the small proving rings brought

to their position to be attached to the anchor rods. The anchor rods were threaded and had a length of 2 mm turned to the root diameter which greatly assisted in the placement of the nuts to secure the proving rings. A nut was screwed onto the rod, followed by the proving ring, a bearing pad and a securing nut to fix the ring in position (see Fig. 4.4). The bearing pad was machined of steel and was half a cylinder in shape, with a 2.4 mm diameter hole perpendicular to the centre line of the cylinder, the cylinder being 5.00 mm in diameter and 10 mm long. This was attached with its curved side resting on the inner circumference of the proving ring and with the securing nut resting on its flat side. The bearing pad insured secure attachment of the ring, and it also prevented stress concentration which would have resulted by the nut resting directly on the proving ring, and it eliminated any hysteresis in the readings of the ring.

When all seven proving rings had been attached, their zero readings were recorded on both the data logger and the digital voltmeter.

The remaining components of the anchor load transducers were then placed. These comprised a slotted tube, a cover plate, a brass washer and a loading nut (see Fig. 4.4). Care was taken during placement of all these components not to disturb the proving rings. However, all readings were recorded again to ensure no measurable disturbance.

The miniature size of the different components of the load transducers made the connecting process very delicate and time-consuming; however, they produced an elegant method for load application and monitoring.

(c) Stressing the anchors

A special device was prepared to facilitate the stressing process and to prevent any rotation of the proving rings. This consisted of a steel plate 910 mm long, 55 mm high and 6.5 mm thick, with a support at each end. The plate was drilled with seven holes 25 mm in diameter spacing at 130 mm. A special attachment comprising two washers, a bolt, a nut, a locking screw and a screw driver was fitted in each hole, as shown in Fig. 5.3. A number of steel brackets were fixed to the timber lining of the sides of the flume in front of the wall. The number and position of the brackets varied for each group of tests, being dependent on the number, inclination and level of the anchor rows. These brackets assisted in supporting the stressing device opposite to each row of anchors.

The stressing device was connected to the brackets opposite to the first row of anchors. Each screw driver was introduced into the slot of the appropriate protruding rod connected to each proving ring. The locking screw (see Fig. 5.3) on each screw driver was then tightened. Special tables labelled with the proving ring numbers and their calibration constants calculated from the calibration curves were prepared to record the zero reading of all proving rings. These helped in carrying out quick calculations for the anticipated output reading of the digital voltmeter corresponding to each stress increment to be applied to the anchors.

The anchors were prestressed to 100 percent of their design load in increments of 5 Newtons. The load increments were applied to the seven anchors in each row one at a time, starting at one end and

proceeding to the other end. Stressing was simply accomplished by turning the nut of each transducer and watching the reading of the digital voltmeter until it reached the predetermined tabulated value corresponding to each stress increment. Incremental stressing was continued until all anchors attained their design load.

A time lapse of ten minutes was allowed before recording all the instruments and reading all the gauge readings. The stressing device was then removed and another group of readings was recorded after twenty minutes.

Excavation was then continued and the above mentioned procedure repeated for all the remaining anchor levels. After the final level of anchors had been stressed and all readings obtained, excavation was carried out to reach the bottom of the wall. Great care was taken not to disturb the wall bottom movement gauge and not to over-excavate below the level of the base of the wall. This was carried out to enable the complete behaviour of the wall to be obtained, although it does not simulate the actual field construction. Fig. 5.4 illustrates the excavation and stressing procedure for a typical test with three rows of horizontal anchors.

5.3.3 Surcharge loading

In an attempt to examine the post-construction behaviour of the wall when subjected to severe loading conditions, the wall was subjected to a strip surcharge loading 0.4 m wide and 0.44 m from the back of the wall. This was carried out as follows:-

i) the last five gauges of the series of sand subsidence gauges

were carefully dismantled to make room for the loading frame;

ii) the loading frame was connected to the top of the testing flume, care being taken not to disturb any of the vertical movement gauges;

iii) the pressure bag was carefully accommodated between the top sand surface and the loading frame, and connected via a flexible tubing to the pressure system;

iv) prior to applying the pressure, all dial gauges and cell readings were recorded. No measurable disturbance was recorded in any of the measuring devices. Fig. 5.5 shows a typical test at that stage of testing;

v) the bag was inflated with pressure increments of 5 KN/m^2, care being taken not to create any creases between the bag and the top sand surface;

vi) a five minutes lapse was allowed after each pressure increment before recording any readings;

vii) pressure increments were continued to a maximum value of 25 KN/m^2, when a final set of readings was recorded.

5.3.4 Procedure after testing

The test was completed by emptying the flume and recording zero readings of the pressure cells and wall base load transducers. Movement gauges and all mechanical dial gauges were removed, and anchor units were dismantled. The narrow polythene strips at the wall edges were removed and acetone was used to clean the sides of the wall.

Group Number	Design Method	Test Number	Free Anchor Length (mm)				Fixed Anchor Dimensions+ (mm)			
			First Row	Second Row	Third Row	Fourth Row	First Row	Second Row	Third Row	Fourth Row
Group One Two Row Systems	A	A_2	640	400			132/33/3	45/25/2		
	B	B_2	730	400			132/33/3	45/25/2		
	C	C_2	520	320			132/33/3	45/25/2		
	D	D_2	605	460			112/20/3	44/20/3		
Group Two Three Row Systems	A	*A_3	610	560	280		96/30/3	80/20/2	31.5/18/2	
	B	B_3	750	490	280		96/30/3	80/20/2	31.5/18/2	
	C	*C_3	515	348	138		96/30/3	80/20/2	31.5/18/2	
	D	D_3	605	530	330		54/18/2	54/18/2	22.5/18/2	
Group Three Four Row Systems	A	A_4	610	380	340	310	96/30/3	36/18/3	28.6/13/2	30/15/2
	B	B_4	750	520	400	260	96/30/3	36/18/3	28.6/13/2	30/15/2
	C	C_4	520	351	256	146	96/30/3	36/18/3	28.6/13/2	30/15/2
	D	D_4	605	530	460	330	54/18/2	30/12/2	26/15/2	30/12/2
Group Four Three Row Inclined Systems	A	*A_I	400	335	130		50/25/2	64/20/3	49/20/2	
	B	B_I	500	330	150		50/25/2	64/20/3	49/20/2	
	C	C_I	370	240	120		50/25/2	64/20/3	49/20/2	
	D	D_I	550	385	165		15/15/2	30/20/2	20/20/2	

* Denotes repeatability test

+ The three figures represent (Anchorage length/Anchor plate height/Number of anchor plates respectively)

Table 5.1. Test Programme.

Test Number	Anchor Loads (N)				Anchor Depth *				Excavation Depth *			
	First Row	Second Row	Third Row	Fourth Row	First Row	Second Row	Third Row	Fourth Row	First Excavation	Second Excavation	Third Excavation	Fourth Excavation
A_2	61.1	85.5			100 0.17H	400 0.67H			120 0.2H	420 0.7H		
B_2	61.1	85.5			100	400			120	420		
C_2	61.1	85.5			100	400			120	420		
D_2	24.0	63.3			100	400			120	420		
A_3	48.90	48.90	48.90		100 0.17H	300 0.5H	500 0.83H		120 0.2H	320 0.53H	520 0.87H	
B_3	48.90	48.90	48.90		100	300	500		120	320	520	
C_3	48.90	48.90	48.90		100	300	500		120	320	520	
D_3	15.10	39.2	33.00		100	300	500		120	320	520	
A_4	48.90	36.70	12.40	36.70	100 0.17H	300 0.5H	400 0.67H	500 0.83H	120 0.2H	320 0.53H	420 0.7H	520 0.87H
B_4	48.90	36.70	12.40	36.70	100	300	400	500	120	320	420	520
C_4	48.90	36.70	12.40	36.70	100	300	400	500	120	320	420	520
D_4	15.10	17.10	30.10	24.90	100	300	400	500	120	320	420	520
A_I	56.40	56.40	56.40		100 0.17H	300 0.5H	500 0.83H		120 0.2H	320 0.53H	520 0.87H	
B_I	56.40	56.40	56.40		100	300	500		120	320	520	
C_I	56.40	56.40	56.40		100	300	500		120	320	520	
D_I	17.40	45.2	38.10		100	300	500		120	320	520	

* Expressed as mm or as a function of wall height, H

Table 5.1 (continued) Test Programme.

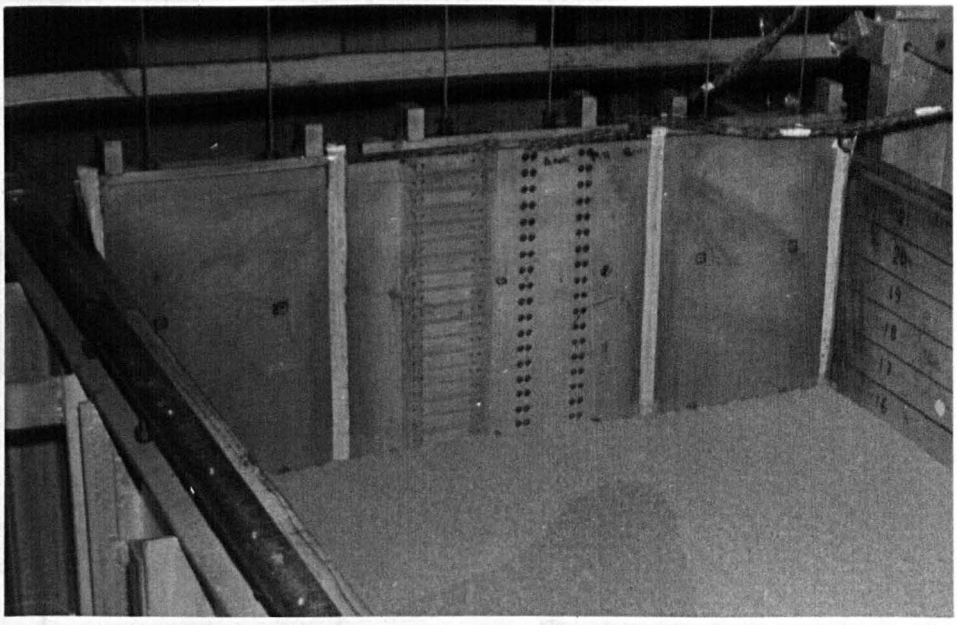

FIG. 5.1 THE TEST WALL DURING SAND FILLING

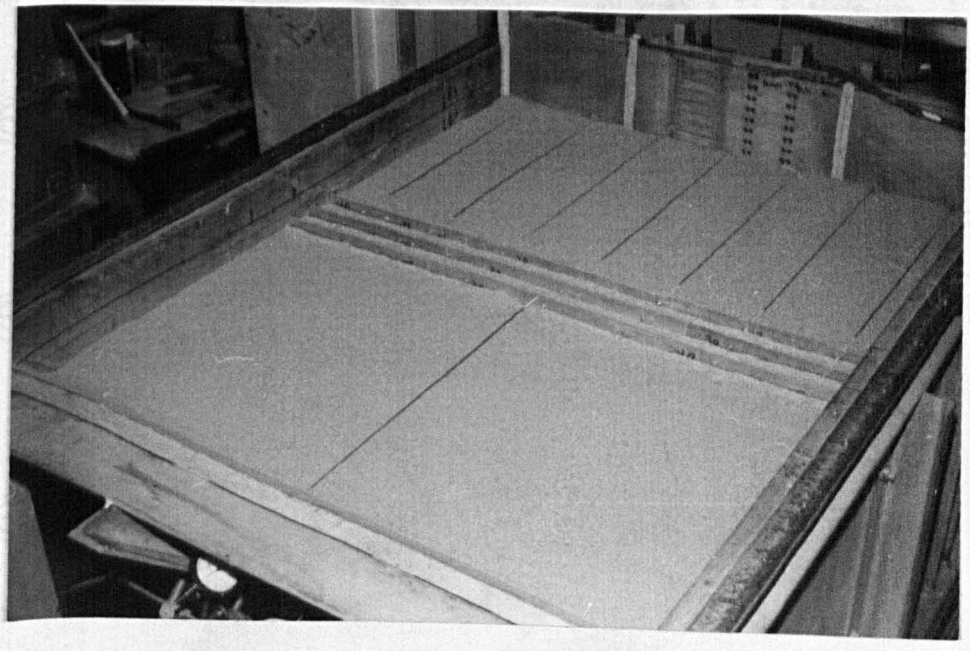

FIG. 5.2 ANCHORS INSTALLATION

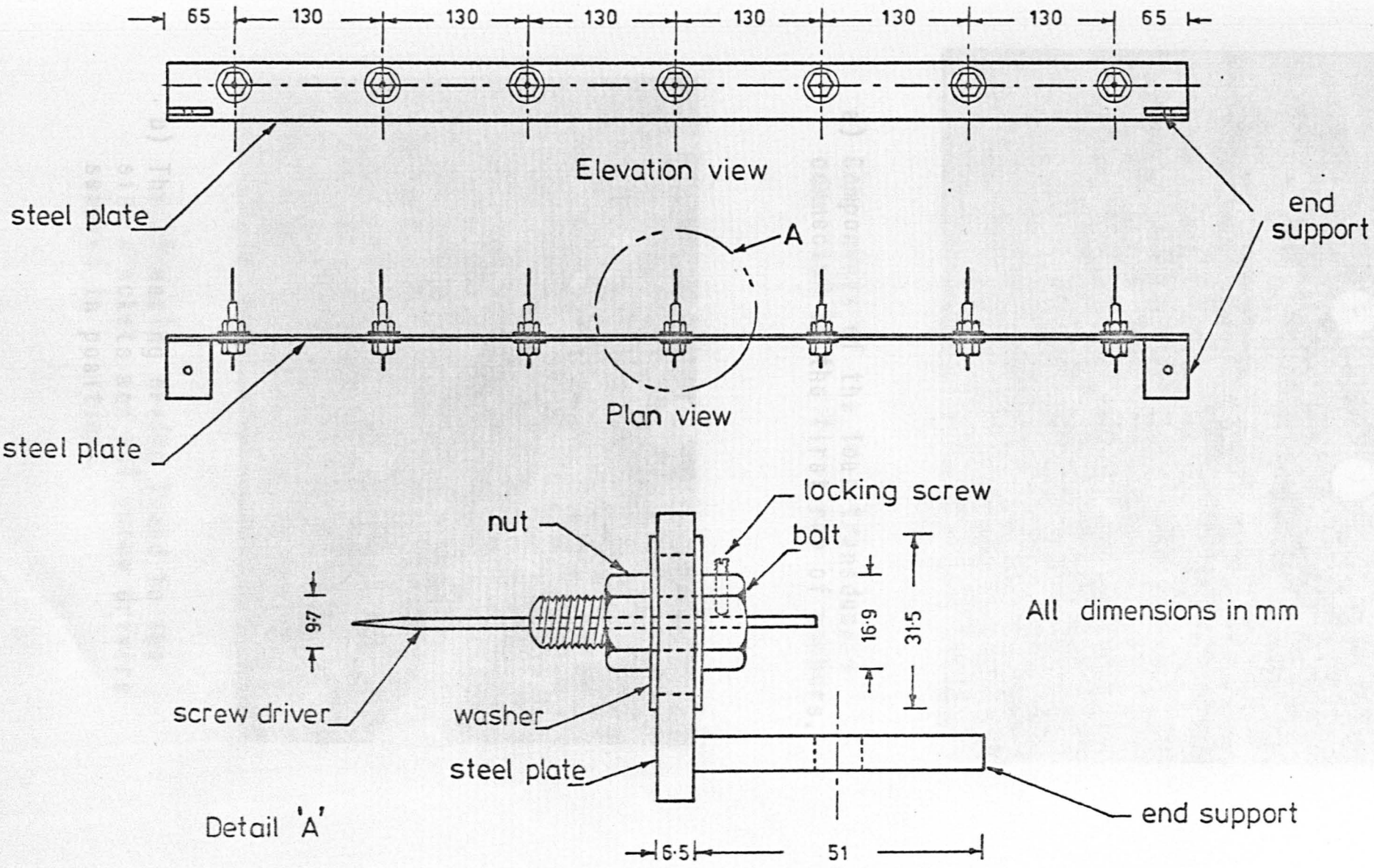

FIG. 5·3 STRESSING DEVICE

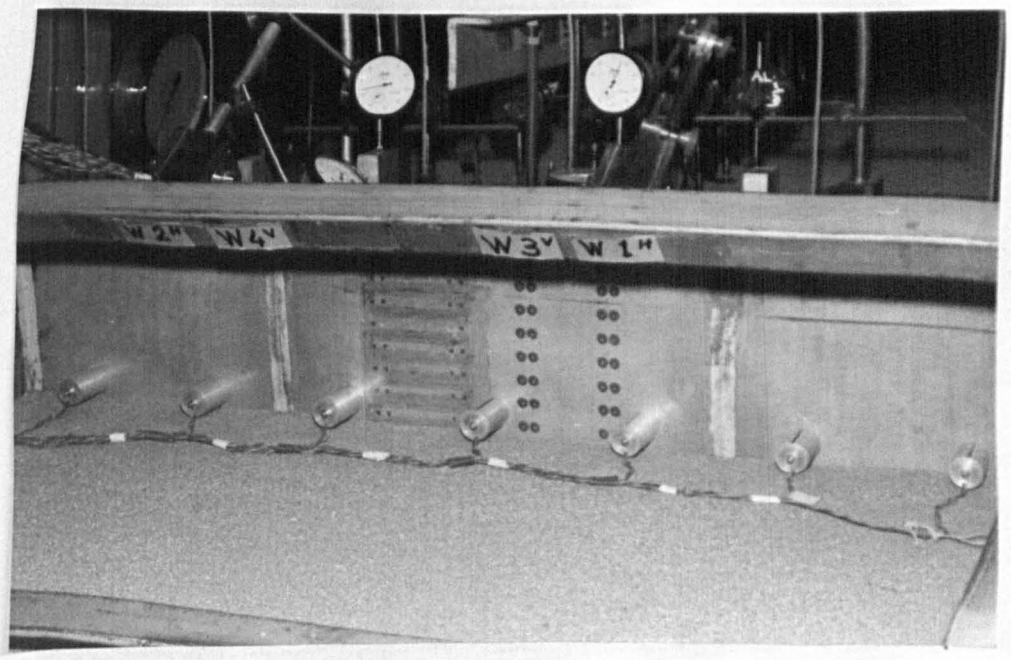

a) Components of the load transducers connected to the first row of anchors.

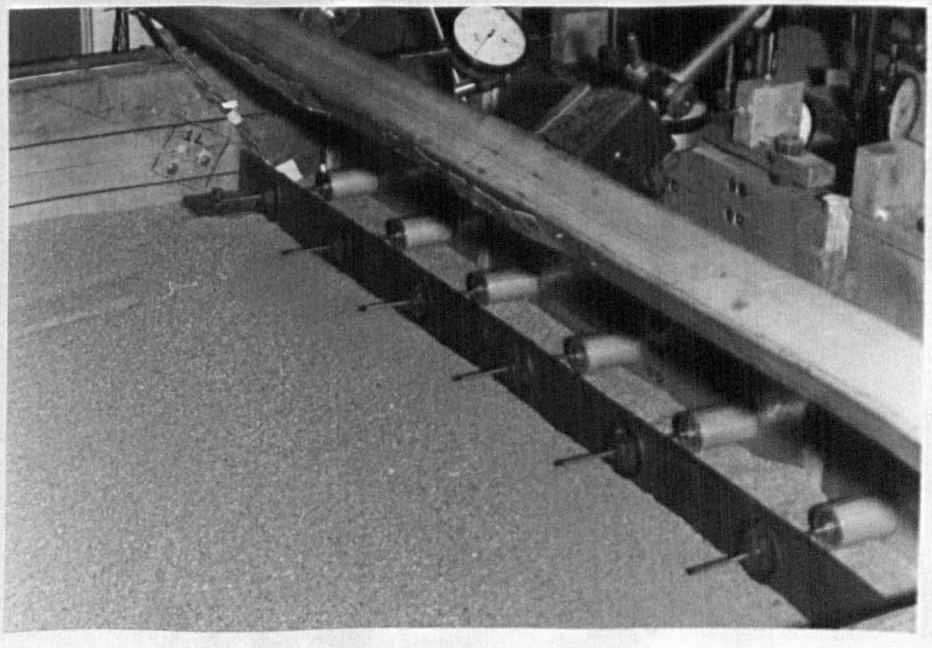

b) The stressing device fixed to the side brackets and all screw drivers secured in position.

FIG. 5.4 EXCAVATION AND STRESSING PROCEDURE

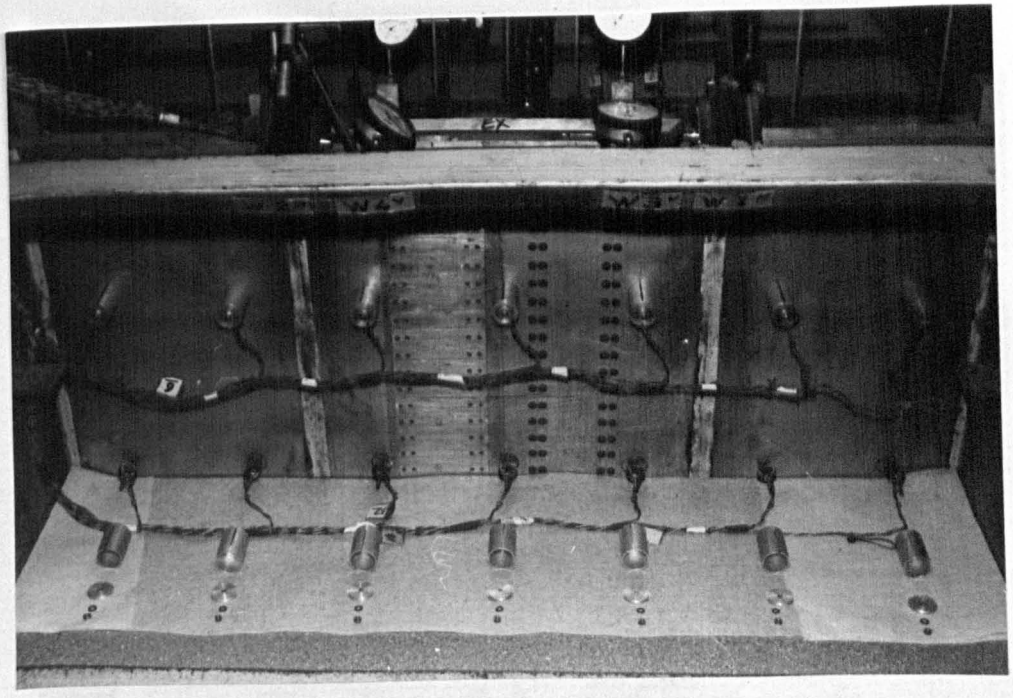

c) Proving rings connected to the second row of anchors and the rest of the load transducer components ready for connecting.

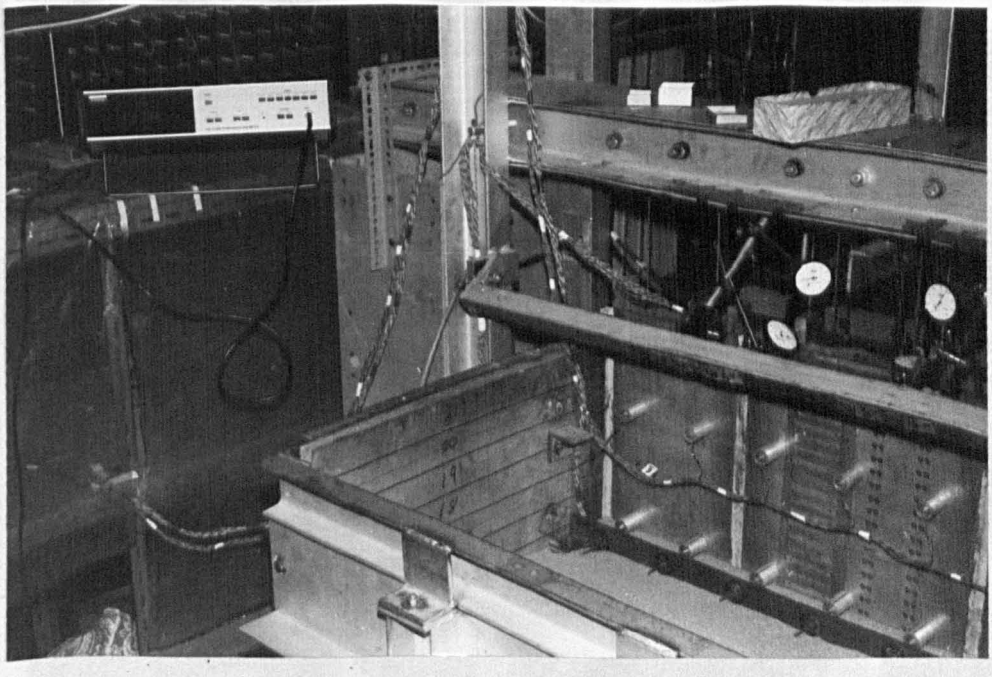

d) Stressing the second row of anchors

Cont. FIG. 5.4 EXCAVATION AND STRESSING PROCEDURE

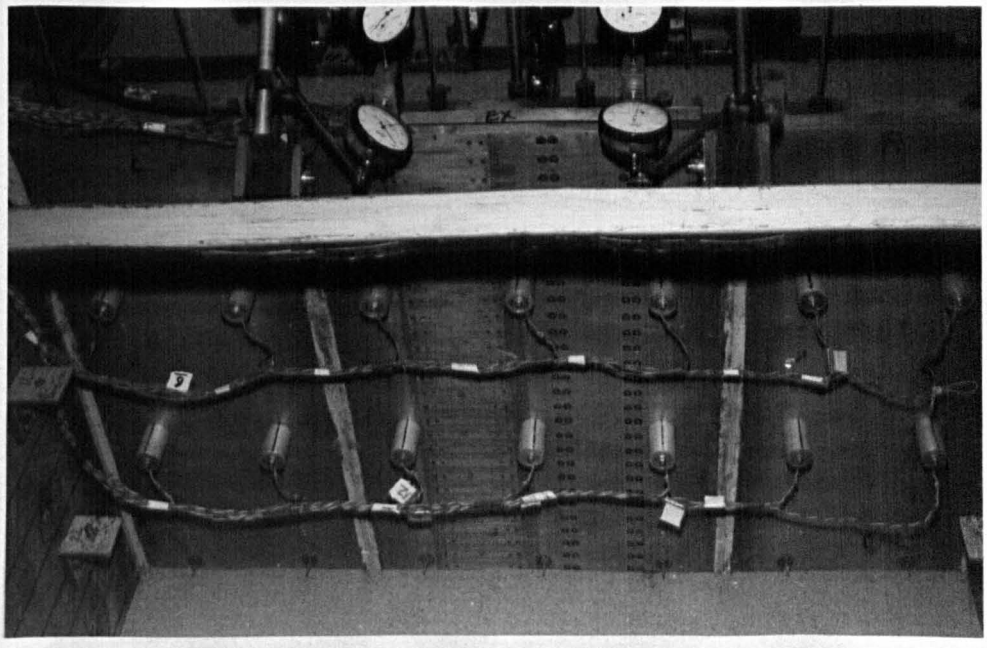

e) Excavation to the third level of anchors

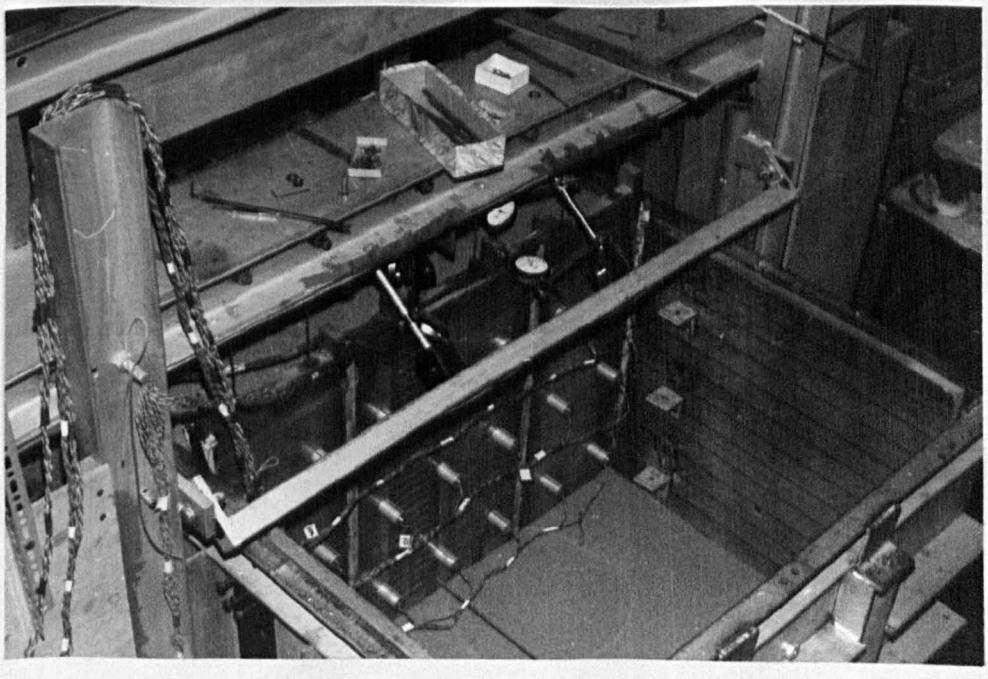

f) The test wall at the final excavation stage

Cont. FIG. 5.4 EXCAVATION AND STRESSING PROCEDURE

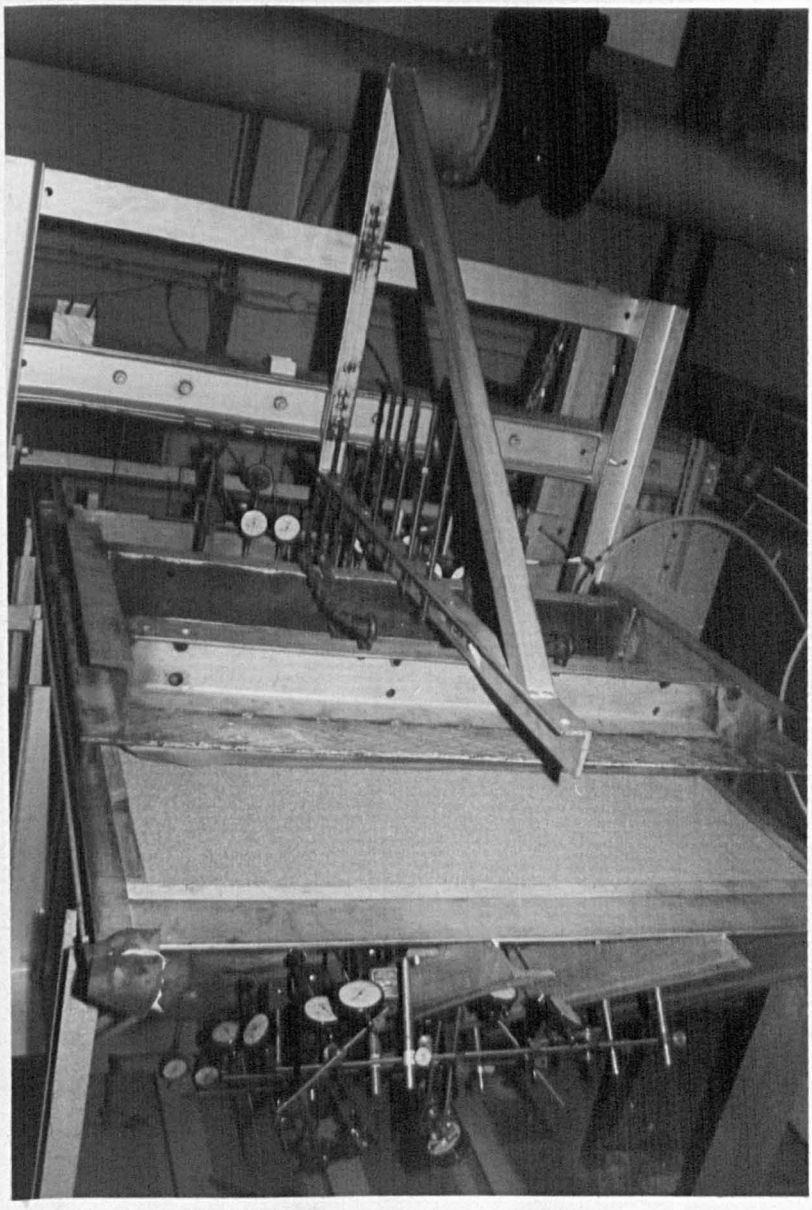

FIG. 5.5 LOADING FRAME AND PRESSURE BAG ON THE BACKFILL

CHAPTER 6

PRESENTATION OF THE EXPERIMENTAL RESULTS

CHAPTER 6

PRESENTATION OF THE EXPERIMENTAL RESULTS

6.1 Introduction

The nineteen tests carried out yielded a large quantity of experimental data and in consequence all the information obtained from each test will not be reported here. Results are presented which are considered typical of the tests performed, while also showing the essential differences. Important factors such as wall movements and anchor load changes are considered as fully as possible. Table 6.1 summarises the legend used throughout Chapters 6 and 7 to identify the different construction stages, as well as the subsequent steps of surcharge application to examine post-construction behaviour.

6.2 Wall Movements

6.2.1 Wall movements during construction

The wall movement profiles with construction progress are shown in Figs. 6.1 to 6.4 for each test. The same scale was used for both vertical and horizontal movements. These are expressed either as absolute movements in millimetres or as a function of the wall height, H.

In all tests, during the first stage of excavation the top of the wall moved towards the excavation by a very small amount. On stressing the first row of anchors, the wall moved towards the backfill by an amount dependent on the anchor lengths and the prestress load applied to that first row of anchors. Greater movements were

generally associated with longer anchors and higher prestress loads.

During the subsequent excavation and stressing stages, wall movement was always towards the excavation.

Stressing stages, after the first one, eliminated the excessive wall movements. However, a slight movement of the wall, parallel to its initial position before stressing, was observed.

The final stage of excavation, which was carried out to the base level of the wall, generally caused the greatest incremental movement compared to that in all previous stages.

In comparing the wall movements during Group Two tests (three row horizontal systems) with movements during Group Four tests (three row inclined systems) it will be noticed that greater vertical and horizontal movements were experienced in all tests with inclined anchors.

The pattern of wall movement observed in all tests associated with design methods A, B and C (Kranz, Ostermayer and The French Code of Practice respectively) was more or less the same, tending to be one of rotation about a point of fixity near the toe of the wall during the first two construction stages and then one of rotation about a point near the top of the wall during the rest of the construction stages. However, tests associated with design method D (the James and Jack method) exhibited a different behaviour. The movements observed during all construction stages, excluding the last stage, tended to be either translation or rotation about a point near the toe of the wall. Lower prestress loads at all anchor levels, especially the top one, during this group of tests were considered mainly responsible for this mode of

movement.

6.2.2 Post-construction wall movements

The wall movement profiles for the different stages of incremental surcharge loading are plotted in Figs. 6.5 to 6.8. Due to the larger movements experienced, a different scale than that used for previous wall movement profiles has been used. The wall movements are expressed in either millimetres or as a function of the wall height, H.

Generally a surcharge load of 5 KN/m^2 caused little movement to the wall compared with the movements monitored after higher surcharge loads had been applied. In all tests designed according to methods A, B and D, the magnitude of wall displacements associated with the subsequent increments of surcharge load was of the same order for each individual test, indicating no tendency for any of the systems to approach failure.

Relative to the final wall profile at full excavation, the wall movement was found to be either translational or rotational. Translational motion was associated with all tests in Group Four (three row inclined systems) and all tests designed according to method D. It was also observed in tests No. C_3, A_4 and C_4. In all other tests the wall tended to rotate rather than to translate, and the rotational motion was more pronounced in tests with horizontal anchors designed according to method B (Ostermayer method).

6.3 Sand Subsidence

6.3.1 Sand subsidence during construction

Sand surface subsidence profiles at the different construction

stages are shown for the sixteen tests in Figs. 6.9 to 6.12. Also shown on each diagram is the relative position of the anchor block of the top row of anchors. Sand subsidence is expressed both in millimetres and as a function of wall height, H, whereas the positions of the measuring points are expressed as a function of H, the wall height.

In the early stages of each test the magnitude of sand subsidence behind the wall was small. With increasing depth of excavation the subsidence increased with the greatest amount of subsidence occurring during the final excavation stage to wall base level.

The magnitude of sand subsidence was greatly reduced using four rows of anchors, whereas the greatest values of sand subsidence were observed with inclined anchors. Generally, early excavation stages caused less subsidence than later ones. However, no change in the shape of the sand subsidence profiles was observed as excavation progressed.

When the top row of anchors was near to the surface, this greatly disturbed the surface. When the ratio D/B (anchor depth/anchor plate height) was very small, of the order of 3, the sand surface was greatly affected when stressing the anchors and during the subsequent excavation and stressing stages. A heave occurred in the front of the anchor block and a considerable amount of subsidence occurred at the back of the anchor block. In tests D_2, D_3 and D_4, where the ratio D/B was of the order of 5, the sand surface was less affected. Heave and subsidence were both much less than those observed when D/B was 3. In Group Four, with the inclined anchors, where the anchor blocks of the first row were comparatively deep (D/B values were 12.0, 7.0, 11.5 and 25 for

tests A_I, B_I, C_I and D_I respectively), the sand surface suffered less disturbance. However, it was still slightly affected. These findings are in agreement with pin model observations (of Chapter 3).

6.3.2 Post-construction sand subsidence

The installation of the loading frame and the pressure bag for load application necessitated the removal of five of the sand subsidence measuring gauges. Consequently it was only possible to monitor the sand subsidence at the first four points near to the wall. Sand subsidence profiles for the different load increments are shown in Figs. 6.13 to 6.16.

In general, the subsidence caused by the first increment of surcharge load was very small compared to subsequent increments. However, during the final loading stage, the magnitude of sand subsidence more than doubled its initial value at full excavation. While the profiles did not change in shape during the construction stages, they did vary during surcharge loading. This is discussed in section 7.4.2.

6.4 Anchor Loads and Anchor Movements

6.4.1 Anchor loads

Figs. 6.17 to 6.20 show the measured anchor loads expressed as a percentage of the theoretical design value for the different construction and post-construction stages. The anchor loads were obtained by averaging the values recorded for the central wall section. At each anchor level, three anchor rods supported the central wall and little variation was observed between the behaviour of each. Table 6.2 shows

the measured anchor loads for the individual anchor rods for test No. A_3 during the different construction stages, which indicates fairly consistent values over the wide range of anchor load changes.

From the figures, the general trend observed can be summarised as follows:

i) Horizontal anchor tests: In all tests designed according to methods A, B and C, a reduction in the anchor load of the top row of anchors was observed as construction progressed until full excavation was reached. This was followed by an increase in the anchor load when surcharge load was applied. At full excavation, loads in the bottom row of anchors attained a value either slightly higher or nearly equal to their design value. On applying surcharge an increase in the anchor loads was observed. The middle rows experienced different behaviour for the different tests.

A different behaviour was observed in tests designed according to method D (the James and Jack method). Anchor loads in all rows increased as construction progressed to full excavation. This was followed by a further increase when the surcharge load was applied.

ii) Inclined anchor tests: In test D_I, all rows experienced an increase in the anchor loads during construction and post-construction stages and this was similar to horizontal anchor tests designed according to design method D. A different behaviour was observed for tests A_I, B_I and C_I. A decrease in the anchor loads was observed in all three rows as construction

progressed until full excavation was reached. When surcharge load was applied, all three rows exhibited an increase in the anchor loads.

6.4.2 Anchor movements

The measured anchor movements for the central wall are plotted against the different construction and post-construction stages in Figs. 6.17 to 6.19, together with the variations in the anchor loads. Anchor movements in all tests with inclined anchors were not measured due to experimental difficulties.

Initial movements associated with anchor stressing were a function of anchor depth. The top rows generally experienced greater movements than bottom ones during stressing. However, as construction progressed, movements increased in all rows. The magnitude of anchor movement slightly increased with applying the first increment of surcharge load. With subsequent increments the movements increased dramatically, but in all cases linear load displacement curves were observed.

6.5 Earth Pressure Distribution

6.5.1 General

When considering the results of the earth pressure measurements it should always be kept in mind that a number of difficulties are encountered in monitoring earth pressures. Plant (1972) detailed these difficulties and they can be summarised as follows:

a) the modulus of deformation of the soil is different from the modulus of deformation of the pressure cell material. This causes

a redistribution of stresses around the cell to produce a higher pressure if the cell is stiffer than the soil;

b) arching due to the deflection of the pressure responsive diaphragm may lead to the under-registration of pressure in granular media;

c) differences in values of pressures recorded under identical conditions might be attributed to the fact that the granular particles do not rest in the same manner on the diaphragm on each occasion, and the degree of particle interlocking differs in each case;

d) local variations in density produce variations in the measured earth pressure.

However, despite these difficulties, the measurements recorded throughout the test programme highlighted the trends and allowed a better understanding of the mode of earth pressure mobilization during and after construction to be made.

6.5.2 Earth pressures during construction

The general trend for the earth pressure distribution, which was observed for all tests, is illustrated in Figs. 6.21 and 6.22 which represent a plot of the measured normal earth pressure distribution for the different stages of construction for two typical tests (tests No. B_3 and D_3, three rows horizontal anchors). The at-rest earth pressure after sand filling gave an approximately triangular-shaped distribution on both sides of the central wall. The slight differences between each side of the wall are attributed to the shape of the test flume and the presence of the anchors which slightly affected the sand stirring

operation. The value of Ko, the coefficient of earth pressure at rest, was calculated from the measured normal earth pressure load acting on the wall. This was found to be 1.25 times the theoretical value according to Jaky (1944).

In all tests performed, and during the different construction stages, the earth pressure changes were observed to be related to the wall movements. During the first excavation stage a reduction in the earth pressure on the back of the wall occurred due to wall movement towards the excavation. A reduction also occurred on the front of the wall due to the reduction in the overburden pressure. On stressing the first row of anchors, the earth pressure increased on the back of the wall and decreased on the front. However, near the toe, a slight decrease was observed on the back and a slight increase on the front due to the wall rotation. This general pattern of behaviour continued for the subsequent stages. At the deeper excavation levels a triangular-shaped passive earth pressure distribution developed on the front of the wall and on the back of the wall the earth pressure distribution became trapezoidal-shaped.

The trends explained above were common to all tests. However, different magnitudes of earth pressures were observed at the different construction stages in different tests.

The influence of wall movements and prestress loads can be appreciated from a comparison of Figs. 6.21 and 6.22. At any construction stage, the difference between the earth pressure on excavation and after stressing the anchors at that stage, was much greater in test B_3 than in test D_3. This can be mainly attributed to higher prestress loads in

test B_3 than in test D_3. The earth pressure on the back of the wall at full excavation is remarkably smaller for test D_3 than for test B_3. In the former test, wall displacements were 3.6 times greater at the top and 1.3 times greater at the bottom.

Figs. 6.23 to 6.26 show plots for the at-rest pressure distribution on the back of the wall, the normal pressure distribution after stressing the bottom row of anchors and the normal pressure distribution at full excavation for all tests carried out.

Significant differences occurred in the magnitude and shape of the normal pressure distribution during the last two stages of construction i.e. after stressing the bottom row and at full excavation. A slight increase in the magnitude of the normal earth pressure was observed on the back of the top half of the wall, whereas a significant decrease occurred on the lower parts. After the final stressing stage the normal earth pressure distribution was generally triangular in shape, whereas at full excavation it tended to be trapezoidal-shaped. In the two row systemsthe trapezoidal distribution was tending to have equal abscissas all over the height of the wall. However, in the three and four row systems higher pressure intensities were observed on the lower parts of the wall. These tended to change the shape of the distribution to be more like a quadrilateral with larger abscissas near the bottom of the wall. Bulges were more pronounced in the earth pressure distribution near the points of anchoring in all tests with inclined anchors.

Smallest values of normal earth pressures were associated with all tests designed according to design method D (the James and Jack method).

This demonstrates the dependence of the magnitude of earth pressure mobilized on the prestress loads induced in the anchors. With lower prestress loads, lower values of the normal earth pressure are mobilized on the back of the wall.

6.5.3 Post-construction earth pressure distribution

Figs. 6.27 to 6.30 show plots of the normal earth pressure distribution on the back of the wall at full excavation, together with the earth pressures at the stages of surcharge application for all tests carried out.

The figures indicate an increase in the magnitude of the normal earth pressure with increase in the surcharge load. The shape of the earth pressure distribution varied significantly depending on the performance of the different systems. In general, higher pressure intensities were observed in front of the anchored part of the wall, i.e. between the top and bottom rows of anchors. However, opposite to the top and toe the pressure either decreased or remained constant depending on the pattern of the wall movement. This will be discussed in more detail in section 7.4.4.

6.6 Wall Base Reaction

6.6.1 Normal reaction at the wall base

Fig. 6.31 shows typical plots for the variation of the normal component of the wall base reaction during filling and testing for tests No. B_2, A_3, D_4 and C_I. The normal component of the reaction is expressed as a percentage of its value after filling.

As a general trend, the normal component of reaction at the wall base gradually increased during sand filling. At the first excavation stage this decreased by approximately 12 to 15%. On stressing the first row of anchors the normal reaction increased by an amount mainly dependent on the anchor inclination. With inclined anchors the magnitude of the increase was greater than with horizontal anchors as expected, because of the vertical component of the anchor loads being transferred to the wall member pulling it downward. As construction progressed, the normal reaction at the wall base decreased during the excavation stages and increased on subsequent stressing of the anchors. In all tests the greatest reduction in the normal reaction occurred at the final excavation stage. In tests with horizontal anchors the value of the normal component of the reaction at full excavation was generally less than its value after filling. However, in tests with inclined anchors this value varied between 90 and 120 per cent of its value after filling.

On application of the surcharge load the normal component of the reaction started to increase and continued to increase with the subsequent increments of surcharge load, the magnitude of increase being greatest in the tests where two rows of anchors supported the wall, and least in tests where four rows of anchors were employed.

6.6.2 Shear reaction at the wall base

Fig. 6.32 shows typical plots for the variation of the shear component of the reaction at the wall base during construction and post-construction stages for test No. B_3 and test No. B_4. Also shown

in the same figure is the sign convention used. The two curves illustrate the general behaviour observed in all tests and are considered to be representative.

The measured shear component of reaction at the wall base was generally at, or near, zero after sand filling. When excavating to the first level, the shear component became very small and of a positive magnitude, i.e. the toe of the wall is moving towards the backfill. On stressing the first row of anchors a stress reversal on the wall base occurred and the positive value of the shear component of reaction either decreased or changed to be negative, i.e. the toe of the wall moved towards the excavation. During the subsequent excavation and stressing stages this value continued to be negative. In general, excavation caused an increase in its negative magnitude, whereas stressing of any row of anchors lying below the mid-height of the wall tended to decrease the negative value of the shear component of reaction.

The final excavation stage caused the greatest decrease in the negative value of the shear component, and either changed it to a positive value or caused it to be very small and negative (see Fig. 6.32).

With the subsequent increments of surcharge load a negative value of the shear component of reaction was observed. This continued to be negative and its value increased continuously with the applied surcharge up to the final value of 25 KN/m^2.

It should be noted that these observations are in agreement with the wall movements presented and discussed earlier.

6.7 Sand Movements

6.7.1 General

Sand movements within the retained sand mass were measured in all tests. The purpose of these measurements was to examine the movements at various stages during any test, and to compare the magnitude and direction of the movements at any stage in one test with movements at a similar stage in any other test.

It is believed that with the number of sand movement gauges used, their influence on the wall behaviour was very small as the scale of testing was very large. Plant (1972), in his study on the behaviour of multi-anchored retaining walls, carried out two typical tests with and without the sand movement gauges. A comparison between the wall movement pattern for both tests showed good repeatability at all stages of construction. Also, it has been shown during a study of the pull-out capacity of single vertical anchors (Carr and Hanna, 1971), that the influence of movement gauge instrumentation on the uplift load-anchor movement diagram was negligible at loads less than 50 per cent of the ultimate value, and at failure a load increase of about 5 per cent was observed. In these tests sixteen movement gauge positions were used in a sand box 1.2 m square and 0.91 m deep.

6.7.2 Sand movements during and post-construction

Figs. 6.33 to 6.36 show the vectorial sand movements at the eight measuring points at the different construction stages for all tests carried out. The different construction stages are indicated by subscripts corresponding to the legend in Table 6.1. Shown also in the

figures are the position of the embedded anchor units in the vicinity of the measuring points.

In general, with the first excavation and stressing stages the movements observed, if any, were very small compared to the final movements at full excavation. With the subsequent excavation stages larger movements developed. However, stressing any row decreased the magnitude of the movement. The greatest magnitude of movement was associated with the final excavation stage. This is similar to what was observed for the wall movements, with the greatest movement associated with the last excavation stage to wall base level.

The least movements were observed in all tests in Group Three, where four rows of anchors were used to support the wall. The greatest movements were observed in Group Four tests, where inclined anchors were employed. Within the individual groups, tests designed according to design method C (The French Code of Practice) exhibited the largest movements.

Fig. 6.37 shows a typical plot of the vectorial sand movements for the four tests of Group Two (three row systems) during the different stages of surcharge application. The different stages are indicated by subscripts corresponding to the legend in Table 6.1. A different scale, five times smaller than that used in Figs. 6.33 to 6.36, was used as larger movements were experienced. The figure shows the general trend observed in all the tests performed. It indicates a similar pattern of movements in all four tests but with different magnitude.

Symbol	Construction Stage
E_1	Excavation to 20 mm below the first level of anchors
S_1	Stressing the first row of anchors
M_1	30 minutes after stressing the first row
E_2	Excavation to 20 mm below the second level of anchors
S_2	Stressing the second row of anchors
M_2	30 minutes after stressing the second row
E_3	Excavation to 20 mm below the third level of anchors
S_3	Stressing the third row of anchors
M_3	30 minutes after stressing the third row
E_4	Excavation to 20 mm below the fourth level of anchors
S_4	Stressing the fourth row of anchors
M_4	30 minutes after stressing the fourth row
F.E.	Excavation to the base of the wall
G_5	Applying surcharge of 5 KN/m^2
G_{10}	Applying surcharge of 10 KN/m^2
G_{15}	Applying surcharge of 15 KN/m^2
G_{20}	Applying surcharge of 20 KN/m^2
G_{25}	Applying surcharge of 25 KN/m^2

Table 6.1. Legend for Different Stages of a Test.

Anchor Row		Construction Stage								
		S1	M1	E2	S2	M2	E3	S3	M3	F.E.
First Row	Individual Anchor Loads *	49.15	49.76	48.54	38.62	39.93	30.43	30.82	31.43	28.61
		49.15	48.52	47.27	37.89	38.70	30.68	29.06	29.68	28.81
		48.96	49.28	48.64	39.24	38.88	31.20	30.56	31.52	30.56
	Average Value	49.08	49.18	48.15	38.58	39.17	30.77	30.15	30.88	29.33
	Maximum difference from average	0.12	0.66	0.88	0.69	0.76	0.43	1.09	1.20	1.23
Second Row	Individual Anchor Loads				47.68	46.40	56.96	54.40	53.76	59.88
					48.36	46.82	56.98	55.13	54.82	59.83
					47.12	46.27	58.83	55.75	55.75	61.14
	Average Value				47.72	46.27	57.59	55.09	54.78	60.28
	Maximum difference from average				0.64	0.55	1.24	0.69	1.02	0.86
Third Row	Individual Anchor Loads							47.77	46.51	48.40
								48.50	46.78	46.06
								47.47	45.88	47.75
	Average Forces							47.91	46.39	47.40
	Maximum difference from average							0.59	0.51	1.34

* All loads in Newton

Table 6.2. Measured Anchor Loads in Individual Anchors at the Central Wall Test A3.

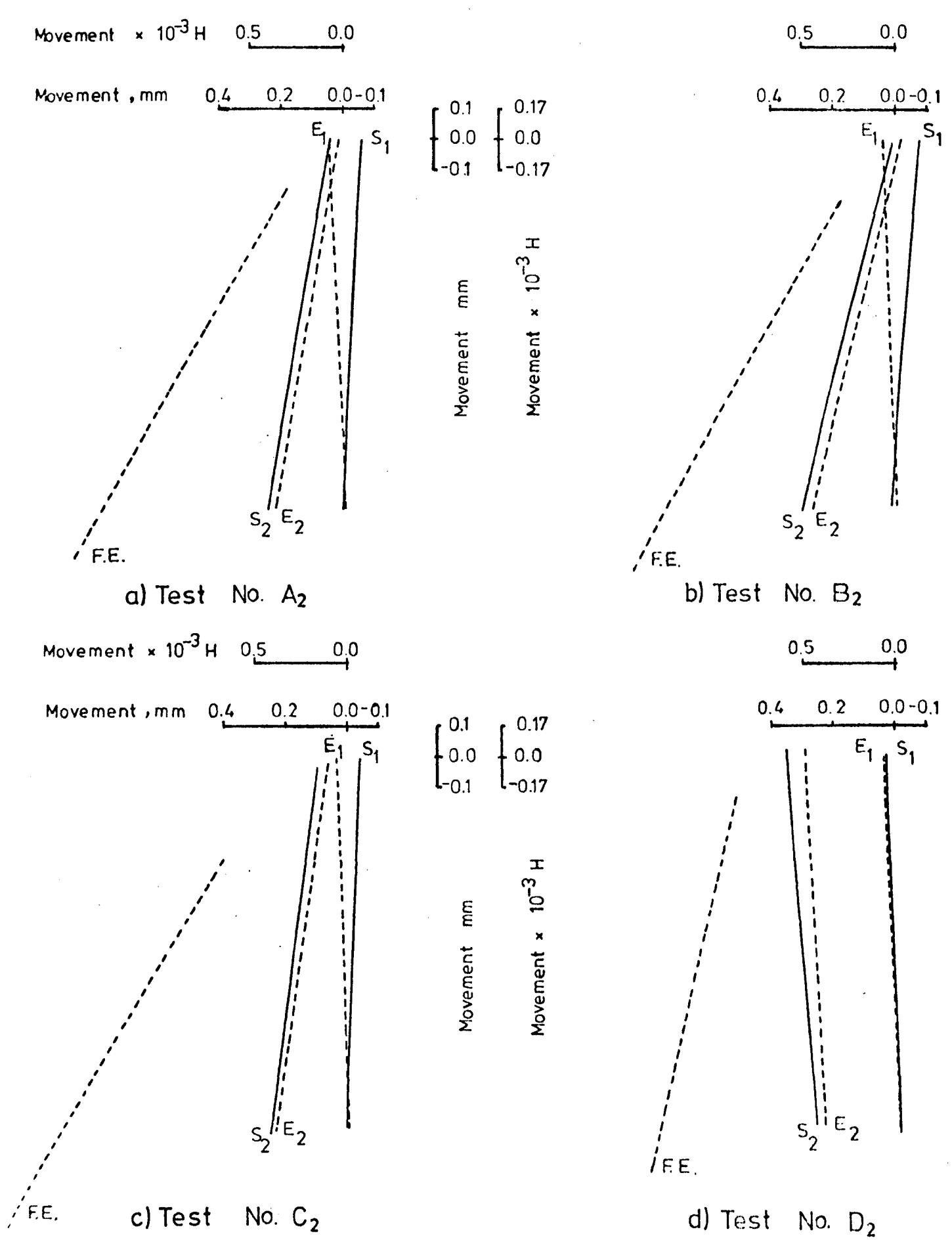

FIG. 6.1 WALL MOVEMENTS AT THE DIFFERENT CONSTRUCTION STAGES FOR GROUP ONE TESTS (TWO ROW SYSTEMS)

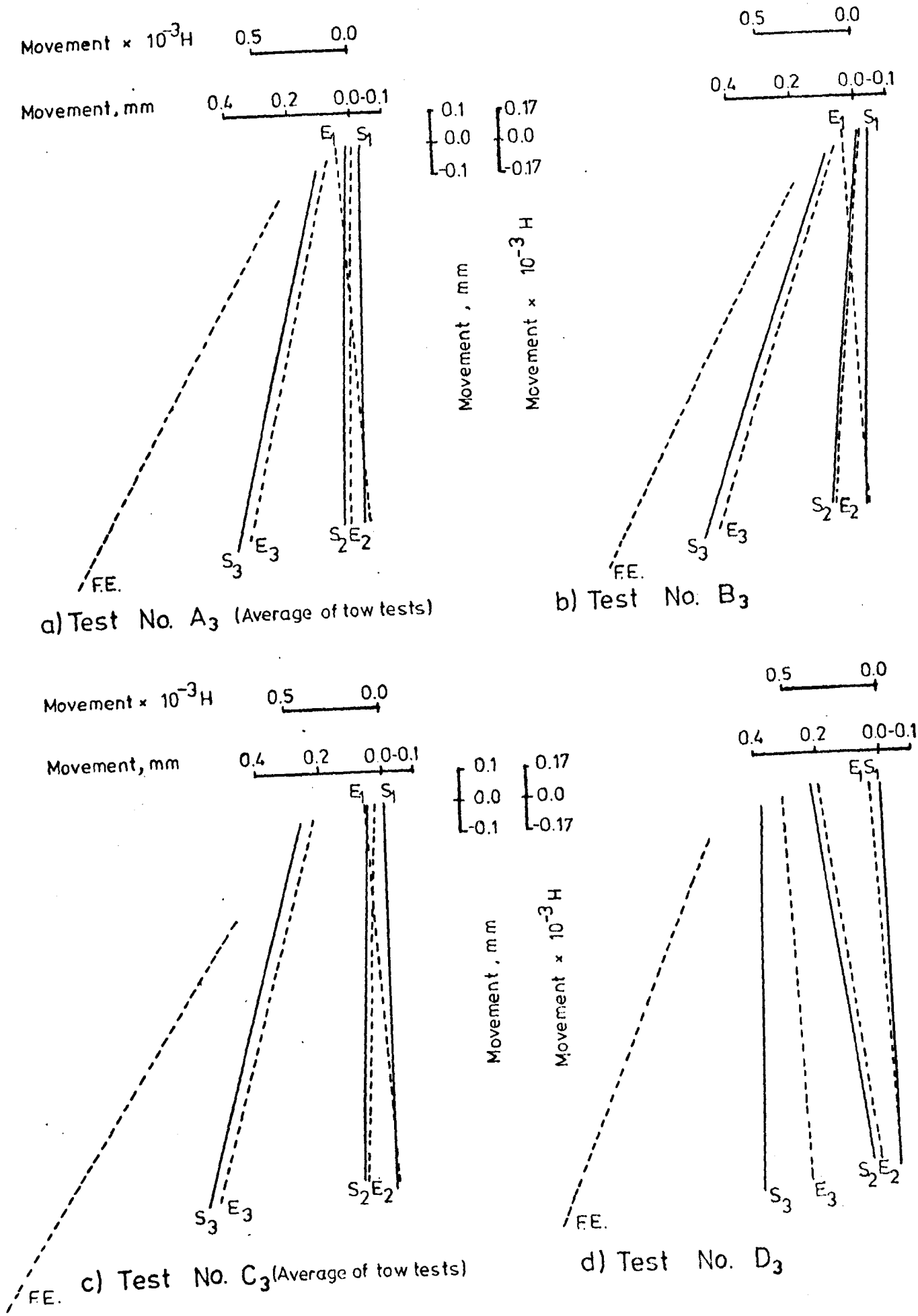

FIG. 6.2 WALL MOVEMENTS AT THE DIFFERENT COSTRUCTION STAGES FOR GROUP TWO TESTS (THREE ROW SYSTEMS)

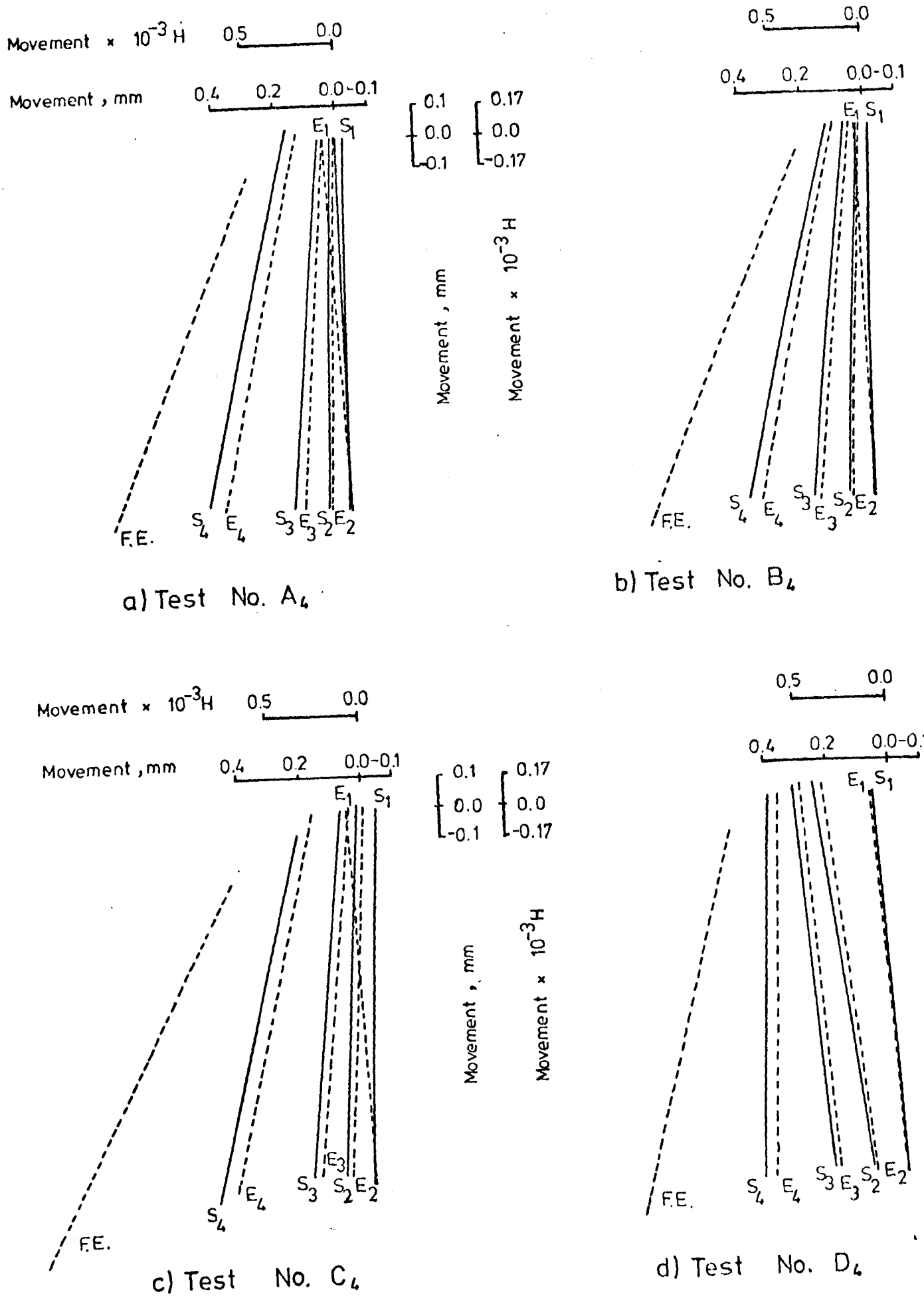

FIG. 6.3 WALL MOVEMENTS AT THE DIFFERENT CONSTRUCTION STAGES FOR GROUP THREE TESTS (FOUR ROW SYSTEMS)

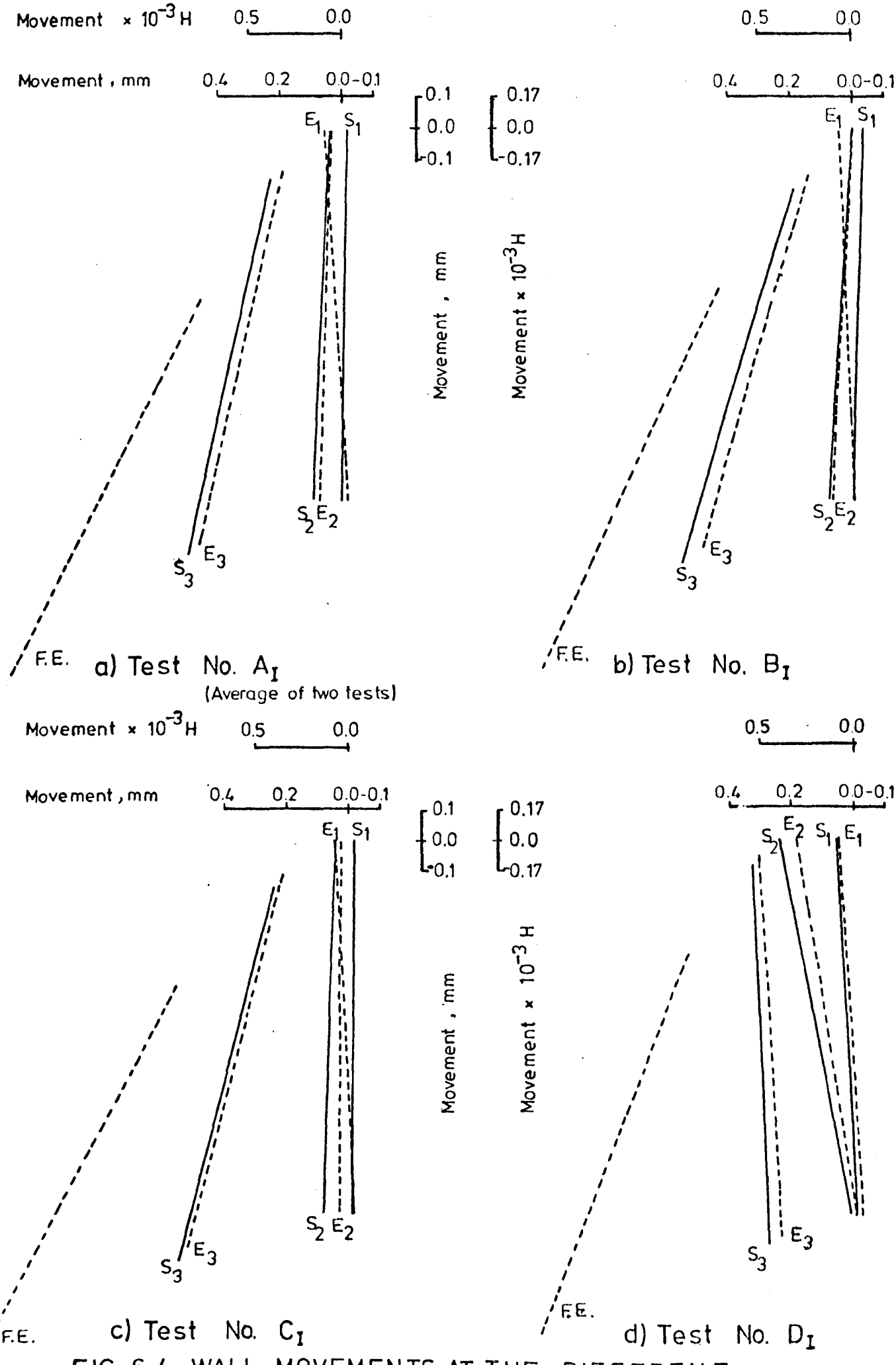

FIG. 6.4 WALL MOVEMENTS AT THE DIFFERENT CONSTRUCTION STAGES FOR GROUP FOUR TESTS (THREE ROW INCLINED SYSTEMS)

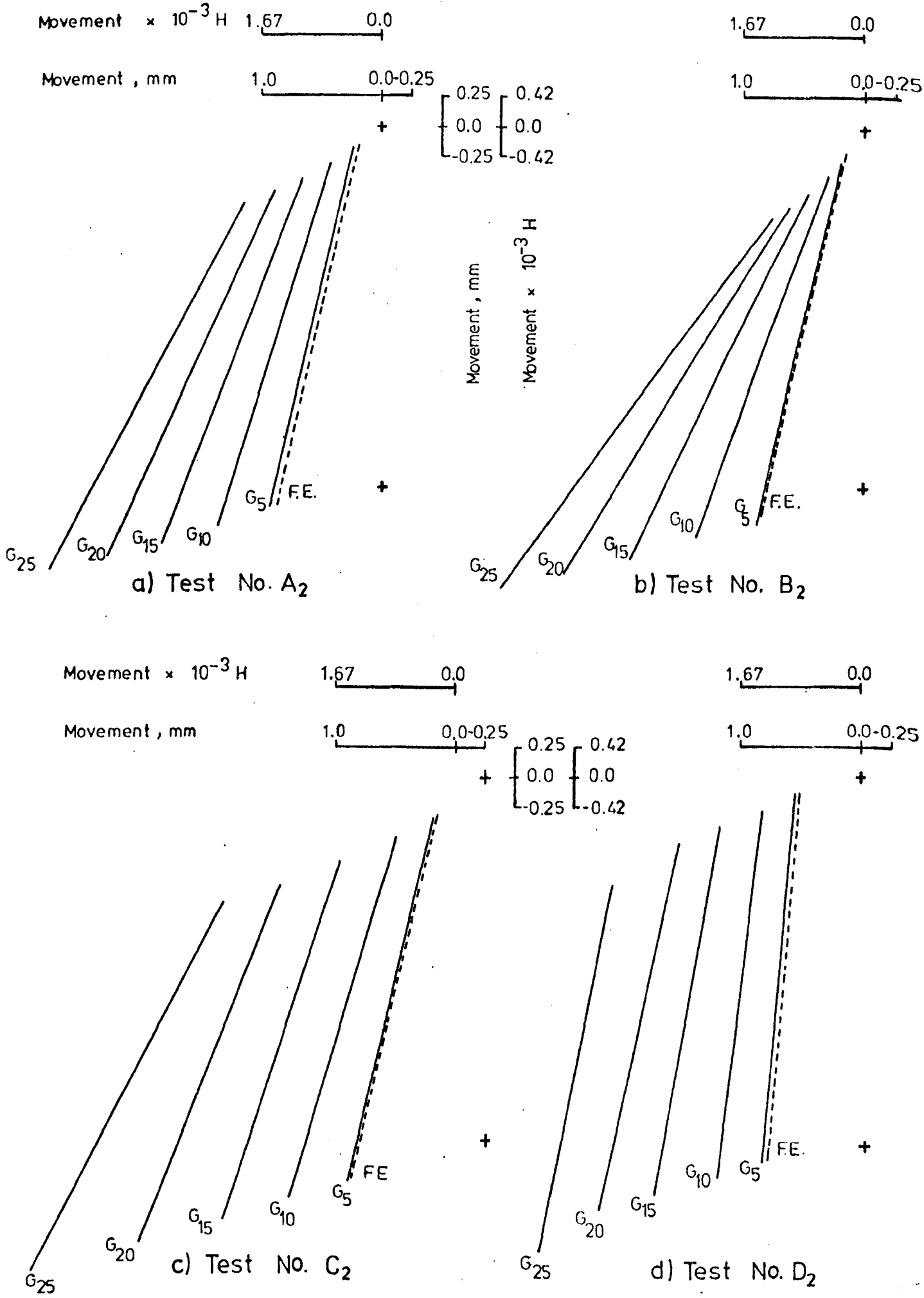

FIG 6.5 WALL MOVEMENTS DURING THE DIFFERENT STAGES OF SURCHARGE LOADING FOR GROUP ONE TESTS (TWO ROW SYSTEMS)

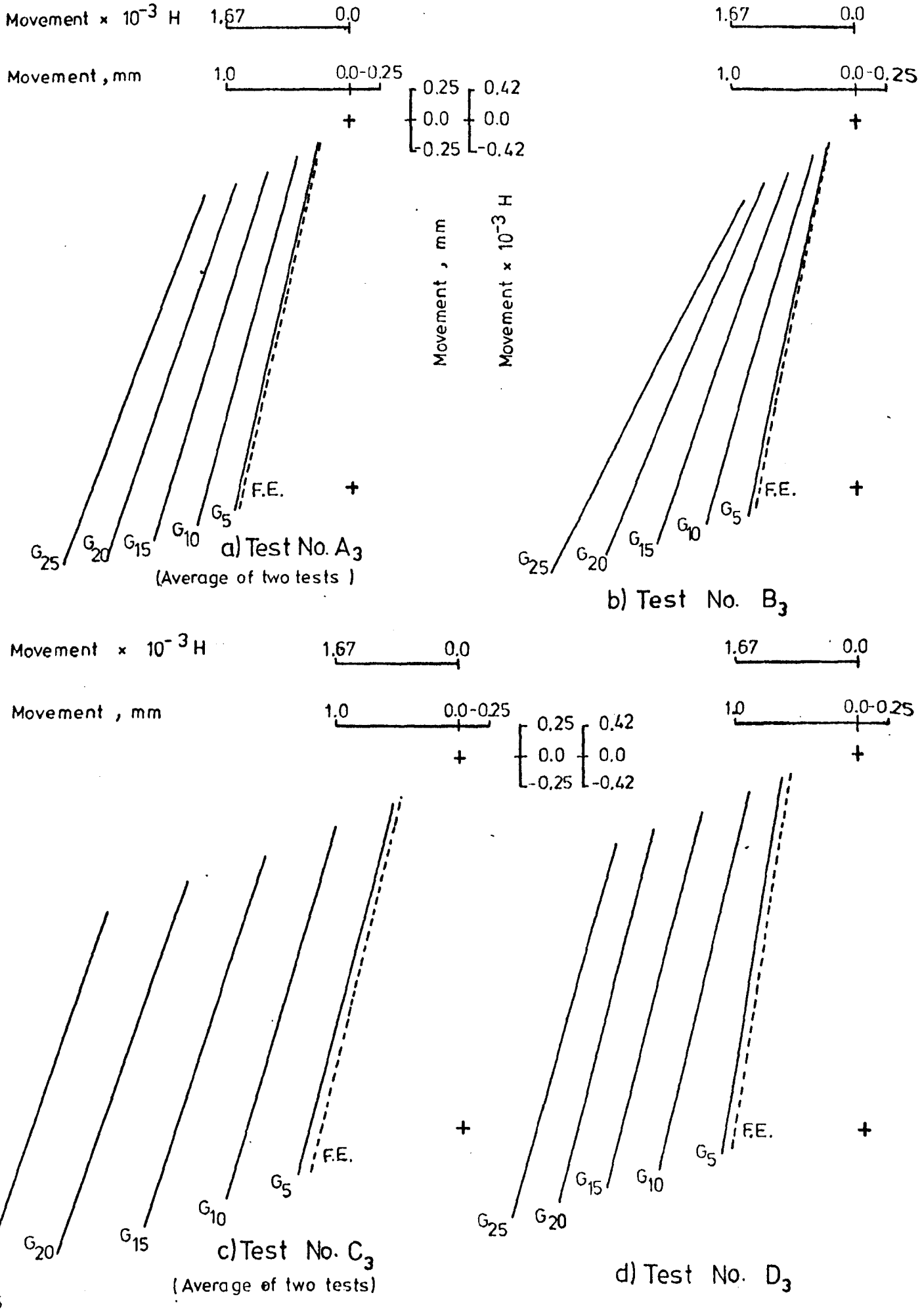

FIG. 6.6 WALL MOVEMENTS DURING THE DIFFERENT STAGES OF SURCHARGE LOADING FOR GROUP TWO TESTS (THREE ROW SYSTEMS)

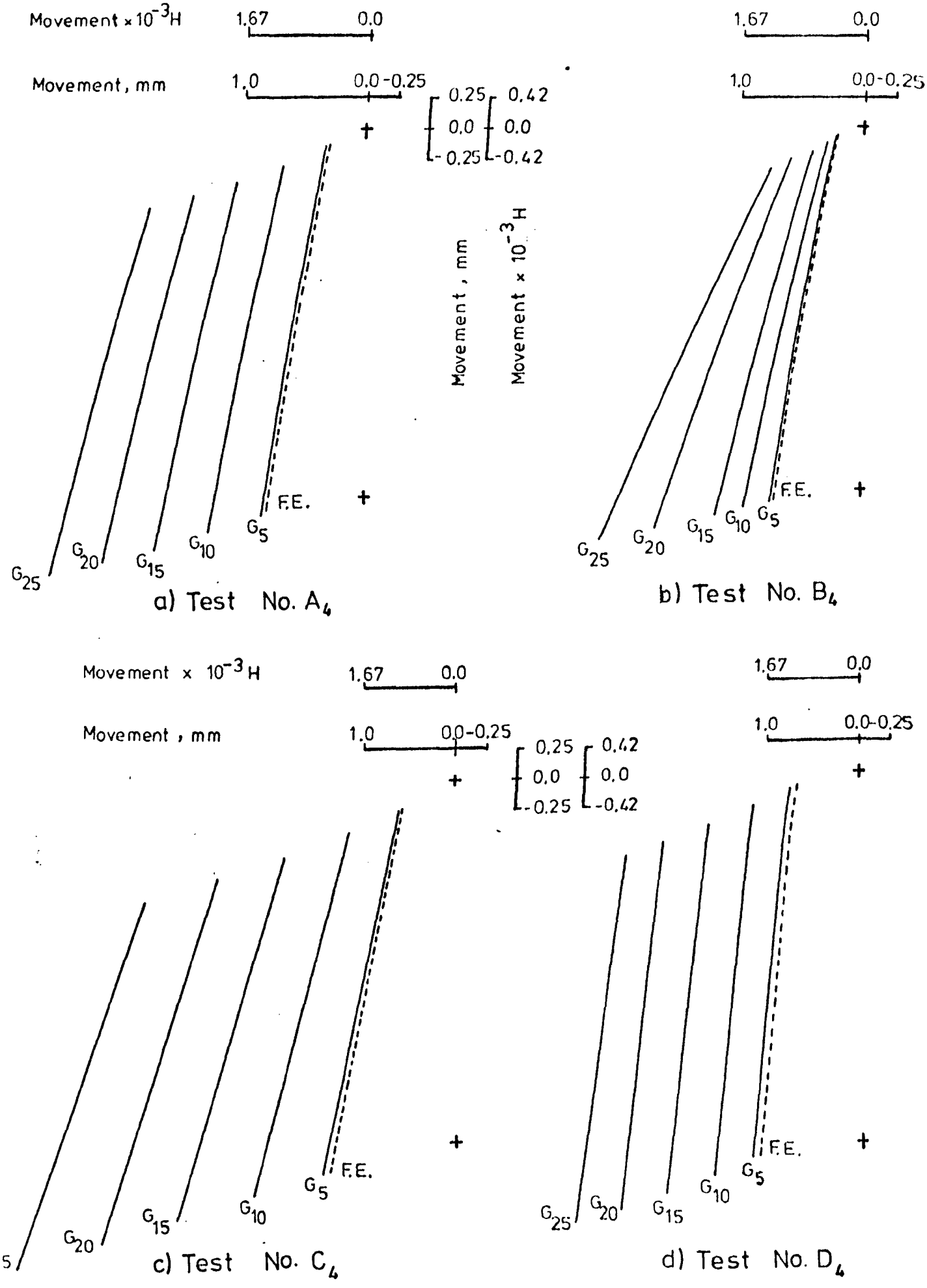

FIG. 6.7 WALL MOVEMENS DURING THE DIFFERENT STAGES OF SURCHARGE LOADING FOR GROUP THREE TESTS (FOUR ROW SYSTEMS)

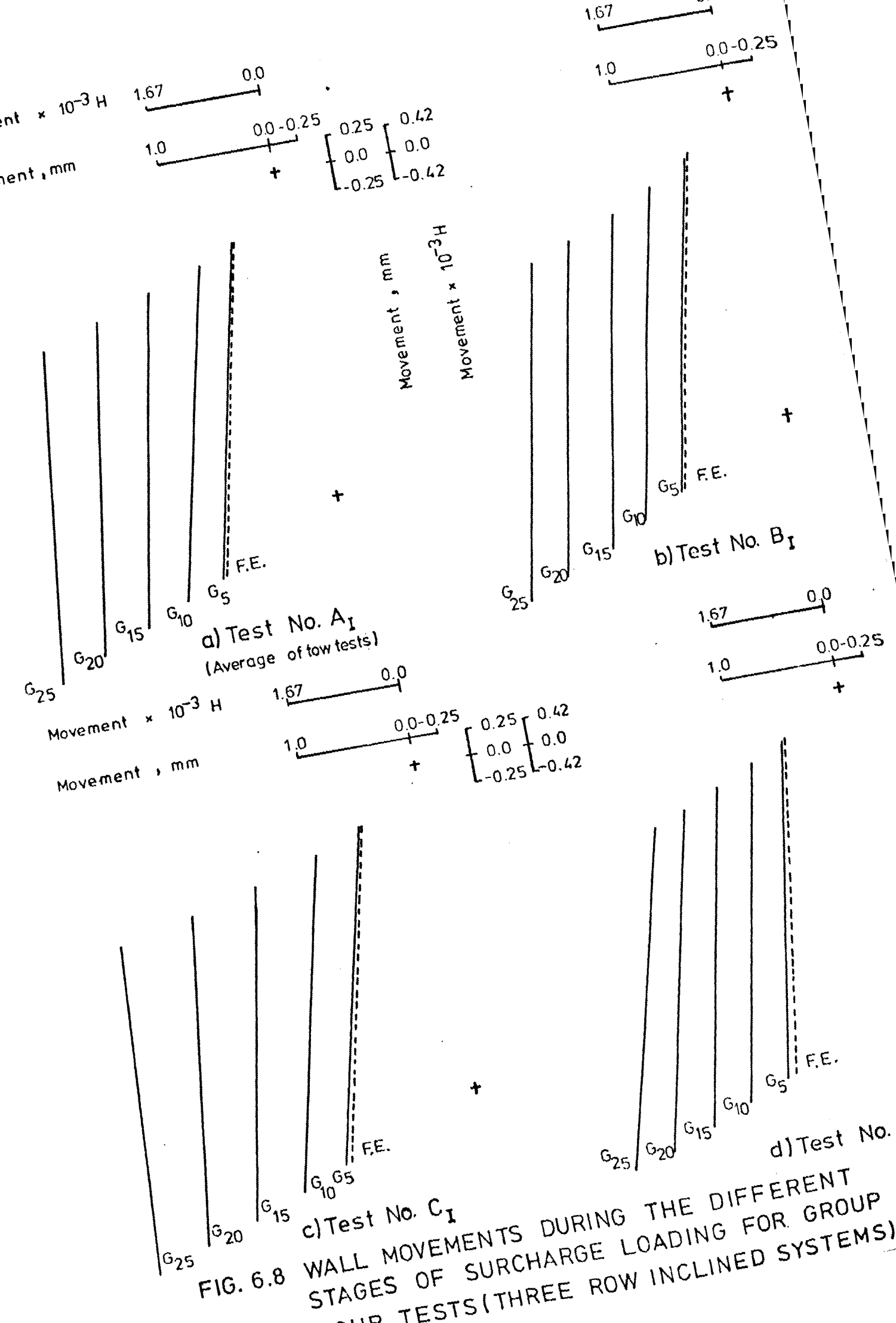

FIG. 6.8 WALL MOVEMENTS DURING THE DIFFERENT STAGES OF SURCHARGE LOADING FOR GROUP FOUR TESTS (THREE ROW INCLINED SYSTEMS)

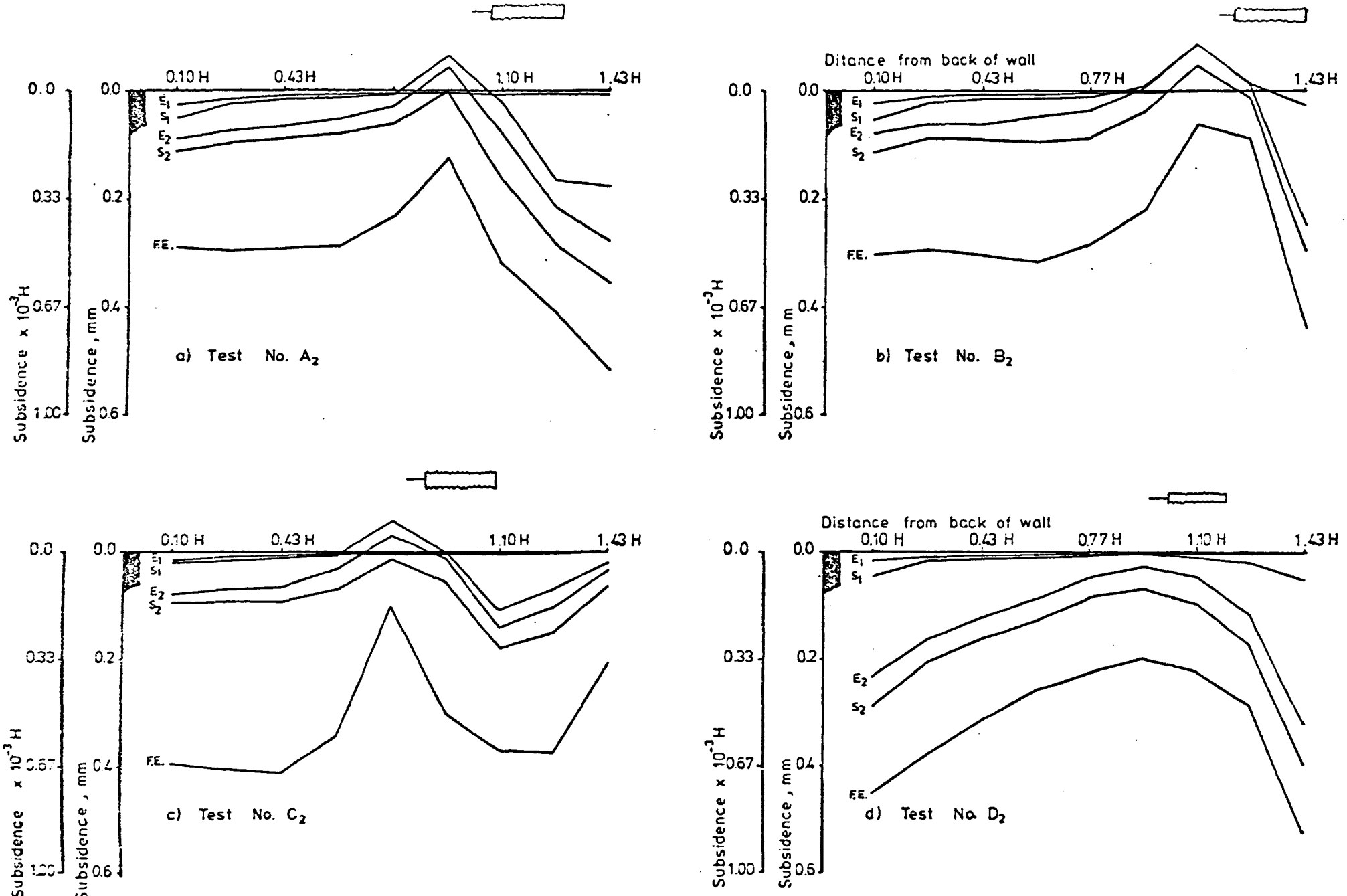

FIG. 6.9 SAND SUBSIDENCE PROFILES FOR EACH CONSTRUCTION STAGE FOR GROUP ONE TESTS (TWO ROW SYSTEMS)

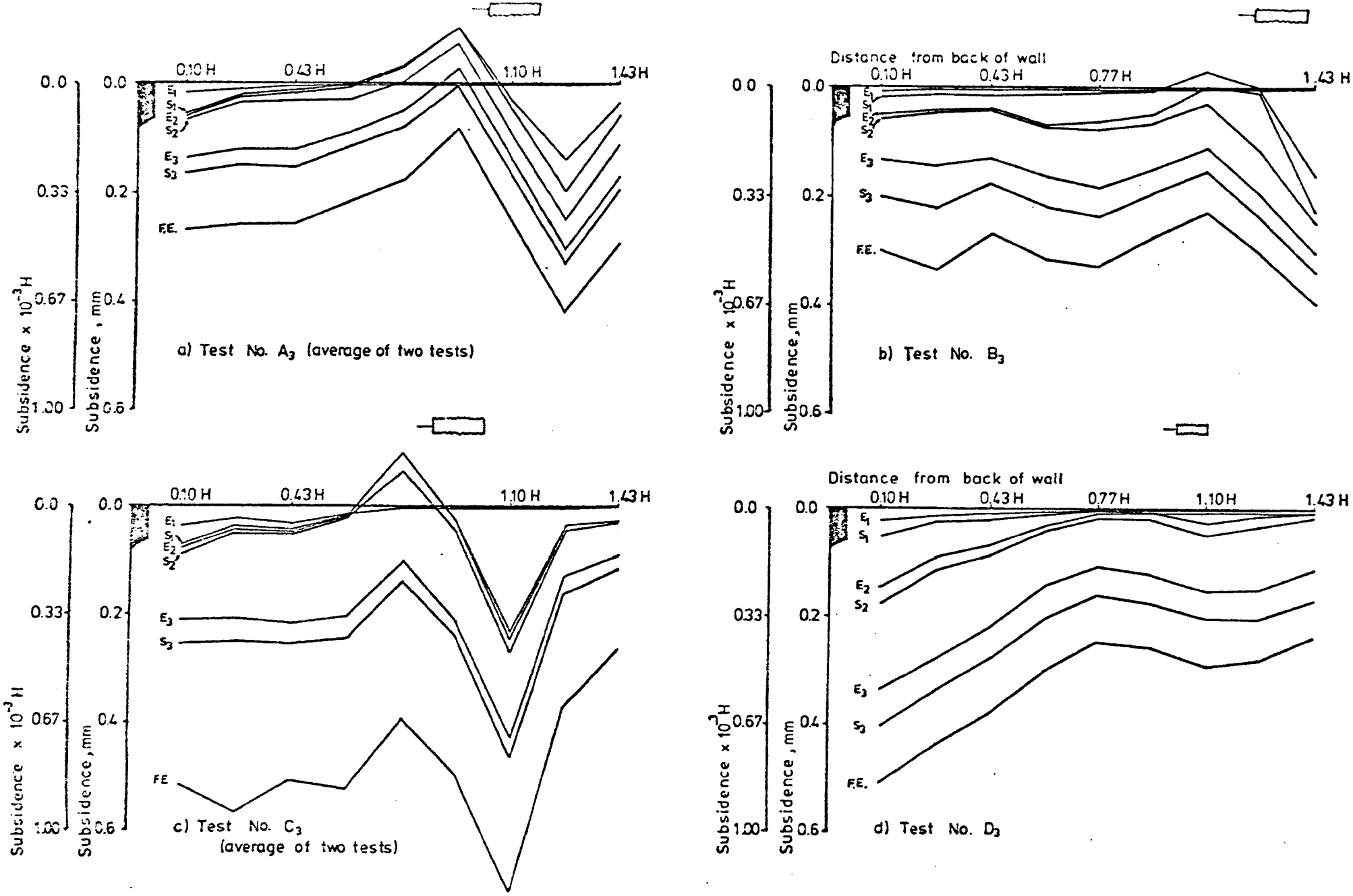

FIG. 6.10 SAND SUBSIDENCE PROFILES FOR EACH CONSTRUCTION STAGE FOR GROUP TWO TESTS (THREE ROW SYSTEMS)

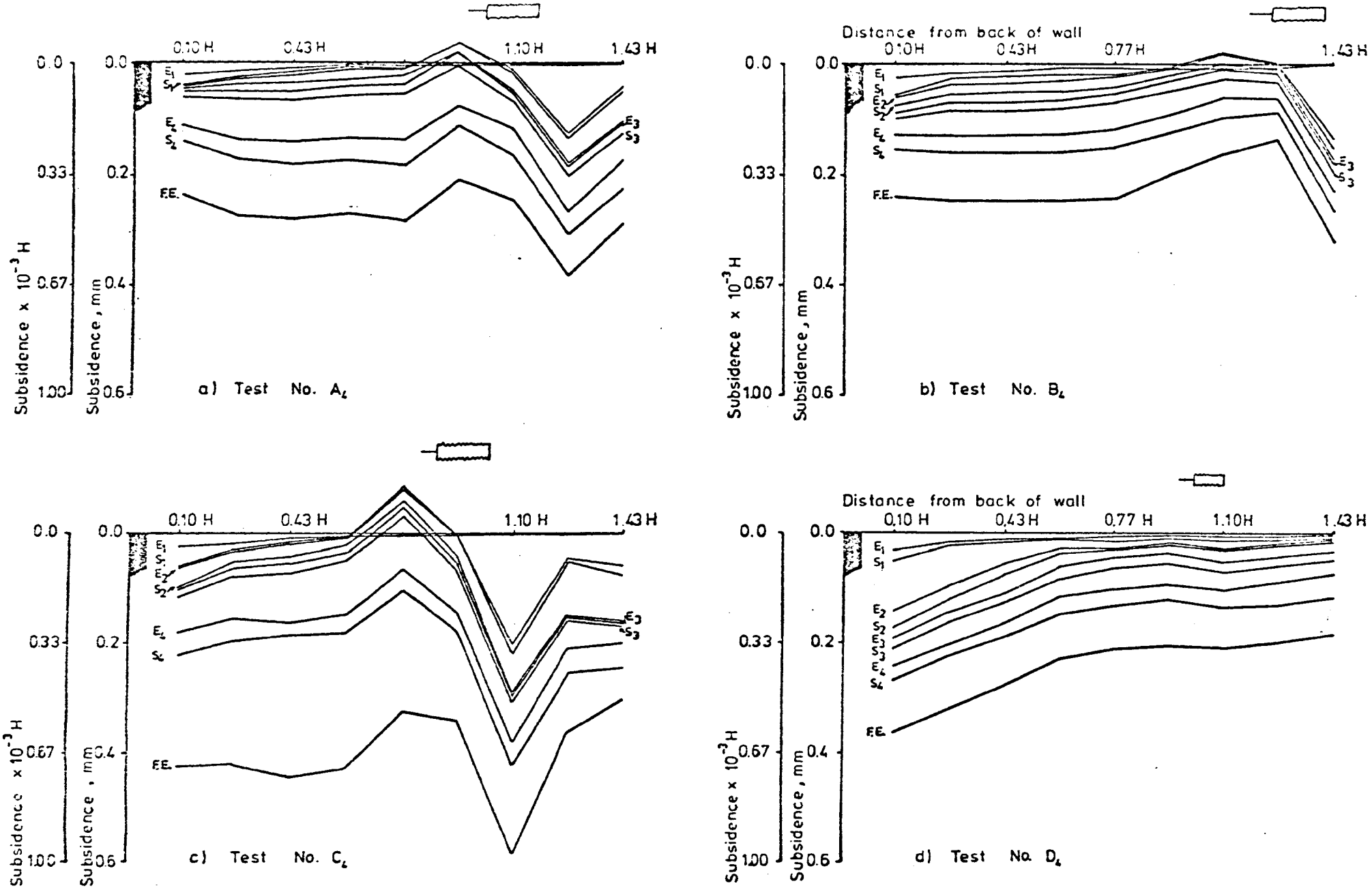

FIG. 6.11 SAND SUBSIDENCE PROFILES FOR EACH CONSTRUCTION STAGE FOR GROUP THREE TESTS
(FOUR ROW SYSTEMS)

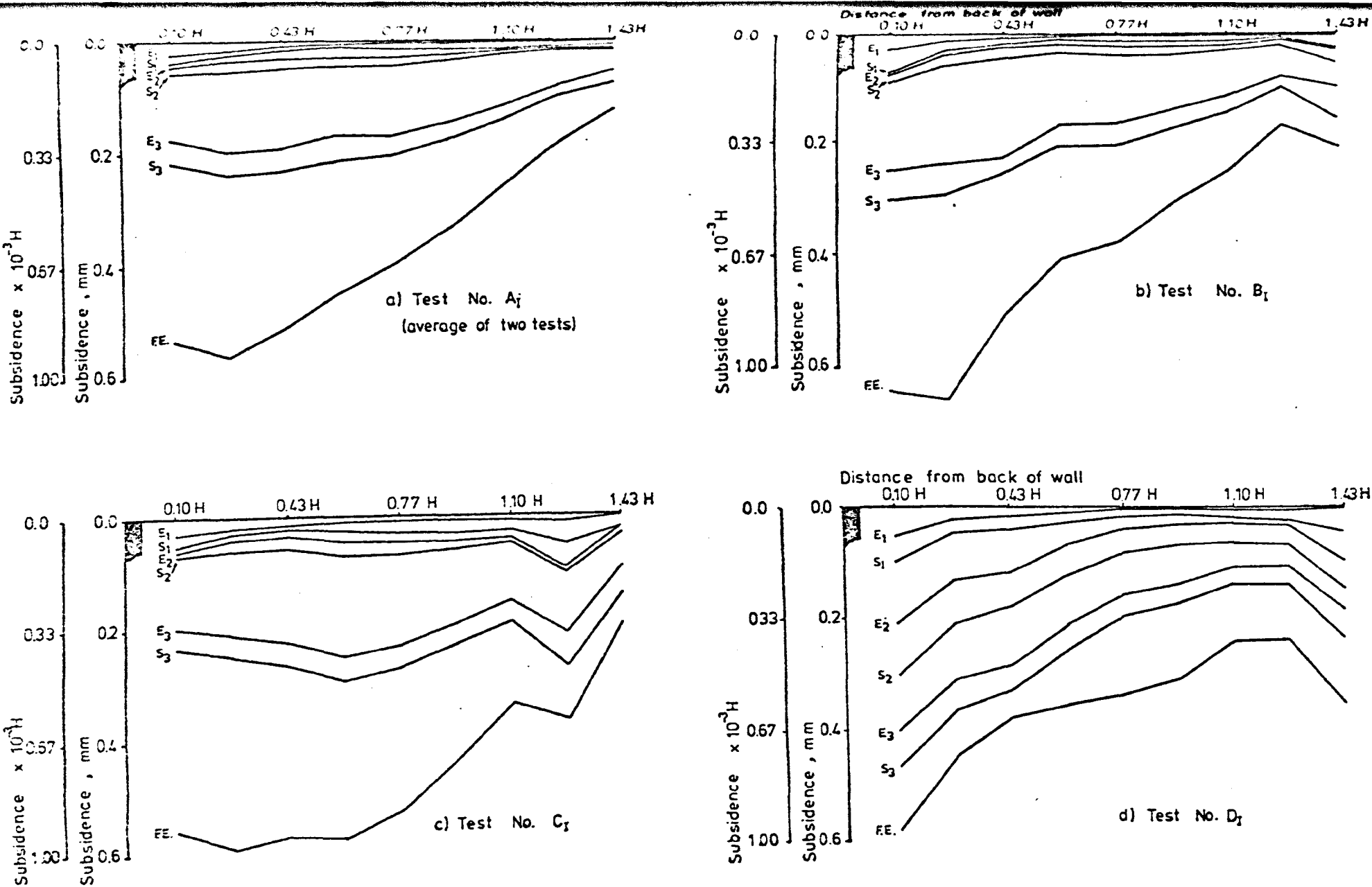

FIG. 6.12 SAND SUBSIDENCE PROFILES FOR EACH CONSTRUCTION STAGE FOR GROUP FOUR TESTS

(THREE ROW INCLINED SYSTEMS)

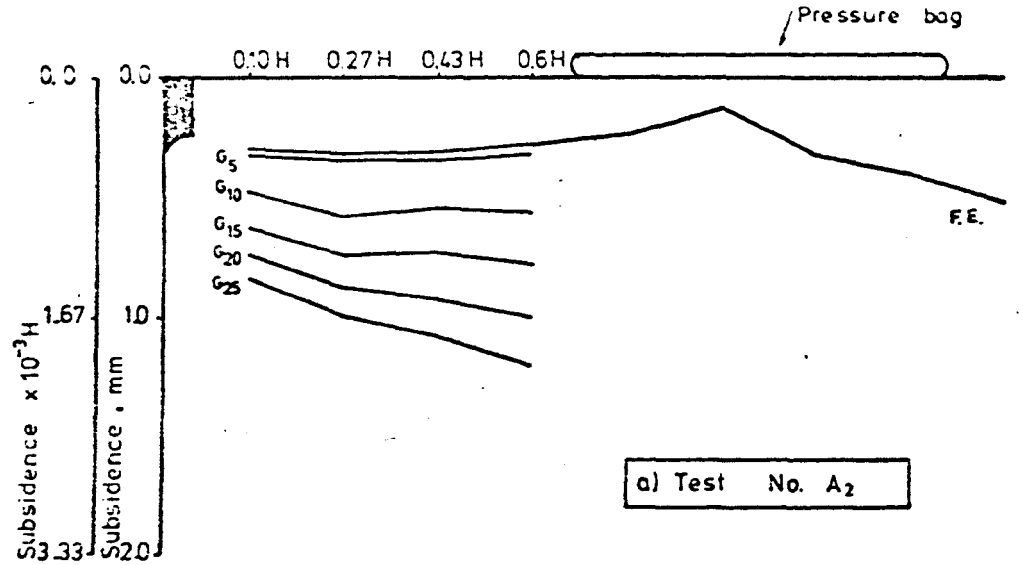

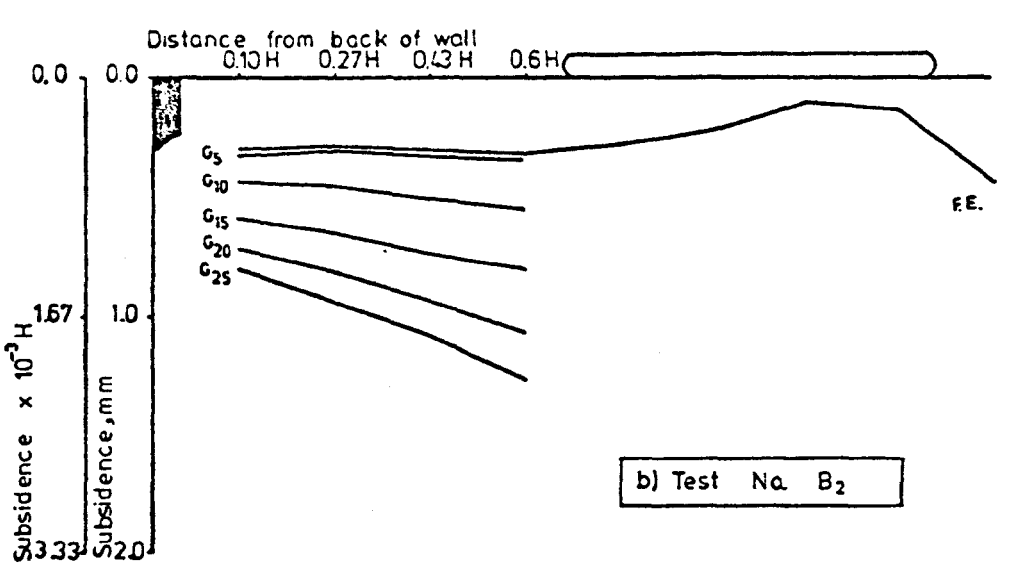

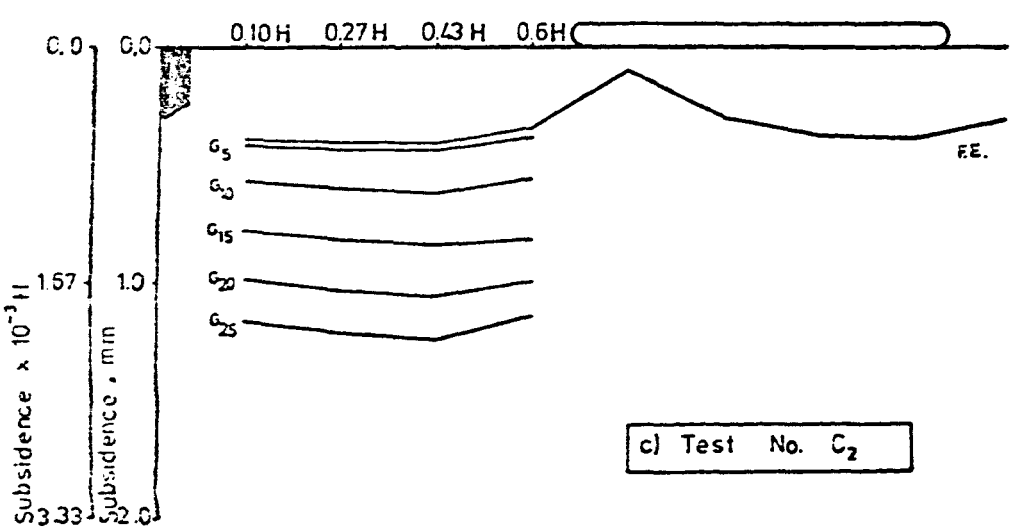

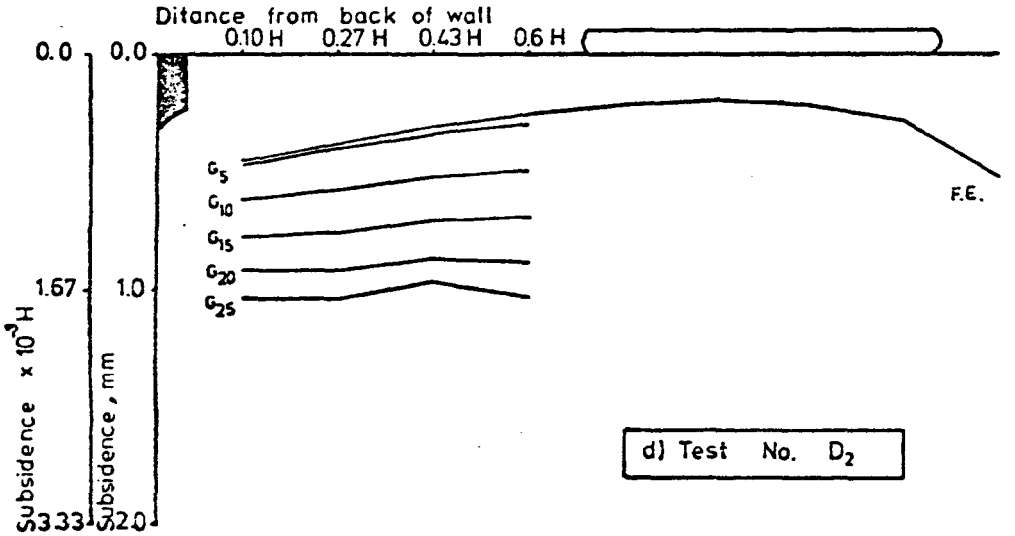

FIG. 6.13 SAND SUBSIDENCE DURING SURCHARGE LOADING STAGES FOR GROUP ONE TESTS

(TWO ROW SYSTEMS)

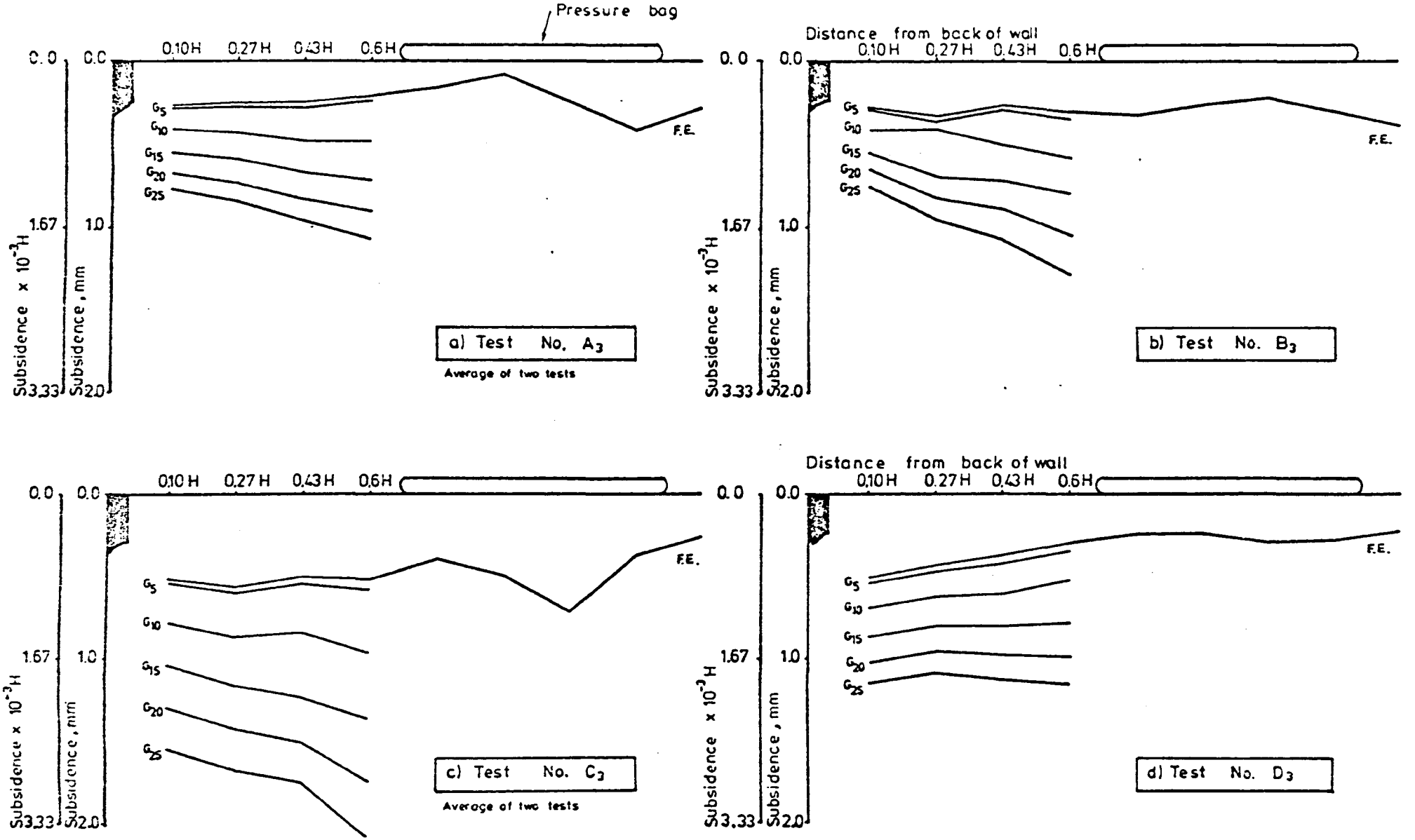

FIG. 6.14 SAND SUBSIDENCE DURING SURCHARG LOADING STAGES FOR GROUP TWO TESTS

(THREE ROW SYSTEMS)

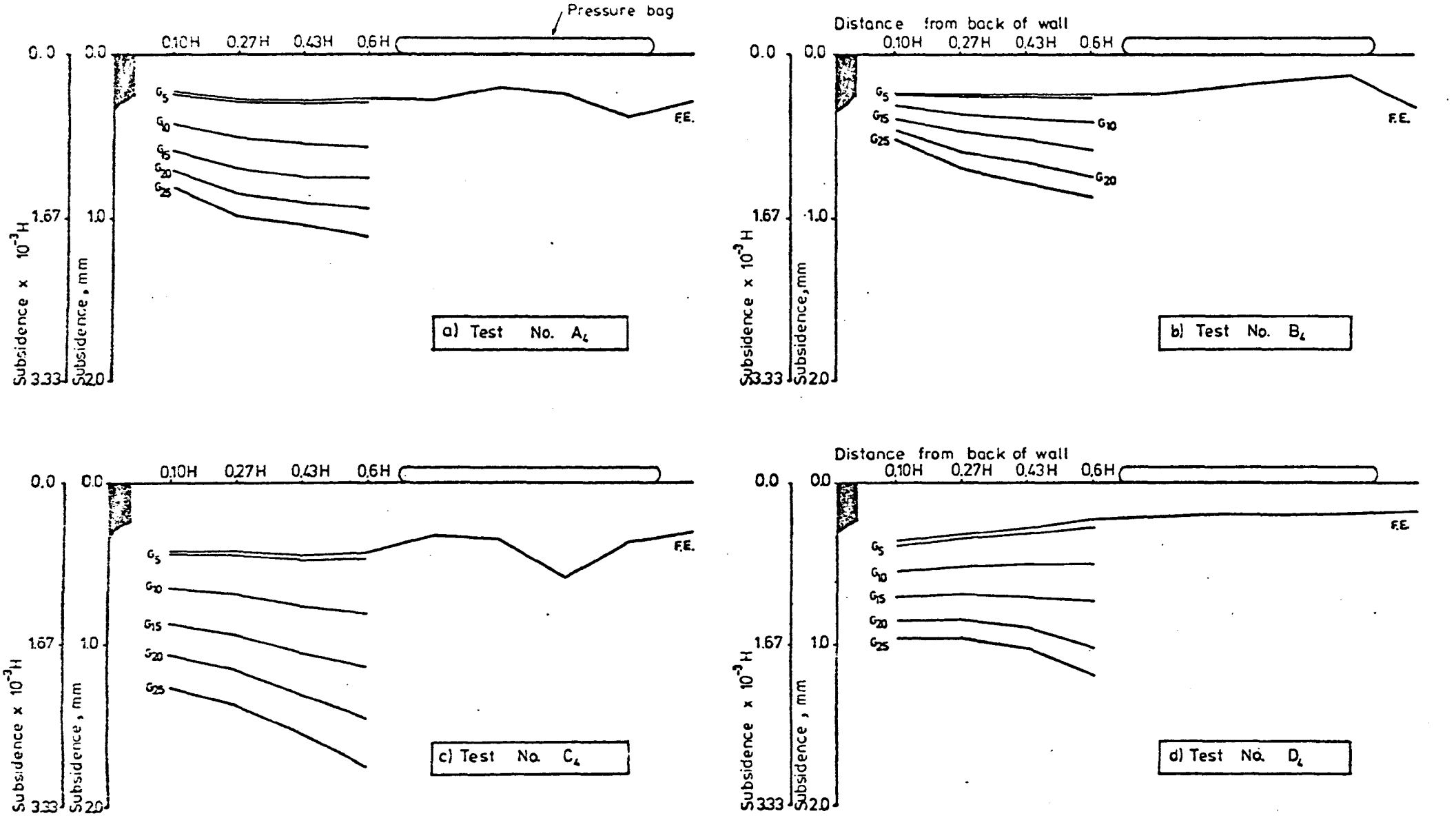

FIG. 6.15 SAND SUBSIDENCE DURING SURCHAGE LOADING STAGES FOR GROUP THREE TESTS

(FOUR ROW SYSTEMS)

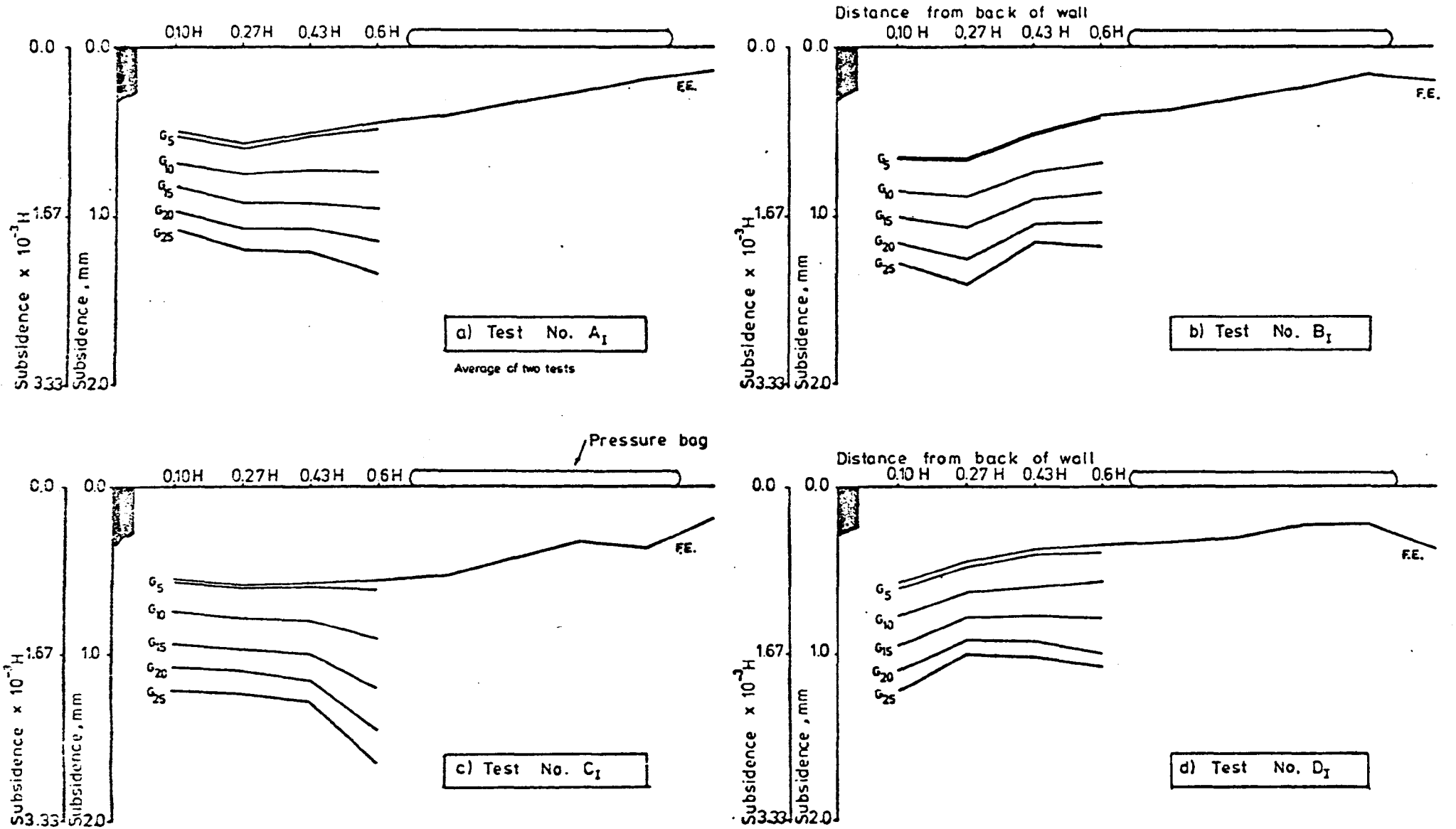

FIG. 6.16 SAND SUBSIDENCE DURING SURCHARGE LOADING STAGES FOR GROUP FOUR TESTS

(THREE ROW INCLINED SYSTEMS)

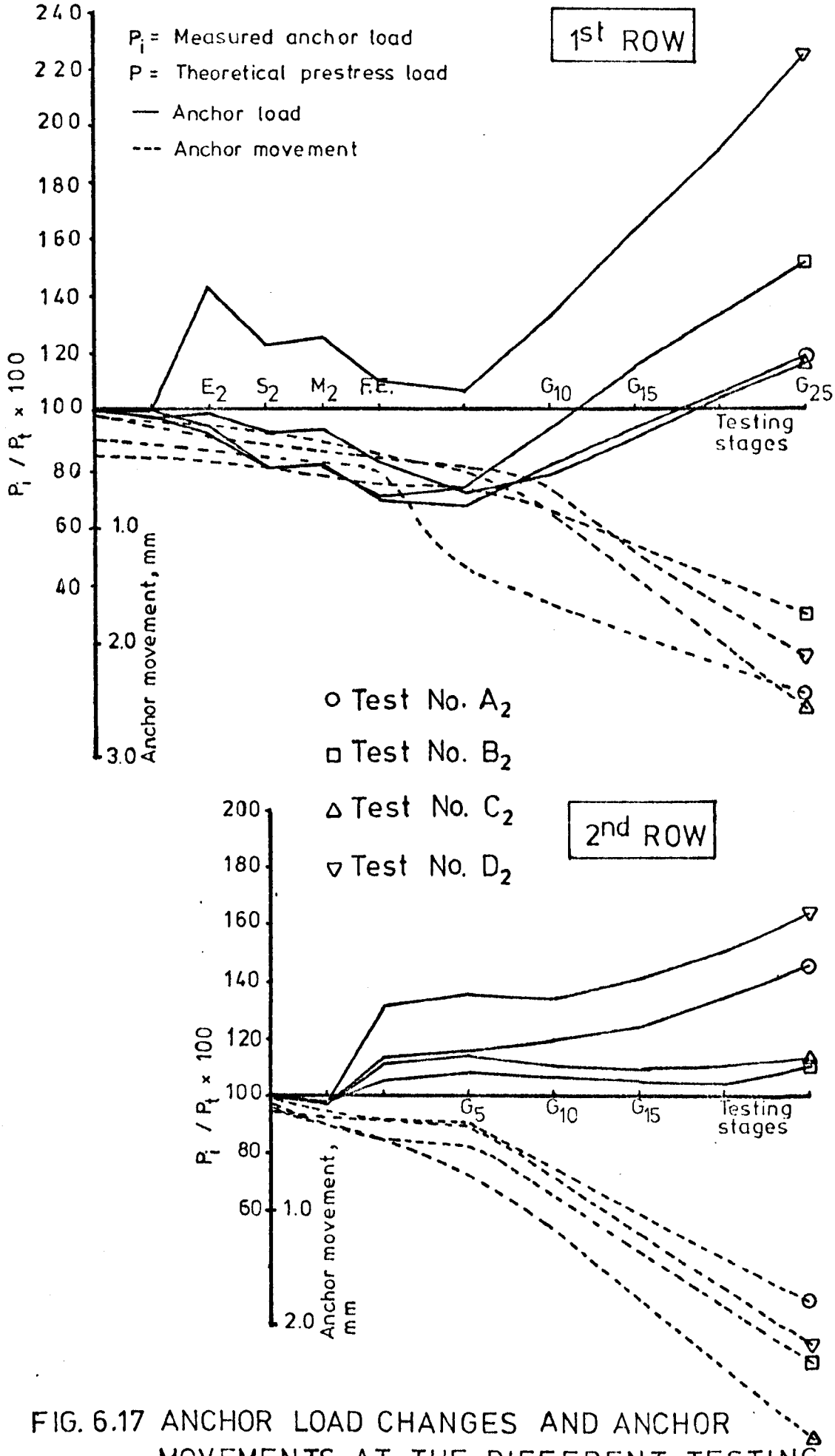

FIG. 6.17 ANCHOR LOAD CHANGES AND ANCHOR MOVEMENTS AT THE DIFFERENT TESTING STAGES FOR GROUP ONE TESTS (TWO ROW SYSTEMS)

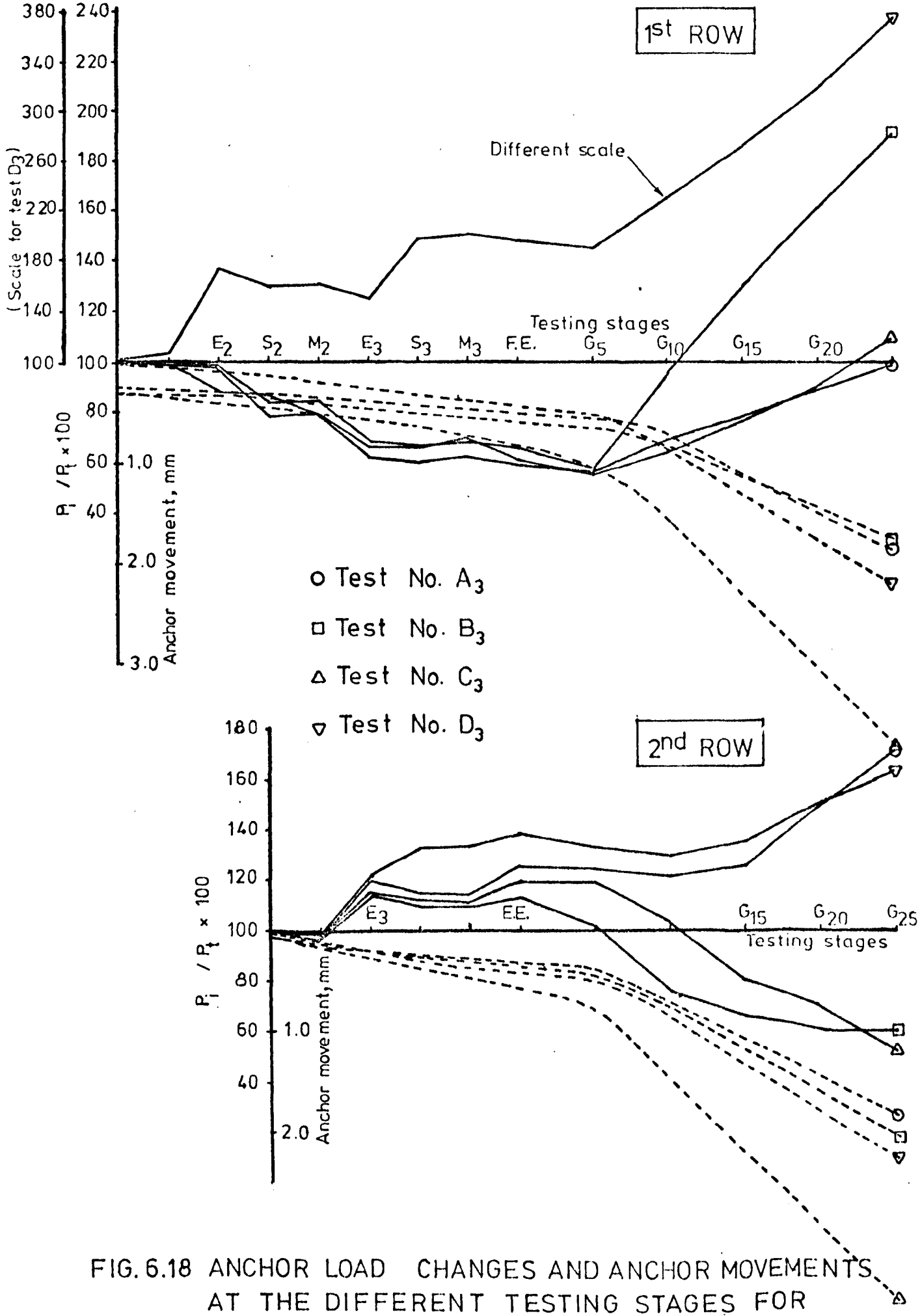

FIG. 6.18 ANCHOR LOAD CHANGES AND ANCHOR MOVEMENTS AT THE DIFFERENT TESTING STAGES FOR GROUP TWO TESTS (THREE ROW SYSTEMS)

P_i = Measured anchor load

P_t = Theoretical prestress load

—— Anchor load

--- Anchor movement

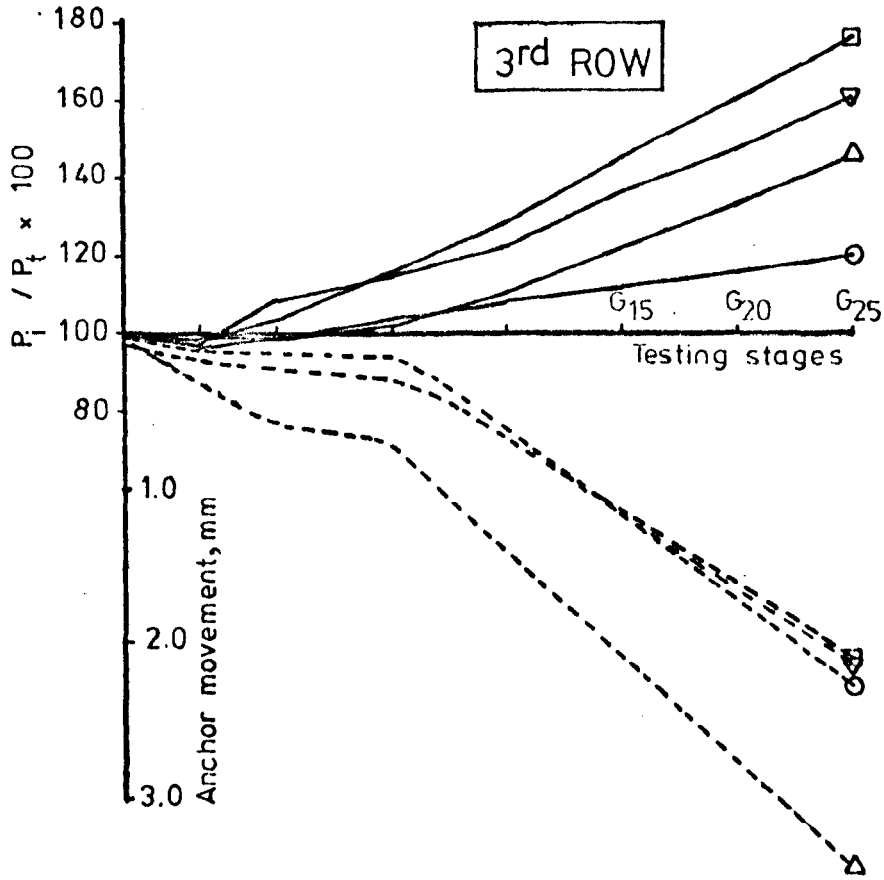

cont. FIG. 6.18 ANCHOR LOAD CHANGES AND ANCHOR MOVEMENTS AT THE DIFFERENT TESTING STAGES FOR GROUP TWO TESTS (THREE ROW SYSTEMS)

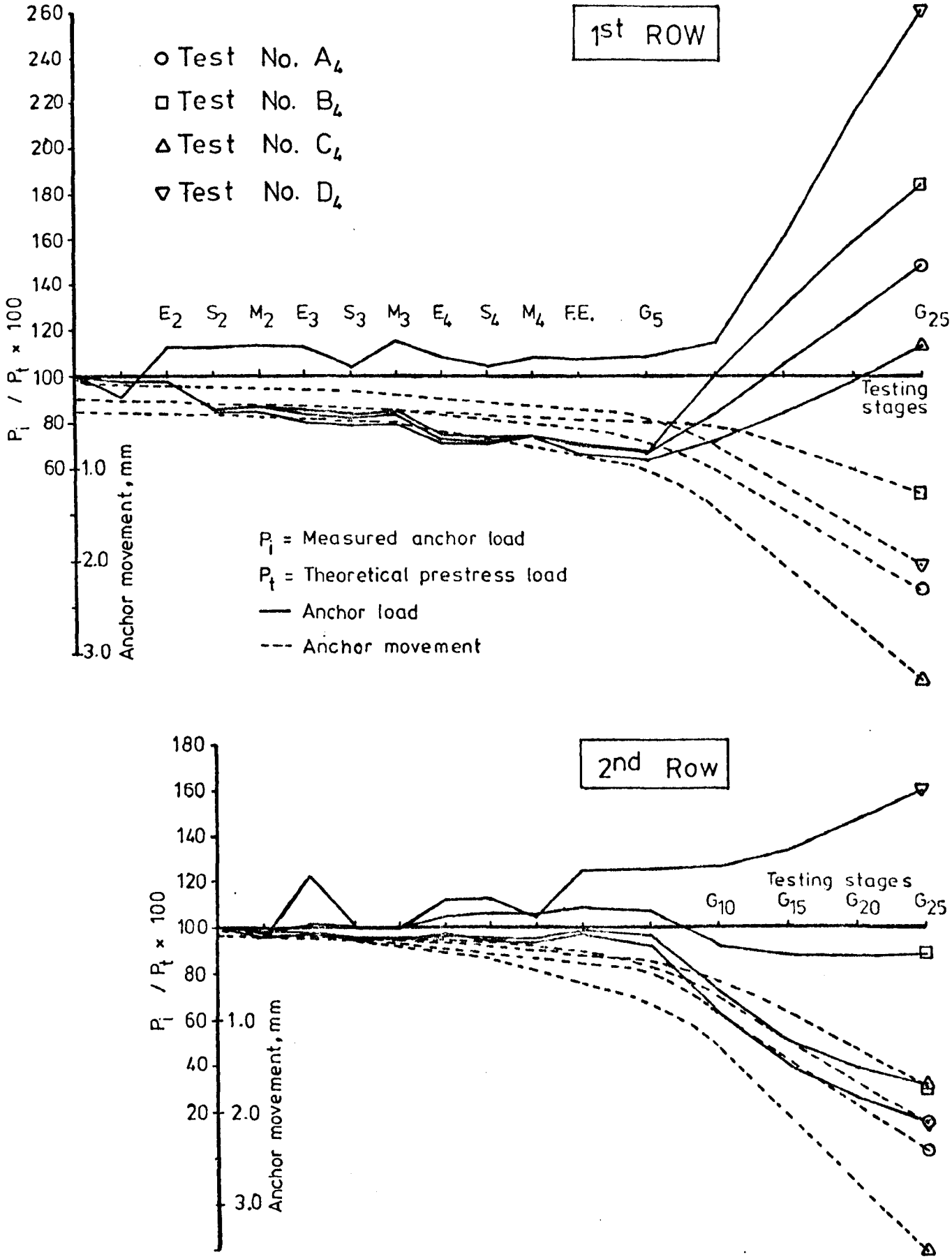

FIG. 6.19 ANCHOR LOAD CHANGES AND ANCHOR MOVEMENTS AT THE DIFFERENT TESTING STAGES FOR GROUP THREE TESTS (FOUR ROW SYSTEMS)

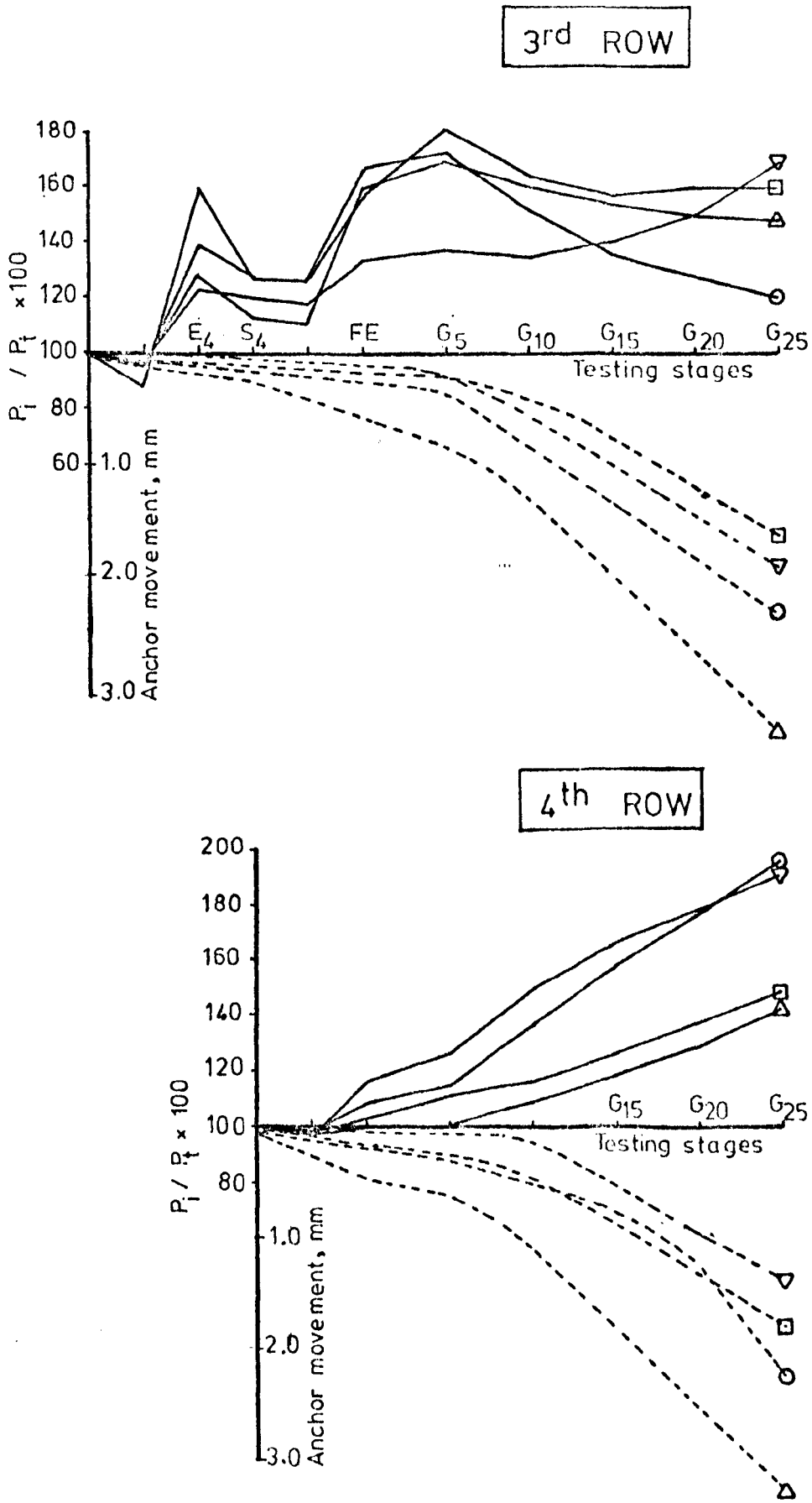

cont.FIG. 6.19 ANCHOR LOAD CHANGES AND ANCHOR MOVEMENTS AT THE DIFFERENT TESTING STAGES FOR GROUP THREE TESTS (FOUR ROW SYSTEMS)

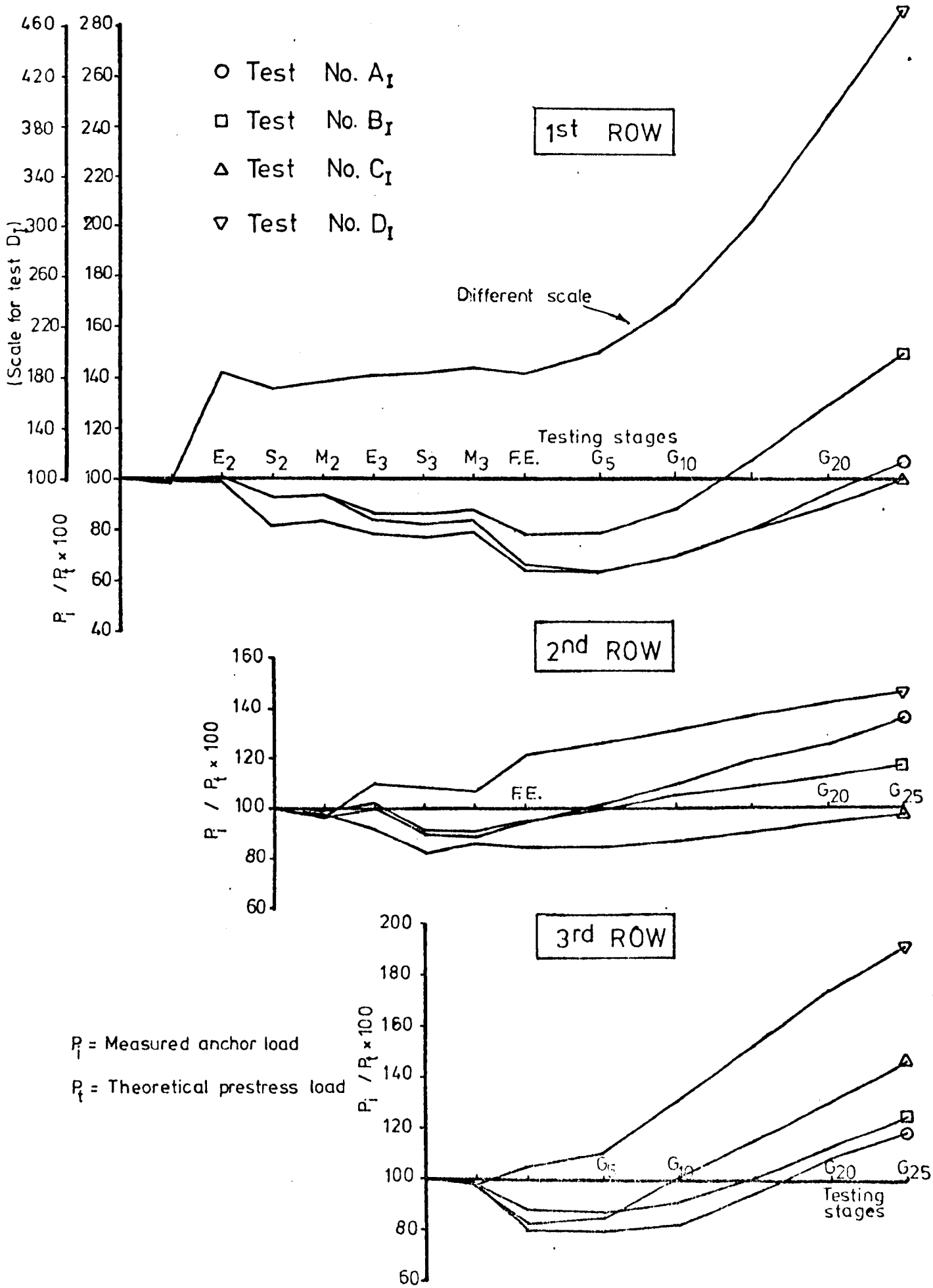

FIG. 6.20 ANCHOR LOAD CHANGES AT THE DIFFERENT TESTING STAGES FOR GROUP FOUR TESTS (THREE ROW INCLINED SYSTEMS)

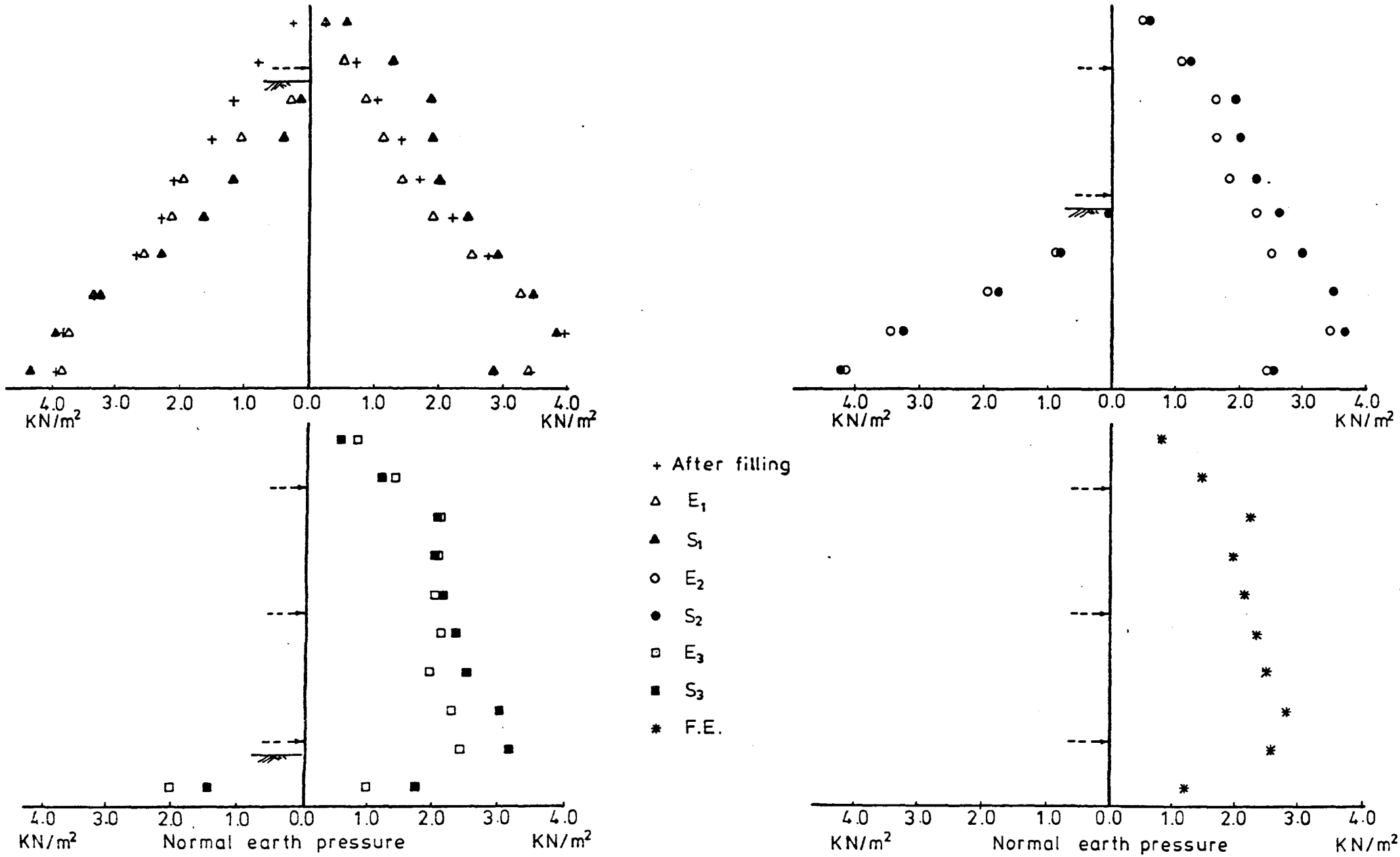

FIG. 6.21 NORMAL EARTH PRESSURE DISTRIBUTION AT THE DIFFERENT CONSTRUCTION STAGES FOR TEST No. B_3 (THREE ROW HORIZONTAL ANCHORS)

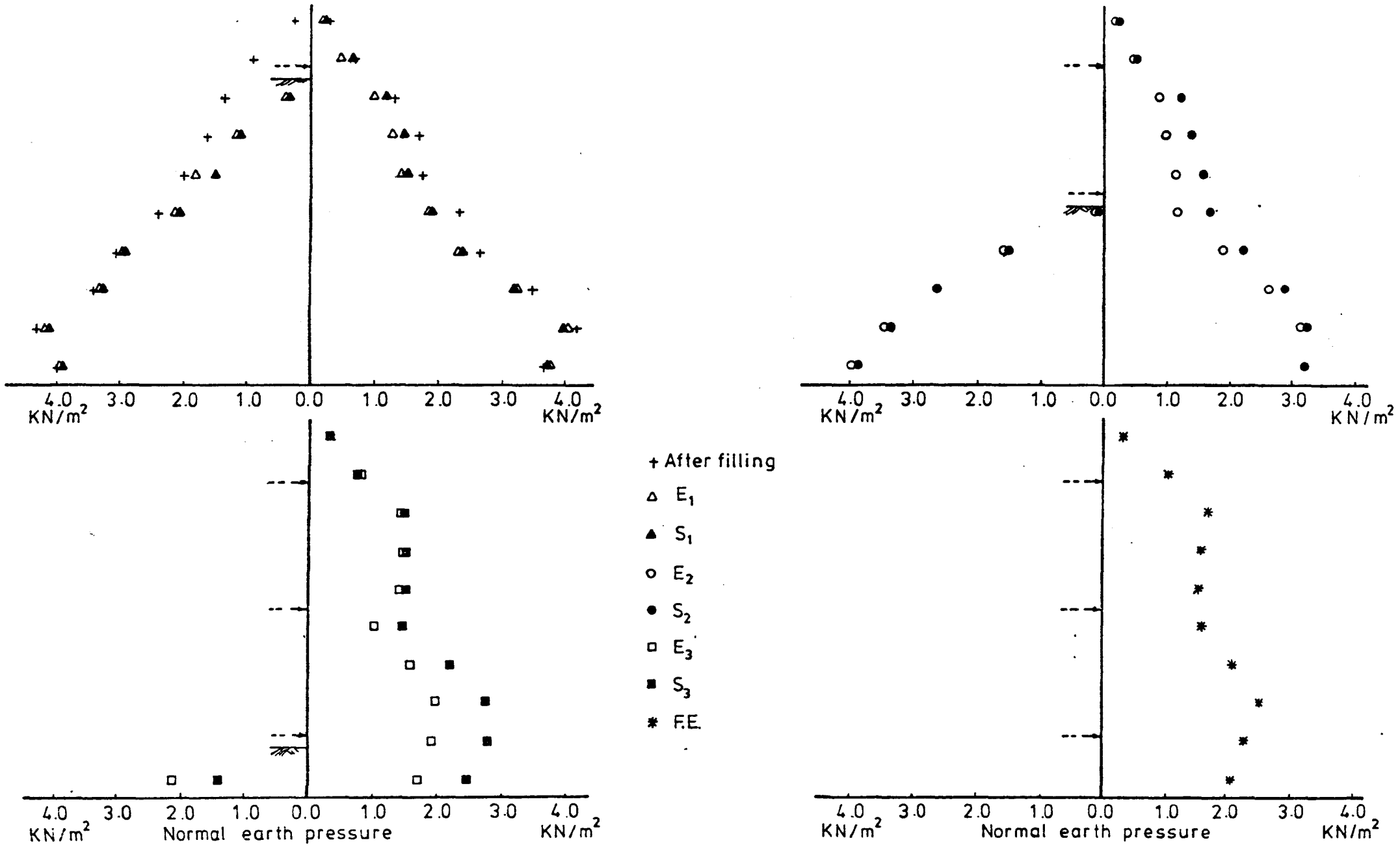

FIG. 6.22 NORMAL EARTH PRESSURE DISTRIBUTION AT THE DIFFERENT CONSTRUCTION STAGES FOR TEST No. D_3 (THREE ROW HORIZONTAL ANCHORS)

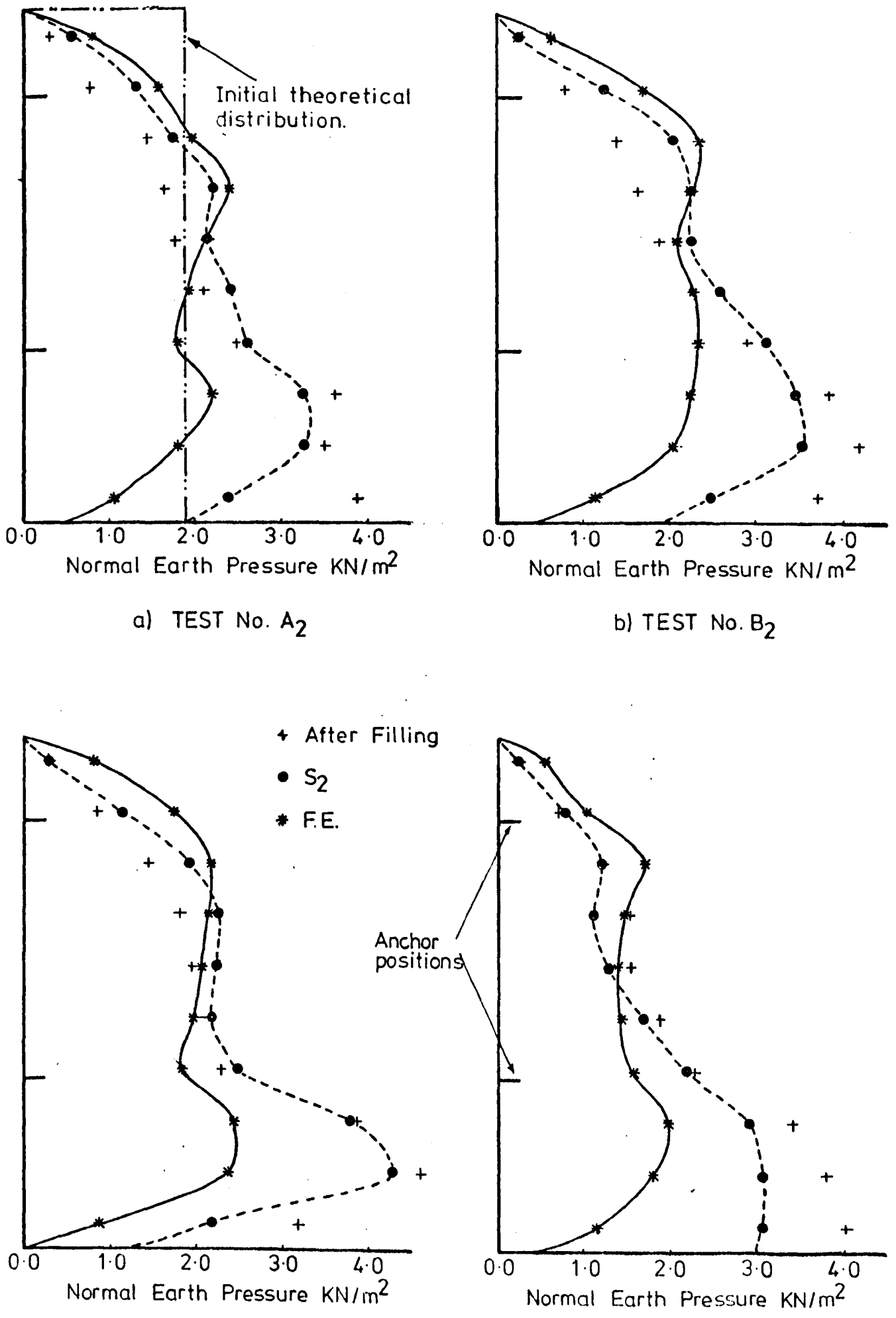

FIG.6.23 EARTH PRESSURE DISTRIBUTION AFTER FILLING AND AT THE FINAL TWO CONSTRUCTION STAGES FOR GROUP ONE TESTS (TWO ROW SYSTEMS)

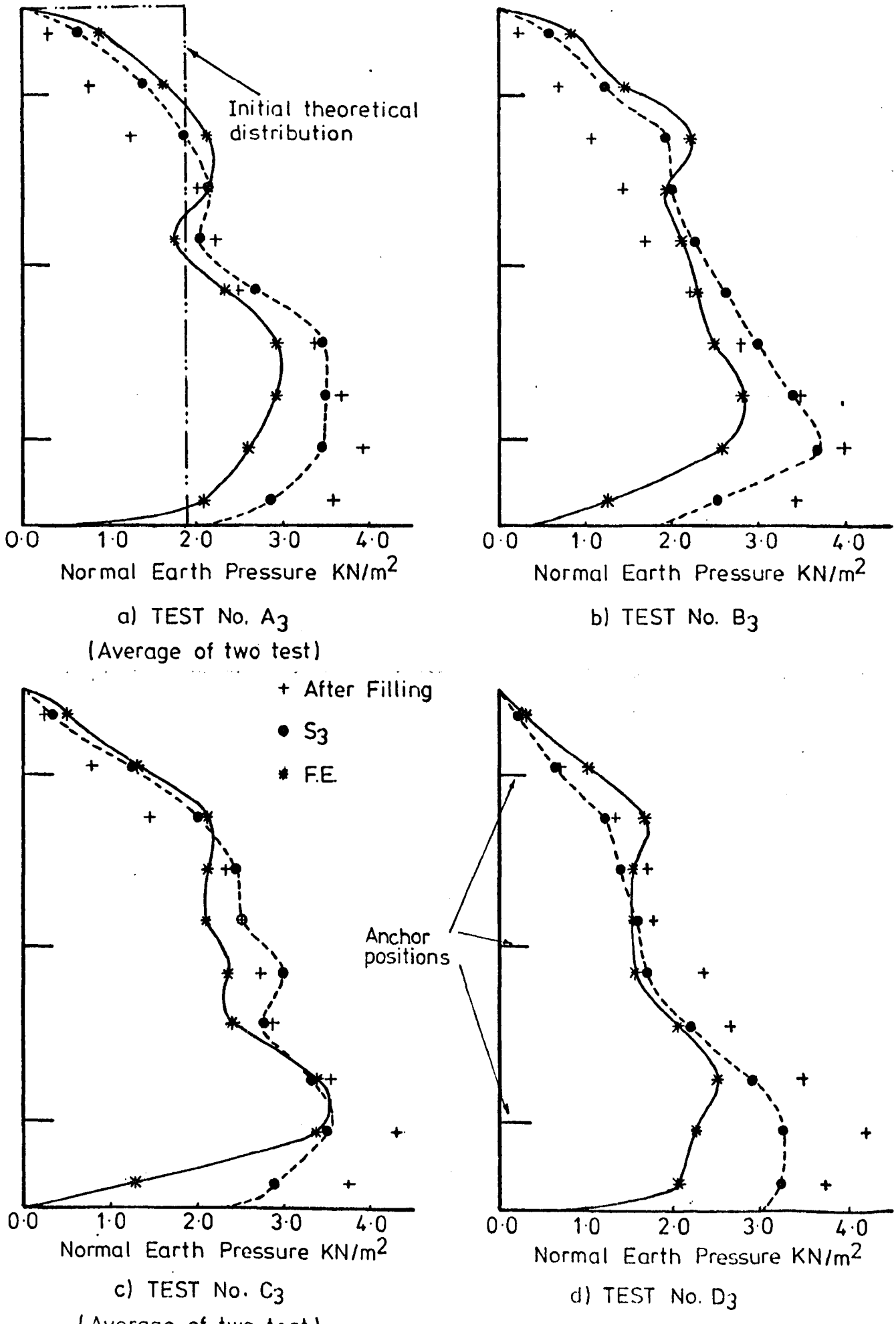

FIG. 6.24 EARTH PRESSURE DISTRIBUTION AFTER FILLING AND AT THE FINAL TWO CONSTRUCTION STAGES FOR GROUP TWO TESTS (THREE ROW SYSTEMS)

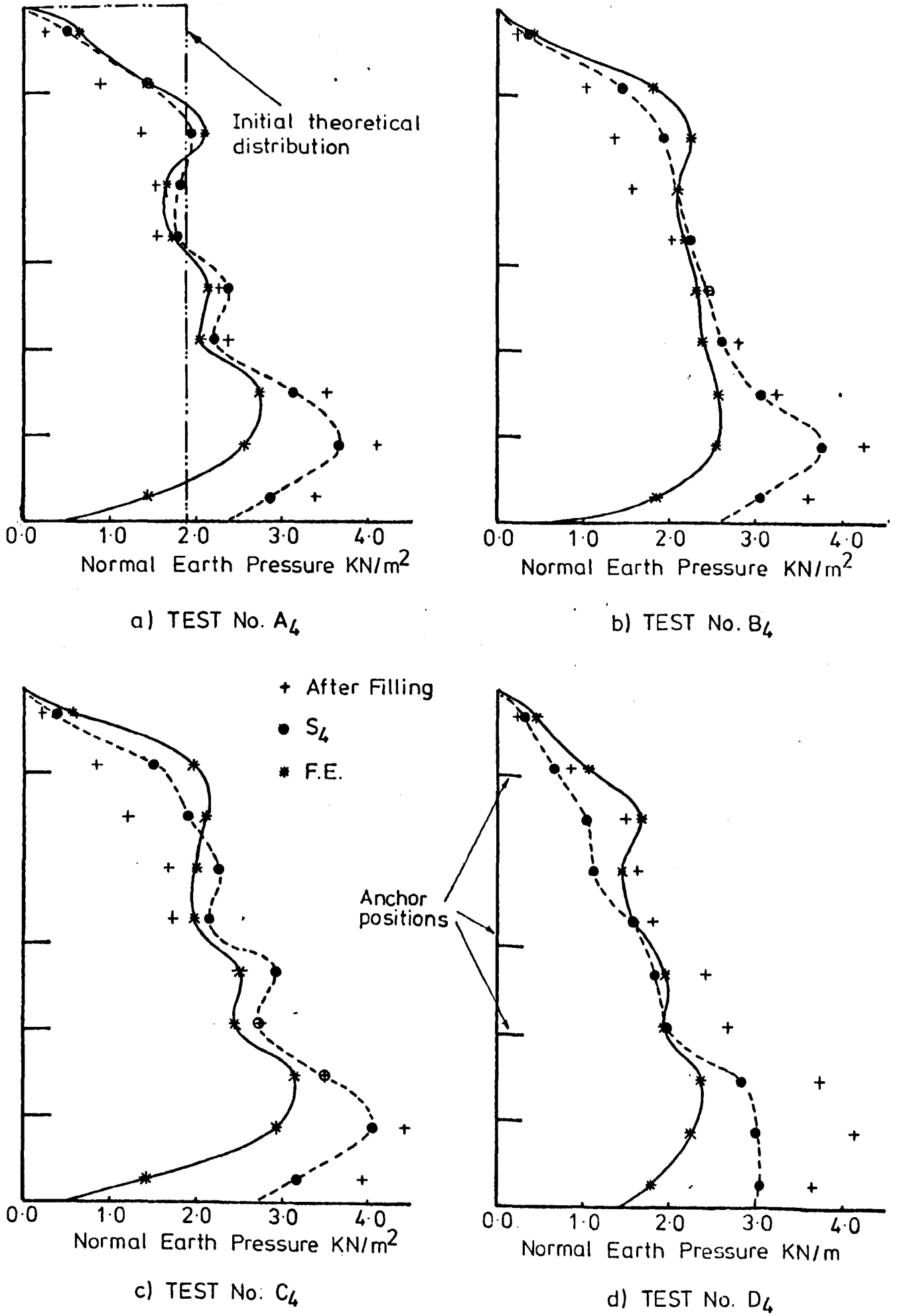

FIG. 6.25 EARTH PRESSURE DISTRIBUTION AFTER FILLING AND AT THE FINAL TWO CONSTRUCTION STAGES FOR GROUP THREE TESTS (FOUR ROW SYSTEMS)

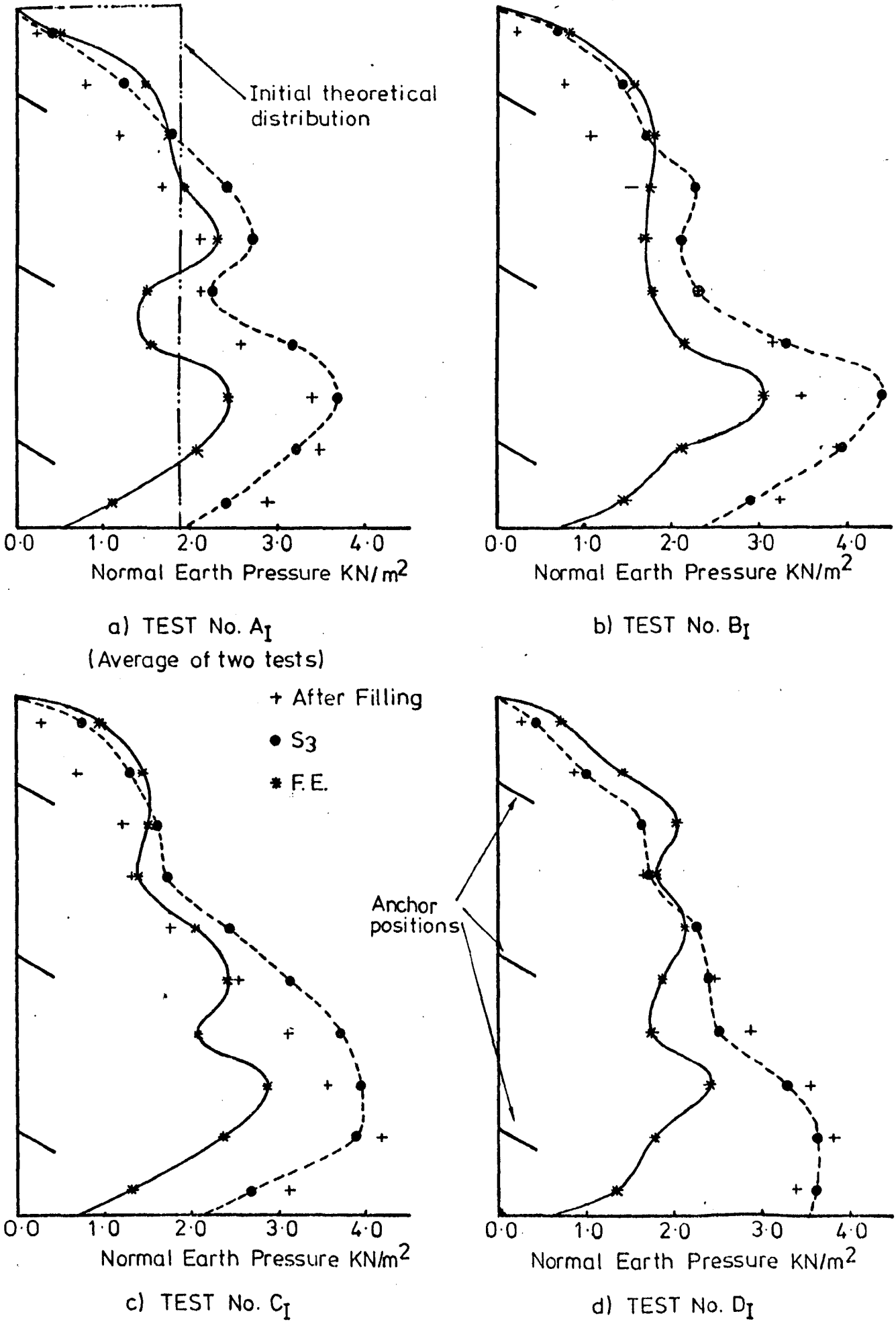

FIG. 6.26 EARTH PRESSURE DISTRIBUTION AFTER FILLING AND AT THE FINAL TWO CONSTRUCTION STAGES FOR GROUP FOUR TESTS (THREE ROW INCLINED SYSTEMS)

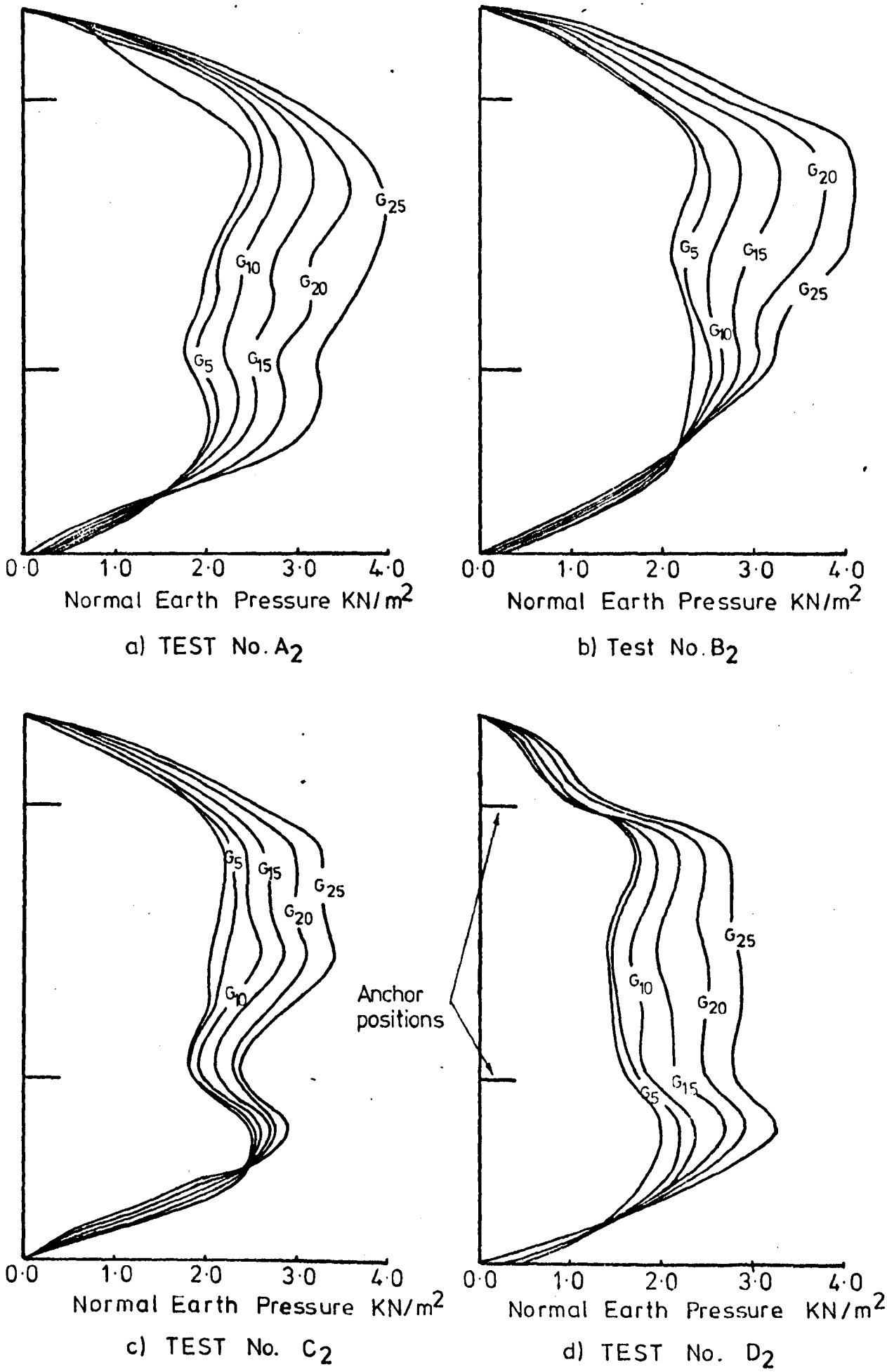

FIG. 6.27 NORMAL EARTH PRESSURE DISTRIBUTION DURING THE DIFFERENT STAGES OF SURCHARGE LOADING FOR GROUP ONE TESTS (TWO ROW SYSTEMS)

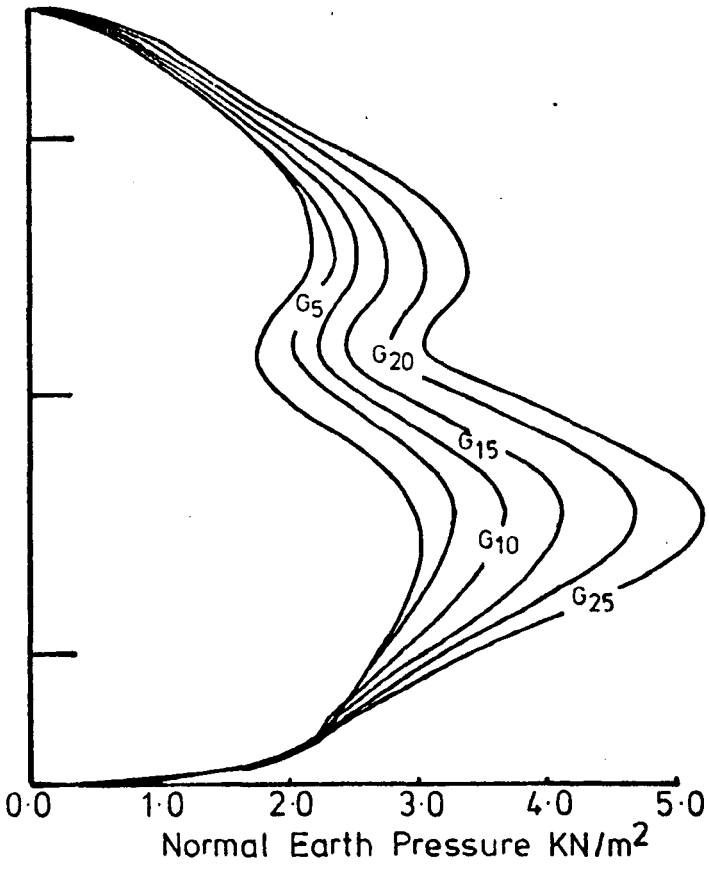

a) TEST No. A_3
(Average of two tests)

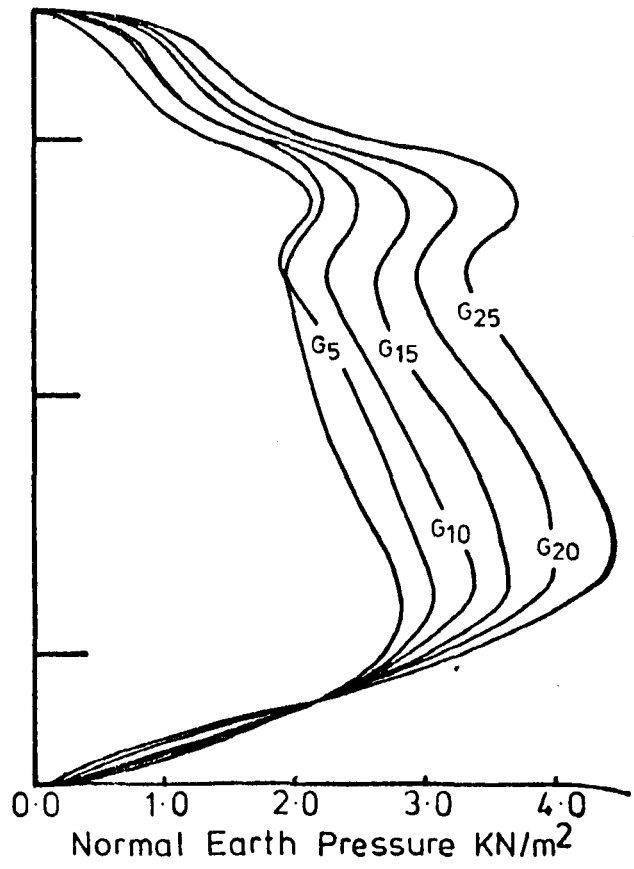

b) TEST No. B_3

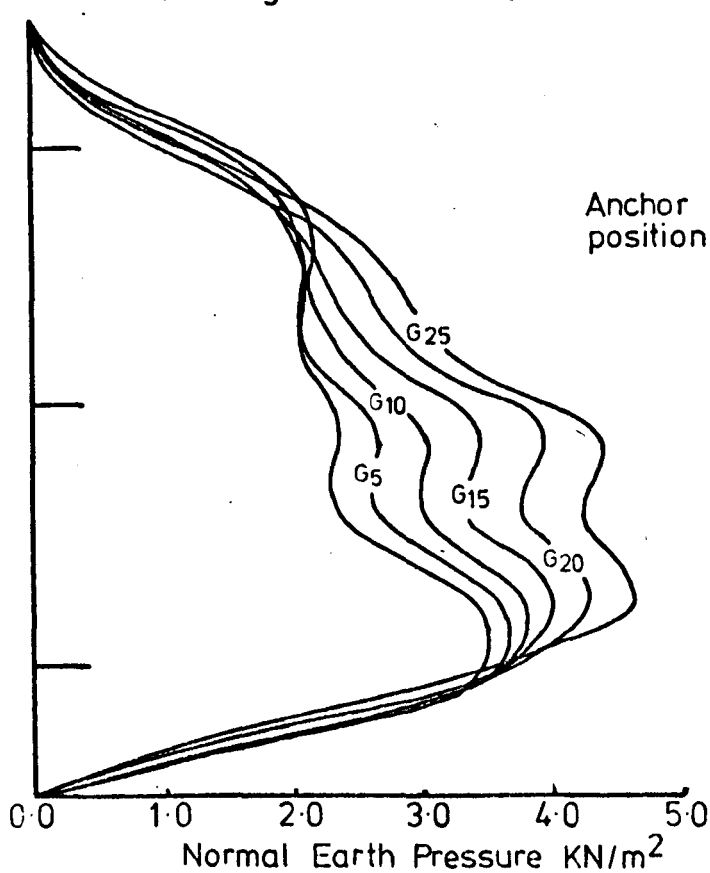

c) TEST No. C_3
(Average of two tests)

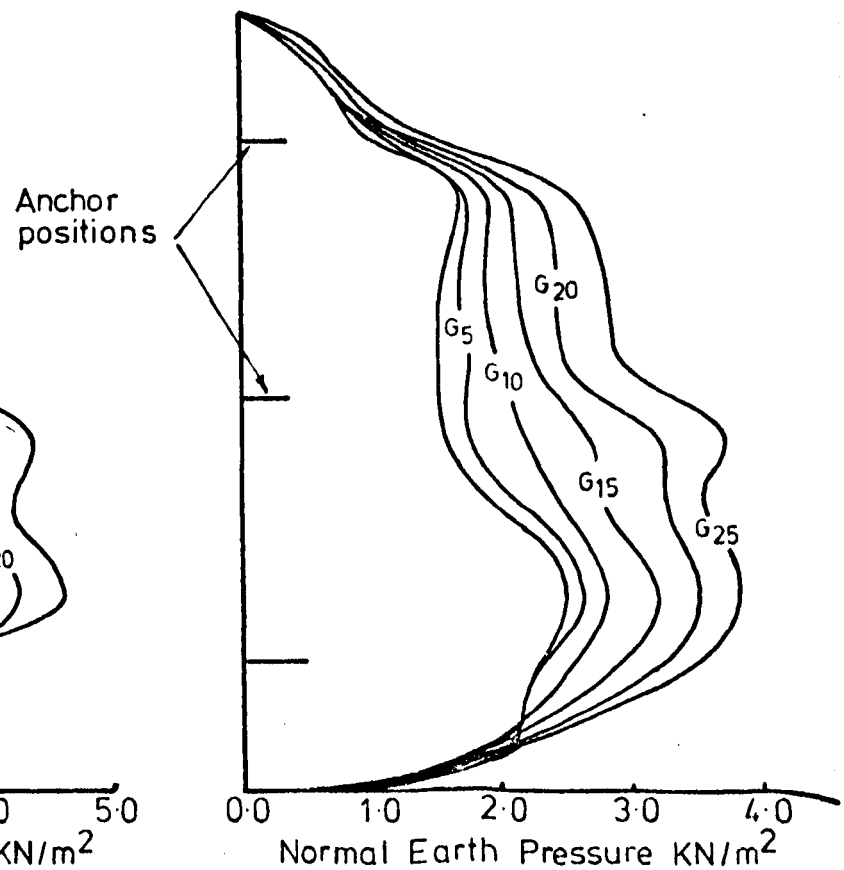

d) TEST No. D_3

FIG. 6.28 NORMAL EARTH PRESSURE DISTRIBUTION DURING THE DIFFERENT STAGES OF SURCHARGE LOADING FOR GROUP TOW TESTS (THREE ROW SYSTEMS)

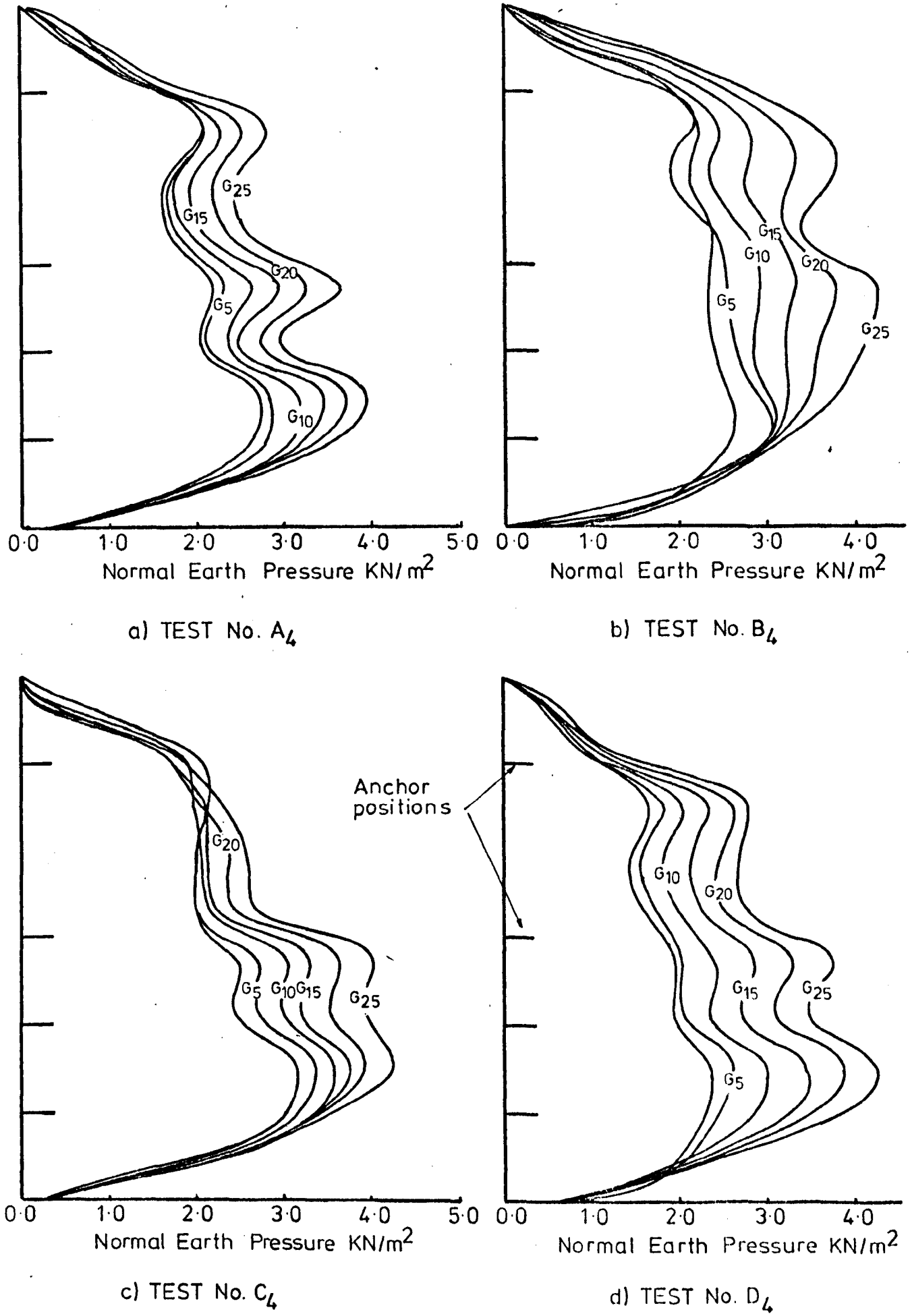

FIG.6.29 NORMAL EARTH PRESSURE DISTRIBUTION DURING THE DIFFERENT STAGES OF SURCHARGE LOADING FOR GROUP THREE TESTS (FOUR ROW SYSTEMS)

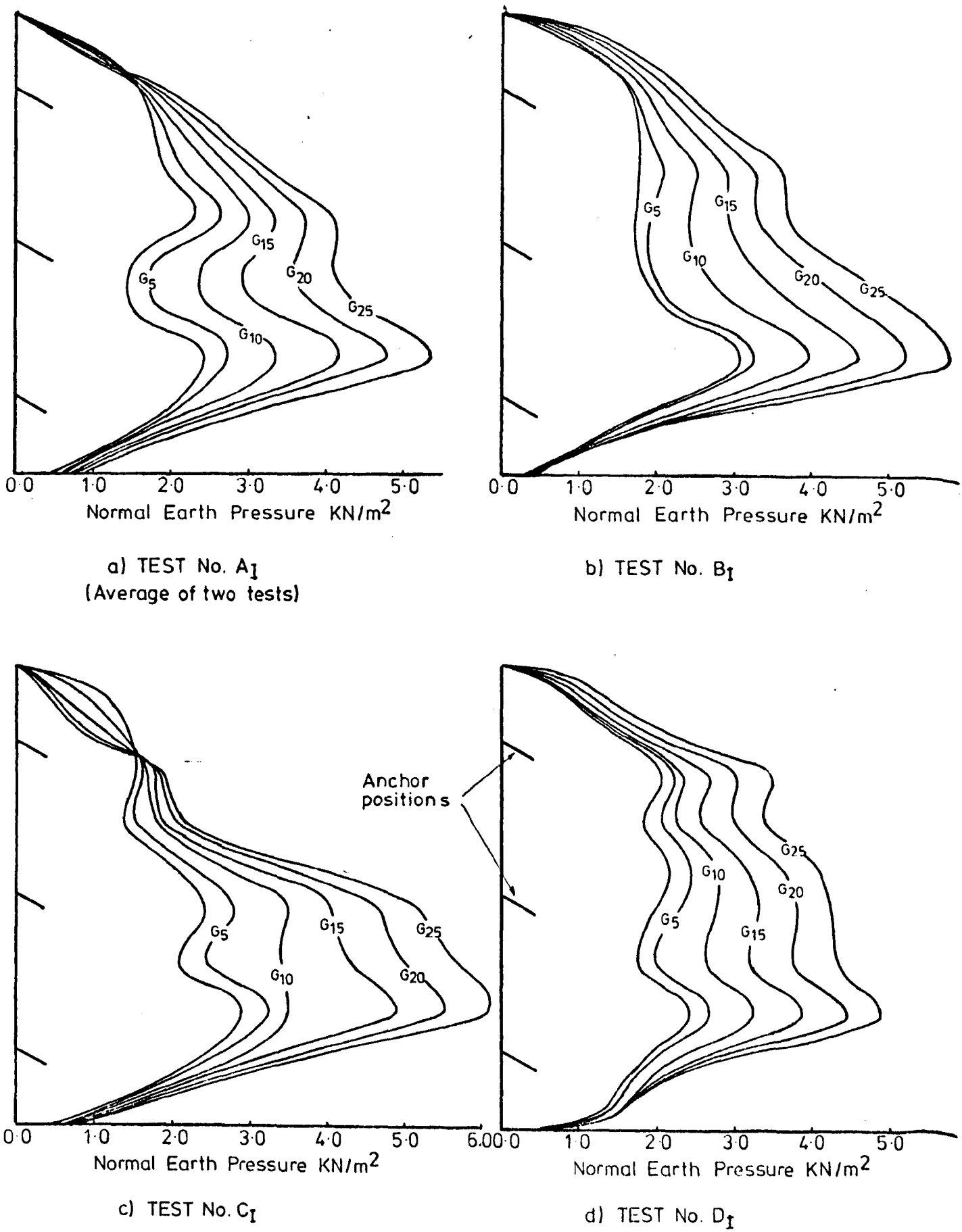

FIG. 6.30 NORMAL EARTH PRESSURE DISTRIBUTION DURING THE DIFFERENT STAGES OF SURCHARGE LOADING FOR GROUP FOUR TESTS (THREE ROW INCLINED SYSTEMS)

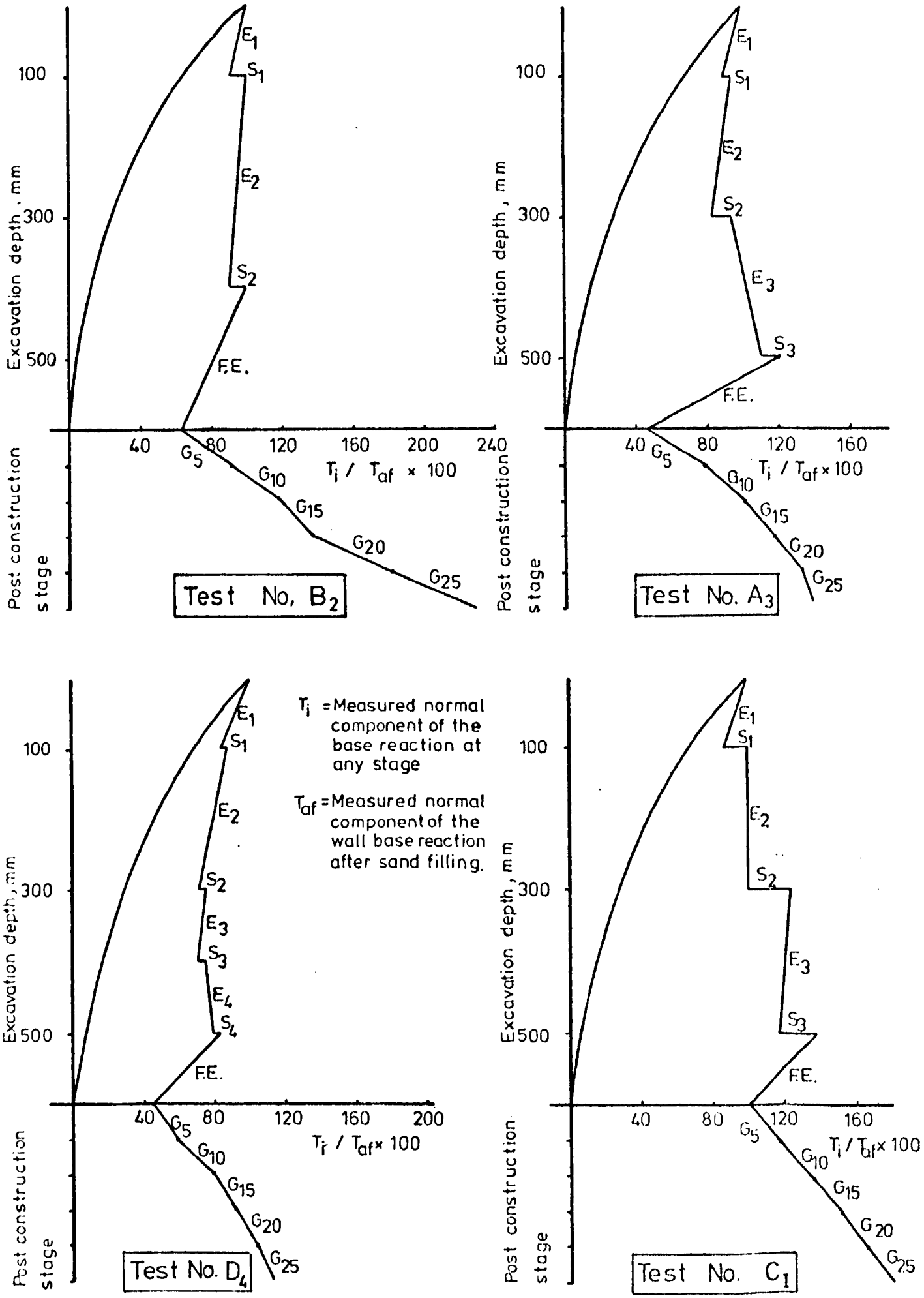

FIG.6.31 VARIATION OF THE NORMAL COMPONENT OF THE WALL BASE REACTION AT THE DIFFERENT TESTING STAGES FOR TESTS B_2, A_3, D_4 AND C_1

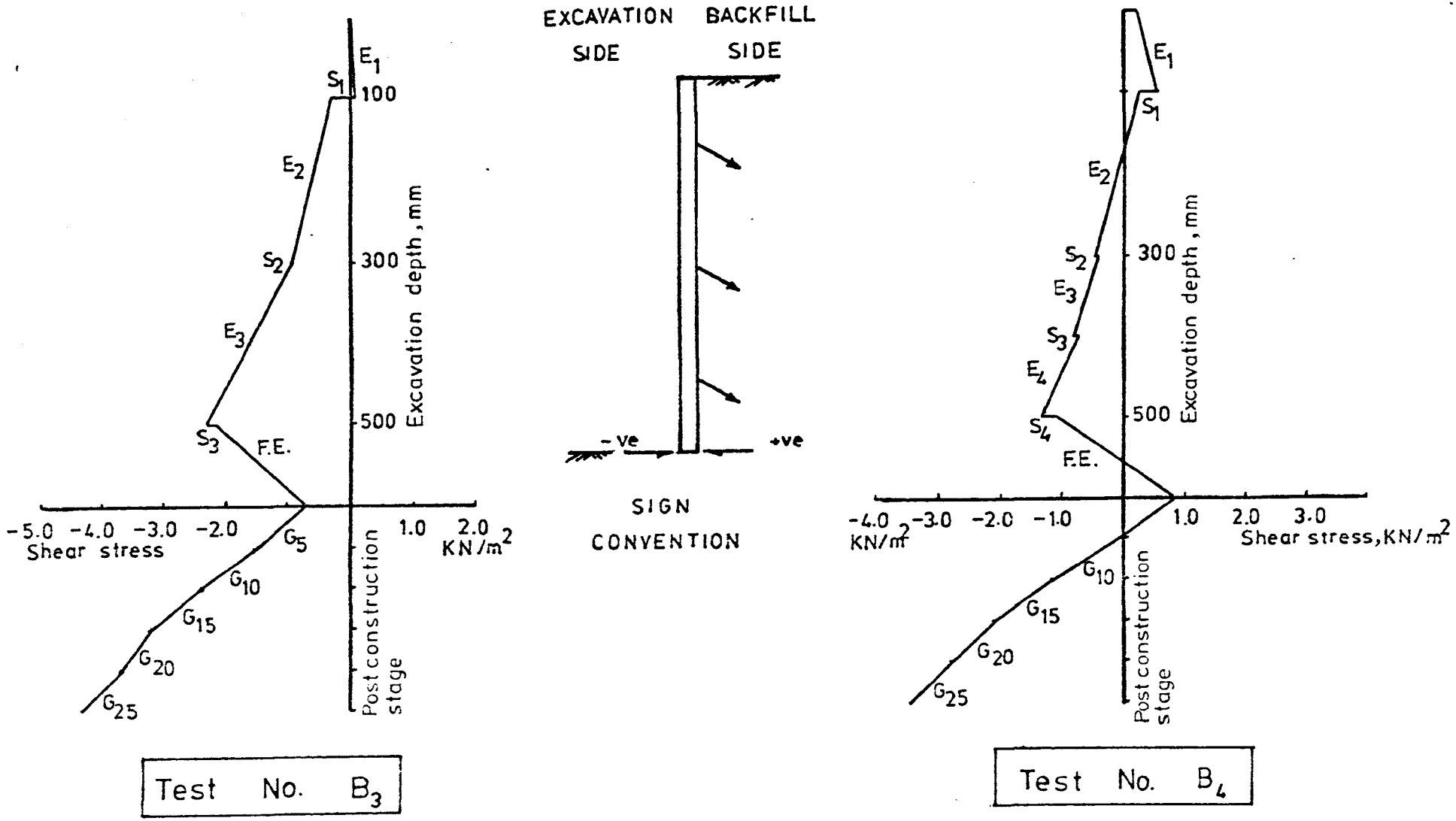

FIG. 6.32 VARIATION OF THE SHEAR COMPONENT OF THE WALL BASE REACTION AT THE DIFFERENT TESTING STAGES FOR TESTS B_3 AND B_4

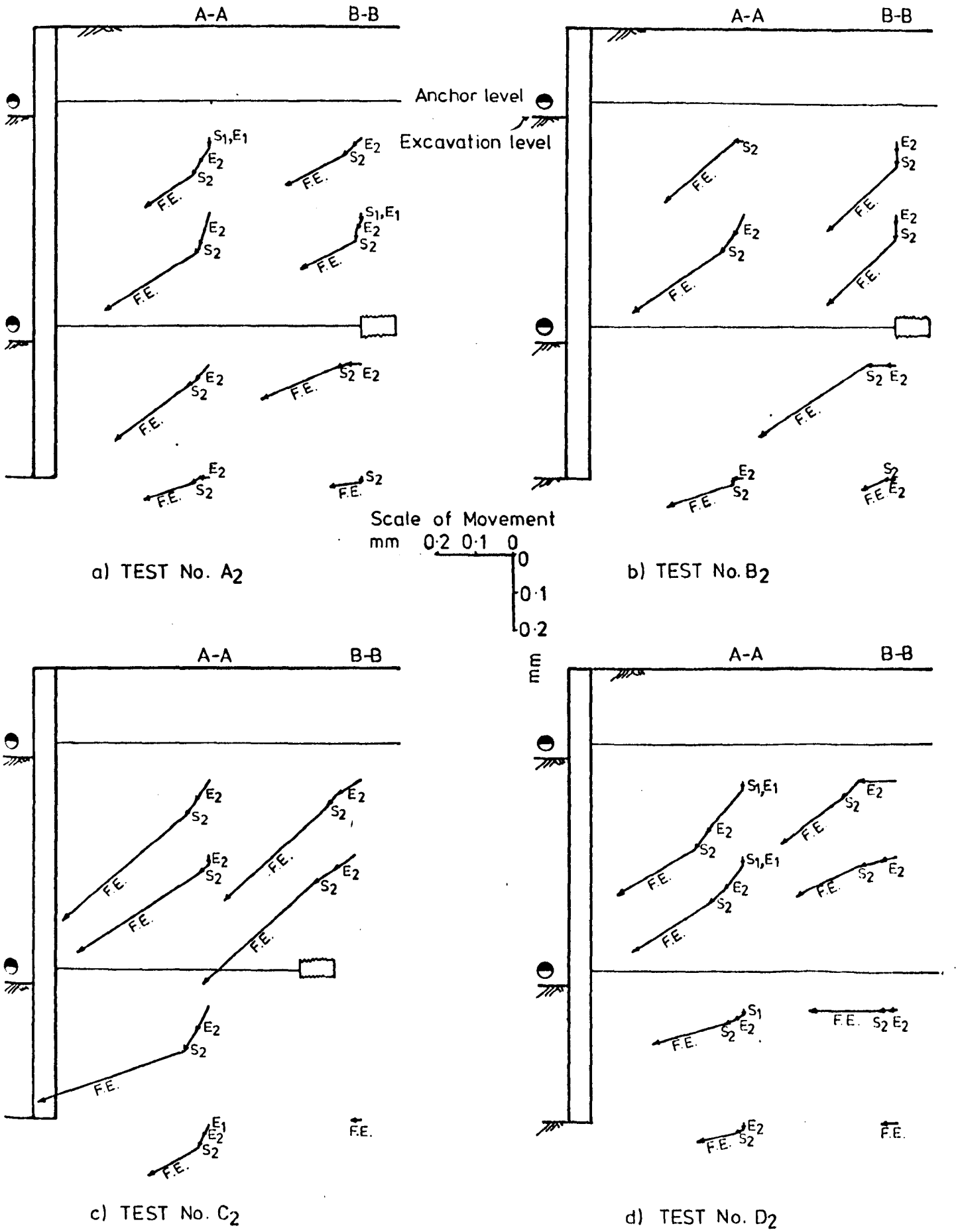

FIG. 6.33 SAND MOVEMENTS WITHIN THE RETAINED SAND MASS DURING THE DIFFERENT CONSTRUCTION STAGES FOR GROUP ONE TESTS (TWO ROW SYSTEMS)

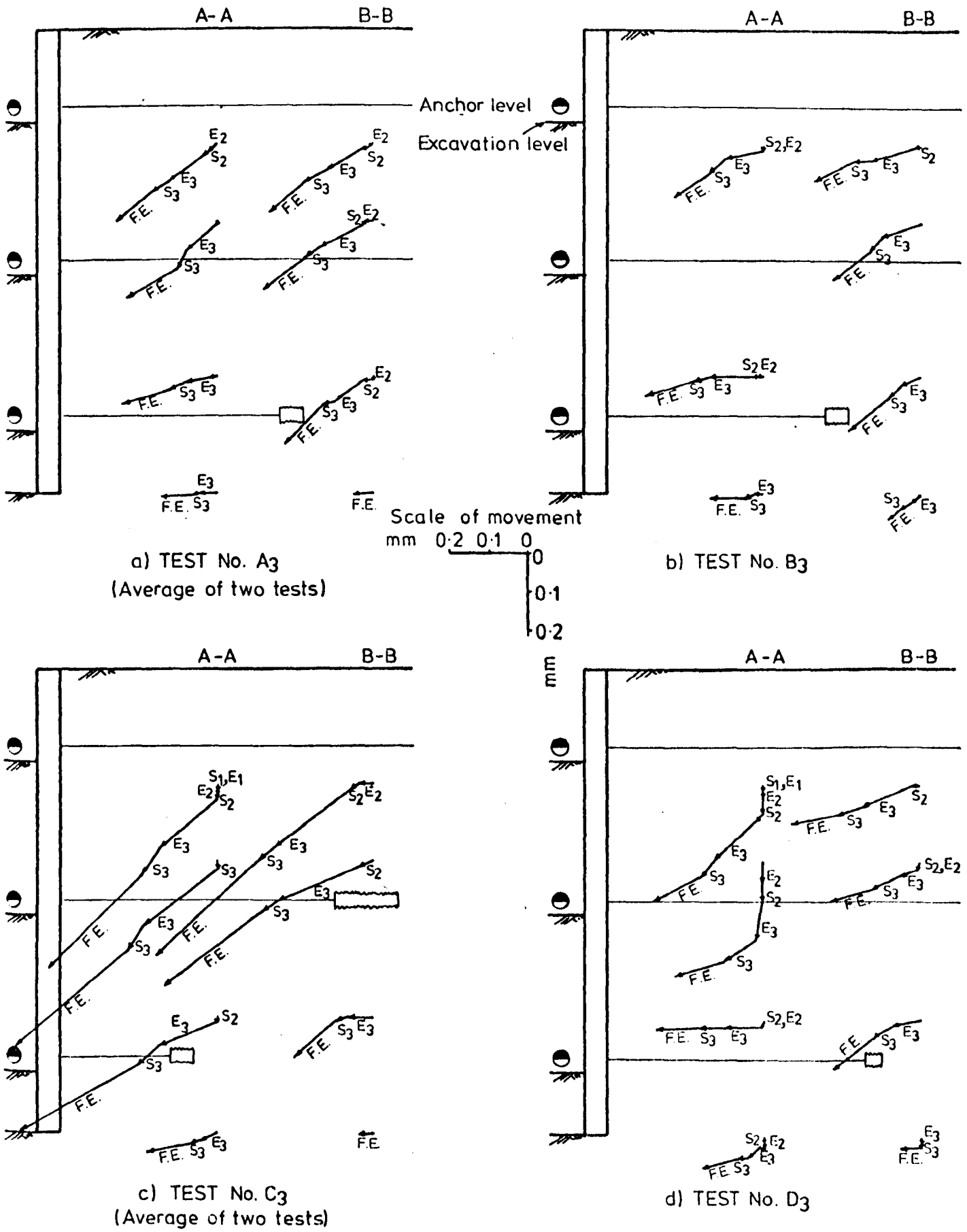

FIG. 6.34 SAND MOVEMENTS WITHIN THE RETAINED SAND MASS DURING THE DIFFERENT CONSTRUCTION STAGES FOR GROUP TWO TESTS (THREE ROW SYSTEMS)

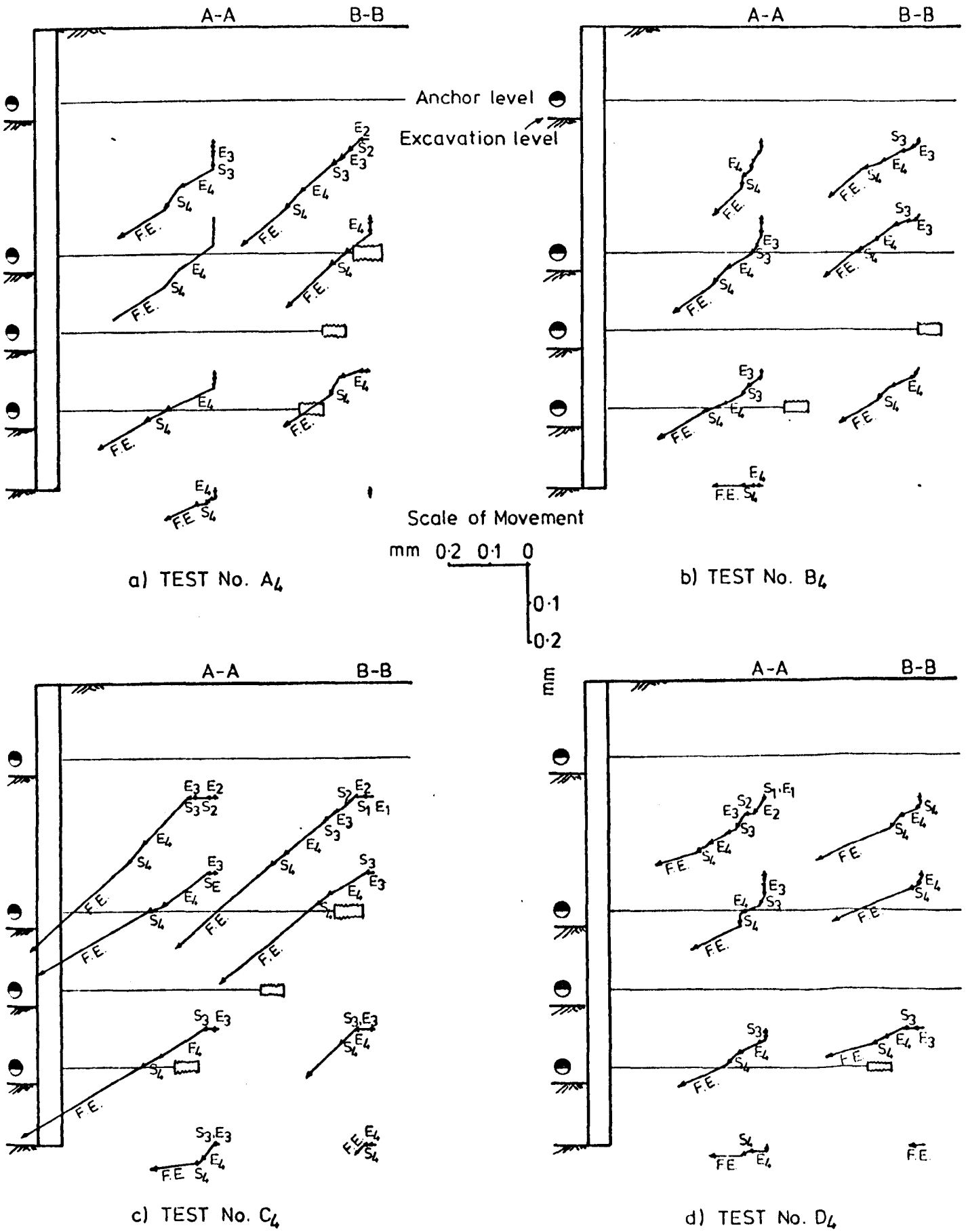

FIG. 6.35 SAND MOVEMENTS WITHIN THE RETAINED SAND MASS DURING THE DIFFERENT CONSTRUCTION STAGES FOR GROUP THREE TESTS (FOUR ROW SYSTEMS)

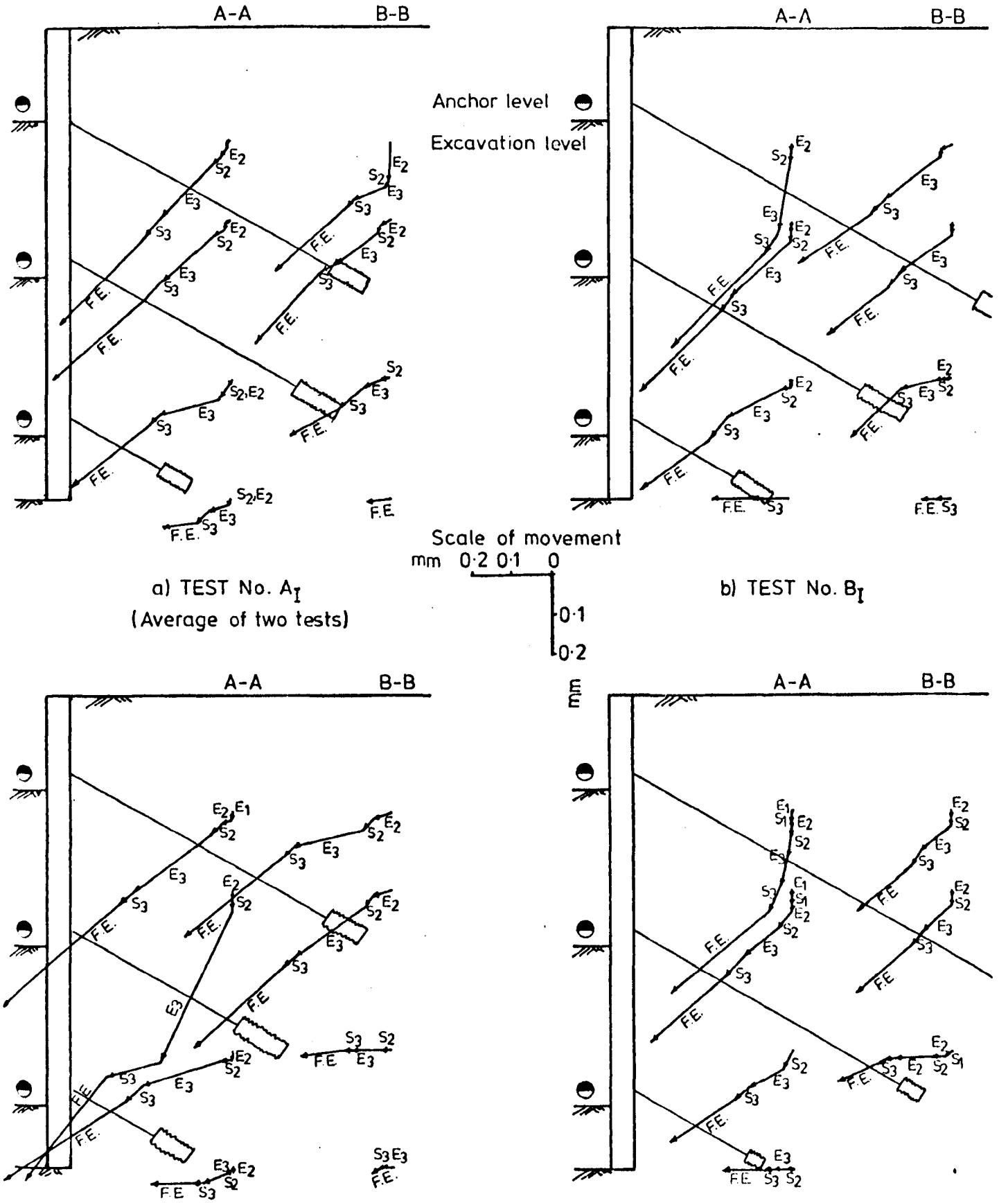

FIG. 6.36 SAND MOVEMENTS WITHIN THE RETAINED SAND MASS DURING THE DIFFERENT CONSTRUCTION STAGES FOR GROUP FOUR TESTS (THREE ROW INCLINED SYSTEMS)

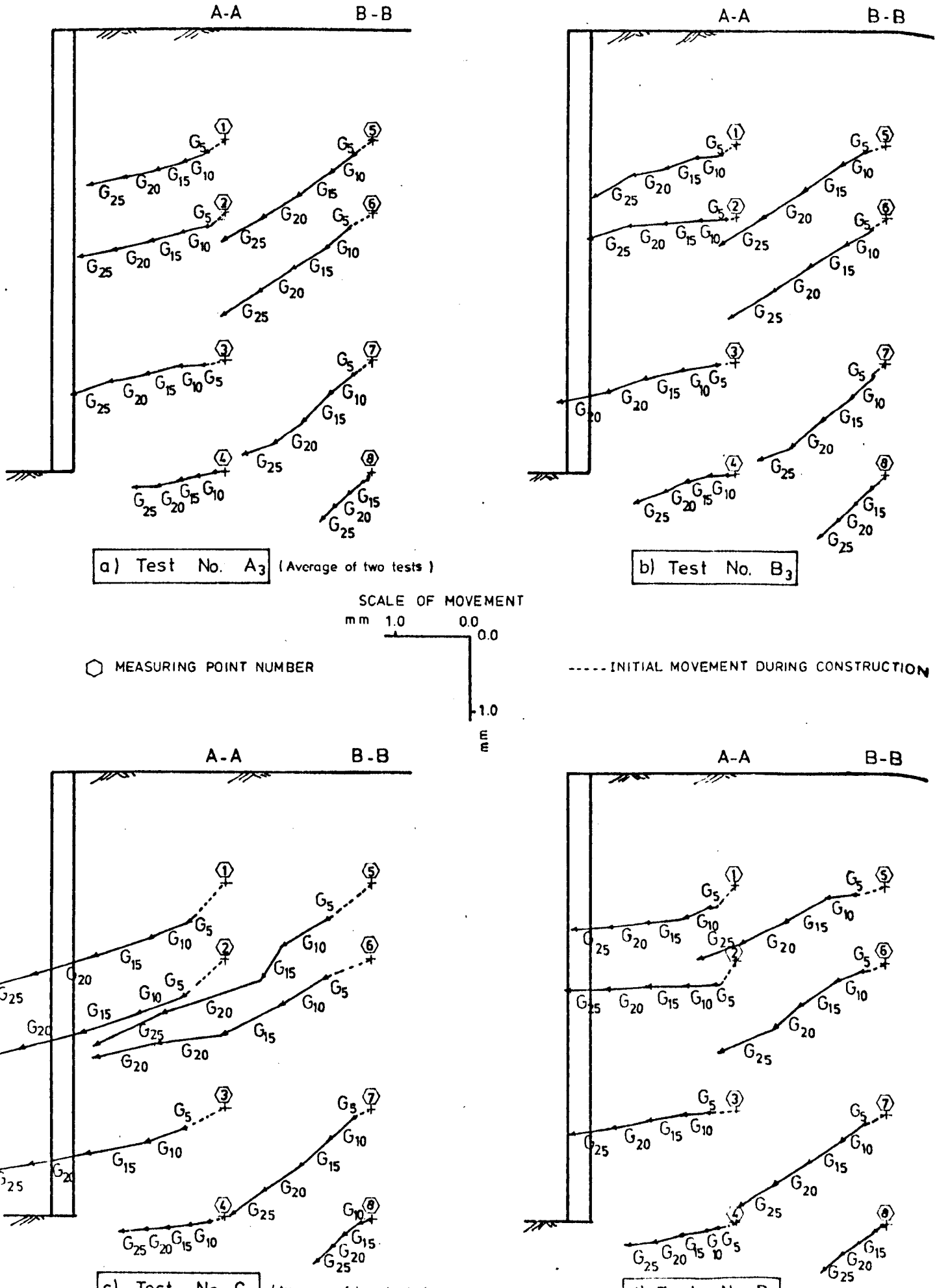

FIG. 6.37 SAND MOVEMENTS WITHIN THE RETAINED SAND MASS DURING THE DIFFERENT STAGES OF SURCHARGE LOADING FOR GROUP TWO TESTS (THREE ROW SYSTEMS)

CHAPTER 7

DISCUSSION AND INTERPRETATION OF THE EXPERIMENTAL RESULTS

CHAPTER 7

DISCUSSION AND INTERPRETATION OF THE EXPERIMENTAL RESULTS

7.1 Introduction

In this chapter the experimental results presented in Chapter 6 are examined in more detail. The wall-anchor-soil system behaviour, at full excavation and on applying surcharge, is examined with respect to the different design methods used. With the aid of the measured earth pressure on the wall, the measured anchor forces and the measured components of reaction at the wall base, and by using simple mechanics and simplifying assumptions, the force system acting on the wall is examined and the average soil strength mobilized in the retained sand is calculated.

In addition the chapter highlights the main differences in behaviour between walls supported by anchor wires and those supported by embedded anchor units.

7.2 Compatibility of the Test Results

In order to assess the validity of the test results, three tests were repeated. These were tests No. A_3, C_3 and A_I. In this section only the results of test A_I, and the repeat test, A_{Ir}, are presented as a typical example.

7.2.1 Wall movements

Fig. 7.1 shows the wall movement profiles during construction for both tests A_I and A_{Ir}. The profiles indicate identical patterns. An examination of the magnitude of movements reveals that during the

different construction stages negligible difference was observed for both the top and bottom horizontal movements and at full excavation the maximum difference observed was 6.5% at the top of the wall and 1.0% at the bottom. The maximum difference in the vertical movement was 10% and this was observed after the final excavation stage. This difference of 10% was the highest difference observed in all repeatibility tests, and may be attributed to over-excavation below the bottom of the wall in test A_{Ir}, allowing some sand particles to escape from underneath the base of the wall and consequently causing larger downward movements of the wall.

The wall movement profiles during the different stages of surcharge application are shown in Fig. 7.2. The patterns are identical with maximum differences of 4% and 5.5% for top and bottom horizontal movements respectively and a maximum difference of 2% for the vertical movement.

7.2.2 Sand subsidence

Sand subsidence profiles for both tests A_I and A_{Ir} are shown in Fig. 7.3. Similarity in both patterns was observed and is indicated by:
i) very small subsidences during the first four stages of construction;
ii) in both tests a value of about 26% of the total subsidence accompanied the third excavation stage, while excavating to the base level of the wall caused about 55% of the total subsidence.

In comparing the final subsidence values a difference of 7% is observed. Greater subsidence of the sand surface occurred in test A_{Ir} and this may be attributed to comparatively larger downward movement of

the wall during this test.

Fig. 7.4 shows the sand subsidence profiles during the post-construction stages. The slight variations observed in both patterns are mainly due to the difference in the original profiles at full excavation. However, when comparing the average magnitude of subsidence at the final stage of surcharge application a difference of 2% is observed.

7.2.3 Anchor loads

The variation in anchor loads with the different stages of testing is illustrated in Fig. 7.5 for tests A_I and A_{Ir}. The figure indicates identical patterns in the way the anchor loads decreased or increased during all construction stages. The maximum differences observed were of the order of 5% and occurred in the first row during the early stages of testing. At full excavation and at the final stage of surcharge loading, the maximum difference was about 4%.

7.2.4 Earth pressure distribution

The normal earth pressure distribution on the back of the wall at full excavation is plotted for both tests, A_I and A_{Ir}, in Fig. 7.6. Both plots show bulges just above the points of anchoring and they both agree to a great extent in the general shape of the distribution. The calculated value of the total earth pressure load on the back of the wall was 83.5% of the theoretical design value for test A_I, and 87.5% for test A_{Ir}.

Fig. 7.7 shows the normal earth pressure distribution on the back

of the wall during post-construction surcharge loading stages. Both patterns indicate a change in the shape of the distribution with increase in the surcharge load. They both show a pressure concentration at a point at a distance of H/3 from the bottom of the wall. Differences between the calculated values of the earth pressure load at the different stages varied between 3% and 5%.

7.2.5 Wall base reaction

The variation of the normal and shear components of the base reaction during testing is shown for both tests A_I and A_{Ir} in Fig. 7.8. In the figure, the normal component of the wall base reaction was expressed as a percentage of its value after filling, whereas the shear component was plotted as an absolute value.

In both tests the variations of the normal component of reaction at the end of each construction and surcharge loading stages showed good agreement. However, in comparing the differences between the absolute values at any stage, a maximum difference of about 8% was observed.

Similarity in patterns was also observed in the variation of the shear component of reaction throughout the different testing stages. Nearly equal magnitudes of the shear component were recorded after filling but with different signs. The initial difference in directions of the shear components is believed to be responsible for the large discrepancies observed at the subsequent stages. The shear cell also suffered from some drift which slightly affected its readings.

7.2.6 Sand movements

Sand movements during construction stages are plotted in Fig. 7.9 for both tests A_I and A_{Ir}. The behaviour is the same in both tests, except for some very slight differences at the initial stages. At full excavation the maximum difference observed between the vectorial displacements was about 9%. This was observed at the top point of section A-A (200 mm behind the back of the wall) and corresponds to the 6.5% difference in the top wall movements mentioned earlier.

Sand movements of the retained sand were also measured during the post-construction stages. These showed good agreement in pattern and magnitude.

7.2.7 Concluding comments

The results presented in the preceding sections are considered to be representative of all repeatibility tests. The measured parameters for all repeatibility tests, when compared, showed a high degree of compatibility.

The results indicated that the different components of the apparatus and instrumentation performed satisfactorily. They also indicated precision in the testing technique adopted.

7.3 Performance of the "Wall-Anchor-Soil" System at Full Excavation

7.3.1 Wall movements

Table 7.1 summarises the wall movements at the final excavation stage to the base level of the wall for all sixteen tests carried out.

Also shown are the individual and total anchor lengths.

The tabulated values for the first three groups of tests (horizontal anchors) indicate that:

i) for the first three design methods A, B and C (Kranz method, Ostermayer method and The French Code of Practice respectively), where the anchor forces were the same, the least top horizontal movement of the wall was associated with design method B, followed by method A, then method C. An increase in the length of the top row of anchors decreased the top horizontal movement;

ii) in all tests associated with design method D (the James and Jack method), and despite the fact that the anchor lengths of the top row were longer than those used for method C and approaching those of method A, larger movements were observed at the top of the wall. These were mainly attributed to comparatively low prestress loads applied to the top row of anchors when designed using method D;

iii) the same behaviour was observed with the bottom horizontal movements with the least movements being associated with systems having longer anchors;

iv) the minimum vertical wall movements were associated with the test wall designed according to method D, whereas method C resulted in the maximum vertical movements.

In tests with inclined anchors (Group Four), among the first three design methods, the least top horizontal movement was associated with method B, followed by methods A and C. However, method D with the longest top row of anchors experienced larger movements than A and B but slightly less than C, which reflects the influence of lower values

of prestress load. Comparison of the bottom horizontal movements in tests A_I, B_I and C_I indicates that the least movement is associated with test B_I having longer anchors, followed by A_I, then C_I. The bottom horizontal movement in test D_I was compatible with that of test B_I, and it seems that a decrease of 40% in the prestress load in test D_I was compensated by an increase of 12% in the total anchor length compared to test B_I. Tests with inclined anchors exhibited larger vertical movements compared to those with horizontal anchors. This is due to the vertical component of the anchor forces being transmitted to the wall and pulling it downward.

The arithmetic mean of both the top and bottom horizontal movements was calculated and defined as the average horizontal movement. From the tabulated values it is clear that the average horizontal movement is inversely proportional to the total anchor length for design methods A, B and C where the anchor forces were the same. Regarding method D, in all tests carried out, the values of the average horizontal movement were found to be greater than those observed for method A and smaller than those observed for method C. In comparing the anchor lengths of the three methods, it is clear that the lengths in method D are larger than those of A and C. On the other hand, a reduction in the prestress load of 40% is associated with method D.

From these observations it is clear that larger movements are associated with lower prestress loads. This is in agreement with the results of the theoretical analysis by Clough and Tsui (1974) which showed a decrease in the wall movement with increasing the prestress load.

Fig. 7.10 presents a plot of the total anchor length against the average horizontal movement for design methods A, B and C, in which the prestress loads were the same. The general trend of the curves indicates that any increase in the anchor length will be accompanied by a decrease in the average horizontal movement of the wall. However, from the shape of the curves it could be concluded that there seems to be a limit beyond which any increase in the anchor length would have little effect on movements. This limiting value was estimated for each system from the plotted curves. The estimated values were divided by the number of anchor rows used in each system and the result expressed as a percentage of the wall height H. For horizontal anchor tests the limiting value was of the order of 95% H. Extrapolating this finding to the field situation suggests that little may be gained by having an average anchor length which exceeds the height of the wall. It also seems that below a certain anchor length any decrease in the anchor length would cause very large movements.

The trend shown in Fig. 7.10 of decreasing movement with increasing total anchor length is in agreement with the observations of Breth and Wolff (1976) in their model tests which indicated smaller wall displacement with longer anchors.

The angle of wall rotation and the centre of wall rotation at full excavation were both calculated using the methods given in Appendices III, IV and are shown in Table 7.2. The tabulated values for the angle of rotation indicate that the least rotational angles were associated with method D, as the wall movement was likely to be mostly translation. This could be attributed to the fact that the prestress

load applied to the first row of anchors was always very small compared to all other methods. This led to large horizontal movements at the top of the wall and as a result less rotational motion. The largest angles of rotation were observed with method C, where the bottom horizontal movements of the wall were the greatest. This could be attributed to having comparatively short anchors in the bottom row. Rotational angles for both methods A and B were greater than those of method D and approaching those of method C.

The centre of wall rotation at full excavation was always above the top of the wall. The calculated values indicate a wide range of variation of the location of the centre of wall rotation. The distance from the top of the wall to the centre of wall rotation varied from a minimum of 0.25 H (the wall height) to a maximum of 1.76 H. However, the calculated values were consistent for all tests, the highest centres of rotation being associated with design method D, followed by method C, then A and B.

7.3.2 Earth pressure distribution

The earth pressure distribution measured by the earth pressure cells on the central wall section provided an estimate of the total horizontal components of earth load acting on the wall at any construction stage.

Values of the normal earth pressure load mobilized on the back of the wall at the final excavation stage were calculated and are shown as absolute values and as a percentage of the rectangular theoretical assumption used in the design of methods A, B and C in Table 7.2. The

calculated values indicate the following:

i) all values ranged between 72% and 107% of the initial theoretical assumed value;

ii) in the two row systems differences between the values of normal earth pressure load mobilized were very small with a maximum difference of 5% from the average value of the three tests, A_2, B_2 and C_2. The value calculated for test D_2 lay far beyond, being 72% of the theoretical value and a difference of 23.5% from the average value of A_2, B_2 and C_2;

iii) in the three row systems a maximum difference of 3% was observed between the earth pressure load values for methods A, B and C, whereas the earth pressure load for method D attained a value 85% of the theoretical value with a difference of 19% of the average of A, B and C;

iv) the values calculated for the four row systems indicate a similar behaviour as the two and three row systems;

v) values calculated for the three row inclined systems were all of the same order with an average of 91% of the theoretical value and a maximum difference of 5% from that average.

From these observations it may be concluded that for all tests with horizontal anchors, there is no significant difference between the values of the earth pressure mobilized for methods A, B and C (Kranz method, Ostermayer method and The French Code of Practice respectively). Lower values were associated with method D (the James and Jack method), and this is mainly attributed to lower prestress loads induced in the anchors compared to the other methods. However, in tests with inclined anchors,

the earth pressure load measured for test D_I was compatible with that of tests A_I, B_I and C_I. It is believed that shorter inclined anchors associated with methods A, B and C were responsible for larger wall movements, especially at the top of the wall, when compared to similar tests with horizontal anchors, i.e. tests No. A_3, B_3 and C_3. As a result, this greatly reduced the mobilized earth pressure.

In a previous study (Plant, 1972), in which embedded anchor units were used to support the wall, it was mentioned that the largest values of normal earth pressure load were associated with tests in which the anchors were shortest. Similar observations were also reported by Breth and Wolff (1976) in their study which was discussed in Chapter 2. In the first study the high earth pressures mobilized were attributed to the comparatively large anchor plates used. Stressing of these large anchors caused a highly stressed wedge of soil to be formed between the anchor plates and the back face of the wall. This had a greater effect on the normal earth pressure than the effect of the wall movements. In the second study, larger wall movements were observed with shorter anchors, yet higher earth pressures were monitored. This is contrary to what would have been expected. However, in the present investigation no significant differences in the value of the mobilized earth pressure loads were observed when different anchor lengths were used.

Comparing the shape of the earth pressure distribution at the last two construction stages, i.e. after stressing the bottom row of anchors and at full excavation, indicates a significant difference as shown in Figs. 6.23 to 6.26 and as pointed out in section 6.5.2. The shape of the distribution suggests that a trapezoidal or rectangular shape

distribution is likely in the case of a strutted wall, where the excavation is carried out to the base level of the wall or in the case of an anchored wall where the excavation is carried out to a considerable depth below the bottom row of anchors. However, if the bottom row of anchors is expected to be very close to the bottom of the excavation, the distribution of the earth pressure will tend to be near triangular in shape. These observations and deductions are in agreement with the argument by Hanna (1968). He pointed out that the use of a trapezoidal diagram is permissible provided that the wall does not penetrate the base of the excavation. However, if it does penetrate the excavation base then a triangular pressure distribution would appear more appropriate.

7.3.3 Force system acting on the wall

In addition to the total horizontal component of earth pressure load calculated, the total anchor force acting on the wall was also determined by summing the measured anchor loads on the central wall. The normal and shear components of reaction at the base of the wall measured by the load cells were converted to equivalent forces for the entire base width of the central wall.

The external theoretical force system acting on the wall at the final excavation stage is shown in Fig. 7.11. The convention adopted is such that when the resultant of the normal force and the shear force on the wall is downward, the average mobilized angle of wall friction, δ_{wm}, is considered positive. An estimate of the magnitude of the wall friction was made from the equilibrium equation in Fig. 7.11. Table 7.2

shows the calculated average mobilized angles of wall friction, δ_{wm}, for all tests at full excavation.

In all tests with horizontal anchors, the value of the mobilized angle of wall friction, δ_{wm}, at full excavation was positive and values ranged from 3.3° to 13.4°. With inclined anchors the mobilized angle of wall friction at full excavation, δ_{wm}, was always negative and ranged from -0.2° to -7.2°.

In order to form a basis for comparison of the earth pressure acting on the back of the wall at full excavation, the concept of a mobilized earth pressure coefficient was introduced. This mobilized earth pressure coefficient, Km, was calculated by dividing the total earth pressure load by $\frac{1}{2}\gamma H^2 L_w$, where L_w is the length of the central wall. The calculated values of Km for each series are shown in Table 7.2. Values of Km varied between a minimum of 0.303 and a maximum of 0.449. All values were greater than the value of the active earth pressure of 0.249, calculated on the assumption of an angle of shearing resistance ϕ' equal to 37°. Also the calculated values were smaller than the "at-rest" coefficient of earth pressure of 0.519, calculated from the normal earth pressure load on the back of the wall after filling.

From the calculated values of the average mobilized angle of wall friction, δ_{wm}, the calculated values of the coefficient of earth pressure mobilized, Km, at full excavation and using the equation due to Coulomb*,

---

* $$K = \frac{\sin^2(\alpha + \phi)}{\sin^2\alpha \sin(\alpha - \delta)\left[1 + \sqrt{\frac{\sin(\phi + \delta)\sin(\phi - \beta)}{\sin(\alpha - \delta)\sin(\alpha + \beta)}}\right]^2}$$ (see Bowles, 1968)

N.B.: $\beta = 0$ for horizontal backfill and $\alpha = 90$ for a vertical wall

an estimate was made of the average angle of friction mobilized in the retained sand mass ϕ'_m. It is worthwhile mentioning that there are limitations to this analysis. These include any slight errors in the measured values of the earth pressures, normal reaction at the wall base and the anchor loads since they influence the calculated value of δ_{wm}, the average value of the wall friction. Also, the use of Coulomb's equation assumes a triangular-shaped earth pressure distribution, whereas the earth pressure distribution at full excavation was observed to be more like a trapezoidal shape. All these factors should be noted when examining the calculated values of the average mobilized angle of friction in the retained sand, ϕ'_m, shown in Table 7.2.

The calculated values ranged from a minimum of 19.5° to a maximum of 30.5°. If a factor of safety was defined as $F = \tan\phi'/\tan\phi'_m$, and if a value of $F = 1.5$ was assumed and the value of $\phi' = 37°$ was adopted, the critical value of ϕ'_m would be 26.7°. Examining the values of ϕ'_m shown in Table 7.2 indicates that values above or approaching this critical value are associated with all tests in which inclined anchors were used, as well as all tests designed according to method D.

The highest value of ϕ'_m of 30.5° was associated with test D_2, where the smallest values of the normal earth pressure load on the back of the wall were measured. In Fig. 7.12 the earth pressure distribution at full excavation for test D_2 is compared with two theoretical distributions for a wall failing by either pure translation or by rotation about the top of the wall. These were determined by the method proposed by Dubrova (1963), and the approach she adopted is described in Appendix V. Also shown in the figure is the normal earth pressure

distribution at full excavation observed for a wall supported by three rows of 45^{o} inclined anchor wires in which the measured angle of internal friction was found to be equal to the angle of shearing resistance of the sand material, and the wall exhibited pure translational motion (see Plant, 1972). In comparing the experimental distribution of test D_2 with the two theoretical distributions, it should be noted that the wall in test D_2 neither rotated about its top nor perfectly translated but it exhibited a combination of both movements. It should also be noted that the value of ϕ'_m was below the peak value of 37^{o}. On the other hand comparing the experimental earth pressure distribution after Plant with the theoretical distribution of a wall failing by pure translation shows a good agreement. From these observations it would appear that the analysis made by Dubrova is quite realistic and the values of the earth pressures calculated by her method are close to those measured by Plant (1972).

Values of ϕ'_m, the average mobilized angle of shearing resistance in the retained sand mass, are plotted against the number of anchor rows in Fig. 7.13. In the figure an average value from the tests designed according to methods A, B and C was considered, while values from tests designed according to method D are plotted separately. Both curves indicate that an increase in the number of anchor rows decreased the mobilized angle of shearing resistance. This finding is in agreement with the results presented by Rowe and Briggs (1961) on their work on strutted walls. However, the shape of the curves indicates that, over the limited height of the wall, the decrease in the value of ϕ'_m when the number of rows was increased from three to four was not as much as

that when the number of rows was increased from two to three. It also seems that adding more anchor rows would have very little effect in reducing the value of ϕ'_m.

7.3.4 Sand subsidence

The sand surface subsidence profiles (Figs. 6.9 to 6.12) were far more difficult to interpret due to the significant influence of the lateral displacement of the anchor blocks of the first row of anchors. These caused substantial local subsidence behind, as well as some heave in front of, the anchor blocks. However, some indication of the relative behaviour can be observed by comparison of the measured sand subsidence of the first three measuring points near to the back of the wall, which are believed to be least affected by the displacement of the anchor block.

The calculated values for the average sand subsidence of the above mentioned three points are shown in Table 7.3 together with the wall movements. The values showed reasonable agreement with the average wall movements. For all horizontal anchor tests, the greatest values of subsidence were associated with method C (The French Code of Practice), whereas methods A (Kranz method) and B (Ostermayer method) resulted in the least values and method D (the James and Jack method) gave values ranging between the two extremes.

The dependence of sand subsidence on both the vertical and horizontal wall movements is illustrated in Fig. 7.14. The figure represents a relationship between the volume of sand subsidence at full excavation - calculated from the measured subsidences of the

first three points near to the wall - and a hypothetical wall movement calculated as the geometrical mean of both the vertical and the average horizontal wall movements. The curve shows an increase in the sand subsidence with increasing wall movement, and indicates that settlement behind an anchored wall can be effectively reduced by reducing the lateral movement of the wall.

The calculated values of sand subsidence were also plotted against the corresponding values of the mobilized angle of shearing resistance ϕ'_m in Fig. 7.15. The curve shows a certain trend, despite some scatter which was mainly associated with design method C. The general trend is an increase in the mobilized angle of shearing resistance, ϕ'_m, with increased subsidence, which is the same finding reported by Rowe and Briggs (1961) and Plant (1972).

It is worthwhile mentioning that the sand surface disturbance observed in the subsidence profiles in the vicinity of the anchor block (e.g. Fig. 6.9) exaggerated but highlighted the importance of taking into account the influence of anchor installation on the adjacent buildings. Ostermayer (1977) pointed out that among other things, settlement or heave of the ground could result due to anchor installation. These effects have to be taken into consideration before fixing the position of the fixed anchor zone to avoid any damage to neighbouring buildings.

7.3.5 Anchor loads

Table 7.4 shows the measured anchor loads at full excavation expressed as a percentage of the theoretical design values. The

different values attained by the different rows in all tests demonstrate the dependence of anchor loads on the initial prestress loads applied, the degree of displacement of the wall at the point of fixity with the anchor and the anchor inclination. In all tests with horizontal anchors designed according to methods A, B and C the top row of anchors experienced a loss in load, reflecting a relatively smaller movement at the top of the wall compared to the bottom movement. Lower rows exhibited an increase in the anchor loads demonstrating larger displacement at the bottom of the wall. Tests with inclined anchors associated with the same design methods A, B and C, showed different behaviour. A reduction in the anchor loads was observed in all three rows. However, the bottom rows suffered less reduction than the top row.

The most significant load increases were associated with all tests designed according to design method D. An increase of up to 97% was observed indicating that the initial theoretical prestress loads were rather small. These observations are in agreement with test results reported by James and Jack (1974), where the same design method was adopted to determine the anchor loads (see Section 2.2.1). Their test results showed that the final loads developed in the anchors exceeded the design predictions for all rows. It is worthwhile mentioning that design method D assumes the mobilization of both the full passive and active earth pressures, at the front and the back of the wall respectively, at the different construction stages. However, the measured values for the earth pressure mobilized in the tests carried out in the present investigation indicate that the earth

pressure mobilized on the front of the wall, at any stage, never reached the passive value and was always less than half the theoretical passive earth pressure. Also, the earth pressure mobilized on the back of the wall, at any stage, was generally greater than the theoretical active earth pressure. This would lead to the conclusion that the initial assumptions of design method D are far from correct and they lead to an underestimation of the anchor loads.

7.3.6 Sand movements

The vectorial sand movements shown in Figs. 6.33 to 6.36, especially those nearest to the wall, are reflecting the wall movements shown in Figs. 6.1 to 6.4 and summarised in Tables 7.1 and 7.2.

In tests with horizontal anchors, the magnitude of the angle of rotation, as well as the position of the centre of rotation, both affected the pattern of the vectorial displacements. Greater angles of rotation were associated with longer vectors near the bottom of the wall compared to those near the top. Meanwhile, the greater the distance between the top of the wall and the centre of rotation, the greater the magnitude of the vectorial displacement. Smaller angles of rotation were associated with longer vectors near the top of the wall compared to those near the bottom. Tests designed according to design method D represent the latter case, while tests designed according to methods A, B and C represent the first case, with method C associated with the highest centres of rotation.

Larger sand movements were observed in all tests with inclined anchors and were attributed to larger vertical and horizontal wall

displacements. The larger vertical wall displacements tended to increase the vertical component of the vectorial displacement, and as a result the movements were more likely to be towards the toe of the wall.

7.4 Performance Under Loading Conditions

7.4.1 Wall movements

Figs. 6.5 to 6.8 show the wall movement profiles during the different stages of surcharge application for all tests carried out. Comparing the different profiles indicates that surcharge loading effectively revealed the effect of anchor lengths and prestress loads on the wall performance. The wall movements for Group One (two rows horizontal anchors) are plotted in Fig. 6.5. The figure shows that for test B_2 where the top anchors were the longest, a very restricted top horizontal movement is observed and this results in severe rotational motion. Rotational motion was also observed in tests A_2 and C_2 but the top horizontal movement was greater than that observed for test B_2. At the final stage of surcharge loading the top horizontal movement of test A_2 was 52% greater than that of B_2 and this corresponds to a reduction of 12% in the length of the top anchors. The top horizontal movement of both tests C_2 and D_2 were of the same order, being 180% greater than that of test B_2. It is believed that comparatively shorter anchors at the top row in test C_2 and smaller prestress loads of the top row in test D_2 were responsible for these large top horizontal movements. The largest bottom horizontal movement was observed in test C_2 associated with the shortest anchors in the

bottom row. The least bottom horizontal movement was observed in both tests A_2 and D_2 and it seems that a decrease of 25% in the prestress load of the bottom row of test D_2 compared to that of test A_2 was compensated by an increase of 15% in the anchor length of the bottom row.

Similar trends were observed with the three and four row systems. However, the effect of the individual anchor lengths or prestress loads was not as pronounced because of the interaction of the different parameters.

The effect of prestress load is illustrated on comparing the wall movement profiles of Fig. 6.5 a, b, c (two row systems) to those of Fig. 6.6 a, b, c (three row systems). The distribution of the prestress load among three rows of anchors instead of two reduced the value of the prestress load induced in the top row, and as a result the wall exhibited slightly larger top horizontal movement in tests A_3, B_3 and C_3 compared to tests A_2, B_2 and C_2. On the other hand having two rows of anchors in the bottom half of the wall in Group Two instead of one row in Group One increased the magnitude of the prestress load applied to the bottom half of the wall, which in turn tended to decrease the bottom horizontal movement.

Tests with inclined anchors (Fig. 6.8) showed a similar behaviour. Comparing the wall movements of tests A_I, B_I and C_I it is clear that the least movements are associated with systems having longer anchors. However, as mentioned before, the stability analysis for design methods A, B and C yielded shorter inclined anchors when compared to those determined according to method D, with the result that, despite a

decrease of 40% in the prestress load applied to the anchors in test D_I compared to tests A_I, B_I and C_I, the wall movements were the least. Compared to the wall profile at full excavation, the movements were almost translation in tests A_I, B_I and C_I. This is believed to be due to shorter anchors in the top row compared to very long ones used when the same design methods were applied to systems with horizontal anchors. Longer anchors in the latter restricted the top wall movement and caused the wall to rotate.

7.4.2 Sand subsidence and sand movements

(a) Sand subsidence

Figs. 6.13 to 6.16 showed plots of the measured sand subsidence of the first four points near to the back of the wall at the different stages of surcharge loading. The sand subsidence was affected by both the wall movement and the surcharge load which might have increased the subsidence of the points in the vicinity of the pressure bag. Excluding the effect of the surcharge load which should have been the same for all tests, the profiles indicate the following:

i) smallest wall movements were accompanied by the least subsidence, e.g. test No. B_4, Fig. 6.15b;

ii) a rotational motion about a point near the top of the wall was accompanied by an uneven subsidence, with the sand surface sloping away from the wall. This was also observed when the wall experienced large horizontal movements, e.g. tests No. C_3 and C_4;

iii) a translation motion was accompanied by nearly uniform subsidence

compared to the final profile at full excavation, e.g. tests No. A_I and B_I (Fig. 6.16) and tests designed according to design method D.

Fig. 7.16 gives plots of the volume of sand subsidence at the different stages of surcharge loading for the different tests carried out. The plots indicate that for all tests with horizontal anchors, design method C exhibited a rather high rate of subsidence compared to all other methods. However, tests with inclined anchors showed similar trends for all design methods. On the basis of the findings discussed in section 7.3.4, whereupon an increase in the subsidence indicates an increase in the mobilized angle of shearing resistance, Fig. 7.16 therefore indicates that horizontal anchor systems designed according to design method C (The French Code of Practice) are likely to approach the peak value of the angle of shearing resistance before other systems.

(b) Sand movements

Sand movements within the retained sand mass are plotted in Fig. 6.37 for Group Two (three row horizontal anchors).

The vectorial displacements reflected the wall movements. Also they agreed with the profiles of the top sand subsidence. Larger wall movements in test C_3 were associated with larger vectorial displacements. The higher degree of rotation in test B_3 was accompanied by longer vectors near the bottom of the wall (point 3) compared to those near the top half of the wall (points 1 and 2). Nearly equal vectors were observed at points 1, 2 and 3 in test D_3 indicating a translation motion of the wall. An uneven subsidence at the top sand surface was

reflected in the vectorial displacements of points 5, 6, 7 and 8, being steeper in tests A_3 and B_3 compared to test D_3 where a uniform subsidence was observed. The vectorial displacements at points 4 and 8, both being at the same level of the bottom of the wall, indicate a flow of the sand towards and underneath the toe of the wall. It is believed that movement gauges below the bottom of the wall would be particularly informative.

7.4.3 Anchor loads and anchor movements

(a) Anchor loads

Anchor load variations with the different stages of surcharge loading were shown in Figs. 6.17 to 6.20. The different trends observed indicate the following:

i) in all tests associated with design method D, where the anchor forces were derived from the method proposed by James and Jack (1974), the variation in anchor loads in all rows showed similar behaviour. All rows experienced an increase in the anchor loads with surcharge application. However, the rate of anchor load increasing was different for the different rows, with the highest rate at the top row and decreasing downward;

ii) in all other tests, i.e. those associated with design methods A, B and C, where the anchor forces were derived from a rectangular earth pressure distribution, the trends were almost similar. However, quantitative differences were observed regarding the rate with which the anchor loads increased or decreased.

In the four row systems, anchor loads in the first and fourth rows increased, while anchor loads in the second and third rows decreased. The rate of anchor load increasing in the first and fourth rows was either constant or increasing. On the other hand the rate of anchor load decreasing in the second and third rows was declining, as can be seen in the third row of test B_4, where the anchor load decreased to a certain value and then started to increase again.

The three row systems showed similar behaviour with the top and bottom rows exhibiting an increase in the anchor loads, while anchor loads in the middle row decreased with a decreasing rate which reached a minimum in test A_3 and then started to increase.

Both rows in the two row systems experienced an increase in the anchor loads. However, the rate of anchor load increasing in the top row was much greater than that of the bottom row.

All three rows, in tests with inclined anchors, exhibited an increase in the anchor loads. However, the rate of anchor load increasing in the top and bottom rows was greater than that of the middle row.

(b) Anchor movements

During the loading of an anchor the stretch or elongation of the top end of the anchor system is easily recorded. This record of elongation and applied load provides a practical method of checking the anchor performance. However, care is needed in the interpretation of such a diagram, as a number of variables control its shape. Hanna (1968) summarised these variables as:

i) the elastic stretch of the anchor;

ii) vertical movement of the wall;

iii) horizontal movement of the wall;

iv) bending of the wale beams; and

v) yield and creep of the anchor.

He emphasised the importance of taking into account the effect of these variables when interpreting the shape of the load-elongation diagram. On the other hand, a direct measurement of the displacement of the anchor block (grouted body), which is rather difficult to achieve in the field, would directly yield enough information about the anchor performance. To the knowledge of the author, the only field study in which such measurements were taken was performed by Shannon and Strazer (1970). Measurements were made of the anchor displacement by embedding a wire in the anchor grout. The wire extended out through a hole to the surface and over a pulley, where a suspended weight tensioned the wire. As the rod was tensioned, anchor displacement was indicated by downward movement of the weight as measured by a dial extensometer independently supported. Approval of the anchor design was based on a linear load-anchor displacement characteristic to a load equivalent to 1.5 times the design anchor load.

Anchor movements during the different stages of surcharge loading are shown in Figs. 6.17 to 6.19. In all tests carried out, the load displacement diagrams for the different anchor rows showed a linear characteristic indicating a satisfactory performance of the anchors. The characteristic of wall movement was reflected in the load displacement curves. When the wall translated, the load displacement

curves for all rows of anchors were equally sloping, e.g. test No. C_3. When the wall experienced rotational motion, the load displacement curves for the bottom anchors were steeper than those for the top rows indicating larger displacements for the bottom anchors, e.g. test No. B_2.

7.4.4 Earth pressure distribution and force system acting on the wall

The different shapes of the earth pressure distribution shown in Figs. 6.27 to 6.30 indicate that the application of the surcharge load was accompanied by an increase in the total earth pressure acting on the wall. The measured values of the mobilized earth pressure load indicate that, up to the maximum surcharge load applied, a linear relation existed between the increase in the surcharge load and the corresponding increase in the earth pressure load. Higher pressure intensities were observed over the middle portion of the wall. However, the pressure intensities over the top and bottom parts of the wall were influenced by the mode of wall movement. This can be explained as follows:

i) when the wall exhibited very small displacements and the movement was purely translation, e.g. test No. B_I (see Fig. 6.8b), a very slight increase in the pressure intensity was observed over the top and bottom parts of the wall;

ii) when the wall exhibited a rotational motion around a point near its top, e.g. test No. B_2 (see Fig. 6.5b), and due to comparatively larger bottom horizontal movements, the pressure intensity over the bottom of the wall decreased, whereas an increase was observed

over the top of the wall;

iii) a rotational motion about a point near the toe of the wall, e.g. test No. C_I (see Fig. 6.8c), decreased the pressure intensity over the top of the wall and increased it over the bottom of the wall;

iv) excessive displacements, e.g. test No. C_3 (see Fig. 6.6c), caused a decrease in the pressure intensities over both the top and bottom portions of the wall.

Values of the total earth pressure load mobilized at the different stages of surcharge loading are plotted in Fig. 7.17. The four plots for the four groups indicate similar behaviour for the different design methods. The rate of earth pressure mobilization was of the same order for methods A, B and D, whereas a smaller rate was observed for method C. This indicates that excessive movements are associated with all tests designed according to method C compared to all other methods. It also indicates that all systems designed according to method C are approaching failure before all other systems.

In addition to the total horizontal component of earth pressure load calculated from the earth pressure distributions, it was also possible to calculate the total anchor forces, the normal and shear components of reaction at the wall base at the different stages of surcharge loading.

Using the equilibrium equation in Fig. 7.11, the different values of δ_{wm}, the average mobilized angle of wall friction, were calculated for the different stages of surcharge loading. Fig. 7.18 represents plots of the variation of δ_{wm}, with surcharge loading, for the different

tests carried out. As can be seen, δ_{wm} had a positive value at the final excavation stage in all tests with horizontal anchors, indicating a downward movement of the backfill relative to the wall. When surcharge load was applied the value of δ_{wm} increased and continued to increase until it reached a peak value in almost all tests and then decreased. Tests with inclined anchors showed a different behaviour where δ_{wm} at full excavation had a negative value, indicating a downward movement of the wall relative to the backfill. However, this negative value of δ_{wm} started to decrease in magnitude with surcharge loading. It either changed to be positive or remained very small and negative, but in both cases the curves indicate that δ_{wm} reached a peak and then decreased.

Previous work (Ponniah, 1973; Shah, 1975) showed that the determination of Km, the coefficient of earth pressure mobilized, or ϕ'_m, the mobilized angle of shearing resistance determined using Coulomb's theory, is not realistic in the case of surcharged backfill or when the retained sand is overconsolidated.

7.5 Wall-Anchors-Soil Interaction

7.5.1 General

The use of embedded anchor units to support the wall simulated the real behaviour in the field and allowed for the interaction between the different elements comprising the system. Consequently it was believed that a comparative study of the general trends between tests carried out with embedded anchor units and those carried out using anchor wires tied to the back of the flume would be of value. In the

following sections test results of the present study are compared with the results of similar tests carried out by Plant (1972) using anchor wires.

7.5.2 Wall movements

The wall profiles at the final excavation stage are shown for each group of tests in separate plots in Fig. 7.19. Also shown are the wall profiles for the identical test of each group which was carried out by Plant, using anchor wires.

Comparison of the different profiles of the first three plots a, b and c, which represent systems with horizontal anchors, indicates the following:

i) in all tests using embedded anchor units the wall exhibited larger horizontal displacements than those measured in tests using anchor wires;

ii) the top horizontal movement of the wall demonstrated a fundamental difference between the two cases. When embedded anchor units were used the top of the wall moved towards the excavation, while with anchor wires the wall moved towards the backfill and away from the excavation. It is worth mentioning, however, that in the field observations reported in section 2.3.2, the only case where the top of the wall moved towards the backfill was observed when the top row of anchors was fixed to a rock stratum (Gould, 1970; Sexena, 1974). In the rest of the field studies it was observed that the wall moved continuously towards the excavation, i.e. similar to the behaviour of the

model wall with embedded anchor units. These findings illustrate a fundamental difference between a model wall supported by embedded anchor units and one supported by anchor wires fixed to the back of the apparatus. In the latter case, the only deformations in the anchor system are those due to a stretch in the anchor wire, while with embedded anchor units a full interaction between the anchor and the surrounding soil was allowed;

iii) at full excavation the centre of wall rotation lay within the wall height in tests with anchor wires, whereas walls with embedded anchors rotated around a point above the top of the wall.

Fig. 7.19 (d) shows the wall profiles of tests with inclined anchors. The wall supported by anchor wires exhibited large vertical movements, nearly four times greater than those exhibited by walls supported by embedded anchor units. Both the top and bottom horizontal movements of the wall supported by anchor wires were greater than those experienced by the walls supported by embedded anchor units. This behaviour is the reverse of the behaviour of walls supported by horizontal anchors. The difference could be attributed to a misleading pattern of movement when inclined anchor wires were used to support the wall. With the anchors being fixed to the back of the flume, any downward movement of the wall was accompanied by an outward movement due to an apparent increase in the anchor lengths. As a result, when the inclined anchor wires were stressed, large horizontal movements were observed which exceeded the movements observed for walls supported by embedded anchor units.

7.5.3 Sand subsidence and sand movements

The existence of embedded anchor units near the top of the sand surface greatly affected the sand subsidence profiles, which in turn did not allow for a complete comparison. However, to demonstrate the general trend, the subsidence profiles of the four measuring points nearest to the back of the wall are plotted in Fig. 7.20, together with the sand subsidence profiles for similar tests with anchor wires.

As expected, in tests with horizontal anchors, the sand subsidences measured when using anchor wires were less than those in tests with embedded anchor units. This reflects the wall movements. Fig. 7.20 (d) shows a significant difference in the magnitude of sand subsidence between tests with inclined anchor wires and the tests with inclined embedded anchor units, the former being associated with larger subsidences. Comparing these observations with the corresponding wall movement profiles (Fig. 7.19 (d)) reveals that the vertical wall movement has a great effect on the sand subsidence.

In general, tests with inclined anchor wires exaggerated the magnitude of subsidence due to the wall exhibiting large vertical movements. On the other hand the use of horizontal anchor wires resulted in very conservative values for both the sand subsidence and the wall movements.

The only identical test in which Plant monitored the sand movements within the retained soil mass was that with three rows of horizontal anchors. Consequently the only possible comparison was between this test and an identical one with embedded anchor units. Fig. 7.21 shows the vectorial displacements in test B_3 (three rows

horizontal embedded anchor units) and in the identical test with anchor wires. The figure indicates two main differences:

i) with anchor wires, the top of the wall moved towards the backfill, and as a result the vectorial displacements behind the top half of the wall were directed away from the excavation. In the second case, with embedded anchor units, all displacements were towards the excavation following the wall movement;

ii) the magnitude of movements was larger in the test with embedded anchor units as a result of larger wall movements.

The pattern of the vectorial displacements observed in tests with embedded anchor units resembles that reported by Sills et al. (1977), following a wall movement towards the excavation (see Fig. 2.35).

7.5.4 Anchor loads

The anchor load variations were similar when embedded anchor units were used and when anchor wires supported the wall. In all tests the trend for anchor load increase or decrease for the different rows during construction was identical as illustrated by Fig. 7.22, which shows the anchor load variations with construction progress for tests No. A_3, B_3 and C_3 and a similar test with anchor wires. Anchor loads at full excavation for tests designed according to design methods A, B and C are shown in Table 7.5, together with the anchor loads for similar tests with anchor wires. All loads are expressed as a percentage of the theoretical prestress value. The tabulated values indicate that embedded anchor units suffered more variations in the anchor loads than anchor wires. However, the final values attained

at full excavation showed similar trends but with different magnitudes.

7.5.5 Values of derived parameters at full excavation

Table 7.5 gives the values of δ_{wm}, the mobilized angle of wall friction, Km, the coefficient of earth pressure mobilized and ϕ'_m, the mobilized angle of shearing resistance in the soil mass for tests with embedded anchor units designed according to design methods A, B and C and for the identical tests with anchor wires.

The values of δ_{wm} indicate similar trends in both cases, with positive values associated with horizontal anchors and negative values with inclined anchors.

Values of Km in tests with horizontal embedded anchors showed a general trend for an increase with increasing the number of anchor rows. However, with anchor wires a similar value was observed for both the two and four row systems and a slightly lower value for the three row systems. With inclined embedded anchors the value of Km was much greater than that observed for tests with inclined anchor wires.

The angle of shearing resistance, ϕ'_m, attained the same value in all tests with horizontal anchor wires, whereas a general trend for ϕ'_m to decrease with increasing the number of rows was observed in tests with embedded anchor units. The maximum value of ϕ'_m was observed with inclined anchors in both cases. However, a larger value was observed in the test with inclined anchor wires as a result of larger wall movements.

7.6 General Discussion

The preceding sections illustrate the effect of the individual parameters on the performance of the different elements comprising the wall-anchors-soil system. However, it is worthwhile having a broad look at the different systems and the different design methods used.

In all tests carried out the different systems performed satisfactorily. The calculated values of the mobilized angle of shearing resistance, at full excavation, were all below the peak value for the sand, and no failures have been indicated even under the severe loading conditions to which the systems were subjected. However, it should be noted that the problem of tied back retaining walls is a deformation problem in which the main task is to control the movements to avoid any damage either to the structure or to surrounding buildings.

A comparison between the measured wall displacements and those reviewed earlier in the field studies indicates that all displacements at the final excavation stage were within tolerable limits. The maximum measured wall displacement did not exceed 0.2% of the wall height, whereas values up to 0.63% of the wall height were observed in the field (Sills et al., 1977).

Values up to 0.1% of the wall height were observed for the sand surface subsidence at full excavation. These are considered quite reasonable compared to reported values of 0.3% of the wall height (James and Phillips, 1972).

The measured wall displacements and the measured mobilized earth pressure load for the tests designed according to method D in Groups Two and Four (three row horizontal anchors and three row inclined

anchors), showed great similarity. For the three row systems larger movements and lower earth pressure loads were observed with systems designed according to methods A, B and C when inclined anchors were used. This might be attributed to the comparatively shorter anchors which resulted when the stability analysis of methods A, B and C was applied to inclined anchor systems. These observations might indicate that the stability analysis of method D using a logarithmic spiral as suggested by Littlejohn (1972) is more suitable than the other analyses, especially in the case of inclined anchors which represent the majority of field situations.

The measured earth pressures at the different construction stages and the measured anchor forces indicate that the method proposed by James and Jack (1974) for calculating the anchor loads is far from correct. The assumption of the full mobilization of both active and passive earth pressures on the back and the front of the wall is unrealistic and leads to the underestimation of the anchor loads. However, it is worthwhile mentioning that when the surcharge load was applied, a purely translational motion was observed for all tests designed according to method D, indicating a more consistent behaviour than that observed in tests designed by the other methods, in which there were complex movements. This probably shows that the distribution of the anchor loads amongst the different rows is realistic. However, to overcome the drawback of underestimating the anchor loads, the principle proposed by James and Jack can be modified in a way to increase the assumed mobilized active earth pressure on the back of the wall and to decrease the assumed passive resistance on the front of the

wall. This would increase the magnitude of the anchor loads, while keeping the same proportional distribution of the anchor loads. Values ranging between the active and the "at-rest" earth pressures could be used for the mobilized earth pressure on the back of the wall, while a value of not more than 50% of the theoretical passive earth pressure could be considered for the mobilized earth pressure on the front of the wall.

On the other hand it seems that the use of a rectangular earth pressure distribution for calculating the anchor loads overestimates the load in the top row of anchors and probably a trapezoidal distribution similar in shape to that shown in Fig. 2.55 (c) and recommended for loose sand is more realistic.

The wall movements observed during the different construction stages indicate that two patterns of movements could be expected in a tied back retaining wall system. Whichever pattern occurs depends mainly on the anchor prestress loads. If the anchors are prestressed according to a triangular earth pressure distribution, as in method D, a rotation about a point near the toe is to be expected. However, if the prestress load is calculated from a rectangular earth pressure distribution, as in methods A, B and C, the wall will rotate about a point near its top.

A comparison of the values of the earth pressure load mobilized in all tests with horizontal anchors indicates that lower values of the normal earth pressure load were observed when lower prestress loads were applied to the anchors, i.e. in design method D. This would suggest that within certain limits the pressure distribution may

be controlled by giving suitable prestress loads to the anchors.

Quite often any system could be subjected to loading conditions which were not taken into consideration during the design. The application of surcharge loading effectively revealed the response of the different systems to such loading conditions. The different tests designed according to method D (the James and Jack method) were more consistent in behaviour. The increase in the intensity of the normal earth pressure was nearly uniformly distributed over the anchored part of the wall, the wall exhibited a translational motion and a nearly uniform surface subsidence was observed in all method D tests. Tests designed according to method B (Ostermayer method) suffered from higher normal earth pressure intensities over some parts of the wall, e.g. tests No. B_2 and B_I, which in the field case could result in higher stresses on the wall member. Also, the excessive rotation of the wall observed for test B_2 was accompanied by an uneven surface subsidence which might cause damage to neighbouring structures, and might not be easily detected in the field if the settlement points were located near the wall. Tests designed according to design methods A and C (Kranz method and The French Code of Practice) suffered from the same problem of higher pressure intensities over some parts of the wall. This was more pronounced with tests designed according to method C. Excessive wall movements were also observed with method C tests and these resulted in the largest surface subsidence, indicating that probably a higher factor of safety is needed in the design.

Group and System	Test Number	Wall Movement at Full Excavation (mm) +				Anchor Lengths (mm)				
		Horizontal		Vertical ++ (mm)	Average Horizontal (mm)	First Row (mm)	Second Row (mm)	Third Row (mm)	Fourth Row (mm)	Total Length (mm)
		Top (mm)	Bottom (mm)							
Group 1 Two Row Systems	A_2	0.18	0.87	0.155	0.525	640	400			1040
	B_2	0.17	0.845	0.190	0.508	730	400			1130
	C_2	0.405	1.12	0.33	0.763	520	320			840
	D_2	0.510	0.80	0.13	0.655	605	460			1065
Group 2 Three Row Systems	*A_3	0.230	0.914	0.17	0.572	610	560	280		1450
	B_3	0.198	0.825	0.168	0.512	750	490	280		1520
	*C_3	0.484	1.241	0.358	0.862	515	348	138		1001
	D_3	0.545	1.065	0.160	0.805	605	530	330		1465
Group 3 Four Row Systems	A_4	0.290	0.790	0.12	0.540	610	380	340	310	1640
	B_4	0.218	0.720	0.08	0.469	750	520	400	260	1930
	C_4	0.426	1.050	0.228	0.738	520	351	256	146	1273
	D_4	0.512	0.832	0.11	0.672	605	530	460	330	1925
Group 4 Three Row Inclined Systems	*A_I	0.455	1.075	0.550	0.765	400	335	130		865
	B_I	0.430	1.000	0.520	0.715	500	330	150		980
	C_I	0.56	1.198	0.470	0.879	370	240	120		730
	D_I	0.540	1.025	0.37	0.783	550	385	165		1100

\+ The true wall displacements were calculated from the measured displacements as shown in Appendix III.
++ Both the top and bottom vertical movements of the wall were identical (see Appendix III).
* Indicates an average value for two repeated tests.

Table 7.1. Wall Displacements and Anchor Lengths.

Test No.	Angle of Rotation at Full Excavation in Mins	Secs	Centre of Wall Rotation at Full Excavation (Measured from the Wall Base, upwards positive)+ (mm)		Calculated Value of the Earth Pressure Load Mobilized at Full Excavation (Newtons)++		Calculated Average Mobilized Angle of Wall Friction, δ_{wm} (Degrees)	Equivalent Average Earth Pressure Coefficient, Km	Calculated Average Mobilized Angle of Friction in the Retained Sand ϕ'_m (Degrees)
A_2	3	57	756	1.26H	407.0	93.0%	+8.3	0.390	23.9
B_2	3	51	750	1.25H	435.0	99.0%	+6.0	0.416	22.8
C_2	4	6	939	1.57H	416.4	94.5%	+3.6	0.389	24.5
D_2	1	40	1655	2.76H	317.0	72.0%	+9.4	0.303	30.5
*A_3	3	55	802	1.34H	467.7	106.3%	+6.2	0.447	20.7
B_3	3	35	789	1.32H	458.3	104.0%	+3.3	0.438	22.0
*C_3	4	20	984	1.64H	455.0	103.5%	+7.9	0.436	21.0
D_3	2	59	1229	2.05H	376.4	85.5%	+4.0	0.360	27.0
A_4	2	52	948	1.58H	420.0	95.5%	+12.3	0.402	22.5
B_4	2	52	860	1.43H	465.2	105.3%	+12.7	0.444	19.7
C_4	3	34	1009	1.68H	470.0	106.8%	+13.4	0.449	19.5
D_4	1	50	1560	2.60H	376.4	85.5%	+10.9	0.360	25.4
*A_I	3	33	1040	1.73H	375.9	85.0%	-6.5	0.359	29.4
B_I	3	16	1052	1.75H	401.8	91.0%	-7.2	0.384	28.7
C_I	3	39	1126	1.88H	415.4	94.0%	-0.2	0.397	25.6
D_I	2	47	1267	2.11H	410.6	93.3%	-4.1	0.392	27.1

\+ Expressed in mm and as a function of the wall height H.
++ Expressed in Newtons and as a percentage of the initial theoretical assumption.
* Indicates an average value of two repeated tests.

Table 7.2. Summary of Experimental Data at Full Excavation.

Group	Test Number	Average Sand Subsidence (mm)	Wall Movement at Full Excavation (mm)			
			Horizontal		Vertical	Average Horizontal (mm)
			Top	Bottom		
One	A_2	0.30	0.18	0.87	0.155	0.525
	B_2	0.30	0.17	0.845	0.190	0.508
	C_2	0.40	0.405	1.120	0.330	0.763
	D_2	0.38	0.510	0.80	0.130	0.655
Two	$*A_3$	0.26	0.230	0.914	0.170	0.572
	B_3	0.30	0.198	0.825	0.168	0.512
	$*C_3$	0.53	0.484	1.241	0.358	0.862
	D_3	0.44	0.545	1.065	0.160	0.805
Three	A_4	0.26	0.290	0.790	0.120	0.540
	B_4	0.24	0.218	0.720	0.080	0.469
	C_4	0.43	0.426	1.050	0.228	0.738
	D_4	0.32	0.512	0.832	0.110	0.672
Four	$*A_I$	0.53	0.455	1.075	0.55	0.765
	B_I	0.60	0.430	1.000	0.52	0.715
	C_I	0.57	0.560	1.198	0.47	0.879
	D_I	0.47	0.54	1.025	0.37	0.783

* Indicates an average value for two repeated tests.

Table 7.3. Average Sand Subsidence and Wall Movements at Full Excavation.

Group	System	Test Number	Anchor Loads at Full Excavation as a Percentage of the Theoretical Prestress Value			
			First Row	Second Row	Third Row	Fourth Row
One	Two Rows	A_2	69	113		
		B_2	70	106		
		C_2	82	112		
		D_2	111	132		
Two	Three Rows	$*A_3$	58	124	99	
		B_3	58	113	103	
		$*C_3$	62	120	98	
		D_3	191	138	109	
Three	Four Rows	A_4	72	93	167	115
		B_4	70	109	157	103
		C_4	67	99	160	100
		D_4	108	125	134	116
Four	Three Rows Inclined	$*A_I$	65	94	78	
		B_I	78	95	88	
		C_I	64	84	88	
		D_I	184	121	105	

* Indicates an average value of two repeated tests.

Table 7.4. Anchor Loads at Full Excavation.

Tests with Embedded Anchor Units								Tests with Anchor Wires						
Test No.	Anchor Loads Expressed as a Percentage of the Prestress Value				Mobilized Angle of Wall Friction δ_{wm} (Degrees)	Mobilized Coefficient of Earth Pressure Km	Mobilized Angle of Shearing Resistance ϕ_m (degrees)	System Description	Anchor Loads Expressed as a Percentage of the Prestress Value				Mobilized Angle of Wall Friction δ_{wm} (Degrees)	Mobilized Coefficient of Earth Pressure Km	Mobilized Angle of Shearing Resistance ϕ_m (Degrees)
	1st Row	2nd Row	3rd Row	4th Row					1st Row	2nd Row	3rd Row	4th Row			
A_2	69	113			8.25	0.390	23.9	Two Row Horizontal Anchors	83	106			4.7	0.421	23
B_2	70	106			6.00	0.416	22.8								
C_2	82	112			3.60	0.398	24.5								
*A_3	58	124	99		6.20	0.447	20.7	Three Row Horizontal Anchors	87	108	108		8.2	0.406	23
B_3	58	113	103		3.30	0.438	22.0								
*C_3	62	118	98		7.90	0.436	21.0								
A_4	72	93	167	115	12.34	0.402	22.5	Four Row Horizontal Anchors	92.5	106	112	111	4.3	0.422	23
B_4	70	109	157	103	12.70	0.444	19.7								
C_4	67	99	160	100	13.40	0.449	19.5								
*A_I	65	94	78		-6.5	0.359	29.4	Three Row Inclined Anchors	58	87	97		-11	0.341	32.5
B_I	78	95	38		-7.2	0.384	28.7								
C_I	64	84	83		-0.2	0.397	25.6								

* Indicates an average value of two repeated tests.

Table 7.5. Experimental Data at Full Excavation for Tests with Embedded Anchor Units and Tests with Anchor Wires.

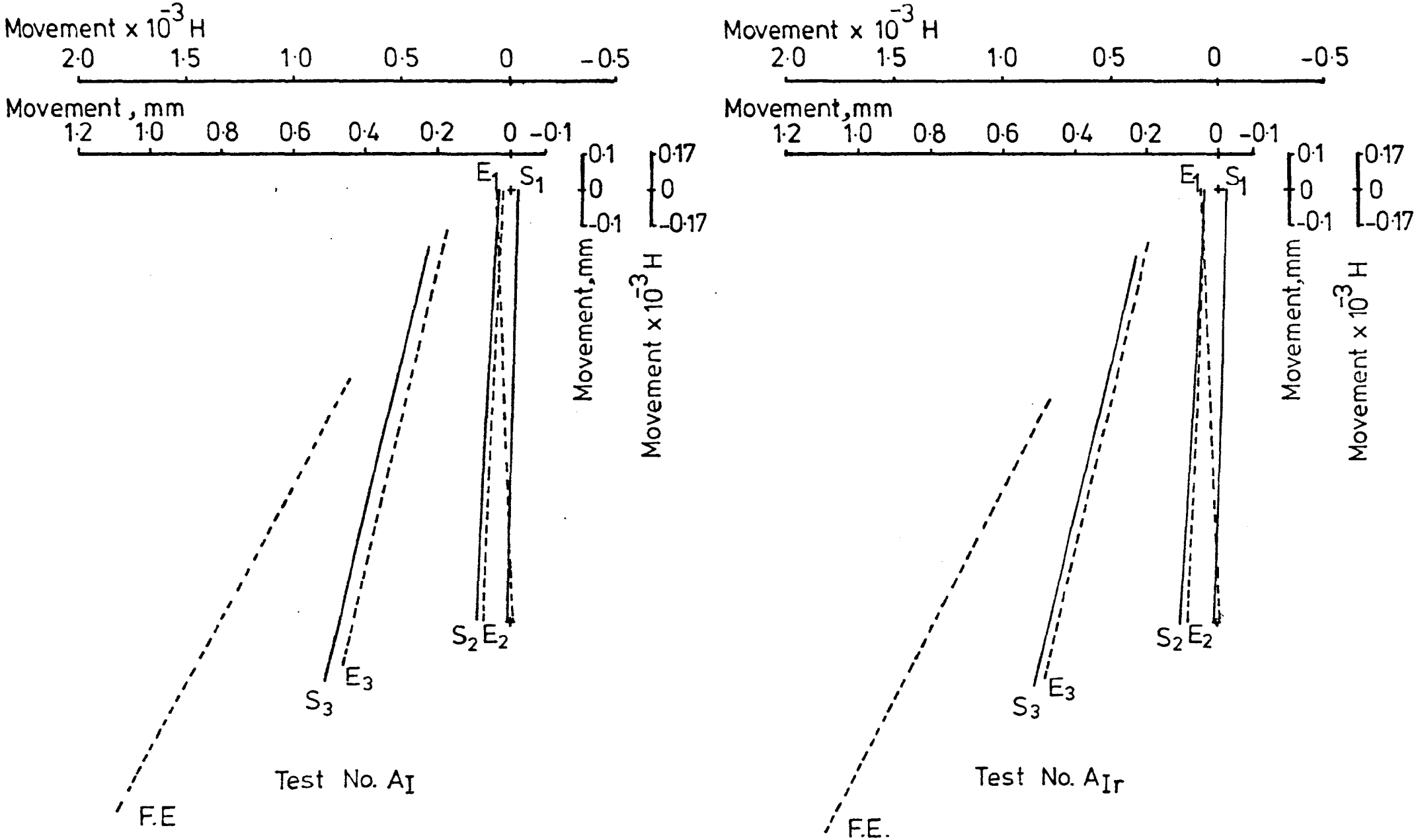

FIG.7·1 COMPARISON OF WALL MOVEMENTS DURING CONSTRUCTION FOR TESTS A_I & A_{Ir}

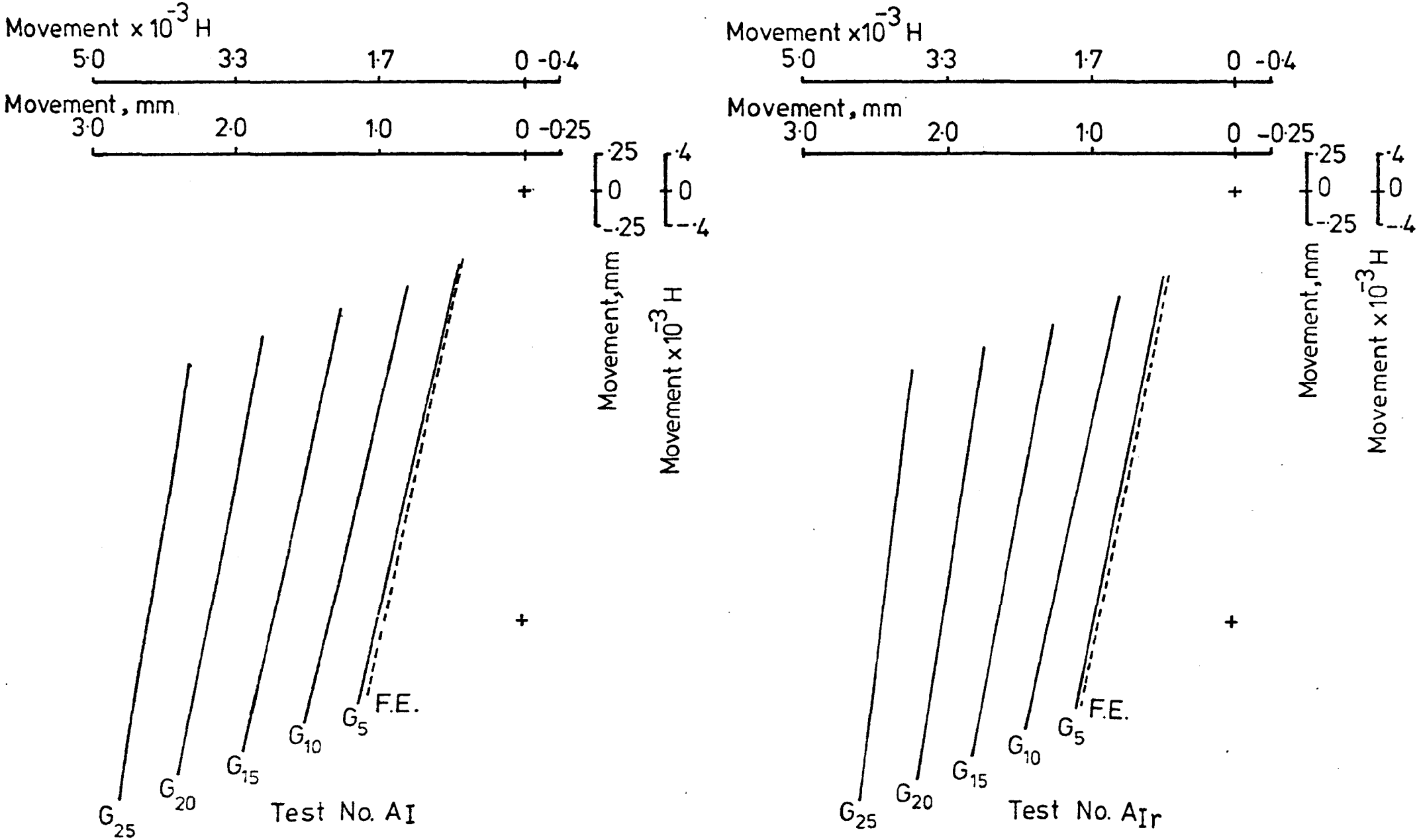

FIG. 7·2 COMPARISON OF WALL MOVEMENT DURING SURCHARGE LOADING FOR TESTS A_I & A_{Ir}

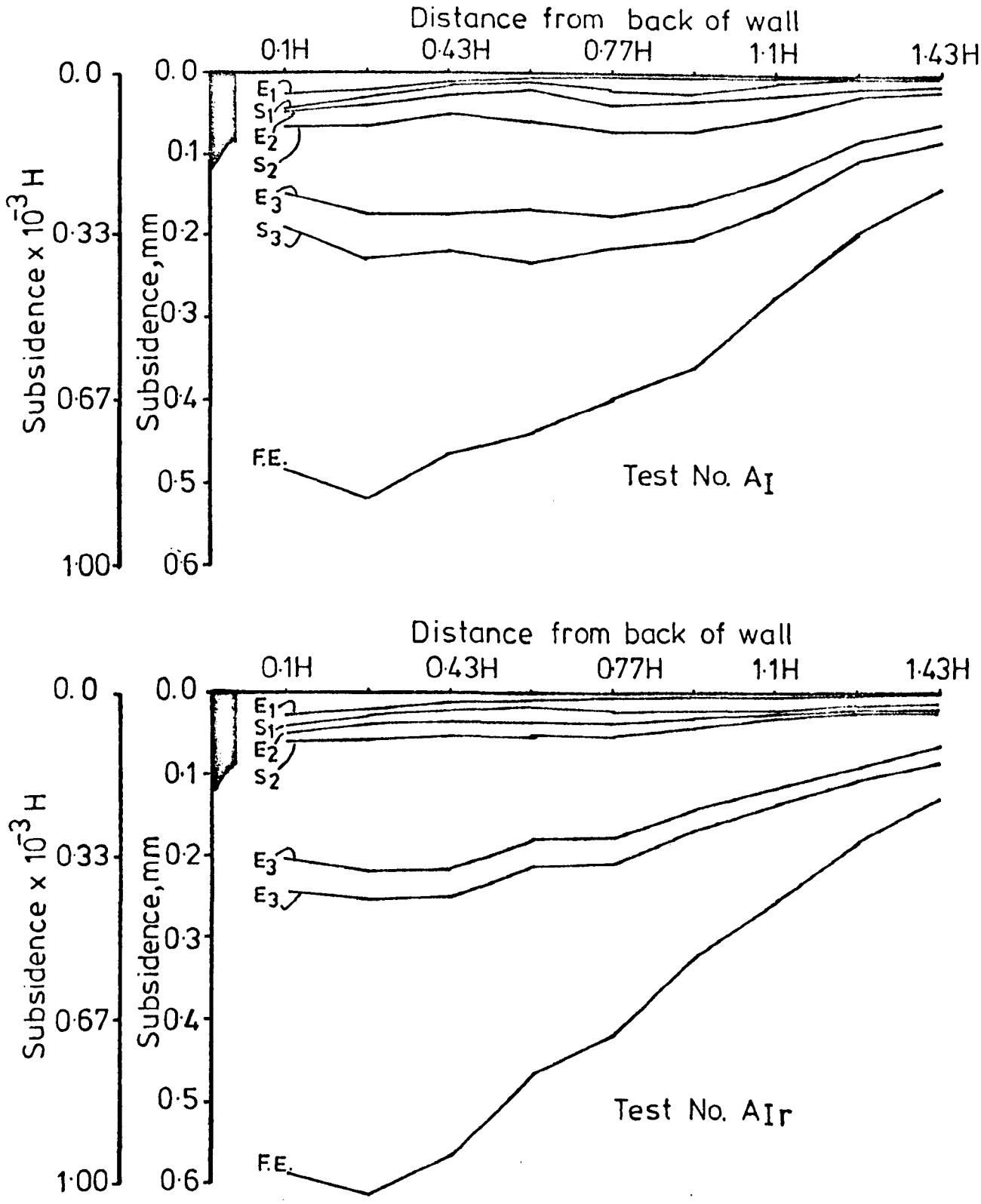

FIG.7.3 COMPARISON OF SAND SUBSIDENCES DURING CONSTRUCTION FOR TESTS A_I & A_{Ir}

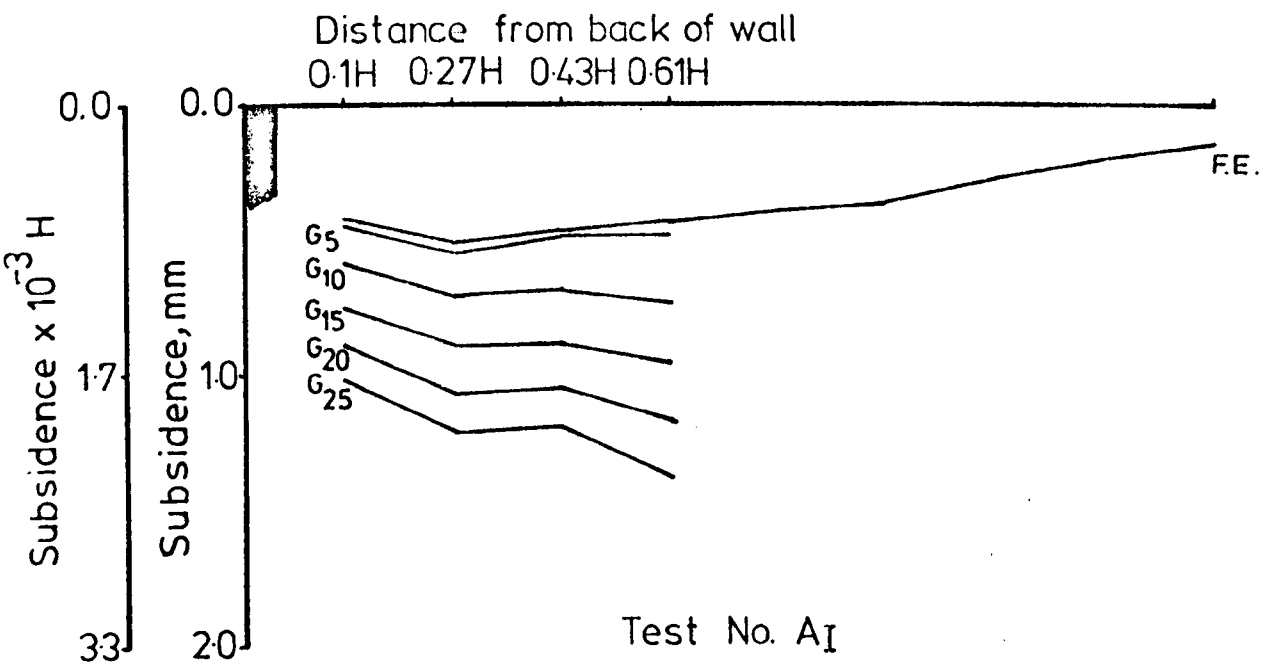

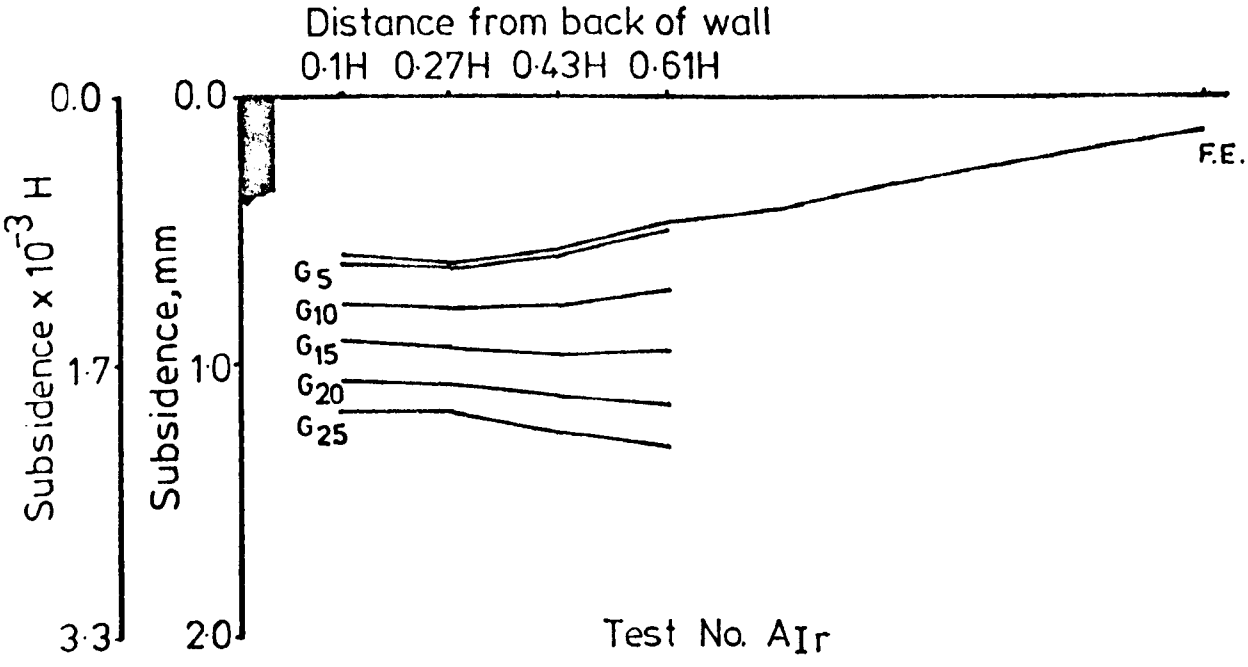

FIG. 7·4 COMPARISON OF SAND SUBSIDENCES DURING SURCHARGE LOADING FOR TESTS AI & AIr

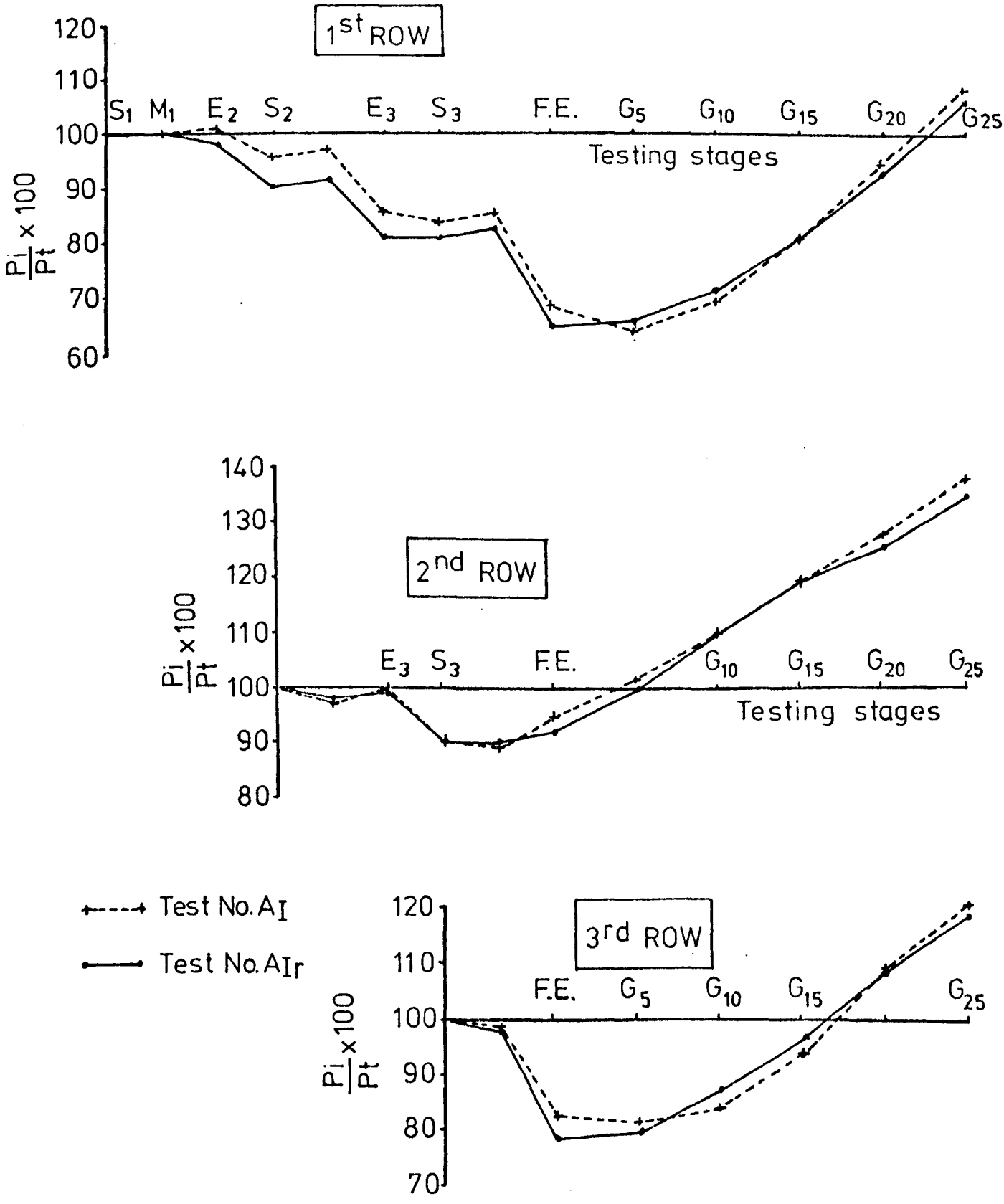

Pi = Measured anchor load

Pt = Theoretical prestress load

FIG. 7·5 ANCHOR LOAD CHANGES FOR THE DIFFERENT TESTING STAGES FOR TESTS A_I & A_{Ir}

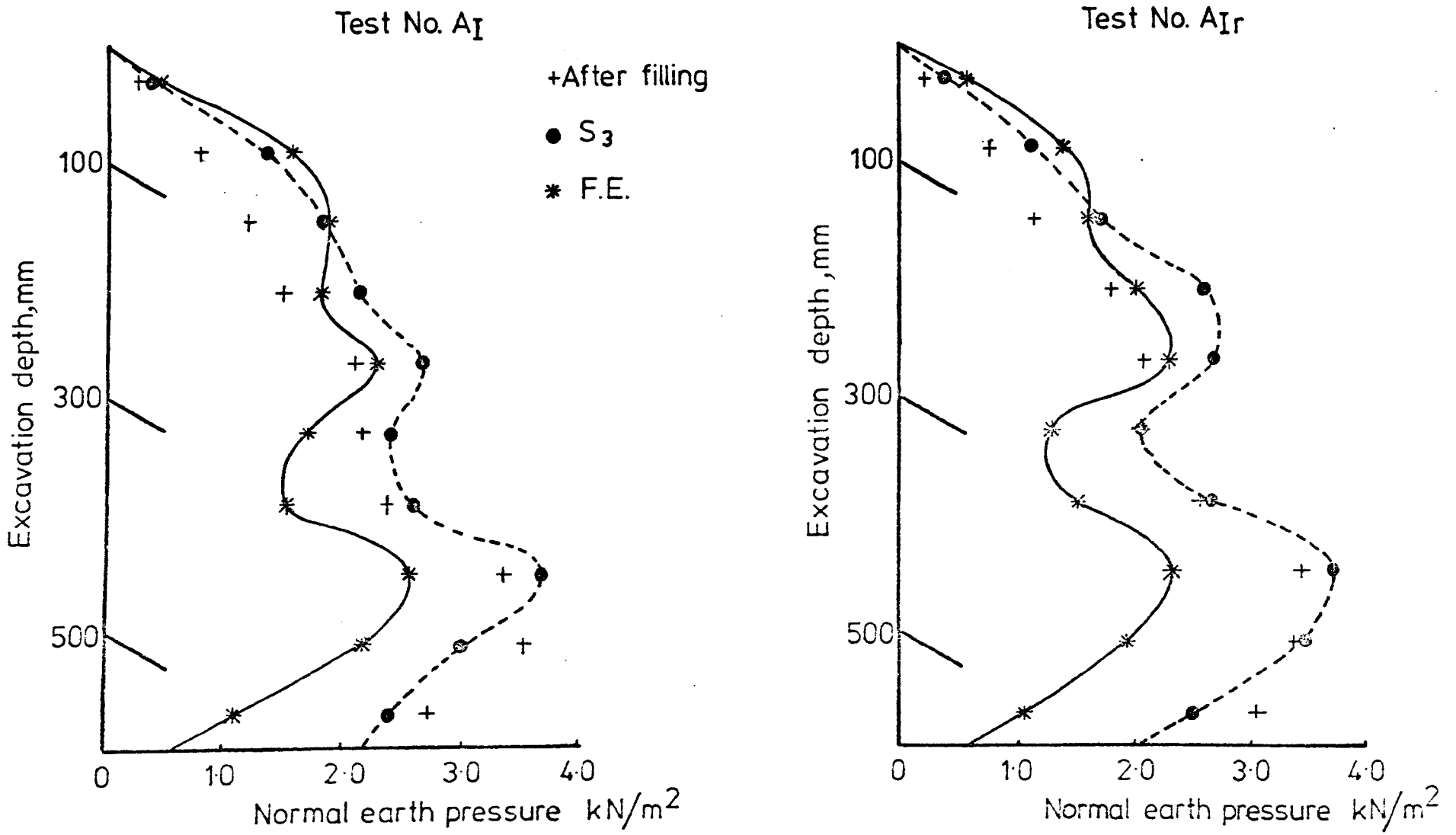

FIG. 7·6 EARTH PRESSURE DISTRIBUTION AFTER FILLING AND AT THE FINAL TWO CONSTRUCTION STAGES FOR TESTS A_I & A_{Ir}

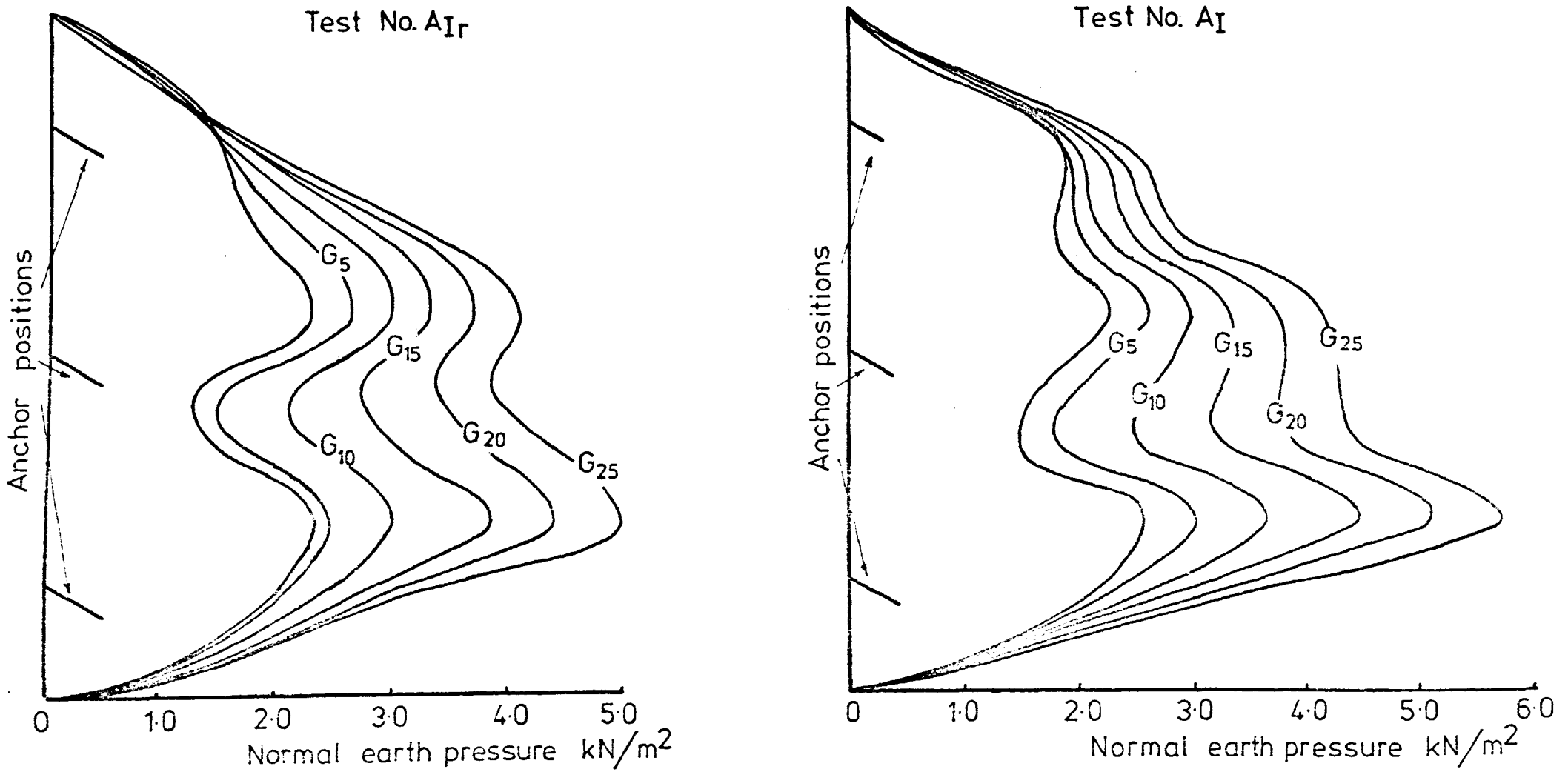

FIG. 7·7 EARTH PRESSURE DISTRIBUTION DURING SURCHARGE LOADING FOR TESTS A_I & A_{Ir}

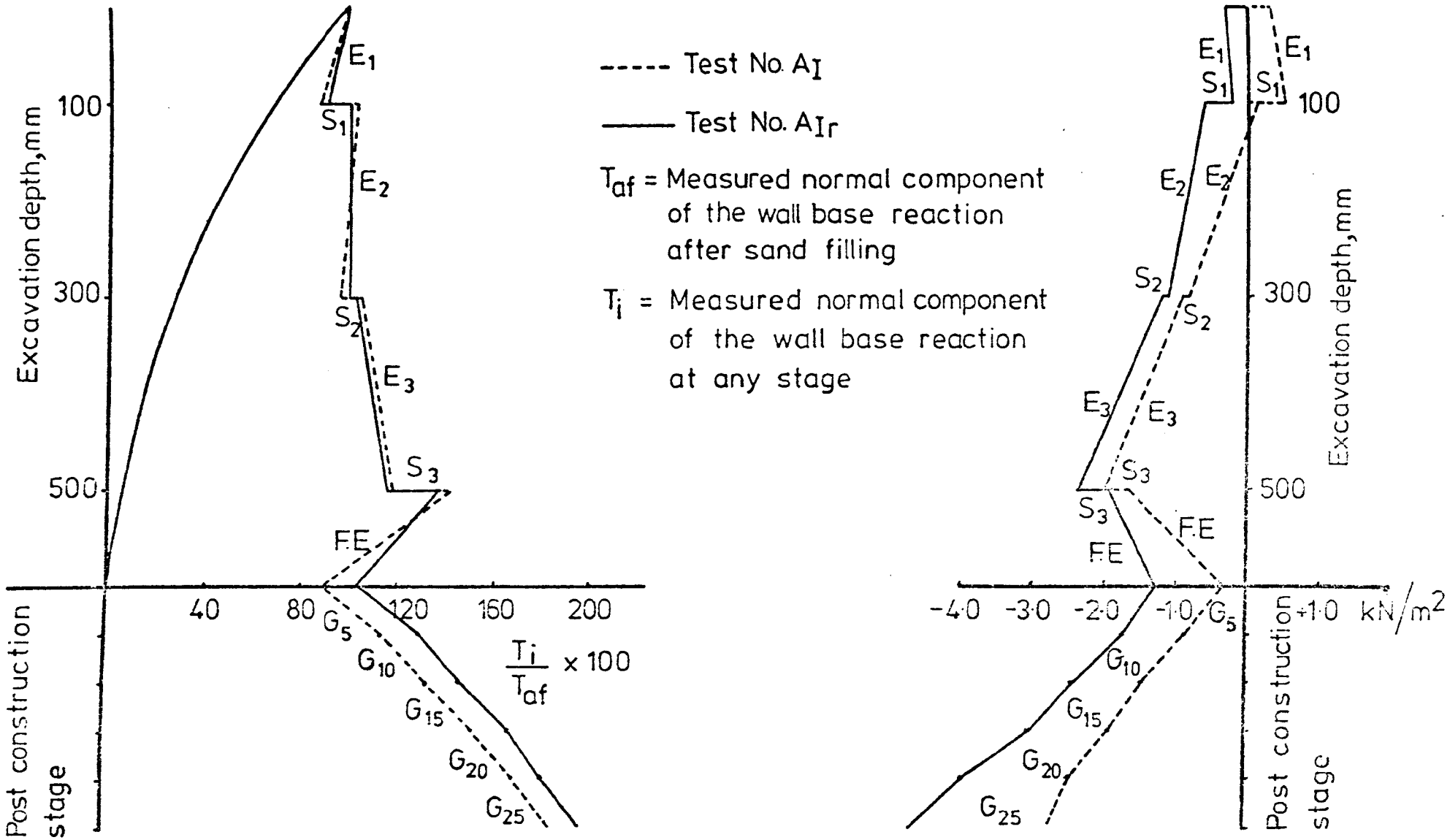

FIG. 7·8 VARIATION OF THE NORMAL AND SHEAR COMPONENTS OF THE WALL BASE REACTION FOR TESTS AI & AIr

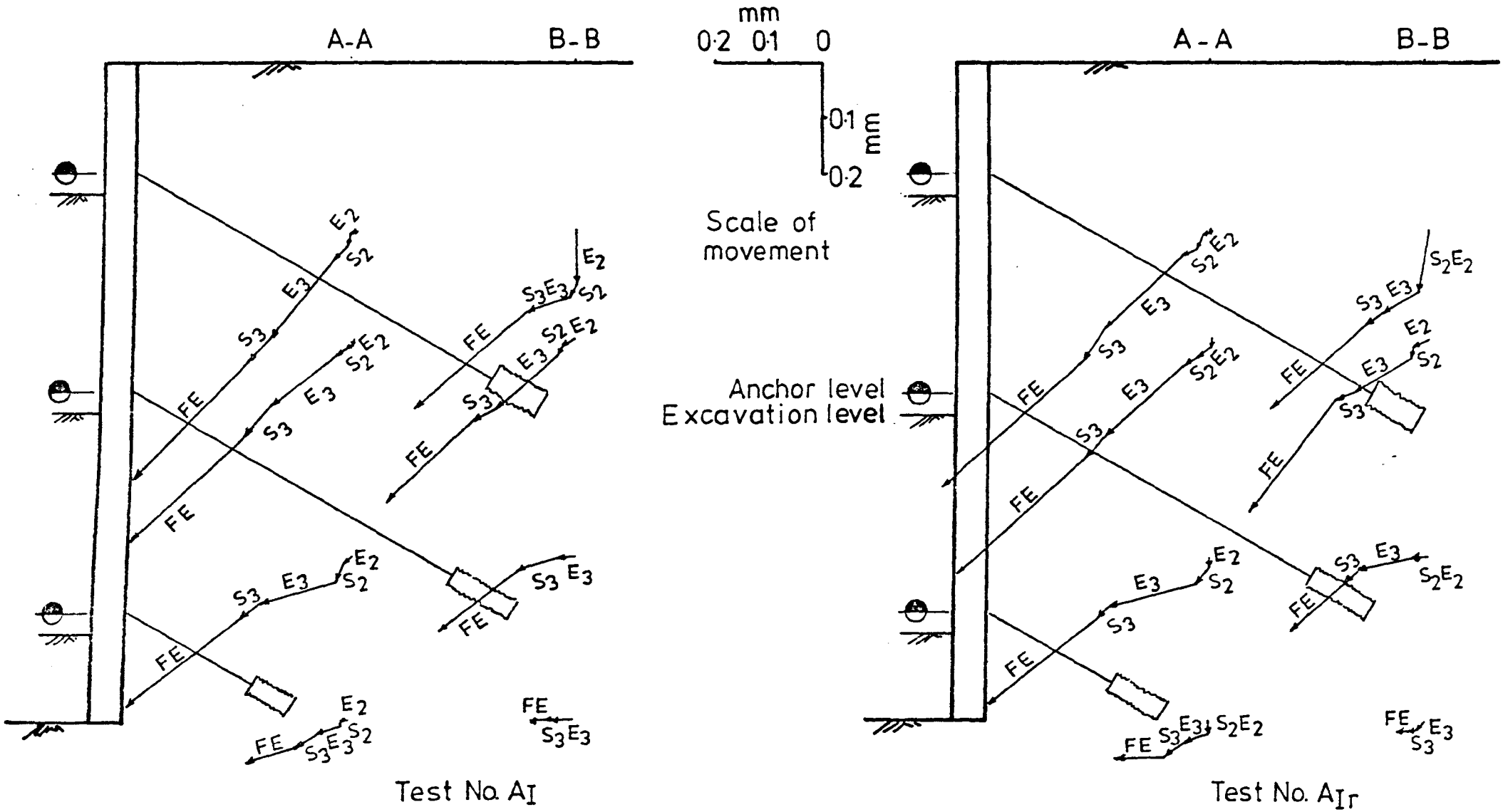

FIG. 7·9 SAND MOVEMENTS WITHIN THE RETAINED SAND MASS FOR TESTS A_I & A_{Ir}

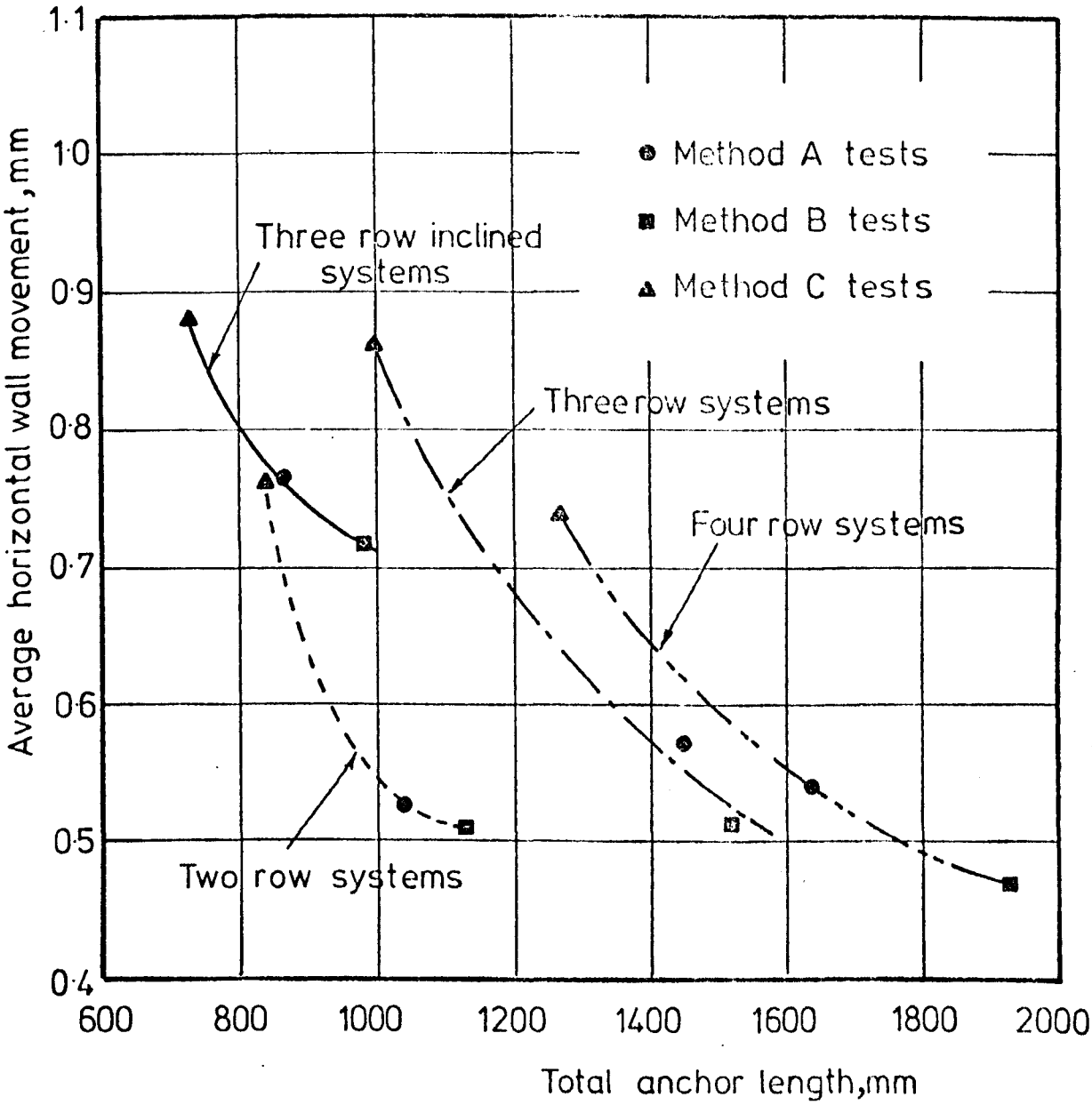

FIG. 7·10 PLOT OF THE AVERAGE HORIZONTAL WALL MOVEMENT V. THE TOTAL ANCHOR LENGTH

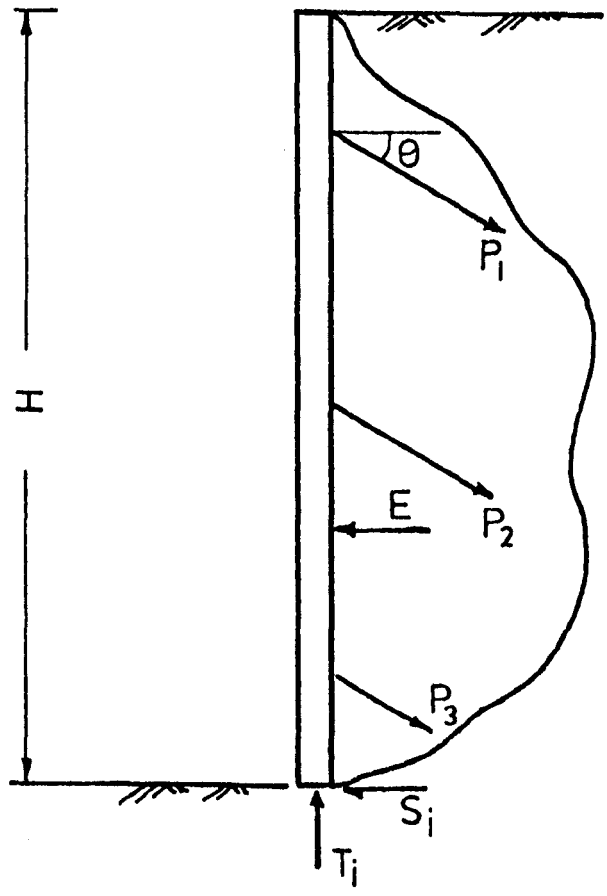

For equilibrium

$T_i - \Sigma P_i \sin\theta - E \tan \delta wm = 0$

$\Sigma P_i \cos\theta - E - S_i = 0$

where δwm is the mobilized angle of wall friction

FIG. 7·11 NOTATION FOR THEORETICAL FORCE SYSTEM ACTING ON THE WALL

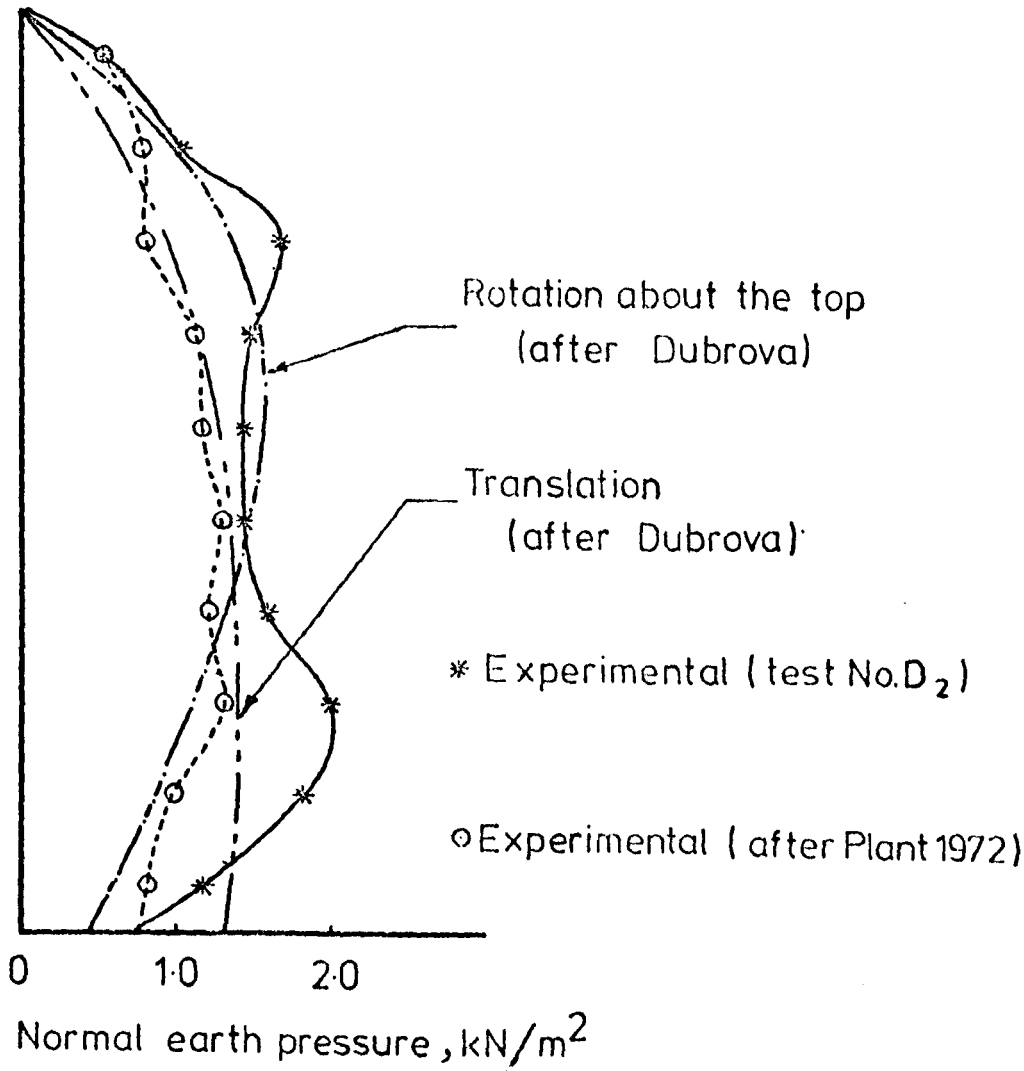

FIG. 7·12 COMPARISON OF THE EXPERIMENTAL EARTH PRESSURE DISTRIBUTION AT FULL EXCAVATION WITH THE THEORETICAL DISTRIBUTION AFTER DUBROVA (1962)

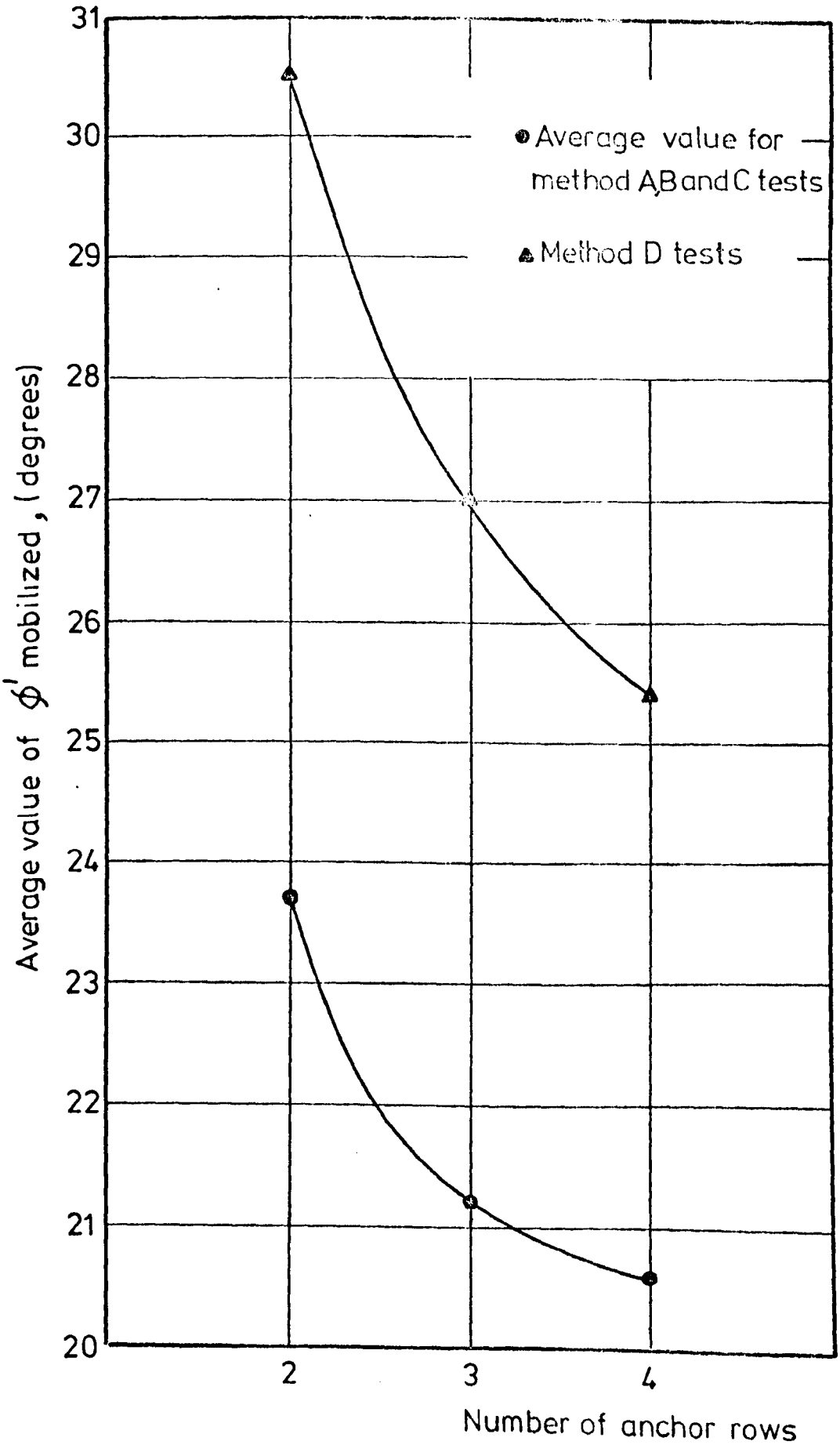

FIG. 7·13 PLOT OF AVERAGE VALUE OF ϕ'_m V. NUMBER OF ANCHOR ROWS

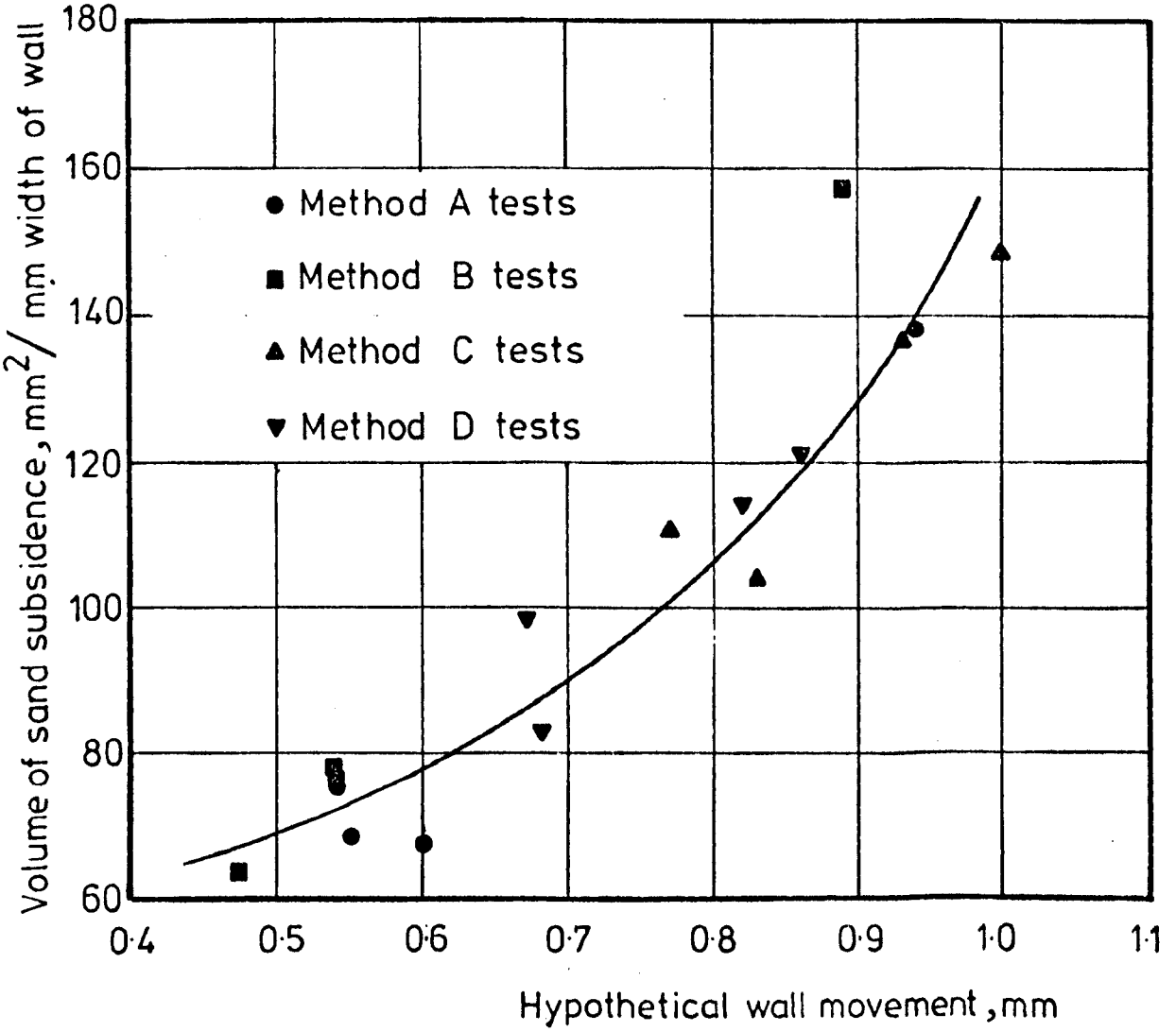

FIG. 7.14 PLOT OF SAND SUBSIDENCE V. HYPOTHETICAL WALL MOVEMENT

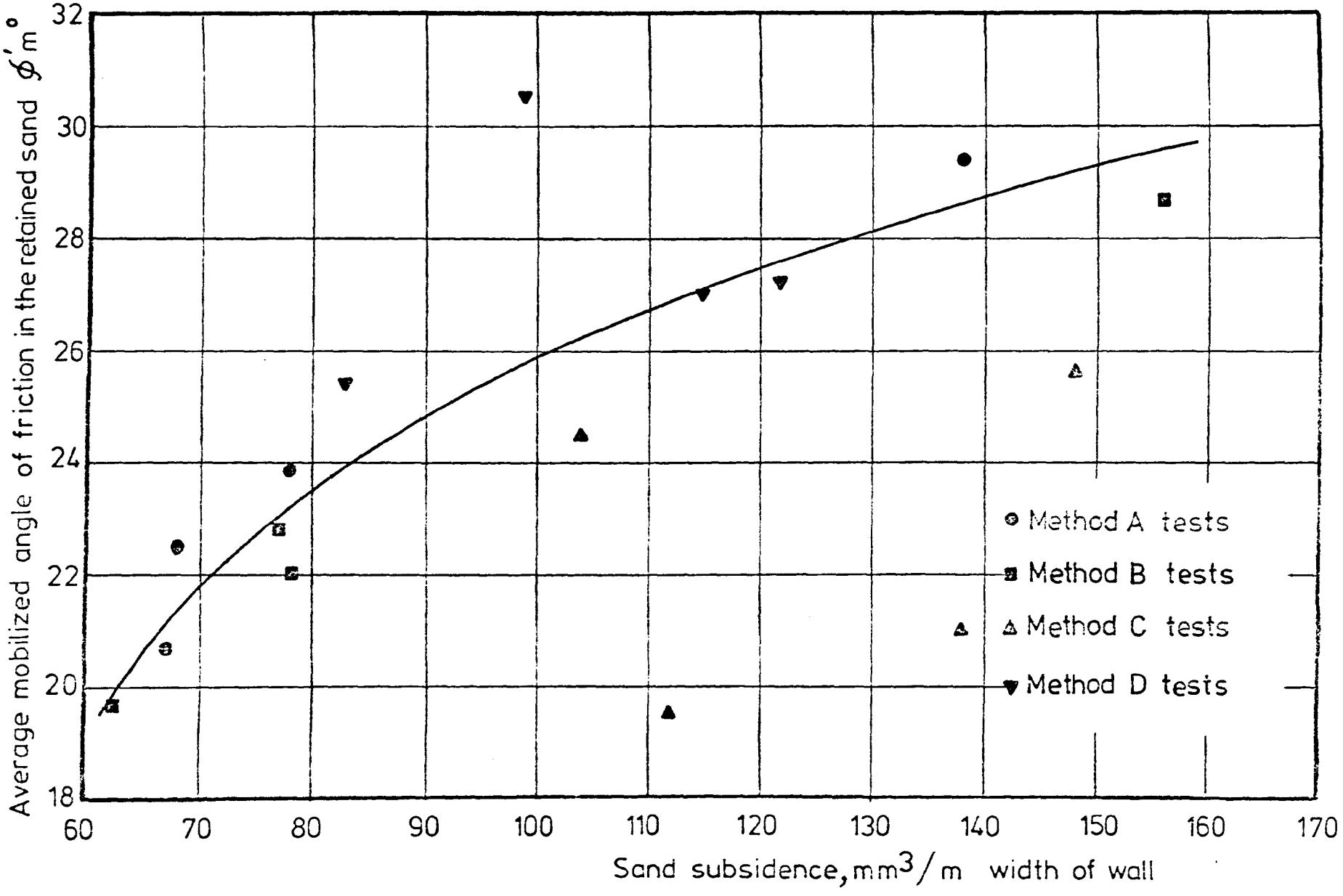

FIG. 7·15 PLOT OF THE AVERAGE MOBILIZED ANGLE OF FRICTION IN THE RETAINED SAND V. SAND SUBSIDENCE

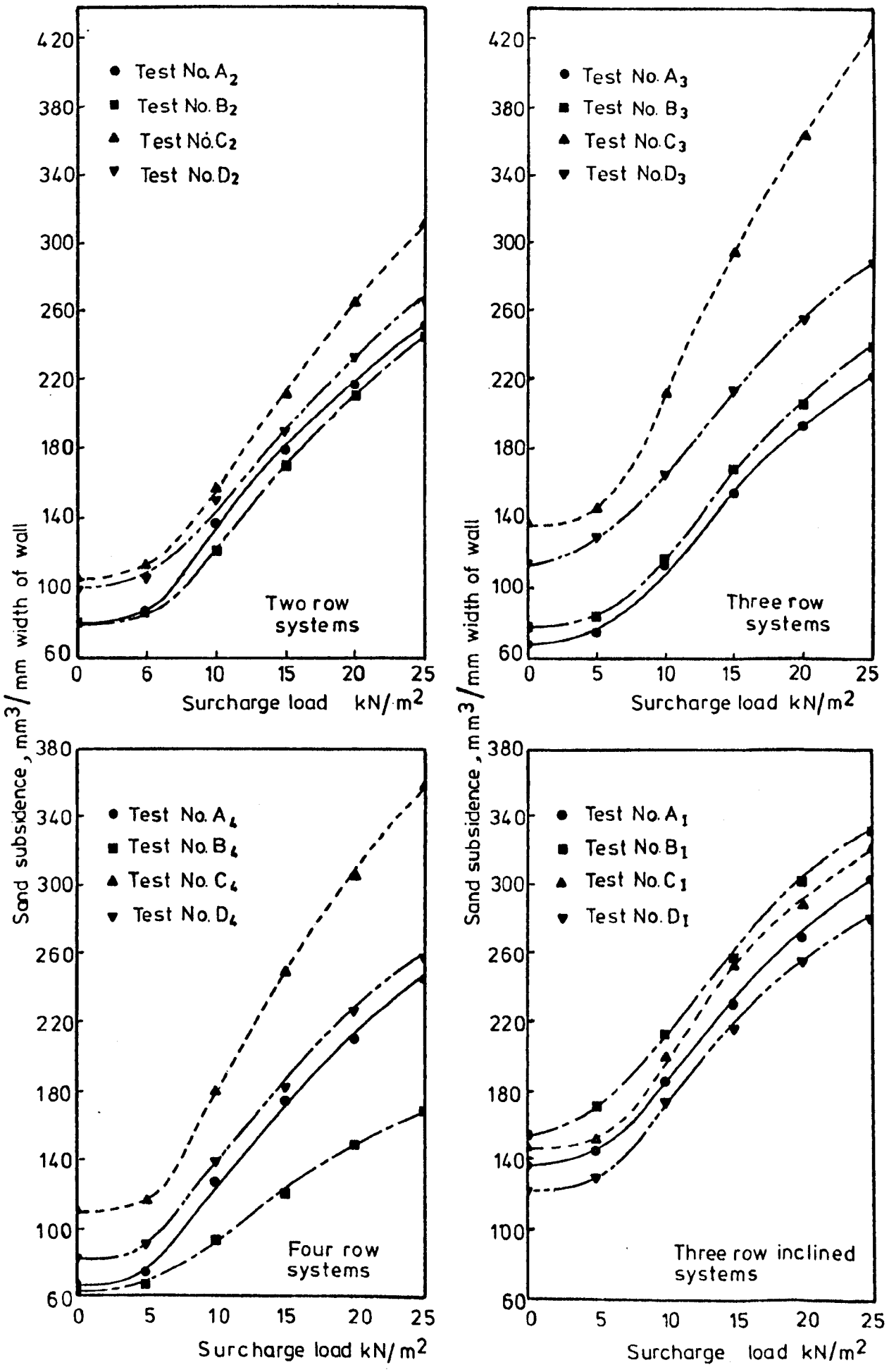

FIG. 7.16 PLOT OF SAND SUBSIDENCE V. SURCHARGE LOAD

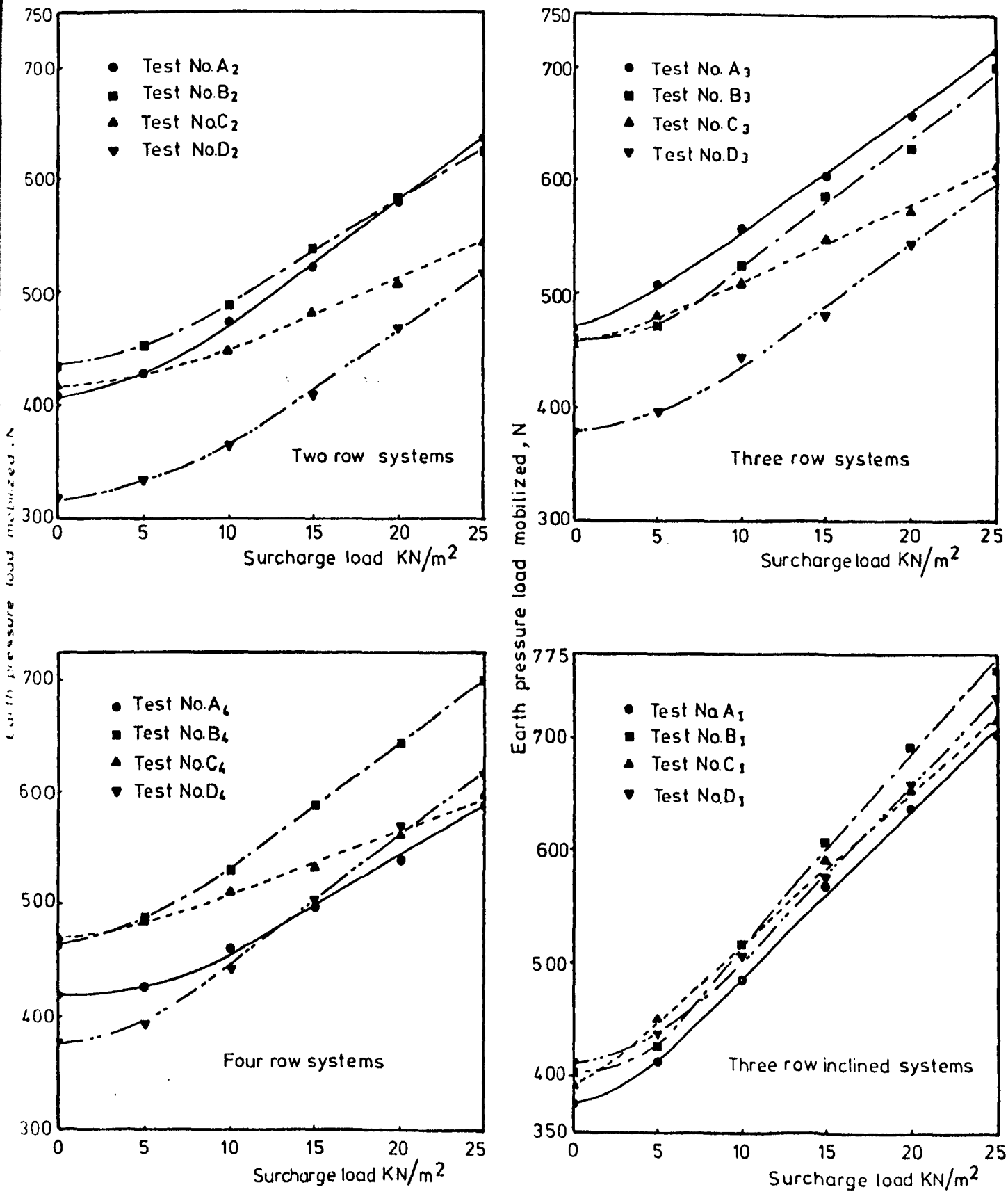

FIG 7.17 PLOT OF NORMAL EARTH PRESSURE LOAD V. SURCHARGE LOAD

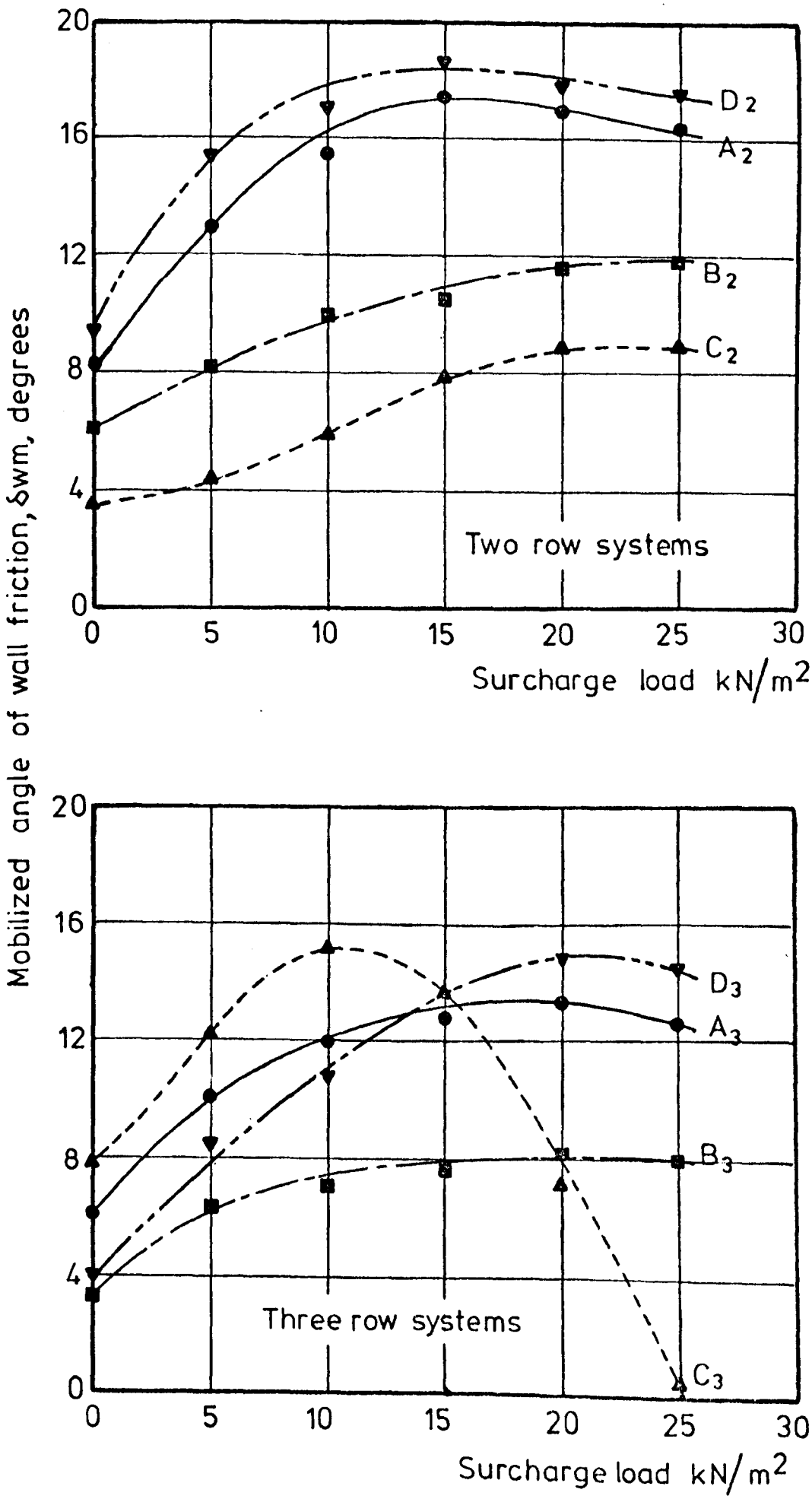

FIG. 7·18 PLOT OF THE MOBILIZED ANGLE OF WALL FRICTION V. SURCHARGE LOAD

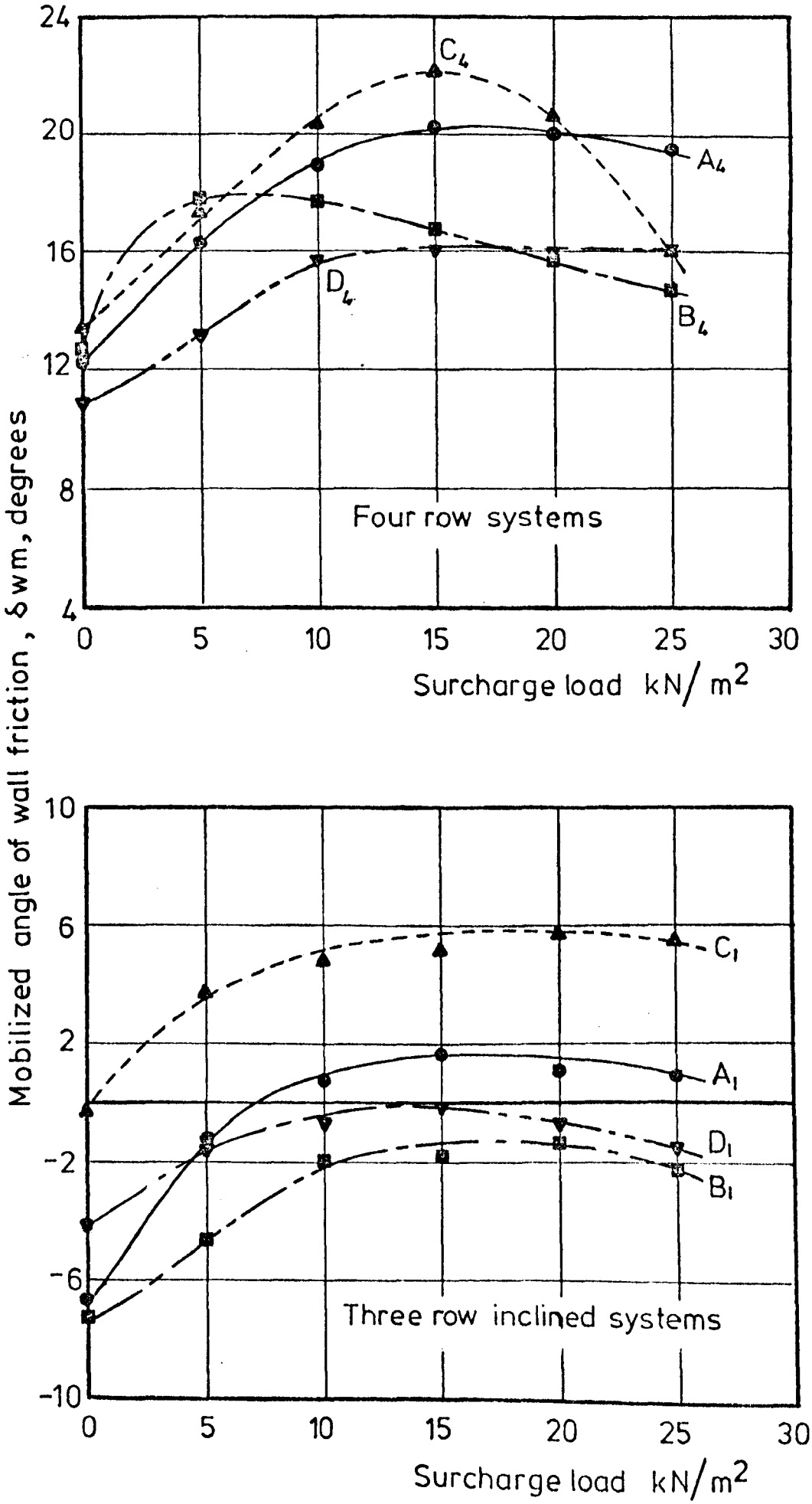

cont. FIG. 7·18 PLOT OF THE MOBILIZED ANGLE OF WALL FRICTION V. SURCHARGE LOAD

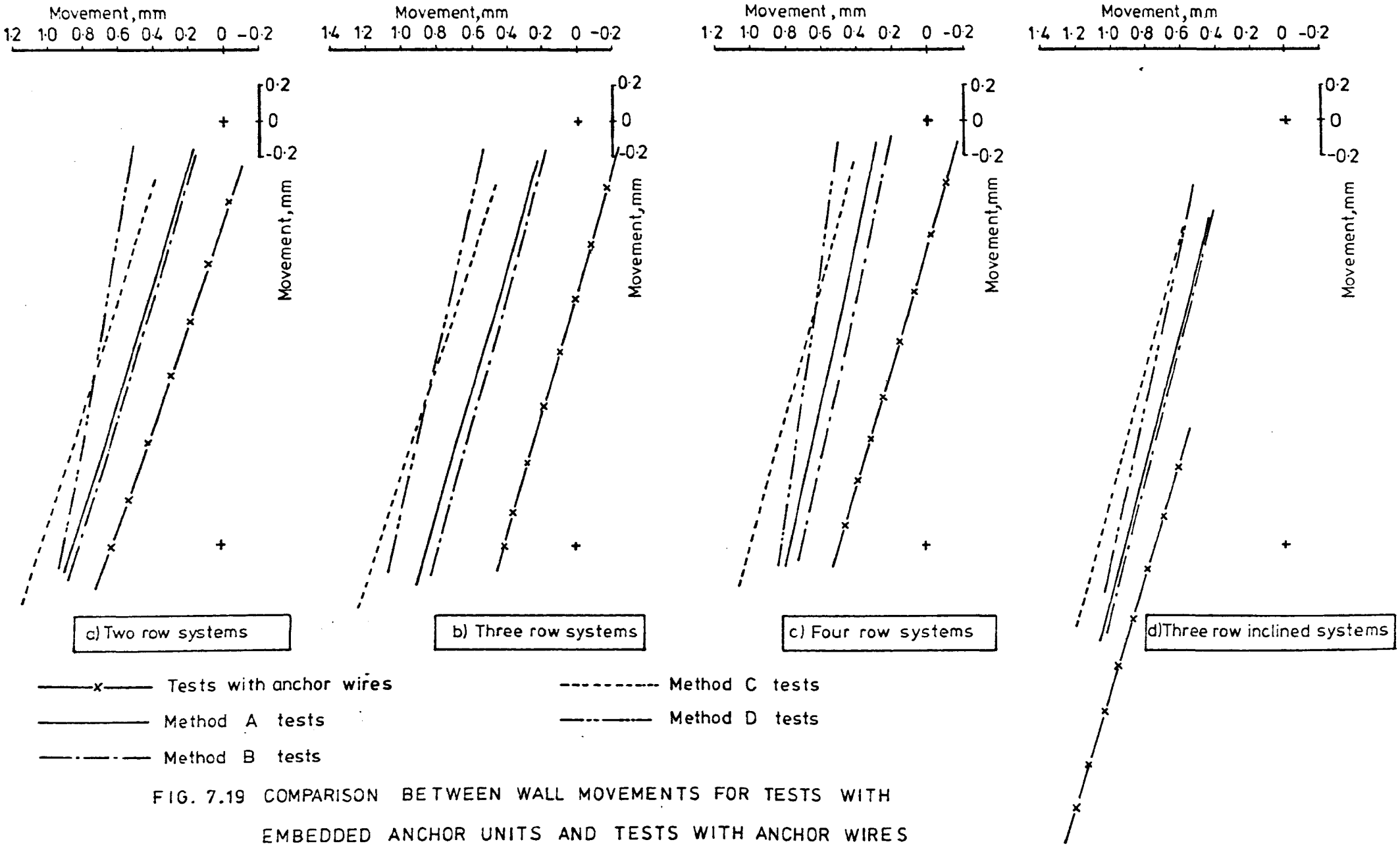

FIG. 7.19 COMPARISON BETWEEN WALL MOVEMENTS FOR TESTS WITH EMBEDDED ANCHOR UNITS AND TESTS WITH ANCHOR WIRES

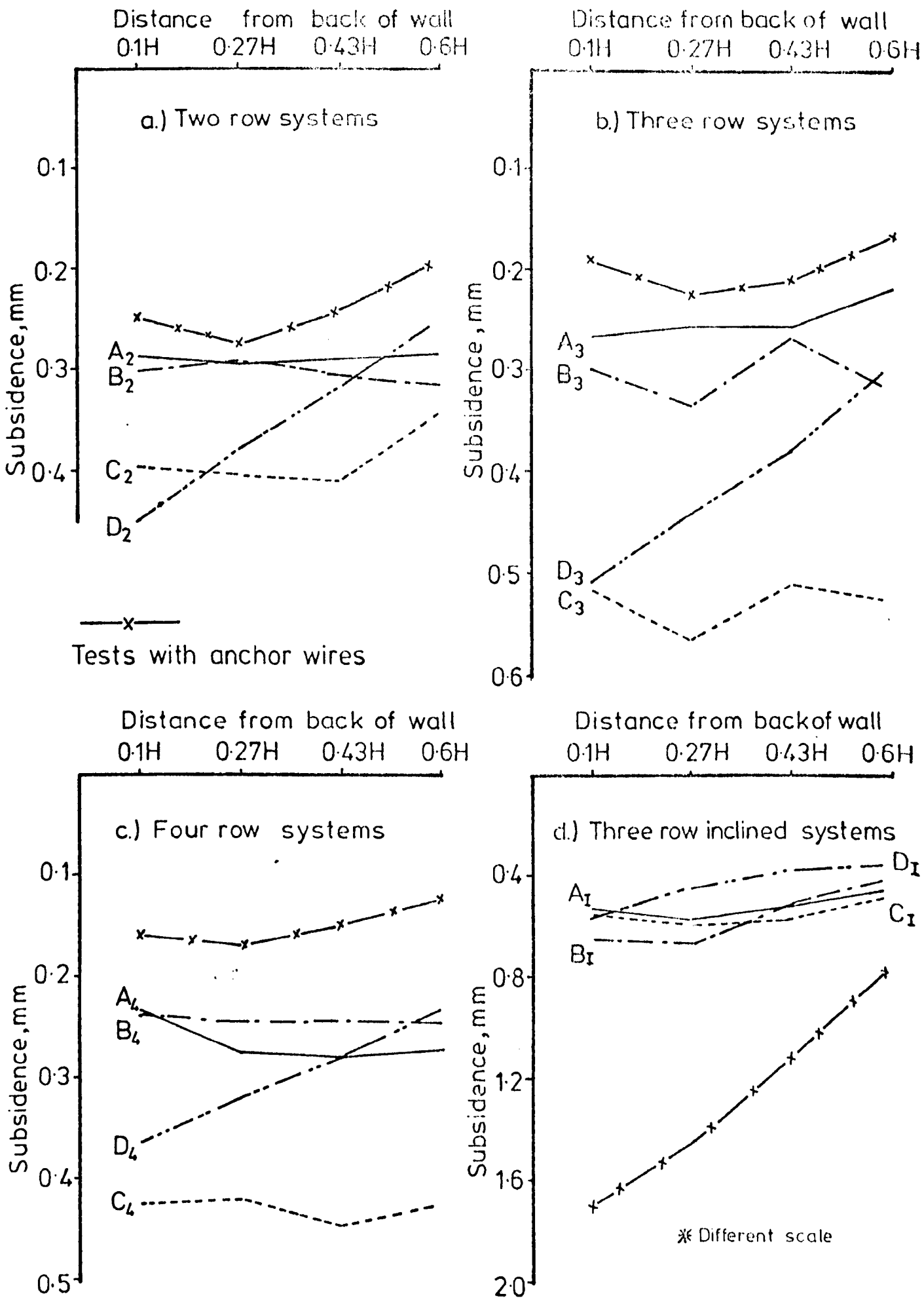

FIG. 7·20 COMPARISON BETWEEN SAND SUBSIDENCE FOR TESTS WITH EMBEDDED ANCHOR UNITS AND FOR TESTS WITH ANCHOR WIRES

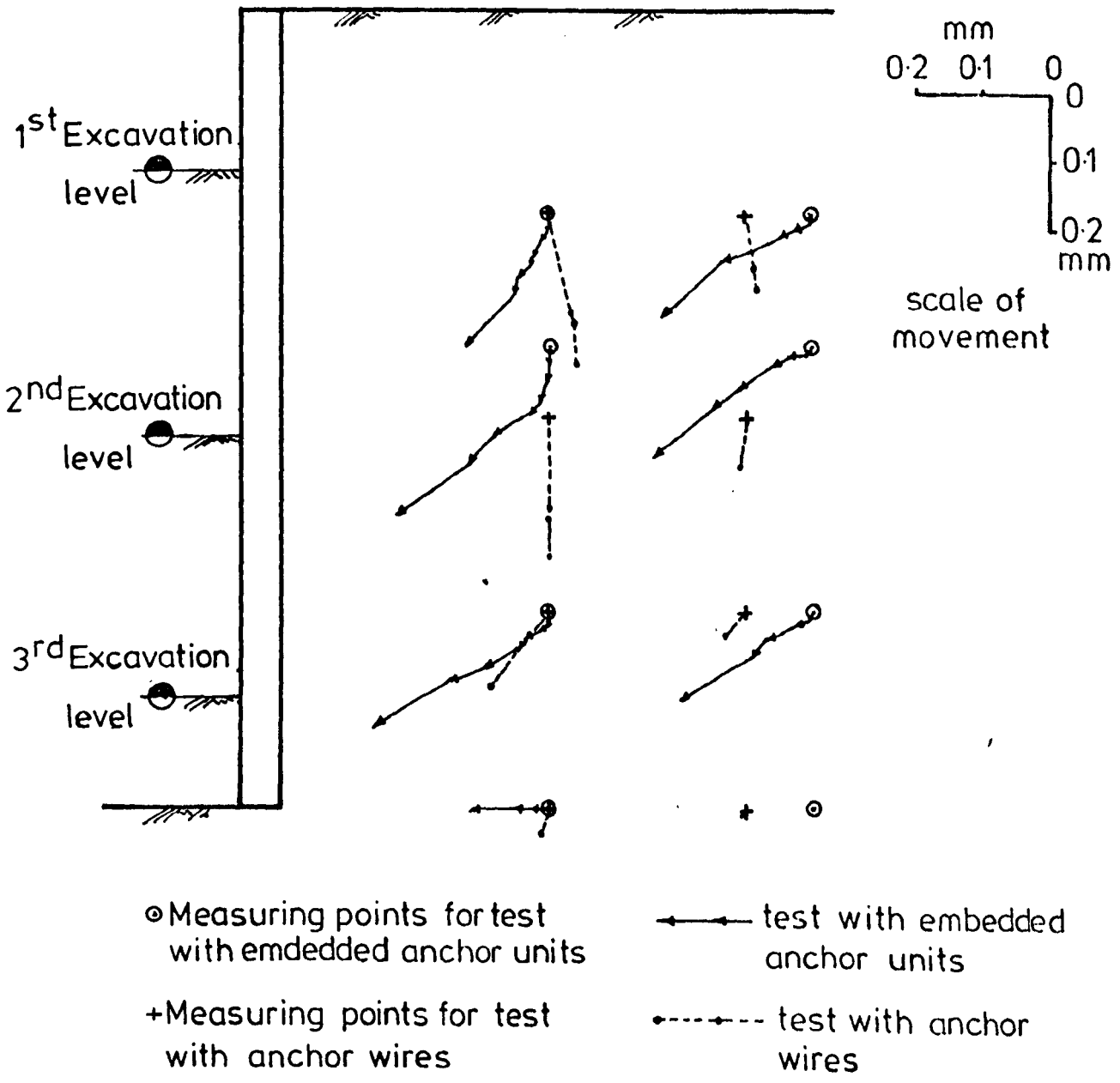

FIG. 7·21 COMPARISON BETWEEN SAND MOVEMENTS WITHIN THE RETAINED SAND MASS FOR TESTS WITH EMBEDDED ANCHOR UNITS AND TESTS WITH ANCHOR WIRES

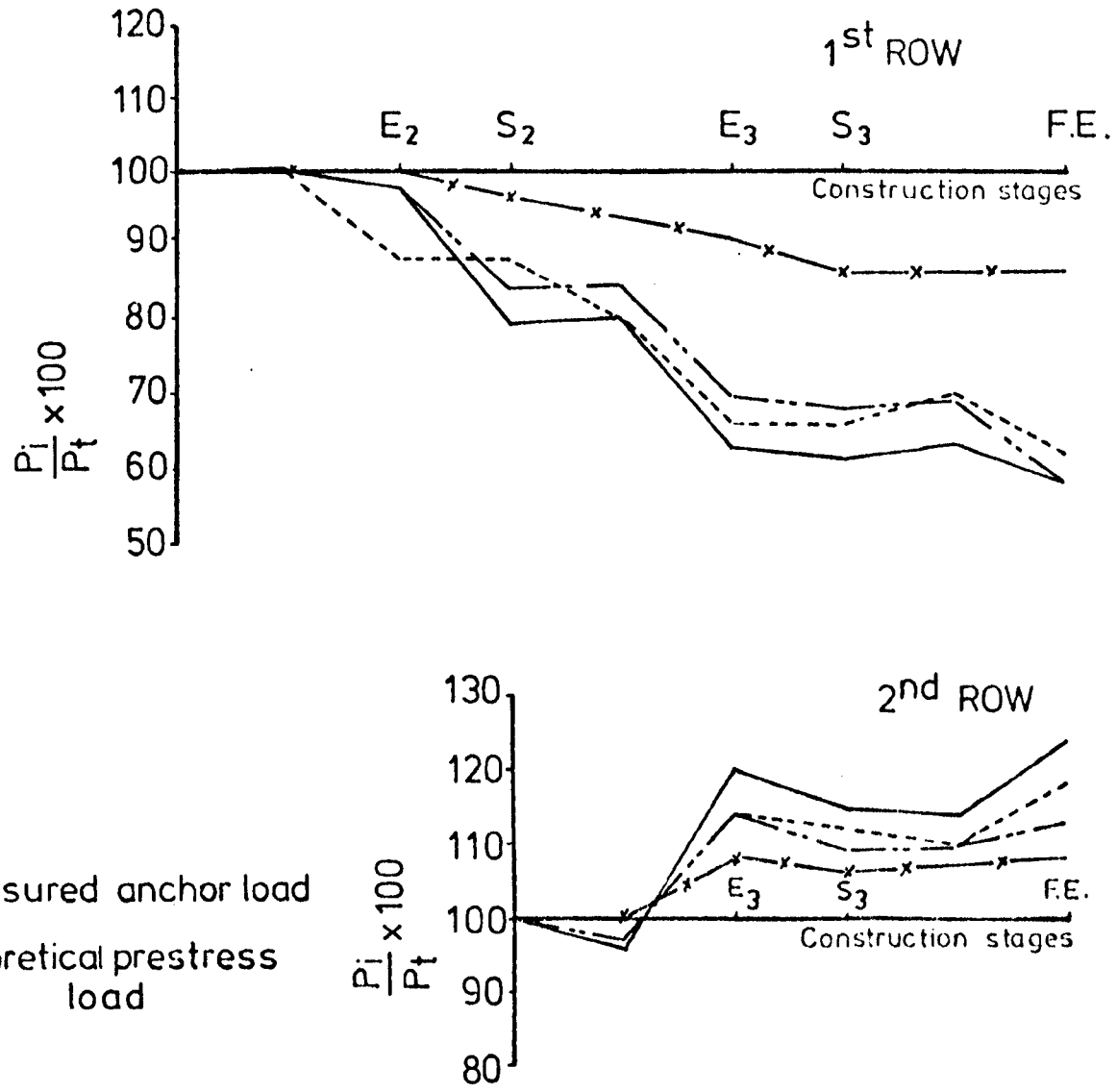

FIG.7·22 ANCHOR LOAD VARIATION FOR TESTS WITH EMBEDDED ANCHOR UNITS AND TESTS WITH ANCHOR WIRES

CHAPTER 8

CONCLUSIONS AND SUGGESTIONS FOR FUTURE WORK

CHAPTER 8

CONCLUSIONS AND SUGGESTIONS FOR FUTURE WORK

8.1 Conclusions

(a) Small scale studies

1. The failure mechanism in the case of a single plate anchor is unique and characterised by the ratio D/B (anchor depth/anchor plate height). In the case of shallow anchors a complete shear failure of the mass extending to the surface was observed, while deep anchors gave a local shear failure.
2. A minimum value of the free anchor length, L, in the case of single plate anchors and multi-plate deep anchors greater than about five times the anchor plate height, was found to be necessary to prevent short-circuiting of the prestress load to the retaining wall.
3. Multi-plate anchors carried more load than a single plate anchor at the same depth and with the same anchor plate height. The difference is mainly attributed to the increase in the size of the failure zone and the frictional force developing along the anchorage length.
4. The position defining shallow and deep anchors in the case of multi-plate anchors is not unique, being dependent on the anchorage length, ℓ.
5. For any particular depth, increasing the number of, or the distance between, the anchor plates increased the pull-out load. However, the effect of increasing the distance between the plates vanishes at a critical spacing after which each single plate develops its own failure zone.

6. Tests carried out on individual strip anchors in the small sand box provided a practical solution for the design of the anchors used in the retaining wall tests.

(b) Retaining wall tests

7. Repeatibility tests showed that the different components of the apparatus and instrumentation as well as the testing technique were satisfactory.

8. With increasing anchor length the wall displacement was reduced. However, if an anchored retaining wall is supported by horizontal anchors, an increase in the average anchor length greater than the wall height may have very little effect on further limiting the displacements.

9. Lower prestress loads resulted in lower values of the normal earth pressure load mobilized on the back of the wall. This indicated that within certain limits the pressure distribution may be controlled by inducing suitable prestress loads in the anchors.

10. From test observations it was found that a trapezoidal earth pressure distribution is realistic when the excavation is carried out to the base level of the wall or if it is at a considerable distance below the bottom row of anchors. However, if the bottom row of anchors is very close to the bottom of the excavation, a triangular distribution is more applicable.

11. The analysis made by Dubrova for determining the earth pressure distribution appears to be realistic and the values of the earth pressure loads calculated according to the proposed method are close to those measured by Plant (1972).

12. The mobilized angle of shearing resistance in the retained sand mass decreased with an increase in the number of anchor rows.

13. Sand surface subsidence was found to be dependent on both the vertical and horizontal wall displacements. Subsidence can be effectively reduced by reducing the lateral movement of the wall.

14. An increase in the magnitude of the sand subsidence was accompanied by an increase in the mobilized angle of shearing resistance, ϕ'_m. This agrees with the findings reported by Rowe and Briggs (1961) and Plant (1972).

15. The observed sand surface disturbance in the vicinity of the anchor blocks exaggerated, but highlighted, the importance of taking into account the influence of anchor installation and stressing on adjacent buildings.

16. Two patterns of wall movement were observed. These were mainly dependent on the earth pressure distribution used for determining the anchor prestress loads. A rectangular distribution resulted in a rotation about a point near the top of the wall whereas a triangular distribution resulted in a rotation about a point near the bottom of the wall.

17. All design methods yielded stable systems, which performed satisfactorily. No failures have been indicated and the deformations and surface subsidence were within tolerable limits. However, it should be pointed out that all design methods are far from ideal. They take no account of the strain or stress distribution in the retained soil, as they assume specific rupture planes, but they provide a practical solution in designing the required anchor lengths.

18. The determination of the anchor loads by the method proposed by James and Jack (method D) proved to be unrealistic. The method grossly underestimates the anchor loads. On the other hand, the stability analysis of method D, using a logarithmic spiral, appeared to be more suitable than the other analyses especially in the case of inclined anchors.

19. Under surcharge loading conditions, tests designed according to method D proved to be more consistent in behaviour. Tests designed according to methods A, B and C suffered from some deficiencies such as higher pressure concentration over some parts of the wall, uneven surface subsidence, severe rotational motion and excessive wall movements.

20. The use of embedded anchor units to support the wall allowed for complete interaction between the soil and the support system.

21. The comparison made between tests with anchor wires and tests with embedded anchor units revealed that the use of horizontal anchor wires resulted in very conservative values for the wall movements and the surface subsidence. However, inclined anchor wires exaggerated the magnitude of subsidence and gave a misleading pattern for the wall movement.

22. The patterns of wall and sand movements observed when embedded anchor units were used were more realistic and resembled field observations.

23. Embedded anchor units suffered more reduction in the anchor loads than anchor wires. However, the trends in anchor load variations were similar but with different magnitudes.

24. The measured parameters Km, δwm and ϕ'_m for tests with anchor wires and tests with embedded anchor units showed similar trends.

8.2 Suggestions for Future Work

1. Further study using the pin model analogy could be carried out to achieve better understanding of the behaviour of multi-plate horizontal and inclined anchors, and to study the optimum arrangement of the plates.
2. A study using the pin model analogy could examine the failure mechanism of walls supported by different numbers of anchor rows. Different combinations of anchor inclinations could be attempted, while the anchor lengths could be determined by different design methods. Failure of the system could be achieved by inducing various modes of movement to the wall.
3. An experimental investigation to study the behaviour of a group of horizontal prestressed anchors to achieve a better understanding of their interaction, performance and design could be carried out. This would be useful when applied to the design of tied-back retaining walls.
4. Theoretical modifications could be applied to the design method proposed by James and Jack for determining anchor loads. This could be investigated experimentally to assess its validity.
5. The effect of a faulty anchor in a group on the response of the other anchors and the overall behaviour of the wall, could be examined if individual circular multi-plate anchors could be used instead of strip multi-plate anchors to support the wall.

6. Parameters which have been fixed in the present study could be investigated.

(a) A similar study could be carried out to assess the behaviour of a flexible wall when supported by embedded anchor units.

(b) The effect of varying the soil density or of using different types of soils could be examined.

(c) The effect of varying the length of fixity of the wall toe on the overall behaviour of the system could be studied.

REFERENCES

REFERENCES

ABU-TALEB, M. G. A. (1971). Laboratory scale studies on tied-back rigid retaining walls in sand. M. Eng. thesis, University of Sheffield.

ABU-TALEB, M. G. A. (1974). The behaviour of anchors in sand. Ph.D. thesis, University of Sheffield.

ANDERSON, W. F., HANNA, T. H. and SHAH, S. A. (1977). Model tests on anchored walls retaining overconsolidated sands. Can. Geotech. J., Vol. 14, No. 2, pp. 214-222.

ARBER, N. R. (1976). A study of the load behaviour of basement-type retaining wall embedded in sand. Ph.D. thesis, University of Sheffield.

BAKER, W. H. and KONDNER, R. L. (1966). Pull out load capacity of a circular earth anchor buried in sand. Highway Res. Rec., No. 108, pp. 1-10.

BALLA, A. (1961). The resistance to breaking out of mushroom foundations for pylons. Proc. 5th Int. Conf. Soil Mech. and Fdn Engng, Paris, Vol. 1, pp. 569-576.

BARLA, G. and MASCARDI, C. (1974). High anchored wall in Genoa. Proc. Conf. Diaphragm Walls and Anchorages, Instn Civil Engrs, London, pp. 123-128.

BIAREZ, J., BOUCRAUT, L. M. and NEGRE, R. (1965). Equilibre limite d'écrans verticaux soumis à une translation ou une rotation. Proc. 6th Int. Conf. Soil Mech. and Fdn Engng, Montreal, Vol. 2, pp. 368-372.

BOUCRAUT, L. M. (1964). Equilibre limite d'un milieu pulverulent à deux dimensions sollicite par un écran rigide. Doctoral thesis, University of Grenoble.

BOWLES, J. E. (1968). Foundation Analysis and Design. Tokyo, McGraw-Hill Kogakusha Ltd.

BRETH, H. and WANOSCHEK, H. R. (1972). The influence of foundation weights upon earth pressure acting on flexible strutted walls. Proc. 5th European Conf. Soil Mech. and Fdn Engng, Madrid, Vol. 3, pp. 251-258.

BRETH, H. and WOLFF, R. (1976). Versuche mit einer mehrfach verankerten modellwand. Die Bautechnik, Vol. 53, Part 2, pp. 38-47.

BROMS, B. B. (1968). Swedish tie-back system for sheet pile walls. Proc. 3rd Budapest Conf. Soil Mech. and Fdn Engng, Budapest, pp. 391-403.

BROOKER, E. W. and IRELAND, H. O. (1965). Earth pressure at-rest related to stress history. Can. Geotech. J., Vol. 2, No. 1, pp. 1-15.

BROWZIN, B. S. (1948). Upon the deflection and strength of anchored bulkheads. Proc. 2nd Int. Conf. Soil Mech., Rotterdam, Vol. 3, pp. 302-308.

BUREAU SECURITAS (1972). Recommendation concernant la conception, le calcul, l'éxecution et le control des tirants d'ancrage. Etablies par le Bureau Securitas. Recommendations TA 72, Paris.

BURLAND, J. B. (1975). Some examples of the influence of field measurements on foundation design and construction. Proc. 6th Regional Conf. for Africa for Soil Mech. and Fdn Engng, Durban, South Africa, Vol. 2, pp. 267-284.

BURLAND, J. B. (1977). Field measurements. Some examples of their influence on foundation design and construction. Ground Engng, Vol. 10, No. 7, pp. 15-22.

BURLAND, J. B. and HANCOCK, R. J. R. (1977). Underground car park at the House of Commons, London. Geotech. aspects, The Struct. Engr, Vol. 55, No. 2, pp. 87-100.

CARR, R. W. (1970). An experimental investigation of plate anchors in sand. Ph.D. thesis, University of Sheffield.

CARR, R. W. and HANNA, T. H. (1971). Sand movement measurements near anchor plates. J. Soil Mech. and Fdn Engng Div., Proc. A.S.C.E., Vol. 97, No. SM5, pp. 833-840.

CASAGRANDE, L. (1973). Comments on conventional design of retaining structures. J. Soil Mech. and Fdn Engng Div., Proc. A.S.C.E., Vol. 99, No. SM2, pp. 181-198.

CLARK, D. A. R. (1951). Advanced Strength of Materials. London, Blackie and Son Ltd.

CLOUGH, G. W. (1976). Excavation support practice in Europe and the West Coast. Presented at pile talk seminar on current practice in pile design and installation, Mariot Hotel, Saddle Brooke, New Jersey, pp. 1-19.

CLOUGH, G. W. and DUNCAN, J. M. (1971). Finite element analysis of retaining wall behaviour. J. Soil Mech. and Fdn Engng Div., Proc. A.S.C.E., Vol. 97, No. SM12, pp. 1657-1673.

CLOUGH, G. W. and TSUI, Y. (1974). Performance of tied-back walls in clay. J. Geotech. Engng Div., Proc. A.S.C.E., Vol. 100, No. GT12, pp. 1259-1273.

CLOUGH, G. W., WEBER, P. R. and LAMONT, J. (1972). Design and observation of a tied-back wall. A.S.C.E. Conf. on Performance of Earth and Earth-Supported Structures, Purdue, Lafayette, Indiana, pp. 1367-1390.

DAS, B. M. and SEELY, G. R. (1975). Vertical and inclined anchors in granular soil. Proc. 2nd Australia-New Zealand Conf. Geomech., Brisbane, Inst. Engng, Australia, Sydney, pp. 99-103.

DE BEER, E. E. and LADANYI, B. (1961). Experimental study of the bearing capacity of sand under circular foundations resting on the surface. Proc. 5th Int. Conf. Soil Mech. and Fdn Engng, Paris, Vol. 1, pp. 577-585.

DINA, A. O. (1973). An investigation of tied-back inclined retaining walls. M. Eng. thesis, University of Sheffield.

DUBROVA, G. A. (1963). Interaction of soil and structures. Izd. Rechnoy Transport, Moscow.

EGGER, P. (1972). Influence of wall stiffness and anchor prestressing on earth pressure distribution. Proc. 5th European Conf. Soil Mech. and Fdn Engng, Madrid, pp. 259-264.

EL-RAYES, M. K. (1965). Behaviour of cohesionless soils under uplift forces. Ph.D. thesis, University of Glasgow.

GERMAN SOCIETY FOR SOIL MECHANICS AND FOUNDATION ENGINEERING (1966). Recommendations of the Committee for Water Front Structures. Berlin, Munich, Wilhelm Ernst and Son.

GOULD, J. P. (1970). Lateral pressures on rigid permanent structures. Proc. A.S.C.E. Speciality Conf., Lateral stresses in the ground and design of earth retaining structures, Cornell, pp. 219-269.

HANNA, T. H. (1968). Factors affecting the loading behaviour of inclined anchors used for the support of tie-back walls. Ground Engng, Vol. 1, No. 5, pp. 38-41.

HANNA, T.H. (1968). Design and behaviour of tie-back retaining walls. Proc. 3rd Budapest Conf. Soil Mech. and Fdn Engng, pp. 410-418.

HANNA, T. H. and ABU-TALEB, M. G. A. (1972). Recent research studies into rigid tie-back supported wall design and their practical implications. Ground Engng, Vol. 5, No. 2, pp. 16-20.

HANNA, T. H. and KURDI, I. I. (1974). Studies on anchored flexible retaining walls in sand. J. Geotech. Engng Div., Proc. A.S.C.E., Vol. 100, No. GT10, pp. 1107-1122.

HANNA, T. H. and MATALLANA, G. A. (1970). The behaviour of tied-back retaining walls. Can. Geotech. J., Vol. 7, No. 4, pp. 372-396.

HANNA, T. H. and SEETON, J. E. (1967). Observations on a tied-back soldier pile and timber-lagging wall. Ontario Hydro. Res. Quarterly, Vol. 19, No. 2, pp. 22-28.

HANNA, T. H., SPARKS, R. and YILMAZ, M. (1972). Anchor behaviour in sand. J. Soil Mech. and Fdn Engng, Proc. A.S.C.E., Vol. 98, No. SM11, pp. 1187-1208.

HANNA, T. H. and SPARKS, R. (1973). The behaviour of preloaded anchors in normally consolidated sands. Proc. 8th Int. Conf. Soil Mech. and Fdn Engng, Moscow, Vol. 2, pp. 137-142.

HENAUER, R. and OTTA, L. (1976). Retaining walls and supervision system for a 16.0 m deep excavation. Proc. 6th European Conf. Soil Mech. and Fdn Engng, Vienna, Vol. 2, pp. 149-156.

HUECKEL, S. (1957). Model tests on anchoring capacity of vertical and inclined plates. Proc. 4th Int. Conf. Soil Mech. and Fdn Engng, London, Vol. 1, pp. 203-206.

INSTITUTION OF STRUCTURAL ENGINEERS (1951). Civil Engineering Code of Practice. Earth retaining structures. CP2.

JAKY, J. (1944). The coefficient of earth pressure at rest. Magyar Menokes Epitesg Egylet Kozloiyc.

JAMES, E. L. and JACK, B. J. (1974). A design study of diaphragm walls. Proc. Conf. Diaphragm Walls and Anchorages, Instn Civil Engrs, London, pp. 41-49.

JAMES, E. L. and PHILLIPS, S. H. E. (1971). Movement of a tied diaphragm wall during excavation. Ground Engng, Vol. 4, No. 4, pp. 14-16.

JAMES, R. G. and BRANSBY, P. L. (1971). A velocity field for some passive earth pressure problems. Geotechnique, Vol. 21, No. 1, pp. 61-83.

KRANZ, E. (1953). Ueber die verankerung von spund wanden. Berlin, W. Ernst and Son.

KURDI, I. I. (1973). Studies on tied-back flexible retaining walls in sand. Ph.D. thesis, University of Sheffield.

LARNACH, W. J. (1972). The pull out resistance of inclined anchors installed singly and in groups in sand. Ground Engng, Vol. 5, No. 4, pp. 14-17.

LARNACH, W. J. (1973). The behaviour of grouped inclined anchors in sand. Ground Engng, Vol. 6, No. 6, pp. 34-41.

LARSEN, M. L., WILLETTE, W. R., HALL, H. C. and GNAEDINGER, J. P. (1972). A case study of a soil anchor tie-back system. Proc. A.S.C.E. Speciality Conf. on Performance of Earth and Earth-Supported Structures, Purdue, Lafayette, Indiana, Vol. 1, Part 2, pp. 1341-1366.

LITTLEJOHN, G. S. (1972). Anchored diaphragm walls in sand - anchor design. Ground Engng, Vol. 5, No. 1, pp. 12-17.

LITTLEJOHN, G. S. and MACFARLANE, I. M. (1974). A case history study of multi tied diaphragm walls. Proc. Conf. Diaphragm Walls and Anchorages, Instn Civil Engrs, London, pp. 113-121.

LIU, T. K. and DUGAN, J. P., Jr. (1972). An instrumented tied-back deep excavation. Proc. A.S.C.E. Speciality Conf. on Earth and Earth-Supported Structures, Purdue, Lafayette, Indiana, Vol. 1, Part 2, June, pp. 1323-1339.

LOCHER, H. G. (1969). See LITTLEJOHN (1972). Anchored diaphragm walls in sand - anchor design. Ground Engng, Vol. 5, No. 1, pp. 12-17.

MAESTRE, M. (1969). Incident produit lors de l'accroissement de la surcharge sur une paroi ancree. Proc. 7th Int. Conf. Soil Mech. and Fdn Engng, Mexico, Speciality Session 14, pp. 43-44.

MANSUR, C. I. and ALIZADEH, M. (1970). Tie-backs in clay to support sheeted excavation. J. Soil Mech. and Fdn Engng Div., Proc. A.S.C.E., Vol. 196, No. SM2, pp. 495-509.

MATALLANA, G. A. (1969). An experimental investigation of anchored model retaining walls. M. Eng. thesis, University of Sheffield.

MAZURKIEWICZ, B. K. (1972). The rupture figure for a double wall cofferdam. Proc. A.S.C.E. Speciality Conf. on Performance of Earth and Earth-Supported Structures, Purdue, Lafayette, Indiana, Vol. 1, Part 2, pp. 1271-1281.

MEYERHOF, G. G. (1973). Uplift resistance of inclined anchors and piles. Proc. 8th Int. Conf. Soil Mech. and Fdn Engng, Moscow, Vol. 2, pp. 167-172.

MEYERHOF, G. G. and ADAMS, J. I. (1968). The ultimate uplift capacity of foundations. Can. Geotech. J., Vol. 5, No. 4, pp. 225-244.

McROSTIE, G. C., BURN, K. N. and MITCHELL, R. J. (1972). The performance of tied-back sheet-piling in clay. Can. Geotech. J., Vol. 9, No. 1, pp. 206-218.

OSTERMAYER, H. (1977). Practice in the detail design applications of anchorages. Proc. of the Seminar on Diaphragm Walls and Anchorages, Instn. Civil Engrs, London, pp. 55-61.

OVESEN, N. K. (1962). Cellular cofferdams, calculation methods and model tests. Danish Geotech. Inst., Copenhagen, Bulletin No. 14.

OVESEN, N. K. (1964). Anchor slabs, calculation methods and model tests. Danish Geotech. Inst., Copenhagen, Bulletin No. 16.

OVESEN, N. K. (1972). Design method for vertical anchor slabs in sand. Proc. A.S.C.E. Speciality Conf. on Earth and Earth-Supported Structures, Purdue, Lafayette, Indiana, pp. 1481-1500.

PECK, R. B. (1943). Earth pressure measurements in open cuts, Chicago, (Ill.) Subway. Transactions A.S.C.E., Vol. 108, pp. 1008-1036.

PECK, R. B. (1969). Deep excavation and tunneling in soft ground. Proc. 7th Int. Conf. Soil Mech. and Fdn Engng, Mexico, State of the art volume, pp. 225-290.

PLANT, G. W. (1972). An assessment of multi-anchored retaining wall behaviour. Ph.D. thesis, University of Sheffield.

PONNIAH, D. A. (1973). A laboratory study on anchored-retaining walls in sand with surcharge loads. M. Eng. thesis, University of Sheffield.

RANKE, A. and OSTERMAYER, H. (1969). Contribution to the investigation of stability of multi-tied walls. Bautechnik, Vol. 46, No. 10, pp. 341-350.

ROSCOE, K. H., ARTHUR, J. R. F. and JAMES, R. G. (1963). The determination of strains in soil by an X-ray method. Civil Engng and Pub. Wks Rev., No. 684, pp. 873-876.

ROWE, P. W. (1952). Anchored sheet pile walls. Proc. Inst. of Civil Engrs, Part 1, Vol. 1, pp. 27-70.

ROWE, P. W. (1956). Sheet pile walls at failure. Proc. Inst. of Civil Engrs, Part 1, Vol. 5, pp. 276-315.

ROWE, P. W. and BRIGGS, A. (1961). Measurements on model strutted sheet pile excavations. Proc. 5th Int. Conf. Soil Mech. and Fdn Engng, Paris, Vol. 2, pp. 437-478.

SAXENA, S. K. (1974). Measured performance of a rigid concrete wall at the World Trade Centre. Proc. Conf. Diaphragm Walls and Anchorages, Instn Civil Engrs, London, pp. 107-112.

SCHNEEBELI, G. (1957). Une analogie mechanique pour l'étude de la stabilité des ouvrages en terre à deux dimensions. Proc. 4th Int. Conf. Soil Mech. and Fdn Engng, London, Vol. 2, pp. 228-232.

SCHULZ, H. (1976). The definition of the factor of safety of multi-tied back walls. Proc. 6th European Conf. Soil Mech. and Fdn Engng, Vienna, Vol. 2, pp. 189-196.

SHAH, S. A. (1975). Tests on tied-back retaining walls in over-consolidated sand with line surcharge load. M. Eng. thesis, University of Sheffield.

SHANNON, W. L. and STRAZER, R. J. (1970). Tied-back excavation wall for Seattle First National Bank. A.S.C.E. Civil Engng, March, pp. 62-64.

SILLS, G. C., BURLAND, J. B. and CZECHOWSKI, M. K. (1977). Behaviour of an anchored diaphragm wall in stiff clay. Proc. 9th Int. Conf. Soil Mech. and Fdn Engng, Tokyo, Japan, pp. 147-154.

STROYER, J. P. R. N. (1935). Earth pressure on flexible walls. J. Instn of Civil Engrs, Vol. 1, November, pp. 94-139.

TERZAGHI, K. (1941). General wedge theory of earth pressure. Transactions A.S.C.E., Vol. 106, pp. 68-94.

TERZAGHI, K. and PECK, R. B. (1967). Soil Mechanics in Engineering Practice. 2nd edition, New York, J. Wiley and Sons, Inc.

TSCHEBOTARIOFF, G. P. (1949). Large scale earth pressure tests with model flexible bulkheads. Final Report, University of Princeton.

TSCHEBOTARIOFF, G. P. (1951). Soil Mechanics, Foundations and Earth Structures. 1st edition, New York, London, McGraw Hill Book Company.

VANDER LINDEN, J. (1969). Controle de mouvements horizontaux d'une paroi moulée dans le sol avec ancrages précentraits. Discussion on Speciality Session 14, Proc. 7th Int. Conf. Soil Mech. and Fdn Engng, Mexico, pp. 103-104.

VESIC, A. (1971). Break-out resistance of objects embedded in ocean bottom. J. Soil Mech. and Fdn Engng Div., Proc. A.S.C.E., Vol. 97, No. SM11, pp. 1183-1205.

WARE, K. R., MIRSKY, M. and LUNIZ, W. E. (1973). Tied-back wall construction results and controls. J. Soil Mech. and Fdn Engng Div., Proc. A.S.C.E., Vol. 99, No. SM12, pp. 1135-1152.

WITTKE, W. and SEMPRICH, S. (1973). Finite element for foundations in soil. Proc. 8th Int. Conf. Soil Mech. and Fdn Engng, Moscow, Vol. 1, Part 3, pp. 271-277.

YILMAZ, M. (1971). The behaviour of groups of anchors in sand. Ph.D. thesis, University of Sheffield.

YILMAZ, M. and HANNA, T. H. (1971). The interaction of groups of anchors in sand. Symposium on Interaction of Structure and Foundations, University of Birmingham, pp. 196-205.

APPENDICES

APPENDIX I

Proving Ring Design

Two sizes of steel proving rings were used in the pin model analogy tests.

Referring to Fig. I-1, and using thick ring theory, the stresses at the different points are calculated from the equation (CLARK, 1951):-

$$f = \frac{N}{A}\left[\frac{ro^2}{\pi(h^2 + ro^2)} + \frac{ro^2}{2h^2}\left(\frac{2ro^2}{\pi(h^2 + ro^2)} - \text{Cos } \beta\right)\frac{\pm t}{ro + t}\right] + \frac{N}{2A} \text{ Cos } \beta$$

where

ro = mean radius,

B = ring width,

2t = ring thickness,

A = cross-sectional area, and

h^2 = function of the geometry of the section

$$= \frac{ro}{2t}\left[\frac{1}{12}\left(\frac{2t}{ro}\right)^2 + \frac{1}{80}\left(\frac{2t}{ro}\right)^4 + \frac{1}{448}\left(\frac{2t}{ro}\right)^6 + \ldots.\right]$$

The dimensions for the first ring were selected as follows:

ro = 16 mm

B = 10 mm

2t = 5 mm

for a design load range of 0 to 900 N. The predicted stresses at the maximum load of 900 N were:-

f_I = +98.4 N/mm^2 (tensile)

f_{II} = -121.4 N/mm^2 (compressive)

f_{III} = -21.1 N/mm^2 (compressive)

f_{IV} = +88.9 N/mm^2 (tensile)

The dimensions for the second ring were selected as follows:

ro = 21.0 mm

B = 10.0 mm

2t = 8.0 mm

for a design load range of 0 to 1800 N. The predicted stresses at the maximum load of 1800 N were:-

f_I = +98.6 N/mm^2 (tensile)

f_{II} = -127.3 N/mm^2 (compressive)

f_{III} = -35.7 N/mm^2 (compressive)

f_{IV} = +98.6 N/mm^2 (tensile)

These conservative values were adopted because no account was taken of the small holes drilled through the proving rings.

All values are less than the allowable limit for steel which is 140 N/mm^2.

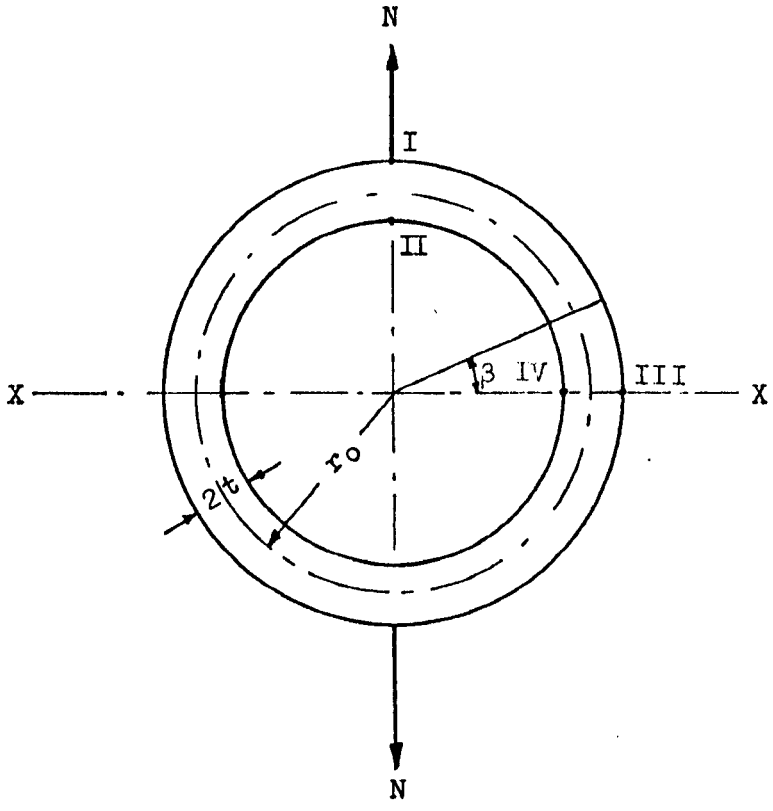

Fig. I-1

β is measured from the X - X axis.

t is positive for points I, III.

t is negative for points II, IV.

APPENDIX II

Design of Duralumin Proving Rings

The same procedure explained in Appendix I was followed. The dimensions and the predicted stresses for a maximum load of 200 Newtons are as follows:

ro = mean radius = 7.62 mm

B = ring width = 7.6 mm

2t = ring thickness = 2.54 mm

f_I	= 51.80	N/mm^2	(tensile)
f_{II}	= -65.0	N/mm^2	(compressive)
f_{III}	= +20.1	N/mm^2	(tensile)
f_{IV}	= +48.0	N/mm^2	(compressive)

All values are less than the allowable limit of 83.7 N/mm^2.

Appendix III

True Wall Displacements and Angle of Rotation

Since the wall displacements were not measured at the base or top of the wall, the true displacements have been calculated using the formulae shown below. Here, the top of the wall refers to the level of the wall at the sand surface, that is 600 mm above the base.

i) Horizontal Displacements

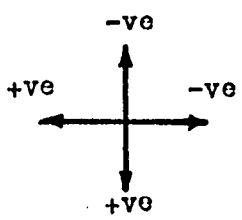

sign convention

X_{tm} = top measured horizontal displacement

X_{bm} = bottom measured horizontal displacement

X_t = true top horizontal displacement

X_b = true bottom horizontal displacement

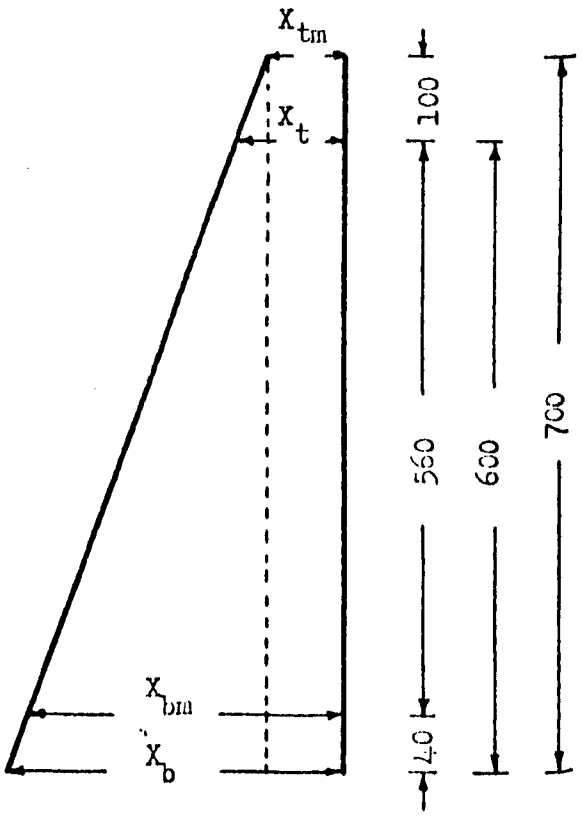

all dimensions in mm

Figure III. 1

Referring to Fig. III.1

$$X_t = \frac{100}{660} \times (X_{bm} - X_{tm}) + X_{tm}$$

$$X_b = \frac{700}{660} \times (X_{bm} - X_{tm}) + X_{tm}$$

Provided that the sign convention is adhered to, the sign and magnitude of X_t and X_b are correct irrespective of the mode of displacement of the wall.

ii) Vertical Displacement

As the order of magnitude of the vertical displacements was very small and because the top of the wall was only 100 mm from the top measuring point, it was considered accurate enough to take the measured vertical displacement as being equal to the displacement of the top of the wall.

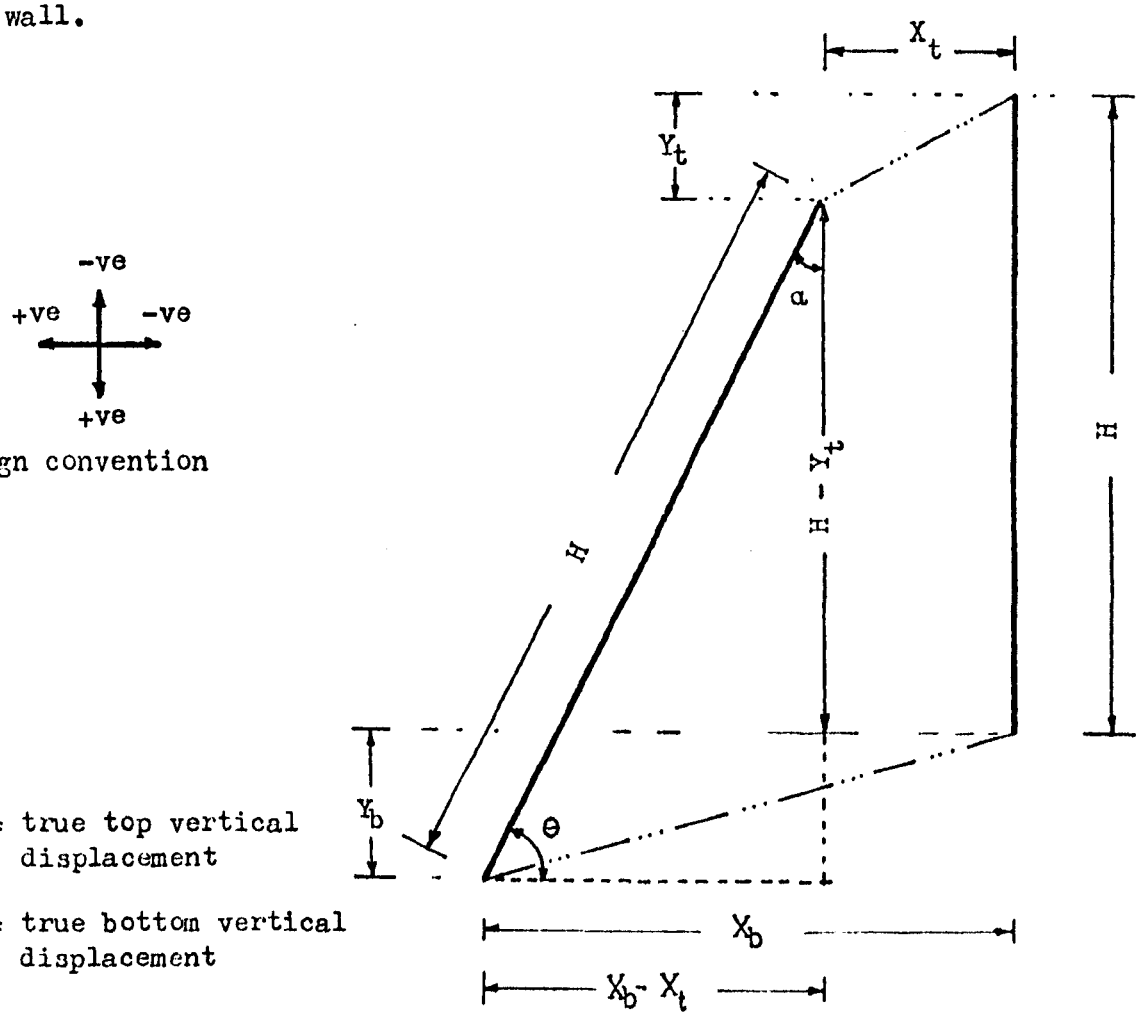

Y_t = true top vertical displacement

Y_b = true bottom vertical displacement

Figure III.2

Referring to Fig. III.2

The true bottom vertical displacement is given by

$$Y_b = H \sin \Theta - (H - Y_t)$$

where $\Theta = \cos^{-1} \frac{X_b - X_t}{H}$

Sample calculations for test C_2 where the wall exhibited the maximum rotation at full excavation.

$$X_t = 0.405 \text{ mm}$$

$$X_b = 1.12 \text{ mm}$$

$$Y_t = 0.33 \text{ mm}$$

Therefore

$$\theta = \cos^{-1} \frac{1.12 - 0.405}{600} = 89.932^{\circ}$$

$$Y_b = 600 \sin 89.932 - (600 - Y_t)$$

$$= 600 \times 0.9999 - (600 - 0.33)$$

$$= 0.3296 \text{ mm}$$

The difference between Y_b calculated and Y_t is 0.12%.

iii) Angle of Rotation

From Fig. III.2

the angle of α is given by $\alpha = 90 - \theta$

Appendix IV

Determination of the Position of the Centre of Wall Rotation

The notation for the calculation given below is as follows:

X_t = horizontal movement at the top of the wall

X_b = horizontal movement at the bottom of the wall

Y_t = vertical movement of the top of the wall

Y_b = vertical movement of the bottom of the wall

Y_c = the distance between the centre of wall rotation and the toe of the wall; a positive value of Y_c indicates that the centre of wall rotation is above the base of the wall

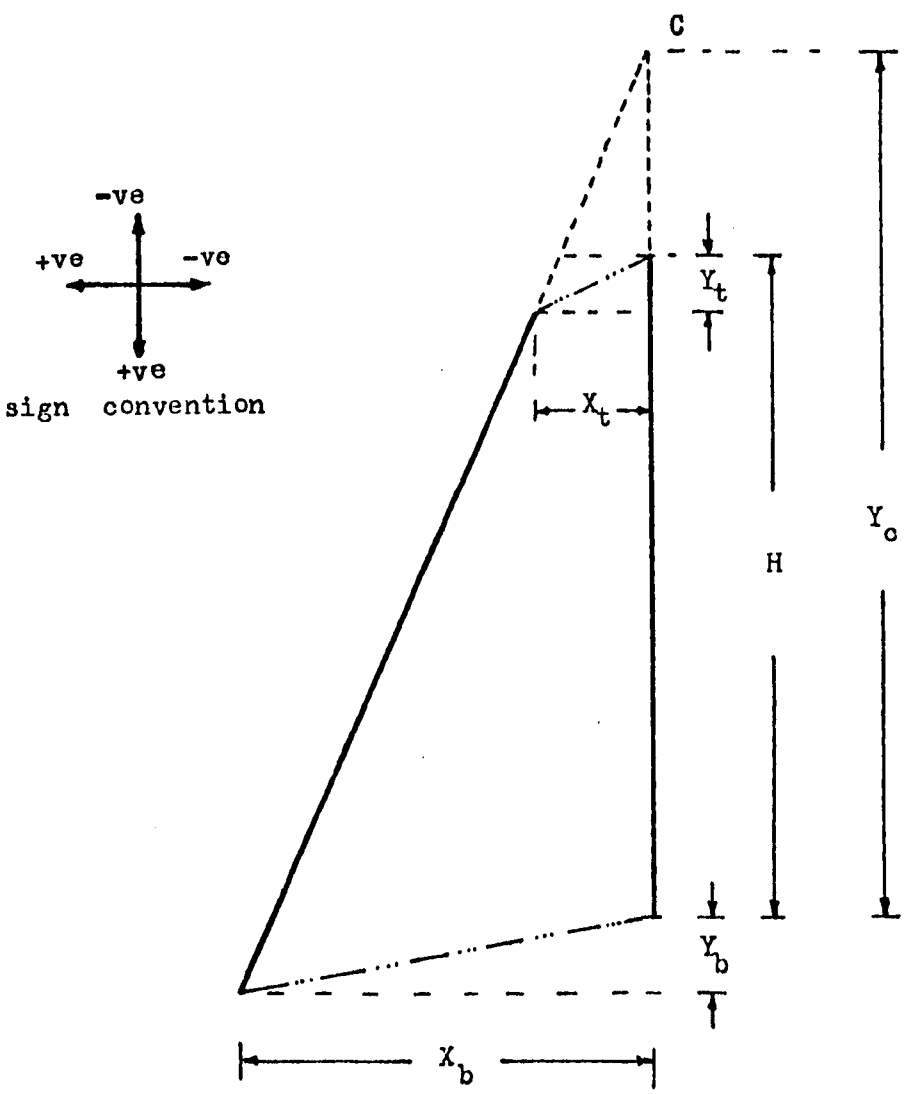

Figure IV.1

From Fig. IV.1 and assuming $Y_t = Y_b$

therefore $$\frac{X_b}{Y_c + Y_b} = \frac{X_t}{(Y_c - H) + Y_t}$$

$$X_b \left[Y_c - H + Y_t \right] = X_t \left[Y_c + Y_t \right]$$

$$X_b Y_c - X_b H + X_b Y_t = X_t Y_c + X_t Y_t$$

$$Y_c (X_b - X_t) = X_t Y_t - X_b Y_t + X_b H$$

$$Y_c (X_b - X_t) = - Y_t (X_b - X_t) + X_b H$$

$$Y_c = \frac{X_b H}{X_b - X_t} - Y_t$$

Appendix V

Lateral Earth Pressure as a Function of Wall Movement

The effect of wall movement on lateral earth pressure may be examined by the method proposed by Dubrova (1963) called the method of redistribution of pressure.

Fig. V.1 shows a rigid wall which rotates about its mid-height. Dubrova suggested the model shown in Fig. V.1 and assumed that the limiting passive condition exists only at the wall top, the limiting active condition only at the bottom, and that they occur simultaneously. The resultant force, F, on the rupture line BC is inclined at an angle $+\phi$ to the normal, while the rupture line for the limiting passive state passes through point A (exaggerated in the figure) and the angle between the resultant force and the normal is $-\phi$. Between these extremes it is assumed that an infinite number of quasi-rupture lines exist. Defining the angle between the force and the normal on any line, Ψ, Dubrova assumed that the variation of this angle with Z, the point along the wall that the line intersects is linear. That is therefore

$$\Psi = \frac{2\phi Z}{H} - \phi$$

Also, since the strength mobilization is dependent on the permitted wall movement, the resultant force, F_0, will be normal to its quasi-rupture line Ob. This is because there is displacement at O, and effectively $\phi = 0$ along Ob.

Dubrova assumed the validity of Coulomb's solution so that the angle that the quasi-rupture line makes with the horizontal for any Z is

$$\Theta = \frac{\pi}{4} + \frac{\Psi}{2} = \frac{\pi}{4} - \frac{\phi}{2} + \frac{\phi Z}{H}$$

Neglecting the effect of wall friction, the force against the wall for any Z is:

$$p = \frac{\gamma}{2}\left[\frac{Z}{1/\cos\Psi + \tan\Psi}\right]^2 = \frac{\gamma}{2}\left[\frac{Z\cos\Psi}{1+\sin\Psi}\right]$$

To determine the distribution of pressure against the wall this is differentiated with respect to Z to give:

$$p_{(Z)o} = \gamma \tan^2(45 - \Psi/2)\left[Z - \frac{2\phi Z^2}{H\cos\Psi}\right]$$

Similarly for rotation about the top, taking $\Psi = \frac{\phi Z}{H}$

$$p_{1(Z)} = \gamma \tan^2(45 - \Psi/2)\left[Z - \frac{\phi Z^2}{H\cos\Psi}\right]$$

and for rotation about the wall toe

$$p_{2(Z)} = \gamma Z\left[\frac{\cos\phi}{1+\sin\phi}\right]^2$$

The case of wall translation was treated as the average of the two latter conditions.

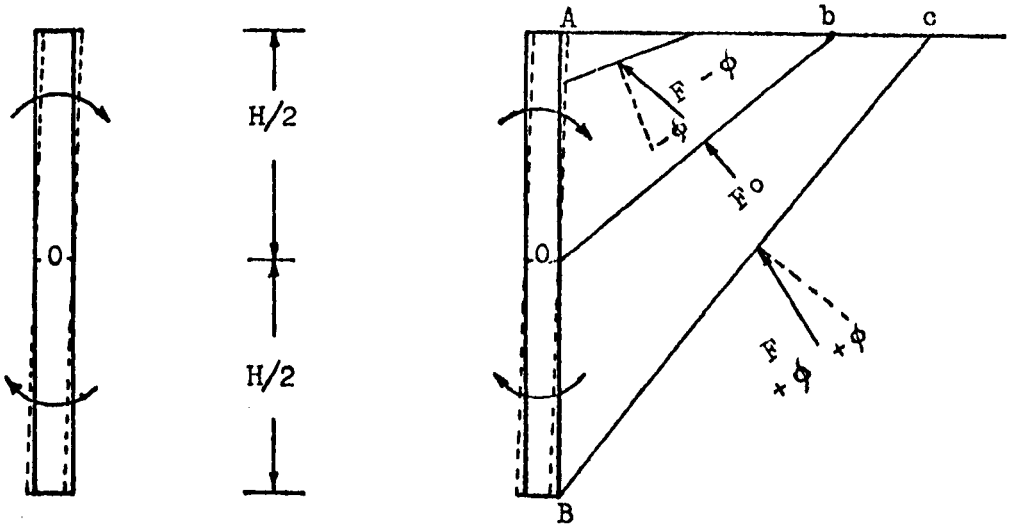

Wall Rotation and Assumed Rupture Lines

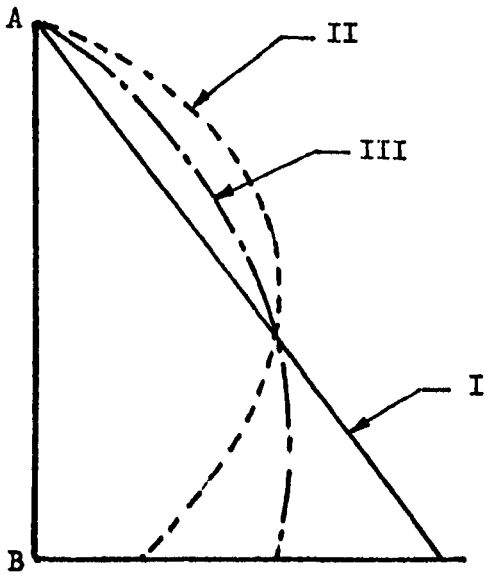

I Rotation about B

II Rotation about A

III Translation

Theoretical Earth Pressure Distribution

Figure V.1. Lateral Earth Pressure as a Function of Wall Movement (After Dubrova, 1963).